LYNN C. ROGERS

AD0613081

FDL-TDR-64-25

TRANSIENT DYNAMIC RESPONSE OF ORBITING SPACE STATIONS

20080820 062

TECHNICAL DOCUMENTARY REPORT No. FDL-TDR-64-25

FEBRUARY 1965

AIR FORCE FLIGHT DYNAMICS LABORATORY
RESEARCH AND TECHNOLOGY DIVISION
AIR FORCE SYSTEMS COMMAND
WRIGHT-PATTERSON AIR FORCE BASE, OHIO

Project No. 1370, Task No. 137008

(Prepared under Contract No. AF 33(657)-10219 by the
Space and Information Systems Division,
North American Aviation, Incorporated, Downey, California;
C. L. Tai, L. V. Andrew, M. M. H. Loh, P. C. Kamrath, Authors)

NOTICES

300 - March 1965 - 448-31-713

AD613081

FOREWORD

This report covers the research conducted by the Space and Information Systems Division of North American Aviation Company, Inc., Downey, California, for the Aerospace Dynamics Branch, Vehicle Dynamics Division, AF Flight Dynamics Laboratory, Wright-Patterson Air Force Base, Ohio, under Contract No. AF33(657)-10219. This work was performed to advance the dynamic loads state of the art for flight vehicles as part of the Research and Technology Division, Air Force Systems Command's exploratory development program. This research was conducted under Project No. 1370, "Dynamic Problems in Flight Vehicles," and Task No. 137008, "Prediction and Prevention of Dynamic Load Problems". Mr. Lynn C. Rogers, and later Mr. T. D. Lemley, of the Vehicle Dynamics Division, AF Flight Dynamics Laboratory, were the Project Engineers.

Mr. L. V. Andrew, who was the Program Manager for North American Aviation, defined a preliminary form of the technical approach and performed part of the technical work. Dr. C. L. Tai, Principal Investigator, refined the technical approach and directed most of the technical work. Mr. M. Pleskys conducted numerical analyses, and Mrs. T. Bryce wrote the computer programs. Mr. M. Lukoff contributed to the analysis of control forces applied to the cable-connected space station.

This report has been reviewed and is approved.

Walter J. Mykytow

WALTER J. MYKYTOW
Asst. for Research & Technology
Vehicle Dynamics Division
AF Flight Dynamics Laboratory

ABSTRACT

The stability and dynamic response of thirteen rotating space station configurations when subjected to various applied disturbances were investigated first by approximate exploratory analyses to determine the significant configurations and the relative significance of transient inputs to each configuration. Detailed analyses of ten selected combinations of configurations and forcing functions were then carried out in depth with special attention given to internal mass motions, docking, angular acceleration, and control forces. In view of the unique dynamic response problems associated with the gravitational gradient and structural elasticity, separate detailed analyses of the cable-connected configuration, the Y-configuration, and the H-configuration were also conducted.

TABLE OF CONTENTS

Section Page

Section Page

ILLUSTRATIONS

Figure		Page
29	Longitudinal Vibration— Normal Mode	124
30	Lateral Vibration— Normal Mode	124
31	Torsional Vibration —Normal Mode	125
32	Lateral Vibration with Rotary Inertia of Compartment and Counterweight— Normal Mode	125
33	Two-Compartment Configuration Connected with Cables; Modes 1, 2, and 3	126
34	Two-Compartment Configuration Connected with Cables; Modes 4, 5, and 6	127
35	Two-Compartment Configuration Connected with Cables; Modes 7 and 8	128
36	Two-Compartment Configuration Connected by 5-Foot-Diameter Spokes — In-Plane Vibration Mode Shapes.	129
37	Two-Compartment Configuration Connected by 5-Foot-Diameter Spokes —Normal-To-Plane Vibration Mode Shapes	130
38	Two-Compartment Configuration Connected by 10-Foot-Diameter Spokes — In-Plane Vibration Mode Shapes	131
39	Two-Compartment Configuration Connected by 10-Foot-Diameter Spokes — Normal-To-Plane Vibration Mode Shapes	132
40	Y-Configuration — In-Plane Vibration Mode Shapes .	133
41	Y-Configuration — Normal-To-Plane Vibration Mode Shapes	134
42	Inertial Coordinate System	135
43	Earth-Fixed Coordinate System	136
44	Euler Rotation Angles	138
45	Idealized Cable-Counterweight Space Station	149
46	Moving Coordinate Frame Through the Center of Mass of a Compartment-Cable-Counterweight System . . .	170
47	Coordinate Systems of Y-Configuration	181
48	Coordinate Systems of H-Configuration	191
49	Four-Degrees-of-Freedom Equations Without Damping ($R, \dot{\theta}, r, \dot{\phi}$)	206
50	Four-Degrees-of-Freedom Equations With One-Percent Critical Damping Factor ($R, \dot{\theta}, r, \dot{\phi}$)	207
51	Seven-Degrees-of-Freedom Equations Without Damping ($R, \dot{\theta}, r, \dot{\phi}, q_1, q_2, q_3$)	208
52	Seven-Degrees-of-Freedom Equations With One-Percent Critical Damping Factor ($R, \dot{\theta}, r, \dot{\phi}, q_1, q_2, q_3$) . . .	211
53	Coordinate Systems	217
54	Internal Mass Motions, Artificial Gravity 1/2-g (Configuration 1-A, Case 1)	236

Figure		Page

Figure		Page

TABLES

NOMENCLATURE

a	Sub-length
A	Cross-sectional area
C	A constant, shape factor of torsional rigidity
E	Modulus of elasticity
F	Force; control force
G	Gravity force; modulus of rigidity
H	Moment of momentum
i	Imaginary unit
I	Moment of inertia; the sum $m_1 \ell_1^2 + m_2 \ell_2^2 + \frac{P}{3}(\ell_1^3 + \ell_2^3)$
k	Constant, spring constant, torsional rigidity of a segment of cable
K	Product of universal gravitational constant and mass of earth; shape factor of shear stress
ℓ	Length of cable from center of gravity at steady state
L	Length of compartment; total length of cable; Laplace transform
m	Mass; mass per unit length
M	Mass; moment; the sum $m_1 + m_2 + \rho r_o$
p	Angular rotation rate about the vehicle x body axis; natural frequency
P	Force
q	Angular rotation rate about the vehicle y body axis; generalize coordinate
Q	Shear force, generalized force

r	Angular rotation rate about the vehicle z body axis; length of cable
R	Distance from center of earth to center of mass of a system, radius of compartment
s	Independent variable of the Laplace transform
S	Stress, cable tension
t	Time
T	Kinetic energy (twice the kinetic energy in Section 4.0)
u	Displacement
U	Strain energy
v	Displacement, velocity
V	Potential energy, velocity
w	Displacement
W	Weight
A_{ij}, B_{ij}, C_{ij}...	Transfer matrix for section or compartment a, b, c,...

Greek Symbols

α	An angle in general; phase angle; nutation angle of x-axis from angular momentum vector
β	A constant; deviation of R
δ	Elongation
ζ	A moving coordinate; body axis
	A moving coordinate; body axis
θ	Euler angle about y body axis; angular displacement
κ	A constant
λ	Mode function; angle between a body fixed plane and a space fixed plane passing through angular momentum vector
ρ	Mass per unit length of cable

ϕ	Euler angle about x body axis; angular displacement; normal mode function
ψ	Euler angle about z body axis; angular displacement
ω	Natural frequency; angular velocity of a system
θ_1	$\tan^{-1}\left(\frac{\partial \delta}{\partial \eta}\right) \eta = \ell_1$
θ_2	$\tan^{-1}\left(\frac{\partial \delta}{\partial \eta}\right) \eta = \ell_2$

Definition of Superscripts

$\cdot$	Derivative with respect to time
$-$	A vector
a, b, c, . . .	Compartment a, b, c, . . .

Definition of Subscripts

H	Hub
1	Compartment (mass 1)
2	Counterweight (mass 2)
c	Cable, center
I	Inertial or in plane
N	Normal to plane; moments (Appendix A); constant
o	Steady state; zero station; initial
n	n^{th} station; a number in general
ot	Zero tension
x	About or along x axis
y	About or along y axis
z	About or along z axis

e	Extensional
ℓ	Lateral
m	Mass
i	A number in general
1, 2, 3,	First, second, etc., vibration modes

1.0 INTRODUCTION AND SUMMARY

1.1 BACKGROUND

A space station revolving in orbit is subject to numerous small disturbing forces from space environments and operating systems. These forces are dynamic in origin and are generally transient in nature. In order to determine the extent of the perturbations, optimize the relations between light weight and structural strength, exploit the possibilities of control, and ensure a comfortable living environment from shock and vibration surroundings, the dynamic response of the station to these disturbing forces at different levels of artificial gravity falling within the human factors envelope (Appendix C) must be fully understood.

The stability and response of various selected configurations of orbiting space stations subjected to rapidly applied disturbances were investigated first by approximate exploratory analyses to determine the significant configurations of space stations and the relative significance of transient inputs to each configuration. A detailed analysis of ten selected combinations of configurations and forcing functions was then carried out in depth. The problem areas to be considered include the internal mass motions, launch and docking forces, angular acceleration, and control forces.

In view of the unique dynamic response problems of some specific configurations which may not be solved by general studies, complete analyses of the compartment-cable-counterweight space station, Y-space station, and H-configuration subjected to the influence of the gravitational gradient, control forces and elastic effects were conducted separately.

The report is divided into nine sections. Generally, the materials listed before section six are exploratory analyses and the remaining sections are detailed analyses.

1.2 SUMMARY AND RESULTS

1.2.1 Configurations

To initiate the study, a number of representative configurations were selected for exploratory investigation. Two or three compartments (and/or counterweights) with ratios of length to width of 1:10, spinning about a common axis interconnected with either compression or tension members, were considered in the configuration analysis. The radius of rotation from compartment to the spin axis is generally set at 100 feet. For tension

Manuscript released by authors May 1964 for publication as an [illegible] Technical Documentary Report.

member-connected configurations, cable lengths of 1,000 and 6,000 feet were used. The configurations which were investigated in the exploratory analysis are discussed in Section 2.0 of this report.

1.2.2 Disturbances and Forcing Functions

The disturbances that act on the space station are classified as external and internal disturbances. In the category of external disturbances, the gravity gradient is the main consideration in the complete analysis of a cable-connected space station, because it is essential to establish that the satellite's motion about its mass center is stable even though a feasible damper may be required. The docking operation was simulated by an increase in the total mass and a change in the moments of inertia of the space station and by a rectangular moment pulse of short duration. The dynamic cross-coupling created by the internal mass transfer was handled by treating the moments of inertia as functions of the mass movements with respect to time. The various inputs were summarized in the form of rectangular, ramp, and sinusoidal functions which in turn were expressed by the general Fourier's series.

1.2.3 Exploratory Analysis - Stability

It is important that the dynamic properties associated with any given configuration of a space station be considered in the design. The distribution of masses relative to the spin axis markedly affects the stabilization and control problem. It has been observed that a nonrigid satellite which is spin-stabilized about its axis of minimum moment of inertia will tumble. The cause is attributed to the dissipation of mechanical energy in the structure due to internal friction. The minimum energy condition which corresponds to the condition of the vehicle spinning about its axis of maximum moment of inertia represents the only stable state for a rotating, non-rigid vehicle. However, when the difference between the maximum and intermediate moments of inertia is small when compared to the minimum moment of inertia, the rotation is less stable. The stability criteria of the various configurations are fully discussed in Section 4.0 of this report.

1.2.4 Exploratory Analysis - Particular Disturbances

From the viewpoint of the designer, the choice of a space station configuration may be based on the rotational stability of the spacecraft and its response to various disturbing forces. In Section 5. 0, the rigid body angular response motions of thr representative configurations are investigated. The motions are obtained by linearizing the Euler's moment equations. The moments exerted on the space stations are expressed in the form of Fourier series. Different levels of artificial gravity, with attention to the human factors associated with a rotating vehicle, were introduced in analyzing the configurations. Fifty-two combinations of configurations and forcing functions have been examined and tabulated for comparison. (See Tables 6 through 11.)

The human factor considerations associated with rotation are discussed in Appendix C. From the results, a selection of 10 combinations of configurations and forcing functions were made for further detailed study in Section 9.0 of this report.

1.2.5 System Vibration Modes

In view of the adaptability of a lumped parameter method to digital computer operations, the method has been developed and applied successfully to most of the selected configurations. For an elastically stable system, one may consider that each normal coordinate corresponds to an independent mode of vibration of the system. In general, any arbitrary motion of the system may be expressed as a superposition of the motions in the normal modes. To apply this theory to systems with an infinite number of degrees of freedom, we begin by seeking the normal modes of vibration. Section 6.0 is devoted to the calculation of the frequencies of free vibration and mode shapes of the different configurations.

1.2.6 General Analysis of the Motion of an Orbiting Space Station

In a general analysis of the motion of an orbiting space station during a six-month period or more, it is desirable that the inertial frame of reference consider, at least, the earth's orbit angle about the sun as a degree of freedom. Thus, eight rigid body degrees of freedom and an unlimited number of elastic degrees of freedom were introduced in the system. The formulations of the kinetic energy and gravitational potential were carried out in detail. The analysis is applied to an idealized cable-counterweight space station. Motion analysis was restricted to the direction of the cable, and gravitational forces up to the second order were included in the study of small perturbations from the steady state. By linearizing the equations of motion, i.e. retaining only first order terms in the perturbations, a stable orbit was achieved and the small perturbations on that orbit due to the gravity gradient were determined. In this preliminary analysis the change in angular momentum due to elastic deformations was neglected and the linearized equations for the elastic degrees of freedom were solved separately. This leads to an unstable root of the elastic equations. It was thus established that the coupled non-linear equations should be solved simultaneously in the subsequent detailed analyses.

1.2.7 Planar Motion of Orbiting Space Stations

Because of the unique dynamic response problems of the compartment-cable-counterweight configuration, the Y-configuration, and the H-configuration of space stations when subjected to the influence of the gravitational gradient and elastic effects, separate detailed analyses of the planar motions were conducted in Section 8.0. The important feature in this analysis is the

inclusion of the coupling effect between the rotational motion and the orbital motion. The effects of flexibility and vibrational motion are also included in the formulation of the equations of motion. Under the assumption of a spherical gravitational potential and the neglect of dissipation forces, the computer solution of the equations of planar motion of the compartment-cable-counterweight configuration shows that the circular orbital motion of the cable system is stable, and that the spinning configuration has neutral elastic stability in the same sense that a simple spring-mass system has neutral elastic stability and oscillates with some finite amplitude in response to an externally applied periodic force when the period is different than the natural period of the system. The introduction of viscous damping terms representing a small percentage of the critical factor resulted in highly damped oscillations indicating a high sensitivity to damping forces. The results confirm those of other researchers although the interpretation of the results differs slightly.

1.2.8 Spin Dynamics of Rotating Space Stations

Normal operations of a rotating space station present several types of disturbances which affect its orientation. In Section 9.0, the rigid body angular motion of ten combinations of configurations and forcing functions were investigated in detail. To facilitate the study of the response of the space station to a time variant mass distribution, to an angular acceleration, and to proportional control forces, the Euler's moment equation with variable moments and products of inertia was solved by a fourth-order Runge-Kutta numerical integration procedure.

1.3 CONCLUSIONS AND RECOMMENDATIONS

It is extremely important that in any analysis of an orbiting elastic vehicle that (1) orders of magnitude of forces be balanced separately (only when the relationships of forces of equal order of magnitude are established can their effects on the motion of the vehicle be determined accurately); (2) initial conditions be consistent with the initial assumptions (i.e., if small amplitudes of elastic deformation are assumed in the derivation at least the initial response amplitudes should be small); (3) care be taken to differentiate between types of instability (i.e., unstable rotational motion may describe tumbling of the vehicle, an unstable orbit has a specific meaning, and unstable elastic deformations may exist under conditions of stable spin and a stable orbit).

The results of this study indicate: (1) that elastic deformations caused by gravity gradients will not cause an otherwise stable orbit to become unstable, (2) a space station with the intermediate moment of inertia very close to the largest moment of inertia will, if disturbed, eventually spin with large amplitudes of wobble - elastic deformations will result in damped

wobble motion until the spin axis is coincident with the axis of maximum moment of inertia, (3) the presence of a very small amount of viscoelastic or purely viscous damping (expected to be inherent in most manned space systems), should be adequate to achieve a satisfactory margin of stability of elastic deformations.

It is recommended that the study of cable-connected space stations be continued. Specifically, it is recommended that the configurations be limited to no less than two counterweights so that a wide separation of the maximum and the intermediate moments of inertia, and thus good spin stability, exists in the deployed configuration. It is believed that the cable-connected system is an attractive one because it provides a large amount of livable volume per unit of weight. It is also recommended that a quantitative study, including experiments, be conducted to establish whether artificial damping devices will be required to achieve a satisfactory margin of stability of elastic deformations.

Consideration of the approximations used in this study reveals that if serious consideration is to be given to the application of tension members to connect living modules of a future space station, an extensive research program must be conducted with emphasis in three-dimensional cable dynamics, the cable material and its internal dissipating mechanism, the non-linear phase of slacking cable, deployment and control problems, and other areas.

The equations of planar motion of the Y- and H-configurations described in Sections 8. 3 and 8. 4 may be investigated in a manner similar to that of the cable-connected compartment-counterweight configuration. A continuation of the study is recommended in order to extend the solution of the equations of motion of these configurations.

A preliminary investigation of the mechanics of deployment of a cable-connected space station has been conducted. A clear relationship is shown between the deployed length of the cable and the rotational velocity of the system. An extension of the analysis to include the effect of dissipation of energy during the deployment and the effect of a control couple to avoid the reverse wind-up is suggested for future study. It is also suggested that other deployment procedures and mechanisms be studied.

2.0 CONFIGURATION ANALYSIS

During the initial exploratory analysis, a number of representative configurations of manned space stations were investigated to determine their inherent stability and rigid body response to various disturbances. The configurations which were studied are shown in Figure 1 and Tables 1 and 2. These configurations are described below.

2.1 SINGLE-CABLE-CONNECTED COMPARTMENTS OR COUNTERWEIGHTS

These configurations, in which the crew compartment is connected by a long flexible cable to a counterweight or a secondary system, represent the simplest model of a space station. The system is spun up to a desired angular velocity about a centroidal axis to simulate varying degrees of artificial gravity.

Configurations 1 and 2 are composed of a cylindrical compartment 10 feet in diameter by 100 feet in length and are connected to a 5-foot-diameter spherical counterweight. The cylindrical compartment is assumed to weigh 260 pounds per linear foot, including the shell structure and equipment, and the counterweight is assumed to have a total weight of 3,250 pounds. The spin axis is designated as the x axis. Configuration 1 is rotating about the centroidal axis of maximum moment of inertia, i.e., the axis normal to the cable and the longitudinal axis of the compartment. Configuration 2 is rotating about a centroidal axis parallel to the longitudinal axis of the compartment. This is an axis of intermediate moment of inertia. From the stability analysis as described in Section 4.0, Configuration 2 is unstable. The compartment and counterweight of Configurations 1-A and 2-A are separated by a flexible cable 1,000 feet in length, while those of Configurations 1-B and 2-B are 6,000 feet apart. The increased cable length provides better environment for the crew by a more realistic simulation of earth gravity, but the ratio of maximum-to-intermediate moments of inertia is reduced and, consequently, so is the stability of the station. The cable is assumed to be 5/8-inch diameter steel strand, with an extensional rigidity (EA) of 4.37×10^6 pounds.

The CC configuration is another single-cable-connected space station that is composed of a 40,000 pound compartment and a 5,000 pound counterweight linked together by a 1,000-foot cable. The compartment is assumed to consist of a cylinder 60 feet long and 15 feet in diameter. The cable is 1-inch diameter steel strand, with an extensional rigidity of 10.94 $\times 10^6$ pounds.

2.2 MULTIPLE-CABLE-CONNECTED COMPARTMENTS OR COUNTERWEIGHTS

Configurations 4 and 6 represent space stations that are composed of two or three compartments linked together by several flexible cables. Each compartment in Configurations 4-A, 4-B, and 6-A is a cylindrical shell 100 feet long and 10 feet in diameter; the compartment of 6-B is a cylinder 20 feet in length and 20 feet in diameter. The total weight of each compartment is assumed to be 26,000 pounds. A hub of 15,000 pounds, located at the centroid of the system, has moments of inertia equal to those of Configuration 7-A. The axis of maximum moment of inertia is chosen as the axis of rotation. For Configurations 6-A and 6-B, the spin axis is normal to the longitudinal axes of the compartments. For Configurations 4-A and 4-B, the spin axis is the centroidal axis parallel to the longitudinal axes of the three compartments. In the case of Configurations 4-A and 4-B, the radial connecting cables that cross each other in pairs, increase the rotational stiffness of the connected members.

2.3 COMPRESSION-MEMBER-CONNECTED COMPARTMENTS

Configurations 7-A and Y-A have standard compartments 10 feet in diameter and 100 feet long. These compartments are connected to the central hub by radial spokes. The 5-foot diameter spokes, which also serve as passageways between the compartments and the hub, provide the necessary bending and torsional stiffness of the structural system. The flexural rigidities are 0.638×10^{12} lb-in.^{2} and 0.645×10^{11} lb-in.^{2}, and the torsional rigidities are 0.48×10^{12} lb-in.^{2} and 0.49×10^{11} lb-in.^{2} for the compartments and spokes, respectively. The compartments behave like rigid bodies even when the spokes are strengthened to have flexural stiffness equal to that of the compartments. A 15,000-pound hub is located at the centroid of the system that has a mass moment of inertia of 0.26×10^6 in.-lb-sec^2 about the symmetric axis and 1.52×10^6 in.-lb-sec^2 about the lateral axis. The station is spinning about the axis of maximum moment of inertia, i.e., the central axis normal to the longitudinal axes of the compartments. In Configuration 7-B, compartments 20 feet in diameter by 20 feet in length are used to reduce the margin of inertia difference between the two larger moments of inertia.

2.4 Y-CONFIGURATION

The Y-Configuration is one of the self-erecting space stations under study by the NASA in which the rigid compartments can be clustered into a compact payload during launching and self-deployed after boosting into orbit. This configuration consists of a central hub, similar to the one of Configuration 7-A, and three large compartments that are extended radially at 120 degrees apart. The compartments are shell structures 15 feet in diameter and 75 feet in length, with flexural and torsional rigidities of 2.2×10^{12} lb-in.^{2} and 1.08×10^{12} lb-in.^{2}, respectively. The total weight

of each compartment, including equipment, is 41,000 pounds. The central hub, as in the other configurations, provides docking facilities for logistic vehicles, and makes a zero-g laboratory possible. Most of the internal volume of this configuration is not concentrated at an optimized radius. It is necessary that living and working quarters for the crew be located at the outer ends of the radial compartments, where the most satisfactory gravitational environments exist.

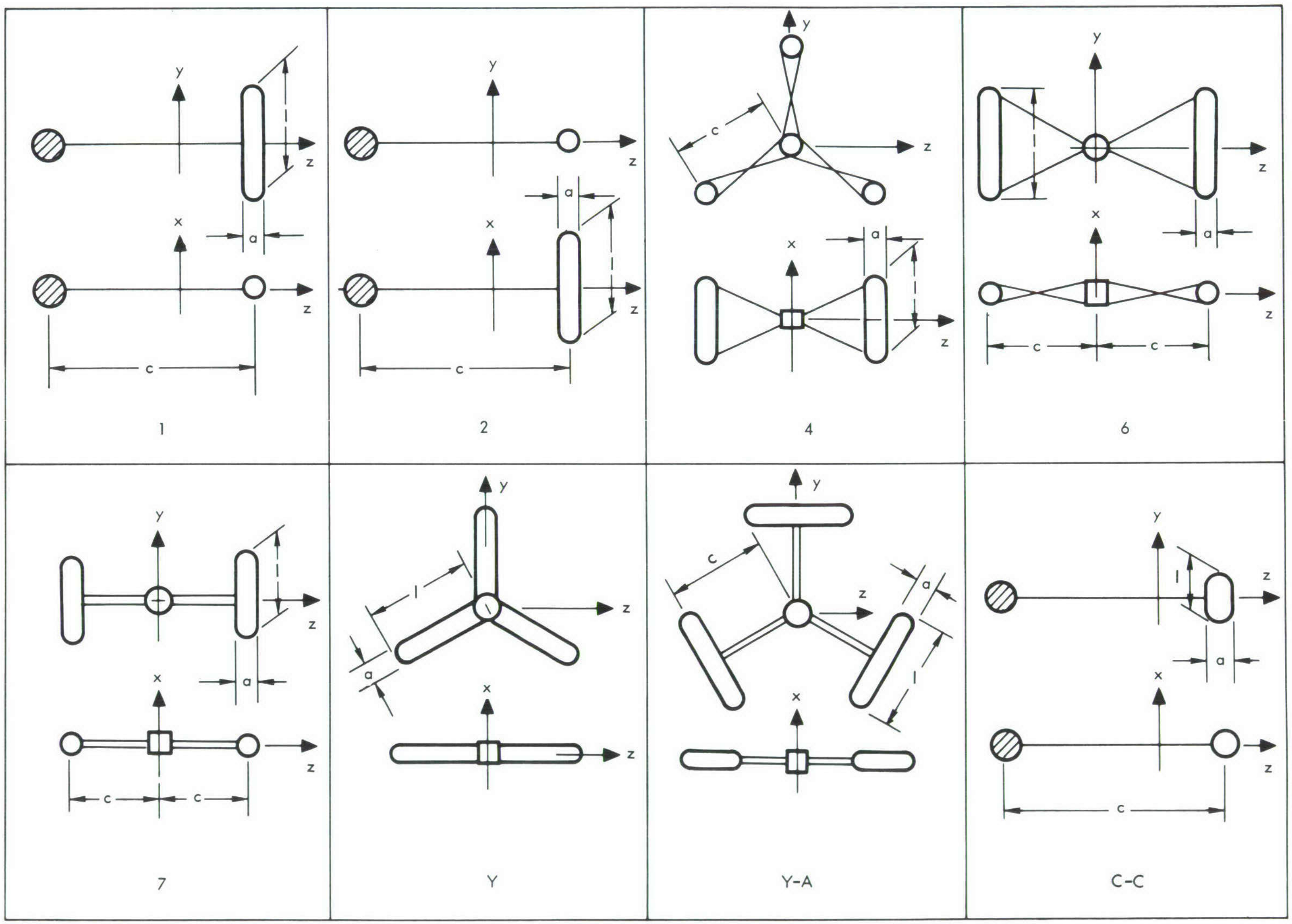

NOTE: X-AXIS IS THE AXIS OF ROTATION

Figure 1. Manned Space Station Configurations

Table 1. Physical Dimensions of the Manned Space Station Configurations

Configuration	Each Compartment			Counterweight		Hub Weight (pounds)	Cable or Spoke		C
	Length, ℓ (feet)	Diameter, a (feet)	Weight (pounds)	Diameter (feet)	Weight (pounds)		Diameter (feet)	Weight (pounds)	
1-A	100	10	26,000	5	3,250			800	1000
1-B	100	10	26,000	5	3,250			4,800	6000
2-A	100	10	26,000	5	3,250			800	1000
2-B	100	10	26,000	5	3,250			4,800	6000
4-A	100	10	26,000			15,000		50.4	100
4-B	100	10	26,000			15,000		252	500
6-A	100	10	26,000			15,000		56.4	100
6-B	20	20	26,000			15,000		50.4	100
7-A	100	10	26,000			15,000	5	7,300	100
7-B	20	20	26,000			15,000	5	7,300	100
Y	75	15	41,000			19,300			
Y-A	100	10	26,000			15,000	5	7,350	100
CC	60	15	40,000	10	5,000			2,200	1000

Table 2. Physical Properties of the Manned Space Station Configurations

Configuration	Cable		Mass Moment of Inertia			Ratio of Mass Moment of Inertia	
	Size (inches ϕ)	Wt/ft (pounds)	$I_x \times 10^{-6}$ (slug - ft.^{2})	$I_y \times 10^{-6}$ (slug - ft.^{2})	$I_z \times 10^{-6}$ (slug - ft.^{2})	$\frac{I_x}{I_y}$	$\frac{I_x}{I_z}$
1-A 1-B	5/8	0.8	96.2283 4489.31	95.5655 4488.65	0.683220 0.683220	1.006935 1.0001477	140.8452 6570.812
2-A 2-B	5/8	0.8	95.5655 4488.65	96.2283 4489.31	0.683220 0.683220	0.9931125 0.999852	135.8751 6569.842
4-A 4-B	1/2	0.504	24.3271 609.575	14.1862 306.813	14.7026 306.810	1.71484 1.986795	1.654615 1.9868159
6-A 6-B	1/2	0.504	17.5558 16.3186	16.2225 16.3167	1.38147 0.171194	1.019353 1.000119	12.70806 95.32235
7-A 7-B			19.0394 17.8080	17.7119 17.8061	1.38697 0.182529	1.07495 1.0001085	13.7273 95.76264
Y			6.1034	3.30830	3.30845	1.844876	1.844794
Y-A			28.5533	13.3159	10.2823	2.1442994	2.776933
CC	1	2.2	154.462	153.124	0.409163	1.0087363	377.5074

3.0 DISTURBANCES AND FORCING FUNCTIONS

3.1 EXTERNAL DISTURBANCES

The disturbances that will act on the space station may be classified as external or internal disturbances. The external disturbances are those that change the resultant angular momentum of the system. Generally, the external disturbances must be countered through the application of an external torque by the control system. Typical external disturbances are gravity gradient, docking and launching, meteorite impacts, and solar pressure.

3.1.1 Gravity Gradient

The gravity gradient disturbance is a force of extremely small magnitude and a torque the magnitude and direction of which are functions of the distribution of mass of the space station and the orientation of the vehicle with respect to the radius vector from the center of the earth to the center of mass of the space station. The torque exists unless the vehicle mass distribution is symmetrical about an axis along the aforementioned radius vector. In case the spin axis of the space station is directed toward the sun at all times and the orbit plane of the space station is not precisely coincident with the earth-orbit plane, a gravity gradient torque will always exist. Generally, over any single orbit, the gravity gradient will produce both a sinusoidal and a unidirectional torque component. Because of the very large angular momentum about the spin axis in comparison with gravity gradient torques, the space station will behave as a gyroscope and its spin axis will slowly precess in response to the applied torque. The response of the rigid station to the sinusoidal component is insignificant. The unidirectional torque is the component which must be compensated to maintain the station orientation.

The disturbance torques on the space station due to the earth's gravitational field are small in magnitude, but their integrated effects over long periods of time are found to be significant.

3.1.2 Docking and Launching

Docking and launching operations present two types of disturbances to the rotating station: (1) an impulsive torque, and (2) a change in mass and moments of inertia. For a resupply vehicle of mass (m) approaching the station with a relative velocity (V), with an attitude error resulting in a misalignment (d), the impulsive torque is

$$T\ (\delta t) = m\,Vd$$

For a representative resupply vehicle of 500 slugs, approaching at a relative docking velocity of 2 fps, with a misalignment of 1 foot, the impulsive torque is 1000 ft-lb-sec. An impact on the y-axis of the station results in a body angular velocity of

$$q = \frac{T(\delta t)}{I_y}$$

when

$I_{xy} = I_{yz} = 0$ and produces wobble motion.

The instantaneous change in mass and moments of inertia due to docking and launching operations can cause large disturbances to the rotating station. The added or subtracted mass of a large resupply vehicle or a weapon system will reduce or increase the station spin rate, shift the position of the mass center, and may introduce mass-unbalance in the system. This problem can be studied as an extension of the internal mass motion problem, since the same parameters are involved.

3.1.3 Meteorite Impact

A space station is subject to collisions with meteorites. The problem of a particular meteorite puncturing the skin of the vehicle and causing a system failure is of paramount importance. However, those punctures that do not cause failure, and those that fail to penetrate, apply torque impulses to the system. Information regarding meteorite frequency, energy, and degree of momentum-transfer in an impact, as well as the distributions of presented areas and impact location is necessary to determine the frequency and magnitude of the torque impulses of meteorites. A meteorite with a mass of 0.04 grams and a relative velocity of 130,000 fps would give a torque impulse of approximately 48 ft-lb-sec. For the space station configurations under consideration, a wobble angle of approximately 4×10^{-4} degree would result. The transient oscillations of the orientation angles imparted to a large space station by individual impacts appear to be very small. Even over a period of one year, the net impulse from meteorite impacts will probably be so small that the attitude control system will not be significantly disturbed.

3.1.4 Solar Pressure

The impact of photons striking the space station produce a pressure or force commonly known as solar wind or solar pressure. The solar pressure is approximately 9×10^{-8} lb/ft^2 for zero reflectivity of the vehicle surfaces[1] The torque on the station is the product of the solar pressure, the vehicle area projected toward the sun, and the distance between the center of mass and the center of solar pressure. This torque is very small, even for stations that are geometrically unsymmetrical. For a sun-oriented space station, with geometric symmetry about the spin axis, the torque due to solar pressure is zero.

---

[1] Reference 28

3.2 INTERNAL DISTURBANCES

Internal disturbances are those that do not change the total system angular momentum but are capable of producing wobble. Typical internal disturbances arise from mass unbalance, rotating machinery, circulating fluids and fluid ejection. These disturbances can generally be countered by a mass conservative wobble damper, such as the momentum wheel precession type.

3.2.1 Mass Unbalance and Mass Transfer

It is well known that a vehicle rotating in space spins about its instantaneous mass center and spins with the highest degree of stability about its largest instantaneous principal axis of inertia. However, due to mass unbalance, the mass center may be displaced from the geometric center and the largest principal axis of inertia may not be in perfect alignment with the spin axis of the station. The effect of rotation about this principal axis of inertia of the combined systems is a rotation of the artificial acceleration of gravity vector that appears to the crew as a tilting motion of the space station floor. The displacement of the mass center results in accelerations at the geometric center that can seriously affect zero-g experiments and docking operations on stations with a central hub.

Mass transfer, such as crew motion, results in transient changes in the moments and products of inertia, and can be a significant source of vehicle wobble. It is necessary to consider the load imposed by such disturbances on the damper system as a function of the magnitude of the inertia changes and the frequency of occurrence. After the wobble has been damped, the vehicle is spinning about its new principal axis with the geometric axis describing a cone about the system momentum vector. The attitude errors corresponding to the products of inertia for crew motions are further discussed in Section 9.0 of this report.

3.2.2 Rotating Machinery and Circulating Fluids

Circulating fluids and rotating machinery can exert disturbing torques on any rotating vehicle. Specifically, rotating machinery in the space station will consist of such devices as pumps and fans for the environmental control system. Circulating fluids used as heat transfer agents also will be present in this system. The circulation of air in each of the modules in the system also represents a possible source of disturbance torques.

If the inertial direction of an angular momentum vector is to be changed, it is accomplished with an external torque. Thus, the angular momentum vectors of rotating machinery or circulating fluids can impose a disturbance on the vehicle if these vectors are forced to change direction in space as the vehicle rotates. However, if these momentum vectors are parallel to the vehicle spin axis, their inertial direction is not affected by normal vehicle rotation. In other words, it appears desirable to mount the pumps and fans in such a way that the spin axis of their rotors is parallel to the vehicle spin axis. A similar specification for circulating fluids would require that the path of circulation lie in the plane of rotation of the vehicle. A second method of minimizing the disturbance would be to oppose the momentum vectors of machines or fluids in one module with those in the diametrically opposite module. For example, in two diametrically opposite modules the fans would be mounted in such a way that the spin axes of their rotors would be parallel, and the rotation of one rotor would be opposite in sense to the rotation of the other.

3.2.3 Fluid Ejection

Fluid ejection from the station by a faulty open reaction jet, puncture or failure of a pressurized compartment, and seal leakage, constitute a decrease in the total mass of the station and may transmit a net torque to the space station. The ejection of low-pressure fluid, such as compartment atmosphere, is not expected to represent a major attitude disturbance to the vehicle.

3.3 FORCING FUNCTIONS

Preliminary and detailed studies were conducted to determine the effects of major disturbances on the rigid body angular response of the space station configurations. These disturbances were idealized by mathematical representation to facilitate the analysis of the problem.

The response of the space station configuration was examined under the action of various external moments. The moments applied were expressed in the form of rectangular, ramp, and sinusoidal functions. The results of these investigations are presented in Section 5.3 of this report.

Transient internal mass transfer of a rotating space station may lead to dynamic cross-coupling moments created by the variation in system mass distribution. The moments and products of inertia of the system about its body axes were formulated as time functions of the mass movements. The disturbance effect on the vehicle due to the time-varying coefficients in the equations of motion was investigated by means of a computer analysis. Results of this analysis are included in Section 9.2 of this report.

Docking of a vehicle on the despun hub of a space station was simulated by a transient increase in the total mass and change in moments and products of inertia. The impulsive torque produced by misaligned docking was represented by a rectangular moment pulse of short duration. Because common parameters exist in both docking and moving mass problems, parallel approaches were used in analyzing these problems.

Control forces were studied with regard to reaction jet wobble damping, spin-up, and spin control. The proportional control equations that were used for spin control and wobble damping are

$$M_x = -k_1 (p - p_c)$$

$$M_y = -k_2 q,$$

$$M_z = -k_3 r,$$

where

p_c = the spin rate required to develop the desired artificial gravity level

k_1, k_2 and k_3 = control gain constants that are partially dependent upon the mass distribution of the space station.

In the preceding control equations, M_x serves to control small variations in the spin velocity and M_y and M_z damp wobble motions.

Spin-up generally involves a large change in the spin velocity and requires the application of a large external moment about the spin axis. Since reaction jets are most efficient under full thrust operations, a rectangular moment pulse was applied until the desired spin rate was achieved.

4.0 ROTATIONAL STABILITY OF A SPINNING SPACE STATION ABOUT ITS PRINCIPAL AXES IN A GRAVITY-FREE FIELD

The rotational stability of a spinning space station is defined below.

If the spin axis deviates slightly from the resultant angular momentum vector, and if there is no tendency for this deviation to grow, then the rotation is considered stable. On the other hand, if it is possible for a small deviation of the spin axis to develop into a large deviation and, eventually, result in a complete change in attitude of the body, then the rotation is considered unstable. Within this definition, the stability criteria of a moment-free unsymmetric station, either a perfectly rigid body or an elastic body, will be established in the following paragraphs.

4.1 ROTATIONAL STABILITY OF A SPINNING RIGID SPACE STATION

When the body axes are the principal axes, the Euler's equations of a torque-free body are

$$\begin{aligned} I_x \dot{p} - (I_y - I_z)\, q\, r &= 0, \\ I_y \dot{q} - (I_z - I_x)\, r\, p &= 0, \\ I_z \dot{r} - (I_x - I_y)\, p\, q &= 0. \end{aligned} \tag{1}$$

We find that

$$\begin{aligned} p &= \text{constant, if } q = r = 0, \\ q &= \text{constant, if } r = p = 0, \\ r &= \text{constant, if } p = q = 0. \end{aligned} \tag{2}$$

This indicates that permanent rotations are possible about each of the principal axes. It will now be shown that these permanent rotations are stable only when they are about the axes of maximum and minimum I.

If a constant rotation p_o is assumed about the x axis, and a small perturbation is allowed to determine its stability, we have an initial condition of $p = p_o$; $q = r = 0$, and a perturbed condition of $p = p_o + e$, with small q and r.

The linearized equations are

$$\begin{cases} I_x \dot{p} = 0 \\ I_y \dot{q} - (I_z - I_x)\, r\, p_o = 0 \\ I_z \dot{r} - (I_x - I_y)\, p_o\, q = 0 \end{cases} \tag{3}$$

Differentiating the last two equations and substituting for $\dot{q}$ and $\dot{r}$ from equation (3)

$$\ddot{q} + \frac{(I_x - I_z)(I_x - I_y)}{I_y I_z} p_o^2 q = 0$$

$$\ddot{r} + \frac{(I_x - I_y)(I_x - I_z)}{I_y I_z} p_o^2 r = 0 \tag{4}$$

which is stable, provided

$$(I_x - I_y)(I_x - I_z) > 0 \tag{5}$$

The above condition is satisfied only when $I_x > I_y$, and $I_x > I_z$; i. e., I_x is a major principal axis, or $I_y > I_x$, and $I_z > I_x$; i. e., I_x is a minor principal axis. When I_x is an intermediate moment of inertia, $(I_x - I_y)(I_x - I_z) < 0$ and small values of q and r will increase with the time. Thus, the permanent rotation is unstable about the axis of intermediate moment of inertia.

4.2 ROTATIONAL STABILITY OF A SPINNING ELASTIC SPACE STATION

The rotation of a rigid space station about its own minimum moment of inertia has been shown to represent a stable motion. In an elastic body, deformations between particles will always take place, resulting in some dissipation of energy by internal friction of the body. It can be shown that the rotation of an elastic space station about its minimum moment of inertia will not be stable. Due to the elastic deformation of the body and the dissipation of mechanical energy, the station begins to nutate with increasing angle. Finally, the station rotates about its axes of maximum moment of inertia.

The stability of an elastic body at different energy levels has been discussed in various classic mechanics texts. The essential feature of the transitional motion is described below.

When the body axes are the principal axes, the first integral of Euler's equations for a torque-free body can be combined to give

$$I_x p^2 + I_y q^2 + I_z r^2 = T \tag{6}$$

and a second integral, by multiplying Euler's equations by $I_x p$, $I_y q$, $I_z r$, yields

$$I_x^2 p^2 + I_y^2 q^2 + I_z^2 r^2 = G^2 \tag{7}$$

where T and G are two arbitrary constants, T equals twice the kinetic energy, and G^2 is the square of total angular momentum.

Suppose that $I_x > I_y > I_z$, and that the station initially spins about its z axis with

$$r = \Omega, \quad p = q = 0 \tag{8}$$

Thus,

$$G^2 = I_z^2 \Omega^2, \quad T_o = I_z \Omega^2, \quad \frac{G^2}{T_o} = I_z \tag{9}$$

During the transition period, the total angular momentum (G) will remain constant because of the absence of external moment, while the total kinetic energy (T) will decrease continuously, due to the dissipation of internal mechanical energy. Finally, the body will have a spin rate

$$p_e = \frac{I_z}{I_x} \Omega, \quad q_e = r_e = 0 \tag{10}$$

and

$$T_e = I_x p_e^2 = \frac{I_z^2}{I_x} \Omega^2, \quad \frac{G^2}{T_e} = I_x \tag{11}$$

Since the quantity G^2/T varies from I_z to I_x, the motion during the transitional period may be divided into three phases as listed in Table 3.

Table 3. Angular Motion at Different Energy Levels

Initial	Transitional			Final
$\frac{G^2}{T_o} = I_z$	$\frac{G^2}{T} < I_y$	$\frac{G^2}{T} = I_y$	$\frac{G^2}{T} > I_y$	$\frac{G^2}{T_e} = I_x$
$r = \Omega$		$q = \frac{I_z}{I_y}\Omega$		$p = \frac{I_z}{I_x}\Omega$
$T_o = I_z \Omega^2 = \frac{G^2}{I_z}$	$\frac{G^2}{I_z} > T > \frac{G^2}{I_y}$	$T = I_y q^2 = \frac{I_z}{I_y} T_o = \frac{G^2}{I_y}$	$\frac{G^2}{I_y} > T > \frac{G^2}{I_x}$	$T_e = I_x p_e^2 = \frac{I_z}{I_x} T_o = \frac{G^2}{I_x}$
rotating about I_z		rotating about I_y		rotating about I_x
I_z is the smallest		I_y is the medium		I_x is the largest

The transitional motion can be described analytically by Kirchhoff's solution[1] in three phases according to whether $I_z < G^2/T < I_y$, $G^2/T = I_y$, or $I_y < G^2/T < I_x$.

4.2.1 The First Phase ($I_z < G^2/T < I_y$ or $G^2/I_z > T > G^2/I_y$)

If we define

$$\Delta(\phi) = \sqrt{1 - k^2 \sin^2 \phi}$$

$$F(\phi) = \int_0^{\phi} \frac{d\phi}{\sqrt{1 - k^2 \sin^2 \phi}} \tag{12}$$

then, k is a modulus of F, and $k < 1$ is a necessary requirement if F is to be real for all values of ϕ; ϕ is the amplitude of the elliptic integral F, written as amF, thus the functions $\sin \phi$, $\cos \phi$, and $\Delta\phi$ may be written as sin amF, cos amF, and Δ amF. These functions may also be written as snF, cnF, and dnF.

By differentiation

$$\frac{d \cos \phi}{d F} = - \sin \phi \frac{d\phi}{dF} = -\sin \phi \, \Delta(\phi)$$

$$\frac{d \sin \phi}{d F} = \cos \phi \frac{d\phi}{dF} = \cos \phi \, \Delta(\phi)$$

$$\frac{d \Delta(\phi)}{d F} = - k^2 \sin \phi \cos \phi \left(1 - k^2 \sin^2 \phi\right)^{-1/2} \frac{d\phi}{dF} = - k^2 \sin\phi \cos\phi \tag{13}$$

The above equations can be made identical with Euler's equations. Since in this phase the polhode includes the axis I_x, if we define

$$\lambda (t - \tau) = F(\phi) = \int_0^{\phi} \frac{d\phi}{\sqrt{1 - k^2 \sin^2 \phi}} ,$$

$$p = c \cos \phi = c \operatorname{cn} \lambda (t - \tau) ,$$

$$q = b \sin \phi = b \operatorname{sn} \lambda (t - \tau) ,$$

$$r = a \Delta(\phi) = a \operatorname{dn} \lambda (t - \tau) , \tag{14}$$

(1) Reference 29, Ch. IV.

Euler's equations become

$$\begin{cases} \dfrac{I_y - I_z}{I_x} = \dfrac{\dot{p}}{qr} = \dfrac{-c \sin\phi \, \Delta(\phi) \, \lambda}{b \, a \sin\phi \, \Delta(\phi)} = -\dfrac{c\lambda}{ab} \\[2ex] \dfrac{I_x - I_z}{I_y} = \dfrac{-\dot{q}}{rp} = \dfrac{-b \cos\phi \, \Delta(\phi) \, \lambda}{a \, c \, \Delta(\phi) \cos\phi} = -\dfrac{b\lambda}{ca} \\[2ex] \dfrac{I_x - I_y}{I_z} = \dfrac{\dot{r}}{pq} = \dfrac{-a k^2 \sin\phi \cos\phi \, \lambda}{c \, b \cos\phi \sin\phi} = -k^2 \dfrac{a\lambda}{bc} \end{cases} \tag{15}$$

when

$$t = \tau$$

$$F = 0$$

$$\phi = 0$$

$$\Delta\phi = 1$$

$$p = c$$

$$q = 0$$

$$r = a$$

From the two first integrals of Euler's equations

$$\begin{cases} I_x c^2 + 0 + I_z a^2 = T \\ I_x^2 c^2 + 0 + I_z^2 a^2 = G^2 \end{cases}$$

where

$$a^2 = \frac{I_x T - G^2}{I_z (I_x - I_z)}$$

and

$$c^2 = \frac{G^2 - I_z T}{I_x (I_x - I_z)} \tag{16}$$

From Euler's equations

$$\frac{I_x - I_z}{I_y} \cdot \frac{I_x}{I_y - I_z} = \frac{b^2}{c^2}, \quad b^2 = \frac{G^2 - I_z T}{I_y (I_y - I_z)}$$

$$\frac{I_x - I_z}{I_y} \cdot \frac{I_y - I_z}{I_x} = \frac{\lambda^2}{a^2}, \quad \lambda^2 = \frac{(I_y - I_z)(I_x T - G^2)}{I_x I_y I_z},$$

$$\frac{I_x - I_y}{I_z} \cdot \frac{I_y}{I_x - I_z} = \frac{k^2 a^2}{b^2}, \quad k^2 = \frac{(I_x - I_y)(G^2 - I_z T)}{(I_y - I_z)(I_x T - G^2)} \tag{17}$$

and $I - k^2 = \dfrac{(I_x - I_z)(I_y T - G^2)}{(I_y - I_z)(I_x T - G^2)}$ is positive since $I_x > I_y > I_z$, a^2, b^2, c^2, and λ^2 are all positive, and $k^2 < 1$. Thus, the assumed solution for the energy range, $G^2/I_z > T > G^2/I_y$, is correct, and indicates that the body oscillates about the x and y axes with $p_{max} = c$, and $q_{max} = b$. The motion about the z axis is the rotation of the angular velocity and always rotates in the same direction. The periods of the oscillation are given by the complete elliptic integral, ana are equal to $4K(k)/\lambda$. For the fluctuating r, the period is $2K(k)/\lambda$. After more energy is dissipated, the motion reaches the second phase.

4.2.2 The Second Phase $\left(\frac{G^2}{T} = I_y\right)$

For $G^2 = I_y T$, we have $1 - k^2 = 0$, $k = 1$, and

$$F = \int_o^{\phi} \frac{d\phi}{\cos\phi} = \frac{1}{2} \log \frac{1 + \sin\phi}{1 - \sin\phi} \tag{18}$$

Thus,

$$\frac{e^F}{e^{-F}} = \frac{1 + \sin\phi}{1 - \sin\phi} \tag{19}$$

so that

$$\sin\phi = \frac{e^{F} - e^{-F}}{e^{F} + e^{-F}} = \tanh F,$$

$$\cos\phi = \sqrt{1 - \tanh^2 F} = \operatorname{sech} F = \frac{1}{\cosh F},$$

$$\Delta\phi = \sqrt{1 - k^2 \sin^2\phi} = \cos\phi = \frac{1}{\cosh F}. \tag{20}$$

therefore

$$\left\{\begin{aligned} p &= c \operatorname{cn} \lambda (t - \tau) = \frac{c}{\cosh \lambda (t - \tau)} \\ q &= b \operatorname{sn} \lambda (t - \tau) = b \tanh \lambda (t - \tau) \\ r &= a \operatorname{dn} \lambda (t - \tau) = \frac{a}{\cosh \lambda (t - \tau)} \end{aligned}\right. \tag{21}$$

when

$t = \tau$

$p = c$

$q = 0$

$r = a$

from Euler's equations and the first two integrals

$$a^2 = \frac{I_x T - G^2}{I_z (I_x - I_z)} = \frac{\left(\frac{I_x}{I_y} - 1\right) G^2}{I_z (I_x - I_z)}$$

$$b^2 = \frac{G^2 - I_z T}{I_y (I_y - I_z)} = \frac{G^2 \left(1 - \frac{I_z}{I_y}\right)}{I_y (I_y - I_z)} = \frac{G^2}{I_y^2}$$

$$c^2 = \frac{G^2 - I_z T}{I_x (I_x - I_z)} = \frac{G^2 \left(1 - \frac{I_z}{I_y}\right)}{I_x (I_x - I_z)}$$

$$\lambda^2 = \frac{(I_y - I_z) \left(\frac{I_x}{I_y} - 1\right) G^2}{I_x I_y I_z} \tag{22}$$

Because $I_x > I_y > I_z$ and a^2, b^2, c^2, and λ^2 are all positive for $t \to \infty$, $p = 0$, $r = 0$, $q = b = I_z/I_y \Omega = G/I_y$, then the body would settle on a rotation about the intermediate axis, I_y, if twice the kinetic energy remains $T = G^2/I_y$. However, T is still dissipated by the irregular motion. The motion will then enter the third phase.

4.2.3 The Third Phase $I_y < \frac{G^2}{T} < I_x$ or $\frac{G^2}{I_y} > T > \frac{G^2}{I_x}$

In the third phase, the polhode encloses the axis of largest moment of inertia, I_x, and the solution of Euler's equation becomes

$$\begin{cases} p = a \operatorname{dn} \lambda \ (t - \tau) \\ q = b \operatorname{sn} \lambda \ (t - \tau) \\ r = c \operatorname{cn} \lambda \ (t - \tau) \end{cases} \tag{23}$$

and a, b, c, λ, and k are determined as before:

$$a^2 = \frac{G^2 - I_z T}{I_x (I_x - I_z)},$$

$$b^2 = \frac{I_x T - G^2}{I_y (I_x - I_y)},$$

$$c^2 = \frac{I_x T - G^2}{I_z (I_x - I_z)},$$

$$\lambda^2 = \frac{(I_x - I_y)(G^2 - I_z T)}{I_x I_y I_z}$$

$$1 - k^2 = \frac{I_x - I_z}{I_x - I_y} \; \frac{G^2 - I_y T}{G^2 - I_z T} \qquad (24)$$

where a^2, b^2, c^2, and λ^2 are all positive and $k^2 < 1$.

The solution explains that the body oscillates about the y and z axes with $q_{max} = b$, $r_{max} = c$, while the body rotates about the x axis with angular velocity p fluctuating in the same direction.

4.3 ROTATIONAL STABILITY OF AN ELASTIC SPACE STATION SPINNING ABOUT ITS AXIS OF MAXIMUM MOMENT OF INERTIA (I_x) WHEN I_x IS SLIGHTLY GREATER THAN ITS INTERMEDIATE MOMENT OF INERTIA (I_y)

The previous discussion shows that the rotation of a moment-free station about the axis of maximum moment of inertia (I_x) is rotationally stable for both unsymmetric rigid and elastic bodies. Now the discussion of the stability of rotation about the I_x axis is extended to the case where $I_x - I_y$ is small with respect to I_z. By Poinsot's construction, the separating polhode closes up about the I_x axis and thus, since a small displacement may lead to a considerable departure from the original pole, the rotation is less stable. This motion can be described more clearly by establishing relations between the nutation angle and the energy dissipation in the fixed-space system.

In a finite time interval, the kinetic energy and angular momentum in a moment-free rotating system can be considered as invariants. Because the total angular momentum vector (OL') is fixed in space, it will be convenient to refer the motion to OL' as the inertia axis. Describe a unit sphere around the center O of the body. The invariable line OL', the instantaneous axis OI, and the principal axes are allowed to cut this sphere in the points L, I, A, B, and C. The direction cosines against OL are α, β, and γ, λ, μ, and ν are angles of the planes LOA, LOB, LOC against some fixed plane LOX passing through OL. During the rotation, the I_x axis is used as the body reference line, α is the nutation angle, and $d\alpha/dt$ is the angular velocity of nutation (Figure 2). Because the body is turning around the instantaneous axis (OI) with an angular velocity (ω), the point A is moving perpendicular to the plane defined by the arc IA with velocity $\omega \sin IA$. By resolving this perpendicularly to the plane LOA,

$$\omega \sin IA \cos LAI = \frac{d\lambda}{dt} \sin \alpha$$

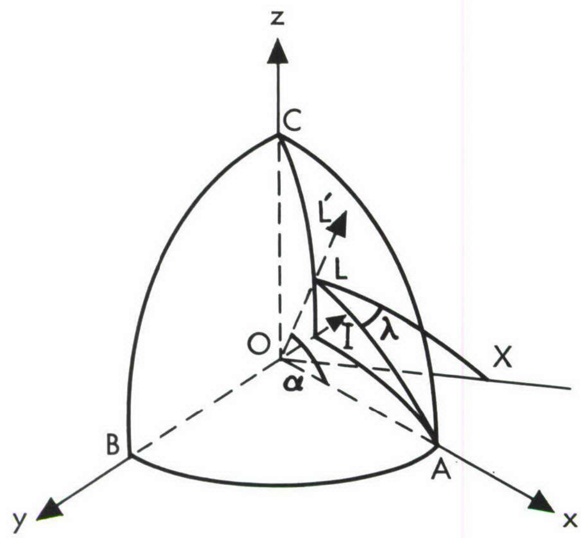

Figure 2. Angular Motion of Principal Axes

By using the cosine law of spherical trigonometry,

$$\cos LAI = \frac{\cos LI - \cos LA \cos IA}{\sin LA \sin IA}$$

then

$$\sin \alpha \frac{d\lambda}{dt} = \omega \frac{\cos LI - \cos \alpha \cos IA}{\sin \alpha}$$

since

$$\omega \cos LI = \frac{I_{OL}\, \omega_{OL}}{I_{OL}} \cdot \frac{\omega_{OL}}{\omega_{OL}} = \frac{T}{G}$$

and

$$\omega \cos IA = p.$$

so that

$$\sin^2 \alpha \frac{d\lambda}{dt} = \frac{T}{G} - p \cos \alpha \tag{25}$$

with

$$G \cos \boldsymbol{\alpha} = I_x p, \qquad \text{or} \qquad p = \frac{G}{I_x} \cos \boldsymbol{\alpha}$$

then

$$\frac{d\lambda}{dt} = \frac{T}{G} \csc^2 \alpha - \frac{G}{I_x} \cot^2 \alpha$$

or

$$\frac{d\lambda}{dt} = \frac{T}{G} + \frac{I_x T - G^2}{I_x G} \cot^2 \alpha \tag{26}$$

The angular velocity of nutation is determined by substituting the direction cosines of the angular momentum OL

$$\cos \alpha = \frac{I_x p}{G}, \qquad \cos \beta = \frac{I_y q}{G}, \qquad \cos \gamma = \frac{I_z r}{G}$$

into the first Euler's equation

$$I_x \dot{p} - (I_y - I_z) q r = 0$$

thus

$$- G \sin \alpha \frac{d\alpha}{dt} - (I_y - I_z) \frac{G^2}{I_y I_z} \cos \beta \cos \gamma = 0$$

or

$$\sin^2 \alpha \left(\frac{d\alpha}{dt}\right)^2 = \left(\frac{1}{I_y} - \frac{1}{I_z}\right)^2 G^2 \cos^2 \beta \cos^2 \gamma = 0 \tag{27}$$

The unknown direction cosines $\cos\beta$ and $\cos\gamma$ can be eliminated by use of the relation $\cos^2\alpha + \cos^2\beta + \cos^2\gamma = 1$ and by the first integral of Euler's equations, $I_x p^2 + I_y q^2 + I_z r^2 = T$, which can be written as

$$\frac{\cos^2\alpha}{I_x} + \frac{\cos^2\beta}{I_y} + \frac{\cos^2\gamma}{I_z} = \frac{T}{G^2}$$

From these two relations,

$$\cos^2\beta = \left[\frac{G^2 - I_z T}{G^2} - \frac{I_x - I_z}{I_x}\cos^2\alpha\right]\frac{I_y}{I_y - I_z}$$

$$\cos^2\gamma = \left[-\frac{G^2 - I_y T}{G^2} + \frac{I_x - I_y}{I_x}\cos^2\alpha\right]\frac{I_z}{I_y - I_z}$$

Thus, the angular velocity of nutation $d\alpha/dt$ may be determined from the equation

$$\sin^2\alpha\left(\frac{d\alpha}{dt}\right)^2 = -\frac{G^2}{I_y I_z}\left[\frac{G^2 - I_z T}{G^2} - \frac{I_x - I_z}{I_x}\cos^2\alpha\right]\left[\frac{G^2 - I_y T}{G^2} - \frac{I_x - I_y}{I_x}\cos^2\alpha\right]$$

or

$$\sin^2\alpha\left(\frac{d\alpha}{dt}\right)^2 = -\frac{G^2}{I_y I_z}\left(\frac{I_x - I_z}{I_x}\right)\left(\frac{I_x - I_y}{I_x}\right)\left[\frac{(G^2 - I_z T)\, I_x}{G^2 (I_x - I_z)} - \cos^2\alpha\right]\left[\frac{(G^2 - I_y T)\, I_x}{G^2 (I_x - I_y)} - \cos^2\alpha\right] \qquad (28)$$

In order to obtain a non-imaginary rate of nutation, $d\alpha/dt$, the expressions in brackets must have opposite signs. This leads to the condition

$$\frac{(G^2 - I_z T) I_x}{G^2 (I_x - I_z)} < \cos^2 \alpha < \frac{(G^2 - I_y T) I_x}{G^2 (I_x - I_y)} \tag{29}$$

The motion is described by the nutation angle α of the I_x axis against the angular momentum vector OL and the angle λ between the body-fixed plane through LOA and some space-fixed plane LOX. The nutation angle varies from the maximum condition

$$\cos^2 \alpha_{max} = \frac{(G^2 - I_y T) I_x}{G^2 (I_x - I_y)}$$

or

$$\sin^2 \alpha_{max} = \frac{I_y}{I_x - I_y} \frac{I_x T - I_x^2 p_e^2}{I_x^2 p_e^2} = \frac{1}{\frac{I_x}{I_y} - 1} \frac{\Delta T}{T_e}$$

so

$$\alpha_{max} = \sin^{-1} \sqrt{\frac{1}{\frac{I_x}{I_y} - 1} \frac{\Delta T}{T_e}} \tag{30}$$

and the minimum condition

$$\cos^2 \alpha_{min} = \frac{(G^2 - I_z T) I_x}{G^2 (I_x - I_z)}$$

or

$$\sin^2 \alpha_{min} = \frac{I_z}{I_x - I_z} \frac{I_x T - I_x^2 p_e^2}{I_x^2 p_e^2} = \frac{1}{\frac{I_x}{I_z} - 1} \frac{\Delta T}{T_e}$$

and, therefore

$$\alpha_{min} = \sin^{-1} \sqrt{\frac{1}{\frac{I_x}{I_z} - 1} \quad \frac{\Delta T}{T_e}} \tag{31}$$

The rate of nutation $d\alpha/dt$ and rate of precession $d\lambda/dt$ can also be expressed in terms of the energy dissipation:

$$\sin^2 \alpha \left(\frac{d\alpha}{dt}\right)^2 = - \frac{G^2}{I_y I_z} \left[- \frac{I_z (I_x T - G^2)}{I_x G^2} + \frac{I_x - I_z}{I_x} \sin^2 \alpha \right]$$

$$\left[- \frac{I_y (I_x T - G^2)}{I_x G^2} + \frac{I_x - I_y}{I_x} \sin^2 \alpha \right]$$

Since

$$G^2 = I_x^2 p_e^2, \qquad T_e = I_x p_e^2, \qquad \Delta T = T - T_e,$$

$$p_e = \frac{I_z \Omega}{I_x}$$

it follows that

$$\frac{d\alpha}{dt} = p_e \sqrt{\left[- \frac{1}{\sin^2 \alpha} \frac{\Delta T}{T_e} + \frac{I_x}{I_z} - 1 \right] \left[\frac{\Delta T}{T_e} - \left(\frac{I_x}{I_y} - 1 \right) \sin^2 \alpha \right]} \tag{32}$$

and

$$\frac{d\lambda}{dt} = p_e \left[1 + \frac{\Delta T}{T_e} + \frac{\Delta T}{T_e} \cot^2 \alpha \right] \tag{33}$$

Hence,

$$d\lambda = \frac{1 + (1 + \cot^2 \alpha)\frac{\Delta T}{T_e}}{\sqrt{\left[\frac{I_x}{I_z} - 1 - \frac{1}{\sin^2 \alpha} \frac{\Delta T}{T_e}\right]\left[\frac{\Delta T}{T_e} - \left(\frac{I_x}{I_y} - 1\right)\sin^2 \alpha\right]}} d\alpha \tag{34}$$

For prescribed moments of inertia, the value of α_{max} and α_{min} and the relations of α to λ can be computed at different energy-dissipation levels. These computed results will indirectly reveal the stability of the configurations studied.

4.4 NUMERICAL RESULTS

The equation

$$d\lambda = \frac{1 + (1 + \cot^2 \alpha)\frac{\Delta T}{T_e}}{\sqrt{\left[\frac{I_x}{I_z} - 1 - \frac{1}{\sin^2 \alpha} \frac{\Delta T}{T_e}\right]\left[\frac{\Delta T}{T_e} - \left(\frac{I_x}{I_y} - 1\right)\sin^2 \alpha\right]}} d\alpha \tag{35}$$

and the lower and upper bounds of α

$$\alpha_{min} = \sin^{-1} \sqrt{\frac{1}{\frac{I_x}{I_z} - 1} \frac{\Delta T}{T_e}} \tag{36}$$

$$\alpha_{max} = \sin^{-1} \sqrt{\frac{1}{\frac{I_x}{I_y} - 1} \frac{\Delta T}{T_e}} \tag{37}$$

were programmed for the prescribed moments of inertia of various configurations (Table 4) at different energy-dissipation levels. These computed results were plotted in polar coordinates, Figures 3 to 9. In general, the plots are rose-like figures with an infinite number of leaves. The graphs show the path of a point on the I_x axis as seen from a space-fixed observer looking in the direction of the angular momentum vector.

Table 4. Nutation of Elastic Space Stations

Configuration		$\frac{I_x}{I_y}$	$\frac{I_x}{I_z}$	Energy-Dissipation Ratio $\Delta T/T_e$									
				0.0001		0.001		0.01		0.03		0.05	
				Nutation Angles in Degrees									
				α_{max}	α_{min}	α_{max}	α_{min}	α_{max}	α_{min}	α_{max}	α_{min}	α_{max}	α_{min}
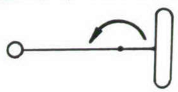	1-A	1.006935	140.8452	6.89	0.048	22.32	0.153						
	1-B	1.00148	6570.812	55.37	0.007								
	2-A	0.993113	139.8751			UNSTABLE							
	2-B	0.999852	6569.842			UNSTABLE							
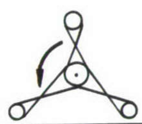	4-A	1.714840	1.654615			2.24	2.14	7.10	6.79	12.36	11.82		
	4-B	1.986795	1.986816			STABLE							
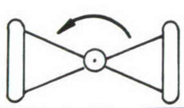	6-A	1.019353	12.70806			3.73	0.49	11.87	1.56	20.87	2.70	27.39	3.49
	6-B	1.000119	95.32235	66.45	0.059								
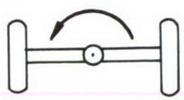	7-A	1.07495	13.7273			5.02	0.49	16.05	1.54	28.61	2.67	38.18	3.45
	7-B	1.000108	95.76264	73.75	0.059								
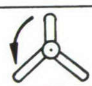	Y	1.844876	1.844794			STABLE							
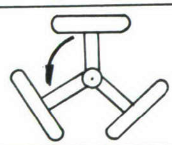	Y-A	2.144299	2.776933			1.69	1.36	5.36	4.30	9.32	7.47	12.07	9.66
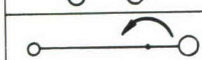	CC	1.008736	377.5074	6.14	0.030	19.78	0.093						

The range of nutation angles shows clearly that for a higher energy-dissipation level the motion of the space station has a larger nutation range about its total angular momentum vector. These graphs also show that for a fixed energy-dissipation level the configuration with a smaller ratio of I_x/I_y has a lower stability about the I_x - axis than the configuration with a higher ratio of I_x/I_y. When the range of nutation is excessively larger than the allowable wobbling angle, the configuration is considered to be rotationally unstable.

In order to keep a real and positive α, the magnitude of $\Delta T/T_e$ is restricted by the ratio of I_x/I_y. The smaller the ratio of I_x/I_y, the more sensitive is the stability of the configuration to the magnitude of energy dissipation. This can be seen from the plots of α versus λ for Configurations 1-A and 1-B. In Configuration 1-A, because the I_x/I_y ratio is equal to 1.006935, the maximum possible value of $\Delta T/T_e$ is around 0.001. For $\Delta T/T_e = 0.001$, the nutation angle α varies between $\alpha_{min} = 0.153$ and $\alpha_{max} = 22.317$. For a smaller $\Delta T/T_e = 0.0001$, the angle α varies between $\alpha_{min} = 0.048$ and $\alpha_{max} = 6.897$. In Configuration 1-B, because $I_{mx}/I_{my} = 1.0001477$, the maximum possible value of $\Delta T/T_e$ is only around 0.0001, and even at this small energy-dissipation level the nutation angle α has a much wider oscillating range of $\alpha_{min} = 0.00707$ and $\alpha_{max} = 55.369$.

The set of equations can be applied as well to other configurations that have a given ratio of I_x/I_y. For instance, in Configuration 7-A, $I_x/I_y = 1.1308$ and $I_x/I_z = 14.8158$, the variation of α at different levels of $\Delta T/T_e$ can be seen from the following:

$\Delta T/T_e$	α_{min} (degrees)	α_{max} (degrees)
0.001	0.487	5.015
0.01	1.542	16.049
0.03	2.671	28.61
0.05	3.449	38.183

For Configuration 7-B the ratio of $I_x/I_y = 1.0001085$. This ratio is nearly equal to one, because the longitudinal and lateral dimensions of the compartments are in 1-to-1 ratio. The low stability of this configuration can easily be detected from the polar plot for $\Delta T/T_e = 0.0001$, in which the nutation angle α increases gradually from $\alpha_{min} = 0.0589$ to $\alpha_{max} = 73.750$ in one half-cycle and then retreats gradually back to $\alpha_{min} = 0.0589$ in the next half-cycle.

If I_x/I_y is nearly equal to I_x/I_z, then α_{min} is nearly equal to α_{max}. This means that the configuration is stable and the motion is close to regular precession. Configurations 4-A and Y fall into this category; therefore, the investigation of nutation for the moment-free condition is not made.

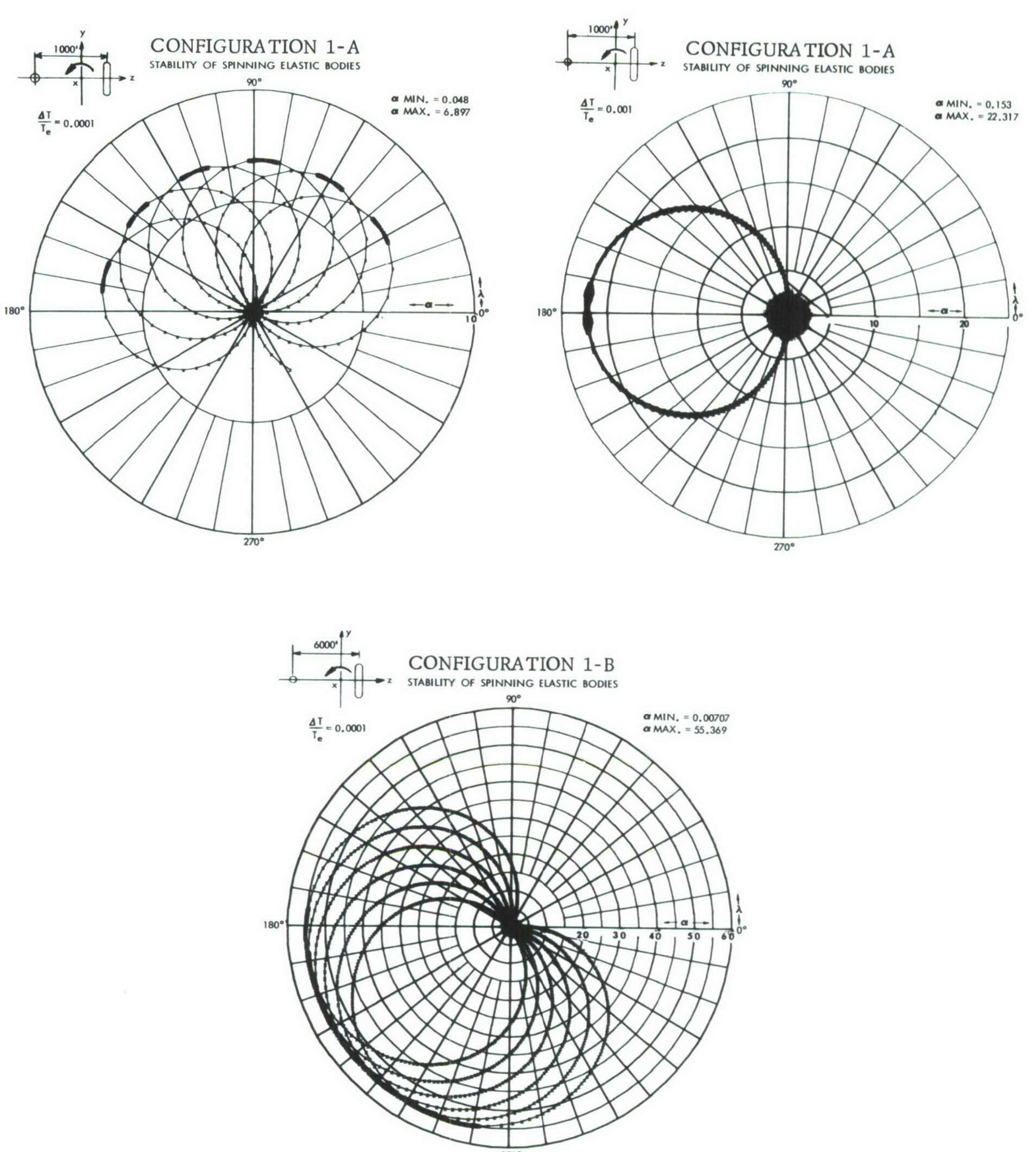

Figure 3. α Versus λ for Configurations 1-A and 1-B.

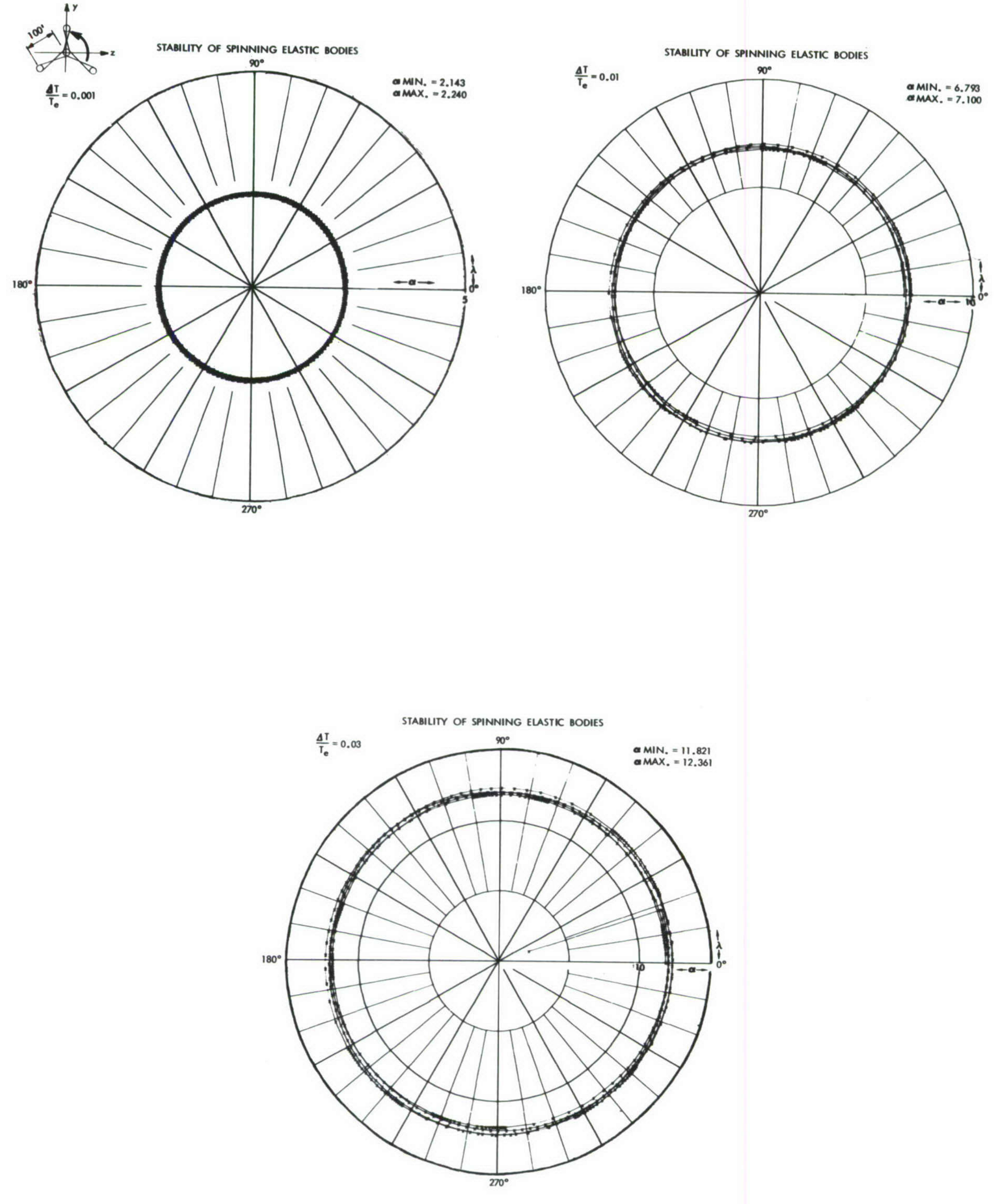

Figure 4. α Versus λ for Configuration 4-A.

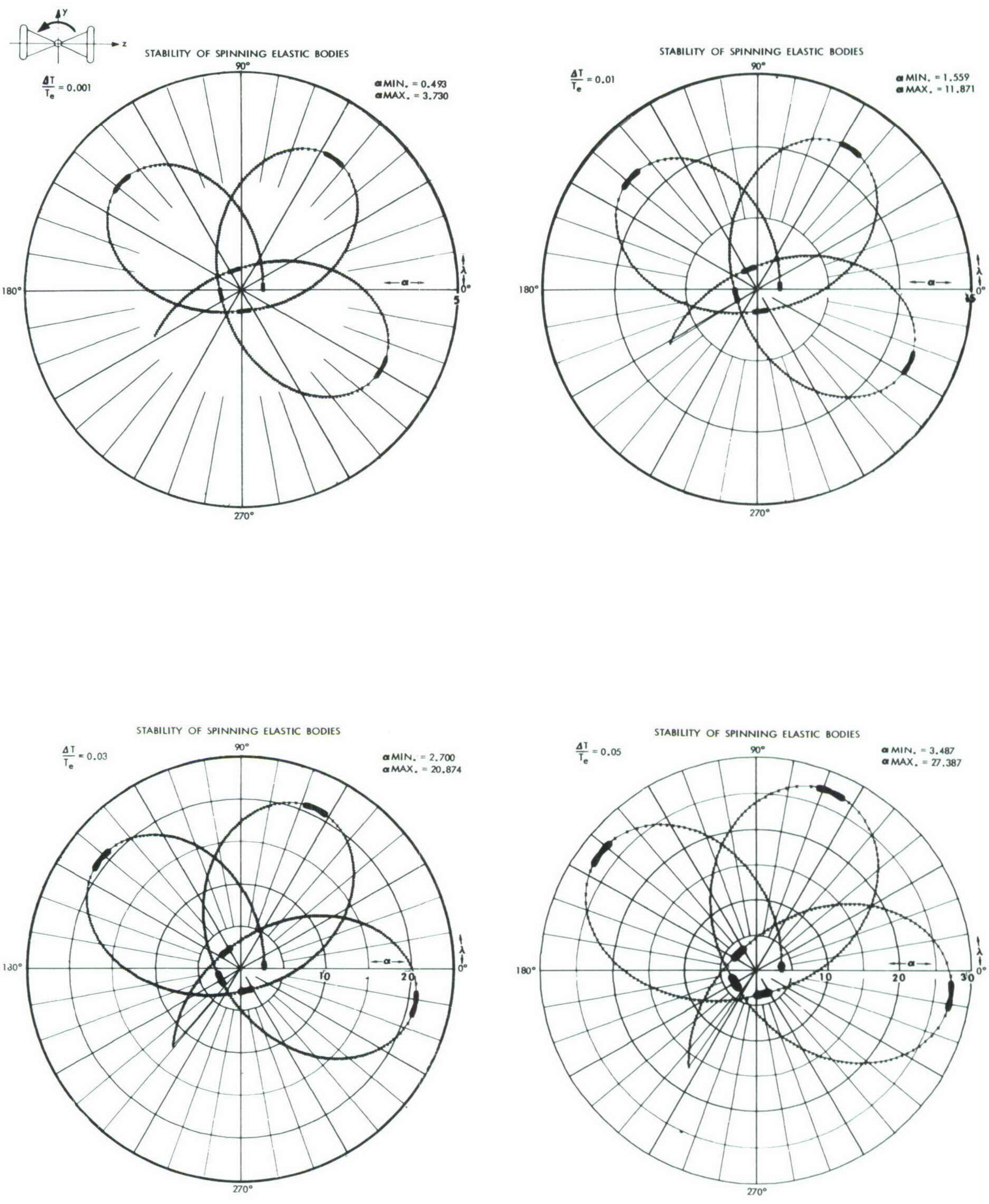

Figure 5. α Versus λ for Configuration 6-A.

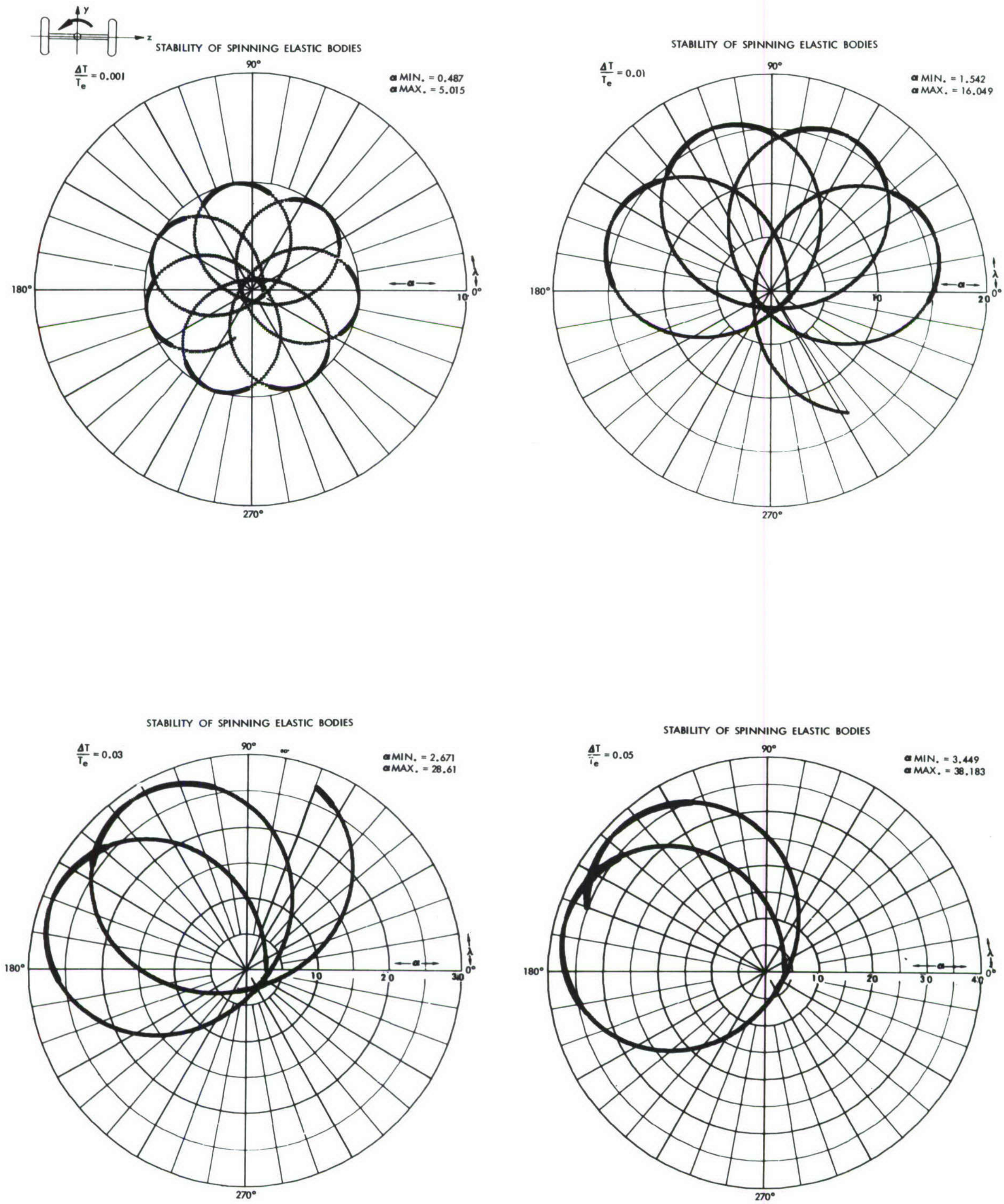

Figure 6. α Versus λ for Configuration 7-A.

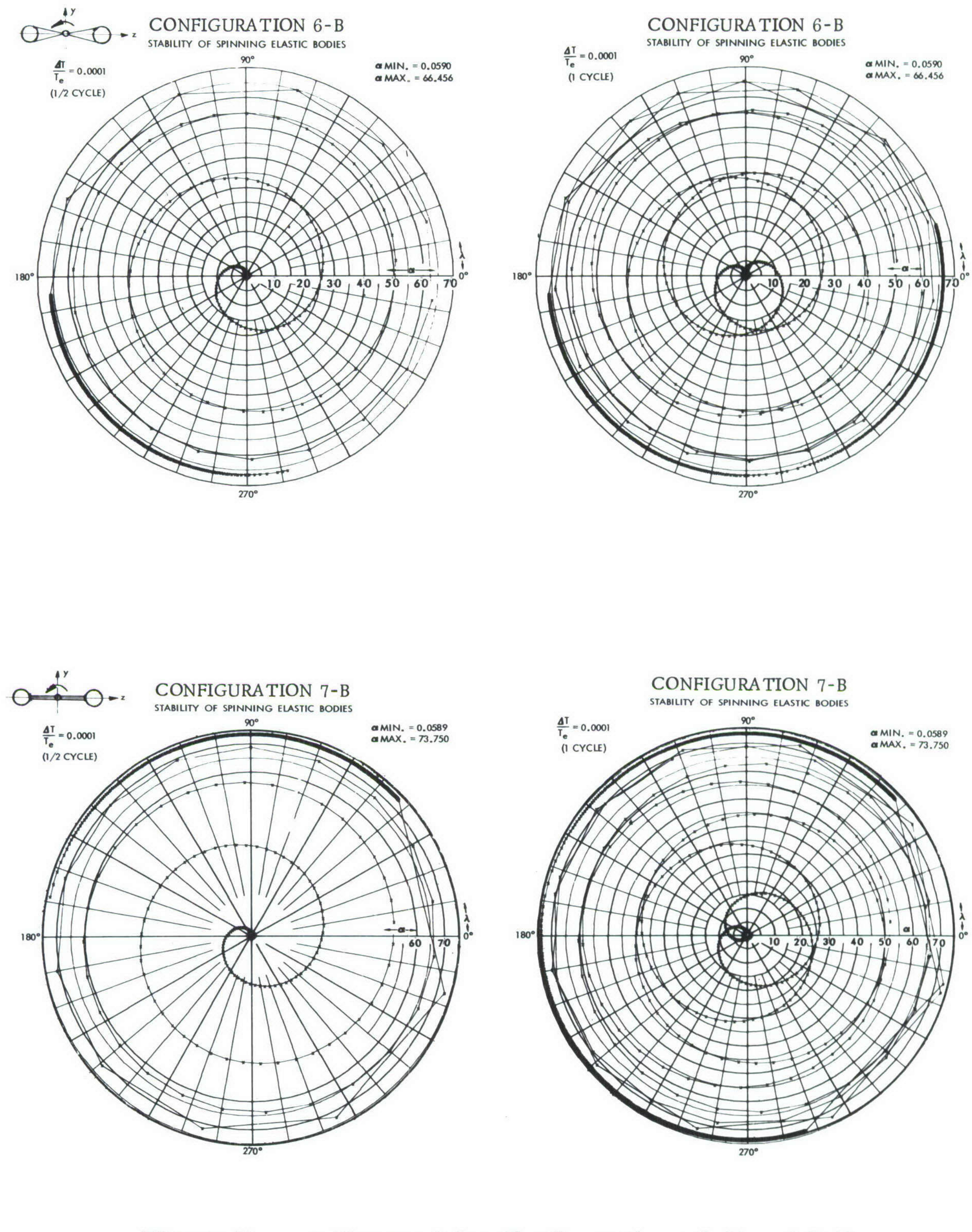

Figure 7. α Versus λ for Configurations 6-B and 7-B.

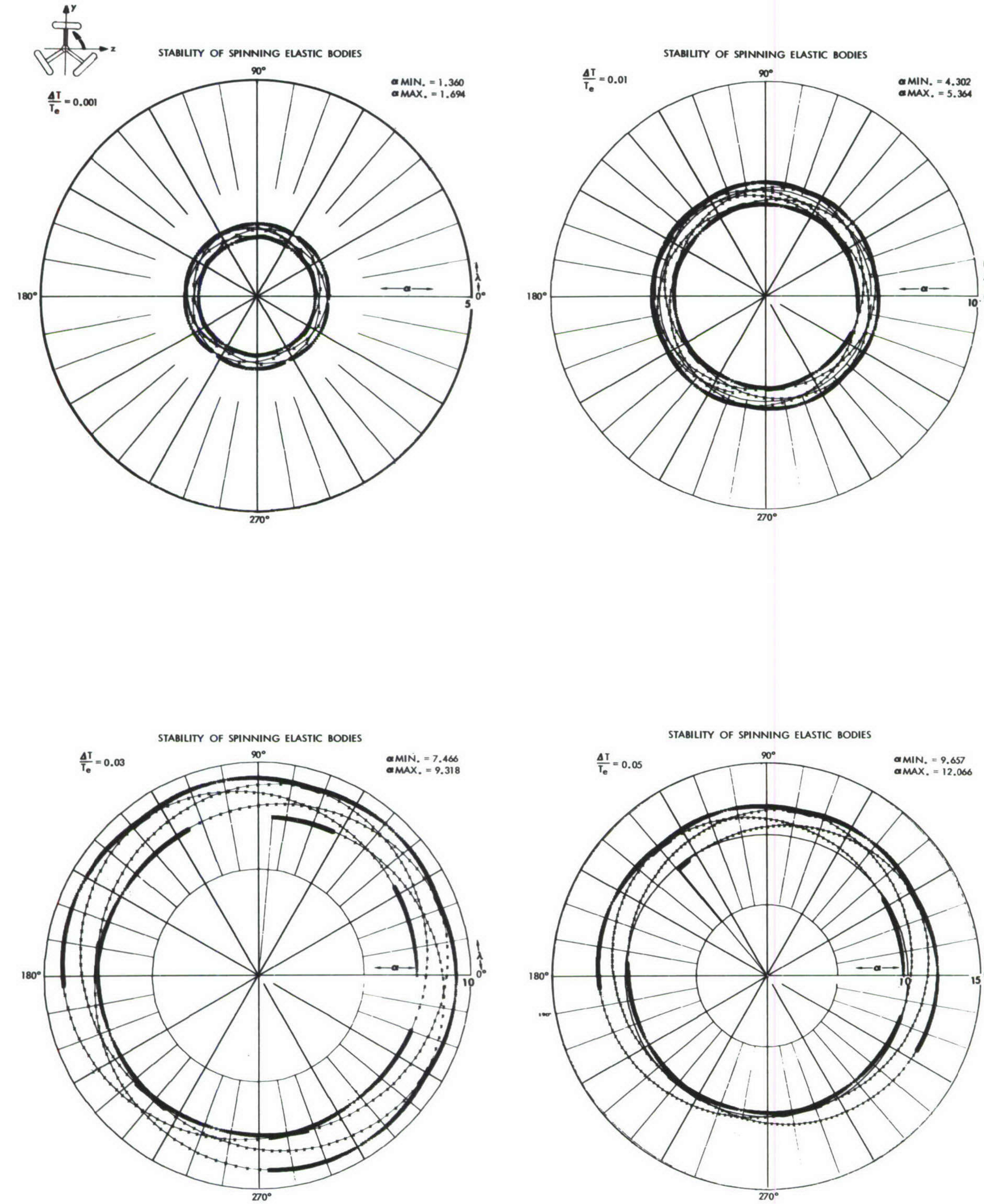

Figure 8. α Versus λ for Configuration Y-A.

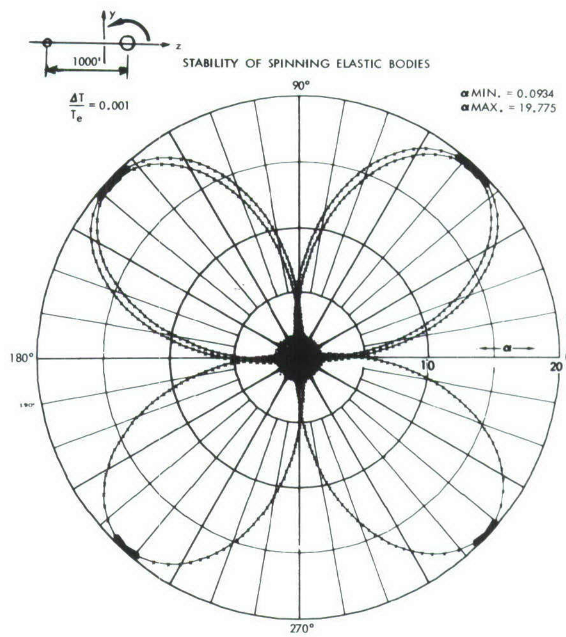

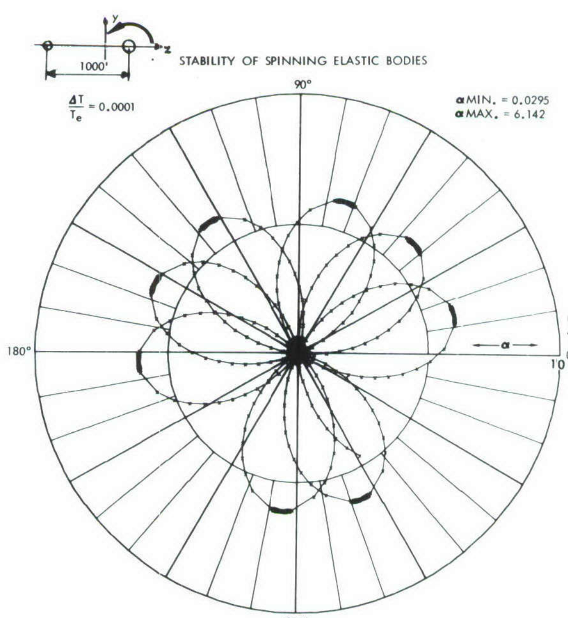

Figure 9. α Versus λ for Configuration C-C

5.0 LINEARIZED MOMENT EQUATIONS FOR PARTICULAR DISTURBANCES

Preliminary studies were conducted to determine the effects of arbitrary transverse moments on the rigid body response of the space station configurations. For these studies, the equations of motion were linearized and an analytical solution was obtained for configurations of constant principal moments of inertia. The external transverse moments were expressed in general form by Fourier series. The results of these studies and the stability evaluation discussed in Section 4.0 of this report were used as guides in the selection of configurations for detailed analysis.

The general equations of motion of a rotating space station in a gravity-free field are presented in Section 9.1 of this report. An analytical solution can be obtained if the x, y, z body axes are taken as principal axes of inertia. Then the components of angular momentum are

$$\begin{Bmatrix} H_x \\ H_y \\ H_z \end{Bmatrix} = \begin{bmatrix} I_x & o & o \\ o & I_y & o \\ o & o & I_z \end{bmatrix} \begin{Bmatrix} p \\ q \\ r \end{Bmatrix}, \qquad (38)$$

where I_x, I_y and I_z are constant principal moments of inertia and the x, y, z axes system is fixed to the rotating space station. The basic equations to be used are the equations for moments about the principal body axes

$$\frac{d\overline{H}}{dt} + \overline{\omega} \times \overline{H} = \overline{M}.$$

Resolving into components along the x, y and z body axes, the moment equations are

$$\begin{aligned} I_x \dot{p} + (I_z - I_y)\, qr &= M_x \\ I_y \dot{q} + (I_x - I_z)\, pr &= M_y \\ I_z \dot{r} - (I_x - I_y)\, pq &= M_z \end{aligned} \qquad (39)$$

The relations between Euler angular velocities and body angular velocities are

$$\dot{\phi} = p + \dot{\psi} \sin \theta$$

$$\dot{\theta} = q \cos \phi - r \sin \phi \quad (40)$$

$$\dot{\psi} = \frac{1}{\cos \theta} (r \cos \phi + q \sin \phi)$$

These non-linear equations are solved analytically under the assumptions discussed in the subsections which follow.

5.1 LINEARIZED EQUATIONS OF ANGULAR MOTION AND THEIR SOLUTION.

Equations (39) are linearized and solved analytically by assuming a constant spin rate, i.e. $p = p_o$ = a constant and $\dot{p} = 0$. Thus, the moment equations become

$$(I_z - I_y) qr = M_x \quad (41)$$

$$\dot{q} + ar = \frac{M_y}{I_y} \quad (42)$$

$$\dot{r} - bq = \frac{M_z}{I_z} \quad (43)$$

where,

$$a = p_o \frac{(I_x - I_z)}{I_y}$$

$$b = p_o \frac{(I_x - I_y)}{I_z} \quad .$$

Utilizing the Laplace transforms, equations (42) and (43) become

$$q(S) = \frac{(M_y(S) + I_y q_o) I_z S - (M_z(S) + I_z r_o) I_y a}{I_y I_z (S^2 + \Omega^2)}$$

$$r(S) = \frac{(M_z(S) + I_z r_o) I_y S + (M_y(S) + I_y q_o) I_z b}{I_y I_z (S^2 + \Omega^2)} \tag{44}$$

where Ω, the undamped natural frequency of angular motion, is

$$\Omega = \sqrt{a b} = p_o \sqrt{\frac{(I_x - I_y)(I_x - I_z)}{I_y I_z}}$$

Equations (40) may be linearized by assuming that

(1) The angle θ is small, i.e., $\cos\theta = 1$, $\sin\theta = \theta$,

(2) $\psi \sin\theta \ll p_o$, define $\lambda = \dot{\psi}\theta / p_o \ll 1$,

Then,

$$\begin{aligned} \phi &= p_o t + \phi_o \\ \dot{\theta} &= q \cos\phi - r \sin\phi \\ \dot{\psi} &= r \cos\phi + q \sin\phi \end{aligned} \tag{45}$$

The general solutions for θ and ψ are obtained by substituting the inverse transforms of equations (44) into equations (45) and integrating

$$\begin{aligned} \theta &= \int_o^t \Big[L^{-1} \left\{ q(S) \right\} \cos(p_o t + \phi_o) \\ &\quad - L^{-1} \left\{ r(S) \right\} \sin(p_o t + \phi_o) \Big] dt + \theta_o \\ \psi &= \int_o^t \Big[L^{-1} \left\{ r(S) \right\} \cos(p_o t + \phi_o) \\ &\quad + L^{-1} \left\{ q(S) \right\} \sin(p_o t + \phi_o) \Big] dt + \psi_o \end{aligned} \tag{46}$$

These solutions depend upon the existence of the Laplace transforms of the disturbing moments M_y and M_z.

5.2 FOURIER REPRESENTATION OF THE DISTURBING MOMENTS

A general approach is possible when the moments M_y and M_z are expressed as Fourier series. The expressions for the moments M_y and M_z are

$$M_y = \frac{a_{yo}}{2} + \sum_{n=1}^{N} a_{yn} \cos \alpha t + \sum_{n=1}^{N} b_{yn} \sin \alpha t$$
$$M_z = \frac{a_{zo}}{2} + \sum_{m=1}^{M} a_{zm} \cos \beta t + \sum_{m=1}^{M} b_{zm} \sin \beta t, \tag{47}$$

where

$\alpha = \frac{n\pi}{t_y}$; t_y is 1/2-period of M_y.

$\beta = \frac{m\pi}{t_z}$; t_z is 1/2-period of M_z.

The Laplace transforms of the disturbing moments M_y and M_z are

$$M_y(S) = \frac{a_{yo}}{2S} + \sum_{n=1}^{N} a_{yn} \frac{S}{S^2 + \alpha^2} + \sum_{n=1}^{N} b_{yn} \frac{\alpha}{S^2 + \alpha^2}$$
$$M_z(S) = \frac{a_{zo}}{2S} + \sum_{m=1}^{M} a_{zm} \frac{S}{S^2 + \beta^2} + \sum_{m=1}^{M} b_{zm} \frac{\beta}{S^2 + \beta^2} \quad . \tag{48}$$

Substituting $M_y(S)$ and $M_z(S)$ into $q(S)$ and $r(S)$ and taking the inverse Laplace transforms, we have

$$q = \left(\frac{a_{yo}}{2I_y} - r_o a\right)\frac{1}{\Omega}\sin\Omega t + q_o\cos\Omega t - \frac{a_{zo}}{2I_z}\frac{a}{\Omega^2}(1 - \cos\Omega t)$$

$$+ \sum_{n=1}^{N}\frac{a_{yn}}{I_y}\frac{(\Omega\sin\Omega t - \alpha\sin\alpha t)}{(\Omega^2 - \alpha^2)} - \sum_{n=1}^{N}\alpha\frac{b_{yn}}{I_y}\frac{(\cos\Omega t - \cos\alpha t)}{(\Omega^2 - \alpha^2)}$$

$$+ \sum_{m=1}^{M} a\frac{a_{zm}}{I_z}\frac{(\cos\Omega t - \cos\beta t)}{(\Omega^2 - \beta^2)}$$

$$+ \sum_{m=1}^{M} a\beta\frac{b_{zm}}{I_z}\frac{\left(\frac{1}{\Omega}\sin\Omega t - \frac{1}{\beta}\sin\beta t\right)}{(\Omega^2 - \beta^2)} \qquad (49)$$

$$r = \left(\frac{a_{zo}}{2I_z} + q_o b\right)\frac{1}{\Omega}\sin\Omega t + r_o\cos\Omega t + \frac{a_{yo}}{2I_y}\frac{b}{\Omega^2}(1 - \cos\Omega t)$$

$$+ \sum_{m=1}^{M}\frac{a_{zm}}{I_z}\frac{(\Omega\sin\Omega t - \beta\sin\beta t)}{(\Omega^2 - \beta^2)} - \sum_{m=1}^{M}\beta\frac{b_{zm}}{I_z}\frac{(\cos\Omega t - \cos\beta t)}{(\Omega^2 - \beta^2)}$$

$$- \sum_{n=1}^{N} b\frac{a_{yn}}{I_y}\frac{(\cos\Omega t - \cos\alpha t)}{(\Omega^2 - \alpha^2)} - \sum_{n=1}^{N}\alpha b\frac{b_{yn}}{I_y}\frac{\left(\frac{1}{\Omega}\sin\Omega t - \frac{1}{\alpha}\sin\alpha t\right)}{(\Omega^2 - \alpha^2)} \qquad (50)$$

Substituting q and r into equations (40), and performing the required integration, taking $\phi_o = 0$, gives the following expressions for θ and ψ :

When, $\phi_o = 0$

$$
\theta = \left\{ \frac{a_{yo}}{I_y} \frac{1}{2\Omega} \left(1 - \frac{b}{\Omega}\right) + r_o \left(1 - \frac{a}{\Omega}\right) + \sum_{n=1}^{N} \frac{a_{yn}}{I_y} \frac{\Omega}{(\Omega^2 - \alpha^2)} \left(1 - \frac{b}{\Omega}\right) \right.
$$

$$
\left. - \sum_{m=1}^{M} \frac{b_{zm}}{I_z} \frac{\beta}{(\Omega^2 - \beta^2)} \left(1 - \frac{a}{\Omega}\right) \right\} \left(\frac{1}{2(p_o - \Omega)} \right) \left[\cos (p_o - \Omega) t - 1 \right]
$$

$$
- \left\{ \frac{a_{yo}}{I_y} \frac{1}{2\Omega} \left(1 + \frac{b}{\Omega}\right) - r_o \left(1 + \frac{a}{\Omega}\right) + \sum_{n=1}^{N} \frac{a_{yn}}{I_y} \frac{\Omega}{(\Omega^2 - \alpha^2)} \left(1 + \frac{b}{\Omega}\right) \right.
$$

$$
\left. + \sum_{m=1}^{M} \frac{b_{zm}}{I_z} \frac{\beta}{(\Omega^2 - \beta^2)} \left(1 + \frac{a}{\Omega}\right) \right\} \left(\frac{1}{2(p_o + \Omega)} \right) \left[\cos (p_o + \Omega) t - 1 \right]
$$

$$
- \left\{ \frac{a_{zo}}{I_z} \frac{1}{2\Omega} \left(1 - \frac{a}{\Omega}\right) - q_o \left(1 - \frac{b}{\Omega}\right) + \sum_{n=1}^{N} \frac{b_{yn}}{I_y} \frac{\alpha}{(\Omega^2 - \alpha^2)} \left(1 - \frac{b}{\Omega}\right) \right.
$$

$$
\left. + \sum_{m=1}^{M} \frac{a_{zm}}{I_z} \frac{\Omega}{(\Omega^2 - \beta^2)} \left(1 - \frac{a}{\Omega}\right) \right\} \left(\frac{1}{2(p_o - \Omega)} \right) \sin (p_o - \Omega) t
$$

$$
+ \left\{ \frac{a_{zo}}{I_z} \frac{1}{2\Omega} \left(1 + \frac{a}{\Omega}\right) + q_o \left(1 + \frac{b}{\Omega}\right) - \sum_{n=1}^{N} \frac{b_{yn}}{I_y} \frac{\alpha}{(\Omega^2 - \alpha^2)} \left(1 + \frac{b}{\Omega}\right) \right.
$$

$$
\left. + \sum_{m=1}^{M} \frac{a_{zm}}{I_z} \frac{\Omega}{(\Omega^2 - \beta^2)} \left(1 + \frac{a}{\Omega}\right) \right\} \left(\frac{1}{2(p_o + \Omega)} \right) \sin (p_o + \Omega) t
$$

$$
+ \frac{a_{yo}}{I_y} \frac{b}{2\Omega^2 p_o} (\cos p_o t - 1) - \frac{a_{zo}}{I_z} \frac{a}{2\Omega^2 p_o} \sin p_o t
$$

$$
- \sum_{n=1}^{N} \frac{a_{yn}}{I_y} \frac{\alpha}{(\Omega^2 - \alpha^2)} \left(1 - \frac{b}{\alpha}\right) \left(\frac{1}{2(p_o - \alpha)} \right) \left[\cos (p_o - \alpha) t - 1 \right]
$$

$$+ \sum_{n=1}^{N} \frac{a_{yn}}{I_y} \frac{\alpha}{(\Omega^2 - \alpha^2)} \left(1 + \frac{b}{\alpha}\right) \left(\frac{1}{2\,(p_o + \alpha)}\right) \left[\cos\,(p_o + \alpha)\,t - 1\right]$$

$$+ \sum_{n=1}^{N} \frac{b_{yn}}{I_y} \frac{\alpha}{(\Omega^2 - \alpha^2)} \left(1 - \frac{b}{\alpha}\right) \left(\frac{1}{2\,(p_o - \alpha)}\right) \sin\,(p_o - \alpha)\,t$$

$$+ \sum_{n=1}^{N} \frac{b_{yn}}{I_y} \frac{\alpha}{(\Omega^2 - \alpha^2)} \left(1 + \frac{b}{\alpha}\right) \left(\frac{1}{2\,(p_o + \alpha)}\right) \sin\,(p_o + \alpha)\,t$$

$$+ \sum_{m=1}^{M} \frac{b_{zm}}{I_z} \frac{\beta}{(\Omega - \beta^2)} \left(1 - \frac{a}{\beta}\right) \left(\frac{1}{2\,(p_o - \beta)}\right) \left[\cos\,(p_o - \beta)\,t - 1\right]$$

$$+ \sum_{m=1}^{M} \frac{b_{zm}}{I_z} \frac{\beta}{(\Omega^2 - \beta^2)} \left(1 + \frac{a}{\beta}\right) \left(\frac{1}{2\,(p_o + \beta)}\right) \left[\cos\,(p_o + \beta)\,t - 1\right]$$

$$+ \sum_{m=1}^{M} \frac{a_{zm}}{I_z} \frac{\beta}{(\Omega^2 - \beta^2)} \left(1 - \frac{a}{\beta}\right) \left(\frac{1}{2\,(p_o - \beta)}\right) \sin\,(p_o - \beta)\,t$$

$$- \sum_{m=1}^{M} \frac{a_{zm}}{I_z} \frac{\beta}{(\Omega^2 - \beta^2)} \left(1 + \frac{a}{\beta}\right) \left(\frac{1}{2\,(p_o + \beta)}\right) \sin\,(p_o + \beta)\,t$$

$$+ \theta_o \tag{5.1}$$

and

$$\psi = \left\{ \frac{a_{zo}}{I_z} \frac{1}{2\,\Omega} \left(1 - \frac{a}{\Omega}\right) - q_o \left(1 - \frac{b}{\Omega}\right) + \sum_{n=1}^{N} \frac{b_{yn}}{I_y} \frac{\alpha}{(\Omega^2 - \alpha^2)} \left(1 - \frac{b}{\Omega}\right) \right.$$

$$\left. + \sum_{m=1}^{M} \frac{a_{zm}}{I_z} \frac{\Omega}{(\Omega^2 - \beta^2)} \left(1 - \frac{a}{\Omega}\right) \right\} \left(\frac{1}{2\,(p_o - \Omega)}\right) \left[\cos\,(p_o - \Omega)\,t - 1\right]$$

$$- \left\{ \frac{a_{zo}}{I_z} \frac{1}{2\,\Omega} \left(1 + \frac{a}{\Omega}\right) + q_o \left(1 + \frac{b}{\Omega}\right) - \sum_{n=1}^{N} \frac{b_{ny}}{I_y} \frac{\alpha}{(\Omega^2 - \alpha^2)} \left(1 + \frac{b}{\Omega}\right)\right.$$

$$\left. + \sum_{m=1}^{M} \frac{a_{zm}}{I_z} \frac{\Omega}{(\Omega^2 - \beta^2)} \left(1 + \frac{a}{\Omega}\right)\right\} \left(\frac{1}{2\,(p_o + \Omega)}\right) \left[\cos\,(p_o + \Omega)\,t - 1\right]$$

$$+ \left\{ \frac{a_{yo}}{I_y} \frac{1}{2\Omega} \left(1 - \frac{b}{\Omega}\right) + r_o \left(1 - \frac{a}{\Omega}\right) + \sum_{n=1}^{N} \frac{a_{yn}}{I_y} \frac{\Omega}{(\Omega^2 - \alpha^2)} \left(1 - \frac{b}{\Omega}\right)\right.$$

$$\left. - \sum_{m=1}^{M} \frac{b_{zm}}{I_z} \frac{\beta}{(\Omega^2 - \beta^2)} \left(1 - \frac{a}{\Omega}\right)\right\} \left(\frac{1}{2\,(p_o - \Omega)}\right) \sin\,(p_o - \Omega)\,t$$

$$- \left\{ \frac{a_{yo}}{I_y} \frac{1}{2\Omega} \left(1 + \frac{b}{\Omega}\right) - r_o \left(1 + \frac{a}{\Omega}\right) + \sum_{n=1}^{N} \frac{a_{yn}}{I_y} \frac{\Omega}{\Omega^2 - \alpha^2} \left(1 + \frac{b}{\Omega}\right)\right.$$

$$\left. + \sum_{m=1}^{M} \frac{b_{zm}}{I_z} \frac{\beta}{(\Omega^2 - \beta^2)} \left(1 + \frac{a}{\Omega}\right)\right\} \left(\frac{1}{2\,(p_o + \Omega)}\right) \sin\,(p_o + \Omega)\,t$$

$$+ \frac{b}{2\,\Omega^2\,p_o} \frac{a_{yo}}{I_y} \sin p_o\,t + \frac{a}{2\,\Omega^2\,p_o} \frac{a_{zo}}{I_z} \left(\cos p_o\,t - 1\right)$$

$$- \sum_{n=1}^{N} \frac{b_{yn}}{I_y} \frac{\alpha}{(\Omega^2 - \alpha^2)} \left(1 - \frac{b}{\alpha}\right) \left(\frac{1}{2\,(p_o - \alpha)}\right) \left[\cos\,(p_o - \alpha)\,t - 1\right]$$

$$- \sum_{n=1}^{N} \frac{b_{yn}}{I_y} \frac{\alpha}{(\Omega^2 - \alpha^2)} \left(1 + \frac{b}{\alpha}\right) \left(\frac{1}{2\,(p_o + \alpha)}\right) \left[\cos\,(p_o + \alpha)\,t - 1\right]$$

$$- \sum_{n=1}^{N} \frac{a_{yn}}{I_y} \frac{\alpha}{(\Omega^2 - \alpha^2)} \left(1 - \frac{b}{\alpha}\right) \left(\frac{1}{2\,(p_o - \alpha)}\right) \sin\,(p_o - \alpha)\,t$$

$$+ \sum_{n=1}^{N} \frac{a_{yn}}{I_y} \frac{\alpha}{(\Omega^2 - \alpha^2)} \left(1 + \frac{b}{\alpha}\right)\left(\frac{1}{2\,(p_o + \alpha)}\right) \sin\,(p_o + \alpha)\,t$$

$$- \sum_{m=1}^{M} \frac{a_{zm}}{I_z} \frac{\beta}{(\Omega^2 - \beta^2)} \left(1 - \frac{a}{\beta}\right)\left(\frac{1}{2\,(p_o - \beta)}\right) \left[\cos\,(p_o - \beta)\,t - 1\right]$$

$$+ \sum_{m=1}^{M} \frac{a_{zm}}{I_z} \frac{\beta}{(\Omega^2 - \beta^2)} \left(1 + \frac{a}{\beta}\right)\left(\frac{1}{2\,(p_o + \beta)}\right) \left[\cos\,(p_o + \beta)\,t - 1\right]$$

$$+ \sum_{m=1}^{M} \frac{b_{zm}}{I_z} \frac{\beta}{(\Omega^2 - \beta^2)} \left(1 - \frac{a}{\beta}\right)\left(\frac{1}{2\,(p_o - \beta)}\right) \sin\,(p_o - \beta)\,t$$

$$+ \sum_{m=1}^{M} \frac{b_{zm}}{I_z} \frac{\beta}{(\Omega^2 - \beta^2)} \left(1 + \frac{a}{\beta}\right)\left(\frac{1}{2\,(p_o + \beta)}\right) \sin\,(p_o + \beta)\,t + \psi_o \qquad (52)$$

5.3 GENERAL DESCRIPTION OF COMPUTED RESULTS

The linearized equations were programmed to the IBM 7094 digital computer. Typical responses are shown in Figures 10 through 19 Table 5 gives the values of the constant spin rate p_o, the natural frequency, Ω, and the natural period, τ_o, for each of the configurations when the artifical gravity level in the manned modules at a distance, R_g, from the mass center is 1/2-g, 1/4-g, and 1/10-g. Tables 6 through 11 contain ranges of the variables which describe the rigid body responses of the space station configurations to various types of disturbances.

It should be noted that all computations in this section were based on the values of moments of inertia for the configurations given in Section 2.0 except for the following two values:

Configuration 6-A: I_x = 20,055,800 slug-ft^2

Configuration 7-A: I_x = 20,029,400 slug-ft^2

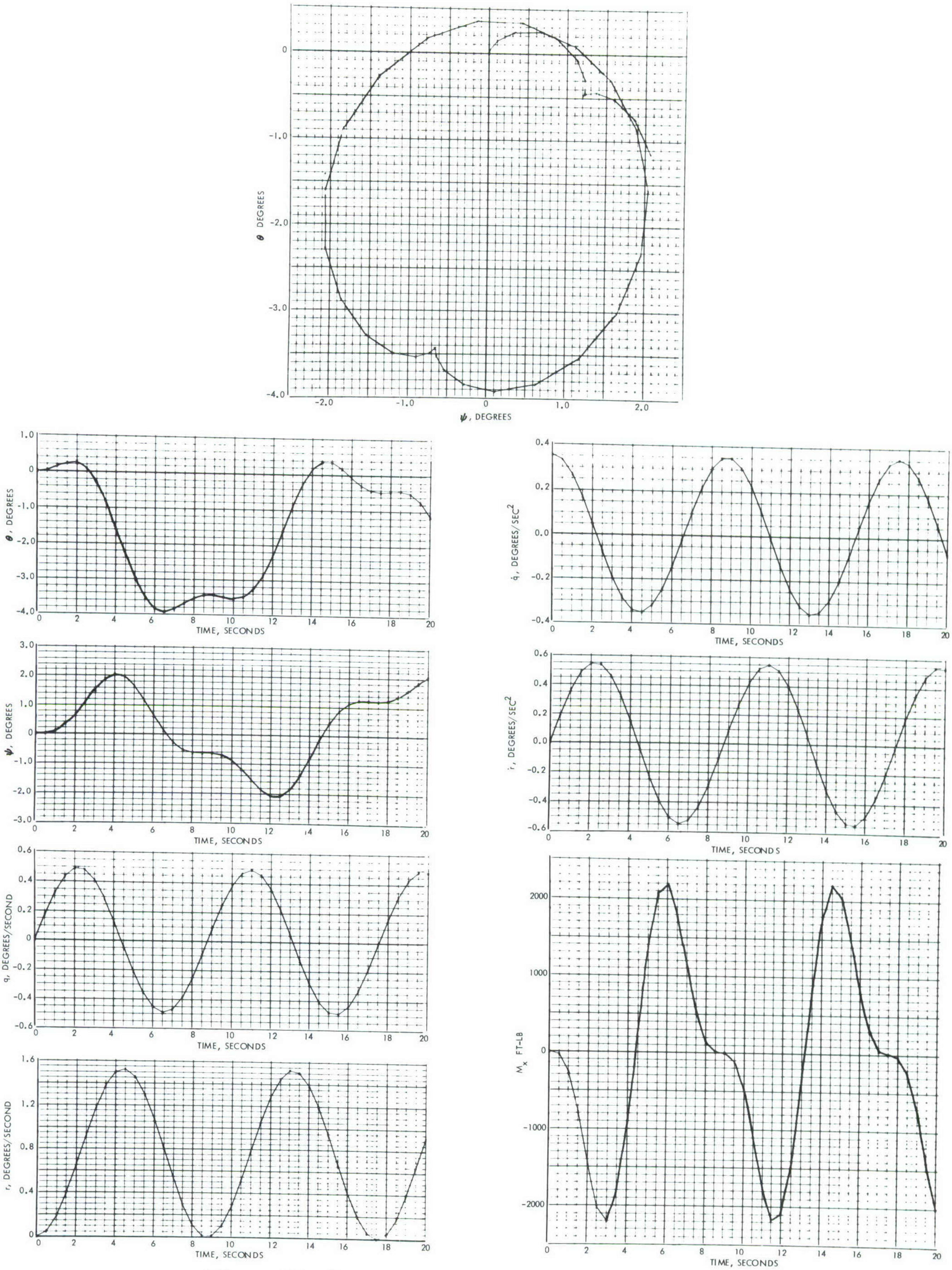

Figure 10. Rigid Body Angular Motions, Configuration 6-A; 1/2-g; M_y = 100, 000 ft-lb

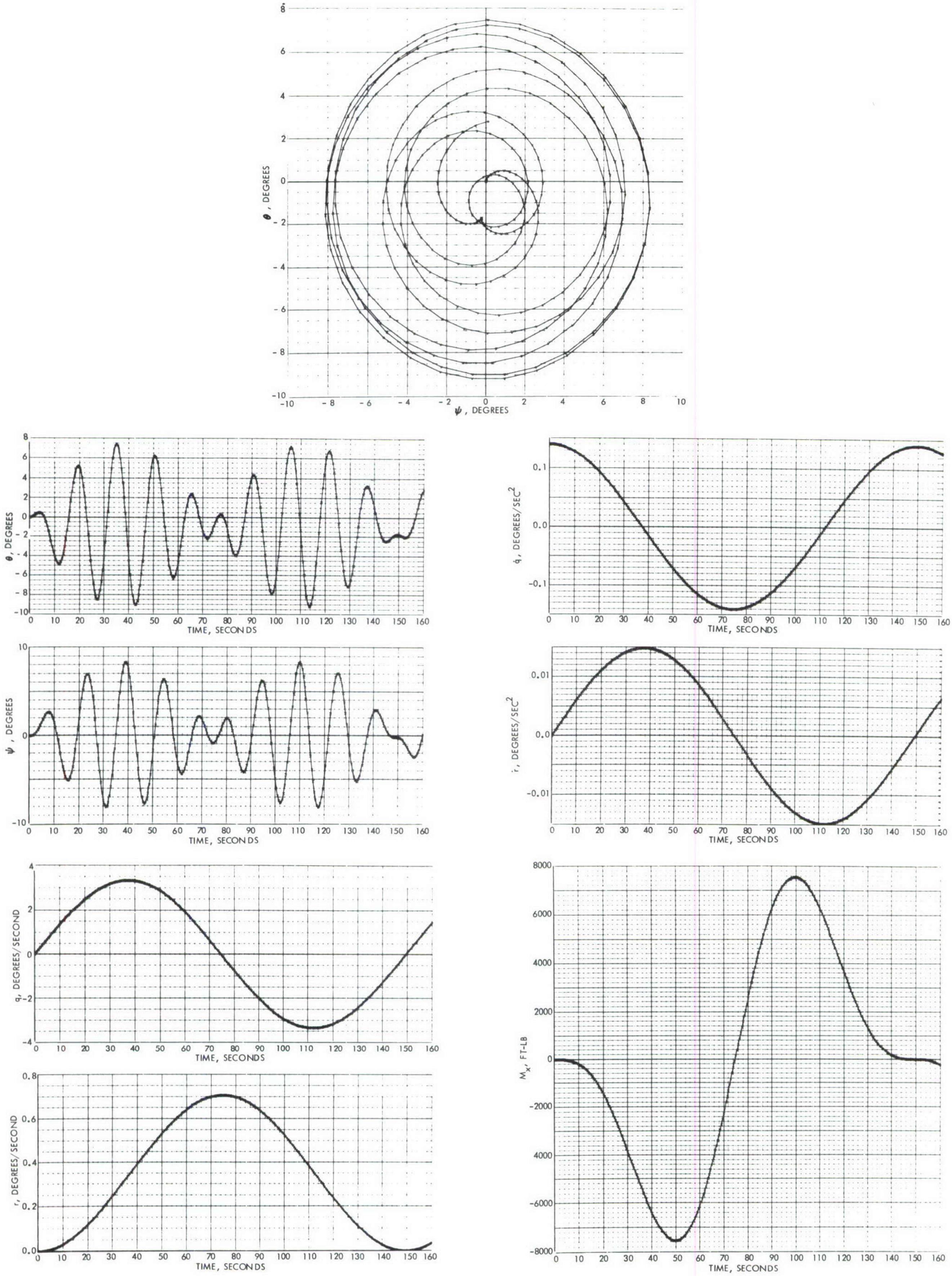

Figure 11. Rigid Body Angular Motions, Configuration 6-B; 1/2-g; M_y = 40, 000 ft-lb

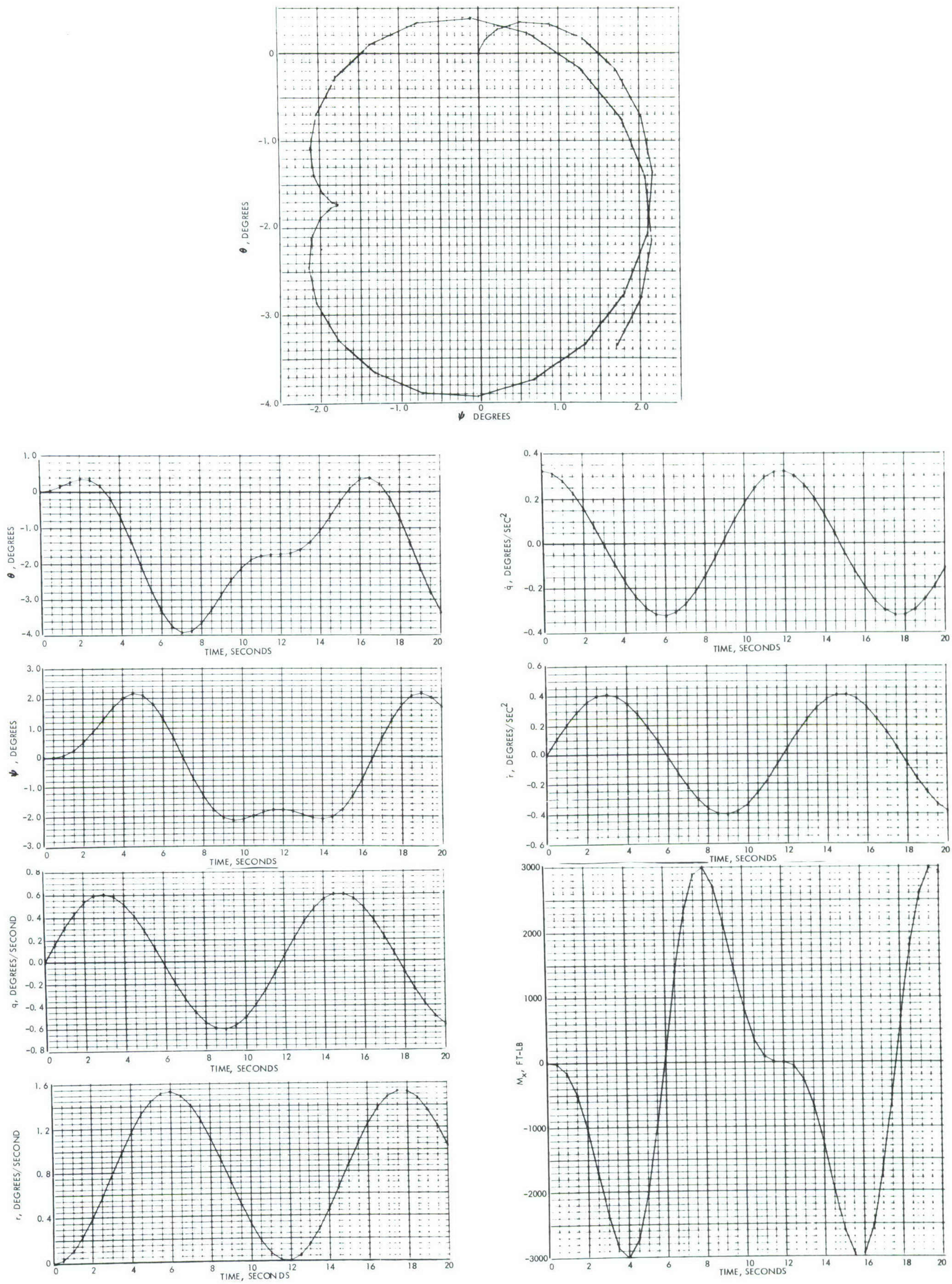

Figure 12. Rigid Body Angular Motions, Configuration 7-A; 1/2-g; M_y = 100, 000 ft-lb

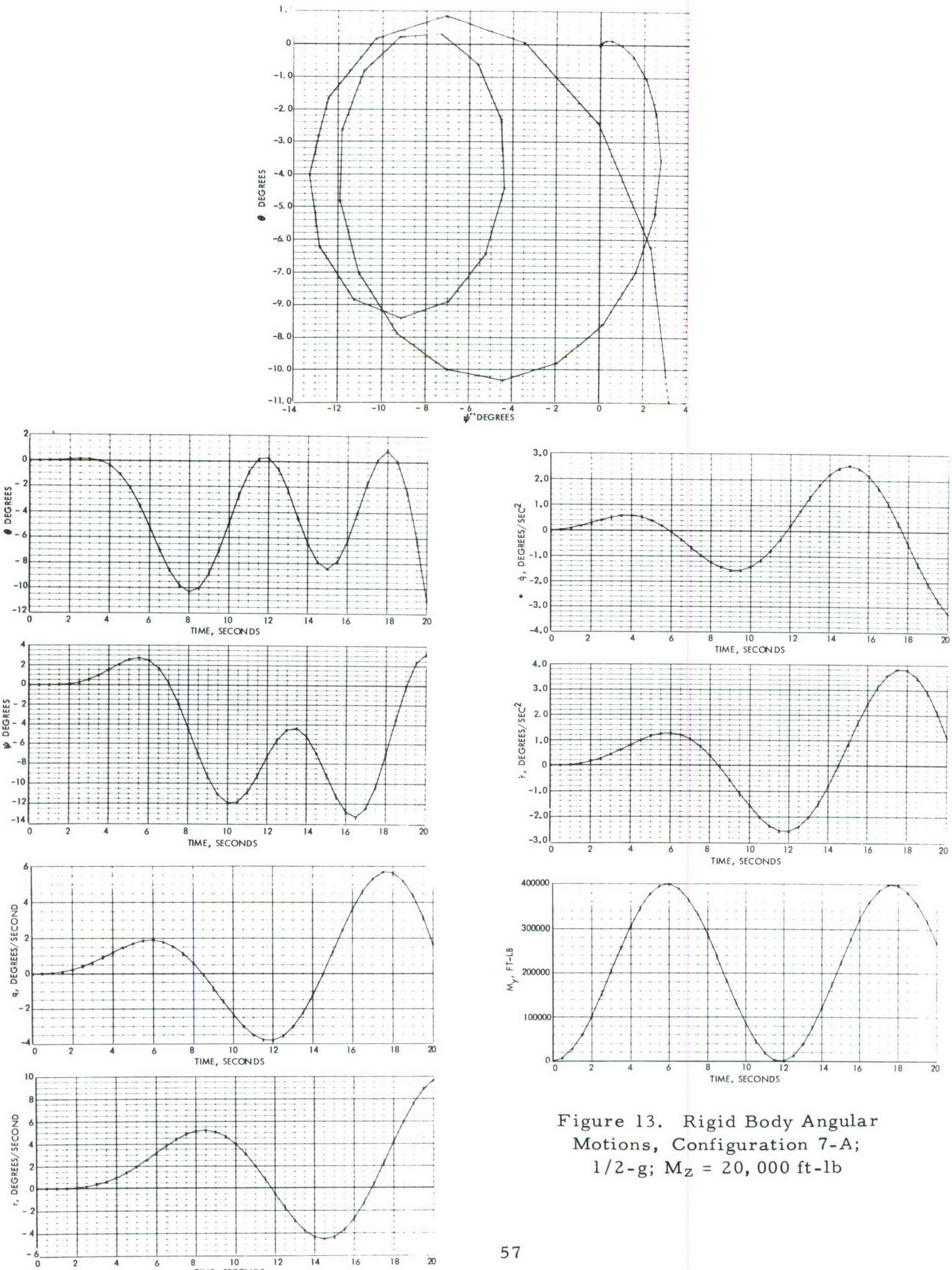

Figure 13. Rigid Body Angular Motions, Configuration 7-A; 1/2-g; M_Z = 20, 000 ft-lb

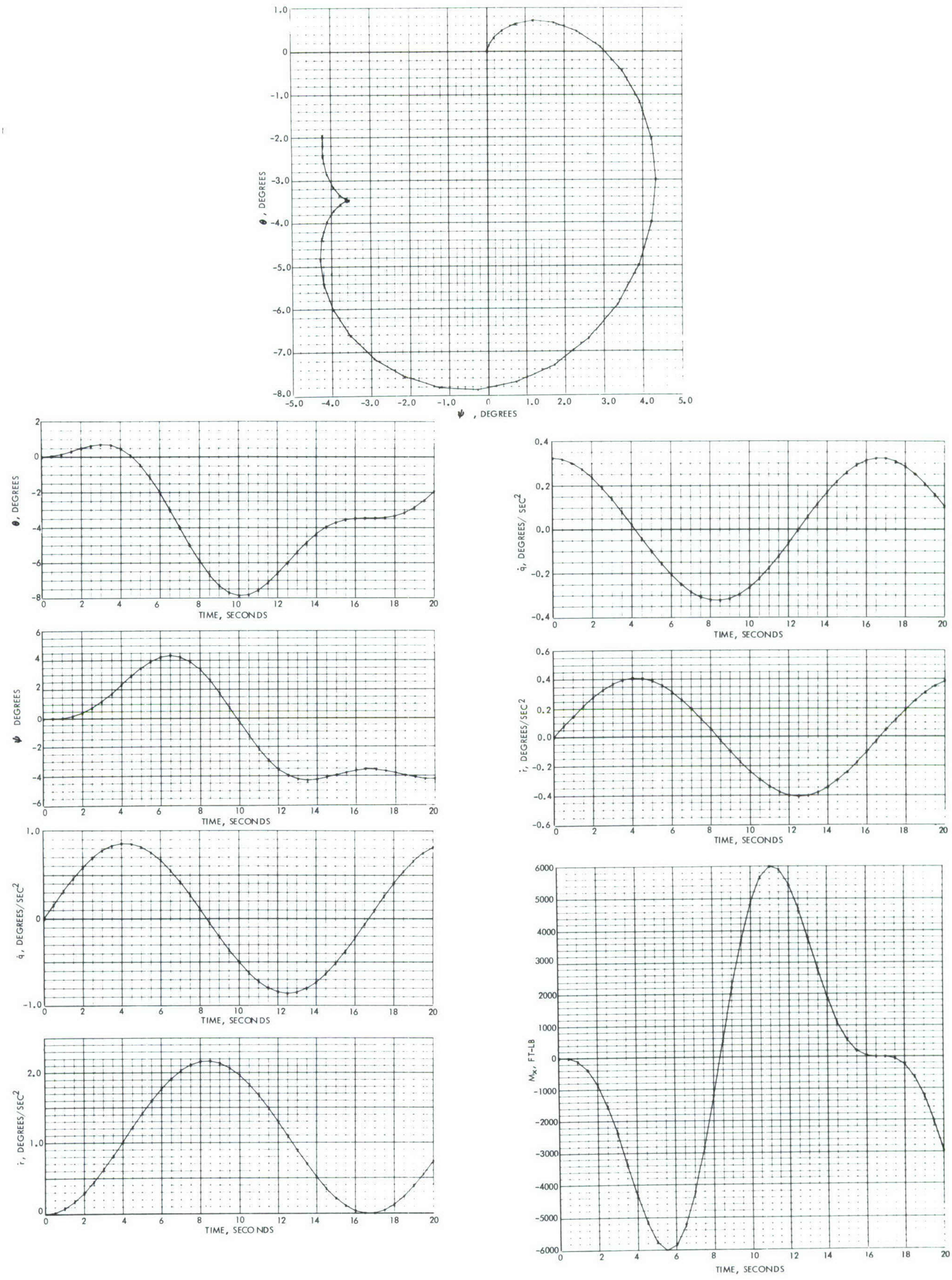

Figure 14. Rigid Body Angular Motions, Configuration 7-A; 1/4-g; M_y = 100, 000 ft-lb

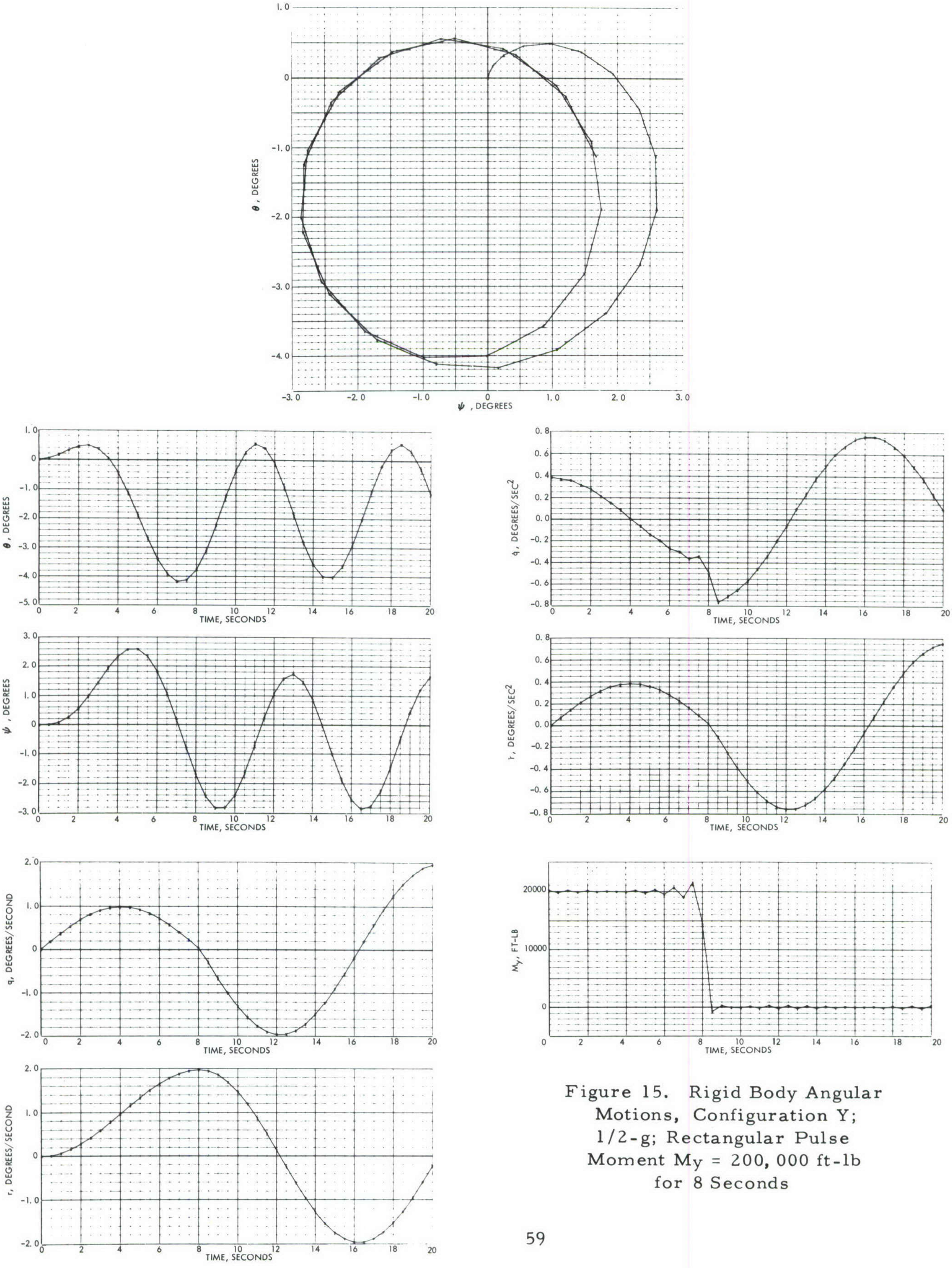

Figure 15. Rigid Body Angular Motions, Configuration Y; 1/2-g; Rectangular Pulse Moment My = 200, 000 ft-lb for 8 Seconds

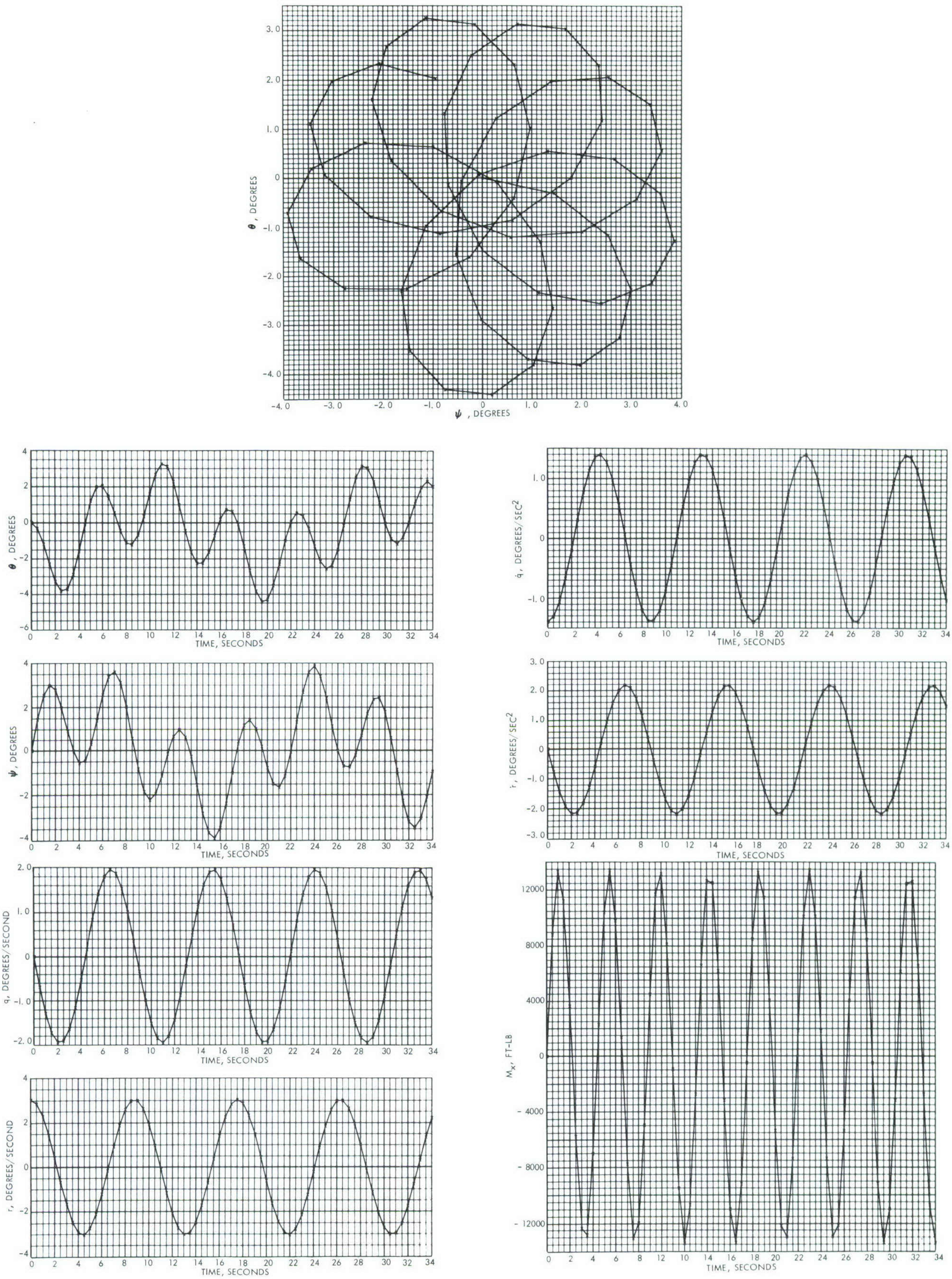

Figure 16. Rigid Body Angular Motions, Configuration 6-A; 1/2-g; q = 0, r = 3.04 Degrees per Second at t = 0

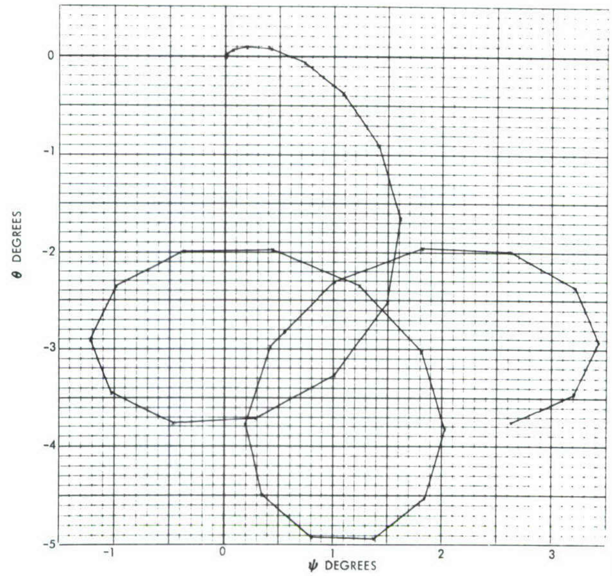

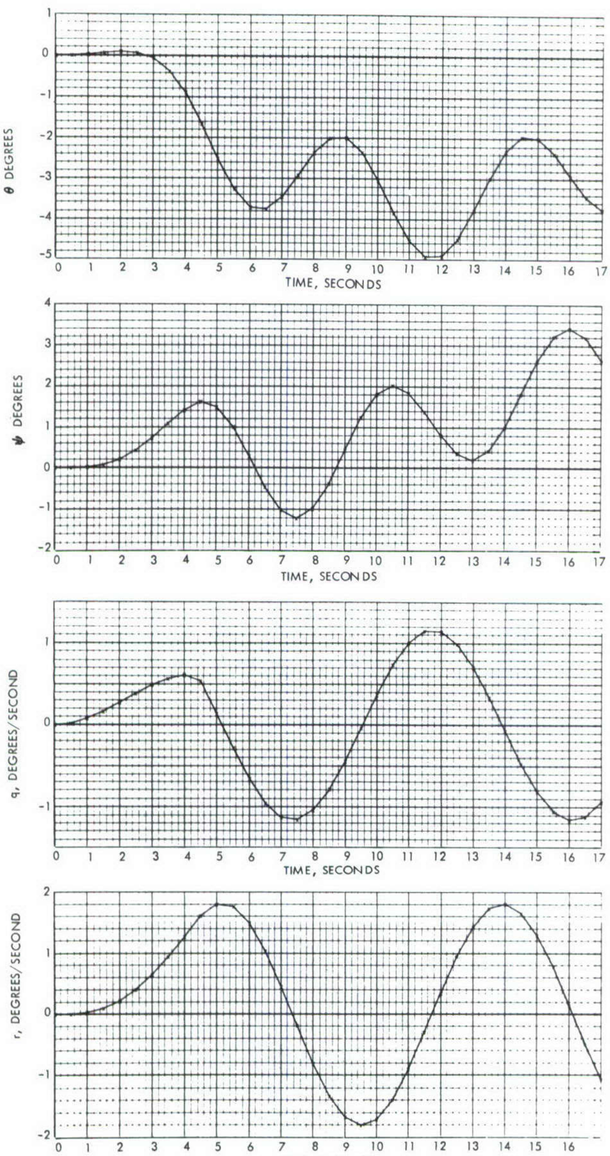

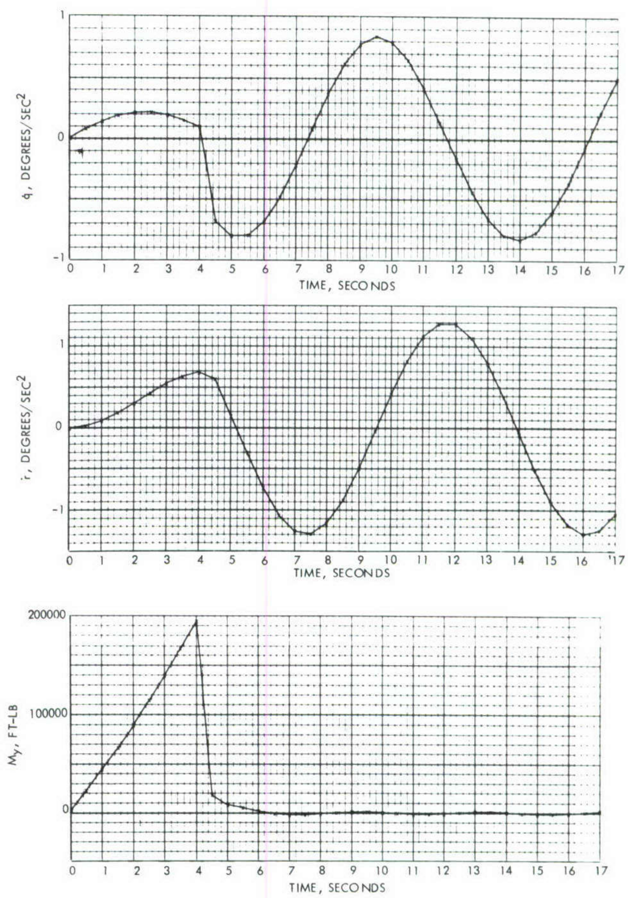

Figure 17. Rigid Body Angular Motions, Configuration 6-A; 1/2-g; Ramp Moment M_y = 190, 000 ft-lb at 4 Seconds

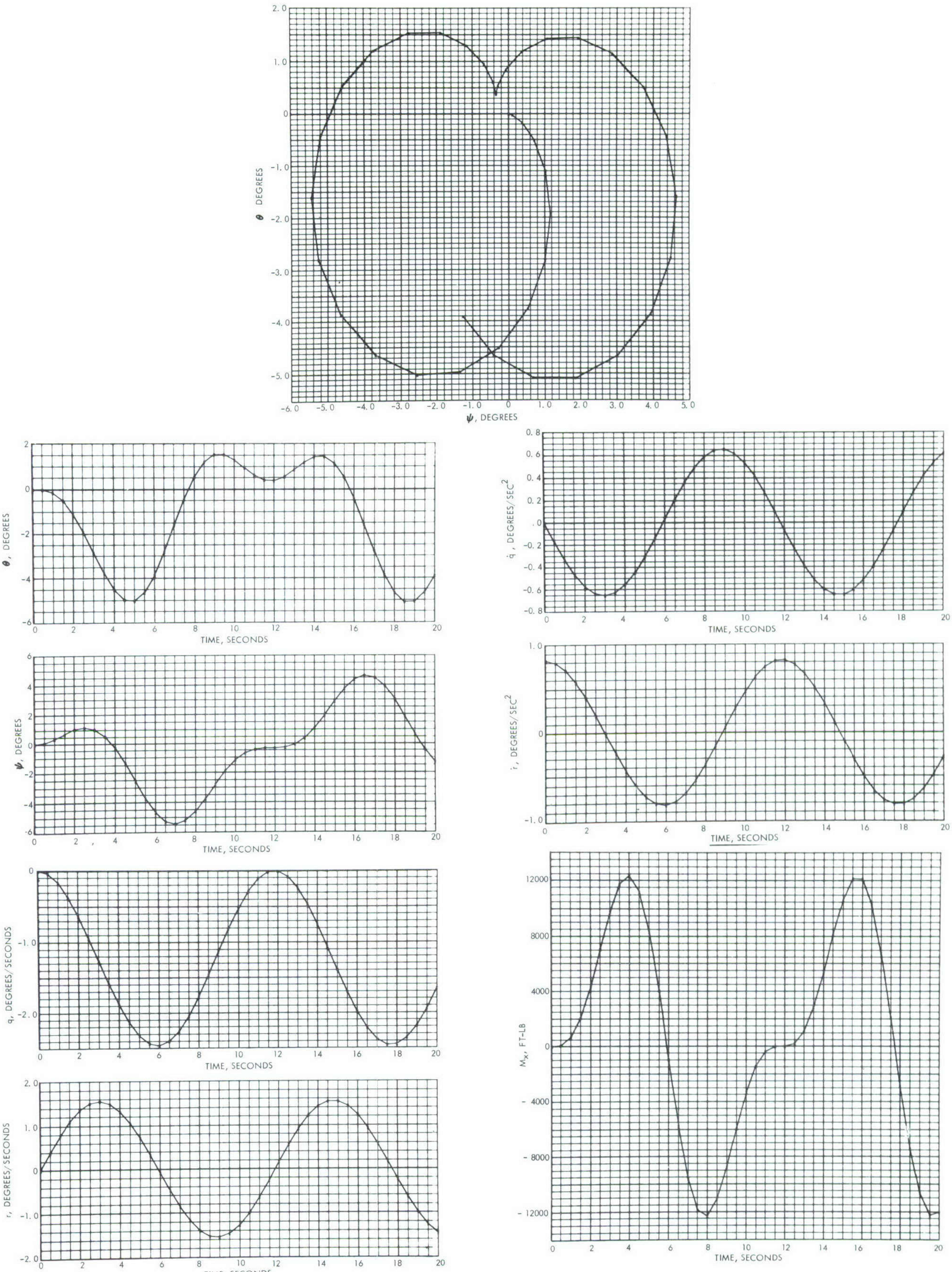

Figure 18. Rigid Body Angular Motions, Configuration 7-A; 1/2-g; $M_y = 200,000\ (1 - \cos \frac{\pi t}{0.5\ \tau_o})$ ft-lb

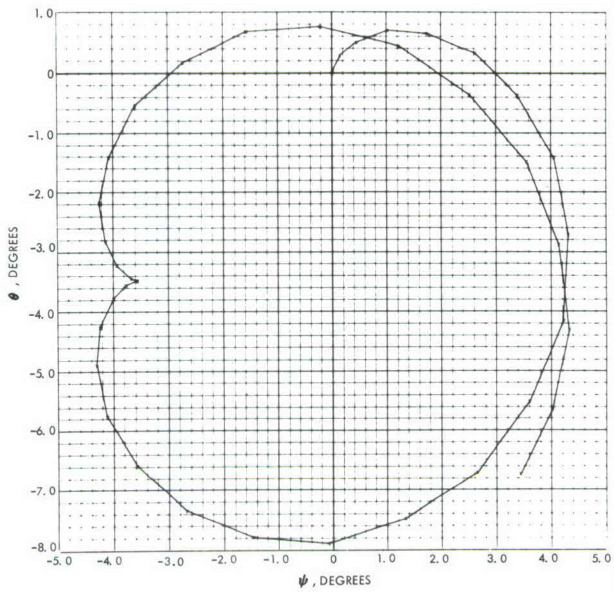

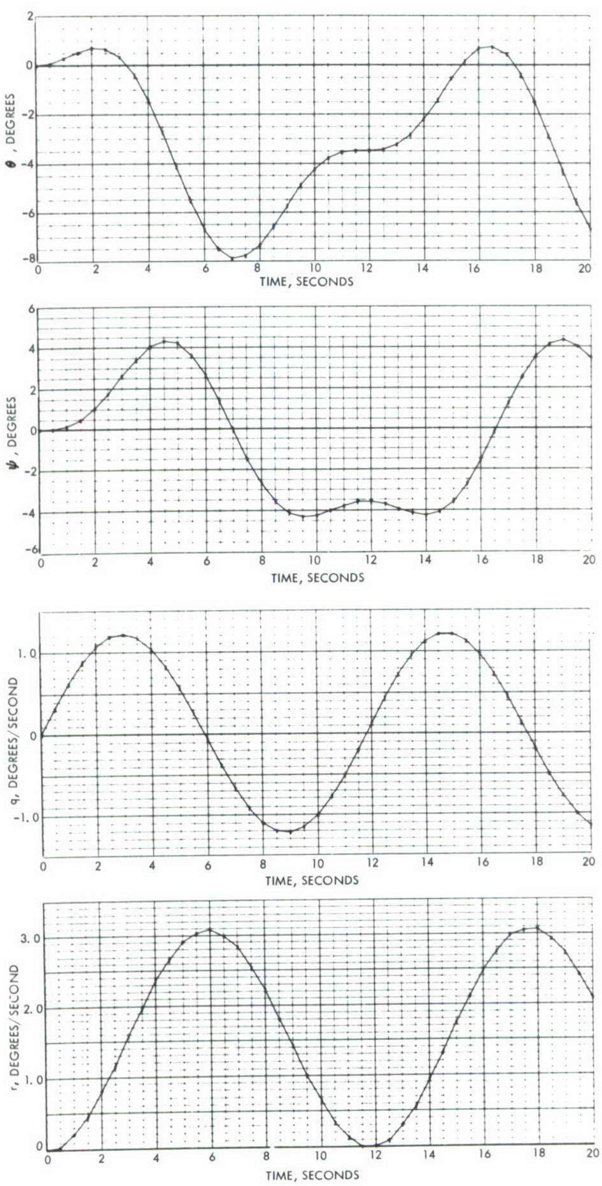

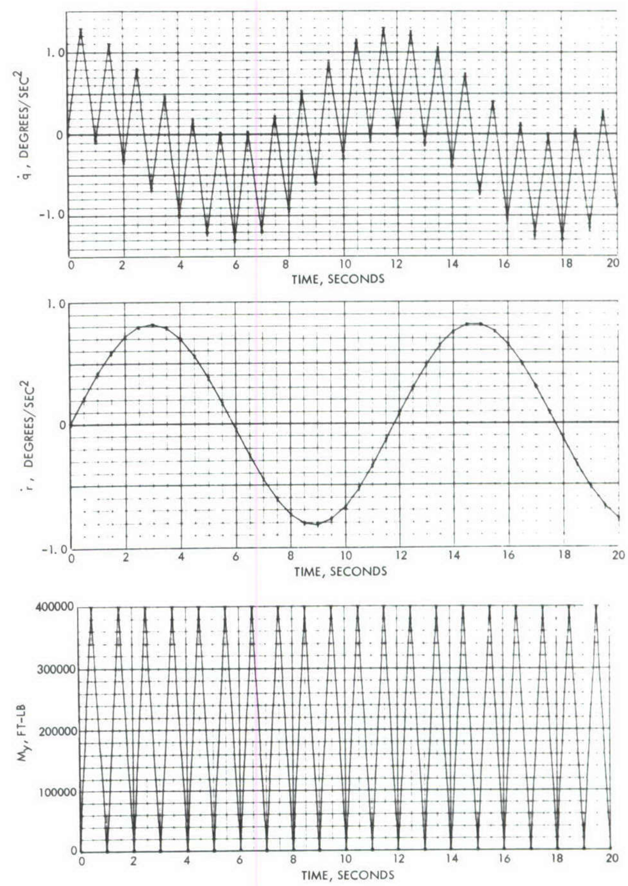

Figure 19. Rigid Body Angular Motion, Configuration 7-A; 1/2-g; M_y = 200, 000 $(1 - \cos \frac{\pi t}{0.5})$ ft-lb

The initial conditions for all computations were such that the x, y, z body axes were initially coincident with the X, Y, Z inertial axes, i.e., $\phi_o = \theta_o = \psi_o = 0$ at $t = 0$. Also, the initial transverse body velocities were $q_o = r_o = 0$ at $t = 0$ unless otherwise noted.

Tables 6 and 7 give the ranges of the response variables for constant external moment disturbances at 1/2-g and 1/4-g artificial gravity levels respectively. M_y and M_z are the values of the constant moments. M_x is the moment about x-axis, as defined by equation (41), which is required to keep the spin rate constant. The variable $\lambda = \dot{\psi}\, \theta / p_o$ is an indication of the error resulting from linearizing equations (40). The accuracy of this transformation from body axes to inertial axes is dependent upon $\lambda << 1$.

Figure 10 shows the response of Configuration 6-A, for 1/2-g artificial gravity, to 100,000 ft-lb constant moment about the y-axis. Under any constant moment forcing function, the body angular velocities q and r both take on values of zero at $t = n\,\tau_o$, $n = 1, 2, 3, \cdots$ which is represented on the θ - ψ curve as a cusp. The moment-free wobble does not exist when the constant moment forcing function is instantaneously reduced to zero at these points. The moment-free wobble motion is greatest when the constant moment forcing function is instantaneously reduced to zero at $t = n\,\tau_o/2$, $n = 1, 3, 5, \ldots$.

Figure 11 shows the response of Configuration 6-B, for 1/2-g artificial gravity, to 40,000 ft-lb constant moment about the y-axis. The natural period is very long, 149 seconds, and the wobble angle is large compared to the disturbance.

Figures 12 and 13 show the response of Configuration 7-A, for 1/2-g artificial gravity, to 100,000 ft-lb constant moment about the y-axis and 20,000 ft-lb constant moment about the z-axis respectively. The dissimilarity in the responses is due to the large differences in transverse moment of inertia values.

Figure 14 shows the response of Configuration 7-A, for 1/4-g artificial gravity, to 100,000 ft-lb constant moment about the y-axis. The wobble angle and the moment M_x are about twice as large as that for 1/2-g artificial gravity, in the case shown in Figure 12.

Table 8 gives the ranges of the response variables for rectangular pulse moment disturbances about the x-axis at 1/2-g artificial gravity. The time duration of the pulse is τ seconds.

Figure 15 shows the response of Configuration Y, for 1/2-g artificial gravity, to 200,000 ft-lb rectangular pulse moment about the y-axis for approximately 8 seconds. The moment-free wobble response for the configuration is also shown.

Table 9 shows the ranges of the response variables for moment-free wobble motion at 1/2-g artificial gravity for seven cases. During the moment-free wobble, both transverse moment components, M_y and M_z are identically zero. The initial values of the transverse body velocity components, q_o and r_o, are not both zero.

Figure 15 shows an example where part of the motion is moment-free wobble; i.e., for $t \geq 9.0$ seconds both M_y and M_z equal zero and the body velocities, q and r, are not both zero. The values of q = 0.7 deg/sec and r = 1.85 deg/sec (at t = 9.0 seconds in Figure 15) could not be used as the initial velocity values q_o and r_o in a moment-free wobble response study.

Figure 16 shows the response on Configuration 6-A, for 1/2-g artificial gravity, to 3.04 deg/sec initial transverse body angular velocity. The type of moment-free wobble motion is dependent upon the mass distribution of the vehicle.

Table 10 gives the ranges of the response variables for ramp function moment disturbances about the y-axis at 1/2-g artificial gravity. The duration of the moment is indicated in the table.

Figure 17 shows the response of Configuration 6-A, for 1/2-g artificial gravity, to a ramp function moment about the y-axis for approximately 4 seconds. The amplitude of the moment at 4 seconds is about 190,000 ft-lb. Moment-free wobble motion exists after approximately 4 seconds.

Table 11 gives the ranges of the response variables for $M_y = a_y (1 - \cos \pi t/t_y)$ moment disturbances at 1/2-g artificial gravity.

Figures 18 and 19 show the responses of Configuration 7-A, for 1/2-g artificial gravity, of the moment function, to $M_y = 200{,}000 (1 - \cos \pi t/t_y)$ moments where the period, $2t_y$, is equal to τ_o and 1.0 seconds, respectively. The response in Figure 18 appears to be diverging during the time interval considered. The response in Figure 19 has the identical form as the response to a constant moment about the y-axis as shown in Figure 12, except $\dot{q}$ and q are the intermodulation of two sinusoidal curves, one with a period of τ_o and the other with a period of 1.0 seconds. The intermodulation does not show on q since the computing interval is 0.5 second.

Angular acceleration out of the plane of rotation of the space station stimulates the semicircular canals and produces a form of canal sickness known as nystagmus, an involuntary jerky motion of the eyes. The angular acceleration threshold for stimulation has been reported to be within the range of 0.2 to 2.0 deg/sec^2. The figures and tables shown indicate that in the greater number of cases studied, the transverse body angular acceleration ($\dot{q}$, $\dot{r}$) are within or below this range. The moment-free wobble response of Configuration 6-A (Figure 16) is one case where the peak transverse body acceleration is greater than 2.0 deg/sec^2 and stimulation

of the semicircular canals can be expected. The effects of artificial gravity on human factors are further discussed in Appendix C.

Table 5. Response Properties of the Configurations

Configuration		1/2-g at R_g			1/4-g at R_g			1/10-g at R_g		
	R_g (ft)	p_o (rad/sec)	Ω (rad/sec)	τ_o (sec)	p_o (rad/sec)	Ω (rad/sec)	τ_o (sec)	p_o (rad/sec)	Ω (rad/sec)	τ_o (sec)
1-A	111.11	0.38066	0.37489	16.760	0.26916	0.26508	23.703	0.17024	0.16765	37.477
1-B	666.66	0.15540	0.15274	41.138	0.10989	0.10800	58.178	0.069499	0.068306	91.986
2-A	111.11	-	-	-	-	-	-	-	-	-
2-B	666.66	-	-	-	-	-	-	-	-	-
4-A	100	0.40125	0.27448	22.891	0.28372	0.19409	32.373	0.17944	0.12275	51.186
4-B	500	0.17544	0.17313	36.293	0.12688	0.12521	50.182	0.080250	0.079191	79.342
6-A	100	0.40125	0.71712	8.734	0.28372	0.50708	12.391	0.17944	0.32071	19.592
6-B	100	0.40125	0.042052	149.416	0.28372	0.029735	211.306	0.17944	0.018806	334.105
7-A	100	0.40125	0.53211	11.808	0.28372	0.37628	16.698	0.17944	0.23796	26.404
7-B	100	0.40125	0.040730	154.265	0.28372	0.028800	218.166	0.17944	0.018215	344.947
Y	75	0.46332	0.38689	16.240	0.32762	0.27358	22.966	0.20720	0.17303	36.314
Y-A	100	0.40125	0.57216	10.282	0.28372	0.40458	15.530	0.17944	0.25588	24.555
C C	111.11	0.38066	0.69044	9.100	0.26916	0.48822	12.870	0.17024	0.30878	20.349

Table 6. Response to Constant Moment Function, 1/2-g Artificial Gravity

			Limits of Response Range					
Configuration	M_y (ft-lb)	M_z (ft-lb)	θ (deg)	ψ (deg)	$\dot{q}$ (deg/sec^2)	$\dot{r}$ (deg/sec^2)	M_x (ft-lb)	$\lambda = \frac{\dot{\psi}\theta}{p_o}$
1-A	1,000,000	0	+1.2 -8.2	+5.4 -5.3	±0.6	±0.59	±94,000	0.021
	0	10,000	+8.0 -7.5	+1.2 -12.9	±0.85	±0.84	190,000	0.0255
1-B	5,000,000	0	+0.8 -5.25	+3.5 -3.4	±0.064	±0.065	±303,000	0.0085
	0	1,000	+4.8 -4.5	+1.0 -7.2	±0.085	±0.084	±541,000	0.0093
4-A	200,000	0	+7.8 -13.9	+8.3 -11.8	±0.8	±0.81	±1780	0.058
	0	200,000	+11.0 -8.0	+7.2 -13.3	±0.77	±0.775	±1630	0.047
4-B	1,000,000	0	+1.9 -12.3	±8.0	±0.188	±0.188	±1.38	0.046
	0	1,000,000	±8.0	+1.7 -12.3	±0.185	±0.188	±1.38	0.0264
6-A	100,000	0	+0.4 -3.9	+2.0 -2.1	±0.35	±0.55	±2200	0.0032
	0	20,000	+3.1 -3.3	+2.2 -2.3	±0.53	±0.81	±5000	0.0037
6-B	40,000	0	+7.4 -9.3	+8.2 -8.1	±0.14	±0.0149	±7550	0.0222
	0	25	+9.3 -9.2	±9.2	±0.078	±0.0083	±2380	0.0265

Table 6. Response to Constant Moment Function, 1/2-g Artificial Gravity (Cont)

Configuration	M_y (ft-lb)	M_z (ft-lb)	Limits of Response Range: θ (deg)	ψ (deg)	$\dot{q}$ (deg/sec^2)	$\dot{r}$ (deg/sec^2)	M_x (ft-lb)	$\lambda = \frac{\dot{\psi}\theta}{p_o}$
7-A	100,000	0	+0.4 -3.9	±2.15	±0.32	±0.4	±3000	0.0043
	0	20,000	+1.5 -5.0	+4.6 -5.4	±0.65	±0.81	±12,300	0.0092
7-B	50,000	0	+8.7 -11.0	±10.0	±0.16	±0.016	±11,200	0.032
	0	25	±9.3	±9.3	±0.077	±0.008	±2530	0.0265
Y	50,000	0	+3.5 -10.5	+6.5 -7.8	±0.95	±0.95	±0.95	0.033
	0	50,000	+7.8 -6.5	+3.5 -10.5	±0.95	±0.95	±0.95	0.245
Y-A	20,000	0	+2.7 -7.4	+5.2 -4.0	±0.86	±0.9	±2800	0.0165
	0	200,000	+4.5 -6.5	+4.2 -8.6	±1.08	±1.2	±4400	0.018
C C	500,000	0	+0.2 -3.2	±1.5	±0.184	±0.33	±9300	0.0019
	0	5,000	+3.2 -3.4	+1.9 -1.75	±0.395	±0.7	±40,000	0.0036

Table 7. Response to Constant Moment Function, 1/4-g Artificial Gravity

			Limits of Response Range					
Configuration	M_y (ft-lb)	M_z (ft-lb)	θ (deg)	ψ (deg)	$\dot{q}$ (deg/sec^2)	$\dot{r}$ (deg/sec^2)	M_x (ft-lb)	$\lambda = \frac{\dot{\psi}\theta}{p_o}$
1-A	500,000	0	-1.2 +8.3	+5.4 -5.3	±0.3	±0.295	±47,000	0.021
	0	5,000	+8.0 -7.5	+1.7 -11.9	±0.42	±0.42	±95,000	0.0255
1-B	5,000,000	0	+1.5 -10.6	+6.9 -6.8	±0.064	±0.063	±610,000	0.034
	0	1,000	+9.7 -9.2	+2.0 -14.3	±0.085	±0.084	1,080,000	0.0375
4-A	100,000	0	+7.8 -13.9	+8.3 -11.8	±0.4	±0.41	±890	0.058
	0	100,000	+11.0 -8.0	+7.2 -13.3	±0.39	±0.39	±820	0.047
4-B	500,000	0	+7.7 -7.6	+1.6 -11.7	±0.093	±0.093	±0.66	0.042
	0	500,000	+7.7 -7.6	+1.6 -11.7	±0.093	±0.093	±0.66	0.0244
6-A	100,000	0	+0.5 -7.8	+4.1 -1.3	±0.35	±0.54	±4400	0.0127
	0	20,000	+0.3 -6.7	+2.0 -4.6	±0.53	±0.82	±10,000	0.015

Table 7. Response to Constant Moment Function, 1/4 Artificial Gravity (Cont)

			Limits of Response Range					
Configuration	M_y (ft-lb)	M_z (ft-lb)	θ (deg)	ψ (deg)	$\dot{q}$ (deg/sec^2)	$\dot{r}$ (deg/sec^2)	M_x (ft-lb)	$\lambda = \frac{\dot{\psi}\theta}{p_o}$
7-A	100,000	0	+0.7 -7.8	±4.3	±0.32	±0.41	±6000	0.017
	0	20,000	+3.0 -10.0	+2.3 -10.8	±0.65	±0.81	24,800	0.087
Y-A	100,000	0	+1.0 -7.5	+5.2 -2.9	±0.43	±0.45	±1400	0.0164
	0	100,000	+3.1 -6.5	+1.3 -8.7	±0.53	±0.56	±2200	0.018
CC	500,000	0	+0.3 -6.4	+3.2 -3.1	±0.183	±0.375	±18,600	0.0076
	0	5,000	+6.3 -6.8	+4.6 -5.5	±0.39	±0.7	±8000	0.014

Table 8. Response to Rectangular Pulse Moment Function of τ Seconds Duration, 1/2-g Artificial Gravity

			Limits of Response Range					
Configuration	M_y (ft-lb)	M_z (ft-lb)	θ (deg)	ψ (deg)	$\dot{q}$ (deg/sec^2)	$\dot{r}$ (deg/sec^2)	M_x (ft-lb)	$\lambda = \frac{\dot{\psi}\theta}{p_o}$
1-A	1,000,000 $\tau = \frac{\tau_o}{2}$	0	+0 -8.3	+4.5 -4.0	±1.2	±1.19	±145,000	0.021
4-A	200,000 $\tau = \frac{\tau_o}{2}$	0	+5.8 -12.0	+5.8 -12.0	±1.6	±1.61	±2730	0.052
6-A	200,000 $\tau = \frac{\tau_o}{2}$	0	+0 -8.0	+8.0 -0	+1.4 -1.35	+2.5 -2.2	±13,500	0.012
7-A	200,000 $\tau = \frac{\tau_o}{2}$	0	-1.0 to -10.0	+8.0 -2.6	±1.3	±1.6	±18,000	0.019
Y	200,000 $\tau = \frac{\tau_o}{2}$	0	+0.6 -4.2	+2.6 -3.82	±076	±0.76	0.0235	0.0054
Y-A	200,000 $\tau = \frac{\tau_o}{2}$	0	-0.9 to -7.0	+4.8 -1.5	±1.7	±1.8	±4300	0.017

Table 9. Moment-Free Wobble Response to Initial Transverse Velocity, 1/2-g Artificial Gravity

			Limits of Response Range					
Configuration	q_o (deg/sec)	r_o (deg/sec)	θ (deg)	ψ (deg)	$\dot{q}$ (deg/sec^2)	$\dot{r}$ (deg/sec^2)	M_x (ft-lb)	$\lambda = \frac{\dot{\psi}\theta}{p_o}$
1-A	-4.7	0	±6.2	+0 -12.4	±1.75	±1.73	±315,000	0.025
4-A	+2.97	+3.0	+1.7 -11.0	+11.0 -1.7	±1.18	±1.18	±14,200	0.036
6-A	+0.5	+1.5	+1.9 -2.3	+3.2 -1.2	±0.78	±1.2	±4000	0.002
7-A	-1.0	+2.0	±3.7	+1.9 -6.3	±1.0	±1.83	±11,000	0.0054
Y	-1.0	+2.0	+0.2 -6.0	+1.4 -3.8	±0.86	±0.86	±0.03	0.0073
Y-A	0	+3.12	+0.6 -6.2	+3.5 -3.4	±1.7	±1.8	±4300	0.0014
CC	-1.0	+2.0	+4.1 -3.9	+1.2 -6.4	±0.95	±1.7	±93,000	0.0054

Table 10. Response to Ramp Function Moment About Y-Axis, 1/2-g Artificial Gravity

			Limits of Response Range				
Configuration	M_y (Ft-lb)	θ (Deg)	ψ (Deg)	$\dot{q}$ (Deg/Sec^2)	$\dot{r}$ (Deg/Sec^2)	M_x (Ft-lb)	$\lambda = \frac{\dot{\psi}\theta}{P_o}$
1-A	0 to 1,000,000 at t_{max} = 15 sec	> +3.8 -2.6	+0.85 -4.2	+0.115 -0.105	+0.21 -0	+0 -18,000	0.0044
4-A	0 to 160,000 at 12 sec	> +2.0 -4.15	+1.3 < -7.2	+0.2 -0.07 at 13 sec	+0.39 -0	> +620 -0	0.0066
4-B	0 to 1,000,000 at 30 sec	>+3.7 -4.2	+1.3 -6.8	+0.038 -0.04	+.052 -0	+0 -0.36	0.0068
6-A	0 to 190,000 at 4 sec	+ .1 -0.9	+1.4 -0	+0.22 -0	+0.7 -0	+0 -3500	0.0004
7-A	0 to 170,000 at 5 sec	+0.1 -1.3	+1.5 -0	+0.2 -0	+0.5 -0	+0 -4000	0.0003
Y	0 to 50,000 at 15 sec	+5.2 -2.7	+3.3 -4.5	+0.18 -0.15	+0.325 -0	+0.0173 -0	0.009
Y-A	0 to 200,000 at 15 sec	> +3.7 -2.2	+0.7 -3.4	+0.095 -0.082	+0.21 -0	+5 -225	0.0036

Table 11. Response to Moment Function $M_y = A_y (1 - \cos \pi t/t_y)$ 1/2-g Artificial Gravity

			Limits of Response Range					
Configuration	a_y (ft/lb)	t_y (sec)	θ (deg)	ψ (deg)	$\dot{q}$ (deg/sec^2)	$\dot{r}$ (deg/sec^2)	Mx (ft/lb)	$\lambda = \frac{\dot{\psi}\theta}{P_o}$
1-A	1,000,000	0.5 $0 \le t \le 20$	-8.2 +1.2	-5.3 +5.4	±1.2	±0.59	±94,000	0.021
4-A	200,000	12.0 $0 \le t \le 34$	+23. -9.5	+15.0 -20.0	+3.0 -1.85	>3.5 -2.5	+6300 -7000	0.180
4-B	1,000,000	10.0 $0 \le t \le 40$	+3.5 -4.5	+7.3 -0.2	+0.4 -0.35	+0.216 -0.29	+0.94 -1.03	0.010
6-A	200,000	$6.55 = \frac{3}{4}\tau_o$ $0 \le t \le 20$	+0. -15.0	+2.0 -13.3	+1.13 -9.2	±2.1	+22,000 -23,000	0.035
	200,000	$8.73 = \tau_o$ $0 \le t \le 20$	-6.8 +3.9	-12.7 +1.2	-4.8 +2.7	±0.96	±11,000	0.0206
7-A	200,000	$11.81 = \frac{1}{2}\tau_o$ $0 \le t \le 20$	-11.4 +0.8	-13.3 +2.7	-1.6 +2.6	-2.6 +3.8	+50,000 -165,000	0.040
Y	50,000	12 sec $0 \le t \le 25$	+15.5 -5.8	+11.5 -13.0	+1.6 -1.3	+1.13 -1.85	±0.19	0.080
Y-A	200,000	8.0 $0 \le t \le 25$	>+8.5 -5.6	+3.0 -10.5	+0.85 -0.9	+0.95 -1.3	+4200 -3500	0.0125

6.0 SYSTEM VIBRATION MODES

6.1 LUMPED PARAMETER METHOD

For the system vibration analysis, a lumped parameter approach was generally used. The fundamental characteristics of the vibration of a system would not be altered in character if the system is divided into a number of small parts with the mass of each part concentrated at its center. By using a sufficiently large number of parts, a lumped mass system, although of finite freedom, may represent the original structure with any desired accuracy.

For the single-cable-connected station (Configurations 1, 2, and CC) the compartment and counterweight, having small dimensions in comparison with the length of the cable, are treated as point masses. The cable is divided into 10 equal parts initially, and into 50 equal parts in the final analysis. The method of Lagrange's equation is used in the analysis. For Configurations 4 and 6, (Figure 1) the cable mass, which has little influence on the dynamics of the system, is not considered. For other configurations, where the longitudinal and lateral dimensions of the compartment have a ratio of 10-to-1, the vibration analysis is conducted by the use of transfer matrices. Equations of equilibrium and elastic compatibility are established from the boundary conditions. The frequencies are computed by iteration from the characteristic equations. After the natural frequencies of the system have been computed, the mode shapes that correspond to each frequency are calculated by matrix operation.

6.2 VIBRATION OF CABLE-CONNECTED SPACE STATIONS

6.2.1 Single Cable-Connected Configuration

The vibration of a space station that consists of two compartments (or a compartment and a counterweight) connected by a cable may be divided into three classes – longitudinal, lateral and torsional.

Longitudinal vibrations are characterized by the periodic motion of points along the center line. The potential energy stored in the stretched cable depends on the change of tension that occurs in the various parts of the cable as a result of the increased or diminished extension.

Lateral vibrations are characterized by the movement of points on the cable in planes perpendicular to the mean line of the cable. In this case, the stored potential energy depends on the steady-state tension,

however the small variation of tension accompanying the additional stretching may be left out. It is assumed that the stretching due to the lateral displacement may be neglected in comparison with that due to inertial forces. The most general lateral vibrations may be resolved into two sets of normal vibrations executed in perpendicular planes. It is sufficient for most purposes to regard the motion as entirely confined to a single plane that passes through the line of the cable.

Due to the large rotary inertia of the compartment and counterweight, the angular displacement may change the vibration characteristic of the system. The lateral vibration equations include the effect of end rotations.

These three classes of vibration are considered independently of each other. The two compartments, considerably heavier than the cable, are considered to be spinning at a constant rate about the center of gravity of the system, with torsion about the mean line of the cable. The amplitude of vibration is assumed to be small so that no coupling effect is introduced between the three classes.

6.2.1.1 Longitudinal Vibration

For a better understanding of the fundamental vibration characteristics of the two-compartment, cable-connected configuration, the lumped-mass approach is adopted. For a preliminary analysis, the entire cable is divided into 10 equal parts, with the mass of each part concentrated at its center. See Figure 20.

Assume that u_1 through u_{11} are the longitudinal displacements of mass points 1 through 11 during vibration along the cable which retains its straightness. M_1, M_2, and m are lumped masses. The total kinetic energy may be expressed by

$$T = \frac{1}{2}\left[(M_1 + \frac{m}{2})\,\dot{u}_1^{\,2} + m\,(\dot{u}_2^{\,2} + \dot{u}_3^{\,2} + \ldots + \dot{u}_{10}^{\,2}) + (M_2 + \frac{m}{2})\,\dot{u}_{11}^{\,2}\right]$$

The potential energy of the displacement depends not on the total tension, but on the increments of tension that occur in the various parts of the string as a result of the incremental extension. Usually, the displacement is small. The change of tension due to rotational motion is not considered in this report.

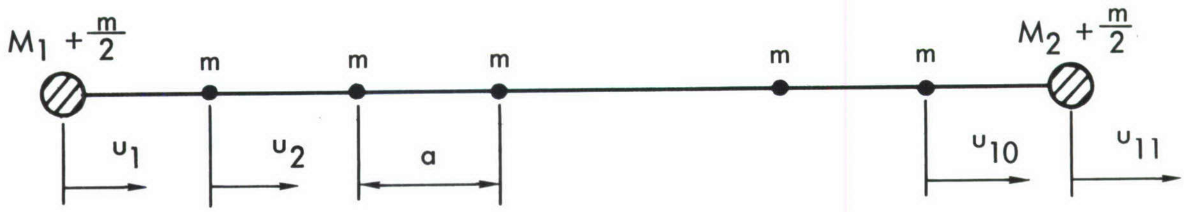

Figure 20. Longitudinal Vibration of Cables

If the average tension in the various segments of the cable is denoted as S_{12}, S_{23}, etc., the expression of potential energy is

$$V = \frac{1}{2} \Delta S_{12} (u_2 - u_1) + \frac{1}{2} \Delta S_{23} (u_3 - u_2) + \ldots .$$

$$= \frac{AE}{2a} \left[(u_2 - u_1)^2 + (u_3 - u_2)^2 + \ldots . + (u_{11} - u_{10})^2 \right]$$

By Lagrange's method, the equations of motion are

$$(M_1 + \frac{m}{2}) \ddot{u}_1 - \frac{AE}{a} (u_2 - u_1) = 0$$

$$m \ddot{u}_2 - \frac{AE}{a} (u_3 - 2 u_2 + u_1) = 0$$

$$m \ddot{u}_3 - \frac{AE}{a} (u_4 - 2 u_3 + u_2) = 0$$

. . . .

. . . .

$$\left(M_2 + \frac{m}{2}\right) \ddot{u}_{11} - \frac{AE}{a}\left(- u_{11} + u_{10}\right) = 0$$

Let the solutions of the above equations be

$$u_i = \lambda_i \sin (pt + \alpha)$$

where

$i = 1, 2, 3, 4, 5, 6, 7, 8, 9, 10, 11$

and introduce the notations

$$\beta_1 = \frac{1}{M_1 + \frac{m}{2}} \cdot \frac{AE}{a}$$

$$\beta_2 = \frac{1}{m} \cdot \frac{AE}{a}$$

$$\beta_3 = \frac{1}{M_2 + \frac{m}{2}} \cdot \frac{AE}{a}$$

The frequency equation, that gives the value of p^2, will assume the form

$$\begin{array}{ccccccc} \lambda_1 & \lambda_2 & \lambda_3 & \lambda_4 \cdots & \lambda_{10} & \lambda_{11} \\ \left|\begin{matrix} p^2 - \beta_1 & \beta_1 & & & & \\ \beta_2 & p^2 - 2\beta_2 & \beta_2 & & & \\ & \beta_2 & p^2 - 2\beta_2 & \beta_2 & & \\ & & \beta_2 & p^2 - 2\beta_2 & \beta_2 & \\ & & & \cdots\cdots & & \\ & & & \cdots\cdots & & \\ & & & \cdots\cdots & & \\ & & & \beta_2 & p^2 - 2\beta_2 & \beta_2 \\ & & & & \beta_3 & p^2 - \beta_3 \end{matrix}\right| \end{array} = 0$$

6.2.1.2 Lateral Vibration

For this analysis the length of the cable is divided into 10 equal parts so that m denotes the lumped mass, and S_{12}, S_{23} .... denote the average tension in each segment. See Figure 21.

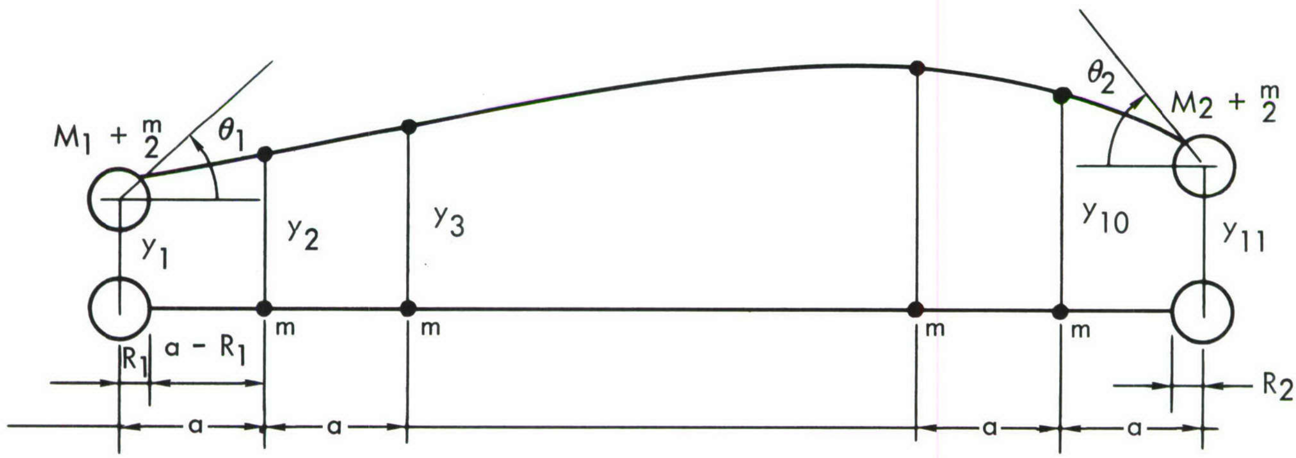

Figure 21. Lateral Vibration of Cable

If y_1 through y_{11} are the lateral displacements of the mass point, the elongations in the various segments of cable are

$$\delta_{1,2} = \left[(a - R_1 \cos\theta_1)^2 + (y_2 - y_1 - R_1 \sin\theta_1)^2\right]^{1/2} - (a - R_1)$$

Assuming θ_1 is small, $\cos\theta_1 = 1$, and $\sin\theta_1 = \theta_1$, then

$$\delta_{1,2} = \left[(a - R_1)^2 + (y_2 - y_1 - R_1\,\theta_1)^2\right]^{1/2} - (a - R_1)$$

$$= \frac{1}{2}\,\frac{(y_2 - y_1 - R_1\,\theta_1)^2}{a - R_1}$$

$$\delta_{2,3} = \frac{1}{2\,a}\,(y_3 - y_2)^2$$

$$\cdots\cdots$$

$$\delta_{9,10} = \frac{1}{2\,a}\,(y_{10} - y_9)^2$$

$$\delta_{10,11} = \frac{1}{2}\,\frac{(y_{11} - y_{10} - R_2\,\theta_2)^2}{a - R_2}$$

The potential energy is

$$V = \frac{S_{1,2}}{2}\,\frac{(y_2 - y_1 - R_1\,\theta_1)^2}{a - R_1} + \frac{S_{2,3}}{2\,a}(y_3 - y_2)^2 + \frac{S_{3,4}}{2\,a}(y_4 - y_3)^2 + \ldots$$

$$+ \frac{S_{9,10}}{2\,a}\,(y_{10} - y_9)^2 + \frac{S_{10,11}}{2}\,\frac{(y_{11} - y_{10} - R_2\,\theta_2)^2}{a - R_2}$$

If the rotary inertia of M_1 and M_2 is denoted by I_1 and I_2 respectively, and the rotary inertia of the cable is neglected, the kinetic energy is

$$T = \frac{1}{2}\,I_1\,\dot{\theta}_1^2 + \frac{1}{2}\,(M_1 + \frac{m}{2})\,\dot{y}_1^2 + \frac{m}{2}\,(\dot{y}_2^2 + \dot{y}_3^2 + \ldots + \dot{y}_{10}^2)$$

$$+ \frac{1}{2}\,(M_2 + \frac{m}{2})\,\dot{y}_{11}^2 + \frac{1}{2}\,I_2\,\dot{\theta}_2^2$$

By Lagrange's method, the equations of motion are

$$I_1\,\ddot{\theta}_1 - R_1\,S_{1,2}\left[\frac{y_2 - y_1}{a - R_1} - \frac{R_1}{a - R_1}\,\theta_1\right] = 0$$

$$(M_1 + \frac{m}{2})\ \ddot{y}_1 - S_{1,2}\left[\frac{y_2 - y_1}{a - R_1} - \frac{R_1}{a - R_1}\ \theta_1\right] = 0$$

$$m\ddot{y}_2 + S_{1,2}\left[\frac{y_2 - y_1}{a - R_1} - \frac{R_1}{a - R_1}\ \theta_1\right] - S_{2,3}\ \frac{y_3 - y_2}{a} = 0$$

$$m\ddot{y}_3 + S_{2,3}\ \frac{y_3 - y_2}{a} - S_{3,4}\ \frac{y_4 - y_3}{a} = 0$$

. . . .

. . . .

$$m\ddot{y}_{10} + S_{9,10}\ \frac{y_{10} - y_9}{a} - S_{10,11}\left[\frac{y_{11} - y_{10}}{a - R_2} - \frac{R_2}{a - R_2}\ \theta_2\right] = 0$$

$$(M_2 + \frac{m}{2})\ \ddot{y}_{11} + S_{10,11}\left[\frac{y_{11} - y_{10}}{a - R_2} - \frac{R_2}{a - R_2}\ \theta_2\right] = 0$$

$$I_2\ \ddot{\theta}_2 - R_2\, S_{10,11}\left[\frac{y_{11} - y_{10}}{a - R_2} - \frac{R_2}{a - R_2}\ \theta_2\right] = 0$$

If the compartment and counterweight are considered as point masses, I_1, I_2, R_1, and R_2 vanish from the above equations. Let the solutions of the above equations be

$$y_i = \lambda_i \sin (pt + \alpha)$$

$$\theta_1 = \Theta_1 \sin (pt + \alpha)$$

$$\theta_2 = \Theta_2 \sin (pt + \alpha)$$

and use the notations

$$b_{11} = \frac{S_{1,2}}{I_1 (a - R_1)} , \qquad b_{12} = \frac{S_{1,2}}{(M_1 + \frac{m}{2}) (a - R_1)} ,$$

$$\beta_1 = \frac{S_{1,2}}{m (a - R_1)} , \qquad \beta_2 = \frac{S_{2,3}}{m a} ,$$

$$\beta_3 = \frac{S_{3,4}}{m a} , \; . \; . \; . \; . \; . \; \beta_9 = \frac{S_{9,10}}{m a} ,$$

$$\beta_{10} = \frac{S_{10,11}}{m (a - R_2)} ,$$

$$b_{21} = \frac{S_{10,11}}{I_2 (a - R_2)} , \qquad b_{22} = \frac{S_{10,11}}{(M_2 + \frac{m}{2}) (a - R_2)}$$

Substituting into the equations of motion, the frequency equation will assume the form

$$\begin{array}{c}
\begin{array}{ccccccccc}
\Theta_1 & \lambda_1 & \lambda_2 & \lambda_3 & & & \lambda_{10} & \lambda_{11} & \Theta_2
\end{array} \\
\left| \begin{array}{ccccccccc}
(-p^2 + R_1^2 b_{11}) & R_1 b_{11} & -R_1 b_{11} & & & & & & \\
R_1 b_{12} & (-p^2 + b_{12}) & -b_{12} & & & & & & \\
-R_1 \beta_1 & -\beta_1 & (-p^2 + \beta_1 + \beta_2) & \beta_2 & & & & & \\
 & & -\beta_2 & (-p^2 + \beta_2 + \beta_3) & -\beta_3 & & & & \\
 & & & & -\beta_8 & (-p^2 + \beta_8 + \beta_9) & -\beta_9 & & \\
 & & & & & -\beta_9 & (-p^2 + \beta_9 + \beta_{10}) & -\beta_{10} & R_2 \beta_{10} \\
 & & & & & & -b_{22} & (-p^2 + b_{22}) & -R_2 b_{22} \\
 & & & & & & R_2 b_{21} & -R_2 b_{21} & (-p^2 + R_2^2 b_{21})
\end{array} \right| = 0
\end{array}$$

From the above equation, the values of p_1 through p_{11} may be solved; for each p_i there is a corresponding set of λ_1 through λ_{11}.

6.2.1.3 Torsional Vibration (Figure 22)

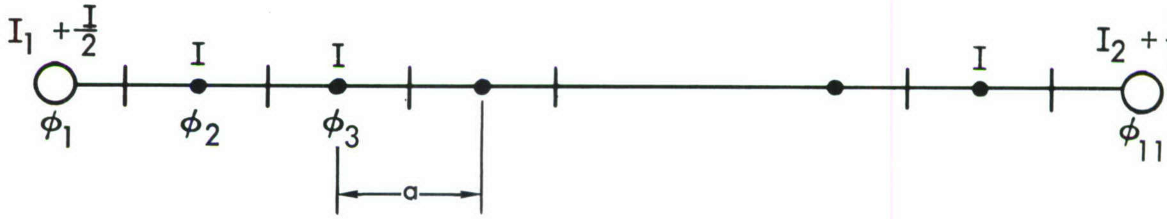

Figure 22. Torsional Vibration of Cable

If ϕ_1 through ϕ_{11} are the angles of twist at each mass point, and k is the torsional rigidity of each segment of cable, then the torsional moments for segments 1-2, 2-3, etc., are

$$k(\phi_2 - \phi_1), \quad k(\phi_3 - \phi_2), \quad \ldots \quad k(\phi_{11} - \phi_{10})$$

If the moment of inertia of M_1, M_2, and m is denoted by I_1, I_2, and I, respectively, the expressions for T and V will be

$$T = \frac{1}{2}\left[(I_1 + \frac{I}{2})\,\dot{\phi}_1^2 + I\,(\dot{\phi}_2^2 + \dot{\phi}_3^3 + \ldots + \dot{\phi}_{10}^2) + (I_2 + \frac{I}{2})\,\dot{\phi}_{11}^2\right]$$

$$V = \frac{k}{2}\left[(\phi_2 - \phi_1)^2 + (\phi_3 - \phi_2)^2 + \ldots + (\phi_{11} - \phi_{10})^2\right]$$

The equations of motion are

$$\left(I_1 + \frac{I}{2}\right) \ddot{\phi}_1 + k\,(\phi_1 - \phi_2) = 0$$

$$I\,\ddot{\phi}_2 - k\,(\phi_1 - \phi_2) + k\,(\phi_2 - \phi_3) = 0$$

$$I\,\ddot{\phi}_3 - k\,(\phi_2 - \phi_3) + k\,(\phi_3 - \phi_4) = 0$$

$$\cdots\cdots\cdots$$

$$\left(I_2 + \frac{I}{2}\right) \ddot{\phi}_{11} - k\,(\phi_{10} - \phi_{11}) = 0$$

Let the solutions of the above equations be

$$\phi_i = \lambda_i \sin\,(pt + \alpha)$$

$$\ddot{\phi}_i = -\,\lambda_i\, p^2 \sin\,(pt + \alpha)$$

where

$$i = 1, 2, \ldots, 11$$

and use the notations

$$\beta_1 = \frac{k}{I_1 + \frac{I}{2}}\,, \qquad \beta_2 = \frac{k}{I} \qquad \text{and } \beta_3 = \frac{k}{I_2 + \frac{I}{2}}$$

the frequency equation can be expressed as

$$\begin{array}{c}
\begin{array}{cccccc} \lambda_1 & \lambda_2 & \lambda_3 & & \lambda_{10} & \lambda_{11} \end{array} \\
\left|\begin{array}{cccccc}
(p^2 - \beta_1) & \beta_1 & & & & \\
\beta_2 & (p^2 - 2\beta_2) & \beta_2 & & & \\
 & \beta_2 & (p^2 - 2\beta_2) & \beta_2 & & \\
 & & \cdots\cdots & & & \\
 & & \cdots\cdots & \beta_2 & (p^2 - 2\beta_2) & \beta_2 \\
 & & & & \beta_3 & (p^2 - \beta_3)
\end{array}\right| = 0
\end{array}$$

6.2.1.4 Vibration Modes

The natural frequencies of the system can be determined from the frequency equations. For each frequency, a corresponding mode can be computed. Following this procedure, the vibratory motion of the cable system is obtained without the investigation of partial differential equations. For the compartment-cable-counterweight configuration, the cable is lumped into 50 equal parts. The lowest five natural frequencies, and their corresponding modes of longitudinal, lateral, torsional, and modified-lateral vibration, including end rotations, are shown in Figures 29 through 32, at the end of this section.

6.2.2 Multiple Cable-Connected Configuration

6.2.2.1 Frequency Equation

The space station that consists of two compartments connected by multiple cables (Configuration 6-A) is described in Figure 23. In analyzing the free vibration of this configuration, the mass of the cables is not considered; however, the extensional rigidity of the cables is considered. The two compartments (A and B) are lumped into a multi-mass system, and the transfer matrices of all the masses are computed by the equations given in Section 6.3. The transfer matrices of each complete compartment are computed by successive multiplication of those matrices at each mass, and are denoted by A_{ij} and B_{ij}, respectively.

If the displacements at the terminals of the cables are v_o^a, v_n^a, v_o^b, v_n^b, and y^c in the y-direction, and $-w_o^a$, $-w_n^a$, $-w_o^b$, $-w_n^b$, $-w_n^b$, and x^c in the x-direction, then the components of the cable tensions are

$$F_{Aox} = \frac{AE}{L}\,\frac{a}{L}\left[\frac{a}{L}\,(-w_o^a - x^c) + \frac{b}{L}\,(v_o^a - y^c)\right]$$

$$F_{Aoy} = \frac{AE}{L}\,\frac{b}{L}\left[\frac{a}{L}\,(-w_o^a - x^c) + \frac{b}{L}\,(v_o^a - y^c)\right]$$

$$F_{Anx} = \frac{AE}{L}\,\frac{a}{L}\left[\frac{a}{L}\,(-w_n^a - x^c) - \frac{b}{L}\,(v_n^a - y^c)\right]$$

$$F_{Any} = \frac{AE}{L}\left(-\frac{b}{L}\right)\left[\frac{a}{L}\,(-w_n^a - x^c) - \frac{b}{L}\,(v_n^a - y^c)\right]$$

$$F_{Box} = \frac{AE}{L}\left(-\frac{a}{L}\right)\left[\left(-\frac{a}{L}\right)(-w_o^b - x^c) + \frac{b}{L}\,(v_o^b - y^c)\right] \qquad (53)$$

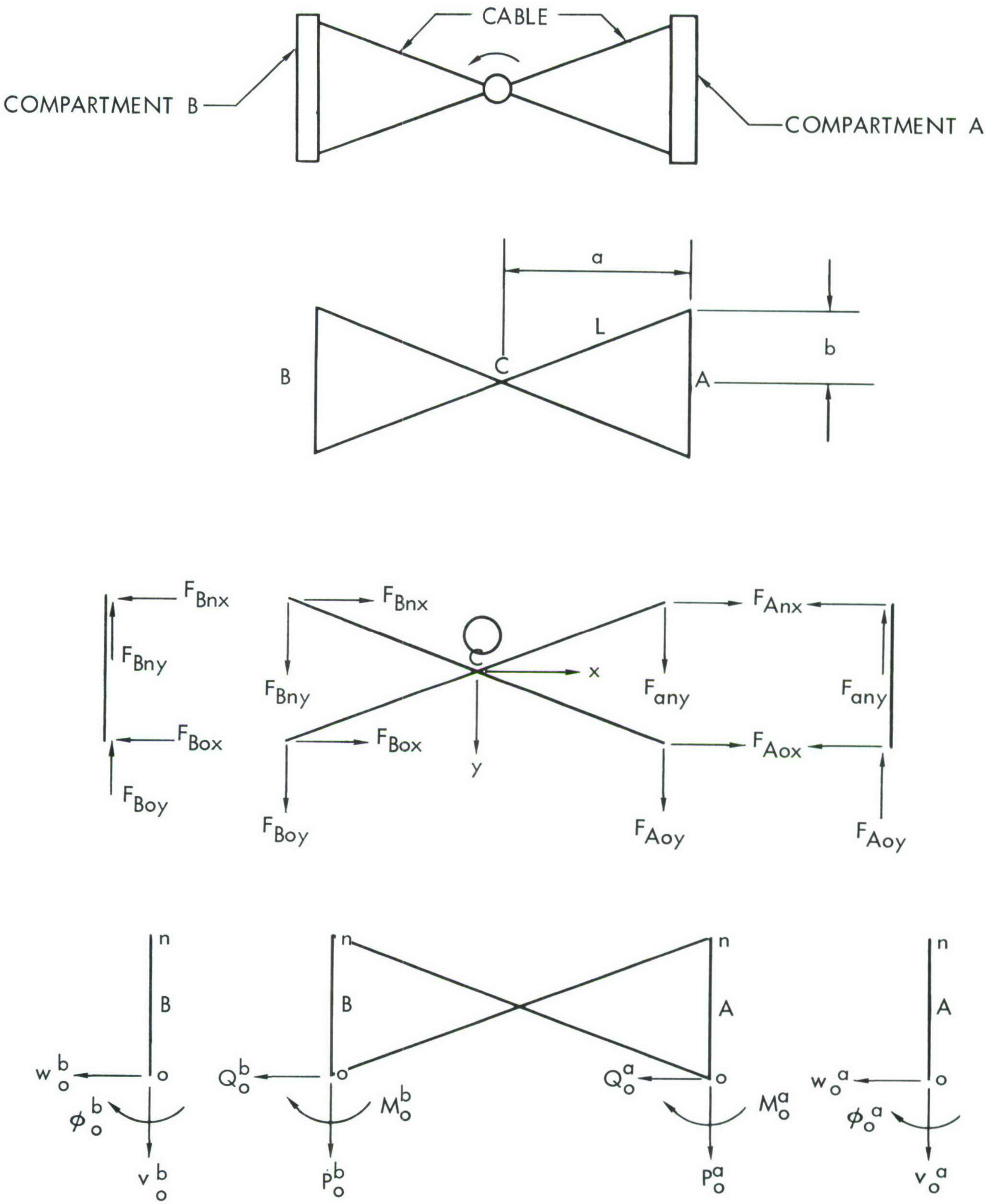

Figure 23. Configuration 6-A

$$F_{Boy} = \frac{AE}{L} \frac{b}{L} \left[(-\frac{a}{L})(-w_o^{\ b} - x^c) + \frac{b}{L}(v_o^{\ b} - y^c)\right]$$

$$F_{Bnx} = \frac{AE}{L}(-\frac{a}{L}) \left[-\frac{a}{L}(-w_n^{\ b} - x^c) - \frac{b}{L}(v_n^{\ b} - y^c)\right]$$

$$F_{Bny} = \frac{AE}{L}(-\frac{b}{L}) \left[-\frac{a}{L}(-w_n^{\ b} - x^c) - \frac{b}{L}(v_n^{\ b} - y^c)\right]$$

Using the notations

$$k_1 = AE\frac{a^2}{L^3}, \quad k_2 = AE\frac{ab}{L^3}, \quad \text{and } k_3 = AE\frac{b^2}{L^3} \tag{54}$$

the load vectors at A_o and B_o are

$$\begin{aligned}
Q_o^{\ a} &= F_{Aox} = -k_1 w_o^{\ a} + k_2 v_o^{\ a} - k_1 x^c - k_2 y^c \\
P_o^{\ a} &= F_{Aoy} = k_2 w_o^{\ a} - k_3 v_o^{\ a} + k_2 x^c + k_3 y^c \\
Q_o^{\ b} &= F_{Box} = -k_1 w_o^{\ b} - k_2 v_o^{\ b} - k_1 x^c + k_2 y^c \\
P_o^{\ b} &= F_{Boy} = -k_2 w_o^{\ b} - k_3 v_o^{\ b} - k_2 x^c + k_3 y^c \\
M_o^{\ a} &= M_o^{\ b} = 0
\end{aligned} \tag{55}$$

The state vectors at A_n and B_n may be expressed by transfer matrices as

$$
\begin{bmatrix} w_n^{\,a} \\ v_n^{\,a} \\ \phi_n^{\,a} \\ Q_n^{\,a} \\ P_n^{\,a} \\ M_n^{\,a} = 0 \end{bmatrix}
= \left[A\right]
\begin{bmatrix} w_o^{\,a} \\ v_o^{\,a} \\ \phi_o^{\,a} \\ Q_o^{\,a} \\ P_o^{\,a} \\ M_o^{\,a} = 0 \end{bmatrix}
= \left[A\right]
\begin{bmatrix} 1 & 0 & 0 & 0 & 0 \\ 0 & 1 & 0 & 0 & 0 \\ 0 & 0 & 1 & 0 & 0 \\ -k_1 & k_2 & 0 & -k_1 & -k_2 \\ k_2 & -k_3 & 0 & k_2 & k_3 \\ 0 & 0 & 0 & 0 & 0 \end{bmatrix}
\begin{bmatrix} w_o^{\,a} \\ v_o^{\,a} \\ \phi_o^{\,a} \\ x^c \\ y^c \end{bmatrix}
\tag{56}
$$

and

$$
\begin{bmatrix} w_n^{\,b} \\ v_n^{\,b} \\ \phi_n^{\,b} \\ Q_n^{\,b} \\ P_n^{\,b} \\ M_n^{\,b} = 0 \end{bmatrix}
= \left[B\right]
\begin{bmatrix} w_o^{\,b} \\ v_o^{\,b} \\ \phi_n^{\,b} \\ Q_o^{\,b} \\ P_o^{\,b} \\ M_o^{\,b} = 0 \end{bmatrix}
= \left[B\right]
\begin{bmatrix} 1 & 0 & 0 & 0 & 0 \\ 0 & 1 & 0 & 0 & 0 \\ 0 & 0 & 1 & 0 & 0 \\ -k_1 & -k_2 & 0 & -k_1 & k_2 \\ -k_2 & -k_3 & 0 & -k_2 & k_3 \\ 0 & 0 & 0 & 0 & 0 \end{bmatrix}
\begin{bmatrix} w_o^{\,b} \\ v_o^{\,b} \\ \phi_o^{\,b} \\ x^c \\ y^c \end{bmatrix}
\tag{57}
$$

Equations (56) and (57) may be rewritten as

$$
\left\{ w_n^{\,a},\ v_n^{\,a},\ \phi_n^{\,a},\ Q_n^{\,a},\ P_n^{\,a},\ M_n^{\,a} \right\} = \left[E\right] \left\{ w_o^{\,a},\ v_o^{\,a},\ \phi_o^{\,a},\ x^c,\ y^c \right\} \tag{58}
$$

and

$$
\left\{ w_n^{\,b},\ v_n^{\,b},\ \phi_n^{\,b},\ Q_n^{\,b},\ P_n^{\,b},\ M_n^{\,b} \right\} = \left[F\right] \left\{ w_o^{\,b},\ v_o^{\,b},\ \phi_o^{\,b},\ x^c,\ y^c \right\} \tag{59}
$$

Equilibrium conditions at the n-end of compartment A yield the equations

$$
\begin{aligned}
Q_n^{\ a} + F_{Anx} &= Q_n^{\ a} - k_1 w_n^{\ a} - k_2 v_n^{\ a} - k_1 x^c + k_2 y^c = 0 \\
P_n^{\ a} - F_{Any} &= P_n^{\ a} - k_2 w_n^{\ a} - k_3 v_n^{\ a} - k_2 x^c + k_3 y^c = 0 \qquad (60) \\
M_n^{\ a} &= 0
\end{aligned}
$$

Similarly, equilibrium conditions at the n-end of compartment B, yield the equations

$$
\begin{aligned}
Q_n^{\ b} + F_{Bnx} &= Q_n^{\ b} - k_1 w_n^{\ b} + k_2 v_n^{\ b} - k_1 x^c - k_2 y^c = 0 \\
P_n^{\ b} - F_{Bny} &= P_n^{\ b} + k_2 w_n^{\ b} - k_3 v_n^{\ b} + k_2 x^c + k_3 y^c = 0 \qquad (61) \\
M_n^{\ b} &= 0
\end{aligned}
$$

Equations (60) and (61) may be expressed in matrix form as

$$
\begin{bmatrix} 0 \\ 0 \\ 0 \end{bmatrix} = \underbrace{\begin{bmatrix} -k_1 & -k_2 & 0 & 1 & 0 & 0 & -k_1 & k_2 \\ -k_2 & -k_3 & 0 & 0 & 1 & 0 & -k_2 & k_3 \\ 0 & 0 & 0 & 0 & 0 & 1 & 0 & 0 \end{bmatrix}}_{\left[K_{an}\right]} \begin{bmatrix} w_n^{\ a} \\ v_n^{\ a} \\ \phi_n^{\ a} \\ Q_n^{\ a} \\ P_n^{\ a} \\ M_n^{\ a} \\ x^c \\ y^c \end{bmatrix}
$$

$$
= \left[K_{an}\right] \left[\begin{array}{ccc} & \mathbf{E} & \\ & (6\text{x}5) & \\ \hline & & \begin{array}{cc} 1 & 0 \\ 0 & 1 \end{array} \end{array}\right] \begin{bmatrix} w_o^a \\ v_o^a \\ \phi_o^a \\ x^c \\ y^c \end{bmatrix} = \left[G\right] \begin{bmatrix} w_o^a \\ v_o^a \\ \phi_o^a \\ x^c \\ y^c \end{bmatrix} \tag{62}
$$

and

$$
\begin{bmatrix} 0 \\ 0 \\ 0 \end{bmatrix} = \underbrace{\begin{bmatrix} -k_1 & k_2 & 0 & 1 & 0 & 0 & -k_1 & -k_2 \\ k_2 & -k_3 & 0 & 0 & 1 & 0 & k_2 & k_3 \\ 0 & 0 & 0 & 0 & 0 & 1 & 0 & 0 \end{bmatrix}}_{\left[K_{bn}\right]} \begin{bmatrix} w_n^b \\ v_n^b \\ \phi_n^b \\ Q_n^b \\ P_n^b \\ M_n^b \\ x^c \\ y^c \end{bmatrix}
$$

$$= \left[K_{bn}\right] \left[\begin{array}{ccc} & F & \\ \hline & 1 & 0 \\ & 0 & 1 \end{array}\right] \begin{bmatrix} w_o^b \\ v_o^b \\ \phi_o^b \\ x^c \\ y^c \end{bmatrix} = \left[H\right] \begin{bmatrix} w_o^b \\ v_o^b \\ \phi_o^b \\ x^c \\ y^c \end{bmatrix} \tag{63}$$

If the mass of the central hub is denoted by M^H, the inertial forces at the hub are $M^H \omega^2 x^c$, and $M^H \omega^2 y^c$. By considering the cables and the hub as a free body, the summation of forces in the x and y directions are zero. Thus,

$$-k_1 \left(w_o^a + w_n^a + w_o^b + w_n^b\right) + k_2 \left(v_o^a - v_o^b - v_n^a + v_n^b\right)$$

$$-4 k_1 x^c + M^H x^c \omega^2 = 0 \tag{64}$$

$$k_2 \left(-w_o^a + w_o^b + w_n^a - w_n^b\right) + k_3 \left(v_o^a + v_o^b + v_n^a + v_n^b\right)$$

$$-4 k_3 y^c + M^H y^c \omega^2 = 0 \tag{65}$$

If the extensional deformations of the compartments are assumed to be small in comparison with the remaining elastic deformations, then $v_o^a = v_n^a$, and $v_o^b = v_n^b$. By introducing the transfer matrices in equations (58) and (59), the two preceding equations become

$$k_1 (1 + E_{11}) w_o^a + k_1 E_{12} v_o^a + k_1 E_{13} \phi_o^a + k_1 (1 + F_{11}) w_o^b$$

$$+k_1 F_{12} v_o^b + k_1 F_{13} \phi_o^b + \left(4 k_1 + k_1 E_{14} + k_1 F_{14}\right.$$

$$\left.-M^H \omega^2\right) x^c + k_1 (E_{15} + F_{15}) y^c = 0 \tag{66}$$

$$
\begin{aligned}
&k_2 (-1 + E_{11}) w_o^{\,a} + (k_2 E_{12} + 2k_3) v_o^{\,a} + (k_2 E_{13}) \phi_o^{\,a} \\
&+ k_2 (1 - F_{11}) w_o^{\,b} + (-k_2 F_{12} + 2k_3) v_o^{\,b} - k_2 F_{13} \phi_o^{\,b} \\
&+ (k_2 E_{14} - k_2 F_{14}) x^c + \Big(k_2 E_{15} - k_2 F_{15} - 4k_3 \\
&+ M^H \omega^2 \Big) y^c = 0
\end{aligned}
\tag{67}
$$

Equations (62), (63), (66), and (67) may be combined to become Equation (68). This is the characteristic equation from which the natural frequencies can be computed.

$$
\begin{bmatrix}
G_{11} & G_{12} & G_{13} & 0 & 0 & 0 & G_{14} & G_{15} \\
G_{21} & G_{22} & G_{23} & 0 & 0 & 0 & G_{24} & G_{25} \\
G_{31} & G_{32} & G_{33} & 0 & 0 & 0 & G_{34} & G_{35} \\
0 & 0 & 0 & H_{11} & H_{12} & H_{13} & H_{14} & H_{15} \\
0 & 0 & 0 & H_{21} & H_{22} & H_{23} & H_{24} & H_{25} \\
0 & 0 & 0 & H_{31} & H_{32} & H_{33} & H_{34} & H_{35} \\
\begin{matrix} k_1 E_{11} \\ +k_1 \end{matrix} & k_1 E_{12} & k_1 E_{13} & \begin{matrix} k_1 F_{11} \\ +k_1 \end{matrix} & k_1 F_{12} & k_1 F_{13} & \begin{matrix} k_1 E_{14} \\ +k_1 F_{14} \\ +4 k_1 \\ -M^H \omega^2 \end{matrix} & \begin{matrix} k_1 E_{15} \\ +k_1 F_{15} \end{matrix} \\
\begin{matrix} k_2 E_{11} \\ -k_2 \end{matrix} & \begin{matrix} k_2 E_{12} \\ +2 k_3 \end{matrix} & k_2 E_{13} & \begin{matrix} -k_2 F_{11} \\ +k_2 \end{matrix} & \begin{matrix} -k_2 F_{12} \\ +2k_3 \end{matrix} & -k_2 F_{13} & \begin{matrix} k_2 E_{14} \\ -k_2 F_{14} \end{matrix} & \begin{matrix} k_2 E_{15} \\ -k_2 F_{15} \\ -4 k_3 \\ +M^H \omega^2 \end{matrix}
\end{bmatrix}
\begin{bmatrix}
w_o^a \\ v_o^a \\ \phi_o^a \\ w_o^b \\ v_o^b \\ \phi_o^b \\ x^c \\ y^c
\end{bmatrix}
= 0
\tag{68}
$$

6.2.2.2 Vibration Modes

The equations of free vibration of Configuration 6-A were programmed on the IBM 7094. The natural frequencies and the corresponding modes were calculated and are plotted in Figures 33 through 35. These figures show that in the third and fourth modes a translational displacement of the hub occurs.

6.3 VIBRATION OF COMPRESSION-MEMBER-CONNECTED SPACE STATIONS

The vibrations of the space station configurations under consideration may be divided into two classes, which are practically independent of each other: (1) vibration in the plane of the configuration which contains the central axes of all the compartments and spokes and (2) vibration normal to the plane of the configuration involving both flexural displacement and twist. In the following analysis, the space stations are idealized by mathematical

models of multiple-mass systems. The solution of the problem is obtained by using transfer matrices that consist of arrays of coefficients that relate conditions of load (moment and torque) and deformation (longitudinal and lateral translation, rotation and twist) across an element of the system. The effects of rotary inertia and shear deformation are included in the consideration.

For in-plane vibration, the transfer equation at each lumped mass may be expressed by

$$\{w,\ v,\ \phi,\ Q,\ P,\ M_I\}_{i+1} = [R_I]\ \{w,\ v,\ \phi,\ Q,\ P,\ M_I\}_i$$

where, Q, P, and M_I are respectively transverse force, longitudinal force, and moment, and w, v, and ϕ are displacements and rotation in the direction of Q, P, and M.

Similar equations for vibration normal to the plane at each lumped mass can be written as

$$\{u,\ \theta,\ \psi,\ F,\ M_N,\ T\}_{i+1} = [R_N]\ \{u,\ \theta,\ \psi,\ F,\ M_N,\ T\}_i$$

where F, M_N, and T are force normal to plane, moment and torque, and u, θ, and ψ are displacement and rotations in the direction of F, M_N, and T, respectively.

R_I and R_N are transfer matrices for the i-th element, which is a point mass and rotary inertia equivalent to the inertias of the adjoining half-segments. R_I and R_N are derived by the energy method (also known as Castigliano's Theorem) and lead to the following results:

$$[R_I] = \begin{array}{c} \begin{array}{cccccc} \quad w \quad & \quad v \quad & \quad \phi \quad & \quad Q \quad & \quad P \quad & \quad M \quad \end{array} \\ \left[\begin{array}{cccccc} 1 + m_i\,\omega^2\left(\dfrac{\ell_i^3}{6EI_{yi}} - \dfrac{\ell}{KGA_i}\right) & 0 & -\ell_i + I_{myi}\,\omega^2\,\dfrac{\ell_i^2}{2EI_{yi}} & \dfrac{\ell_i^3}{6EI_{yi}} - \dfrac{\ell_i}{KGA_i} & 0 & \dfrac{\ell_i^2}{2EI_{yi}} \\ 0 & 1 & 0 & 0 & 0 & 0 \\ -m_i\,\omega^2\,\dfrac{\ell_i^2}{2EI_{yi}} & 0 & 1 - I_{myi}\,\omega^2\,\dfrac{\ell_i}{EI_{yi}} & -\dfrac{\ell_i^2}{2EI_{yi}} & 0 & -\dfrac{\ell_i}{EI_{yi}} \\ m_i\,\omega^2 & 0 & 0 & 1 & 0 & 0 \\ 0 & m_i\,\omega^2 & 0 & 0 & 1 & 0 \\ m_i\,\omega^2\,\ell_i & 0 & I_{myi}\,\omega^2 & \ell_i & 0 & 1 \end{array}\right] \end{array}$$

$$
\begin{array}{c}
\begin{matrix} \quad u \quad & \quad \theta \quad & \quad \psi \quad & \quad F \quad & \quad M \quad & \quad T \quad \end{matrix} \\
[R_N] = \begin{bmatrix}
1 + m_i\,\omega^2\left(\frac{\ell_i^3}{6EI_{xi}} - \frac{\ell_i}{KGA_i}\right) & -\ell_i + I_{mxi}\,\omega^2\,\frac{\ell_i^2}{2EI_{xi}} & 0 & \frac{\ell_i^3}{6EI_{xi}} - \frac{\ell_i}{KGA_i} & \frac{\ell_i^2}{2EI_{xi}} & 0 \\
-m_i\,\omega^2\,\frac{\ell_i^2}{2EI_{xi}} & 1 - I_{mxi}\,\omega^2\,\frac{\ell_i}{EI_{xi}} & 0 & -\frac{\ell_i^2}{2EI_{xi}} & -\frac{\ell_i}{EI_{xi}} & 0 \\
0 & 0 & 1 - I_{mzi}\,\omega^2\,\frac{\ell_i}{GC_i} & 0 & 0 & -\frac{\ell_i}{GC_i} \\
m_i\,\omega^2 & 0 & 0 & 1 & 0 & 0 \\
m_i\,\omega^2\,\ell_i & I_{mxi}\,\omega^2 & 0 & \ell_i & 1 & 0 \\
0 & 0 & I_{mzi}\,\omega^2 & 0 & 0 & 1
\end{bmatrix}
\end{array}
$$

The transfer matrices of the compartment or a section of the space station are obtained by successive multiplication of transfer matrices at each lumped mass. The frequency equations for in-plane and normal-to-plane vibrations are formed from boundary conditions.

6.3.1 Configuration 7-A

The two-compartment space station is idealized and divided into sections a, b, d, and e as shown in Figure 24. Let the transfer matrix of each section be denoted by A_{ij}, B_{ij}, D_{ij} and E_{ij} which are computed by successive multiplication of transfer matrices of lumped masses in each section. From the boundary conditions at the joint of intersection of sections a, d, and e, we have for in-plane vibration

$$
\begin{aligned}
w_o^e &= w_n^d = -v_o^a \\
v_o^e &= v_n^d = w_o^a \\
\phi_o^e &= \phi_n^d = \phi_o^a \\
Q_o^e &= Q_n^d + P_o^a \\
P_o^e &= P_n^d - Q_o^a \\
M_o^e &= M_n^d - M_o^a
\end{aligned}
\qquad (69)
$$

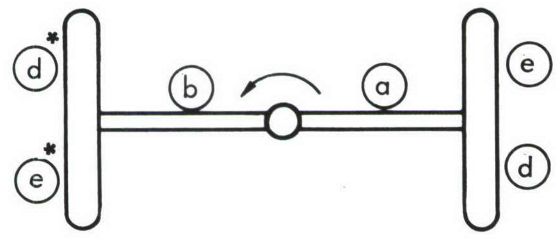

a. TWO-COMPARTMENT SPACE STATION

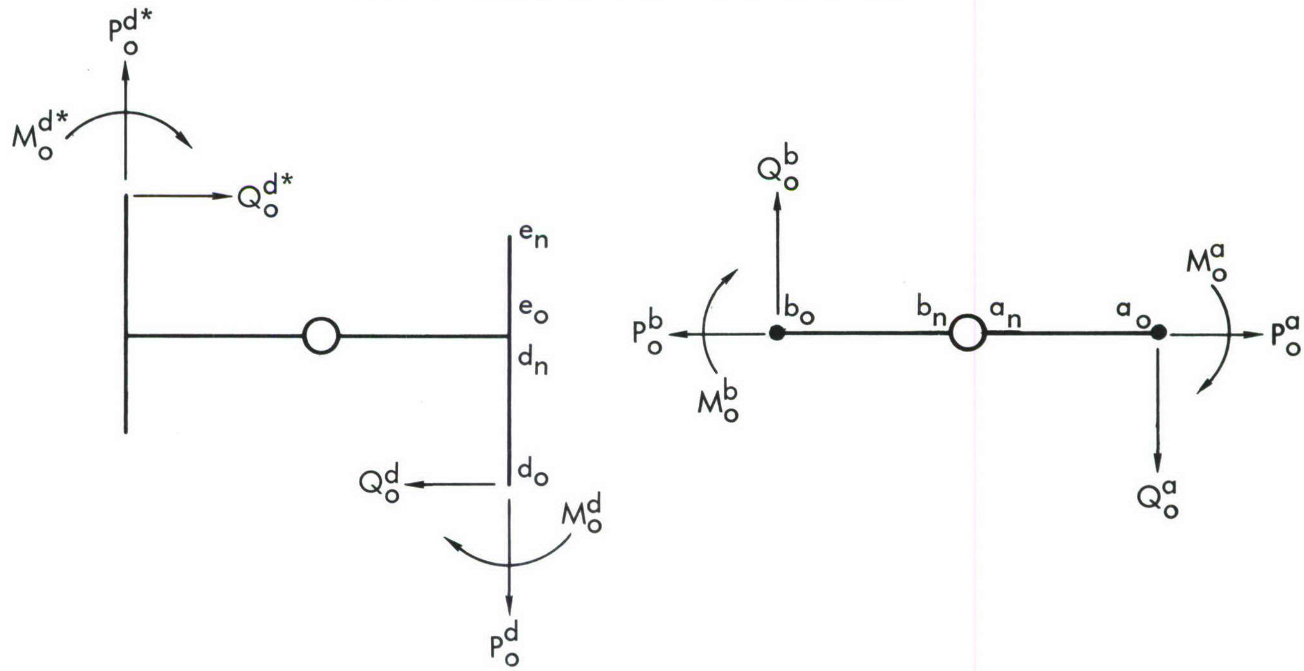

b. IN-PLANE VIBRATION

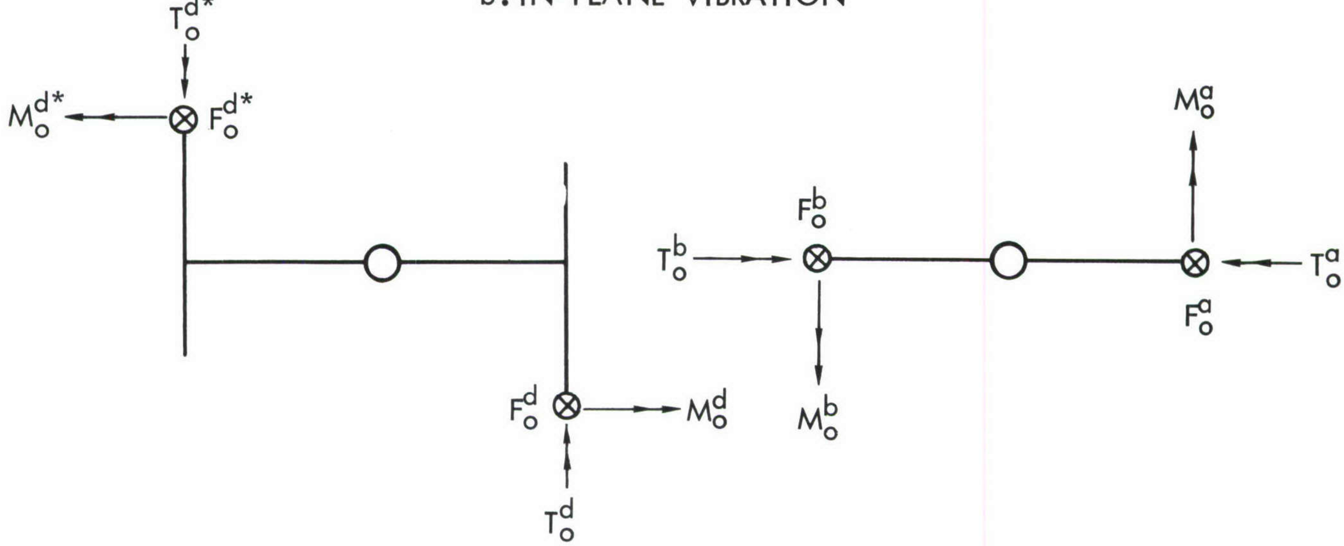

c. NORMAL-TO-PLANE VIBRATION

Figure 24. Configuration 7-A

Therefore

$$\begin{bmatrix} w \\ v \\ \phi \\ Q \\ P \\ M \end{bmatrix}_n^e = [E] \begin{bmatrix} w \\ v \\ \phi \\ Q \\ P \\ M \end{bmatrix}_o^e = [E]\,[D] \begin{bmatrix} w \\ v \\ \phi \\ 0 \\ 0 \\ 0 \end{bmatrix}_o^d + [E] \begin{bmatrix} 0 \\ 0 \\ 0 \\ P \\ -Q \\ -M \end{bmatrix}_o^a$$

Since $Q_n^e = P_n^e = M_n^e = 0$, by introducing $[F] = [E]\,[D]$

$$\begin{bmatrix} 0 \\ 0 \\ 0 \end{bmatrix} = \begin{bmatrix} F_{41} & F_{42} & F_{43} \\ F_{51} & F_{52} & F_{53} \\ F_{61} & F_{62} & F_{63} \end{bmatrix} \begin{bmatrix} w \\ v \\ \phi \end{bmatrix}_0^d + \begin{bmatrix} -E_{45} & E_{44} & -E_{46} \\ -E_{55} & E_{54} & -E_{56} \\ -E_{65} & E_{64} & -E_{66} \end{bmatrix} \begin{bmatrix} Q \\ P \\ M \end{bmatrix}_o^a$$

If the preceding equation is written as

$$[S] \begin{bmatrix} w \\ v \\ \phi \end{bmatrix}_o^d + [T] \begin{bmatrix} Q \\ P \\ M \end{bmatrix}_o^a = \{0\}$$

then

$$\begin{bmatrix} Q \\ P \\ M \end{bmatrix}_o^a = -\,[T]^{-1}\,[S] \begin{bmatrix} w \\ v \\ \phi \end{bmatrix}_o^d = -\,[U] \begin{bmatrix} w \\ v \\ \phi \end{bmatrix}_o^d$$

where $[U] = [T]^{-1} [S]$. Similarly, for spoke b,

$$\begin{bmatrix} Q \\ P \\ M \end{bmatrix}_o^b = - [U] \begin{bmatrix} w \\ v \\ \phi \end{bmatrix}_o^{d*}$$

By combining the load vectors at a_o and b_o

$$\begin{bmatrix} \begin{Bmatrix} Q \\ P \\ M \end{Bmatrix}_o^a \\ \begin{Bmatrix} Q \\ P \\ M \end{Bmatrix}_o^b \end{bmatrix} = \begin{bmatrix} -U & O \\ O & -U \end{bmatrix} \begin{bmatrix} \begin{Bmatrix} w \\ v \\ \phi \end{Bmatrix}_o^d \\ \begin{Bmatrix} w \\ v \\ \phi \end{Bmatrix}_o^{d*} \end{bmatrix} \tag{70}$$

From equation (69)

$$\begin{bmatrix} w \\ v \\ \phi \end{bmatrix}_o^a = \begin{bmatrix} v \\ -w \\ \phi \end{bmatrix}_n^d = \begin{bmatrix} D_{21} & D_{22} & D_{23} \\ -D_{11} & -D_{12} & -D_{13} \\ D_{31} & D_{32} & D_{33} \end{bmatrix} \begin{bmatrix} w \\ v \\ \phi \end{bmatrix}_o^d = [V] \begin{bmatrix} w \\ v \\ \phi \end{bmatrix}_o^d$$

Similarly

$$\begin{bmatrix} w \\ v \\ \phi \end{bmatrix}_o^b = [V] \begin{bmatrix} w \\ v \\ \phi \end{bmatrix}_0^{d*}$$

Combining the preceding two equations

$$\begin{bmatrix} \begin{Bmatrix} w \\ v \\ \phi \end{Bmatrix}_o^a \\ \begin{Bmatrix} w \\ v \\ \phi \end{Bmatrix}_o^b \end{bmatrix} = \begin{bmatrix} V & O \\ O & V \end{bmatrix} \begin{bmatrix} \begin{Bmatrix} w \\ v \\ \phi \end{Bmatrix}_o^d \\ \begin{Bmatrix} w \\ v \\ \phi \end{Bmatrix}_o^{d*} \end{bmatrix} \tag{71}$$

From the condition of continuity at the intersection of spokes a and b

$$\begin{bmatrix} w \\ v \\ \phi \\ Q \\ P \\ M \end{bmatrix}_n^a + \begin{bmatrix} w \\ v \\ -\phi \\ -Q \\ -P \\ M \end{bmatrix}_n^b = [A] \begin{bmatrix} w \\ v \\ \phi \\ Q \\ P \\ M \end{bmatrix}_o^a + \begin{vmatrix} B_{1j} \\ B_{2j} \\ -B_{3j} \\ -B_{4j} \\ -B_{5j} \\ B_{6j} \end{vmatrix} \begin{vmatrix} w \\ v \\ \phi \\ Q \\ P \\ M \end{vmatrix}_o^b = \{0\}$$

The preceding equations may be rewritten as

$$\begin{bmatrix} \bar{A}_{11} & \bar{A}_{12} \\ \bar{A}_{21} & \bar{A}_{22} \end{bmatrix} \begin{bmatrix} \begin{Bmatrix} w \\ v \\ \phi \end{Bmatrix}_o^a \\ \begin{Bmatrix} Q \\ P \\ M \end{Bmatrix}_o^a \end{bmatrix} + \begin{bmatrix} \bar{B}_{11} & \bar{B}_{12} \\ \bar{B}_{21} & \bar{B}_{22} \end{bmatrix} \begin{bmatrix} \begin{Bmatrix} w \\ v \\ \phi \end{Bmatrix}_o^b \\ \begin{Bmatrix} Q \\ P \\ M \end{Bmatrix}_o^b \end{bmatrix} = \{0\}$$

which can be rearranged

$$\begin{bmatrix} \bar{A}_{11} & \bar{B}_{11} \\ \bar{A}_{21} & \bar{B}_{21} \end{bmatrix} \begin{bmatrix} \begin{Bmatrix} w \\ v \\ \phi \end{Bmatrix}_o^a \\ \begin{Bmatrix} w \\ v \\ \phi \end{Bmatrix}_o^b \end{bmatrix} + \begin{bmatrix} \bar{A}_{12} & \bar{B}_{12} \\ \bar{A}_{22} & \bar{B}_{22} \end{bmatrix} \begin{bmatrix} \begin{Bmatrix} Q \\ P \\ M \end{Bmatrix}_o^a \\ \begin{Bmatrix} Q \\ P \\ M \end{Bmatrix}_o^b \end{bmatrix} = \{0\}$$

By substituting equations (70) and (71) into the above equations.

$$\begin{bmatrix} \bar{A}_{11} & \bar{B}_{11} \\ \bar{A}_{21} & \bar{B}_{21} \end{bmatrix} \begin{bmatrix} V & 0 \\ 0 & V \end{bmatrix} \begin{bmatrix} \begin{Bmatrix} w \\ v \\ \phi \end{Bmatrix}_o^d \\ \begin{Bmatrix} w \\ v \\ \phi \end{Bmatrix}_o^{d*} \end{bmatrix} + \begin{bmatrix} \bar{A}_{12} & \bar{B}_{12} \\ \bar{A}_{22} & \bar{B}_{22} \end{bmatrix} \begin{bmatrix} -U & 0 \\ 0 & -U \end{bmatrix} \begin{bmatrix} \begin{Bmatrix} w \\ v \\ \phi \end{Bmatrix}_o^d \\ \begin{Bmatrix} w \\ v \\ \phi \end{Bmatrix}_o^{d*} \end{bmatrix} = 0 \qquad (72)$$

The preceding equation is the characteristic equation. The frequencies are computed from the condition that the determinant of the coefficients of the equation (the residue) must be zero.

For normal-to-plane vibration, the following equations are obtained at the intersection of sections a, d, and e

$$u_o^e = u_n^d = u_o^a$$

$$\theta_o^e = \theta_n^d = -\psi_o^a$$

$$\psi_o^e = \psi_n^d = \theta_o^a$$

$$F_o^e = F_n^d - F_o^a$$

$$M_o^e = M_n^d + T_o^a$$

$$T_o^e = T_n^d - M_o^a \tag{73}$$

therefore

$$\begin{bmatrix} u \\ \theta \\ \psi \\ F \\ M \\ T \end{bmatrix}_n^e = [E^N] \begin{bmatrix} u \\ \theta \\ \psi \\ F \\ M \\ T \end{bmatrix}_o^e = [E^N]\,[D^N] \begin{bmatrix} u \\ \theta \\ \psi \\ 0 \\ 0 \\ 0 \end{bmatrix}_o^d + [E^N] \begin{bmatrix} 0 \\ 0 \\ 0 \\ -F \\ T \\ -M \end{bmatrix}_o^a$$

Since $F_n^e = M_n^e = T_n^e = 0$, with the notation $[F^N] = [E^N]\,[D^N]$

$$\begin{bmatrix} F_{41} & F_{42} & F_{43} \\ F_{51} & F_{52} & F_{53} \\ F_{61} & F_{62} & F_{63} \end{bmatrix}^N \begin{bmatrix} u \\ \theta \\ \psi \end{bmatrix}_o^d + \begin{bmatrix} -E_{44} & -E_{46} & E_{45} \\ -E_{54} & -E_{56} & E_{55} \\ -E_{64} & -E_{66} & E_{65} \end{bmatrix}^N \begin{bmatrix} F \\ M \\ T \end{bmatrix}_o^a = \{0\}$$

The above equation may be written as

$$[S^N] \begin{bmatrix} u \\ \theta \\ \psi \end{bmatrix}_o^d + [T^N] \begin{bmatrix} F \\ M \\ T \end{bmatrix}_o^a = \{0\}$$

Thus,

$$\begin{bmatrix} F \\ M \\ T \end{bmatrix}_o^a = - [T^N]^{-1} [S^N] \begin{bmatrix} u \\ \theta \\ \psi \end{bmatrix}_o^d = - [U^N] \begin{bmatrix} u \\ \theta \\ \psi \end{bmatrix}_o^d$$

where $[U^N] = [T^N]^{-1} [S^N]$.

Similarly

$$\begin{bmatrix} F \\ M \\ T \end{bmatrix}_o^b = - [U^N] \begin{bmatrix} u \\ \theta \\ \psi \end{bmatrix}_o^{d*}$$

By combining the load vectors at a_o and b_o

$$\begin{bmatrix} \begin{Bmatrix} F \\ M \\ T \end{Bmatrix}_o^a \\ \begin{Bmatrix} F \\ M \\ T \end{Bmatrix}_o^b \end{bmatrix} = \begin{bmatrix} -U^N & O \\ O & -U^N \end{bmatrix} \begin{bmatrix} \begin{Bmatrix} u \\ \theta \\ \psi \end{Bmatrix}_o^d \\ \begin{Bmatrix} u \\ \theta \\ \psi \end{Bmatrix}_o^{d*} \end{bmatrix} \qquad (74)$$

From equation (73)

$$\begin{bmatrix} u \\ \theta \\ \psi \end{bmatrix}_o^a = \begin{bmatrix} u \\ \psi \\ -\theta \end{bmatrix}_n^d = \begin{bmatrix} D_{11} & D_{12} & D_{13} \\ D_{31} & D_{32} & D_{33} \\ -D_{21} & -D_{22} & -D_{23} \end{bmatrix}^N \begin{bmatrix} u \\ \theta \\ \psi \end{bmatrix}_o^d = [V^N] \begin{bmatrix} u \\ \theta \\ \psi \end{bmatrix}_o^d$$

Similarly

$$\begin{bmatrix} u \\ \theta \\ \psi \end{bmatrix}_o^b = [V^N] \begin{bmatrix} u \\ \theta \\ \psi \end{bmatrix}_o^{d*}$$

Combining the above two equations

$$\begin{bmatrix} \begin{Bmatrix} u \\ \theta \\ \psi \end{Bmatrix}_o^a \\ \begin{Bmatrix} u \\ \theta \\ \psi \end{Bmatrix}_o^b \end{bmatrix} = \begin{bmatrix} V^N & O \\ O & V^N \end{bmatrix} \begin{bmatrix} \begin{Bmatrix} u \\ \theta \\ \psi \end{Bmatrix}_o^d \\ \begin{Bmatrix} u \\ \theta \\ \psi \end{Bmatrix}_o^{d*} \end{bmatrix} \tag{75}$$

From the condition of continuity at the hub

$$\begin{bmatrix} u \\ \theta \\ \psi \\ F \\ M \\ T \end{bmatrix}_n^a + \begin{bmatrix} -u \\ \theta \\ \psi \\ F \\ -M \\ -T \end{bmatrix}_n^b = \left[A^N\right] \begin{bmatrix} u \\ \theta \\ \psi \\ F \\ M \\ T \end{bmatrix}_o^a + \begin{bmatrix} -B_{1j} \\ B_{2j} \\ B_{3j} \\ B_{4j} \\ -B_{5j} \\ -B_{6j} \end{bmatrix}^N \begin{bmatrix} u \\ \theta \\ \psi \\ F \\ M \\ T \end{bmatrix}_o^b = \{0\}$$

The above equation may be rewritten as

$$\begin{bmatrix} \overline{A}_{11} & \overline{A}_{12} \\ \overline{A}_{21} & \overline{A}_{22} \end{bmatrix}^N \begin{bmatrix} \begin{Bmatrix} u \\ \theta \\ \psi \end{Bmatrix}_o^a \\ \begin{Bmatrix} F \\ M \\ T \end{Bmatrix}_o^a \end{bmatrix} + \begin{bmatrix} \overline{B}_{11} & \overline{B}_{12} \\ \overline{B}_{21} & \overline{B}_{22} \end{bmatrix}^N \begin{bmatrix} \begin{Bmatrix} u \\ \theta \\ \psi \end{Bmatrix}_o^b \\ \begin{Bmatrix} F \\ M \\ T \end{Bmatrix}_o^b \end{bmatrix} = \{0\}$$

which may be rearranged as

$$\begin{bmatrix} \bar{A}_{11} & \bar{B}_{11} \\ \bar{A}_{21} & \bar{B}_{21} \end{bmatrix}^N \begin{bmatrix} \begin{Bmatrix} u \\ \theta \\ \psi \end{Bmatrix}_o^a \\ \begin{Bmatrix} u \\ \theta \\ \psi \end{Bmatrix}_o^b \end{bmatrix} + \begin{bmatrix} \bar{A}_{12} & \bar{B}_{12} \\ \bar{A}_{22} & \bar{B}_{22} \end{bmatrix}^N \begin{bmatrix} \begin{Bmatrix} F \\ M \\ T \end{Bmatrix}_o^a \\ \begin{Bmatrix} F \\ M \\ T \end{Bmatrix}_o^b \end{bmatrix} = \{0\}$$

By substituting equations (74) and (75) into the above equations

$$\begin{bmatrix} \bar{A}_{11} & \bar{B}_{11} \\ \bar{A}_{21} & \bar{B}_{21} \end{bmatrix}^N \begin{bmatrix} V^N & O \\ O & V^N \end{bmatrix} \begin{bmatrix} \begin{Bmatrix} u \\ \theta \\ \psi \end{Bmatrix}_o^d \\ \begin{Bmatrix} u \\ \theta \\ \psi \end{Bmatrix}_o^{d*} \end{bmatrix} + \begin{bmatrix} \bar{A}_{12} & \bar{B}_{12} \\ \bar{A}_{22} & \bar{B}_{22} \end{bmatrix}^N \begin{bmatrix} -U^N & O \\ O & -U^N \end{bmatrix} \begin{bmatrix} \begin{Bmatrix} u \\ \theta \\ \psi \end{Bmatrix}_o^d \\ \begin{Bmatrix} u \\ \theta \\ \psi \end{Bmatrix}_o^{d*} \end{bmatrix} = \{0\}$$

The preceding equation is the characteristic equation from which the frequencies of normal-to-plane vibration can be computed.

The natural frequencies for both in-plane and normal-to-plane vibration of Configuration 7-A with 5-foot diameter spokes are computed with the aid of the IBM-7094. The mode shapes corresponding to each frequency have been calculated and plotted in Figures 36 and 37. The mode shapes for the same configuration with 10-foot diameter spokes are shown in Figures 38 and 39. Figures 36 through 39 will be found at the end of this section.

6.3.2 Configuration Y-A

In analyzing the Y-A configuration, the space station is divided into sections a, b, c, d, and e as shown in Figure 25. The transfer matrix of each section is designated respectively as A_{ij}, B_{ij}, C_{ij}, D_{ij}, and E_{ij},

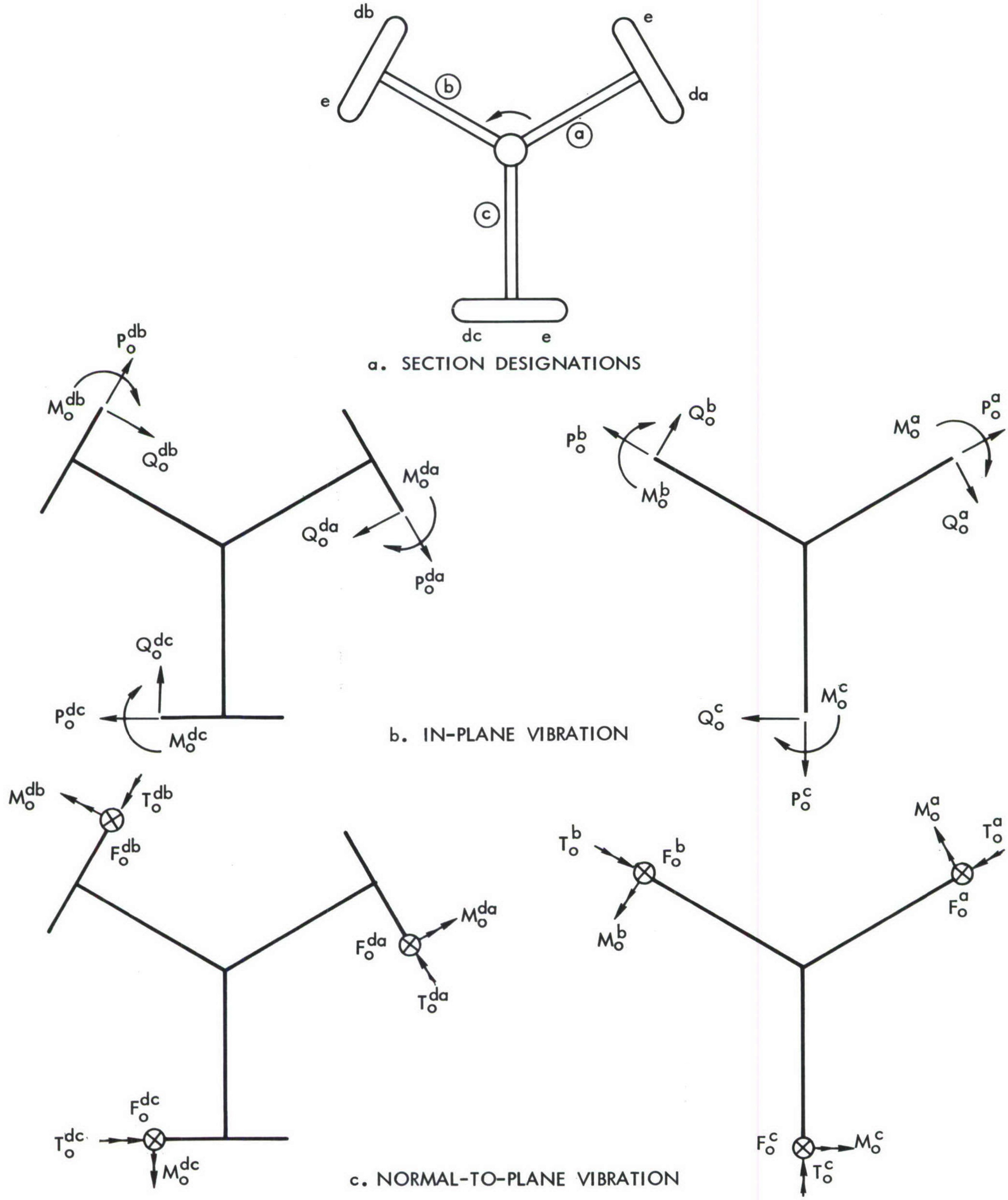

Figure 25. Y-A Configuration

which are computed by successive multiplication of the transfer matrices of lumped masses in each section. By an approach similar to that employed in analyzing Configuration 7-A, the load vectors and deformation vectors at a_o, b_o, c_o may be expressed in terms of deformation vector at da_o, db_o, and dc_o. Applying equations (70) and (71), we have for the in-plane vibration

$$\begin{bmatrix} \begin{Bmatrix} Q \\ P \\ M \end{Bmatrix}_o^a \\ \begin{Bmatrix} Q \\ P \\ M \end{Bmatrix}_o^b \\ \begin{Bmatrix} Q \\ P \\ M \end{Bmatrix}_o^c \end{bmatrix} = \begin{bmatrix} -U & 0 & 0 \\ 0 & -U & 0 \\ 0 & 0 & -U \end{bmatrix} \begin{bmatrix} \begin{Bmatrix} w \\ v \\ \phi \end{Bmatrix}_o^{da} \\ \begin{Bmatrix} w \\ v \\ \phi \end{Bmatrix}_o^{db} \\ \begin{Bmatrix} w \\ v \\ \phi \end{Bmatrix}_o^{dc} \end{bmatrix} \tag{76}$$

and

$$\begin{bmatrix} \begin{Bmatrix} w \\ v \\ \phi \end{Bmatrix}_o^a \\ \begin{Bmatrix} w \\ v \\ \phi \end{Bmatrix}_o^b \\ \begin{Bmatrix} w \\ v \\ \phi \end{Bmatrix}_o^c \end{bmatrix} = \begin{bmatrix} V & 0 & 0 \\ 0 & V & 0 \\ 0 & 0 & V \end{bmatrix} \begin{bmatrix} \begin{Bmatrix} w \\ v \\ \phi \end{Bmatrix}_o^{da} \\ \begin{Bmatrix} w \\ v \\ \phi \end{Bmatrix}_o^{db} \\ \begin{Bmatrix} w \\ v \\ \phi \end{Bmatrix}_o^{dc} \end{bmatrix} \tag{77}$$

The spokes a, b, and c are rigidly joined together at the hub. The conditions of equilibrium and elastic compatibility at the joint are expressed in equation (84) in the analysis of the Y-Configuration. By expressing the state vectors at the hub in terms of those at a_o, b_o, and c_o, the equation (84) may be written as

$$\left[G\right] \begin{bmatrix} \begin{Bmatrix} w \\ v \\ \phi \end{Bmatrix}_o^a \\ \begin{Bmatrix} w \\ v \\ \phi \end{Bmatrix}_o^b \\ \begin{Bmatrix} w \\ v \\ \phi \end{Bmatrix}_o^c \end{bmatrix} + \left[H\right] \begin{bmatrix} \begin{Bmatrix} Q \\ P \\ M \end{Bmatrix}_o^a \\ \begin{Bmatrix} Q \\ P \\ M \end{Bmatrix}_o^b \\ \begin{Bmatrix} Q \\ P \\ M \end{Bmatrix}_o^c \end{bmatrix} = 0 \tag{78}$$

Substituting equations (76) and (77) into (78)

$$\left[G\right] \begin{bmatrix} V & 0 & 0 \\ 0 & V & 0 \\ 0 & 0 & V \end{bmatrix} \begin{bmatrix} \begin{Bmatrix} w \\ v \\ \phi \end{Bmatrix}_o^{da} \\ \begin{Bmatrix} w \\ v \\ \phi \end{Bmatrix}_o^{db} \\ \begin{Bmatrix} w \\ v \\ \phi \end{Bmatrix}_o^{dc} \end{bmatrix} + \left[H\right] \begin{bmatrix} -U & 0 & 0 \\ 0 & -U & 0 \\ 0 & 0 & -U \end{bmatrix} \begin{bmatrix} \begin{Bmatrix} w \\ v \\ \phi \end{Bmatrix}_o^{da} \\ \begin{Bmatrix} w \\ v \\ \phi \end{Bmatrix}_o^{db} \\ \begin{Bmatrix} w \\ v \\ \phi \end{Bmatrix}_o^{dc} \end{bmatrix} = 0 \tag{79}$$

By setting the determinant of coefficients of the preceding equations to zero, natural frequencies corresponding to the in-plane vibrations of the system can be computed.

For normal-to-plane vibration, equations (74) and (75) may be applied from which

$$\begin{bmatrix} \begin{Bmatrix} F \\ M \\ T \end{Bmatrix}_o^a \\ \begin{Bmatrix} F \\ M \\ T \end{Bmatrix}_o^b \\ \begin{Bmatrix} F \\ M \\ T \end{Bmatrix}_o^c \end{bmatrix} = \begin{bmatrix} -U^N & 0 & 0 \\ 0 & -U^N & 0 \\ 0 & 0 & -U^N \end{bmatrix} \begin{bmatrix} \begin{Bmatrix} u \\ \theta \\ \psi \end{Bmatrix}_o^{da} \\ \begin{Bmatrix} u \\ \theta \\ \psi \end{Bmatrix}_o^{db} \\ \begin{Bmatrix} u \\ \theta \\ \psi \end{Bmatrix}_o^{dc} \end{bmatrix} \tag{80}$$

and

$$\begin{bmatrix} \begin{Bmatrix} u \\ \theta \\ \psi \end{Bmatrix}_o^a \\ \begin{Bmatrix} u \\ \theta \\ \psi \end{Bmatrix}_o^b \\ \begin{Bmatrix} u \\ \theta \\ \psi \end{Bmatrix}_o^c \end{bmatrix} = \begin{bmatrix} V^N & 0 & 0 \\ 0 & V^N & 0 \\ 0 & 0 & V^N \end{bmatrix} \begin{bmatrix} \begin{Bmatrix} u \\ \theta \\ \psi \end{Bmatrix}_o^{da} \\ \begin{Bmatrix} u \\ \theta \\ \psi \end{Bmatrix}_o^{db} \\ \begin{Bmatrix} u \\ \theta \\ \psi \end{Bmatrix}_o^{dc} \end{bmatrix} \tag{81}$$

By using the conditions of continuity at the hub, the equation (85) in the Y-Configuration analysis is expressed as

$$\left[G^N\right] \begin{bmatrix} \begin{Bmatrix} u \\ \theta \\ \psi \end{Bmatrix}_o^a \\ \begin{Bmatrix} u \\ \theta \\ \psi \end{Bmatrix}_o^b \\ \begin{Bmatrix} u \\ \theta \\ \psi \end{Bmatrix}_o^c \end{bmatrix} + \left[H^N\right] \begin{bmatrix} \begin{Bmatrix} F \\ M \\ T \end{Bmatrix}_o^a \\ \begin{Bmatrix} F \\ M \\ T \end{Bmatrix}_o^b \\ \begin{Bmatrix} F \\ M \\ T \end{Bmatrix}_o^c \end{bmatrix} = 0 \tag{82}$$

Substituting equations (80) and (81) into (82)

$$\left[G^N\right] \begin{bmatrix} V^N & 0 & 0 \\ 0 & V^N & 0 \\ 0 & 0 & V^N \end{bmatrix} \begin{bmatrix} \begin{Bmatrix} u \\ \theta \\ \psi \end{Bmatrix}_o^{da} \\ \begin{Bmatrix} u \\ \theta \\ \psi \end{Bmatrix}_o^{db} \\ \begin{Bmatrix} u \\ \theta \\ \psi \end{Bmatrix}_o^{dc} \end{bmatrix} + \left[H^N\right] \begin{bmatrix} -U^N & 0 & 0 \\ 0 & -U^N & 0 \\ 0 & 0 & -U^N \end{bmatrix} \begin{bmatrix} \begin{Bmatrix} u \\ \theta \\ \psi \end{Bmatrix}_o^{da} \\ \begin{Bmatrix} u \\ \theta \\ \psi \end{Bmatrix}_o^{db} \\ \begin{Bmatrix} u \\ \theta \\ \psi \end{Bmatrix}_o^{dc} \end{bmatrix} = 0 \tag{83}$$

The preceding equation is the characteristic equation from which the frequencies corresponding to the normal-to-plane vibrations are computed.

6.4 VIBRATION OF Y-CONFIGURATION SPACE STATIONS

It is advantageous to consider structural and inertial symmetry of the Y-Configuration. A convenient orientation of an inertially fixed right-handed Cartesian coordinate system is one with the origin at the hub, the positive x-axis coincident with the central axis of Compartment a (Figure 26), and the positive z-axis perpendicular to the plane of the paper and directed toward the reader. In this coordinate system the Y-Configuration is considered to have two planes of structural and inertial symmetry, the X-Y plane and the X-Z plane.

Because of the symmetry relative to the X-Y plane, deflections and accelerations in the plane will cause no interval or inertial loads normal to the plane. The statement is also true when the words "in" and "normal to" are interchanged. Therefore, there is neither elastic nor inertial coupling between the in-plane and normal-to-plane vibrations. The inertial coupling due to coreolis accelerations of the spinning vehicle can be computed during subsequent calculations of stability or responses of the system to externally applied loads.

For those modes which exist in pairs (Figures 40 and 41) it might be expected that there would be three mutually orthogonal pairs, one for each of the possible selections of the X-Z plane of symmetry. This is not the case. The modes rotated by 120 degrees are not orthogonal either to the unrotated pair or to the pair rotated 240 degrees. The dynamic response to a load applied parallel (or perpendicular) to the axis of the compartments b or c, can be computed from the unrotated pair, and the resulting motion will be symmetric (or anti-symmetric) relative to the plane of symmetry containing that compartment axis.

6.4.1 In-Plane Vibration

The radial compartments (a, b, and c, Figure 26) are divided into segments, and the transfer matrices of these segments are computed by the equations given in Section 6.3. Let the transfer matrix of the compartments be denoted A_{ij}, B_{ij}, and C_{ij} which are computed by successive multiplication of transfer matrices of the lumped masses in each segment. By designating the free end of the compartment as station zero and the hub end of the compartment as station n, the transfer matrix of the entire compartment is a product of $[R_n] \ldots [R_2] [R_1] [R_o]$.

It is worthwhile to examine closely the transfer matrices. Because the compartments are considered to be structurally and inertially identical, the transfer matrix from the free end to the hub of each compartment is

identical to that of the others. Also, certain of the elements of this transfer matrix always will be zero. The non-zero elements are indicated below by x's and 1.0's.

$$\begin{Bmatrix} w_n \\ \phi_n \\ Q_n \\ M_n \\ \nu_o \\ P_n \end{Bmatrix} = \begin{bmatrix} x & x & x & x & 0 & 0 \\ x & x & x & x & 0 & 0 \\ x & x & x & x & 0 & 0 \\ x & x & x & x & 0 & 0 \\ 0 & 0 & 0 & 0 & 1.0 & 0 \\ 0 & 0 & 0 & 0 & x & 1.0 \end{bmatrix} \begin{Bmatrix} w_o \\ \phi_o \\ Q_o \\ M_o \\ \nu_o \\ P_o \end{Bmatrix}$$

It also can be seen from the locations of the zeros that no coupling exists between the longitudinal and lateral degrees of freedom along the compartment.

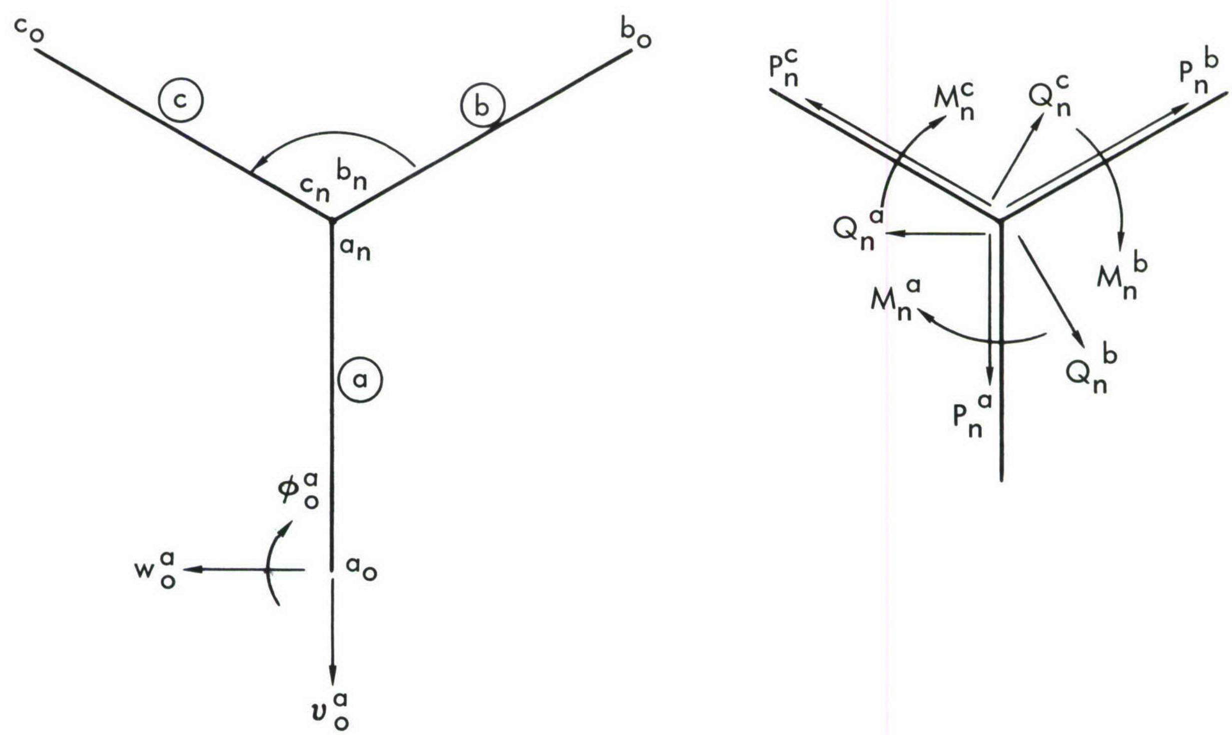

Figure 26. Y-Configuration—In-Plane Vibration Parameters

At the free end of each compartment, the load vectors disappear, i.e., $Q_o = P_o = M_o = 0$. Therefore, we have only three deformation vectors at each free end or a total of nine deformation vectors for the three compartments: $\{w, v, \phi\}_o^a$, $\{w, v, \phi\}_o^b$, and $\{w, v, \phi\}_o^c$. Since the three modules are joined rigidly at the hub, the conditions of static equilibrium and elastic compatibility at the hub yield the following nine equations:

$$
\begin{aligned}
&M_n^a + M_n^b + M_n^c = 0 \\
&-Q_n^a + \frac{\sqrt{3}}{2} P_n^b + \frac{1}{2} Q_n^b - \frac{\sqrt{3}}{2} P_n^c + \frac{1}{2} Q_n^c = 0 \\
&-P_n^a + \frac{1}{2} P_n^b - \frac{\sqrt{3}}{2} Q_n^b + \frac{1}{2} P_n^c + \frac{\sqrt{3}}{2} Q_n^c = 0 \\
&w_n^a + \frac{1}{2} w_n^b + \frac{\sqrt{3}}{2} v_n^b = 0 \\
&v_n^a - \frac{\sqrt{3}}{2} w_n^b + \frac{1}{2} v_n^b = 0 \\
&w_n^a + \frac{1}{2} w_n^c - \frac{\sqrt{3}}{2} v_n^c = 0 \\
&v_n^a + \frac{\sqrt{3}}{2} w_n^c + \frac{1}{2} v_n^c = 0 \\
&\phi_n^a - \phi_n^b = 0 \\
&\phi_n^a - \phi_n^c = 0
\end{aligned}
\tag{84}
$$

When deflections in the X-Y plane are symmetric relative to the X-Z plane, i.e.,

$$w^a \equiv \phi^a \equiv 0, \quad w_n^b = -w_n^c, \quad \nu_n^b = \nu_n^c, \text{ and } \phi_n^b = -\phi_n^c$$

both the interval and inertial forces and moments are also symmetric, i.e.,

$$Q^a \equiv M^a \equiv 0, \quad Q_u^b = -Q_u^c, \quad P_n^b = P_n^c, \text{ and } M_n^b = -M_n^c$$

And, when deflections are anti-symmetric

$$\nu^a \equiv 0, \qquad w_n^b = w_n^c, \qquad \nu_n^b = -\nu_n^c, \text{ and } \phi_n^b = \phi_n^c$$

then

$$P^a \equiv 0, \qquad Q_n^b = Q_n^c, \qquad P_n^b = -P_n^c, \text{ and } M_n^b = M_n^c$$

Substitution of these expressions into equations (84) yields two sets of non-trivial equations:

Symmetric	Anti-Symmetric
$-P_n^a + P_n^b - \sqrt{3}\ Q_n^b = 0$	$M_n^a + 2M_n^b = 0$
$w_n^b + \sqrt{3}\ \nu_n^b = 0$	$-Q_n^a + \sqrt{3}\ P_n^b + Q_n^b = 0$
$2\nu_n^a - \sqrt{3}\ w_n^b + \nu_n^b = 0$	$2w_n^a + w_n^b + \sqrt{3}\ \nu_n^b = 0$
$\phi_n^b = 0$	$\sqrt{3}\ w_n^b - \nu_n^b = 0$
	$\phi_n^a - \phi_n^b = 0$

(85)

Equations (85) may be expressed in the matrix form:

Symmetric

$$\begin{bmatrix} -B_{65} & \sqrt{3}B_{31} & B_{65} & -\sqrt{3}B_{32} \\ 0 & B_{11} & \sqrt{3} & B_{12} \\ 2.0 & \sqrt{3}B_{11} & 1.0 & -\sqrt{3}B_{12} \\ 0 & B_{21} & 0 & B_{22} \end{bmatrix} \begin{Bmatrix} \nu_o^a \\ w_o^b \\ \nu_o^b \\ \phi_o^b \end{Bmatrix} = 0$$

Anti-Symmetric

$$\begin{bmatrix} B_{41} & B_{42} & 2B_{41} & 0 & 2B_{42} \\ -B_{31} & -B_{32} & B_{31} & \sqrt{3}B_{65} & B_{32} \\ 2B_{11} & 2B_{12} & B_{11} & \sqrt{3} & B_{12} \\ 0 & 0 & \sqrt{3}B_{11} & -1.0 & \sqrt{3}B_{12} \\ B_{21} & B_{22} & -B_{21} & 0 & -B_{22} \end{bmatrix} \begin{Bmatrix} w_o^a \\ \phi_o^a \\ w_o^b \\ \nu_o^b \\ \phi_o^b \end{Bmatrix} = 0$$

The expanded determinants of coefficients are set equal to R_s and R_A, respectively

$$R_s^{(I)} = 6S^{(I)} \qquad\qquad R_A^{(I)} = -18\, S^{(I)} A^{(I)}$$

where

$$S^{(I)} = (B_{32}\,B_{21} - B_{31}\,B_{22}) - B_{65}\,(B_{11}\,B_{22} - B_{12}\,B_{21})$$

and

$$A^{(I)} = (B_{11}\,B_{42} - B_{12}\,B_{41})$$

These equations show that whenever the symmetric residue (R_S) equals zero the anti-symmetric residue (R_A) also equals zero, and therefore at each natural frequency at which a symmetric in-plane mode exists an anti-symmetric in-plane mode also exists. Solution of a sub-set of these matrix equations for $w_o^b = 1.0$ yields the deflections at the free ends of the compartments:

	Symmetric	Anti-Symmetric	
	S = 0	S = 0	A = 0
w_o^b	1.0	1.0	1.0
ϕ_o^b	$-B_{21}/B_{22}$	$-B_{21}/B_{22}$	$-B_{41}/B_{42}$
ν_o^b	$-(B_{11} + B_{12}\ \phi_o^b)/\sqrt{3}$	$\sqrt{3}(B_{11} + B_{12}\ \phi_o^b)$	$\sqrt{3}(B_{11} + B_{12}\ \phi_o^b)$
w_o^c	-1.0	1.0	1.0
ϕ_o^c	$-\phi_o^b$	ϕ_o^b	ϕ_o^b
ν_o^c	ν_o^b	$-\nu_o^b$	$-\nu_o^b$
w_o^a	0	-2.0	1.0
ϕ_o^a	0	$-2\phi_o^b$	ϕ_o^b
ν_o^a	$\nu_o^b - \sqrt{3}\ (B_{31} + B_{32}\ \phi_o^b)/B_{65}$	0	0

The natural frequencies and corresponding mode shapes of the in-plane vibration are shown in Figure 40.

6.4.2 Normal-to-Plane Vibration

The radial compartments (a, b, and c, Figure 27) are divided into segments, and the transfer matrices of these segments are computed by the equations given in Section 6.3. The transfer matrices of the whole compartments are computed by successive multiplication of the transfer matrices of each segment and are denoted as A_{ij}, B_{ij}, and C_{ij}, which are identical because of structural and inertial identity. Certain of the elements of this out-of-plane transfer matrix will, as of the in-plane matrix, be zero. Non-zero elements are indicated on the following page by x's.

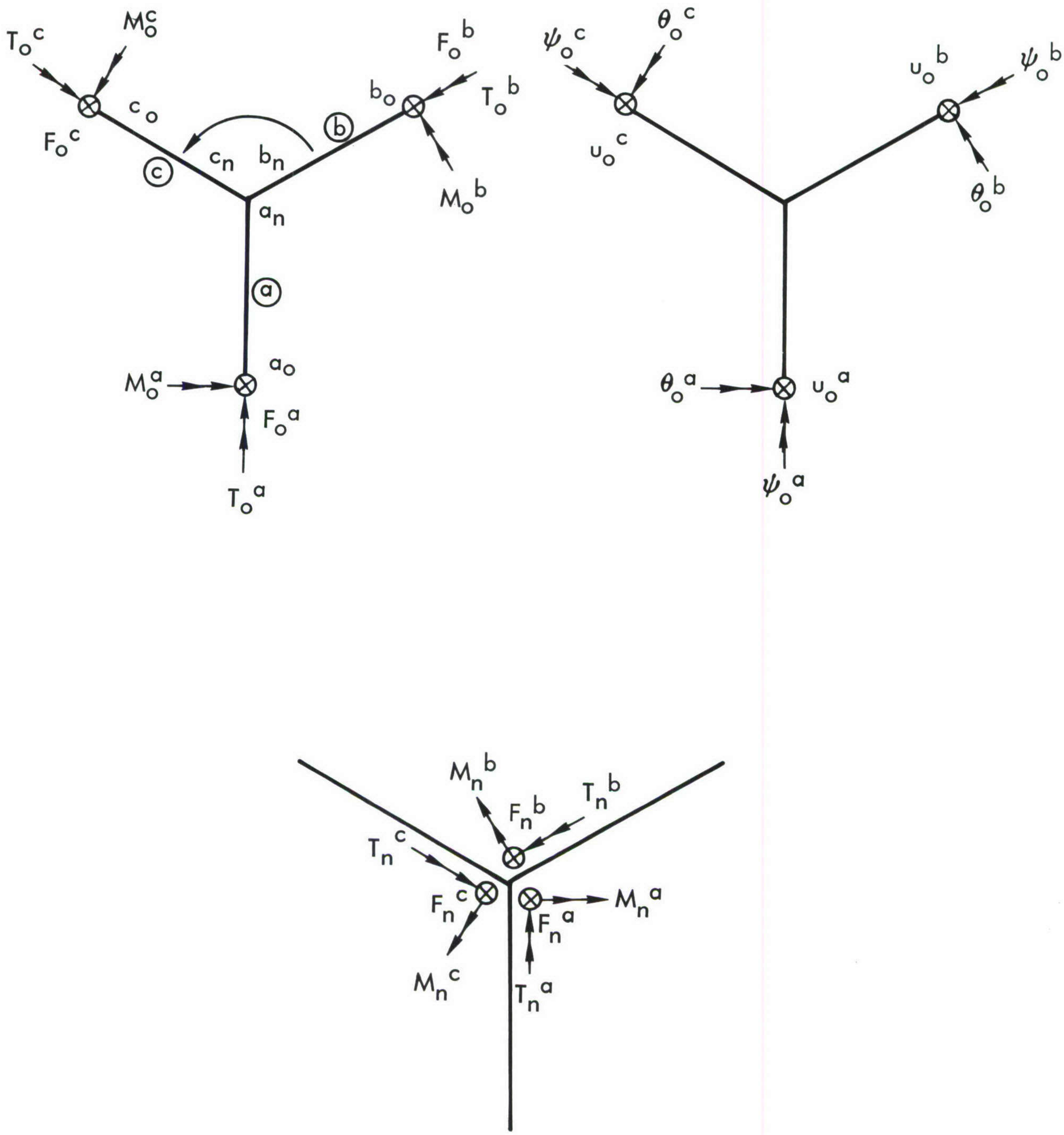

Figure 27. Y-Configuration—Normal-To-Plane Vibration Parameters

$$
\begin{Bmatrix} u_n \\ \theta_n \\ F_n \\ M_n \\ \psi_n \\ T_n \end{Bmatrix}
=
\begin{bmatrix}
x & x & x & x & 0 & 0 \\
x & x & x & x & 0 & 0 \\
x & x & x & x & 0 & 0 \\
x & x & x & x & 0 & 0 \\
0 & 0 & 0 & 0 & x & x \\
0 & 0 & 0 & 0 & x & x
\end{bmatrix}
\begin{Bmatrix} u_o \\ \theta_o \\ F_o \\ M_o \\ \psi_o \\ T_o \end{Bmatrix}
$$

The location of the zeros show that no coupling exists between the torsional and bending degrees of freedom.

At the free end (station zero) of each compartment, the load vectors disappear, i.e., $F_o = M_o = T_o = 0$. Therefore, we have only three deformation vectors at each free end, or a total of nine deformation vectors for the three compartments: $\{u, \theta, \psi\}_o^a$, $\{u, \theta, \psi\}_o^b$, and $\{u, \theta, \psi\}_o^c$. These nine deformation vectors can be determined from the nine equations that resulted from the conditions of static equilibrium and elastic compatibility at the hub. If the state vectors at the hub are denoted as u_n, θ_n, ψ_n, F_n, M_n and T_n, then

$$
\begin{aligned}
& F_n^a + F_n^b + F_n^c = 0 \\
& M_n^a - \frac{1}{2} M_n^b - \frac{\sqrt{3}}{2} T_n^b - \frac{1}{2} M_n^c + \frac{\sqrt{3}}{2} T_n^c = 0 \\
& T_n^a + \frac{\sqrt{3}}{2} M_n^b - \frac{1}{2} T_n^b - \frac{\sqrt{3}}{2} M_n^c - \frac{1}{2} T_n^c = 0 \\
& \psi_n^a - \frac{\sqrt{3}}{2} \theta_n^b + \frac{1}{2} \psi_n^b = 0 \\
& \theta_n^a + \frac{1}{2} \theta_n^b + \frac{\sqrt{3}}{2} \psi_n^b = 0 \\
& \psi_n^a + \frac{\sqrt{3}}{2} \theta_n^c + \frac{1}{2} \psi_n^c = 0 \\
& \theta_n^a + \frac{1}{2} \theta_n^c - \frac{\sqrt{3}}{2} \psi_n^c = 0 \\
& u_n^a - u_n^b = 0 \\
& u_n^a - u_n^c = 0
\end{aligned}
\tag{86}
$$

When deflections normal to the X-Y plane are symmetric relative to the X-Z plane, i.e.,

$$\psi^a \equiv 0, \qquad u_n^b = u_n^c, \qquad \theta_n^b = \theta_n^c, \text{ and } \psi_n^b = -\psi_n^c$$

then

$$T^a \equiv 0, \qquad F_n^b = F_n^c, \qquad M_n^b = M_n^c, \text{ and } T_n^b = -T_n^c$$

and when deflections are anti-symmetric, i.e.,

$$u^a \equiv \theta^a \equiv 0, \qquad u_n^b = -u_n^c, \qquad \theta_n^b = -\theta_n^c, \text{ and } \psi_n^b = \psi_n^c$$

then

$$F^a \equiv M^a \equiv 0, \qquad F_n^b = -F_n^c, \qquad M_n^b = -M_n^c, \text{ and } T_n^b = T_n^c.$$

Substitution of these expressions into equations (86) yields the two sets of non-trivial equations:

Symmetric

$$F_n^a + 2F_n^b = 0$$

$$M_n^a - M_n^b - \sqrt{3}\, T_n^b = 0$$

$$\sqrt{3}\, \theta_n^b - \psi_n^b = 0$$

$$2\theta_n^a + \theta_n^b + \sqrt{3}\, \psi_n^b = 0$$

$$u_n^a - u_n^b = 0$$

or

$$\begin{bmatrix} B_{31} & B_{32} & 2B_{31} & 2B_{32} & 0 \\ B_{41} & B_{42} & -B_{41} & -B_{42} & \sqrt{3}\,B_{65} \\ 0 & 0 & \sqrt{3}\,B_{21} & \sqrt{3}\,B_{22} & -B_{55} \\ 2B_{21} & 2B_{22} & B_{21} & B_{22} & \sqrt{3}\,B_{55} \\ B_{11} & B_{12} & -B_{11} & -B_{12} & 0 \end{bmatrix} \begin{Bmatrix} u_o^a \\ \theta_o^a \\ u_o^b \\ \theta_o^b \\ \psi_o^b \end{Bmatrix} = 0$$

Anti-Symmetric

$$T_n^a + \sqrt{3}\, M_n^b - T_n^b = 0$$

$$2\psi_n^a - \sqrt{3}\, \theta_n^b + \psi_n^b = 0$$

$$\theta_n^b + \sqrt{3}\, \psi_n^b = 0$$

$$u_n^b = 0$$

$$\begin{bmatrix} B_{65} & -B_{65} & \sqrt{3}\,B_{41} & \sqrt{3}\,B_{42} \\ 2B_{55} & B_{55} & \sqrt{3}\,B_{21} & \sqrt{3}\,B_{22} \\ 0 & \sqrt{3}\,B_{55} & B_{21} & B_{22} \\ 0 & 0 & B_{11} & B_{12} \end{bmatrix} \begin{Bmatrix} \psi_o^a \\ \psi_o^b \\ u_o^b \\ \theta_o^b \end{Bmatrix} = 0$$

The expanded determinants of coefficients are set equal to $R_s^{(0)}$ and $R_A^{(0)}$, respectively

$$R_s^{(0)} = 18\, S^{(0)}\, A^{(0)} \qquad \Big| \qquad R_A^{(0)} = 6\, B_{55}\, A$$

where

$$S^{(0)} = B_{31}\, B_{22} - B_{21}\, B_{32}$$

and

$$A^{(0)} - B_{65}\,(B_{12}\, B_{21} - B_{11}\, B_{22}) + B_{55}\,(B_{12}\, B_{41} - B_{11}\, B_{42})$$

The equations show that whenever an anti-symmetric normal-to-plane mode exists a symmetric normal-to-plane mode also exists. The deflections of the free ends of the compartments are given below.

	Symmetric		Anti-Symmetric
	$A = 0$	$S = 0$	$A = 0$
u_o^b	1.0	1.0	1.0
θ_o^b	$-B_n/B_{12}$	$-B_{31}/B_{32}$	$-B_{11}/B_{12}$
ψ_o^b	$\sqrt{3}\,(B_{41} + B_{42}\,\theta_o^b)/B_{65}$	0	$-(B_{21} + B_{22}\,\theta_o^b)/\sqrt{3}\,B_{55}$
u_o^c	1.0	1.0	-1.0
θ_o^c	θ_o^b	θ_o^b	$-\theta_o^b$
ψ_o^c	$-\psi_o^b$	0	ψ_o^b
u_o^a	-2.0	1.0	0
θ_o^a	$-2\theta_o^b$	θ_o^b	0
ψ_o^a	0	0	$2\psi_o^b$

The natural frequencies and corresponding mode shapes of the normal-to-plane vibration are shown in Figure 41.

6.5 CABLE MODES FROM A CONTINUOUS REPRESENTATION BY PARTIAL DIFFERENTIAL EQUATIONS

In transverse oscillation, the arbitrary displacement $\zeta(\eta, t)$ can be represented by the sum of the normal modes $\phi_n(\eta)$ multiplied by the generalized coordinates $q_n(t)$ associated with the mode. See Figure 28.

$$\zeta(\eta, t) = \sum_{n=1}^{\infty} \phi_n(\eta)\, q_n(t)$$

where n denotes the mode number.

The cable tension at any positive η from the center of mass is

$$S_1 = \int_{\eta}^{\ell_1} \omega^2 \eta \rho \, d\eta + \ell_1 m_1 \omega^2 = \frac{\omega^2 \rho \ell_1^2}{2} \left(a_1^2 - \frac{\eta^2}{\ell_1^2} \right)$$

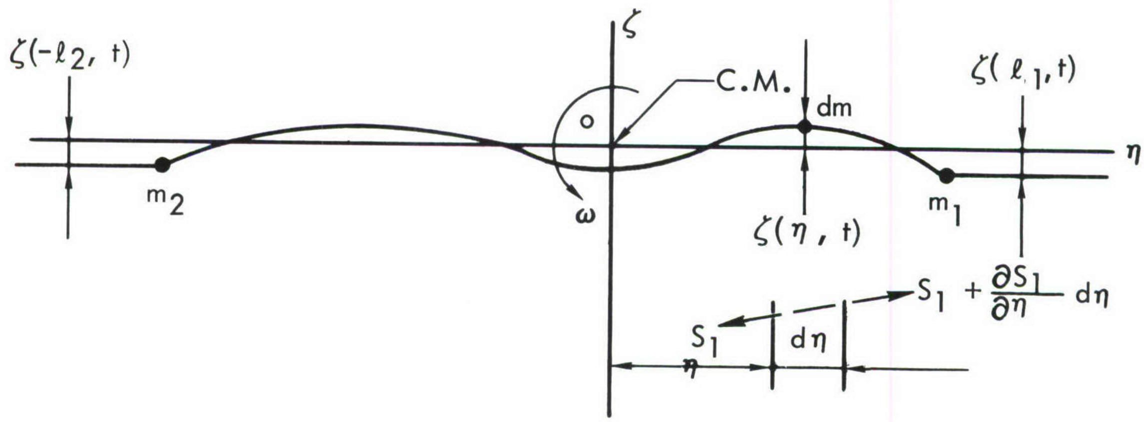

Figure 28. Compartment-Cable-Counterweight Configuration

and the cable tension for the negative η axis is

$$S_2 = \int_{\eta}^{-\ell_2} \omega^2 \eta\rho \, d\eta + \ell_2 m_2 \omega^2 = \frac{\omega^2 \rho \ell_2^2}{2} \left(a_2^2 - \frac{\eta^2}{\ell_2^2} \right)$$

where

$$a_1^2 = 1 + \frac{2m_1}{\rho \ell_1}$$

$$a_2^2 = 1 + \frac{2m_2}{\rho \ell_2}$$

The dynamic equilibrium equation of transverse oscillation of the cable is

$$\left(s_1 \frac{\partial \zeta}{\partial \eta} + \frac{\partial}{\partial \eta} \left(s_1 \frac{\partial \zeta}{\partial \eta} \right) d\eta \right) - s_1 \frac{\partial \zeta}{\partial \eta} = \rho \, d\eta \left(\frac{\partial^2 \zeta}{\partial t^2} - \omega^2 \zeta \right)$$

since

$$\frac{\partial}{\partial \eta} \left(s_1 \frac{\partial \zeta}{\partial \eta} \right) = \frac{\partial s_1}{\partial \eta} \frac{\partial \zeta}{\partial \eta} + s_1 \frac{\partial^2 \zeta}{\partial \eta^2} = \omega^2 \rho \eta \frac{\partial \zeta}{\partial \eta} + \frac{\omega^2 \rho}{2} \left(a_1^2 \ell_1^2 - \eta^2 \right) \frac{\partial^2 \zeta}{\partial \eta^2}$$

thus

$$(a_1^2 \ell_1^2 - \eta^2) \frac{\partial^2 \zeta}{\partial \eta^2} - 2\eta \frac{\partial \zeta}{\partial \eta} - \frac{2}{\omega^2} \frac{\partial^2 \zeta}{\partial t^2} + 2\zeta = 0$$

Similarly, for the negative η axis

$$(a_2^2 \ell_2^2 - \eta^2) \frac{\partial^2 \zeta}{\partial \eta^2} - 2\eta \frac{\partial \zeta}{\partial \eta} - \frac{2}{\omega^2} \frac{\partial^2 \zeta}{\partial t^2} + 2\zeta = 0$$

allowing

$$\zeta_n = \phi_n(\eta) \, e^{ip_n t}, \text{ so } \frac{\partial^2 \zeta}{\partial \eta^2} = e^{ip_n t} \frac{\partial^2 \phi_n}{\partial \eta^2}, \; \frac{\partial^2 \zeta}{\partial t^2} = - p_n^2 \phi_n \, e^{ip_n t},$$

The preceding two equations are reduced to

$$(a_1^2\ell_1^2 - \eta^2) \frac{\partial^2\phi_n}{\partial\eta^2} - 2\eta \frac{\partial\phi_n}{\partial\eta} + 2\left[\left(\frac{p_n}{\omega}\right)^2 + 1\right]\phi_n = 0$$

$$(a_2^2\ell_2^2 - \eta^2) \frac{\partial^2\phi_n}{\partial\eta^2} - 2\eta \frac{\partial\phi_n}{\partial\eta} + 2\left[\left(\frac{p_n}{\omega}\right)^2 + 1\right]\phi_n = 0$$

The preceding equations can be reduced to the standard form of the Legendre equation by letting $\eta = a_1\ell_1 x$, so $\partial^2\phi_n/\partial\eta^2 = (1/a_1^2\ell_1^2)(\partial^2\phi_n/\partial x^2)$ $\partial\phi_n/\partial\eta = (1/a_1\ell_1)(\partial\phi_n/\partial x)$

thus

$$(1 - x^2) \frac{\partial^2\phi_n}{\partial x^2} - 2x \frac{\partial\phi_n}{\partial x} + 2\left[\left(\frac{p_n}{\omega}\right)^2 + 1\right]\phi_n = 0$$

by taking into account that the linear and angular momenta of the vibration modes are zero, i.e.,

$$\rho \int_{-\ell_2}^{\ell_1} \phi_n \, d\eta + m_1\phi_n(\ell_1) + m_2\phi_n(\ell_2) = 0$$

$$\rho \int_{-\ell_2}^{\ell_1} \eta\phi_n \, d\eta + \ell_1 m_1\phi_n(\ell_1) - \ell_2 m_2\phi_n(\ell_2) = 0$$

the two-final equations of transverse vibration can be solved simultaneously for ϕ_n and p_n for given a_1, a_2, ℓ_1, ℓ_2, and satisfying the continuity of slope and displacement at $\eta = 0$.

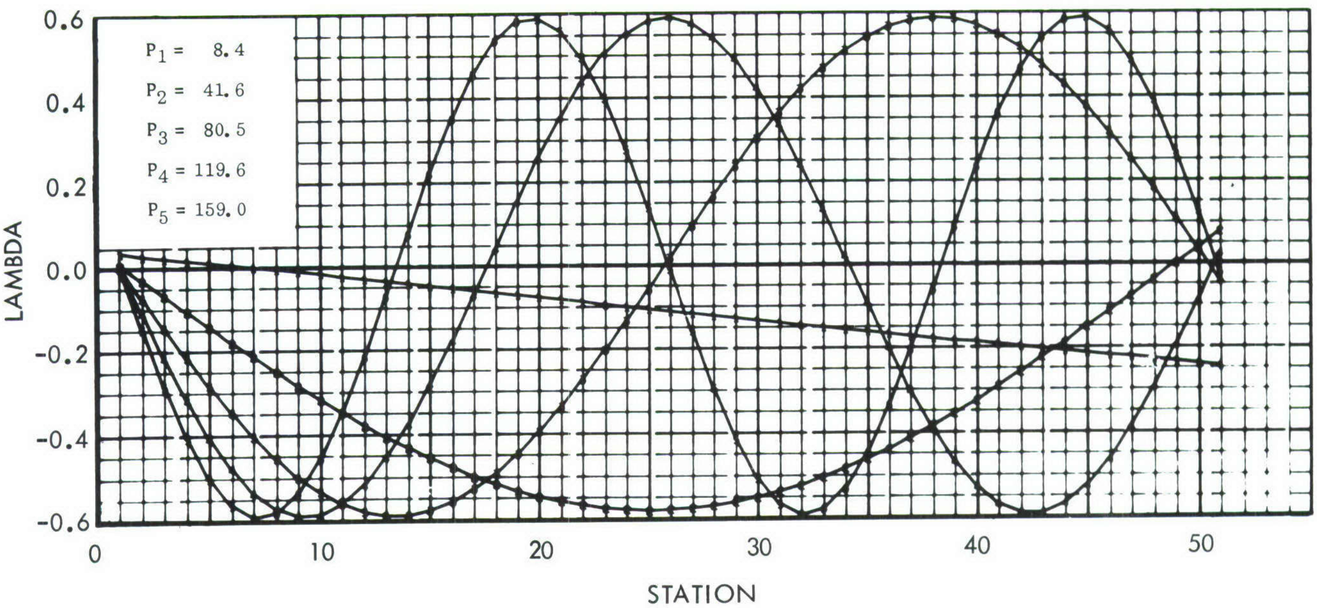

Figure 29. Longitudinal Vibration—Normal Mode

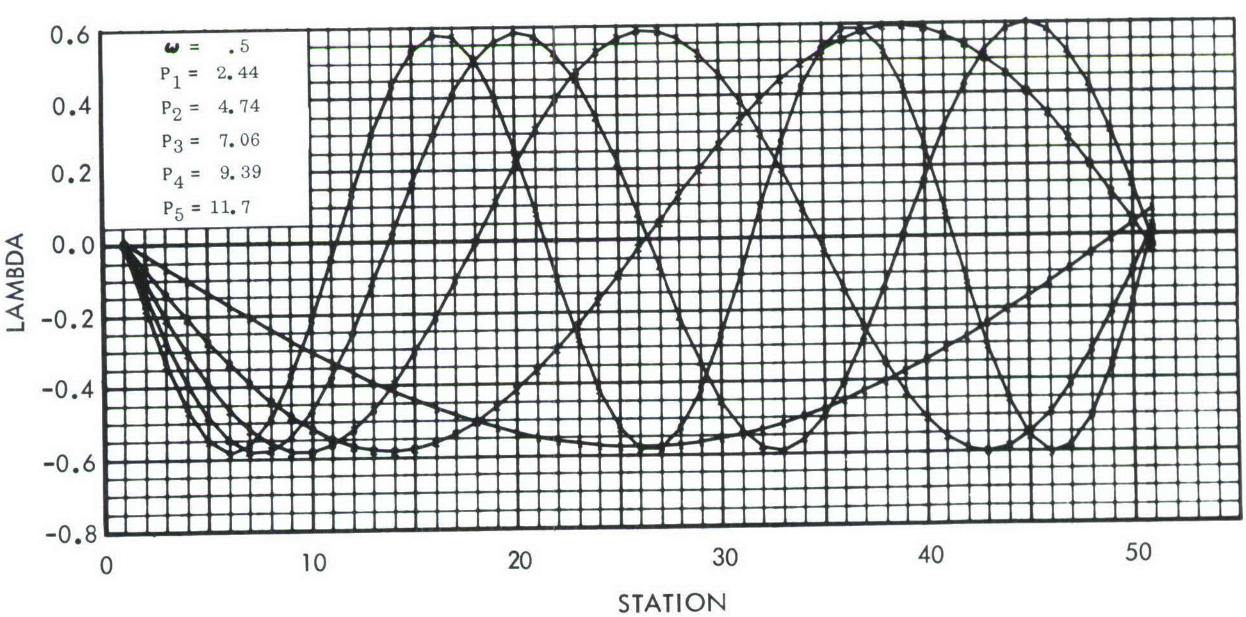

Figure 30. Lateral Vibration—Normal Mode

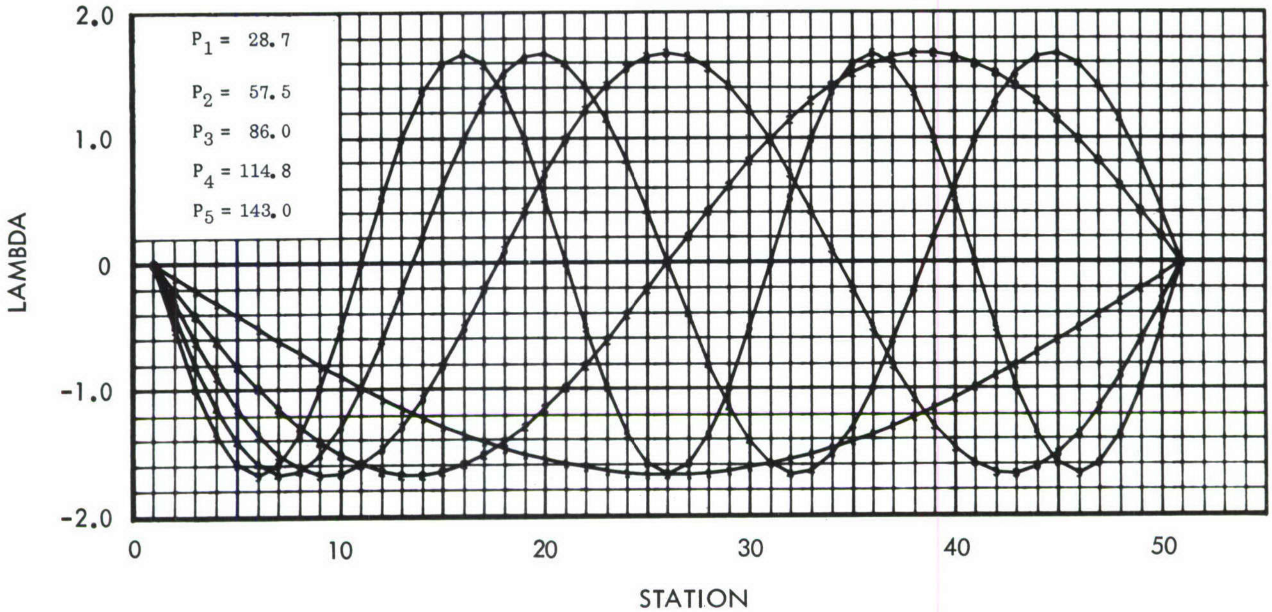

Figure 31. Torsional Vibration—Normal Mode

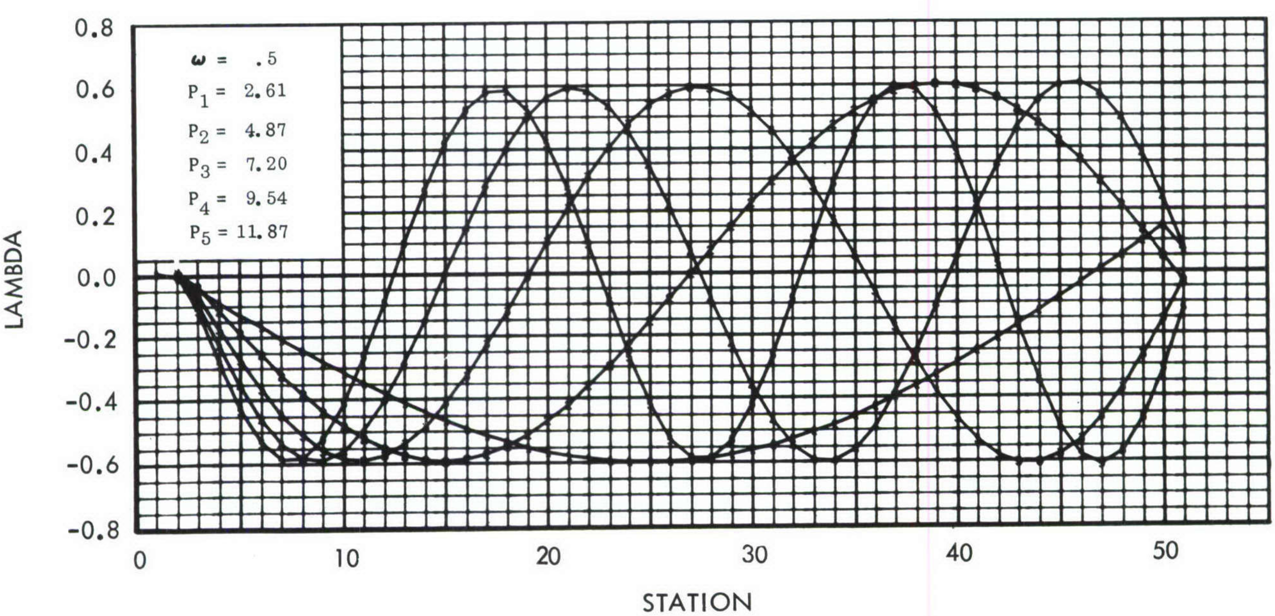

Figure 32. Lateral Vibration With Rotary Inertia of Compartment and Counterweight—Normal Mode

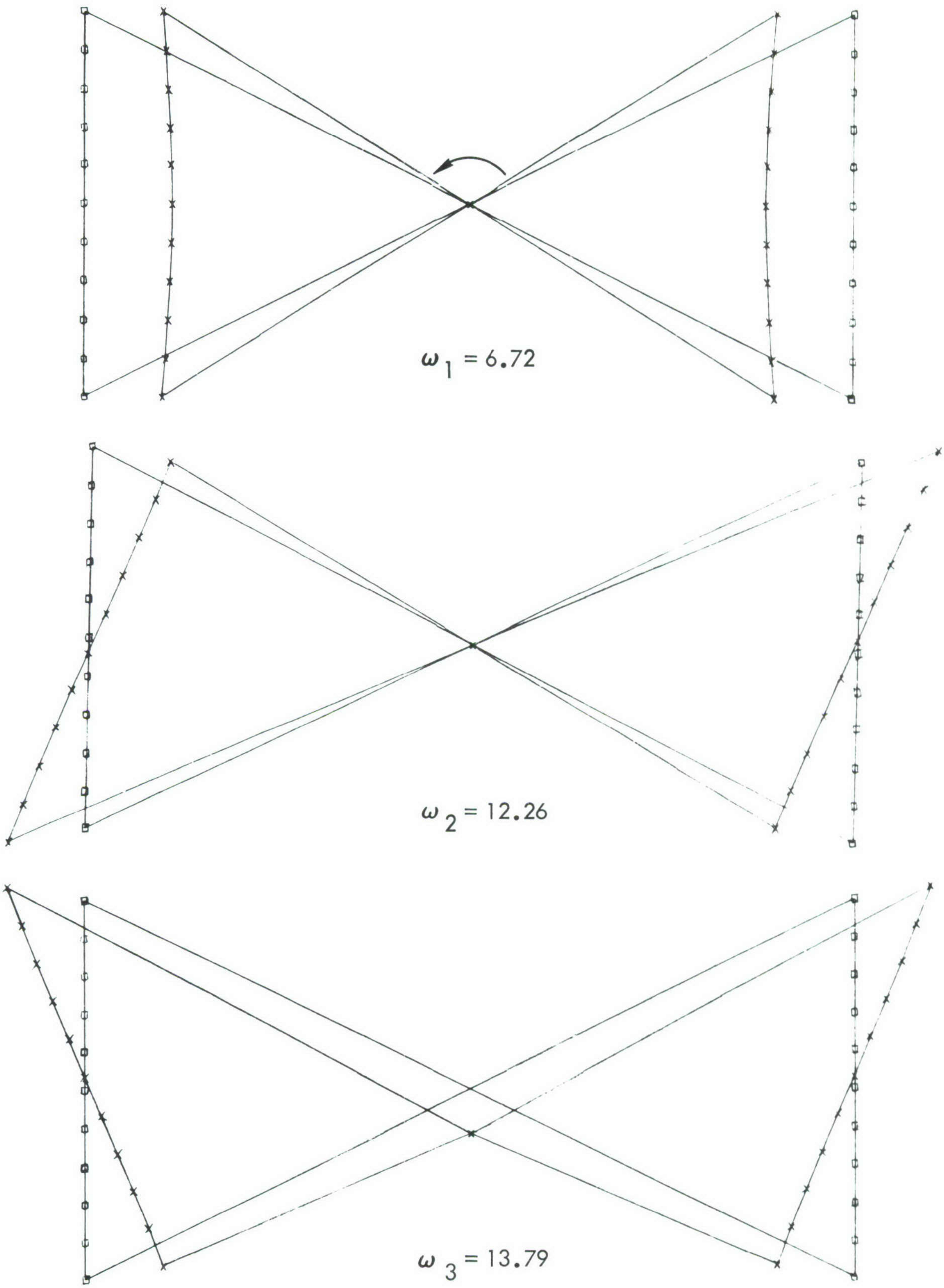

Figure 33. Two-Compartment Configuration Connected With Cables; Modes 1, 2, and 3

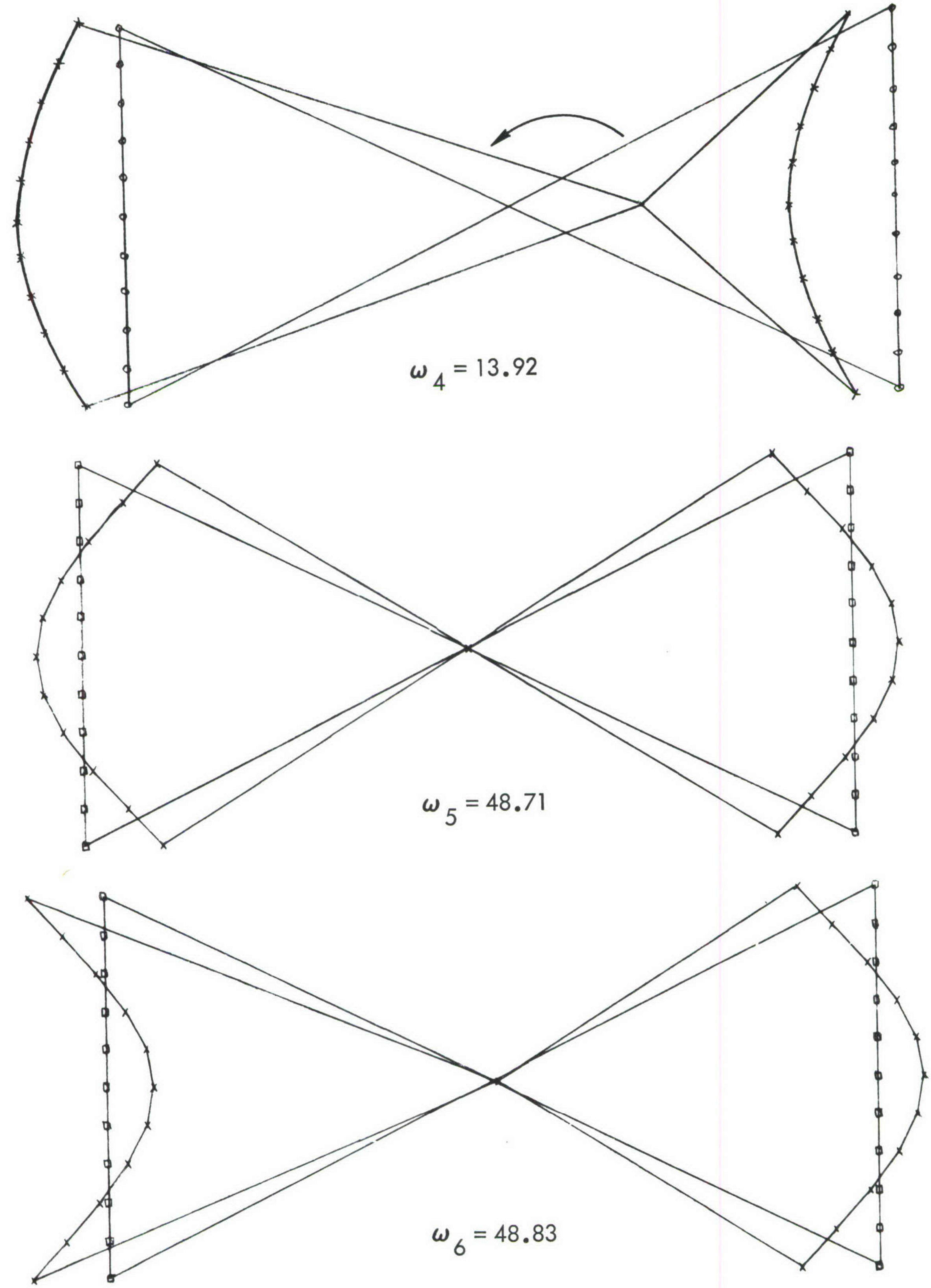

Figure 34. Two-Compartment Configuration Connected With Cables; Modes 4, 5, and 6

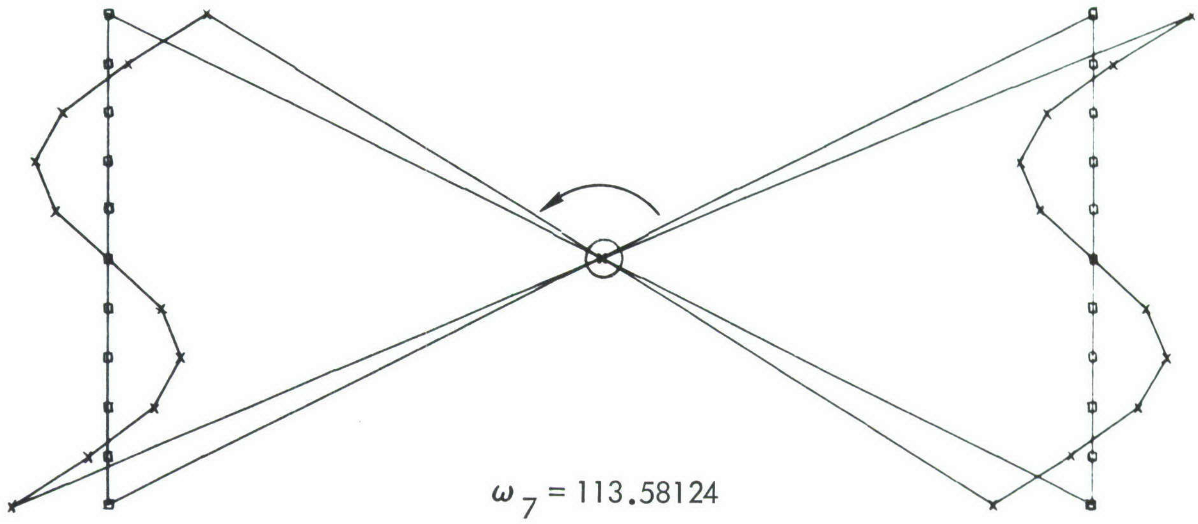

$\omega_7 = 113.58124$

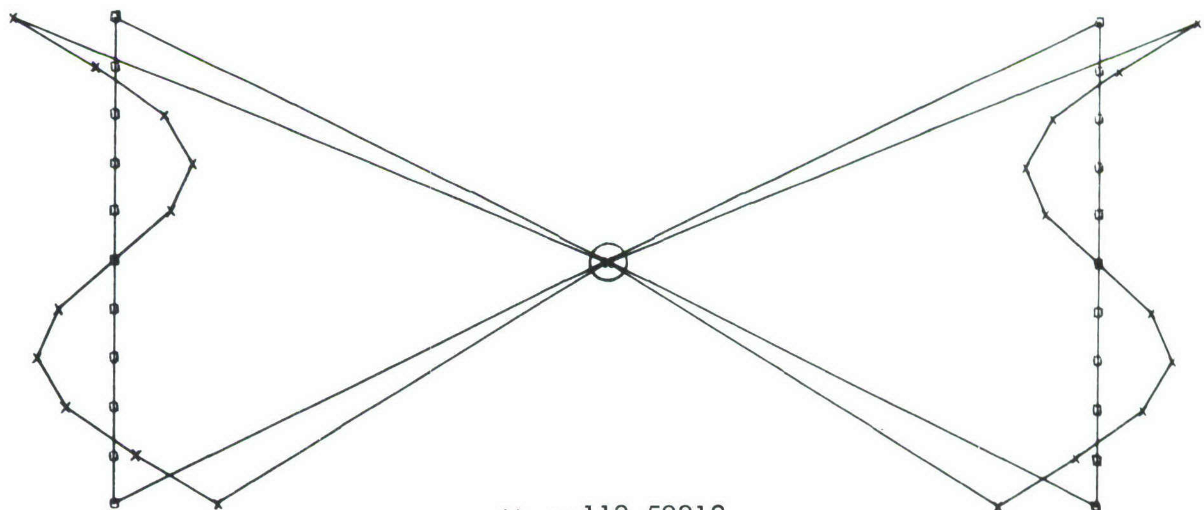

$\omega_8 = 113.58312$

Figure 35. Two-Compartment Configuration Connected With Cables; Modes 7 and 8

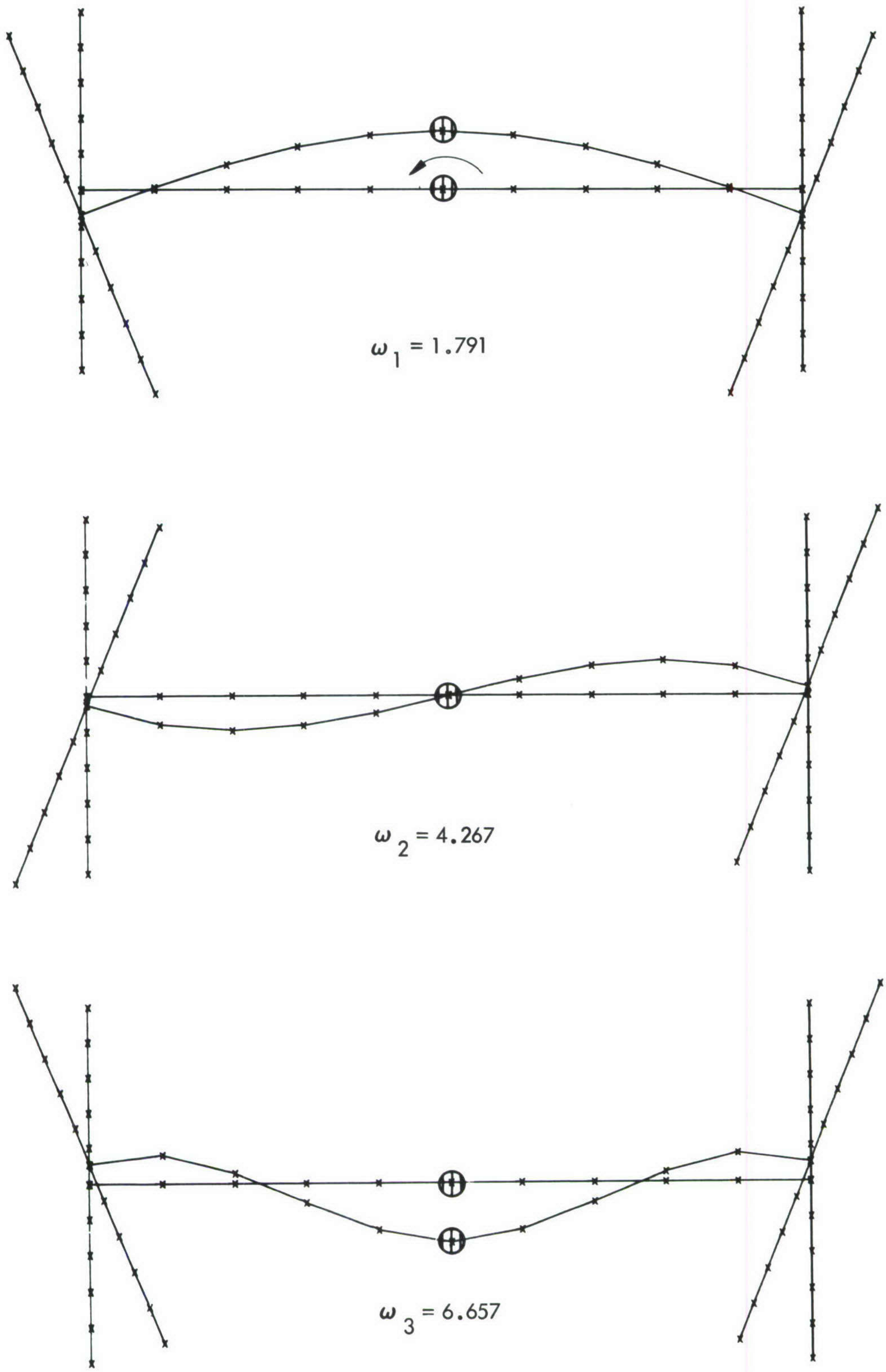

Figure 36. Two-Compartment Configuration Connected by 5-Foot-Diameter Spokes—In-Plane Vibration Mode Shapes

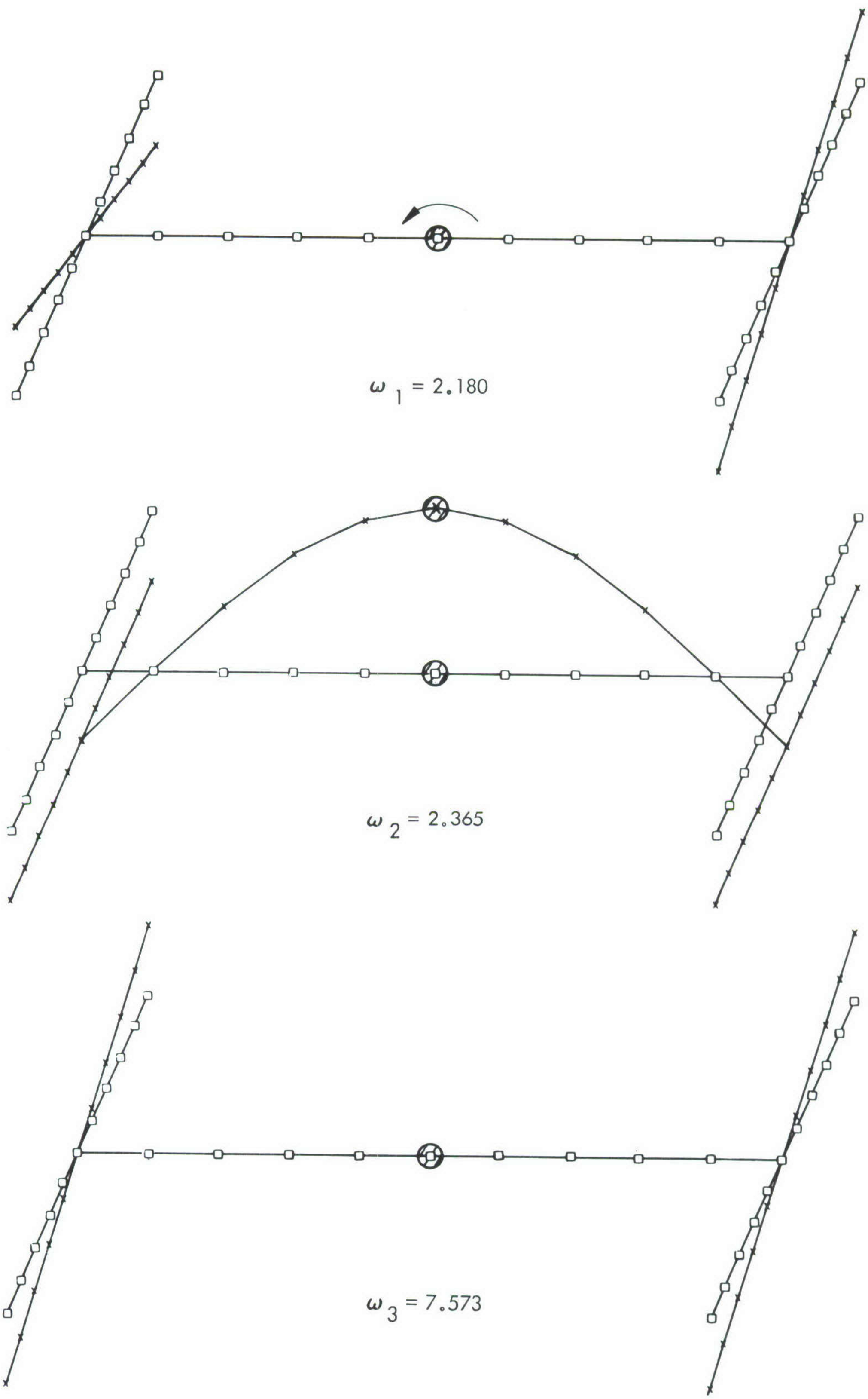

Figure 37. Two-Compartment Configuration Connected by 5-Foot-Diameter Spokes—Normal-To-Plane Vibration Mode Shapes

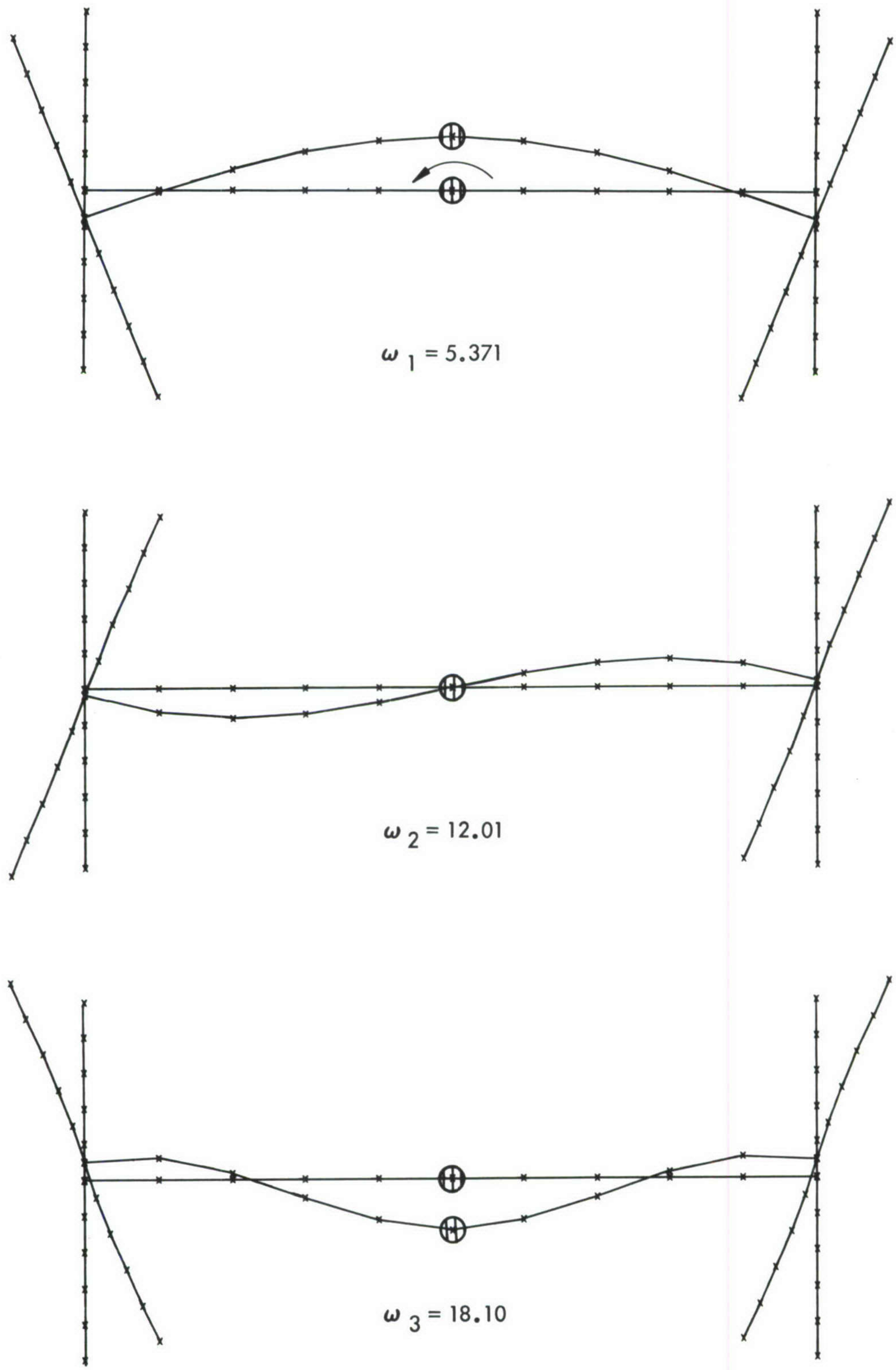

Figure 38. Two-Compartment Configuration Connected by 10-Foot-Diameter Spokes—In-Plane Vibration Mode Shapes

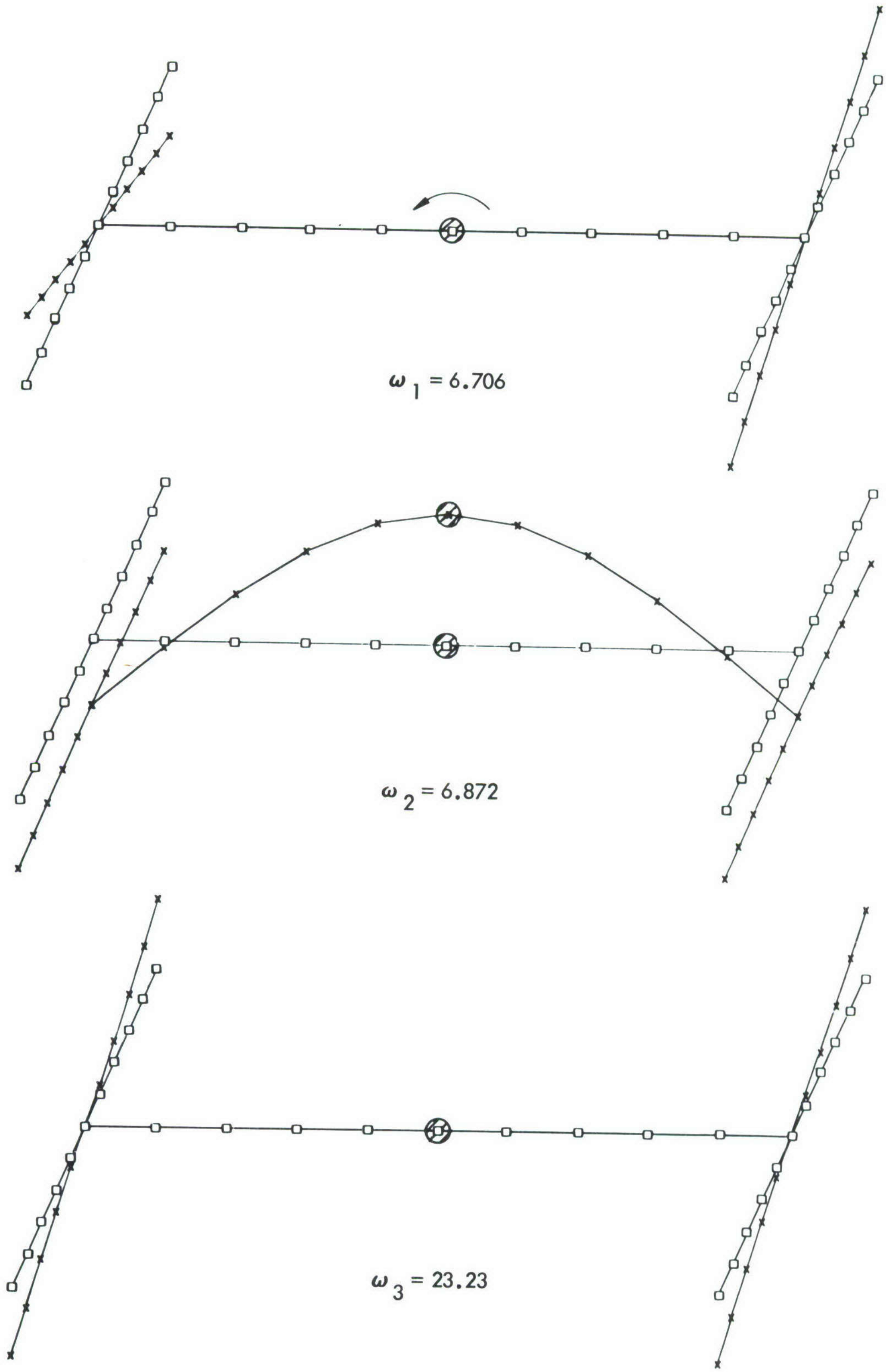

Figure 39. Two-Compartment Configuration Connected by 10-Foot-Diameter Spokes—Normal-To-Plane Vibration Mode Shapes

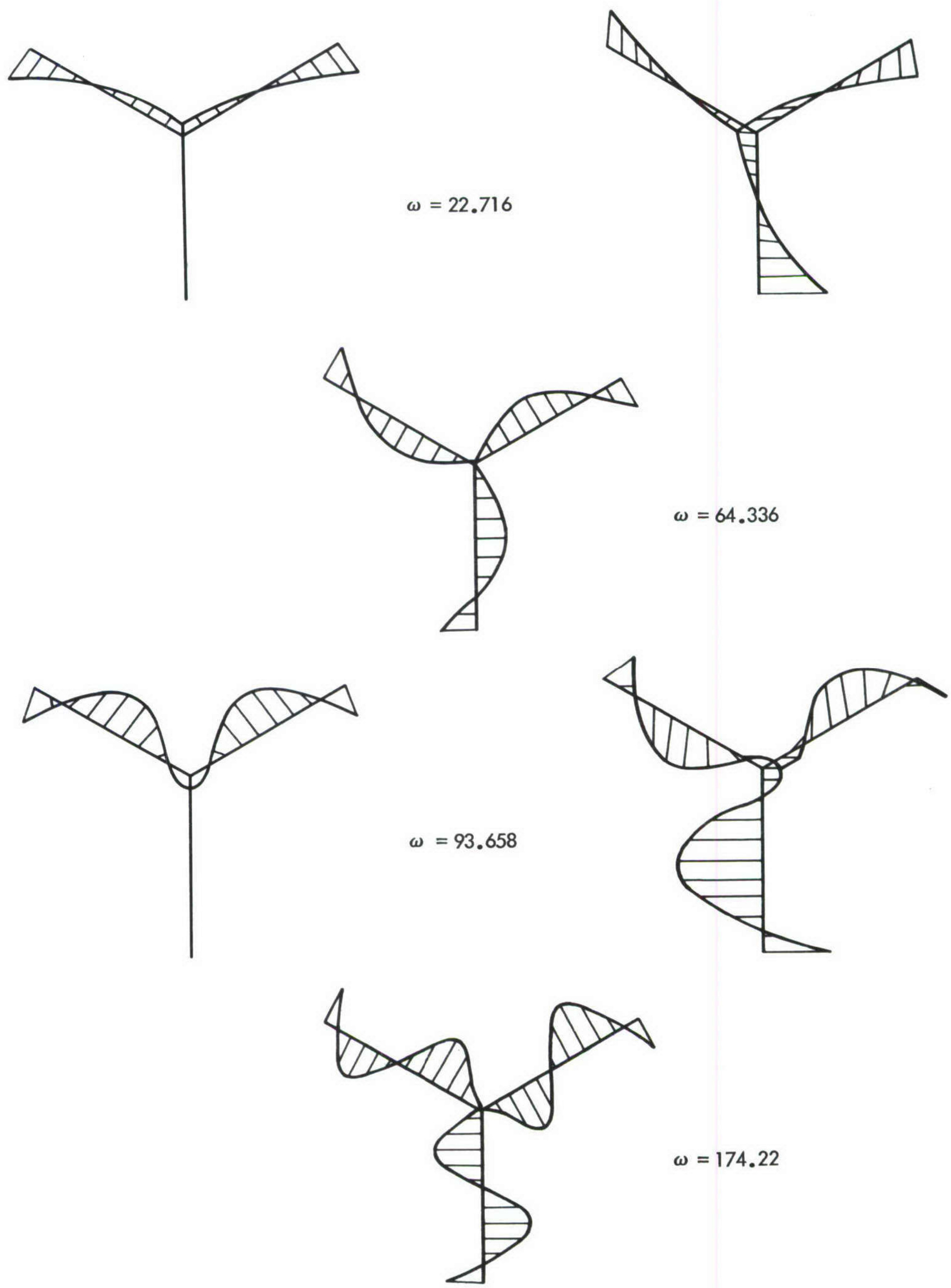

Figure 40. Y-Configuration—In-Plane Vibration Mode Shapes

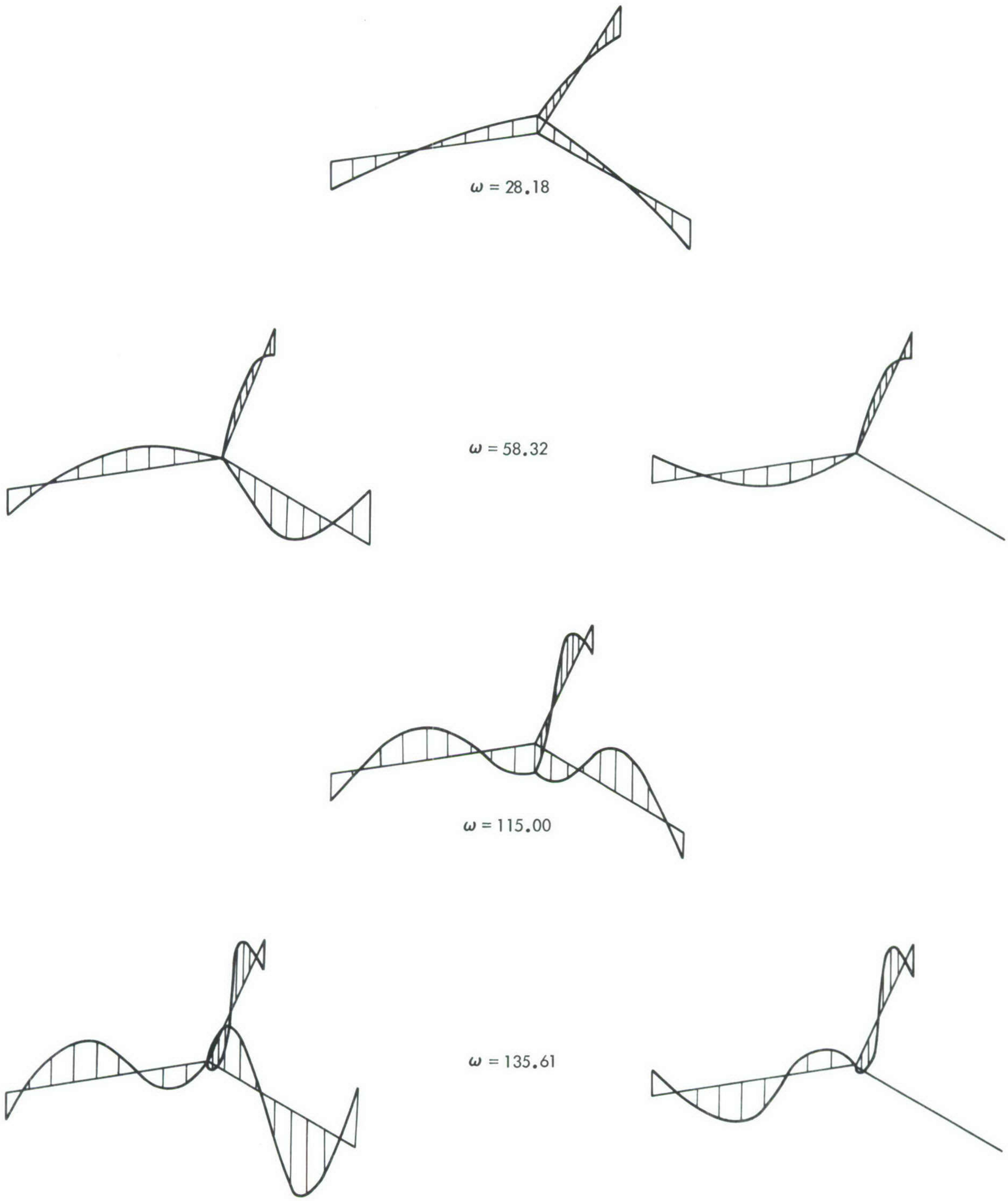

Figure 41. Y-Configuration—Normal-to-Plane Vibration Mode Shapes

7.0 A GENERAL APPROACH TO THE EQUATIONS OF UNSTEADY MOTIONS OF ELASTIC SPACE STATIONS

7.1 ANALYTICAL APPROACH

In a general analysis of the motion of an orbiting elastic space station during a six-month period or more, it is desirable that the earth's orbit angle degree of freedom about the sun be considered in the inertial frame of reference. The ellipticity of the earth's orbit and the perturbations of the orbit due to the moon are sufficiently small to be considered as zero in the analysis. Also, the oblateness of each of these bodies and the gravitational effects of the moon are sufficiently small to be considered as zero.

The unit vectors in this inertial Cartesian coordinate system are shown in Figure 42.

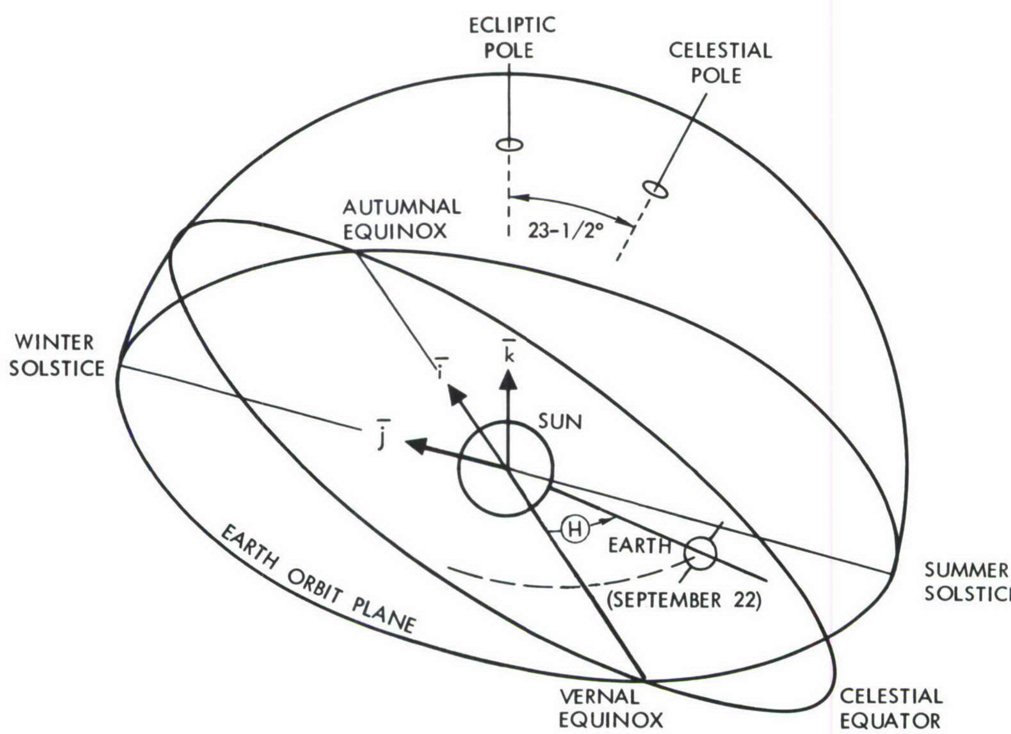

Figure 42. Inertial Coordinate System

The remainder of the development follows the development shown in ASD TR 61-171.[1] It varies only in the sequence of Euler angular rotations of the rigid space station, and in that elastic degrees of freedom of the space station are considered.

---
[1]Reference 12

When the expression for the kinetic energy is obtained and explicit terms are written that lead to expressions of forces that couple the earth orbit angle to the elastic degrees of freedom, it will be assumed that these forces are so small that they will not affect the motion of the system. This assumption will be justified when it is subsequently shown that elastic deformations within elastic limits do not significantly affect even the mean orbit of the space station about the earth.

In this analysis the earth is considered to be spherical and of uniform density. The origin of the earth-fixed coordinate system lies at the center of the earth, and is oriented so that the z_E axis points toward the North Pole, and at the time of some particular autumnal equinox, the x_E axis is coincident with the inertial x_I axis. See Figure 43.

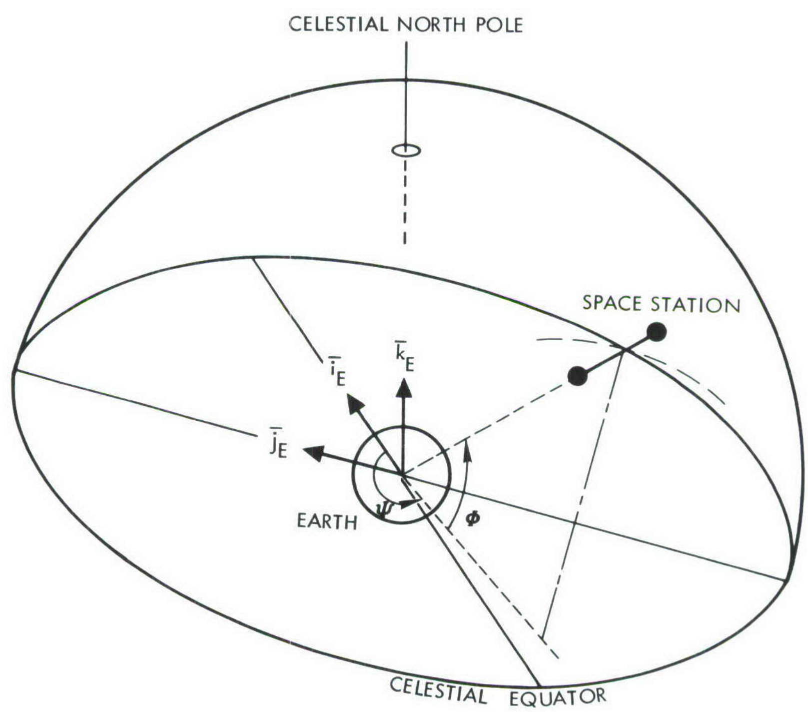

Figure 43. Earth-Fixed Coordinate System

A point located at x_E, y_E, z_E, relative to the center of the earth is, in the inertial system, located at

$$\begin{Bmatrix} x \\ y \\ z \end{Bmatrix}_I = -R_{EC} \begin{Bmatrix} C_{\Theta} \\ S_{\Theta} \\ 0 \end{Bmatrix} + \begin{bmatrix} 1 & 0 & 0 \\ 0 & C_c & -S_c \\ 0 & S_c & C_c \end{bmatrix} \begin{bmatrix} C_{\Omega} & -S_{\Omega} & 0 \\ S_{\Omega} & C_{\Omega} & 0 \\ 0 & 0 & 1 \end{bmatrix} \begin{Bmatrix} x \\ y \\ z \end{Bmatrix}_E \qquad (87)$$

where

R_{EC} = the earth's mean radius of orbit about the sun

Θ = the earth's orbit angle (Figure 42)

$C_{c,\Theta,\Omega}$ = cos (23 1/2°, Θ, Ω t)

$S_{c,\Theta,\Omega}$ = sin (23 1/2°, Θ, Ω t)

Ω = the earth's spin rate

{ } ~ a column matrix

[ ] ~ a rotational transformation matrix

The origin of the vehicle geocentric coordinate system is defined as the center of mass of the space station, and the coordinates are oriented so that the positive z_V axis points toward the center of the earth, and the first quadrant of the x_V - z_V plane contains the North Pole. Thus, a point located at x_V, y_V, z_V, relative to the center of mass of the space station is, in the earth-fixed system, located at

$$\begin{Bmatrix} x \\ y \\ z \end{Bmatrix}_E = \begin{bmatrix} C_{\Psi} & -S_{\Psi} & 0 \\ S_{\Psi} & C_{\Psi} & 0 \\ 0 & 0 & 1 \end{bmatrix} \begin{bmatrix} C_{\Phi} & 0 & -S_{\Phi} \\ 0 & 1 & 0 \\ S_{\Phi} & 0 & C_{\Phi} \end{bmatrix} \begin{bmatrix} 0 & 0 & -1 \\ 0 & 1 & 0 \\ 1 & 0 & 0 \end{bmatrix} \left\{ \begin{Bmatrix} 0 \\ 0 \\ -R_o \end{Bmatrix} + \begin{Bmatrix} x \\ y \\ z \end{Bmatrix}_V \right\} \qquad (88)$$

where

R_o = the space station radius of orbit about the earth

$C_{\Psi, \Phi}$ $\equiv$ cos (Ψ, Φ)

$S_{\Psi, \Phi}$ $\equiv$ sin (Ψ, Φ)

Ψ, Φ are defined by Figure 43.

The transformation from vehicle geocentric axes to vehicle body axes is accomplished by successive right-hand rule rotations about the z, y, and x axes, respectively, as shown in Figure 44.

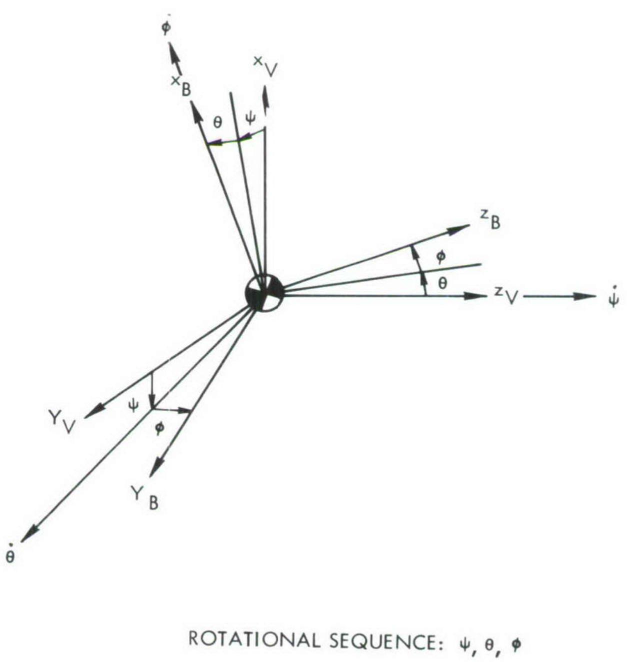

Figure 44. Euler Rotation Angles

Thus, a point at x_B, y_B, z_B, relative to the center of mass of the space station is, in the vehicle geocentric system, located at

$$\begin{Bmatrix} x \\ y \\ z \end{Bmatrix}_V = \begin{bmatrix} C_\psi & -S_\psi & 0 \\ S_\psi & C_\psi & 0 \\ 0 & 0 & 1 \end{bmatrix} \begin{bmatrix} C_\theta & 0 & S_\theta \\ 0 & 1 & 0 \\ -S_\theta & 0 & C_\theta \end{bmatrix} \begin{bmatrix} 1 & 0 & 0 \\ 0 & C_\phi & -S_\phi \\ 0 & S_\phi & C_\phi \end{bmatrix} \begin{Bmatrix} x \\ y \\ z \end{Bmatrix}_B \tag{89}$$

where

$$C_{\psi,\,\theta,\,\phi} \equiv \cos\,(\psi,\,\theta,\,\phi)$$

$$S_{\psi,\,\theta,\,\phi} \equiv \sin\,(\psi,\,\theta,\,\phi)$$

Symbolically, this transformation can be written as

$$\begin{Bmatrix} x \\ y \\ z \end{Bmatrix}_V = T_\psi\, T_\theta\, T_\phi \begin{Bmatrix} x \\ y \\ z \end{Bmatrix}_B \tag{90}$$

The velocities relative to the vehicle geocentric system are

$$\begin{Bmatrix} \dot{x} \\ \dot{y} \\ \dot{z} \end{Bmatrix}_V = T_\psi T_\theta T_\phi \begin{Bmatrix} \dot{x} \\ \dot{y} \\ \dot{z} \end{Bmatrix}_B + \left[\dot{T}_\psi T_\theta T_\phi + T_\psi \dot{T}_\theta T_\phi + T_\psi T_\theta \dot{T}_\phi\right] \begin{Bmatrix} x \\ y \\ z \end{Bmatrix}_B \tag{91}$$

$$\begin{Bmatrix} \dot{x} \\ \dot{y} \\ \dot{z} \end{Bmatrix}_V = T_\psi T_\theta T_\phi \left\{ \begin{Bmatrix} \dot{x} \\ \dot{y} \\ \dot{z} \end{Bmatrix}_B + T_\phi^* \left[\dot{T}_\phi + T_\theta^* \left[\dot{T}_\theta + T_\psi^* \dot{T}_\psi T_\theta\right] T_\phi\right] \begin{Bmatrix} x \\ y \\ z \end{Bmatrix}_B \right\} \tag{92}$$

where the symbol, *, indicates the transpose of the matrix, and

$$\dot{T}_\psi = \dot{\psi} \begin{bmatrix} -S_\psi & -C_\psi & 0 \\ C_\psi & -S_\psi & 0 \\ 0 & 0 & 0 \end{bmatrix} ; \quad \dot{T}_\theta = \dot{\theta} \begin{bmatrix} -S_\theta & 0 & C_\theta \\ 0 & 0 & 0 \\ -C_\theta & 0 & -S_\theta \end{bmatrix} ; \quad \dot{T}_\phi = \dot{\phi} \begin{bmatrix} 0 & 0 & 0 \\ 0 & -S_\phi & -C_\phi \\ 0 & C_\phi & -S_\phi \end{bmatrix} \tag{93}$$

Carrying out the indicated matrix multiplication

$$\begin{Bmatrix} \dot{x} \\ \dot{y} \\ \dot{z} \end{Bmatrix}_V = T_\psi T_\theta T_\phi \left\{ \begin{Bmatrix} \dot{x} \\ \dot{y} \\ \dot{z} \end{Bmatrix}_B + \begin{bmatrix} 0 & (\dot\theta S_\phi - \dot\psi C_\theta C_\phi) & (\dot\theta C_\phi + \dot\psi C_\theta S_\phi) \\ -(\dot\theta S_\phi - \dot\psi C_\theta C_\phi) & 0 & -(\dot\phi - \dot\psi S_\theta) \\ -(\dot\theta C_\phi + \dot\psi C_\theta S_\phi) & (\dot\phi - \dot\psi S_\theta) & 0 \end{bmatrix} \begin{Bmatrix} x \\ y \\ z \end{Bmatrix}_B \right\} \tag{94}$$

The parallel development in vector notation of the velocities relative to the vehicle geocentric system makes use of dyadics. Define

$$II_\sigma \equiv \bar{i}_\sigma \bar{i}_\sigma + \bar{j}_\sigma \bar{j}_\sigma + \bar{k}_\sigma \bar{k}_\sigma \tag{95}$$

Then, the radius vector and velocity vector in the geocentric system can be written as

$$\bar{R}_V = II_V \cdot \bar{R}_B \tag{96}$$

and

$$\dot{\bar{R}}_V = II_V \cdot [\dot{\bar{R}}_B + \bar{\Omega} \times \bar{R}_B] \tag{97}$$

where $\bar{\Omega}$ is the rotation vector of the body axis system relative to the geocentric system. The components of this vector in the body axis system are p, q, and r; i.e.,

$$\bar{\Omega} = p\, \bar{i}_B + q\, \bar{j}_B + r\, \bar{k}_B \tag{98}$$

and

$$\bar{\Omega} \times \bar{R}_B = (q\, z_B - r\, y_B)\, \bar{i}_B + (r\, x_B - p\, z_B)\, \bar{j}_B + (p\, y_B - q\, x_B)\, \bar{k}_B \tag{99}$$

Thus, the velocity in geocentric coordinates can be written

$$\begin{Bmatrix} \dot{x} \\ \dot{y} \\ \dot{z} \end{Bmatrix}_V = \begin{Bmatrix} \bar{i} \\ \bar{j} \\ \bar{k} \end{Bmatrix}_V \cdot \dot{\bar{R}}_V \tag{100}$$

or,

$$\begin{Bmatrix} \dot{x} \\ \dot{y} \\ \dot{z} \end{Bmatrix}_V = \begin{Bmatrix} \bar{i} \\ \bar{j} \\ \bar{k} \end{Bmatrix}_V \cdot \mathrm{II}_V \cdot \begin{bmatrix} \bar{i} & & \\ & \bar{j} & \\ & & \bar{k} \end{bmatrix}_B \left\{ \begin{Bmatrix} \dot{x} \\ \dot{y} \\ \dot{z} \end{Bmatrix}_B + \begin{bmatrix} 0 & -r & q \\ r & 0 & -p \\ -q & p & 0 \end{bmatrix} \begin{Bmatrix} x \\ y \\ z \end{Bmatrix}_B \right\} \tag{101}$$

Term by term comparison with equation (94) gives

$$\left. \begin{aligned} p &= \dot{\phi} - \dot{\psi} \sin \theta \\ q &= \dot{\theta} \cos \phi + \dot{\psi} \cos \theta \sin \phi \\ r &= -\dot{\theta} \sin \phi + \dot{\psi} \cos \theta \cos \phi \end{aligned} \right\} \tag{102}$$

which agree with equations (4.5, 3).[1] In matrix notation these equations are

$$\begin{Bmatrix} p \\ q \\ r \end{Bmatrix} = \begin{Bmatrix} \dot{\phi} \\ 0 \\ 0 \end{Bmatrix} + T_\phi^* \left\{ \begin{Bmatrix} 0 \\ \dot{\theta} \\ 0 \end{Bmatrix} + T_\theta^* \begin{Bmatrix} 0 \\ 0 \\ \dot{\psi} \end{Bmatrix} \right\} \tag{103}$$

Equivalent expressions relative to the inertial frame of reference are obtained by substituting equations (88) and (89) into equation (87) and writing equation (87) in symbolic form as

$$\begin{Bmatrix} x \\ y \\ z \end{Bmatrix}_I = -R_{EC} \begin{Bmatrix} C_{\Theta} \\ S_{\Theta} \\ 0 \end{Bmatrix} + T_C T_\Omega T_\Psi T_\Phi T_V \left\{ \begin{Bmatrix} 0 \\ 0 \\ -R_o \end{Bmatrix} + T_\psi T_\theta T_\phi \begin{Bmatrix} x \\ y \\ z \end{Bmatrix}_B \right\} \tag{104}$$

Differentiation results in

---

[1]Reference 5

$$\left\{\begin{matrix}\dot{x}\\ \dot{y}\\ \dot{z}\end{matrix}\right\}_I = R_{EC}\,\dot{\Theta}\left\{\begin{matrix}S_{\Theta}\\ -C_{\Theta}\\ 0\end{matrix}\right\} + {}_I T_V \left\{\left\{\begin{matrix}0\\ 0\\ -R_o\end{matrix}\right\} + {}_V T_B \left\{\left\{\begin{matrix}\dot{x}\\ \dot{y}\\ \dot{z}\end{matrix}\right\}_B + \begin{bmatrix}0 & -r & 0\\ r & 0 & -p\\ -q & p & 0\end{bmatrix}\left\{\begin{matrix}x\\ y\\ z\end{matrix}\right\}_B\right\}\right.$$

$$\left. + \begin{bmatrix}0 & (\dot{\Psi}+\Omega)S_{\Phi} & -\dot{\Phi}\\ -(\dot{\Psi}+\Omega)S_{\Phi} & 0 & -(\dot{\Psi}+\Omega)C_{\Phi}\\ \Phi & (\dot{\Psi}+\Omega)C_{\Phi} & 0\end{bmatrix}\left\{\left\{\begin{matrix}0\\ 0\\ -R_o\end{matrix}\right\} + {}_V T_B \left\{\begin{matrix}x\\ y\\ z\end{matrix}\right\}_B\right\}\right\}$$

or

$$\left\{\begin{matrix}\dot{x}\\ \dot{y}\\ \dot{z}\end{matrix}\right\}_I = R_{EC}\,\dot{\Theta}\left\{\begin{matrix}S_{\Theta}\\ -C_{\Theta}\\ 0\end{matrix}\right\} + {}_I T_E \left\{\left\{\begin{matrix}R_o\\ 0\\ 0\end{matrix}\right\} + R_o\left\{\begin{matrix}0\\ (\dot{\Psi}+\Omega)C_{\Phi}\\ \dot{\Phi}\end{matrix}\right\}\right\}$$

$$+ {}_I T_B \left\{\left\{\begin{matrix}\dot{x}\\ \dot{y}\\ \dot{z}\end{matrix}\right\}_B + \begin{bmatrix}0 & -r' & q'\\ r' & 0 & -p'\\ -q' & p' & 0\end{bmatrix}\left\{\begin{matrix}x\\ y\\ z\end{matrix}\right\}_B\right\} \qquad (105)$$

where

$${}_I T_V = {}_I T_E T_V$$

$${}_I T_E = T_C T_{\Omega} T_{\Psi} T_{\Phi}$$

$${}_I T_B = {}_I T_V \; {}_V T_B$$

$${}_V T_B = T_{\psi} T_{\theta} T_{\phi}$$

and

$$\begin{bmatrix}0 & -r' & q'\\ r' & 0 & -p'\\ -q' & p' & 0\end{bmatrix} = \begin{bmatrix}0 & -r & q\\ r & 0 & -p\\ -q & p & 0\end{bmatrix} + {}_V T_B^{*}\begin{bmatrix}0 & (\dot{\Psi}+\Omega)S_{\Phi} & -\dot{\Phi}\\ -(\dot{\Psi}+\Omega)S_{\Phi} & 0 & -(\dot{\Psi}+\Omega)C_{\Phi}\\ \dot{\Phi} & (\dot{\Psi}+\Omega)C_{\Phi} & 0\end{bmatrix} {}_V T_B$$

or

$$\begin{Bmatrix} p' \\ q' \\ r' \end{Bmatrix} = \begin{Bmatrix} \dot{\phi} \\ 0 \\ 0 \end{Bmatrix} + T_{\phi}^{*} \left\{ \begin{Bmatrix} 0 \\ \dot{\theta} \\ 0 \end{Bmatrix} + T_{\theta}^{*} \left\{ \begin{Bmatrix} 0 \\ 0 \\ \dot{\psi} \end{Bmatrix} + T_{\psi}^{*} T_{V}^{*} \left\{ \begin{Bmatrix} 0 \\ -\dot{\Phi} \\ 0 \end{Bmatrix} + T_{\Phi}^{*} \begin{Bmatrix} 0 \\ 0 \\ \dot{\psi} + \Omega \end{Bmatrix} \right\} \right\} \right\}$$

Carrying out the indicated operations

$$\begin{Bmatrix} p' \\ q' \\ r' \end{Bmatrix} = \begin{bmatrix} (1) & 0 & (-S_{\theta}) & (C_{\theta} C_{\psi} C_{\Phi} + S_{\theta} S_{\Phi}) & (-C_{\theta} S_{\psi}) \\ (0) & (C_{\phi}) & (C_{\theta} S_{\phi}) & ([S_{\phi} S_{\theta} C_{\psi} - C_{\phi} S_{\psi}]\, C_{\Phi} - S_{\phi} C_{\theta} S_{\Phi} & (-S_{\phi} S_{\theta} S_{\psi} - C_{\phi} C_{\psi}) \\ (0) & (-S_{\phi}) & (C_{\theta} C_{\phi}) & ([C_{\phi} S_{\theta} C_{\psi} + S_{\phi} S_{\psi}]\, C_{\Phi} - C_{\phi} C_{\theta} S_{\Phi}) & (-C_{\phi} S_{\theta} S_{\psi} + S_{\phi} C_{\psi}) \end{bmatrix} \begin{Bmatrix} \dot{\phi} \\ \dot{\theta} \\ \dot{\psi} \\ \dot{\Psi} + \Omega \\ \dot{\Phi} \end{Bmatrix} \qquad (106)$$

From equations (105) and (106) we can write the total kinetic energy (T) of the space station spinning freely and in orbit about the rotating and revolving earth.

$$T = \frac{1}{2} \iiint [\dot{x}\ \dot{y}\ \dot{z}]_{I} \begin{Bmatrix} \dot{x} \\ \dot{y} \\ \dot{z} \end{Bmatrix}_{I} dm$$

or

$$T = \frac{1}{2} \iiint \Bigg(R_{EC}^{2}\, \dot{\Theta}^{2} + 2 R_{EC} \dot{\Theta} [S_{\Theta}\ \ -C_{\Theta}\ \ 0]\ {}_{I}T_{E} \left\{ \begin{Bmatrix} \dot{R}_{o} \\ 0 \\ 0 \end{Bmatrix} + R_{o} \begin{Bmatrix} 0 \\ (\dot{\Psi} + \Omega) C_{\Phi} \\ \dot{\Phi} \end{Bmatrix} \right\}$$

$$+ 2 R_{EC} \dot{\Theta} [S_{\Theta}\ \ -C_{\Theta}\ \ 0]\ {}_{I}T_{B} \left\{ \begin{Bmatrix} \dot{x} \\ \dot{y} \\ \dot{z} \end{Bmatrix}_{B} + \begin{bmatrix} 0 & -r' & q' \\ r' & 0 & -p' \\ -q' & p' & 0 \end{bmatrix} \begin{Bmatrix} x \\ y \\ z \end{Bmatrix}_{B} \right\}$$

$$+ \dot{R}_{0}^{2} + R_{0}^{2} \left((\dot{\Psi} + \Omega)^{2} C_{\Phi}^{2} + \dot{\Phi}^{2} \right)$$

$$+ 2 [\dot{R}_{0}\ \ R_{0}(\dot{\Psi} + \Omega) C_{\Phi}\ \ R_{0}\dot{\Phi}]\ {}_{E}T_{B} \left\{ \begin{Bmatrix} \dot{x} \\ \dot{y} \\ \dot{z} \end{Bmatrix}_{B} + \begin{bmatrix} 0 & -r' & q' \\ r' & 0 & -p' \\ -q' & p' & 0 \end{bmatrix} \begin{Bmatrix} x \\ y \\ z \end{Bmatrix}_{B} \right\}$$

$$+ \left(\dot{x}_B^{\,2} + \dot{y}_B^{\,2} + \dot{z}_B^{\,2}\right) + 2\,[\dot{x}\;\dot{y}\;\dot{z}]_B \begin{bmatrix} 0 & z & -y \\ -z & 0 & x \\ y & -x & 0 \end{bmatrix}_B \begin{Bmatrix} p' \\ q' \\ r' \end{Bmatrix}$$

$$+ [p'\;q'\;r'] \begin{bmatrix} 0 & -z & y \\ z & 0 & -x \\ -y & x & 0 \end{bmatrix}_B \begin{bmatrix} 0 & z & -y \\ -z & 0 & x \\ y & -x & 0 \end{bmatrix}_B \begin{Bmatrix} p' \\ q' \\ r' \end{Bmatrix} \Bigg)\, dm \qquad (107)$$

The total kinetic energy of the earth and space station system would require integration over the volume of the earth, too. The equation (107) has already been specialized to the case in which the earth's orbit radius about the sun is constant. At this point it will be further specialized to the case in which (1) the center of the earth is considered to be fixed in space, i.e., $\Theta = 0$, (2) the earth is not rotating, i.e., $\Omega = 0$, and (3) the space station is in an equatorial orbit, i.e., $\Phi = \dot{\Phi} = 0$. For this specialized case the total kinetic energy can be written as

$$T = \frac{1}{2}\Bigg(m\left(R_0^{\,2} + R_0^{\,2}\dot{\Psi}^2\right) + 2\,[0 \;\; R_0\dot{\Psi} \;\; -\dot{R}_0]\; {}_V T_B \Bigg\{ \iiint \begin{Bmatrix} \dot{x} \\ \dot{y} \\ \dot{z} \end{Bmatrix}_B dm$$

$$+ \iiint \begin{bmatrix} 0 & z & -y \\ -z & 0 & x \\ y & -x & 0 \end{bmatrix}_B dm \begin{Bmatrix} p' \\ q' \\ r' \end{Bmatrix} \Bigg\} + \iiint \left(\dot{x}^2 + \dot{y}^2 + \dot{z}^2\right)_B dm$$

$$+ 2\iiint [\dot{x}\;\dot{y}\;\dot{z}]_B \begin{bmatrix} 0 & z & -y \\ -z & 0 & x \\ y & -x & 0 \end{bmatrix}_B dm \begin{Bmatrix} p' \\ q' \\ r' \end{Bmatrix}$$

$$+ [p'\;q'\;r'] \iiint d \begin{bmatrix} I_{xx} & -I_{xy} & -I_{xz} \\ -I_{xy} & I_{yy} & -I_{yz} \\ -I_{xz} & -I_{yz} & I_{zz} \end{bmatrix}_B \begin{Bmatrix} p' \\ q' \\ r' \end{Bmatrix} \Bigg) \qquad (108)$$

The expression for the kinetic energy can be used to develop equations of motion for systems that are not elastically restrained as well as for those that are elastically restrained. In the latter case, the expression can be further specialized and simplified as shown in Section 7.2.

The expression for the potential energy is needed in order to complete the Lagrangian. The potential energy of an elastically-restrained system can be written as the sum of the potential due to elastic deformations and gravity, i.e.,

$$U = U_E + U_G \tag{109}$$

Generally the potential due to elastic deformations can be written as

$$U_E = \int_\Gamma \overline{F}_E \cdot d\,\overline{R}$$

The more detailed expression will be developed later in this section.

The potential (dU_{G_n}), of an incremental mass (dm_n), due to gravity can be written as

$$dU_{G_n} = \int_{-\infty}^{|\overline{R}_O + \overline{r}_n|} \frac{GM_E\, dr}{r^2}\, dm_n$$

or

$$dU_{G_n} = -\frac{GM_E\, dm_n}{|\overline{R}_0 + \overline{r}_n|} \tag{110}$$

where

G = gravitational constant

M_E = mass of the earth

$|\overline{R}_o + \overline{r}_n|$ = distance of the incremental mass from the center of the earth

The forces due to mutual gravitational attraction are negligible by comparison to the centrifugal forces of the spinning space station.

The location of the n^{th} incremental mass in earth geocentric coordinates is

$$\begin{Bmatrix} x_n \\ y_n \\ z_n \end{Bmatrix}_G = \begin{Bmatrix} R_o \\ o \\ o \end{Bmatrix} + {}_G T_B \begin{Bmatrix} x_n \\ y_n \\ z_n \end{Bmatrix}_B$$

and

$$|\bar{R}_o + \bar{r}_n|^2 = [x_n \; y_n \; z_n]_G \begin{Bmatrix} x_n \\ y_n \\ z_n \end{Bmatrix}_G \tag{111}$$

or

$$|\bar{R}_o + \bar{r}_n|^2 = R_o^2 \left(1 + [2 \;\; 0 \;\; 0]\, {}_G T_B \begin{Bmatrix} x_n/R_o \\ y_n/R_o \\ z_n/R_o \end{Bmatrix}_B + \left(\frac{x_n}{R_o}\right)_B^2 + \left(\frac{y_n}{R_o}\right)_B^2 + \left(\frac{z_n}{R_o}\right)_B^2 \right) \tag{112}$$

Using equations (88) and (89)

$$|\bar{R}_o + \bar{r}_n|^2 = R_o^2 \left(1 + 2\left(\frac{x_n}{R_o}\right)_B S_\theta - 2\left(\frac{y_n}{R_o}\right)_B C_\theta S_\phi - 2\left(\frac{z_n}{R_o}\right)_B C_\theta C_\phi + \left(\frac{x_n}{R_o}\right)_B^2 + \left(\frac{y_n}{R_o}\right)_B^2 + \left(\frac{z_n}{R_o}\right)_B^2 \right) \tag{113}$$

Expanding the binomial, retaining only second order terms, and integrating over the volume of the space station

$$U_G = \frac{-GM_E}{R_o} \iiint \left(1 - \left(\frac{x_n}{R_o}\right) S_\theta + \left(\frac{y_n}{R_o}\right) C_\theta S_\phi + \left(\frac{z_n}{R_o}\right) C_\theta C_\phi \right.$$

$$- \left(\frac{x_n}{R_o}\right)^2 \frac{1 - 3S_\theta^{\,2}}{2} - \left(\frac{y_n}{R_o}\right)^2 \frac{1 - 3C_\theta^{\,2} S_\phi^{\,2}}{2}$$

$$- \left(\frac{z_n}{R_o}\right)^2 \frac{1 - 3C_\theta^{\,2} C_\phi^{\,2}}{2} - 3\left(\frac{x_n}{R_o}\right)\left(\frac{y_n}{R_o}\right) S_\theta C_\theta S_\phi$$

$$\left. - 3\left(\frac{x_n}{R_o}\right)\left(\frac{z_n}{R_o}\right) S_\theta C_\theta C_\phi + 3\left(\frac{y_n}{R_o}\right)\left(\frac{z_n}{R_o}\right) C_\theta^{\,2} S_\phi C_\phi + \cdot\cdot \right) dm \tag{114}$$

Because the origin of the body axes is at the center of mass of the space station

$$\iiint \left(\frac{x_n}{R_o}\right) dm = \iiint \left(\frac{y_n}{R_o}\right) dm = \iiint \left(\frac{z_n}{R_o}\right) dm = 0 \tag{115}$$

The product of inertia terms,

$$\frac{I_{xy}}{R_o^{\,2}} = \iiint \left(\frac{x_n}{R_o}\right)\left(\frac{y_n}{R_o}\right) dm; \quad \frac{I_{xz}}{R_o^{\,2}} = \iiint \left(\frac{x_n}{R_o}\right)\left(\frac{z_n}{R_o}\right) dm;$$

$$\frac{I_{yz}}{R_o^{\,2}} = \iiint \left(\frac{y_n}{R_o}\right)\left(\frac{z_n}{R_o}\right) dm \tag{116}$$

are retained to emphasize that during an analysis of deployment or docking maneuvers, the instantaneous principal axes must be considered in addition to the instantaneous center of mass. Therefore, the gravitational potential is written as

$$U_G = \frac{-GM_E}{R_o}\left(m + \frac{3}{2}\iiint\left(\left(\frac{x_n}{R_o}\right)^2 S_\theta^{\ 2} + \left(\frac{y_n}{R_o}\right)^2 C_\theta^2 S_\phi^{\ 2} + \left(\frac{z_n}{R_o}\right)^2 C_\theta^{\ 2} C_\phi^{\ 2}\right) dm\right.$$

$$- \frac{1}{2}\iiint\left(\left(\frac{x_n}{R_o}\right)^2 + \left(\frac{y_n}{R_o}\right)^2 + \left(\frac{z_n}{R_o}\right)^2\right) dm$$

$$\left. - 3\left(I_{xy} S_\theta C_\theta S_\phi + I_{xz} S_\theta C_\theta C_\phi - I_{yz} C_\theta^{\ 2} S_\phi C_\phi\right)\right) \tag{117}$$

Substituting equation (117) into equation (109), and using equation (108) we can write the Lagrangian using the expression

$$L = T - U_E - U_G \tag{118}$$

and generate the equations of motion from the general equation

$$\frac{d}{dt}\frac{\partial L}{\partial \dot{q}_i} - \frac{\partial L}{\partial q_i} = Q_i, \ i = 1, 2, 3, \ldots \tag{119}$$

7.2 CABLE-COUNTERWEIGHT CONFIGURATION—FULLY DEPLOYED AND SPINNING

The general analysis of a spinning elastic space station in orbit about an inertially fixed earth is applied in this section to an idealized configuration as shown in Figure 45.

The motion of the elements of the space station is restricted to the y_B direction in the spin plane and the spin plane is coincident with the orbit plane, i.e.,

$$\phi = \psi = \frac{\pi}{2}; \ \dot{\phi} = \dot{\psi} = \dot{z}_{n_B} = \dot{x}_{n_B} = 0 \tag{120}$$

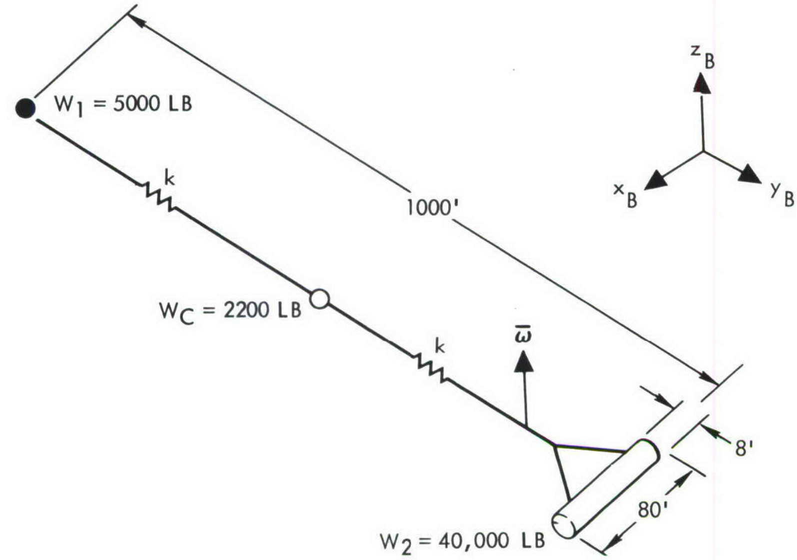

Figure 45. Idealized Cable-Counterweight Space Station

Then

$$
{}_V T_B = \begin{bmatrix} 0 & 0 & 1 \\ C_\theta & S_\theta & 0 \\ -S_\theta & C_\theta & 0 \end{bmatrix} \tag{121}
$$

And from equation (106),

$$
\begin{Bmatrix} p' \\ q' \\ r' \end{Bmatrix} = \begin{bmatrix} 1 & 0 & 0 \\ 0 & 0 & +1 \\ 0 & -1 & 0 \end{bmatrix} \left\{ \begin{Bmatrix} 0 \\ \dot{\theta} \\ 0 \end{Bmatrix} + \begin{bmatrix} C_\theta & 0 & -S_\theta \\ 0 & 1 & 0 \\ S_\theta & 0 & C_\theta \end{bmatrix} \left\{ \begin{bmatrix} 0 & 1 & 0 \\ -1 & 0 & 0 \\ 0 & 0 & 1 \end{bmatrix} \begin{bmatrix} 0 & 0 & 1 \\ 0 & 1 & 0 \\ -1 & 0 & 0 \end{bmatrix} \begin{Bmatrix} 0 \\ 0 \\ \dot{\Psi} \end{Bmatrix} \right\} \right\}
$$

or

$$\begin{Bmatrix} p' \\ q' \\ r' \end{Bmatrix} = \begin{Bmatrix} 0 \\ 0 \\ \dot{\Psi} - \dot{\theta} \end{Bmatrix} \tag{122}$$

$$\begin{Bmatrix} x_n \\ y_n \\ z_n \end{Bmatrix}_B = \begin{Bmatrix} x_{o_n} \\ y_{o_n} \\ z_{o_n} \end{Bmatrix}_B + \begin{Bmatrix} 0 \\ \eta_n \\ 0 \end{Bmatrix} \tag{123}$$

where

η_n = the elastic deflection of the n^{th} mass

and

$$\begin{Bmatrix} \dot{x}_n \\ \dot{y}_n \\ \dot{z}_n \end{Bmatrix}_B = \begin{Bmatrix} 0 \\ \dot{\eta}_n \\ 0 \end{Bmatrix} \tag{124}$$

The approach taken in this analysis is to assume that fluctuating elastic deflections are small, then to determine whether mechanical devices will be required to keep them small. From equation (108) we get

$$\begin{aligned} T = \frac{1}{2} \Bigg(& (\dot{R}_o^{\,2} + R_o^{\,2} \dot{\Psi}^2) \sum m_n + 2 (R_o \dot{\Psi} S_\theta - \dot{R}_o C_\theta) \sum m_n \dot{\eta}_n \\ & + 2 (\dot{\Psi} - \dot{\theta}) \iiint \cancelto{0}{x_{o_2} \dot{\eta}_2} \, dm_2 + \sum m_n \dot{\eta}_n^{\,2} \\ & + (\dot{\Psi} - \dot{\theta})^2 \Big(m_1 (y_{o_1} + \eta_1)^2 + m_C (y_{o_C} + \eta_C)^2 \\ & + \iiint \big(x_2^{\,2} + (y_{o_2} + \eta_2)^2 \big) dm_2 \Big) \Bigg) \end{aligned} \tag{125}$$

and from equation (117)

$$U_G = \frac{-GM_E}{R_o}\left(\sum m_n + \frac{3}{2}\left(m_1\left(\frac{y_{o_1} + \eta_1}{R_o}\right)^2 C_\theta^{\,2} + m_C\left(\frac{y_{o_C} + \eta_c}{R_o}\right)^2 C_\theta^{\,2}\right.\right.$$

$$+ \iiint \left(\left(\frac{x_{o_2}}{R_o}\right)^2 S_\theta^{\,2} + \left(\frac{y_{o_2} + \eta_2}{R_o}\right)^2 C_\theta^{\,2}\right) dm_2\Bigg)$$

$$- \frac{1}{2}\left(m_1\left(\frac{y_{o_1} + \eta_1}{R_o}\right)^2 + m_C\left(\frac{y_{o_C} + \eta_C}{R_o}\right)^2\right.$$

$$+ \iiint\left(\left(\frac{x_{o_2}}{R_o}\right)^2 + \left(\frac{y_{o_2} + \eta_2}{R_o}\right)^2\right) dm_2\Bigg) \tag{126}$$

$$\left. + \text{ product of inertia terms assumed equal to zero}\right)$$

The potential energy caused by deformation of the springs is

$$U_E = \frac{1}{2} k \left((\eta_2 - \eta_C)^2 + (\eta_C - \eta_1)^2\right) \tag{127}$$

Now, by allowing small perturbations on R_o, $\dot{\Psi}$, and θ,

$$\left.\begin{aligned}
R_o &= R_{o_e} + \delta R & \dot{R}_o &= \delta\dot{R} & \ddot{R}_o &= \delta\ddot{R} \\
& & \dot{\Psi} &= \dot{\Psi}_e + \delta\dot{\Psi} & \ddot{\Psi} &= \delta\ddot{\Psi} \\
\theta &= \omega t + \delta\theta & \dot{\theta} &= \omega + \delta\dot{\theta} & \ddot{\theta} &= \delta\ddot{\theta}
\end{aligned}\right\} \tag{128}$$

where

$$\omega = 0.4 \text{ rad/sec}$$

and

$$\sin\theta = \sin\omega t + \delta\theta\cos\omega t;\ \cos\theta = \cos\omega t - \delta\theta\sin\omega t \tag{129}$$

The degree of freedom $q = \delta R$ yields the equation

$$\frac{d}{dt}\frac{\partial T}{\partial \delta R} - \frac{\partial T}{\partial \delta R} = \delta\ddot{R}\sum m_n + (\omega + \delta\dot{\theta})(S_\omega + \delta\theta C_\omega)\sum m_n\dot{\eta}_n$$

$$- (C_\omega - \delta\theta S_\omega)\sum m_n\ddot{\eta}_n - (R_{o_e} + \delta R)(\dot{\Psi}_e + \delta\Psi)^2\sum m_n$$

$$+ (\dot{\Psi}_e + \delta\dot{\Psi})(S_\omega + \delta\theta C_\omega)\sum m_n\dot{\eta}_n$$

and

$$\frac{\partial U}{\partial \delta R} = \frac{GM_E}{R_{o_e}^2}\left[1 - 2\left(\frac{\delta R}{R_{o_e}}\right) + \ldots\right]\sum m_n$$

$$+ 3\frac{GM_E}{R_{o_e}^2}\left(\frac{3(C_\omega - \delta\theta S_\omega)^2 - 1}{2}\iiint\left(\frac{y_o}{R_{o_e}}\right)^2\left(1 + 2\frac{\eta}{y_o} - 4\frac{\delta R}{R_{o_e}} + \ldots\right)dm\right.$$

$$\left.+ \frac{3(S_\omega + \delta\theta C_\omega)^2 - 1}{2}\iiint\left(\frac{x_o}{R_{o_e}}\right)^2\left(1 - 4\frac{\delta R}{R_{o_e}} + \ldots\right)dm\right)$$

By retaining only first-order terms in the perturbations,

$$Q_1 = -R_{o_e}\dot{\Psi}_e^2\sum m_n + \frac{GM_E}{R_{o_e}^2}\sum m_n + 3\frac{GM_E}{R_{o_e}^2}\left(\frac{3C_\omega^2 - 1}{2}\sum m_n\left(\frac{y_{o_n}}{R_{o_e}}\right)^2\right.$$

$$\left.+ \frac{3S_\omega^2 - 1}{2}\sum m_n\left(\frac{x_{o_n}}{R_{o_e}}\right)^2\right) + (\delta\ddot{R} - \dot{\Psi}_e^2\delta R - 2R_{o_e}\dot{\Psi}_e\delta\Psi)\sum m_n$$

$$+ (\omega + \dot{\Psi}_e) S_\omega \sum m_n \dot{\eta}_n - C_\omega \sum m_n \ddot{\eta}_n - 2 \frac{GM_E}{R_{o_e}^2} \frac{\delta R}{R_{o_e}} \sum m_n$$

$$+ 3 \frac{GM_E}{R_{o_e}^2} \left(\frac{3 C_\omega^2 - 1}{2} \iiint \left(\frac{y_o}{R_{o_e}}\right)^2 \left(2 \frac{\eta}{y_o} - 4 \frac{\delta R}{R_{o_e}}\right) dm\right.$$

$$- 3 \, \delta\theta S_\omega C_\omega \sum m_n \left(\frac{y_{o_n}}{R_{o_e}}\right)^2 + \frac{3 S_\omega^2 - 1}{2} \iiint \left(\frac{x_o}{R_{o_e}}\right)^2 \left(- 4 \frac{\delta R}{R_{o_e}}\right) dm$$

$$\left. + 3 \, \delta\theta S_\omega C_\omega \sum m_n \left(\frac{x_{o_n}}{R_{o_e}}\right)^2 \right) \qquad (130)$$

Substituting the relationships

$$\left.\begin{aligned} \frac{3 C_\omega^2 - 1}{2} &= \frac{1 + 3 C_{2\omega}}{4} \\ \text{and} \qquad & \\ \frac{3 S_\omega^2 - 1}{2} &= \frac{1 - 3 C_{2\omega}}{4} \end{aligned}\right\} \qquad (131)$$

into equation (130),

$$\frac{Q_1}{m R_{o_e}} = - \dot{\Psi}_e^2 + \frac{GM_E}{R_{o_e}^3} \sum \frac{m_n}{m} + \frac{3}{4} \frac{GM_E}{R_{o_e}^3} \left(\frac{I_{zz_o}}{mR_{o_e}^2} + \frac{3\bar{I}_{zz_o}}{mR_{o_e}^2} C_{2\omega} \right)$$

$$+ \left(\frac{\delta \ddot{R}}{R_{o_e}} - \dot{\Psi}_e^2 \frac{\delta R}{R_{o_e}} - 2 \dot{\Psi}_e \delta\dot{\Psi} \right) + (\omega + \dot{\Psi}_e) S_\omega \sum \left(\frac{\dot{\eta}_n}{R_{o_e}} \right) \frac{m_n}{m}$$

$$- C_\omega \sum \left(\frac{\ddot{\eta}_n}{R_{o_e}} \right) \frac{m_n}{m} - 2 \frac{GM_E}{R_{o_e}^3} \frac{\delta R}{R_{o_e}} \sum \frac{m_n}{m}$$

$$+\frac{3}{4}\frac{GM_E}{R^3_{o_e}}\left(2\sum\left(\frac{y_{o_n}}{R_{o_e}}\right)\left(\frac{\eta_n}{R_{o_e}}\right)\frac{m_n}{m} - 4\frac{\delta R}{R_{o_e}}\frac{I_{zz_o}}{mR^2_{o_e}}\right.$$

$$\left. - 12\frac{\delta R}{R_{o_e}} C_\omega \frac{\bar{I}_{zz_o}}{mR^2_{o_e}} - 6\,\delta\theta\, S_{2\omega}\frac{\bar{I}_{zz_o}}{mR^2_{o_e}}\right) \tag{132}$$

where

$$\frac{I_{zz_o}}{mR^2_{o_e}} = \sum\left(\left(\frac{y_{o_n}}{R_{o_e}}\right)^2 + \left(\frac{x_{o_n}}{R_{o_e}}\right)^2\right)\frac{m_n}{m};$$

$$\frac{\bar{I}_{zz_o}}{mR^2_{o_e}} = \sum\left(\left(\frac{y_{o_n}}{R_{o_e}}\right)^2 - \left(\frac{x_{o_n}}{R_{o_e}}\right)^2\right)\frac{m_n}{m}$$

and

$$m = \sum m_n$$

At this point $\dot{\Psi}_e$ is defined as

$$\dot{\Psi}_e^{\,2} = \frac{GM_E}{R^3_{o_e}}\left(1 + \frac{3}{4}\frac{I_{zz_o}}{mR^2_{o_e}}\right) \tag{133}$$

In the fully deployed configuration

Y_{o_1} = -870. 763 feet;

Y_{o_C} = -370. 763 feet;

Y_{o_2} = 129. 237 feet

Then

$$\dot{\Psi}_e \cong \sqrt{\frac{GM_E}{R_{o_e}^3}} \left(1 + .828 \times 10^{-10}\right) \tag{134}$$

or

$$\dot{\Psi}_e = 0.001196833 \text{ rad/sec} \tag{135}$$

The elastic limit deflection of a one-inch cable is about 7.04×10^{-3} (ft/ft of cable). Direct substitution of limit deflections and equation (133) shows that equation (132) reduces (when $Q_1 = 0$) to

$$\frac{\delta \ddot{R}}{R_{o_e}} = \dot{\Psi}_e^{\,2} \left(3 \frac{\delta R}{R_{o_e}} - \frac{9}{4} C_{2\omega} \frac{\bar{I}_{zz_o}}{mR_{o_e}^2} \right) + 2 \dot{\Psi}_e \, \delta \dot{\Psi} \tag{136}$$

It may be noted that elastic effects can only enter this equation through $\delta\dot{\Psi}$. The equation of motion in that degree of freedom is

$$Q_2 = \frac{d}{dt} \left(R_o^{\,2} (\dot{\Psi}_e + \delta\dot{\Psi})\, m + R_o S_\theta \sum m_n \dot{\eta}_n + (\dot{\Psi}_e + \delta\dot{\Psi} - \dot{\theta}) \left(\iiint x_2^{\,2}\, dm_2 \right.\right.$$

$$\left.\left. + \sum (y_{o_n} + \eta_n)^2 m_n \right) \right)$$

$$= 2 (R_{o_e} + \delta R)\, \delta\dot{R}\, (\dot{\Psi}_e + \delta\dot{\Psi})\, m + (R_{o_e} + \delta R)^2\, \delta\ddot{\Psi}\, m + \delta\dot{R}\, (S_\omega$$

$$+ \delta\theta\, C_\omega) \sum m_n \dot{\eta}_n + (R_{o_e} + \delta R)(\omega + \delta\dot{\theta})(C_\omega - \delta\theta\, S_\omega) \sum m_n \dot{\eta}_n$$

$$+ (R_{o_e} + \delta R)(S_\omega + \delta\theta\, C_\omega) \sum m_n \ddot{\eta}_n + (\delta\ddot{\Psi} - \delta\ddot{\theta}) \left(\iiint x_2^{\,2}\, dm_2 \right.$$

$$\left. + \sum m_n (y_{o_n} + \eta_n)^2 \right) + (\dot{\Psi}_e - \omega + \delta\dot{\Psi} - \delta\dot{\theta}) \sum 2\, m_n (y_{o_n} + \eta_n)\, \dot{\eta}_n$$

By retaining only first-order terms in the perturbations, one gets

$$\frac{Q_2}{mR_{o_e}^2} \cong \delta\ddot{\Psi}\left(1 + \left(\frac{I_{zz_o}}{mR_{o_e}^2}\right)\right) \quad 2\,\dot{\Psi}_e \frac{\delta\dot{R}}{R_{o_e}}$$

$$+ \omega\ C_\omega \sum\left(\frac{\dot{\eta}_n}{R_{o_e}}\right)\frac{m_n}{m} + S_\omega \sum\left(\frac{\ddot{\eta}_n}{R_{o_e}}\right)\frac{m_n}{m}$$

$$- \delta\ddot{\theta}\left(\frac{I_{zz_o}}{mR_{o_e}^2}\right)$$

$$+ \left(\dot{\Psi}_e - \omega\right)\sum 2\left(\frac{y_{o_n}}{R_{o_e}}\right)\left(\frac{\dot{\eta}_n}{R_{o_e}}\right)\frac{m_n}{m}$$

It can be shown that because of orthogonality of the vibration modes to the rigid body degrees of freedom

$$\sum\left(\frac{\dot{\eta}_n}{R_{o_e}}\right)\frac{m_n}{m} = \sum\left(\frac{\ddot{\eta}_n}{R_{o_e}}\right)\frac{m_n}{m} = 0$$

and that

$$\sum\left(\frac{y_{o_n}}{R_{o_e}}\right)\left(\frac{\dot{\eta}_n}{R_{o_e}}\right)\frac{m_n}{m}$$

is negligibly small. Therefore, when $Q_2 = 0$

$$\delta\ddot{\Psi} = -\,2\,\dot{\Psi}_e \frac{\delta\dot{R}}{R_{o_e}} - \left(\delta\ddot{\Psi} - \delta\ddot{\theta}\right)\frac{I_{zz_o}}{mR_{o_e}^2} \qquad (137)$$

The equation of motion in the spin degree of freedom is

$$Q_3 = \frac{d}{dt}\left((\dot{\Psi} - \dot{\theta})\left((\sum m_n (y_{o_n} + \eta_n)^2 + \sum m_n x_{o_n}^2\right)\right)$$

$$- \left((R_o \dot{\Psi} C_\theta + \dot{R}_o S_\theta) \sum m_n \dot{\eta}_n\right)$$

$$- \frac{GM_E}{R_{o_e}^3}\left(- 3 C_\theta S_\theta \sum m_n (y_{o_n} + \eta_n)^2 + 3 S_\theta C_\theta \sum m_n x_{o_n}^2\right)$$

or

$$\frac{Q_3}{m R_{o_e}^2} = (\delta\ddot{\Psi} \cdot \delta\ddot{\theta}) \left(\frac{I_{zz_o}}{mR_{o_e}^2}\right.$$

$$\left. + 2\sum\left(\frac{y_{o_n}}{R_{o_e}}\right)\left(\frac{\eta_n}{R_{o_e}}\right) \frac{m_n}{R_{o_e}}\right)$$

$$+ (\dot{\Psi}_e - \omega + \delta\dot{\Psi} - \delta\theta) \sum 2 \left(\frac{y_{o_n}}{R_{o_e}}\right)\left(\frac{\dot{\eta}_n}{R_{o_e}}\right) \frac{m_n}{m}$$

$$- \left(\dot{\Psi}_e C_\omega\right) \sum \left(\frac{\dot{\eta}_n}{R_{o_e}}\right) \frac{m_n}{m}$$

$$+ \frac{3}{2}\frac{GM_E}{R_{o_e}^3} \left(1 - 3\frac{\delta R}{R_{o_e}} + \ldots\right) \left(S_{2\omega} + 2\,\delta\theta C_{2\omega}\right)\left(\frac{I_{zz_o}}{mR_{o_e}^2}\right.$$

$$\left. + 2\,\Sigma \left(\frac{y_{o_n}}{R_{o_e}}\right)\left(\frac{\eta_n}{R_{o_e}}\right) \frac{m_n}{m}\right)$$

and for a 100-mile orbit

$$R_{o_e} = 2.142 \times 10^7 \text{ feet}$$

so

$$\frac{y_{o_1}}{R_{o_e}} = -4.065187 \times 10^{-5};$$

$$\frac{y_{o_C}}{R_{o_e}} = -1.730920 \times 10^{-5};$$

$$\frac{y_{o_2}}{R_{o_e}} = 0.603347 \times 10^{-5}$$

and

$$\frac{m_1}{m} = 0.1059325;$$

$$\frac{m_C}{m} = 0.0466102;$$

$$\frac{m_2}{m} = 0.8474601$$

It follows that

$$\sum \left(\frac{y_{o_n}}{R_{o_e}}\right)^2 \frac{m_n}{m} = 2.198 \times 10^{-10}$$

Also

$$\sum \left(\frac{x_{o_n}}{R_{o_e}}\right)^2 \frac{m_n}{m} = 0.010 \times 10^{-10}$$

And retaining only first order terms

$$\frac{Q_3}{m R_{o_e}^2} = (\delta \ddot{\Psi} - \delta \ddot{\theta}) \left(\frac{I_{zz_o}}{m R_{o_e}^2} \right) + \frac{3}{2} \frac{GM_E}{R_{o_e}^3} S_{2\omega} \frac{\overline{I}_{zz_o}}{mR_{o_e}^2}$$

$$+ (\dot{\Psi}_e - \omega) \sum 2 \left(\frac{y_{o_n}}{R_{o_e}} \right) \left(\frac{\dot{\eta}_n}{R_{o_e}} \right) \frac{m_n}{m} - \dot{\Psi}_e C_\omega \sum \cancelto{0}{\frac{\eta_n}{R_{o_e}} \frac{m_n}{m}}$$

$$+ \frac{3}{2} \frac{GM_E}{R_{o_e}^3} \left(2 S_{2\omega} \sum \left(\frac{y_{o_n}}{R_{o_e}} \right) \left(\frac{\eta_n}{R_{o_e}} \right) \frac{m_n}{n} \right.$$

$$\left. - 3 \frac{\delta R}{R_{o_e}} S_{2\omega} \left(\frac{I_{zz_o}}{m R_{o_e}^2} \right) + 2 \delta\theta \, C_{2\omega} \left(\frac{I_{zz_o}}{m R_{o_e}^2} \right) \right)$$

All terms except the first two are considered to be negligible. Thus,

$$\delta \ddot{\Psi} - \delta \ddot{\theta} = - \frac{3}{2} \dot{\Psi}_e^2 \frac{\overline{I}_{zz_o}}{I_{zz_o}} S_{2\omega} \tag{138}$$

Equations (136), (137), and (138) are linear differential equations. They may be solved by substituting equation (138) into equation (137) to get

$$\delta \ddot{\Psi} + 2 \dot{\Psi}_e \frac{\delta \dot{R}}{R_{o_e}} = \frac{3}{2} F \sin 2 \omega t \tag{139}$$

and, similarly, equation (136) may be written

$$\frac{\delta \ddot{R}}{R_{o_e}} - 3\,\dot{\Psi}_e^{\,2}\,\frac{\delta R}{R_{o_e}} - 2\,\dot{\Psi}_e\,\delta\dot{\Psi} = -\frac{9}{4} F \cos 2\omega t \tag{140}$$

where

$$F = \dot{\Psi}_e^{\,2}\,\frac{\overline{I}_{zz_o}}{m R_{o_e}^{2}} = 3.13 \times 10^{-16}$$

The solution of these simultaneous differential equations is

$$\frac{\delta R(t)}{R_{o_e}} = \left[\frac{4\delta R(o)}{R_{o_e}} + 2\,\frac{\delta\dot{\Psi}(o)}{\dot{\Psi}_e} + \frac{3}{2}\,\frac{F}{\omega\Psi_e}\right] - \left[\frac{3\,\dot{\Psi}_e + 9\,\omega/2}{4\omega^2 - \dot{\Psi}_e^{\,2}}\,F\right]\frac{\cos 2\,\omega\,t}{2\omega}$$

$$+ \left[\frac{\delta\dot{R}(o)}{R_{o_e}}\right]\frac{\sin\dot{\Psi}_e\,t}{\dot{\Psi}_e} - \left[2\delta\,\dot{\Psi}(o) + 3\,\dot{\Psi}_e\,\frac{\delta R(o)}{R_{o_e}}\right.$$

$$\left. + \frac{6\,\omega + \frac{9}{4}\,\dot{\Psi}_e}{4\omega^2 - \dot{\Psi}_e^{\,2}}\,F\right]\frac{\cos\dot{\Psi}_e\,t}{\dot{\Psi}_e}$$

and

$$\delta\dot{\Psi}(t) = -\,\dot{\Psi}_e\left[6\,\frac{\delta R(o)}{R_{o_e}} + 3\,\frac{\delta\dot{\Psi}(o)}{\dot{\Psi}_e} + \frac{9}{4}\,\frac{F}{\omega\,\dot{\Psi}_e}\right]$$

$$-\left[\frac{6\,\omega^2 + 9\,\omega\,\dot{\Psi}_e + \frac{9}{2}\dot{\Psi}_e^{\,2}}{4\omega^2 - \dot{\Psi}_e^{\,2}}\right]F\quad\frac{\cos 2\,\omega\,t}{2\,\omega}$$

$$+\left[-2\,\dot{\Psi}_e \frac{\delta\dot{R}(o)}{R_{o_e}}\right] \frac{\sin \dot{\Psi}_e t}{\dot{\Psi}_e} + \left[4\,\dot{\Psi}_e\,\delta\dot{\Psi}(o) + 6\,\dot{\Psi}_e^{\,2} \frac{\delta R(o)}{R_{o_e}}\right.$$

$$\left. + \frac{12\,\omega\,\dot{\Psi}_e + \frac{9}{2}\dot{\Psi}_e^{\,2}}{4\omega^2 - \dot{\Psi}_e^{\,2}} F\right] \frac{\cos \Psi_e t}{\dot{\Psi}_e} \qquad (141)$$

By setting

$$\frac{\delta R(o)}{R_{o_e}} = + \frac{\frac{9}{4} + \frac{3}{2}\frac{\dot{\Psi}_e}{\omega}}{4\omega^2 - \dot{\Psi}_e^{\,2}} F = +1.102 \times 10^{-15}$$

$$\delta\dot{\Psi}(o) = -\frac{3 + \frac{9}{2}\frac{\dot{\Psi}_e}{\omega}\left(1 + \frac{\dot{\Psi}_e}{2\omega}\right)}{4\omega^2 - \dot{\Psi}_e^{\,2}}\,\omega F = -5.984 \times 10^{-15} \qquad (142)$$

and

$$\frac{\delta\dot{R}(o)}{R_{o_e}} = 0$$

the following equations are obtained

$$\left.\begin{aligned} \frac{\delta R(t)}{R_{o_e}} &= \frac{\delta R(o)}{R_{o_e}} \cos 2\,\omega t \\ \delta\dot{\Psi}(t) &= \delta\dot{\Psi}(o) \cos 2\,\omega t \end{aligned}\right\} \qquad (143)$$

And in order to avoid divergence of $\delta\theta$,

$$\delta\dot{\theta}(o) = \delta\dot{\Psi}(o) - \frac{3F}{4\omega \frac{I_{zz_o}}{m R_{o_e}^2}} = -2.658 \times 10^{-6} \qquad (144)$$

and to further simplify calculations, set

$$\delta\Psi(o) = \delta\theta(o) = 0$$

to get

$$\delta\theta(t) = \left(\frac{\delta\Psi(o)}{2\omega} - \frac{3\,F}{8\omega^2 \dfrac{I_{zz_o}}{m\,R_{o_e}^2}} \right) \sin 2\,\omega\,t \tag{145}$$

or

$$\delta\theta(t) = -3.322 \times 10^{-6} \sin 2\,\omega\,t$$

Now it may be stated that within the limitations of the linearized analysis, a stable orbit has been achieved and that the small perturbations on that orbit caused by gravity gradient have been determined. The effects on the elastic degrees of freedom may be determined as follows

$$Q_i = \frac{d}{dt}\left((\dot{R}_o\, \dot{\Psi}\, S_\theta - \dot{R}_o\, C_\theta)\, m_n + m_n\, \dot{\eta}_n \right)$$

$$- \left((\dot{\Psi} - \dot{\theta})^2\, m_n\, (y_{o_n} + \eta_n) \right)$$

$$- \frac{GM_E}{R_o^{\,3}} \left(\frac{1 + 3\,C_{2\theta}}{4} \right) 2\, m_n\, (y_{o_n} + \eta_n) + \frac{\partial U_E}{\partial \eta_n} \tag{146}$$

where

$i = n + 3$

Expanding and retaining only zero and first-order terms gives (after a considerable amount of manipulation and substitution of previous results) the following:

$$
\begin{aligned}
Q_j = m_n \Bigg[& - y_{o_n} \left(\omega^2 + 2\omega\dot{\Psi}_e + \frac{3}{2}\dot{\Psi}_e^2\right) + \left(-\frac{3}{2}\dot{\Psi}_e^2 \, y_{o_n}\right) C_{2\omega} + \left(\omega R_{o_e} \dot{\Psi}_e\right) C_\omega \\
& + S_\omega S_{2\omega} \left(- 2\omega \, \delta R_o \, \dot{\Psi}_e - 2\,\omega R_{o_e} \, \delta \dot{\Psi}_o - \omega R_{o_e} \dot{\Psi}_e \, \delta\dot{\theta}_o - 2\,\omega^2 \, \delta R_o\right. \\
& + S_{2\omega} S_{2\omega} \left(3\,\dot{\Psi}_e^2 \, \delta\dot{\theta}_o \, y_{o_n}\right) + C_{2\omega} C_{2\omega} \left(\frac{9}{2}\dot{\Psi}_e^2 \, y_{o_n} \frac{\delta R_o}{R_{o_e}}\right) \\
& + C_\omega C_{2\omega} \left(2\omega \, \delta\dot{\theta}_o \, R_{o_e} \dot{\Psi}_e + \omega \dot{\Psi}_e \, \delta R_o + \omega R_{o_e} \, \delta \dot{\Psi}_o\right) \\
& + C_{2\omega} \, y_{o_n} \left(- 2\,\dot{\Psi}_e \, \delta\dot{\Psi}_o + 2\omega \, \delta\dot{\Psi}_o + 4\omega \, \delta\dot{\theta}_o \dot{\Psi}_e - 4\,\omega^2 \, \delta\dot{\theta}_o\right. \\
& \left.\left. + \frac{3}{2}\dot{\Psi}_e^2 \frac{\delta R_o}{R_{o_e}}\right)\Bigg] + m_n \eta_n \Bigg[\left(- \omega^2 + 2\omega\dot{\Psi}_e - \frac{3}{2}\dot{\Psi}_e^2\right) \\
& + C_{2\omega} \left(-\frac{3}{2}\dot{\Psi}_e^2\right)\Bigg] + \left(\frac{\partial U_E}{\partial \eta_n} + m_n \ddot{\eta}_n\right)
\end{aligned}
\tag{147}
$$

The trigonometric functions are then expressed in terms of multiple angles and numerical substitutions reveal insignificant terms. When all these terms are eliminated, a set of three simultaneous linear differential equations is the result. The Laplace transform of these equations follow:

$$\begin{bmatrix} \frac{m_1}{m}S^2 + \left(\frac{k}{m} - \frac{m_1}{m}\alpha\right) & -\frac{k}{m} & 0 \\ -\frac{k}{m} & \frac{m_c}{m}S^2 + \left(\frac{2k}{m} - \frac{m_c}{m}\alpha\right) & -\frac{k}{m} \\ 0 & -\frac{k}{m} & \frac{m_2}{m}S^2 + \left(\frac{k}{m} - \frac{m_2}{m}\alpha\right) \end{bmatrix} \begin{Bmatrix} \frac{\eta_1(S)}{R_{o_e}} \\ \frac{\eta_C(S)}{R_{o_e}} \\ \frac{\eta_2(S)}{R_{o_e}} \end{Bmatrix} = L\left(A_1 C_\omega + A_3 C_{3\omega}\right) \begin{Bmatrix} \frac{m_1}{m} \\ \frac{m_C}{m} \\ \frac{m_2}{m} \end{Bmatrix} + L\left(A_o + A_2 S_{2\omega} + A_4 S_{4\omega}\right) \begin{Bmatrix} \frac{m_1}{m} & \frac{y_{o_1}}{R_{o_e}} \\ \frac{m_C}{m} & \frac{y_{o_C}}{R_{o_e}} \\ \frac{m_2}{m} & \frac{y_{o_2}}{R_{o_e}} \end{Bmatrix} \tag{148}$$

where

$$\begin{Bmatrix} \frac{m_1}{m} \\ \frac{m_C}{m} \\ \frac{m_2}{m} \end{Bmatrix} = \begin{Bmatrix} 0.1059326 \\ 0.0466102 \\ 0.8474602 \end{Bmatrix} \quad \text{and } \alpha = 0.159045$$

The spring constant for 500 feet of one-inch steel cable whose solid cross-section area is 0.576 square inches is

$$k = \frac{19 \times 10^6 \times .576}{500} = 21{,}888 \text{ pounds per foot}$$

So

$$\frac{k}{m} = 14.93206$$

And

$$A_0 = +\left(\omega^2 - 2\,\omega\,\dot{\Psi}_e + \frac{3}{2}\,\dot{\Psi}_e^{\,2}\right) + 0\,(-12) \qquad = +0.159045$$

$$A_1 = -(\omega\,\dot{\Psi}_e) + 0\,(-9) \qquad = -0.478732 \times 10^{-3}$$

$$A_2 = -\left(-\frac{3}{2}\,\dot{\Psi}_e^{\,2} + 4\omega\dot{\Psi}_e\,\delta\theta_o\right) + 4\omega^2\,\delta\theta(o) + 0\,(-15) \qquad = +0.02557 \times 10^{-6}$$

$$A_3 = -\left(\frac{3}{2}\,\omega\,\dot{\Psi}_e\,\delta\theta_o\right) + 0\,(-15) \qquad = +2.38618 \times 10^{-9}$$

$$A_4 = -\left(-\frac{3}{2}\,\dot{\Psi}_e^{\,2}\,\delta\theta_o\right) + 0\,(-21) \qquad = -7.13868 \times 10^{-12}$$

The steady state solution (i. e., for the term A_0 on the right hand side) yields

$$\left\{\begin{matrix} \dfrac{\eta_1}{R_{o_e}} \\ \\ \dfrac{\eta_c}{R_{o_e}} \\ \\ \dfrac{\eta_2}{R_{o_e}} \end{matrix}\right\}_{S.S.} = \left\{\begin{matrix} -8.7339 \\ \\ -4.1373 \\ \\ 1.3208 \end{matrix}\right\} \times 10^{-8} \tag{149}$$

The remainder of the analysis shows that a small amount of damping is required to prevent divergence of the flexible degrees of freedom.

The determinant of the coefficients of $\eta_n(S)/R_{o_e}$ in equation (148) yields the polynomial

$$(S^2 - 0.159045)\,(S^2 + 73.2407)\,(S^2 + 726.451) = 0$$

The positive root indicates divergence and gives a measure of the amount of damping required.

Structural damping, as commonly used by the flutter analyst, cannot provide the stabilizing forces for the elastic degrees of freedom. This fact can be anticipated, because there are no forces 90 degrees out of phase with the displacements when aerodynamic forces or other forces proportional to velocity are absent.

If a sinusoidal motion were assumed, i. e.,

$$\left(\frac{\eta_n}{R_{o_e}}\right) = \left(\frac{\bar{\eta}_n}{R_{o_e}}\right) e^{j\omega_N t}$$

$$\left(\frac{\ddot{\eta}_n}{R_{o_e}}\right) = -\omega_N^2 \left(\frac{\eta_n}{R_{o_e}}\right)$$

and then the factor $(1 + jg)$ is applied arbitrarily (to account for forces proportional to displacement but in phase with the velocity) wherever k/m appears in the equations, the determinant

$$0 = \begin{bmatrix} -\frac{m_1}{m}(\omega_N^2 + \alpha) + \frac{k}{m}(1 + jg) & -\frac{k}{m}(1 + jg) & 0 \\ -\frac{k}{m}(1 + jg) & -\frac{m_C}{m}(\omega_N^2 + \alpha) + \frac{2k}{m}(1 + jg) & -\frac{k}{m}(1 + jg) \\ 0 & -\frac{k}{m}(1 + jg) & -\frac{m_2}{m}(\omega_N^2 + \alpha) + \frac{k}{m}(1 + jg) \end{bmatrix} \tag{150}$$

is used to find the natural frequencies of the system, (ω_N) in terms of g_n.

Then

$$\omega_N^2 = -\alpha, \ \frac{k}{2m}(1 + jg)\left[\frac{m_C}{m}\left(\frac{m_1}{m} + \frac{m_2}{m}\right) + 2\frac{m_1}{m}\frac{m_2}{m} \pm\sqrt{\left(\frac{m_c}{m}\right)^2\left(\frac{m_1}{m} - \frac{m_2}{m}\right)^2 + \left(2\frac{m_1}{m}\frac{m_2}{m}\right)^2}\ \right]$$

would force the conclusion that no factor applied to the spring constant, whether real to account for friction forces, or complex to account for hysteresis forces, will avoid getting the root, $\omega_N^2 = -\alpha$.

Thus, it is shown that when the equation representing the change in angular momentum due to elastic deflections is not solved simultaneously with the elastic equations, the result is an unstable root of the elastic equations. This suggests that when determining the elastic response of the system the linearized equation for the spin rate should be expanded to include those terms due to elastic deflections and solved simultaneously with the elastic equations. It appears that if structural or material damping is to be considered in the analysis, it should be divided into two parts: (1) the very small portion that can be shown to be proportional to velocity, and (2) the portion that is proportional to displacement. Artificial viscous dampers and pendulum dampers could also be accounted for in the analysis.

When these damping forces are added to the system, the problem of finding the amplitudes of oscillation becomes one of finding resonant frequencies and amplitudes in response to the forces arising from gravity gradients.

It is suggested that future work be conducted to account for the damping inherent in typical configurations of space stations. An accurate determination can be made of the magnification factors, transfer functions, transient responses and amplitudes of steady-state responses to the gravity gradient and other oscillatory forces only when the elastic deformations can be shown to be damped after an initial displacement or forced response.

It is also suggested that the amplitudes of the elastic responses be used, when the damping is properly accounted for, to check numerically the validity of neglect of higher order terms in the complete set of equations of motion.

8.0 PLANAR MOTION OF ORBITING SPACE STATIONS

8.1 TECHNICAL APPROACH

Past experience in the analysis of orbiting extended bodies in a non-uniform gravitational field indicated that the rotational motion of a system about its center of mass cannot be treated as independent of its orbital motion without violating the law of conservation of energy and the law of conservation of momentum. In the case of manned space stations, when the connecting members are made of long flexible cable or elastic structural members, the stability and control characteristics may be significantly influenced by the distortions of the flexible extended members under transient loading conditions. The effect of flexibility and vibrational motion must also be included in the formulation of equations of motion.

In view of the above stated reasons, comprehensive analyses were conducted of the planar motions of some extended elastic configurations and are presented in sections 8.2, 8.3, and 8.4 of this report. These space stations are assumed to be spinning in the orbital plane around a spherical earth with an inverse-square-law gravitational field. The spin-up phase is not included in the analysis.

The equations of planar motion in the earth-fixed coordinates were derived from the total kinetic energy of the system, the strain energy of the cable, and the generalized forces that resulted from the work done by external disturbances. The external forces included in the derivation are those due to the gravitational gradient over the extended body. The effect of control forces acting on the end modules of the cable-connected configuration is given in Appendix A, Control Forces on the Cable-Connected Space Station.

8.2 PLANAR MOTION OF A COMPARTMENT-CABLE-COUNTERWEIGHT SPACE STATION

Figure 46 shows a moving coordinate frame η and ζ (unit vectors $\bar{i}_3$ and $\bar{j}_3$) through the center of mass of compartment-cable-counterweight system. The inertial axes through the center of earth are x and y (unit vectors $\bar{i}_4$ and $\bar{j}_4$). These two sets of axes are related by R, θ, and ϕ.

Let $\bar{R}_i$ be the vector drawn from the center of mass of the earth to any point on the cable. The inertial velocity of this point is given by

$$\overline{V_i} = \overline{V}_c + \overline{V}_r + \overline{\omega} \times \overline{d}_i \tag{151}$$

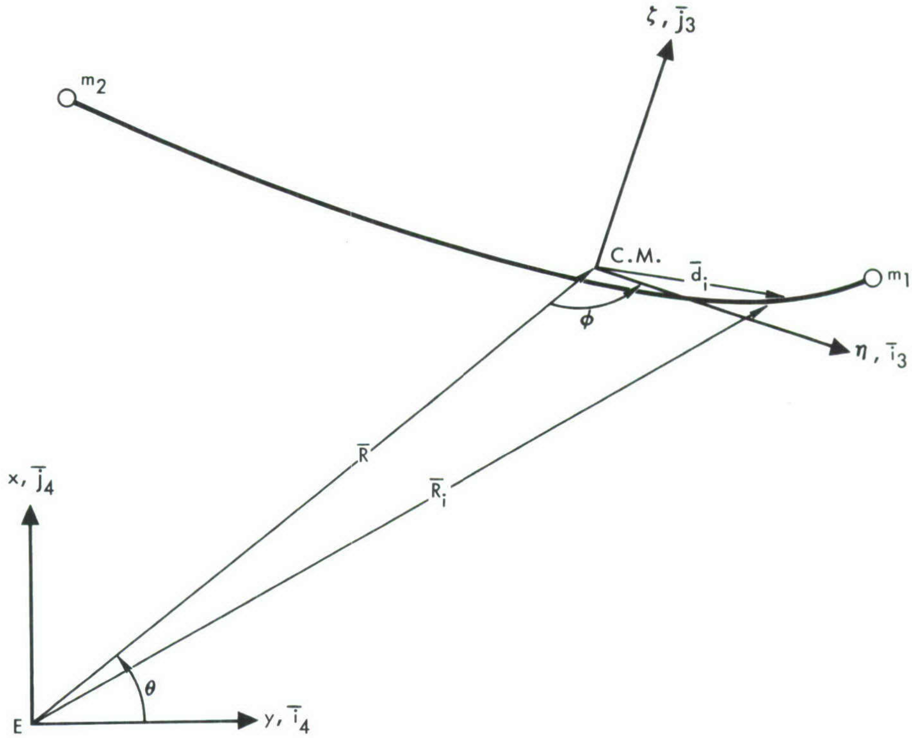

Figure 46. Moving Coordinate Frame Through the Center of Mass of a Compartment-Cable-Counterweight System

Since

$$\overline{V}_c = -\bar{i}_3 \, [R\dot{\theta} \sin \phi + \dot{R} \cos \phi] + \bar{j}_3 \, [\dot{R} \sin \phi - R\dot{\theta} \cos \phi] \tag{152}$$

$$\overline{V}_r = \dot{\eta} \, \bar{i}_3 + \dot{\zeta} \, \bar{j}_3, \tag{153}$$

and

$$\overline{\omega} \times \overline{d}_i = - \bar{i}_3 \, [\zeta \, (\dot{\theta} + \dot{\phi})] + \bar{j}_3 \, [\eta(\dot{\theta} + \dot{\phi})] \tag{154}$$

we get

$$\overline{V}_i = \bar{i}_3 \, [\dot{\eta} - R\dot{\theta} \sin \phi - \dot{R} \cos \phi - \zeta \, (\dot{\theta} + \dot{\phi})]$$

$$+ \bar{j}_3 \, [\dot{\zeta} + \dot{R} \sin \phi - R\dot{\theta} \cos \phi + \eta \, (\dot{\theta} + \dot{\phi})] \tag{155}$$

The kinetic energy of the system, referred to inertial axes, is

$$T = \frac{1}{2} m_1 \Bigg\{ \dot{\eta}_1^2 + \dot{\zeta}_1^2 + \left(\zeta_1^2 + \eta_1^2\right)(\dot{\theta} + \dot{\phi})^2 + \dot{R}^2 + R^2\dot{\theta}^2 - 2\dot{\eta}_1 [R\dot{\theta} \sin \phi$$

$$+ \dot{R} \cos \phi + \zeta_1 (\dot{\theta} + \dot{\phi})] + 2\dot{\zeta}_1 [\dot{R} \sin \phi - R\dot{\theta} \cos \phi + \eta_1 (\dot{\theta} + \dot{\phi})] + 2\zeta_1 (\dot{\theta}$$

$$+ \dot{\phi}) [R\dot{\theta} \sin \phi + \dot{R} \cos \phi] + 2\eta_1 (\dot{\theta} + \dot{\phi}) [\dot{R} \sin \phi - R\dot{\theta} \cos \phi] \Bigg\}$$

$$+ \frac{1}{2} m_2 \Bigg\{ \dot{\eta}_2^2 + \dot{\zeta}_2^2 + \left(\zeta_2^2 + \eta_2^2\right)(\theta + \dot{\phi})^2 + \dot{R}^2 + R^2\dot{\theta}^2 - 2\dot{\eta}_2 [R\dot{\theta} \sin \phi$$

$$+ \dot{R} \cos \phi + \zeta_2 (\dot{\theta} + \dot{\phi})] + 2\dot{\zeta}_2 [\dot{R} \sin \phi - R\theta \cos \phi + \eta_2 (\dot{\theta} + \phi)] + 2\zeta_2 (\dot{\theta}$$

$$+ \dot{\phi}) [R\dot{\theta} \sin \phi + \dot{R} \cos \phi] + 2\eta_2 (\dot{\theta} + \dot{\phi}) [\dot{R} \sin \phi - R\dot{\theta} \cos \phi] \Bigg\}$$

$$+ \frac{1}{2} \int_{-\ell_2}^{\ell_1} \rho \Bigg\{ \dot{\eta}^2 + \dot{\zeta}^2 + (\zeta^2 + \eta^2)(\dot{\theta} + \dot{\phi})^2 + \dot{R}^2 + R^2\dot{\theta}^2 - 2\dot{\eta} [R\dot{\theta} \sin \phi$$

$$+ \dot{R} \cos \phi + \zeta (\dot{\theta} + \dot{\phi})] + 2\dot{\zeta} [\dot{R} \sin \phi - R\dot{\theta} \cos \phi + \eta (\dot{\theta} + \dot{\phi})] + 2\zeta (\dot{\theta}$$

$$+ \dot{\phi}) [R\dot{\theta} \sin \phi + \dot{R} \cos \phi] + 2\eta (\dot{\theta} + \dot{\phi}) [\dot{R} \sin \phi - R\dot{\theta} \cos \phi] \Bigg\} d\eta. \qquad (156)$$

By Lagrange's method, the equations of motion are as follows

$$\frac{d}{dt}\left(\frac{\partial T}{\partial \dot{q}_j}\right) - \frac{\partial T}{\partial q_j} = Q_j \qquad (157)$$

where q_j are the generalized coordinates including R, θ, r, φ and q_n; q_n is the generalized coordinate that gives the displacement in the n^{th} normal mode. Q_j is the component of the generalized force that results from the work done by the external forces. When the external forces are the gravity forces and elastic forces, Q_j will be evaluated from

$$\Sigma Q_j \, \delta q_j = \overline{G}_1 \cdot (\delta x_1 \, \overline{i}_4) + \overline{G}_2 \cdot (\delta x_2 \, \overline{i}_4) + \int d\overline{G}_c \cdot (\delta x_c \, \overline{i}_4) + \overline{G}_1 \cdot (\delta y_1 \, \overline{j}_4)$$

$$+ G_2 \cdot (\delta y_2 \overline{j}_4) + \int d\overline{G}_c \cdot (\delta y_c \, \overline{j}_4) - \frac{\partial U_e}{\partial q_n} \delta r - \frac{\partial U_\ell}{\partial q_n} \delta q_n \qquad (158)$$

These virtual displacements are to be given as functions of virtual displacements of generalized coordinates. This can be done by considering the vector, $\overline{R}_i$, drawn from the center of the earth to any point on the cable.

$$\overline{R}_i = \overline{i}_3 [\eta - R \cos \phi] + \overline{j}_3 [\zeta + R \sin \phi] \tag{159}$$

Transferring the preceding equation to inertia coordinates by the relation

$$\overline{i}_3 = - \overline{i}_4 \cos (\theta + \phi) - \overline{j}_4 \sin (\theta + \phi)$$

$$\overline{j}_3 = \overline{i}_4 \sin (\theta + \phi) - \overline{j}_4 \cos (\theta + \phi) \tag{160}$$

we have

$$\overline{R}_i = \overline{i}_4 [-\eta \cos (\theta + \phi) + \zeta \sin (\theta + \phi) + R \cos \theta]$$

$$+ \overline{j}_4 [-\eta \sin (\theta + \phi) - \zeta \cos (\theta + \phi) + R \sin \theta] \tag{161}$$

Now we will introduce the lateral displacement, $\zeta (\eta_o, t)$, in terms of the summation of the normal modes, $\phi_n (\eta_o)$, multiplied by the generalized coordinates, $q_n (t)$, associated with the mode.

$$\zeta (\eta_o, t) = \sum_{n=1}^{\infty} \phi_n (\eta_o) q_n (t). \tag{162}$$

The extensional displacement of any point at the cable will be incorporated into the abscissa, η_o, by the assumption

$$\eta (\eta_o, t) = \eta_o \frac{r}{r_o}$$

and

$$\rho \, d \eta = \rho_o \, d \eta_o \tag{163}$$

where

r = the length of cable at any unsteady state

r_o = the length of cable at steady state

η_o = the abscissa at steady state; varies from $-\ell_2$ to ℓ_1.

Thus, from equation (161), virtual displacements are determined to be

$$\delta x_i = \delta R (\cos \theta) + \delta r \left[- \frac{\eta_o}{r_o} \cos (\theta + \phi) \right] + \sin (\theta + \phi) \Sigma \phi_n \ \delta q_n$$
$$+ \delta \theta \left[\eta_o \frac{r}{r_o} \sin (\theta + \phi) + \zeta \cos (\theta + \phi) - R \sin \theta \right] + \delta \phi \left[\eta_o \frac{r}{r_o} \sin (\theta \right.$$
$$\left. + \phi) + \zeta \cos (\theta + \phi) \right]$$

$$\delta y_i = \delta R (\sin \theta) + \delta r \left[- \frac{\eta_o}{r_o} \sin (\theta + \phi) \right] - \cos (\theta + \phi) \Sigma \phi_n \ \delta q_n$$
$$+ \delta \theta \left[- \eta_o \frac{r}{r_o} \cos (\theta + \phi) + \zeta \sin (\theta + \phi) + R \cos \theta \right]$$
$$+ \delta \phi \left[- \eta_o \frac{r}{r_o} \cos (\theta + \phi) + \zeta \sin (\theta + \phi) \right] \qquad (164)$$

Replace subscript i by 1, 2, or c for denoting virtual displacements of m_1, m_2 or ρ_o of any point of the cable, with η being given by ℓ_1, $-\ell_2$, and η_o; and ζ being given by ζ_1, ζ_2, and ζ.

The differential gravity force on a small element of the cable is given by

$$d\overline{G}_c = -\overline{i}_4 \frac{K \rho_o d\eta_o}{R_i^3} \left[- \eta_o \frac{r}{r_o} \cos (\theta + \phi) + \zeta \sin (\theta + \phi) + R \cos \theta \right]$$
$$-\overline{j}_4 \frac{K \rho_o d\eta_o}{R_i^3} \left[- \eta_o \frac{r}{r_o} \sin (\theta + \phi) - \zeta \cos (\theta + \phi) + R \sin \theta \right] \qquad (165)$$

From equations (161) and (163),

$$R_i^{\,3} = R^3 \left[1 - \frac{2r\eta_o}{r_o R}\cos\phi + \frac{2\zeta}{R}\sin\phi + \left(\frac{r\eta_o}{r_o R}\right)^2 + \frac{\zeta^2}{R^2}\right]^{3/2}$$

$$R_i^{\,-3} \approx R^{-3}\left[1 + \frac{3r\eta_o}{r_o R}\cos\phi - \frac{3\zeta}{R}\sin\phi + \text{higher order terms}\right] \qquad (166)$$

Thus

$$d\overline{G}_c = -\overline{i}_4 \frac{K\rho_o d\eta_o}{R^3}\left[-\eta_o\frac{r}{r_o}\cos(\theta+\phi) + \zeta\sin(\theta+\phi) + R\cos\theta\right]$$

$$-\overline{j}_4 \frac{K\rho_o d\eta_o}{R^3}\left[-\eta_o\frac{r}{r_o}\sin(\theta+\phi) - \zeta\cos(\theta+\phi) + R\sin\theta\right]$$

$$-\overline{i}_4\left(\frac{3K\rho_o d\eta_o}{R^3}\right)\left[\frac{r\eta_o}{r_o}\cos\phi\cos\theta - \zeta\sin\phi\cos\theta\right.$$

$$-\frac{r^2\eta_o^2}{r_o^2 R}\cos\phi\cos(\theta+\phi) + \frac{r\eta_o\zeta}{r_o R}\cos\phi\sin(\theta+\phi) + \frac{r\eta_o\zeta}{r_o R}\sin\phi\cos(\theta$$

$$\left.+\phi) - \frac{\zeta^2}{R}\sin\phi\sin(\theta+\phi)\right] - \overline{j}_4\left(\frac{3K\rho_o d\eta_o}{R^3}\right)\left[\frac{r\eta_o}{r_o}\cos\phi\sin\theta\right.$$

$$-\zeta\sin\phi\sin\theta - \frac{r^2\eta_o^2}{r_o^2 R}\cos\phi\sin(\theta+\phi) - \frac{r\eta_o\zeta}{r_o R}\cos\phi\cos(\theta+\phi)$$

$$\left.+\frac{r\eta_o\zeta}{r_o R}\sin\phi\sin(\theta+\phi) + \frac{\zeta^2}{R}\sin\phi\cos(\theta+\phi)\right] \qquad (167)$$

For masses m_1 and m_2, the corresponding values of $\overline{G}_1$ and $\overline{G}_2$ are obtained by replacing $\rho_o d\eta_o$ by m_1 or m_2, η_o by ℓ_1 or $-\ell_2$, and ζ by ζ_1 or ζ_2.

In the disturbed state, the strain energy due to elastic extensional motion is

$$U_e = \frac{AE}{2r_{ot}} \left[(r - r_{ot})^2 - (r_o - r_{ot})^2 \right] \tag{168}$$

This leads to

$$\frac{\partial U_e}{\partial r} = \frac{AE\,(r - r_{ot})}{r_{ot}} \tag{169}$$

The strain energy of the cable, due to elastic lateral motion, is obtained from

$$U_\ell = \frac{1}{2} \int_o^{\ell_1} S_1 \left(\frac{d\zeta}{d\eta_o} \right)^2 d\eta_o + \frac{1}{2} \int_o^{\ell_2} S_2 \left(\frac{d\zeta}{d\eta_o} \right)^2 d\eta_o \tag{170}$$

Tensions S_1 and S_2 have now been introduced. These lead to

$$\frac{\partial U_\ell}{\partial q_n} = \frac{\omega^2 \rho_o \ell_1^{\,2}}{2} \int_o^{\ell_1} \left(a_1^{\,2} - \frac{\eta_o^{\,2}}{\ell_1^{\,2}} \right) \left[q_n (\phi_n{}')^2 + \sum_{m \neq n} q_m \phi_m{}' \, \phi_n{}' \right] d\eta_o$$

$$+ \frac{\omega^2 \rho_o \ell_2^{\,2}}{2} \int_o^{\ell_2} \left(a_2^{\,2} - \frac{\eta_o^{\,2}}{\ell_2^{\,2}} \right) \left[q_n (\phi_n{}')^2 + \sum_{m \neq n} q_m \phi_m{}' \, \phi_n{}' \right] d\eta_o \tag{171}$$

where

$$\omega \equiv (\dot{\theta} + \dot{\phi}), \quad \phi_n{}' = \frac{d\phi_n}{d\eta_o}, \quad a_1^{\,2} = 1 + \frac{2m_1}{\rho_o \ell_1}, \quad a_2^{\,2} = 1 + \frac{2m_2}{\rho_o \ell_2} \tag{172}$$

Thus, the total virtual work due to the gravitational potential energy and elastic strain energy in the generalized coordinates is

$$\Sigma Q_j \, \delta q_j = \delta R \left[-\frac{K}{R^2} M \right] + \delta\theta\,[o] + \delta r \left[-\frac{K}{R^3} \left(\frac{r}{r_o^2} \right) I \,(1 - 3\cos^2\phi) - \frac{EA}{r_{ot}} (r - r_{ot}) \right]$$

$$+ \delta\phi \left[-\frac{3K}{R^3} \sin\phi \cos\phi \left(\frac{r^2}{r_o^2} I - \Sigma M_n q_n^2 \right) \right]$$

$$+ \delta q_m \left[-\frac{K}{R_3} M_n q_n \,(1 - 3\sin^2\phi) - (\dot\theta + \dot\phi)\,(N_n q_n + \Sigma q_m N_{mn}) \right] \qquad (173)$$

where

$$M = m_1 + m_2 + \rho_o r_o$$

and

$$I = m_1 \ell_1^2 + m_2 \ell_2^2 + \frac{\rho_o}{3} \left(\ell_1^3 + \ell_2^3 \right) \qquad (174)$$

In deriving equation (173), the important properties of normal modes of free vibration were used, i.e., the zero resultant of linear and angular momenta in each mode and the orthogonality of normal modes.

The values of M_n, N_n and N_{mn} are defined by the following conditions

$$\rho_o \int_{-\ell_2}^{\ell_1} \phi_n \phi_m \, d\eta_o + m_1 \phi_n(\ell_1) \phi_m(\ell_1) + m_2 \phi_n(-\ell_2) \phi_m(-\ell_2) = \begin{cases} M_n & \text{for } n = m \\ O & \text{for } n \neq m \end{cases}$$

$$\frac{\rho_o}{2} \ell_1^2 \int_o^{\ell_1} \left(a_1^2 - \frac{\eta_o^2}{\ell_1^2} \right) \phi'_n \phi'_m \, d\eta_o$$

$$+ \frac{\rho_o}{2} \ell_2^2 \int_o^{\ell_2} \left(a_2^2 - \frac{\eta_o^2}{\ell_2^2} \right) \phi'_n \phi'_m \, d\eta_o = \begin{cases} N_n & \text{for } n = m \\ N_{mn} & \text{for } n \neq m \end{cases} \qquad (175)$$

Routine application of the preceding equations leads to the following set of system equations

R - equation

$$M\ddot{R} - MR\dot{\theta}^2 = -\frac{K}{R^2}M \tag{176}$$

θ - equation

$$\frac{d}{dt}\left[MR^2\dot{\theta} + \frac{I}{r_o^2}(\dot{\theta} + \dot{\phi})r^2 + (\dot{\theta} + \dot{\phi})\Sigma M_n q_n^2\right] = 0 \tag{177}$$

r - equation

$$[\ddot{r} - (\dot{\theta} + \dot{\phi})^2 r]\frac{I}{r_o^2} = -\frac{Kr}{R^3}(1 - 3\cos^2\phi)\frac{I}{r_o^2} - \frac{EA(r - r_{ot})}{r_{ot}} \tag{178}$$

ϕ - equation

$$(\ddot{\theta} + \ddot{\phi})\left(\frac{Ir^2}{r_o^2} + \Sigma M_n q_n^2\right) + 2(\dot{\theta} + \dot{\phi})\left(\frac{Ir\dot{r}}{r_o^2} + \Sigma M_n q_n \dot{q}_n\right)$$

$$= -\frac{3K}{R^3}\sin\phi\cos\phi\left(\frac{Ir^2}{r_o^2} - \Sigma M_n q_n^2\right) \tag{179}$$

q_n - equation

$$M_n \ddot{q}_n = \frac{K M_n}{R^3}[3\sin^2\phi - 1]q_n - (\dot{\theta} + \dot{\phi})(N_n - M_n)q_n$$

$$- (\dot{\theta} + \dot{\phi})\sum_{m \neq n} q_m N_{mn}$$

$$(n = 1, 2, \ldots N;\ m = 1, 2, \ldots, N) \tag{180}$$

The resulting equations reveal that the rotational and vibrational motion about the center of mass represented by equations (178), (179) and

(180) are coupled with the orbital motion represented by equations (176) and (177) through the terms of gravitational gradient, and cannot be treated separately.

In the case where only the extensional motion is assumed, i.e., $q_n = 0$, equations (176) to (180) are reduced to the following form

R-equation

$$\ddot{R} - R\dot{\theta}^2 = -\frac{K}{R^2} \tag{181}$$

θ - equation

$$\frac{d}{dt}\left[MR^2\,\dot{\theta} + \frac{I}{r_o^2}(\dot{\theta} + \dot{\phi})\,r^2\right] = 0 \tag{182}$$

r - equation

$$\ddot{r} - (\dot{\theta} + \dot{\phi})^2\,r = -\frac{Kr}{R^3}(1 - 3\cos^2\phi) - \frac{EA\,(r - r_{ot})\,r_o^2}{I} \tag{183}$$

φ - equation

$$(\ddot{\theta} + \ddot{\phi})\,r + 2\,(\dot{\theta} + \dot{\phi})\,\dot{r} = -\frac{3Kr}{R_o^3}\sin\phi\cos\phi \tag{184}$$

The preceding four equations represent the planar motion of a compartment and a counterweight connected by an elastic cable. Equations (181) to (184) are much more simple in form than equations (176) to (180), but in both cases, satisfactory computer solutions are difficult to achieve. The summation of a very large number, such as the orbital radius to several powers, and a very small number, such as gravity forces, may lose the significant role played by the smaller number. In fact, the effect of small forces is of primary concern.

The computer solutions will be discussed in a subsequent section. However, the stableness of circular orbit of the elastic cable-connected space station (not the stability of configuration), can be shown here from a simplified approach. From the conservation of momentum equation (182),

$$R^2\,\dot{\theta} + \frac{I}{Mr_o^2}(\dot{\theta} + \dot{\phi})\,r^2 = C_o \tag{185}$$

Let $C_1 = \dfrac{I}{M r_o^2}$ and $C_o = R_o^2 \dot{\theta}_o + C_1 (\dot{\theta}_o + \dot{\phi}_o) r_o^2$; equation (185) yields

$$\dot{\theta} = \frac{C_o - C_1 r^2 \dot{\phi}}{R^2 + C_1 r^2} \qquad (186)$$

Substituting equation (186) into equation (181), and neglecting higher order terms in the binomial expansion

$$\ddot{R} - \left(C_o - C_1 r^2 \dot{\phi}\right)^2 \left(1 - 2 C_1 \frac{r^2}{R^2}\right) R^{-3} = - KR^{-2} \qquad (187)$$

Let $R = R_o + \beta$ and substitute into equation (187); after neglecting higher order terms, the equation becomes

$$\ddot{\beta} + \left[3 R_o^{-4} \left(C_o - C_1 r^2 \dot{\phi}\right)^2 - 2 KR_o^{-3}\right]\beta = R_o^{-3} \left(C_o - C_1 r^2 \dot{\phi}\right)^2 - KR_o^{-2}$$

In steady state, $R = R_o$, $\ddot{R}_o = 0$; from equation (181) we obtain

$$- KR_o^{-2} = - R_o^{-3} \left(C_o - C_1 r_o^2 \dot{\phi}_o\right)^2 \left(1 + C_1 \frac{r_o^2}{R_o^2}\right)^{-2}$$

$$= - \left(C_o - C_1 r_o^2 \dot{\phi}_o\right)^2 R_o^{-3}$$

Hence

$$\ddot{\beta} + \left[3 R_o^{-4} \left(C_o - C_1 r^2 \dot{\phi}\right)^2 - 2 K R_o^{-3}\right] \beta = 0 \qquad (188)$$

Thus, only when

$$\alpha^2 = \left[3 R_o^{-4} \left(C_o - C_1 r^2 \dot{\phi}\right)^2 - 2 K R_o^{-3}\right] > 0$$

or

$$\frac{C_o}{2 C_1}\left(\frac{3 C_o^2}{2 K R_o} - 1\right) > r^2 \dot{\phi} \qquad (189)$$

the periodic motion in β of frequency α rad/sec. will give a stable circular orbit.

For the artificial gravity of 1 g in the compartment, and using

$$R_o = 0.21454428 \times 10^8 \text{ ft}$$

$$\dot{\theta} = 0.0011939534 \text{ rad/sec}$$

$$K = 0.140775 \times 10^{17} \text{ ft}^3/\text{sec}$$

$$r_o = 1000 \text{ ft}$$

$$\dot{\phi}_o = \begin{cases} 0.49915338 \text{ rad/sec.; when mass of the cable is included} \\ 0.53811378 \text{ rad/sec.; when mass of the cable is not included} \end{cases}$$

$$m_1 = 1.242236 \times 10^3 \text{ slugs}$$

$$m_2 = 0.1552795 \times 10^3 \text{ slugs}$$

$$\rho_o = 0.06832298 \text{ slugs/ft}$$

we find

$$\frac{C_o}{2\,C_1}\left(\frac{3\,C_o^{\,2}}{2\,K\,R_o} - 1\right) = 0.13113073 \times 10^{13}$$

The value of $\dot{\phi} r^2$ at steady state is

$$r_o^{\,2}\,\dot{\phi}_o = 0.499 \times 10^6 \ll 0.131 \times 10^{13}$$

It is difficult to see that the value of $r^2\,\dot{\phi}$ in the unsteady state will be greater than the value, 0.13×10^{13}. Hence, from the investigation of the R-equation, it is shown that the periodic motion in β will have a stable circular orbit.

8.3 EQUATIONS OF PLANAR MOTION OF THE Y-CONFIGURATION SPACE STATION

Consider the Y-configuration space station rotating in the plane of the orbit. The modules are designated as a, b, and c; x, y (unit vectors $\bar{i}_I$ and $\bar{j}_I$) are inertia coordinates (Figure 47), with their origin at the center of the earth; η and ζ, with subscripts a, b, and c are the coordinates of the modules along, and normal to, their respective longitudinal axes; and η and ζ, with subscript H, are the coordinates of the hub along, and normal to, module "a" $\bar{i}$, $\bar{j}$ and $\bar{k}$ are rotating coordinates with their origin at the center of mass and $\bar{i}$ coincides with module "a" of the undeformed configuration. The vectors $\bar{R}$ and $\bar{R}_a$ are directed from the center of the earth to

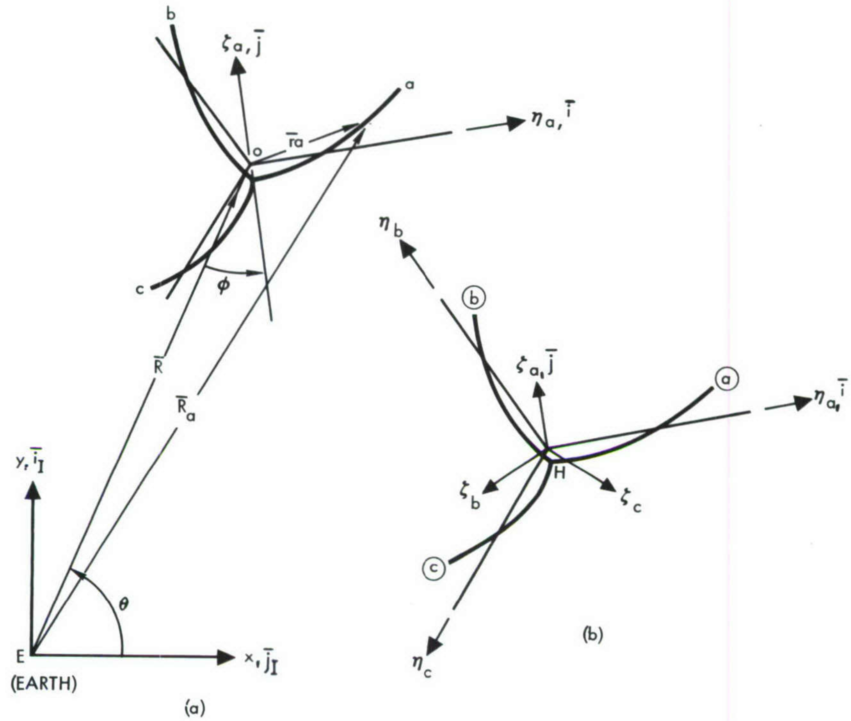

Figure 47. Coordinate Systems of Y-Configuration

the center of mass of the Y-configuration, and a point on module a, respectively. The inertial velocity of the point on module a is

$$\bar{v}_a = \bar{v}_o + [\dot{\bar{r}}_a] + (\dot{\theta} + \dot{\phi})\,\bar{k} \times \bar{r}_a \tag{190}$$

where

$$\bar{v}_o = (\dot{R} \sin\phi - R\,\dot{\theta} \cos\phi)\,\bar{i} + (\dot{R} \cos\phi + R\,\theta \sin\phi)\,\bar{j}$$

$$\bar{r}_a = \eta_a\,\bar{i} + \zeta_a\,\bar{j}, \qquad [\dot{\bar{r}}_a] = \dot{\eta}_a\,\bar{i} + \dot{\zeta}_a\,\bar{j}$$

$$(\dot{\theta} + \dot{\phi})\,\bar{k} \times \bar{r}_a = -\zeta_a\,(\dot{\theta} + \dot{\phi})\,\bar{i} + \eta_a\,(\dot{\theta} + \dot{\phi})\,\bar{j}$$

Therefore,

$$\bar{v}_a = [\dot{\eta}_a + \dot{R} \sin\phi - R\,\dot{\theta} \cos\phi - \zeta_a\,(\dot{\theta} + \dot{\phi})]\,\bar{i} + [\dot{\zeta}_a + \dot{R} \cos\phi + R\,\dot{\theta} \sin\phi + \eta_a\,(\dot{\theta} + \dot{\phi})]\,\bar{j} \tag{191}$$

Equations for $\bar{v}_b$ and $\bar{v}_c$ can be obtained directly from equation (191) with the following substitution.

For $\bar{v}_b$,

$$\left.\begin{aligned} &\text{Replace } \eta_a \text{ by } \left(-\frac{1}{2}\eta_b - \frac{\sqrt{3}}{2}\zeta_b\right) \\ &\text{replace } \zeta_a \text{ by } \left(\frac{\sqrt{3}}{2}\eta_b - \frac{1}{2}\zeta_b\right) \end{aligned}\right\}$$

For $\bar{v}_c$,

$$\left.\begin{aligned} &\text{replace } \eta_a \text{ by } \left(-\frac{1}{2}\eta_c + \frac{\sqrt{3}}{2}\zeta_c\right) \\ &\text{replace } \zeta_a \text{ by } \left(-\frac{\sqrt{3}}{2}\eta_c - \frac{1}{2}\zeta_c\right) \end{aligned}\right\} \tag{192}$$

Thus,

$$\begin{aligned} \bar{v}_b = {} & \left[\left(-\frac{1}{2}\dot{\eta}_b - \frac{\sqrt{3}}{2}\dot{\zeta}_b\right) + \dot{R}\sin\phi - R\dot{\theta}\cos\phi - (\dot{\theta}+\dot{\phi})\left(\frac{\sqrt{3}}{2}\eta_b\right.\right. \\ & \left.\left. - \frac{1}{2}\zeta_b\right)\right]\bar{i} + \left[\left(\frac{\sqrt{3}}{2}\dot{\eta}_b - \frac{1}{2}\dot{\zeta}_b\right) + \dot{R}\cos\phi + R\dot{\theta}\sin\phi\right. \\ & \left. + (\dot{\theta}+\dot{\phi})\left(-\frac{1}{2}\eta_b - \frac{\sqrt{3}}{2}\zeta_b\right)\right]\bar{j} \end{aligned} \tag{193}$$

and

$$\begin{aligned} \bar{v}_c = {} & \left[\left(-\frac{1}{2}\dot{\eta}_c + \frac{\sqrt{3}}{2}\dot{\zeta}_c\right) + \dot{R}\sin\phi - R\dot{\theta}\cos\phi - (\dot{\theta}+\dot{\phi})\left(-\frac{\sqrt{3}}{2}\eta_c\right.\right. \\ & \left.\left. - \frac{1}{2}\zeta_c\right)\right]\bar{i} + \left[\left(-\frac{\sqrt{3}}{2}\dot{\eta}_c - \frac{1}{2}\dot{\zeta}_c\right) + \dot{R}\cos\phi + R\dot{\theta}\sin\phi\right. \\ & \left. + (\dot{\theta}+\dot{\phi})\left(-\frac{1}{2}\eta_c + \frac{\sqrt{3}}{2}\zeta_c\right)\right]\bar{j} \end{aligned} \tag{194}$$

Use subscript, H, in referring to the hub, then,

$$\bar{r}_H = \eta_H\,\bar{i} + \zeta_H\,\bar{j}$$

$$\begin{aligned} \bar{v}_H = {} & \bar{v}_o + \dot{\bar{r}}_H + (\dot{\theta}+\dot{\phi})\,\bar{k}\times\bar{r}_H = [\dot{\eta}_H + \dot{R}\sin\phi - R\dot{\theta}\cos\phi \\ & - \zeta_H(\dot{\theta}+\dot{\phi})]\,\bar{i} + [\dot{\zeta}_H + \dot{R}\cos\phi + R\dot{\theta}\sin\phi + \eta_H(\dot{\theta}+\dot{\phi})]\,\bar{j} \end{aligned} \tag{195}$$

Let m equal the mass per unit length of modules a, b and c, and M_H equal the mass of the hub. The kinetic energy of module a is

$$2T_a = \int_0^{\ell} m\, \bar{v}_a \cdot \bar{v}_a \; d\eta_a = m \int \Big\{ \dot{\eta}_a^{\,2} + \dot{\zeta}_a^{\,2} + \dot{R}^2 + R^2 \dot{\theta}^2 + (\dot{\theta} + \dot{\phi})^2 \left(\eta_a^{\,2} + \zeta_a^{\,2}\right) + 2\dot{\eta}_a \left[\dot{R} \sin \phi - R \dot{\theta} \cos \phi - \zeta_a (\dot{\theta} + \dot{\phi})\right] + 2\dot{\zeta}_a \left[\dot{R} \cos \phi + R \dot{\theta} \sin \phi + \eta_a (\dot{\theta} + \dot{\phi})\right] + 2\zeta_a (\dot{\theta} + \dot{\phi}) \left[-\dot{R} \sin \phi + R \dot{\theta} \cos \phi\right] + 2\eta_a (\dot{\theta} + \dot{\phi}) \left[\dot{R} \cos \phi + R \dot{\theta} \sin \phi\right] \Big\} d\eta_a \tag{196}$$

The kinetic energy, T_b and T_c, of modules b and c can be obtained by introducing equation (192) into equation (196).

The kinetic energy of the hub is

$$2T_H = M_H \bar{v}_H \cdot \bar{v}_H + I_{MH} (\dot{\theta} + \dot{\phi})^2 = M_H \Big\{ \dot{\eta}_H^{\,2} + \dot{\zeta}_H^{\,2} + \dot{R}^2 + R^2 \dot{\theta}^2 + (\dot{\theta} + \dot{\phi})^2 \left(\eta_H^{\,2} + \zeta_H^{\,2}\right) + 2\dot{\eta}_H \left[\dot{R} \sin \phi - R \dot{\theta} \cos \phi - \zeta_H (\dot{\theta} + \dot{\phi})\right] + 2\dot{\zeta}_H \left[\dot{R} \cos \phi + R \dot{\theta} \sin \phi + \eta_H (\dot{\theta} + \dot{\phi})\right] + 2\zeta_H (\dot{\theta} + \dot{\phi}) \left[-\dot{R} \sin \phi + R \dot{\theta} \cos \phi\right] + 2\eta_H (\dot{\theta} + \dot{\phi}) \left[\dot{R} \cos \phi + R \dot{\theta} \sin \phi\right] \Big\} + I_{MH} (\dot{\theta} + \dot{\phi})^2 \tag{197}$$

where

I_{MH} = rotary inertia of the hub

The total kinetic energy is

$$T_{(TOTAL)} = T_H + T_a + T_b + T_c \tag{198}$$

Let the coordinates of the elastic curve of the deformed configuration be expressed in terms of normal modes, thus,

$$
\begin{aligned}
\zeta_a (z_a, t) &= \sum_{n=1}^{\infty} u_{an} (z_a)\, q_n (t) \\
\eta_a (z_a, t) &= z_a + \sum_{n=1}^{\infty} w_{an}\, q_n (t) \\
\zeta_b (z_b, t) &= \sum_{n=1}^{\infty} u_{bn} (z_b)\, q_n (t) \\
\eta_b (z_b, t) &= z_b + \sum_{n=1}^{\infty} w_{bn}\, q_n (t) \\
\zeta_c (z_c, t) &= \sum_{n=1}^{\infty} u_{cn} (z_c)\, q_n (t) \\
\eta_c (z_c, t) &= z_c + \sum_{n=1}^{\infty} w_{cn}\, q_n (t) \\
\zeta_H (z_H, t) &= \sum_{n=1}^{\infty} u_{Hn} (z_H)\, q_n (t) \text{ where } z_H = 0 \\
\eta_H (t) &= \sum_{n=1}^{\infty} w_{Hn}\, q_n (t)
\end{aligned}
\qquad (199)
$$

where

$$
\left.\begin{matrix} u_n \\ w_n \end{matrix}\right\} = \text{components of the } n^{th} \text{ normal mode shapes.}
$$

Subscripts a, b, c and H refer to modules a, b, c and the hub.

q_n (t) = the generalized coordinates, giving the displacement in the n^{th} mode.

z_a, z_b, and z_c = positions of mass elements in the reference steady state.

By Lagrange's method, the equations of motion are

$$\frac{d}{dt}\left(\frac{\partial T}{\partial \dot{q}_j}\right) - \frac{\partial T}{\partial q_j} + \frac{\partial U}{\partial q_j} = Q_j \tag{200}$$

The generalized coordinates are R, θ, ϕ and q_i. Equation (199) represents orthogonal modes. From the orthogonal conditions, it can be shown that

$$m\ell\,[w_{an}\,w_{am} + w_{bn}\,w_{bm} + w_{cn}\,w_{cm}] + m \int [u_{an}\,u_{am}\,dz_a + u_{bn}\,u_{bm}\,dz_b$$

$$+ u_{cn}\,u_{cm}\,dz_c] + M_H\,[w_{Hn}\,w_{Hm} + u_{Hn}\,u_{Hm}] = \begin{cases} 0 & n \neq m \\ M_n & n = m \end{cases} \tag{201}$$

$$EI \int \left[u''_{an}\,u''_{am}\,dz_a + u''_{bn}\,u''_{bm}\,dz_b + u''_{cn}\,u''_{cm}\,dz_c\right] = \begin{cases} 0 & n \neq m \\ N_n & n = m \end{cases} \tag{202}$$

The preceding conditions, in addition to the zero-linear and angular-momentum conditions for each normal mode of free vibration, are used in the derivation of equations of motion. Another condition is also introduced in the derivation. This condition is written as

$$w_a + w_b + w_c = 0 \tag{203}$$

The components of generalized forces, Q_j, are evaluated from the work done by external forces. If the gravitational force is the only consideration,

$$\Sigma\, Q_j\, \delta q_j = \int d\overline{G}_a \cdot (\delta x_a\, \overline{i}_I) + \int d\overline{G}_b \cdot (\delta x_b\, \overline{i}_I) + \int d\overline{G}_c \cdot (\delta x_c\, \overline{i}_I) + \overline{G}_H \cdot (\delta x_H\, \overline{i}_I)$$

$$+ \int d\overline{G}_a \cdot (\delta y_a\, \overline{j}_I) + \int d\overline{G}_b \cdot (\delta y_b\, \overline{j}_I) + \int d\overline{G}_c \cdot (\delta y_c\, \overline{j}_I)$$

$$+ \overline{G}_H \cdot (\delta y_H\, \overline{j}_I) \tag{204}$$

In the rotational coordinate system, the position vector of H, and any point on modules a, b, and c are

$$\overline{R}_H = (\eta_H + R \sin \phi)\,\overline{i} + (\zeta_H + R \cos \phi)\,\overline{j}$$

$$\overline{R}_a = (\eta_a + R \sin \phi)\,\overline{i} + (\zeta_a + R \cos \phi)\,\overline{j}$$

$$\overline{R}_b = \left[\left(-\frac{1}{2}\eta_b - \frac{\sqrt{3}}{2}\zeta_b\right) + R \sin \phi\right]\overline{i} + \left[\left(\frac{\sqrt{3}}{2}\eta_b - \frac{1}{2}\zeta_b\right) + R \cos \phi\right]\overline{j}$$

$$\overline{R}_c = \left[\left(-\frac{1}{2}\eta_c + \frac{\sqrt{3}}{2}\zeta_c\right) + R \sin \phi\right]\overline{i} + \left[\left(-\frac{\sqrt{3}}{2}\eta_c - \frac{1}{2}\zeta_c\right) + R \cos \phi\right]\overline{j} \tag{205}$$

Using the relations between $\overline{i}$, $\overline{j}$ and $\overline{i}_I$, $\overline{j}_I$

$$\overline{i} = \sin(\theta + \phi)\,\overline{i}_I - \cos(\theta + \phi)\,\overline{j}_I$$

$$\overline{j} = \cos(\theta + \phi)\,\overline{i}_I + \sin(\theta + \phi)\,\overline{j}_I \tag{206}$$

The position vectors in the inertial coordinates are

$$\begin{aligned}\overline{R}_H = {} & [R \cos \theta + \eta_H \sin(\theta + \phi) + \zeta_H \cos(\theta + \phi)]\,\overline{i}_I + [R \sin \theta \\ & - \eta_H \cos(\theta + \phi) + \zeta_H \sin(\theta + \phi)]\,\overline{j}_I \\ \overline{R}_a = {} & [R \cos \theta + \eta_a \sin(\theta + \phi) + \zeta_a \cos(\theta + \phi)]\,\overline{i}_I + [R \sin \theta \\ & - \eta_a \cos(\theta + \phi) + \zeta_a \sin(\theta + \phi)]\,\overline{j}_I\end{aligned} \tag{207}$$

The values of $\overline{R}_b$ and $\overline{R}_c$ can be easily obtained from $\overline{R}_a$ by using the relation shown in equation (192).

From the preceding equations, virtual displacements are determined to be

$$\begin{bmatrix} \delta x_H \\ \delta x_a \end{bmatrix} = \cos\theta\,\delta R + \left\{ - R\sin\theta + \begin{bmatrix} \eta_H \\ \eta_a \end{bmatrix} \cos(\theta+\phi) - \begin{bmatrix} \zeta_H \\ \zeta_a \end{bmatrix} \sin(\theta+\phi) \right\} \delta\theta$$

$$+ \left\{ \begin{bmatrix} \eta_H \\ \eta_a \end{bmatrix} \cos(\theta+\phi) - \begin{bmatrix} \zeta_H \\ \zeta_a \end{bmatrix} \sin(\theta+\phi) \right\} \delta\phi$$

$$+ \left\{ \sin(\theta+\phi) \begin{bmatrix} \Sigma\, w_H \\ \Sigma\, w_a \end{bmatrix} + \cos(\theta+\phi) \begin{bmatrix} \Sigma\, u_H \\ \Sigma\, u_a \end{bmatrix} \right\} \delta q_n$$

$$\begin{bmatrix} \delta y_H \\ \delta y_a \end{bmatrix} = \sin\theta\,\delta R + \left\{ R\cos\theta + \begin{bmatrix} \eta_H \\ \eta_a \end{bmatrix} \sin(\theta+\phi) + \begin{bmatrix} \zeta_H \\ \zeta_a \end{bmatrix} \cos(\theta+\phi) \right\} \delta\theta$$

$$+ \left\{ \sin(\theta+\phi) \begin{bmatrix} \eta_H \\ \eta_a \end{bmatrix} + \cos(\theta+\phi) \begin{bmatrix} \zeta_H \\ \zeta_a \end{bmatrix} \right\} \delta\phi$$

$$+ \left\{ -\cos(\theta+\phi) \begin{bmatrix} \Sigma\, w_H \\ \Sigma\, w_a \end{bmatrix} + \sin(\theta+\phi) \begin{bmatrix} \Sigma\, u_H \\ \Sigma\, u_a \end{bmatrix} \right\} \delta q_n \tag{208}$$

Similarly, the virtual displacements, δx_b, δx_c, δy_b, and δy_c can be obtained from δx_a and δy_a by introducing equation (192).

The gravitational forces on the central hub and on a small element of modules a, b, c are given by

$$\bar{G}_H = -\frac{K\,M_H}{R^3} \Big\{ [R\cos\theta + \eta_H \sin(\theta+\phi) + \zeta_H \cos(\theta+\phi)]\,\bar{i}_I$$

$$+ [R\sin\theta - \eta_H\cos(\theta+\phi) + \zeta_H \sin(\theta+\phi)]\,\bar{j}_I$$

$$d\bar{G}_a = -\frac{K\,m\,d\eta_a}{R^3} \Big\{ [R\cos\theta + \eta_a \sin(\theta+\phi) + \zeta_a \cos(\theta+\phi)]\,\bar{i}_I$$

$$+ [R\sin\theta - \eta_a\cos(\theta+\phi) + \zeta_a \sin(\theta+\phi)]\,\bar{j}_I \Big\}$$

$$d\overline{G}_b = -\frac{K\, m\, d\eta_b}{R^3} \left\{ \left[R \cos\theta + \left(-\frac{1}{2}\eta_b - \frac{\sqrt{3}}{2}\zeta_b \right) \sin(\theta + \phi) \right.\right.$$

$$\left. + \left(\frac{\sqrt{3}}{2}\eta_b - \frac{1}{2}\zeta_b \right) \cos(\theta + \phi) \right] \overline{i}_I + \left[R \sin\theta - \left(-\frac{1}{2}\eta_b \right.\right.$$

$$\left.\left. - \frac{\sqrt{3}}{2}\zeta_b \right) \cos(\theta + \phi) + \left(\frac{\sqrt{3}}{2}\eta_b - \frac{1}{2}\zeta_b \right) \sin(\theta + \phi) \right] \overline{j}_I$$

$$d\overline{G}_c = -\frac{K\, m\, d\eta_c}{R^3} \left\{ \left[R \cos\theta + \left(-\frac{1}{2}\eta_c + \frac{\sqrt{3}}{2}\zeta_c \right) \sin(\theta + \phi) \right.\right.$$

$$\left. + \left(-\frac{\sqrt{3}}{2}\eta_c - \frac{1}{2}\zeta_c \right) \cos(\theta + \phi) \right] \overline{i}_I + \left[R \sin\theta - \left(-\frac{1}{2}\eta_c \right.\right.$$

$$\left.\left. + \frac{\sqrt{3}}{2}\zeta_c \right) \cos(\theta + \phi) + \left(-\frac{\sqrt{3}}{2}\eta_c - \frac{1}{2}\zeta_c \right) \sin(\theta + \phi) \right] \overline{j}_I \qquad (209)$$

The assumption

$$R_i^{-3} = R^{-3} \qquad (i = a, b, c, H) \qquad (210)$$

has been imposed on equations (209). Substituting the relation of equations (208) and (209) into equation (204), the components of the generalized forces due to gravitational gradient are computed to be

$$Q_R = -\frac{K}{R^2}[3\, m\ell + M_H]$$

$$Q_\phi = 0$$

$$Q_\theta = 0$$

$$Q_{q_n} = -\frac{K}{R^3} M_n\, q_n \qquad (211)$$

Since the extensional elastic deformation of the modules is neglected in equation (199), because of its small magnitude in comparison to its rigid body movement, the total strain energy of modules a, b, and c is derived from the bending deformation. Thus,

$$U = \frac{EI}{2} \int \left\{ \left(\frac{\partial^2 \zeta_a}{\partial z_a^2} \right)^2 dz_a + \left(\frac{\partial^2 \zeta_b}{\partial z_b^2} \right)^2 dz_b + \left(\frac{\partial^2 \zeta_c}{\partial z_c^2} \right)^2 dz_c \right\}$$

$$= \frac{EI}{2} \int \left\{ \left(\Sigma u_a'' q \right)^2 dz_a + \left(\Sigma u_b'' q \right)^2 dz_b + \left(\Sigma u_c'' q \right)^2 dz_c \right\} \tag{212}$$

and

$$\frac{\partial U}{\partial q_n} = EI \int \left\{ u_{an}'' \Sigma u_{am}'' q_m dz_a + u_{bn}'' \Sigma u_{bm}'' q_m dz_b + u_{cn}'' \Sigma u_{cm}'' q_m dz_c \right\}$$

$$= \begin{cases} 0 & n \neq m \\ N_n q_n & n = m \end{cases} \tag{213}$$

Substituting the values of equations (198), (211) and (213) into Lagrange's equations of motion (200), and using the property of normal modes and conditions in equations (201), (202), and (203), the equations of planar motion of the Y-configuration are

$$\ddot{R} - R\dot{\theta}^2 = - \frac{K}{R^2} \tag{214}$$

$$R^2 \dot{\theta} \; [3m\ell + M_H] + (\dot{\theta} + \dot{\phi}) \left[m\ell^3 + \sum_{n=1}^{\infty} M_n q_n^2 + I_{mH} \right]$$

$$- I_{mH} \sum_{n=1}^{\infty} u_{Hn}' \dot{q}_n = C_1 \tag{215}$$

$$(\dot{\theta} + \dot{\phi}) \left[m\ell^3 + \sum_{n=1}^{\infty} M_n q_n^2 + I_{mH} \right] - I_{mH} \sum_{n=1}^{\infty} u_{Hn}' \dot{q}_n = C_2 \tag{216}$$

$$\ddot{q}_n + \left[\frac{K}{R^3} - (\dot{\theta} + \dot{\phi})^2 + \frac{N_n}{M_n} \right] q_n = (\ddot{\theta} + \ddot{\phi}) \frac{I_{mH}}{M_n} u_{Hn}'$$

$$(n = 1, 2, \ldots) \tag{217}$$

By using equation (216), equation (215) becomes

$$R^2 \dot{\theta} = \frac{C_1 - C_2}{3m\ell + M_H} = C_3 \tag{218}$$

where

K = the product of gravitational constant and mass of earth

C_1, C_2, C_3 = numerical constants determined by initial conditions

M_n and N_n = constants obtained from the orthogonal conditions of normal modes and $u_H = \frac{\partial \zeta_H}{\partial z_H}$.

It can be seen from equations (214) and (218) that the orbital motion is independent from the rotational motion of the station, but the elastic degrees of freedom are coupled with the rotational degree of freedom through equations (216) and (217). If we include the higher order terms in the expansion of R_i^{-3} instead of the assumption made in equation (210), then the resulting equations will show that the orbital and rotational motions are coupled by the gravitational terms, and that the rotational degrees of freedom are coupled with the elastic degrees of freedom.

8.4 EQUATIONS OF PLANAR MOTION OF THE H-CONFIGURATION SPACE STATION

Consider the H-configuration (two compartments connected with compression members) rotating in the plane of the orbit. The compartments, spokes, and hub are designated as a, b, c, d, and H, respectively. Their elastic displacements are denoted by v and w with subscripts a, b, c, d, and H. x_I, y_I (unit vectors $\bar{i}_I$ and $\bar{j}_I$) are inertia coordinates with origin at center of earth. η_a, ζ_a, η_b, ζ_b, η_c, ζ_c, η_d, ζ_d, η_H and ζ_H are the coordinates of the modules, spokes and hub (as shown in Figure(48) $\bar{i}$, $\bar{j}$, $\bar{k}$ are the rotating coordinates with origin at the mass center of the system and $\bar{i}$ coincides with the spoke of undeformed configuration. The vector $\bar{R}$ is directed from the center of earth to the center of mass of the system. The vectors $\bar{r}_a$, $\bar{r}_b$, $\bar{r}_c$, $\bar{r}_d$ and $\bar{r}_H$ are drawn from center of mass of the system to a point on the respective elements. x, y are steady-state coordinates with origin at center of mass of the system. By expressing the coordinates of the elastic curve of the deformed configuration in terms of normal modes, we have

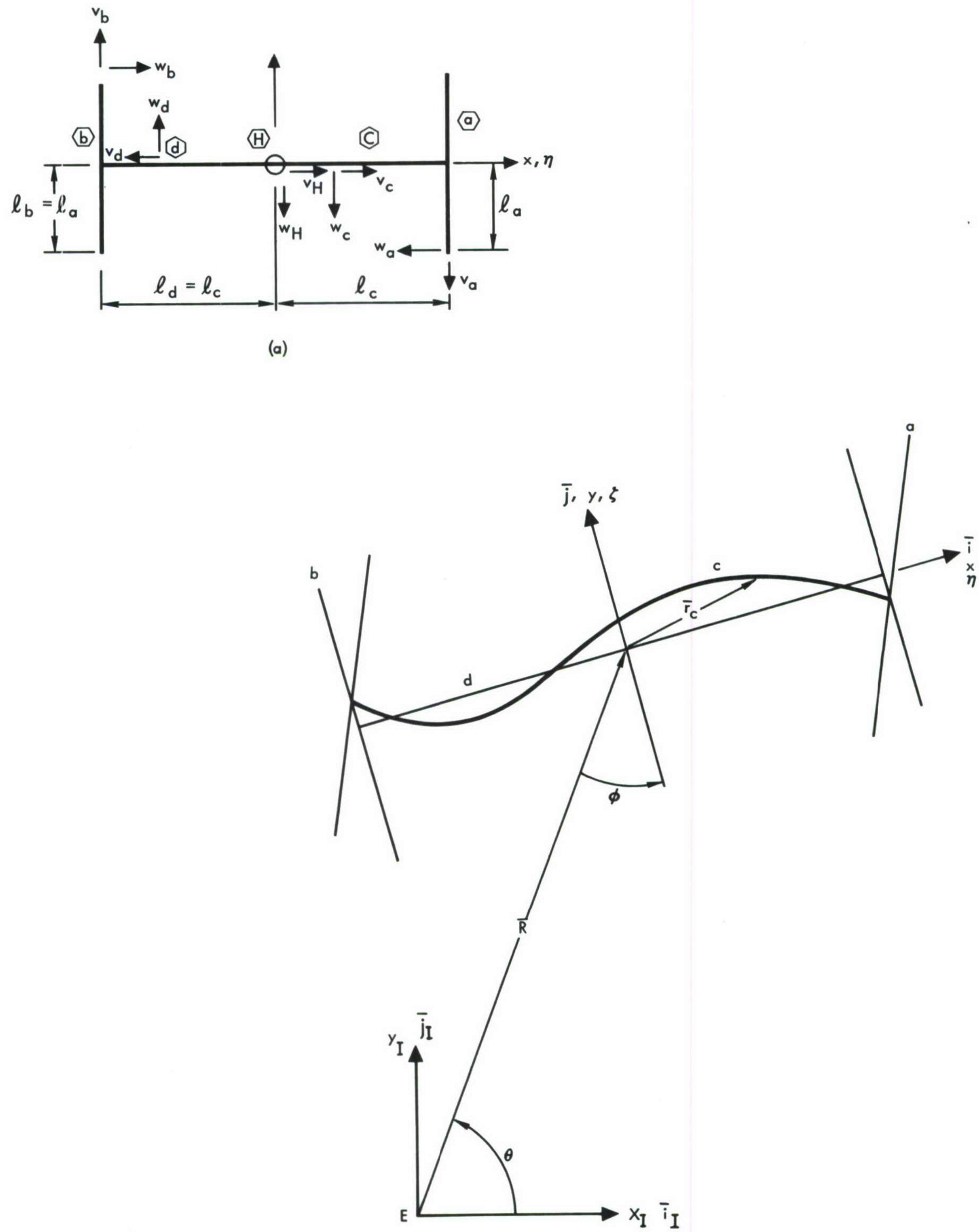

Figure 48. Coordinate Systems of H-Configuration

$$\bar{r}_c = \left[x_c + \sum_{n=1}^{\infty} v_{cn} q_n(t)\right]\bar{i} - \left[\sum_{n=1}^{\infty} w_{cn}(x_c) q_n(t)\right]\bar{j} = \eta_c \bar{i} + \zeta_c \bar{j}$$

$$\bar{r}_d = \left[x_d - \sum_{n=1}^{\infty} v_{dn} q_n(t)\right]\bar{i} + \left[\sum_{n=1}^{\infty} w_{dn}(x_d) q_n(t)\right]\bar{j} = \eta_d \bar{i} + \zeta_d \bar{j}$$

$$\bar{r}_a = \left[\ell_c - \sum_{n=1}^{\infty} w_{an}(y_a) q_n(t)\right]\bar{i} + \left[y_a - \sum_{n=1}^{\infty} v_{an} q_n(t)\right]\bar{j} = \eta_a \bar{i} + \zeta_a \bar{j}$$

$$\bar{r}_b = \left[-\ell_c + \sum_{n=1}^{\infty} w_{bn}(y_b) q_n(t)\right]\bar{i} + \left[y_b + \sum_{n=1}^{\infty} v_{bn} q_n(t)\right]\bar{j} = \eta_b \bar{i} + \zeta_b \bar{j}$$

$$\bar{r}_H = \sum_{n=1}^{\infty} v_{Hn} q_n(t)\bar{i} - \sum_{n=1}^{\infty} w_{Hn}(z_H) q_n(t)\bar{j} = \eta_H \bar{i} + \zeta_H \bar{j}$$

$$z_H = 0 \tag{219}$$

Where

w_n and v_n = the nth mode functions.

$q_n(t)$ = generalized coordinates giving the displacement in the nth mode.

x, y and η, ζ = coordinate systems of steady state and deformed state, respectively.

The inertial velocity of center of mass of the system is

$$\bar{v}_o = (\dot{R} \sin\phi - R\dot{\theta}\cos\phi)\bar{i} + (\dot{R}\cos\phi + R\dot{\theta}\sin\phi)\bar{j}$$

The inertial velocity of a point on spoke c is

$$\bar{v}_c = \bar{v}_o + [\dot{\bar{r}}_c] + (\dot{\theta} + \dot{\phi})\bar{k} \times \bar{r}_c$$

where

$$[\dot{\bar{r}}_c] = \dot{\eta}_c \, \bar{i} + \dot{\zeta}_c \, \bar{j}$$

$$(\dot{\theta} + \dot{\phi}) \, \bar{k} \times \bar{r}_c = - \zeta_c \, (\dot{\theta} + \dot{\phi}) \, \bar{i} + \eta_c \, (\dot{\theta} + \dot{\phi}) \, \bar{j}$$

Therefore

$$\begin{aligned} \bar{v}_c = {} & [\dot{\eta}_c + \dot{R} \sin \phi - R\dot{\theta} \cos \phi - \zeta_c \, (\dot{\theta} + \dot{\phi})] \, \bar{i} \\ & + [\dot{\zeta}_c + \dot{R} \cos \phi + R\dot{\theta} \sin \phi + \eta_c \, (\dot{\theta} + \dot{\phi})] \, \bar{j} \end{aligned} \tag{220}$$

Similarly,

$$\begin{aligned} \bar{v}_d = {} & [\dot{\eta}_d + \dot{R} \sin \phi - R\dot{\theta} \cos \phi - \zeta_d \, (\dot{\theta} + \dot{\phi})] \, \bar{i} \\ & + [\dot{\zeta}_d + \dot{R} \cos \phi + R\dot{\theta} \sin \phi + \eta_d \, (\dot{\theta} + \dot{\phi})] \, \bar{j} \end{aligned} \tag{221}$$

$$\begin{aligned} \bar{v}_a = {} & [\dot{\eta}_a + \dot{R} \sin \phi - R\dot{\theta} \cos \phi - \zeta_a \, (\dot{\theta} + \dot{\phi})] \, \bar{i} \\ & + [\dot{\zeta}_a + \dot{R} \cos \phi + R\dot{\theta} \sin \phi + \eta_a \, (\dot{\theta} + \dot{\phi})] \, \bar{j} \end{aligned} \tag{222}$$

$$\begin{aligned} \bar{v}_b = {} & [\dot{\eta}_b + \dot{R} \sin \phi - R\dot{\theta} \cos \phi - \zeta_b \, (\dot{\theta} + \dot{\phi})] \, \bar{i} \\ & + [\dot{\zeta}_b + \dot{R} \cos \phi + R\dot{\theta} \sin \phi + \eta_b \, (\dot{\theta} + \dot{\phi})] \, \bar{j} \end{aligned} \tag{223}$$

$$\begin{aligned} \bar{v}_H = {} & [\dot{\eta}_H + \dot{R} \sin \phi - R\dot{\theta} \cos \phi - \zeta_H \, (\dot{\theta} + \dot{\phi})] \, \bar{i} \\ & + [\dot{\zeta}_H + \dot{R} \cos \phi + R\dot{\theta} \sin \phi + \eta_H \, (\dot{\theta} + \dot{\phi})] \, \bar{j} \end{aligned} \tag{224}$$

Let m_a, m_b, m_c, and m_d be the mass per unit length of the elements a, b, c and d; and M_a, M_b, M_c, M_d, and M_H be the total mass of the elements a, b, c, d, and the central hub; and designate the rotary inertia of the hub as I_{MH}

$$\int_o^{\ell_c} m_c \, dx_c = m_c \, \ell_c = M_c$$

$$\int_{-\ell_d}^{o} m_d \, dx_d = m_d \, \ell_d = M_d = M_c$$

$$\int_{-\ell_a}^{\ell_a} m_a \, dy_a = 2 m_a \ell_a = M_a$$

$$\int_{-\ell_b}^{\ell_b} m_b \, dy_b = 2 m_b \ell_b = M_b = M_a \tag{225}$$

The total kinetic energy of the system is

$$2T_{(TOTAL)} = \int^{\ell_c} \bar{v}_c \cdot \bar{v}_c \, m_c \, dx_c + \int_{-\ell_d}^{o} \bar{v}_d \cdot \bar{v}_d \, m_d \, dx_d + \int_{-\ell_a}^{\ell_a} \bar{v}_a \cdot \bar{v}_a \, dy_a$$

$$+ \int_{-\ell_b}^{\ell_b} \bar{v}_b \cdot \bar{v}_b \, dy_b + M_H \bar{v}_H \cdot \bar{v}_H + I_{MH} (\dot{\theta} + \dot{\phi})^2$$

$$= \sum m_i \int \Big\{ \dot{\eta}_i^{\,2} + \dot{\zeta}_i^{\,2} + \dot{R}^2 + R^2 \dot{\theta}^2$$

$$+ (\dot{\theta} + \dot{\phi})^2 \left(\eta_i^{\,2} + \zeta_i^{\,2} \right) + 2\dot{\eta}_i \, [\dot{R} \sin \phi - R\dot{\theta} \cos \phi - \zeta_i (\dot{\theta} + \dot{\phi})]$$

$$+ 2\dot{\zeta}_i \, [\dot{R} \cos \phi + R\dot{\theta} \sin \phi + \eta_i (\dot{\theta} + \dot{\phi})] - 2\zeta_i (\dot{\theta} + \dot{\phi}) [\dot{R} \sin \phi$$

$$- R\dot{\theta} \cos \phi] + 2\eta_i (\dot{\theta} + \dot{\phi}) [\dot{R} \cos \phi + R\dot{\theta} \sin \phi] \Big\} \, dx_i + M_H \Big\{ \dot{\eta}_H^{\,2}$$

$$+ \dot{\zeta}_H^{\,2} + \dot{R}^2 + R^2 \dot{\theta}^2 + (\dot{\theta} + \dot{\phi})^2 \left(\eta_H^{\,2} + \zeta_H^{\,2} \right) + 2\dot{\eta}_H \, [\dot{R} \sin \phi$$

$$- R\dot{\theta} \cos \phi - \zeta_H (\dot{\theta} + \dot{\phi})] + 2\dot{\zeta}_H \, [\dot{R} \cos \phi + R\dot{\theta} \sin \phi$$

$$+ \eta_H (\dot{\theta} + \dot{\phi})] - 2\zeta_H (\dot{\theta} + \dot{\phi}) [\dot{R} \sin \phi - R\dot{\theta} \cos \phi]$$

$$+ 2\eta_H (\dot{\theta} + \dot{\phi}) [\dot{R} \cos \phi + R\dot{\theta} \sin \phi] \Big\} + I_{MH} (\dot{\theta} + \dot{\phi})^2 \tag{226}$$

where

i = a, b, c and d.

The equations of motion are obtained by applying Lagrange's method

$$\frac{d}{dt}\left(\frac{\partial T}{\partial \dot{q}_j}\right) - \frac{\partial T}{\partial q_j} + \frac{\partial U}{\partial q_j} = Q_j \qquad (227)$$

The generalized coordinates are R, θ, ϕ and mode coordinates q_n. Because the elastic curves are expressed in terms of normal modes of free vibration, both the linear and angular momentum for each normal mode are zero. From the orthogonal conditions, it can be shown that

$$M_c v_{cn} v_{cm} + M_d v_{dn} v_{dm} + M_a v_{an} v_{am} + M_b v_{bn} v_{bm}$$

$$+ m_c \int w_{cn} w_{cm} dx_c + m_d \int w_{dn} w_{dm} dx_d + M_a \int w_{an} w_{am} dy_a$$

$$+ m_b \int w_{bn} w_{bm} dy_b + M_H v_{Hn} v_{Hm} + M_H w_{Hn} w_{Hm}$$

$$= \begin{cases} 0 & n \neq m \\ M_n & n = m \end{cases} \qquad (228)$$

The following notations are used for simplicity

$$M_c + M_d + M_a + M_b + M_H = M_T$$

$$\frac{1}{3} m_c \ell_c^3 + \frac{1}{3} m_d \ell_d^3 + M_a \ell_c^2 + M_b \ell_c^2 + \frac{2}{3} M_a \ell_a^3 + \frac{2}{3} M_b \ell_b^3 = I_T$$

$$\sum_{n=1}^{\infty} \ell_c \left[M_c v_{cn} + M_d v_{dn} - 2 m_a \int w_{an} dy_a\right.$$

$$\left. - m_b \int w_{bn} dy_b \right] q_n = \Sigma P_n q_n \qquad (229)$$

The components of generalized forces Q_j are evaluated from the work done by external forces. If only the gravitational force is considered, the total work done is

$$\sum Q_j \, \delta q_j = \int d\overline{G}_c \cdot (\delta x_c \, \overline{i}_I) + \int d\overline{G}_d \cdot (\delta x_d \, \overline{i}_I) + \int d\overline{G}_a \cdot (\delta x_a \, \overline{i}_I) + \int d\overline{G}_b \cdot (\delta x_b \, \overline{i}_I)$$

$$+ \overline{G}_H \cdot (\delta x_H \, \overline{i}_I) + \int d\overline{G}_c \cdot (\delta Y_c \, \overline{j}_I) + \int d\overline{G}_d \cdot (\delta Y_d \, \overline{j}_I) + \int d\overline{G}_a \cdot (\delta Y_a \, \overline{j}_I)$$

$$+ \int d\overline{G}_b \cdot (\delta Y_b \, \overline{j}_I) + \overline{G}_H \cdot (\delta Y_H \, \overline{j}_I) \tag{230}$$

In the rotational coordinate system, the position vector of H and any point on modules a and b and at any point on spokes c and d are

$$\overline{R}_i = (\eta_i + R \sin \phi) \, \overline{i} + (\zeta_i + R \cos \phi) \, \overline{j} \tag{231}$$

where

$i = a, b, c, d,$ or H.

Introducing the relations between $\overline{i}$, $\overline{j}$ and $\overline{i}_I$, $\overline{j}_I$ systems

$$\begin{bmatrix} \overline{i} \\ \overline{j} \end{bmatrix} = \begin{bmatrix} \sin (\theta + \phi) & -\cos (\theta + \phi) \\ \cos (\theta + \phi) & \sin (\theta + \phi) \end{bmatrix} \begin{bmatrix} \overline{i}_I \\ \overline{j}_I \end{bmatrix} \tag{232}$$

We have the position vectors in the inertial coordinates

$$\overline{R}_i = \{\eta_i \sin (\theta + \phi) + R \sin \phi \sin (\theta + \phi) + \zeta_i \cos (\theta + \phi)$$

$$+ R \cos \phi \cos (\theta + \phi)\} \, \overline{i}_I + \{-\eta_i \cos (\theta + \phi)$$

$$- R \sin \phi \cos (\theta + \phi) + \zeta_i \sin (\theta + \phi)$$

$$+ R \cos \phi \sin (\theta + \phi)\} \, \overline{j}_I \tag{233}$$

where the subscripts

$i = a, b, c, d,$ or H

From the above equations, the virtual displacements are determined to be

$$\begin{bmatrix} \delta x_c \\ \delta x_d \\ \delta x_a \\ \delta x_b \\ \delta x_H \end{bmatrix} = \cos\theta\,\delta R + \left\{ -R\sin\theta + \begin{bmatrix} \eta_c \\ \eta_d \\ \eta_a \\ \eta_b \\ \eta_H \end{bmatrix} \cos(\theta+\phi) - \begin{bmatrix} \zeta_c \\ \zeta_d \\ \zeta_a \\ \zeta_b \\ \zeta_H \end{bmatrix} \sin(\theta+\phi) \right\} \delta\theta$$

$$+ \left\{ \begin{bmatrix} \eta_c \\ \eta_d \\ \eta_a \\ \eta_b \\ \eta_H \end{bmatrix} \cos(\theta+\phi) - \begin{bmatrix} \zeta_c \\ \zeta_d \\ \zeta_a \\ \zeta_b \\ \zeta_H \end{bmatrix} \sin(\theta+\phi) \right\} \delta\phi$$

$$+ \left\{ \sin(\theta+\phi) \begin{bmatrix} v_{cn} \\ -v_{dn} \\ -w_{an} \\ w_{bn} \\ v_{Hn} \end{bmatrix} + \cos(\theta+\phi) \begin{bmatrix} -w_{cn} \\ w_{dn} \\ -v_{an} \\ v_{bn} \\ -w_{Hn} \end{bmatrix} \right\} \delta q_n$$

$$\begin{bmatrix} \delta Y_c \\ \delta Y_d \\ \delta Y_a \\ \delta Y_b \\ \delta Y_H \end{bmatrix} = \sin\theta\,\delta R + \left\{ R\cos\theta + \begin{bmatrix} \eta_c \\ \eta_d \\ \eta_a \\ \eta_b \\ \eta_H \end{bmatrix} \sin(\theta+\phi) + \begin{bmatrix} \zeta_c \\ \zeta_d \\ \zeta_a \\ \zeta_b \\ \zeta_H \end{bmatrix} \cos(\theta+\phi) \right\} \delta\theta$$

$$+ \left\{ \begin{bmatrix} \eta_c \\ \eta_d \\ \eta_a \\ \eta_b \\ \eta_H \end{bmatrix} \sin(\theta+\phi) + \begin{bmatrix} \zeta_c \\ \zeta_d \\ \zeta_a \\ \zeta_b \\ \zeta_H \end{bmatrix} \cos(\theta+\phi) \right\} \delta\phi$$

$$+ \left\{ -\cos(\theta+\phi) \begin{bmatrix} v_{cn} \\ -v_{dn} \\ -w_{an} \\ w_{bn} \\ v_{Hn} \end{bmatrix} + \sin(\theta+\phi) \begin{bmatrix} -w_{cn} \\ w_{dn} \\ -v_{an} \\ v_{bn} \\ -w_{Hn} \end{bmatrix} \right\} \delta q_n \tag{234}$$

Let K be the product of mass of earth and universal gravitational constant. With the assumption,

$$R_i^{-3} = R^{-3} \qquad (i = a, b, c, d, H) \tag{235}$$

the gravitational forces on a mass element of the modules, spokes, and hub are given by

$$d\overline{G}_c = -\frac{K\, m_c\, dx_c}{R^3}\Big\{[R\cos\theta + \eta_c \sin(\theta+\phi) + \zeta_c \cos(\theta+\phi)]\,\overline{i}_I$$

$$+ [R\sin\theta - \eta_c\cos(\theta+\phi) + \zeta_c \sin(\theta+\phi)]\,\overline{j}_I\Big\}$$

$$d\overline{G}_d = -\frac{K\, m_d\, dx_d}{R^3}\Big\{[R\cos\theta + \eta_d \sin(\theta+\phi) + \zeta_d \cos(\theta+d)]\,\overline{i}_I$$

$$+ [R\sin\theta - \eta_d\cos(\theta+\phi) + \zeta_d \sin(\theta+d)]\,\overline{j}_I\Big\}$$

$$d\overline{G}_a = -\frac{K\, m_a\, dy_a}{R^3}\Big\{[R\cos\theta + \eta_a \sin(\theta+\phi) + \zeta_a \cos(\theta+\phi)]\,\overline{i}_I$$

$$+ [R\sin\theta - \eta_a\cos(\theta+\phi) + \zeta_a \sin(\theta+\phi)]\,\overline{j}_I\Big\}$$

$$d\overline{G}_b = -\frac{K\, m_b\, dy_b}{R^3}\Big\{[R\cos\theta + \eta_b \sin(\theta+\phi) + \zeta_b \cos(\theta+\phi)]\,\overline{i}_I$$

$$+ [R\sin\theta - \eta_b\cos(\theta+\phi) + \zeta_b \sin(\theta+\phi)]\,\overline{j}_I\Big\}$$

$$\overline{G}_H = -\frac{K\, M_H}{R^3}\Big\{[R\cos\theta + \eta_H \sin(\theta+\phi) + \zeta_H \cos(\theta+\phi)]\,\overline{i}_I$$

$$+ [R\sin\theta - \eta_H\cos(\theta+\phi) + \zeta_H \sin(\theta+\phi)]\,\overline{j}_I\Big\} \tag{236}$$

By substituting the relation of equations (234) and (236) into equation (230), the components of the generalized forces caused by gravitational gradient are computed

$$Q_R = -\frac{K}{R^2} M_T$$

$$Q_\phi = 0$$

$$Q_\theta = 0$$

$$Q_{q_n} = -\frac{K}{R}\left[M_n q_n + \frac{1}{2} P_n\right] \tag{237}$$

Because the extensional elastic deformation of the modules and spokes is neglected in equation (219), the total strain energy of the system is derived from flexural deformation of the modules and spokes.

$$U = \frac{EI_c}{2} \int_o^{\ell_c} \left(\frac{\partial^2 \zeta_c}{\partial x_c^2}\right)^2 dx_c + \frac{EI_d}{2} \int_{-\ell_d}^{o} \left(\frac{\partial^2 \zeta_d}{\partial x_d^2}\right)^2 dx_d$$

$$+ \frac{EI_a}{2} \int_{-\ell_a}^{\ell_a} \left(\frac{\partial^2 \eta_a}{\partial y_a^2}\right)^2 dy_a + \frac{EI_b}{2} \int_{-\ell_b}^{\ell_b} \left(\frac{\partial^2 \eta_b}{\partial y_b^2}\right)^2 dy_b$$

$$= \frac{EI_c}{2} \int \left(-\Sigma w''_{cm} q_m\right)^2 dx_c + \frac{EI_d}{2} \int \left(\Sigma w''_{dm} q_m\right)^2 dx_d$$

$$+ \frac{EI_a}{2} \int \left(-\Sigma w''_{am} q_m\right)^2 dy_a + \frac{EI_b}{2} \int \left(\Sigma w''_{bm} q_m\right)^2 dy_b \tag{238}$$

$$\frac{\partial U}{\partial q_n} = EI_c \int \left(\Sigma w''_{cm} q_m\right) w''_{cn} dx_c + EI_d \int \left(\Sigma w''_{dm} q_m\right) w''_{cn} dx_d$$

$$+ EI_a \int \left(\Sigma w''_{am} q_m\right) w''_{an} dy_a + EI_b \int \left(\Sigma w''_{bm} q_m\right) w''_{bn} dy_b$$

$$= \begin{cases} 0 & n \neq m \\ N_n & n = m \end{cases} \tag{239}$$

Substituting the values of equations (226), (237), and (239) into (227), and observing the properties of normal modes and conditions of (228) and (229), the equations of planar motion of the H-configuration are

R-equation

$$\ddot{R} - R\dot{\theta}^2 = -\frac{K}{R^2} \tag{240}$$

θ-equation

$$R^2 \dot{\theta} M_T + (\dot{\theta} + \dot{\phi}) \left[I_T + \Sigma M_n q_n^2 + \Sigma P_n q_n + I_{MH} \right] - I_{MH} \Sigma w'_{Hn} \dot{q}_n = C_1 \tag{241}$$

φ-equation

$$(\dot{\theta} + \dot{\phi}) \left[I_T + \Sigma M_n q_n^2 + \Sigma P_n q_n + I_{MN} \right] - I_{MH} \Sigma w'_{Hn} \dot{q}_n = C_2 \tag{242}$$

q-equation

$$\ddot{q}_n + \left[\frac{K}{R^3} - (\dot{\theta} + \dot{\phi})^2 + \frac{P_n}{M_n} \right] q_n - (\ddot{\theta} + \ddot{\phi}) \frac{I_{MH}}{M_n} w'_{Hn} + \frac{1}{2} \left[\frac{K}{R^3} - (\dot{\theta} + \dot{\phi})^2 \right] \frac{P_n}{M_n} \tag{243}$$

8.5 RESULTS AND DISCUSSIONS

Equations (175) to (180) are coupled nonlinear ordinary differential equations. If the first three normal modes of lateral vibration were introduced into equation (180), i. e., $n = 3$, $m = 3$, there would be seven equations with seven degrees of freedom. After a careful study of these equations which involve some parameters of very large magnitude and some equally important parameters of negligible quantity, it is obvious that not only an analytical solution is out of consideration, but also the computer solution needs careful planning.

From the equation of conservation of momentum (177), the value of $\dot{\theta}$ can be solved in terms of other variables, thus

$$\dot{\theta} = \frac{C_2 - \left(\frac{I_r^2}{r_o^2} + \sum_1^n M_n q_n^2 \right) \dot{\phi}}{M R^2 + \frac{I_r^2}{r_o^2} \sum_1^n M_n q_n^2} \tag{244}$$

where

$$C_2 = M R_o^2 \dot{\theta}_o + I (\dot{\theta}_o + \dot{\phi}_o) + (\dot{\theta}_o + \dot{\phi}_o) \sum_1^n M_n q_n^2 \tag{245}$$

$$n = 1, 2, 3.$$

Eliminating $\dot{\theta}$ from equations (176), (178), (179), and (180) by using equation (244), we have six equations with six degrees of freedom; R, r, ϕ, q_1, q_2, and q_3. Each of these equations is a second order coupled nonlinear differential equation solved in IBM 7094 by using Runge-Kutta numerical integration procedure and by perturbing the variables R and r according to

$$\begin{aligned} R &= R_o + \Delta R \\ r &= r_o + \Delta r \end{aligned} \tag{246}$$

For investigation the effect of different artificial gravities on the motion, the equations of four degrees of freedom (181) to (184) were used. Because this set of equations considers only the extensional motion of cable, only the variation of spin rate changes the length of cable. It differs from the case of seven degrees of freedom, in which, once the spin rate is changed, the lateral vibration modes, the orthogonal constants, and the initial conditions of normal coordinates are changed. Furthermore, by letting the cable mass $\rho = 0$, it will make $I = (m_1 \ell_1^2 + m_2 \ell_2^2)$ and $M = m_1 + m_2$. Now the four equations represent the case of the planar motion of an extensible, massless-cable-connected compartment and counterweight space station. These four equations are solved by the same technique as that for the seven degree equations.

The physical conditions used in the computer solutions are a hundred miles circular orbit and the following initial conditions:

$$
\begin{aligned}
R_o &= 0.21454428 \times 10^8 \text{ ft} \\
K &= 0.140777 \times 10^{17} \text{ ft}^3/\text{sec}^2 \\
m_1 &= 1.242236 \times 10^3 \text{ slug} \\
m_1 &= 0.1552795 \times 10^3 \text{ slug} \\
\rho_o r_o &= 0.06832298 \times 10^3 \text{ slug} \\
r_o &= 1000 \text{ ft} \\
\phi_o &= \frac{\pi}{2} \text{ rad} \\
EA &= 0.10944 \times 10^8 \text{ lb}
\end{aligned}
\tag{247}
$$

The initial spin rate $\dot{\phi}_o$ is determined by the required artificial gravity in the living compartment. In the four degrees of freedom case, the motions under artificial gravities of 1 g, 0.42 g, and 0.25 g are studied separately. In the seven degree case, only the motions having 1 g in the living compartment with two sets of arbitrary initial conditions of q_n, besides the conditions (247) were studied. The initial conditions of q_n are determined from

$$\zeta\,(\eta_o, t) = \sum_{n=1}^{3} \phi_n(\eta_o)\, q_n(t)$$

The conditions of q_n are:

$$
\left.
\begin{aligned}
\zeta\,(\text{station } 1) &= 1 \text{ in.} \\
\zeta\,(\text{station } 50) &= -2 \text{ in.} \\
\zeta\,(\text{station } 101) &= 3 \text{ in.} \\
\dot{\zeta}\,(\text{station } 1) &= -3 \text{ in/sec} \\
\dot{\zeta}\,(\text{station } 50) &= 2 \text{ in/sec} \\
\dot{\zeta}\,(\text{station } 101) &= -1 \text{ in/sec}
\end{aligned}
\right\} \rightarrow
\left\{
\begin{aligned}
q_1 &= 51.4 \\
q_2 &= 58.8 \\
q_3 &= 54.2 \\
\dot{q}_1 &= -111 \\
\dot{q}_2 &= -279 \\
\dot{q}_3 &= -136
\end{aligned}
\right.
\quad \text{at } t = 0 \tag{248}
$$

and,

$$\left.\begin{array}{ll} \zeta\,(\text{station } 1) & = 1'' \\ \zeta\,(\text{station } 50) & = 0 \\ \zeta\,(\text{station } 101) & = 0 \\ \dot{\zeta}_i(\text{station } 1,\ 50,\ 101) & = 0 \end{array}\right\} \rightarrow \left\{\begin{array}{ll} q_1 & = 34.9 \\ q_2 & = 96.7 \\ q_3 & = 44.7 \\ \dot{q}_i & = 0 \ (i = 1, 2, 3) \end{array}\right. \text{at } t = 0 \qquad (249)$$

For the study of damped motion, a viscous damping term was introduced into equation (183), the four degrees of freedom case, and into equations (178) and (180), the seven degrees of freedom case. In both cases, a critical damping factor of 1 percent was considered under the 1-g artificial gravity condition.

Four representative cases of the computer results are shown in Figures 49, 50, 51, and 52. The first two figures represent extensional oscillations of a spinning massless-cable-connected compartment and counterweight space station in a 100-mile circular orbit. The last two figures present the results of extensional and lateral oscillations of the same space station including the mass of the cable.

Figures 49a to 49f show the time histories of Δr, ΔR, $\dot{R}$, $\dot{\phi}$, $\dot{r}$ and $\dot{\theta}$; 1-g in compartment m_1; and without damping. A stable orbit is shown. Δr oscillates around a length a little above the steady state length of the cable and shows a state of neutral stability. $\dot{\phi}$ shows a corresponding fluctuation and decreases very slowly. The natural frequency of the extensional oscillation of the cable is about 35.2 radians per second in comparison with the initial spin rate 0.53833 radians per second.

Figures 50a to 50f show the effect of the addition of 1 percent critical damping into the four degrees of freedom system. It can be seen from Figure 50a that only a very short time is required to damp the transient oscillation of the extensional motion and the spin rate. However, the figures show that as the cable configuration continues spinning, the spin velocity retains a very small, steady oscillatory component. The spin velocity deteriorates continuously at a very slow rate, and the length of the cable decreases correspondingly.

The computer solutions of the four degrees of freedom equations under the artificial gravities of 0.42-g and 0.25-g show a motion similar to that under the 1-g condition. A slight increase in the natural frequencies of the extensional oscillation of the cable, 23.8 rad/sec for 0.42 g and 19.2 rad/sec for 0.25 g, did not warrant repetition of these figures.

Figures 51a through 51d show the time histories of Δr, ΔR, q_1, q_2, q_3, $\dot{R}$, $\dot{\phi}$, $\dot{r}$, $\dot{q}_1$, $\dot{q}_2$, $\dot{q}_3$, and $\dot{\theta}$; 1-g in compartment m_1; and without damping. As in the four degree of freedom case, a stable orbit is shown. Δr oscillates around a length a little below the steady state length of the cable and shows a state of neutral stability. The time histories of q_1, q_2, and q_3 show neutral stability and oscillate around the steady state position; fluctuates about a very slowly decreasing mean value. The natural frequency of the extensional oscillation of the cable is 8.55 rad/sec. The natural frequencies of q_1, q_2, and q_3 are 3.39 rad/sec, 6.72 rad/sec, and 10.1 rad/sec, respectively.

Figures 52a through 521 show the effect of the addition of 1 percent critical damping into the seven degrees of freedom system. The transient extensional and lateral oscillations are damped out completely in a very short time. The damped spin rate shows a very slight tendency to degenerate.

The computer solution of the seven degrees of freedom equations using the second set of initial conditions, q_1, q_2, and q_3, shows results similar to those in Figure 52.

Within the limit of the assumptions established for this specific investigation, and from the results which have been summarized, a conclusion may be drawn for the planar motion of a cable-connected compartment and counter-weight space station as follows:

The spinning cable-connected space station has a stable circular orbit, but the cable will oscillate under the influence of the gravitational gradient and will be neutrally stable. Positive elastic stability can be achieved by the addition of a velocity-proportional damping device. For stabilization of the motion induced by the gravitational gradient alone, only a small percentage of the critical damping factor is required. When the cable tension caused by spin is of the same order of magnitude as the tension caused by gravitational gradient, the cable-connected configuration may no longer be stable because then the cable may go slack during portions of the rotation cycle.

However, physical and mathematical approximations have been assumed in the formulation of equations: the restriction of the motion to the orbital plane, the spherical earth, the neglect of dissipation energy, the neglect of other forces other than the gravity force, the neglect of change of cable length in the derivation of lateral vibration modes, and the neglect of terms of higher than the second degree in the expansion of R_i. If one or more of these approximations are corrected with rigor, it may change the conclusion drawn from this investigation.

Consideration of these approximations reveals that if serious consideration is to be given to the application of tension members to connect living modules of a future space station, an extensive research program must be conducted with emphasis in the areas of three dimensional cable dynamics, the cable material and its internal dissipating mechanism, the non-linear phase of slacking cable, the deployment and control problems, and other areas to be defined.

The equations of planar motion of the Y- and H-Configurations described in Sections 8. 3 and 8. 4 may be investigated in a manner similar to that of the cable-connected compartment-counterweight configuration. A continuation of the study is recommended to extend the solution of the equations of motion for these configurations.

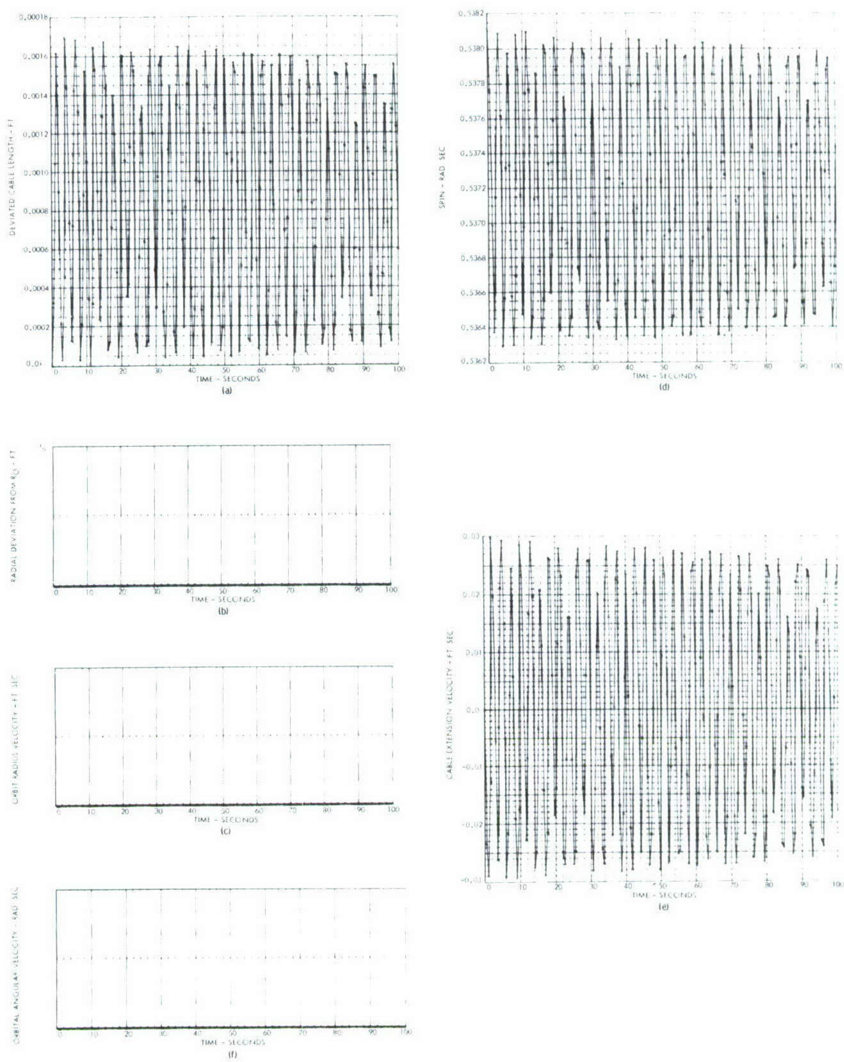

Figure 49. Four-Degrees-of-Freedom Equations Without Damping (R, $\dot{\theta}$, r, $\dot{\phi}$)

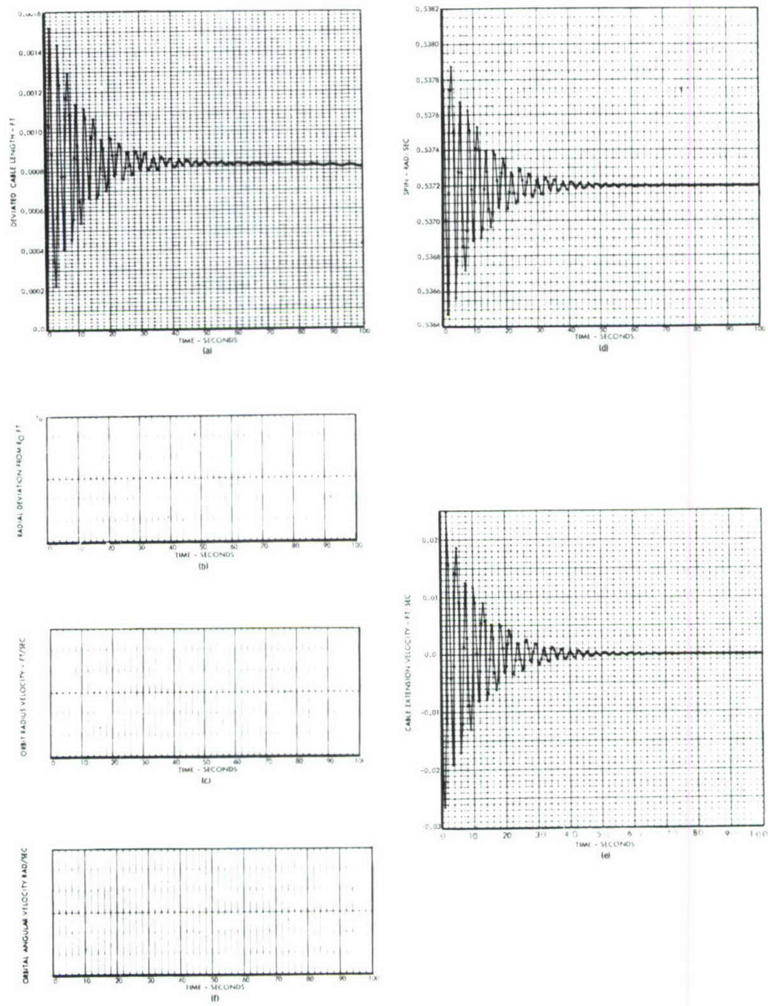

Figure 50. Four-Degrees-of-Freedom Equations With One-Percent Critical Damping Factor (R, $\dot{\theta}$, r, $\dot{\phi}$)

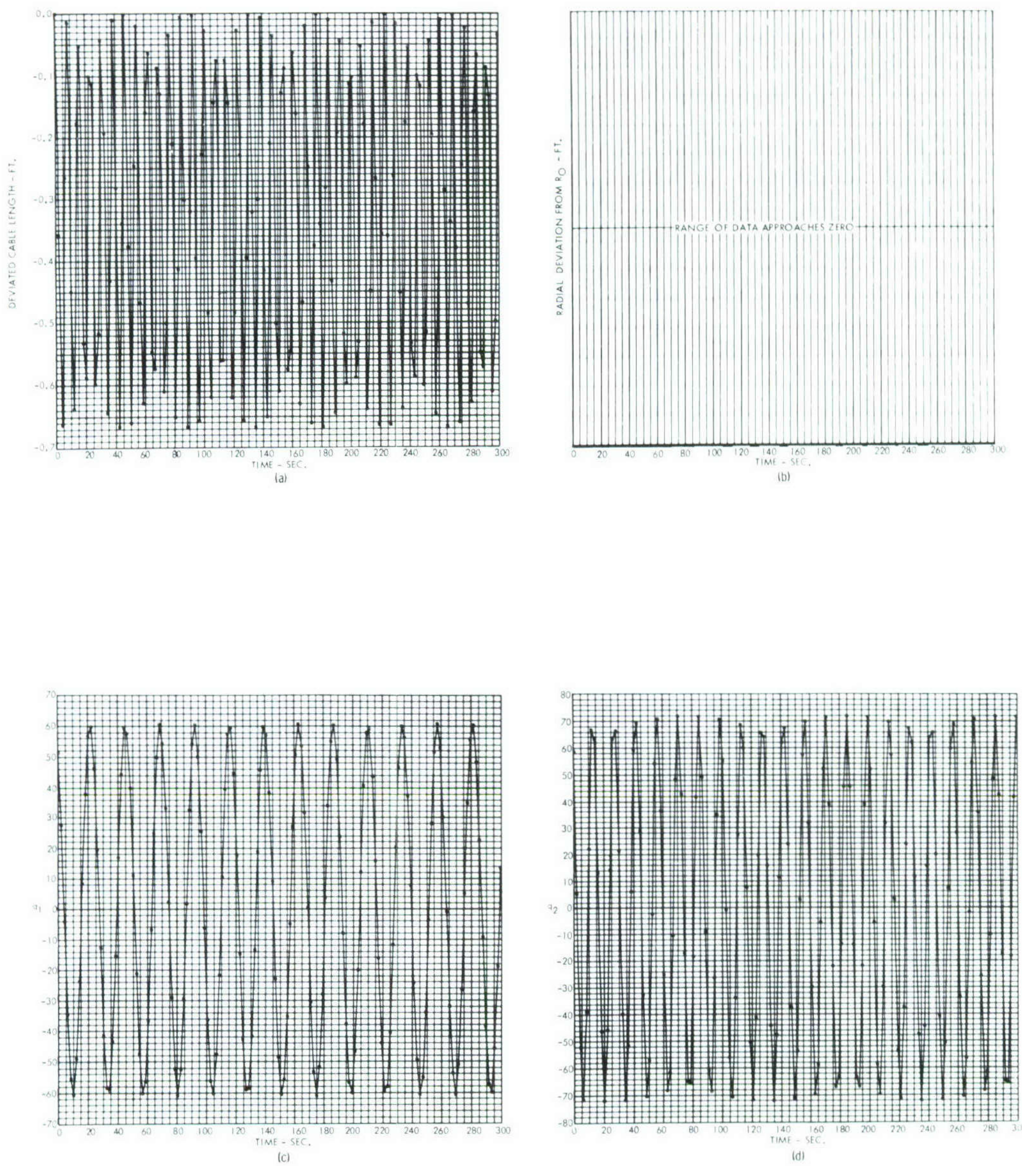

Figure 51. Seven-Degrees-of-Freedom Equations Without Damping (R, $\dot{\theta}$, r, $\dot{\phi}$, q_1, q_2, q_3) (Sheet 1)

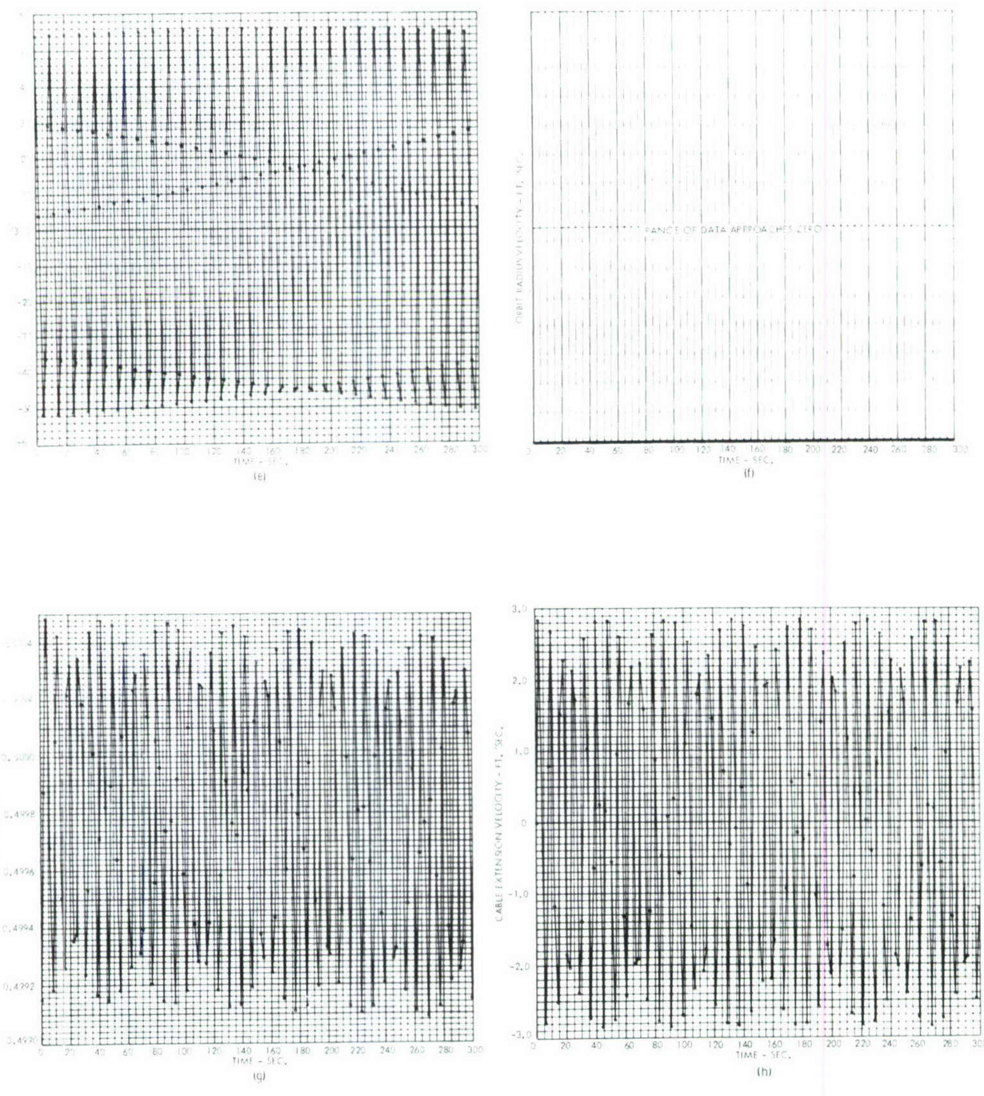

Figure 51. Seven-Degrees-of-Freedom Equations Without Damping (R, $\dot{\theta}$, r, $\dot{\phi}$, q_1, q_2, q_3) (Sheet 2)

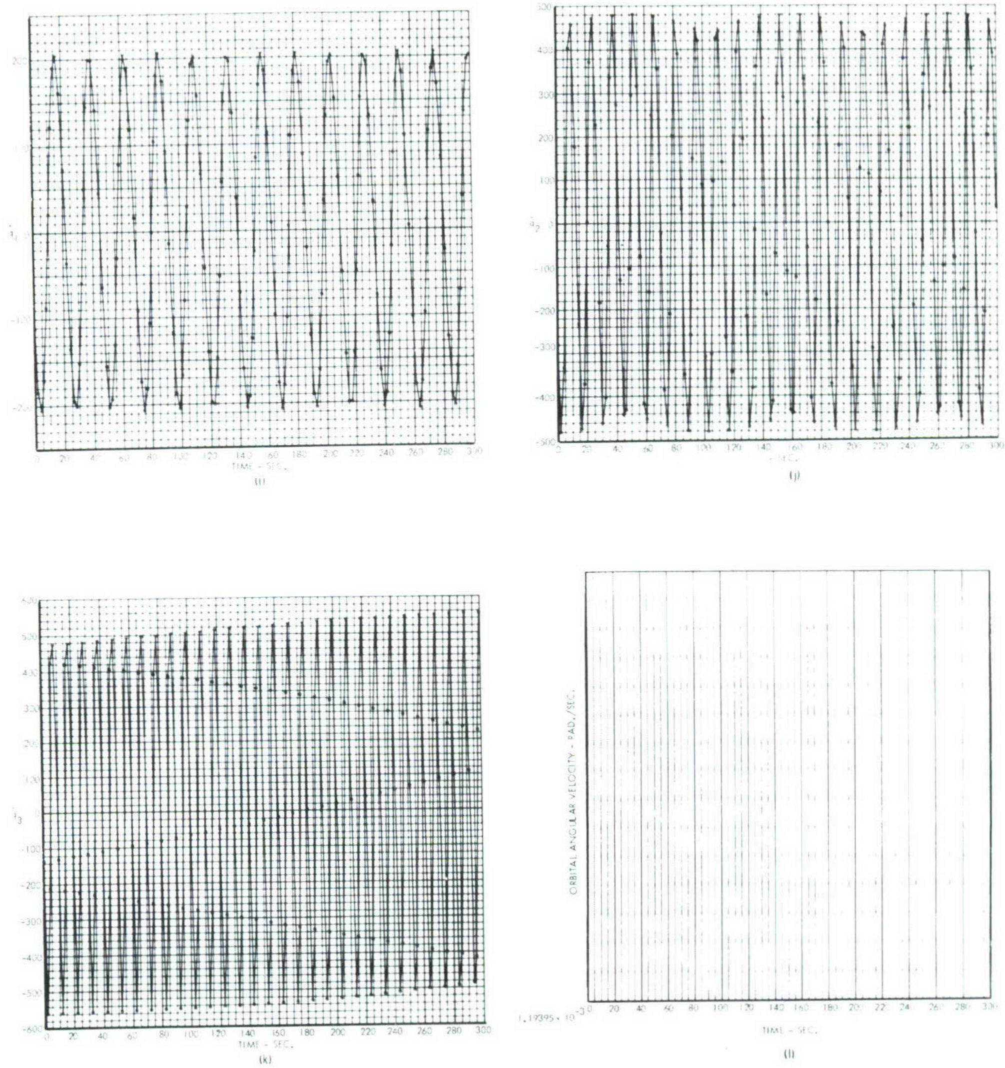

Figure 51. Seven-Degrees-of-Freedom Equations Without Damping ($R, \dot{\theta}, r, \dot{\phi}, q_1, q_2, q_3$) (Sheet 3)

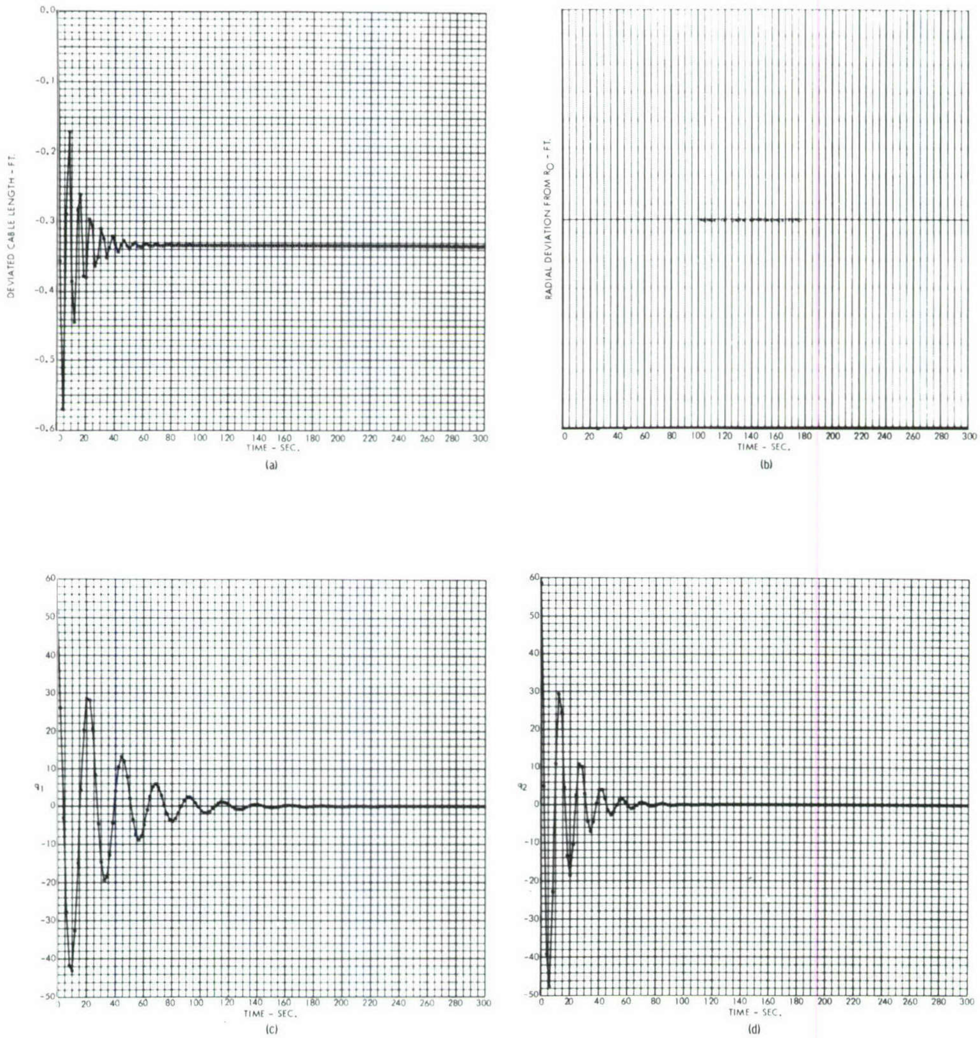

Figure 52. Seven-Degrees-of-Freedom Equations With One-Percent Critical Damping Factor ($R, \dot{\theta}, r, \dot{\phi}, q_1, q_2, q_3$) (Sheet 1)

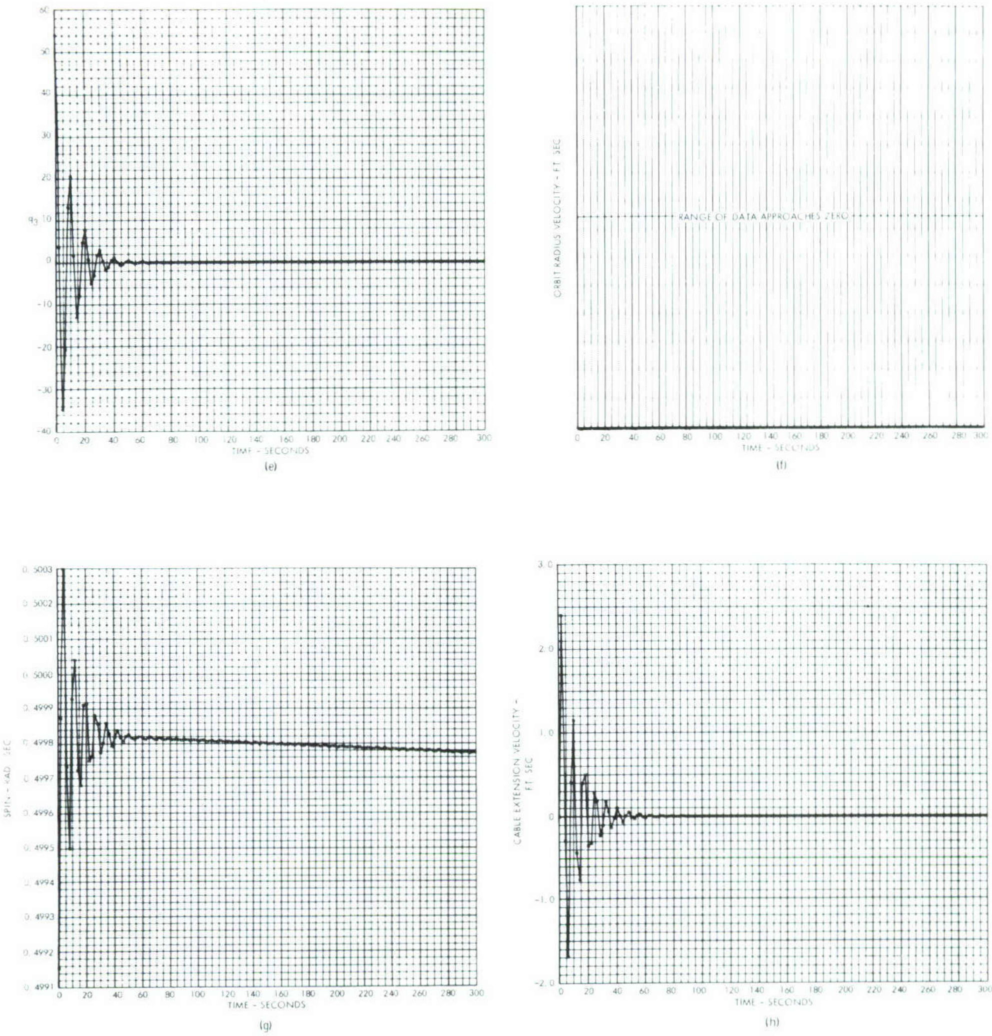

Figure 52. Seven-Degrees-of-Freedom Equations With One-Percent Critical Damping Factor (R, $\dot{\theta}$, r, $\dot{\phi}$, q_1, q_2, q_3) (Sheet 2)

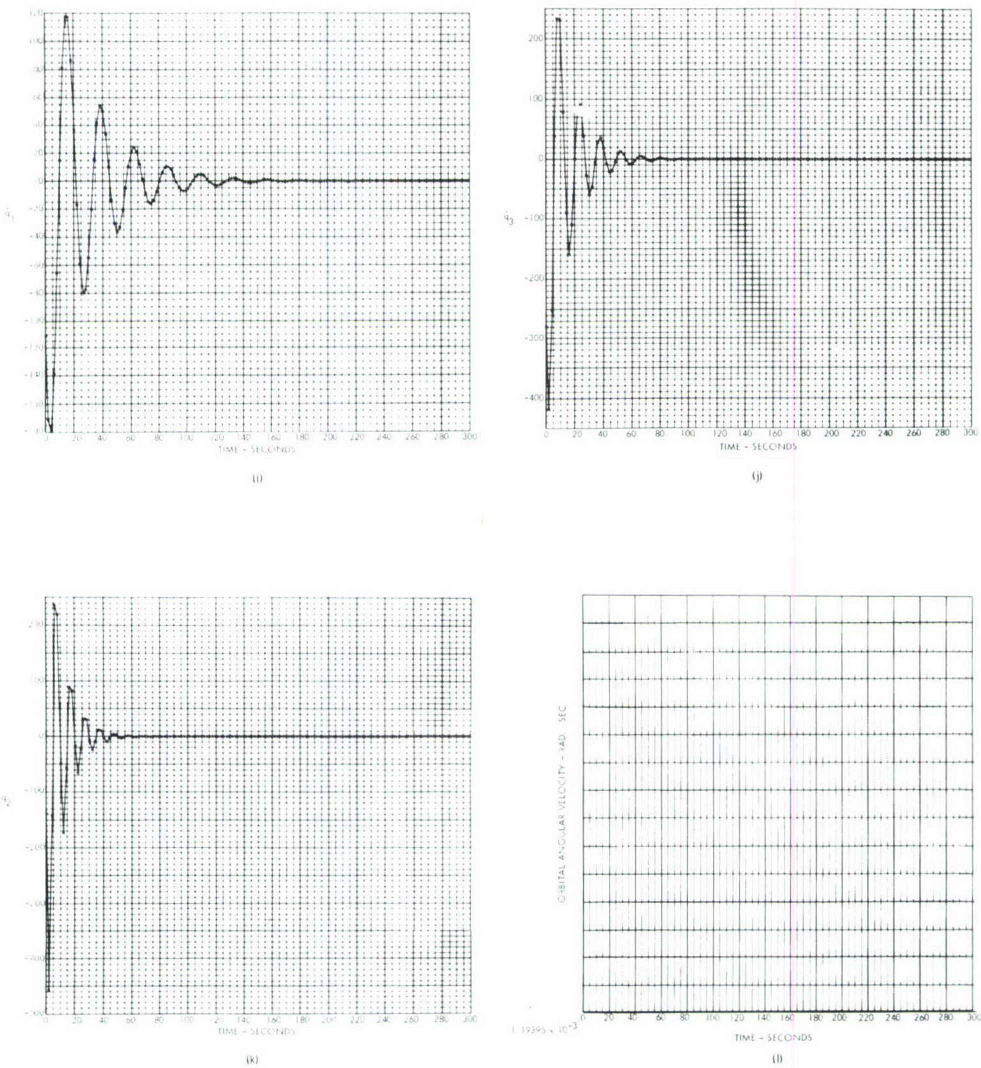

Figure 52. Seven-Degrees-of-Freedom Equations With One-Percent Critical Damping Factor $(R, \dot{\theta}, r, \dot{\phi}, q_1, q_2, q_3)$ (Sheet 3)

9.0 SPIN DYNAMICS OF ROTATING SPACE STATIONS

9.1 GENERAL MOMENT EQUATIONS

The general motion of a rigid body has six degrees of freedom which can be conveniently separated into two sets: (1) three degrees of freedom which define the motion of the mass center of the body, and (2) three degrees of freedom which define the orientation of the body about its mass center. When the body is free from external forces or the angular motion of the body is independent from the linear velocity, only the three rotational degrees of freedom need be considered to determine its orientation.

Consider a body, free from external forces, rotating about its mass center which can be considered fixed in space. The angular momentum vector about the mass center is

$$\overline{H} = \sum_i m_i \left(\overline{r}_i \times \overline{v}_i\right)$$

$$= \sum_i m_i \left(\overline{r}_i \times \left(\overline{\omega} \times \overline{r}_i\right)\right)$$

$$= \sum_i m_i \left(\overline{\omega}\, r_i^2 - \overline{r}_i \left(\overline{r}_i \cdot \overline{\omega}\right)\right), \tag{250}$$

in which $\overline{\omega}$ is the body angular velocity. Resolving the angular momentum vector equation (250) into components along the x, y, z axes system gives

$$\begin{Bmatrix} H_x \\ H_y \\ H_z \end{Bmatrix} = \begin{bmatrix} I_x & -I_{xy} & -I_{xz} \\ -I_{xy} & I_y & -I_{yz} \\ -I_{xz} & -I_{yz} & I_z \end{bmatrix} \begin{Bmatrix} p \\ q \\ r \end{Bmatrix} \tag{251}$$

in which p, q, and r are the components of angular velocity about the body x, y, and z axes, respectively, and I_x, I_y, I_z and I_{xz}, I_{yz} are the instantaneous moments of inertia and products of inertia with respect to the body axes indicated by the subscripts.

The motion of the body is expressed in terms of the external moment about the mass center which is equal to the time derivative of the angular momentum vector about the mass center. Since information regarding the orientation of the space station is desired, the x, y, z body axes system is considered to be fixed to the rotating space station. The vector equation of motion is

$$\overline{M} = \frac{d}{dt}\,\overline{H} + \overline{\omega} \times \overline{H}. \tag{252}$$

The equations of motion for a rotating space station with variable moments of inertia are

$$\begin{bmatrix} I_x & -I_{xy} & -I_{xz} \\ -I_{xy} & I_y & -I_{yz} \\ -I_{xz} & -I_{yz} & I_z \end{bmatrix} \begin{Bmatrix} \dot{p} \\ \dot{q} \\ \dot{r} \end{Bmatrix}$$

$$= \begin{Bmatrix} M_x \\ M_y \\ M_z \end{Bmatrix} - \begin{bmatrix} \dot{I}_x & -\dot{I}_{xy} & -\dot{I}_{xz} \\ -\dot{I}_{xy} & \dot{I}_y & -\dot{I}_{yz} \\ -\dot{I}_{xz} & -\dot{I}_{yz} & \dot{I}_z \end{bmatrix} \begin{Bmatrix} p \\ q \\ r \end{Bmatrix} - \begin{Bmatrix} Cq - Br \\ Ar - Cp \\ Bp - Aq \end{Bmatrix} \tag{253}$$

in which

$$\begin{Bmatrix} A \\ B \\ C \end{Bmatrix} = \begin{bmatrix} I_x & -I_{xy} & -I_{xz} \\ -I_{xy} & I_y & -I_{yz} \\ -I_{xz} & -I_{yz} & I_z \end{bmatrix} \begin{Bmatrix} p \\ q \\ r \end{Bmatrix}.$$

The orientation of the space station relative to inertial space is defined by a set of Euler angles relating the x, y, z body axes to the X, Y, Z, inertially-fixed axes. The transformation is accomplished by successive righthand rule rotations about the z, y', and x'' axes, respectively as shown in Figure 53.

The Euler angular velocities $\dot{\phi}$, $\dot{\theta}$ and $\dot{\psi}$ may be expressed in terms of the body angular velocities p, q, and r

$$\dot{\phi} = p + \dot{\psi} \sin \theta$$

$$\dot{\theta} = q \cos \phi - r \sin \phi$$

$$\dot{\psi} = \frac{1}{\cos \theta} (r \cos \phi + q \sin \phi). \tag{254}$$

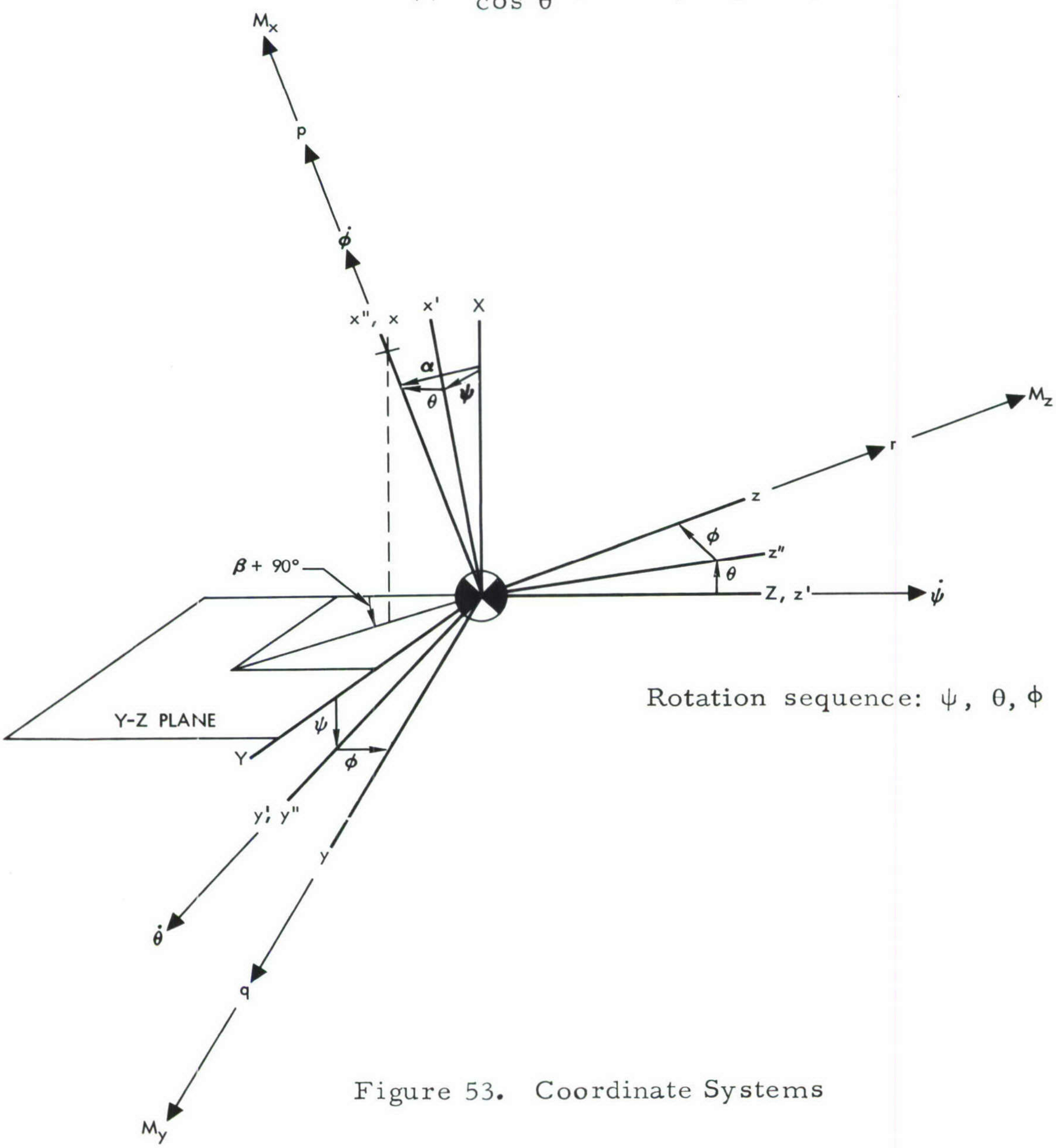

Rotation sequence: ψ, θ, φ

Figure 53. Coordinate Systems

The angular motion of the space station is completely defined by the equations (253) and (254). Numerical solutions of the first set of simultaneous equations for the body angular velocities, and of the second set of equations for the Euler angles were obtained using a fourth-order Runge-Kutta integration procedure with variable time increments programmed for the IBM 7094 digital computer.

The angular motion of the space station is represented by the trace of a point on the x-body axis on the fixed reference plane Y-Z. The angle α is the wobble angle between the x-body axis and the X-fixed axis (Figure 53). The angle β is the angle between the Y-fixed axis and the projection of the x-body axis on the Y-Z fixed reference plane. A polar plot of α in degrees as the radial coordinate against β in degrees gives a simple physical picture of the space station motion with respect to the fixed coordinate system.

The transformation from the body axes system to the fixed axes system is

$$\begin{Bmatrix} X \\ Y \\ Z \end{Bmatrix} = \begin{bmatrix} C_\psi C_\theta & -S_\psi C_\phi + C_\psi S_\theta S_\phi & S_\psi S_\phi + C_\psi S_\theta C_\phi \\ S_\psi C_\theta & C_\psi C_\phi + S_\psi S_\theta S_\phi & -C_\psi S_\phi + S_\psi S_\theta C_\phi \\ -S_\theta & C_\theta S_\phi & C_\theta C_\phi \end{bmatrix} \begin{Bmatrix} x \\ y \\ z \end{Bmatrix} \tag{255}$$

in which S and C represent the sine and cosine of the subscript.

Thus,

$$\alpha = \cos^{-1} (\cos \psi \cos \theta)$$

$$\beta = \tan^{-1} \left(\frac{- \sin \theta}{\sin \psi \cos \theta} \right) . \tag{256}$$

9.2 INTERNAL MASS MOTIONS

The motion of a space station as given by the equations (253) depends upon the moments and products of inertia of the system. The inertia terms are dependent upon the mass distribution of the space station and will, of course, be affected by any mass transfer within the space station system. The moving masses are simulated by discrete point masses, m_n, and the moments and products of inertia are written as functions of the time dependent position coordinates (x_n, y_n, z_n) of the moving masses m_n relative to the x, y, z body axes system as follows.

$$I_x = I_{Mx} + \sum_{n=1}^{N} m_n \left(y_n^2 + z_n^2\right) - \left(M + \sum_{n=1}^{N} m_n\right)\left(y_G^2 + z_G^2\right)$$

$$I_y = I_{My} + \sum_{n=1}^{N} m_n \left(x_n^2 + z_n^2\right) - \left(M + \sum_{n=1}^{N} m_n\right)\left(x_G^2 + z_G^2\right)$$

$$I_z = I_{Mz} + \sum_{n=1}^{N} m_n \left(x_n^2 + y_n^2\right) - \left(M + \sum_{n=1}^{N} m_n\right)\left(x_G^2 + y_G^2\right)$$

$$I_{xy} = I_{Mxy} + \sum_{n=1}^{N} m_n x_n y_n - \left(M + \sum_{n=1}^{N} m_n\right) x_G y_G$$

$$I_{xz} = I_{Mxz} + \sum_{n=1}^{N} m_n x_n z_n - \left(M + \sum_{n=1}^{N} m_n\right) x_G z_G$$

$$I_{yz} = I_{Myz} + \sum_{n=1}^{N} m_n y_n z_n - \left(M + \sum_{n=1}^{N} m_n\right) y_G z_G . \qquad (257)$$

The time rates of change of the inertia expressions in equation (257) are then

$$\dot{I}_x = 2 \left\{ \sum_{n=1}^{N} m_n (y_n \dot{y}_n + z_n \dot{z}_n) - \left(M + \sum_{n=1}^{N} m_n\right) (y_G \dot{y}_G + z_G \dot{z}_G) \right\}$$

$$\dot{I}_y = 2 \left\{ \sum_{n=1}^{N} m_n (x_n \dot{x}_n + z_n \dot{z}_n) - \left(M + \sum_{n=1}^{N} m_n\right) (x_G \dot{x}_G + z_G \dot{z}_G) \right\}$$

$$\dot{I}_z = 2 \left\{ \sum_{n=1}^{N} m_n (x_n \dot{x}_n + y_n \dot{y}_n) - \left(M + \sum_{n=1}^{N} m_n\right) (x_G \dot{x}_G + y_G \dot{y}_G) \right\}$$

$$\dot{I}_{xy} = \sum_{n=1}^{N} m_n (x_n \dot{y}_n + \dot{x}_n y_n) - \left(M + \sum_{n=1}^{N} m_n\right) (x_G \dot{y}_G + \dot{x}_G y_G)$$

$$\dot{I}_{xz} = \sum_{n=1}^{N} m_n (x_n \dot{z}_n + \dot{x}_n z_n) - \left(M + \sum_{n=1}^{N} m_n\right) (x_G \dot{z}_G + \dot{x}_G z_G)$$

$$\dot{I}_{yz} = \sum_{n=1}^{N} m_n (y_n \dot{z}_n + \dot{y}_n z_n) - \left(M + \sum_{n=1}^{N} m_n\right) (y_G \dot{z}_G + \dot{y}_G z_G). \tag{258}$$

In the previous equations (257) and (258),

M = Mass of the space station excluding moving masses

m_n = Mass of the n^{th} moving mass

x_n, y_n, z_n = Instantaneous position coordinates of the n^{th} moving mass relative to the x, y, z body axes

I_{Mx}, I_{My}, I_{Mz} = Moments of inertia of the space station, excluding moving masses

$I_{Mxy}, I_{Mxz}, I_{Myz}$ = Products of inertia of the space station excluding moving masses

The position coordinates and velocity components of the instantaneous mass center of the whole space station relative to the x, y, z body axes are given by the following expressions:

$$\begin{Bmatrix} x_G \\ y_G \\ z_G \end{Bmatrix} = \frac{1}{M + \sum_{n=1}^{N} m_n} \begin{Bmatrix} \sum_{n=1}^{N} m_n x_n \\ \sum_{n=1}^{N} m_n y_n \\ \sum_{n=1}^{N} m_n z_n \end{Bmatrix}$$

$$\begin{Bmatrix} \dot{x}_G \\ \\ \dot{y}_G \\ \\ \dot{z}_G \end{Bmatrix} = \frac{1}{M + \sum_{n=1}^{N} m_n} \begin{Bmatrix} \sum_{n=1}^{N} m_n \dot{x}_n \\ \\ \sum_{n=1}^{N} m_n \dot{y}_n \\ \\ \sum_{n=1}^{N} m_n \dot{z}_n \end{Bmatrix} . \tag{259}$$

The computed responses for several cases of internal mass motion are presented in graphical form in Figures 54 through 66. The period during which the masses are in motion is indicated by the heavy portions of the curves and is marked by the plotting symbol (x); subsequently, the curves are light and are marked by the symbol (•).

In each case, the weight of each of the discrete masses, m_n, is 200 pounds, corresponding to the approximate weight of a space station crew member. Also, the external moment on the vehicle is zero and the initial spin rate, p, is that which is required to develop the artificial gravity level at the command module. Other initial conditions are $q = r = \phi = \theta = \psi = 0$ at $t = 0$. The moments of inertia for each configuration are given in Section 2. 0.

9. 2. 1 Configuration 1-A

The responses for three cases of internal mass motion were computed for Configuration 1-A. The initial positions of moving masses m_n are given below.

n	x_n (ft)	y_n (ft)	z_n (ft)
1	0	+45	+111.11
2	0	0	+111.11
3	0	-45	+111.11

Case 1

The artificial gravity is 1/2-g. Masses move in the x-direction such that $I_{xz} \neq 0$. The final moments and products of inertia are

$$I_x = 96.2237 \times 10^6 \text{ slug-ft}^2$$

$$I_y = 95.5611 \times 10^6 \text{ slug-ft}^2$$

$$I_z = 0.68424 \times 10^6 \text{ slug-ft}^2$$

$$I_{xz} = 6087.0 \text{ slug-ft}^2$$

$$I_{xy} = I_{yz} = 0$$

The time dependent position coordinates of the masses m_n are given below.

n	Time Interval (seconds)	x_n (ft)	y_n (ft)	z_n (ft)
1	$0 \leq t \leq 6$	+0.5 t	+45	+111.11
	$6 < t$	+3	+45	+111.11
2	$0 \leq t \leq 6$	+0.5 t	0	+111.11
	$6 < t$	+3	0	+111.11
3	$0 \leq t \leq 6$	+0.5 t	-45	+111.11
	$6 < t$	+3	-45	+111.11

Figure 54 shows that, for 1/2-g artificial gravity, the maximum wobble angle is 0.4 degrees and the maximum transverse body velocity is 0.15 deg/sec. The maximum body angular acceleration is 0.058 deg/sec^2. The variation in the spin rate is negligible.

Case 2

The artificial gravity is 1/2-g. Masses move in the x-direction such that $I_{xy} \neq 0$. The final moments and products of inertia are

$$I_x = 96.2237 \times 10^6 \text{ slug-ft}^2$$

$$I_y = 95.5611 \times 10^6 \text{ slug-ft}^2$$

$$I_z = 0.68419 \times 10^6 \text{ slug-ft}^2$$

$$I_{xy} = 1677.0 \text{ slug-ft}^2$$

$$I_{xz} = I_{yz} = 0$$

The time dependent position coordinates of the masses m_n are given below:

n	Time Interval (seconds)	x_n (ft)	y_n (ft)	z_n (ft)
1	$0 \leq t \leq 6$	+0.5 t	+45	+111.11
	$6 < t$	3	+45	+111.11
2	$0 \leq t$	0	0	+111.11
3	$0 \leq t \leq 6$	-0.5 t	-45	+111.11
	$6 < t$	-3	-45	+111.11

Figure 55 shows that, for 1/2-g artificial gravity, the maximum wobble angle is 0.26 degrees and the maximum transverse body velocity is 0.1 deg/sec. The maximum body angular acceleration is 0.02 deg/sec. The variation in the spin velocity is negligible.

Case 3

The artificial gravity is 1/2-g. Masses move in the y-direction and oscillates in the x-direction. The final moments and products of inertia are

$I_x = 96.2355 \times 10^6$ slug-ft^2

$I_y = 95.5611 \times 10^6$ slug-ft^2

$I_z = 0.69599 \times 10^6$ slug-ft^2

$I_{xy} = -2463.0$ slug-ft^2

$I_{xz} = 6087.0$ slug-ft^2

$I_{yz} = -91,219$ slug-ft^2

The time dependent position coordinates of the masses m_n are given below ($\omega = 0.31416$ rad/sec):

n	Time Interval (seconds)	x_n (ft)	y_n (ft)	z_n (ft)
1	$0 \le t \le 6$	$+3 \sin \omega t$	$+45-2t$	111.11
	$6 < t$	+3	-45	111.11
2	$0 \le t \le 6$	$+3 \sin \omega t$	$-t$	111.11
	$6 < t$	+3	-45	111.11
3	$0 \le t \le 6$	$+3 \sin \omega t$	-45	111.11
	$6 < t$	+3	-45	111.11

Figure 56 shows that, for 1/2-g artificial gravity, the maximum wobble angle is 3.3 degrees and the maximum transverse body velocity is 1.2 deg/sec. The maximum body angular acceleration is 0.45 deg/sec^2. The maximum variation in the spin rate that is shown is 0.2 percent.

9.2.2 Configuration 6-A

The responses for three cases of internal mass motions were computed for Configuration 6-A. The initial positions of moving masses m_n are given below:

n	x_n (ft)	y_n (ft)	z_n (ft)
1	0	+45	+100
2	0	0	+100
3	0	-45	+100
4	0	-45	-100
5	0	0	-100
6	0	+45	-100

Case 1

Three artificial gravity levels were considered — 1/2-g, 1/4-g, and 1/10-g. Masses move in the x-direction such that $I_{xz} \neq 0$. The final moments and products of inertia are

$$I_x = 17.5558 \times 10^6 \text{ slug-ft}^2$$

$$I_y = 16.2228 \times 10^6 \text{ slug-ft}^2$$

$$I_z = 1.3818 \times 10^6 \text{ slug-ft}^2$$

$$I_{xz} = 11{,}180 \text{ slug-ft}^2$$

$$I_{xy} = I_{yz} = 0$$

Time dependent position coordinates of the masses m_n are given below. The values of y_n and z_n remain the same as the initial values.

n	Time Interval (seconds)	x_n (ft)
1, 2, 3	$0 \leq t \leq 6$	$+0.5\,t$
	$6 < t$	$+3$
4, 5, 6	$0 \leq t \leq 6$	$-0.5\,t$
	$6 < t$	-3

Figure 57 shows that, for 1/2-g artificial gravity, the maximum wobble angle is 0.37 degrees and the maximum transverse body velocity is 0.16 deg/sec. The maximum body angular acceleration is 0.063 deg/sec^2. The variation in the spin rate is negligible.

Figure 58 shows that, for 1/4-g artificial gravity, the maximum wobble angle is 0.4 degrees and the maximum transverse body velocity is 0.13 deg/sec. The maximum body angular acceleration is 0.035 deg/sec^2. The variation in the spin rate is negligible.

Figure 59 shows that, for 1/10-g artificial gravity, the maximum wobble angle is 0.42 degrees and the maximum transverse body velocity is 0.09 deg/sec. The maximum body angular acceleration is 0.0144 deg/sec^2. The variation in the spin rate is negligible.

Case 2

These artificial gravity levels were considered — 1/2-g, 1/4-g, and 1/10-g. Masses move in the x-direction such that $I_{xy} \neq 0$. The final moments and products of inertia are

$$I_x = 17.5558 \times 10^6 \text{ slug-ft}^2$$

$$I_y = 16.2227 \times 10^6 \text{ slug-ft}^2$$

$$I_z = 1.38169 \times 10^6 \text{ slug-ft}^2$$

$$I_{xy} = 3354 \text{ slug-ft}^2$$

$$I_{xz} = I_{yz} = 0$$

Time dependent position coordinates of the masses m_n are listed below. The values of y_n and z_n remain the same as the initial values.

n	Time Interval (seconds)	x_n (ft)
1, 6	$0 \le t \le 6$	+0.5 t
	$6 < t$	+3
2, 5	$0 \le t$	0
3, 4	$0 \le t \le 6$	-0.5 t
	$6 < t$	-3

Figure 60 shows that, for 1/2-g artificial gravity, the maximum wobble angle is 0.26 degrees and the maximum transverse body velocity is 0.108 deg/sec. The maximum body angular acceleration is 0.0193 deg/sec^2. The variation in the spin rate is negligible.

Figure 61 shows that, for 1/4-g artificial gravity the maximum wobble angle is 0.27 degrees and the maximum transverse body velocity is 0.08 deg/sec. The maximum body angular acceleration is 0.0109 deg/sec^2. The variation in the spin rate is negligible.

Figure 62 shows that, for 1/10-g artificial gravity, the maximum wobble angle is 0.28 degrees and the maximum transverse body angular velocity is 0.05 deg/sec. The maximum body angular acceleration is 0.0047 deg/sec^2. The variation in the spin rate is negligible.

Case 3

The artificial gravity is 1/2-g. Masses move in the y-direction and oscillate in the x-direction. The final moments and products of inertia are

$$I_x = 17.5809 \times 10^6 \text{ slug-ft}^2$$

$$I_y = 16.2228 \times 10^6 \text{ slug-ft}^2$$

$I_z = 1.40696 \times 10^6$ slug-ft^2

$I_{xy} = -5,031$ slug-ft^2

$I_{xz} = 11,180$ slug-ft^2

$I_{yz} = -167,702$ slug-ft^2

The time dependent position coordinates of the masses m_n are given below, (ω = 0.31416 rad/sec):

n	Time Interval (seconds)	x_n (ft)	y_n (ft)	z_n (ft)
1	$0 \le t \le 45$	$3 \sin \omega t$	$+45-2t$	+100
	$45 < t$	+3	-45	+100
2	$0 \le t \le 45$	$3 \sin \omega t$	$-t$	+100
	$45 < t$	+3	-45	+100
3	$0 \le t \le 45$	$3 \sin \omega t$	-45	+100
	$45 < t$	+3	-45	+100
4	$0 \le t \le 45$	$-3 \sin \omega t$	$-45+2t$	-100
	$45 < t$	-3	+45	-100
5	$0 \le t \le 45$	$-3 \sin \omega t$	$+t$	-100
	$45 < t$	-3	+45	-100
6	$0 \le t \le 45$	$-3 \sin \omega t$	+45	-100
	$45 < t$	-3	+45	-100

Figure 63 shows that, for 1/2-g artificial gravity, the maximum wobble angle is 2.5 degrees and the maximum transverse body velocity is 1.1 deg/sec. The maximum body angular acceleration is 0.387 deg/sec^2. The variation in the spin rate is 0.3 percent.

9.2.3 Configuration Y-A

The responses for three cases of internal mass motions were computed for Configuration Y-A. The artificial gravity is 1/2-g for these three cases. The initial positions of moving masses m_n are shown below:

n	x_n (ft)	y_n (ft)	z_n (ft)
1	0	-100	+45
2	0	-100	0
3	0	-100	-45
4	0	+11.03	-109.1
5	0	+50	- 86.6
6	0	+88.97	- 64.1
7	0	+88.97	+ 64.1
8	0	+50	+ 86.6
9	0	+11.03	+109.1

Case 1

Masses move in the x-direction such that $I_{xy} \neq 0$. The final moments and products of inertia are:

$$I_x = 28.5533 \times 10^6 \text{ slug-ft}^2$$

$$I_y = 13.3164 \times 10^6 \text{ slug-ft}^2$$

$$I_z = 10.2828 \times 10^6 \text{ slug-ft}^2$$

$$I_{xy} = 11{,}180 \text{ slug-ft}^2$$

$$I_{xz} = I_{yz} = 0$$

Time dependent position coordinates of the masses m_n are listed below. The values of y_n and z_n remain the same as the initial values.

n	Time Interval (seconds)	x_n
1, 2, 3	$0 \leq t \leq 6$ $6 < t$	$-0.5\ t$ -3
4, 5, 6 7, 8, 9	$0 \leq t \leq 6$ $6 < t$	$+0.5\ t$ $+3$

Figure 64 shows that, for 1/2-g artificial gravity, the maximum wobble angle is 0.066 degrees and the maximum transverse body angular velocity is 0.038 deg/sec. The maximum body angular acceleration is 0.0125 deg/sec^2. The variation in the spin rate is negligible.

Case 2

Masses m_5 and m_8 move in the radial direction and oscillate in the x-direction. All other masses remain in their initial positions. The final moments and products of inertia are:

$$I_x = 28.42896 \times 10^6 \text{ slug-ft}^2$$

$$I_y = 13.22276 \times 10^6 \text{ slug-ft}^2$$

$$I_z = 10.25117 \times 10^6 \text{ slug-ft}^2$$

$$I_{xy} = I_{xz} = I_{yz} = 0$$

The maximum value of I_{xz} during the mass motion was + 1520 slug-ft^2. The time dependent position coordinates of the masses m_5 and m_8 are given below (ω = 0.82467 rad/sec):

n	Time Interval (seconds)	x_n (ft)	y_n (ft)	z_n (ft)
5	$0 \leq t \leq 40$ $40 < t$	$-1.5 \sin \omega t$ -1.5	$+50-1.25\ t$ 0	$-86.6+2.165\ t$ 0
8	$0 \leq t \leq 40$ $40 < t$	$+1.5 \sin \omega t$ $+1.5$	$+50-1.25\ t$ 0	$+86.6-2.165\ t$ 0

Figure 65 shows that for 1/2-g artificial gravity, the maximum transverse body angular velocity is 0.013 deg/sec. The maximum body acceleration is 0.0095 deg/sec^2. The wobble angle and the variation in the spin rate are negligible.

Case 3

Masses m_4 and m_9 move in the tangential direction and oscillate in the x-direction. All other masses remain in their initial positions. The final moments and products of inertia are

$$I_x = 28.55302 \times 10^6 \text{ slug-ft}^2$$

$$I_y = 13.21919 \times 10^6 \text{ slug-ft}^2$$

$$I_z = 10.37897 \times 10^6 \text{ slug-ft}^2$$

$$I_{xz} = 2389.0 \text{ slug-ft}^2$$

$$I_{xy} = I_{yz} = 0$$

The time dependent position coordinates of the masses m_4 and m_9 are given below (ω = 0.31416 rad/sec):

n	Time Interval (seconds)	x_n (ft)	y_n (ft)	z_n (ft)
4	$0 \le t \le 45$	$-3 \sin \omega t$	$+11.03+1.732t$	$-109.1+t$
	$45 < t$	-3	$+88.97$	-64.1
9	$0 \le t \le 45$	$+3 \sin \omega t$	$+11.03+1.732t$	$+109.1-t$
	$45 < t$	$+3$	$+88.97$	$+64.1$

Figure 66 shows that, for 1/2-g aritficial gravity, the maximum transverse body velocity is 0.02 deg/sec. The maximum body acceleration is 0.0094 deg/sec^2. The wobble angle and the variation in the spin rate are negligible.

9.3 DOCKING AND LAUNCHING OPERATIONS

Docking and launching disturbances are similar in that both involve a change in the total mass of the rotating space station system. During the docking operation, the space station is also subject to an impulsive force due to impact between the docking vehicle and the space structure. If the

line of action of the impulsive force does not pass through the mass center of the space station as in a misaligned docking maneuver, an impulsive torque will be applied to the space station, as discussed in Section 3. 1. 2.

Docking to and launching from a space station configuration, such as Configuration 1-A which does not have a stationary platform or a despun central hub, present formidable dynamic problems of dubious feasibility unless the entire space station is despun. For this reason, only configurations with central hubs are considered.

The docking vehicle which is used in this study has weight and inertia properties comparable to the Apollo command module (W = 9800 pounds, I_x = 4500 slug-ft^2, I_y = I_z = 4000 slug-ft^2, and 5.4 feet is the distance between the docking face and the mass center along its x-body axis. The docking vehicle is simulated by eight discrete masses distributed in a three-dimensional array, such that the combination has the weight and inertia properties given above.

The vehicle docks directly above the Y inertia axis parallel to the station x-body axis at a misalignment distance of two feet from the x-axis. The time interval for the docking operation is assumed to be three seconds. During this time, the mass of the docking vehicle is added to the space station as a linear function of time and a 400 foot-pound rectangular torque pulse, attributed to docking impact and thrusting of the docking vehicle, is applied.

The docking of this vehicle to Configurations 6-A and 7-A is completely similar. Therefore, only the results for Configurations 7-A and Y-A at 1/2-g artificial gravity are presented below.

9. 3. 1 Configuration 7-A: Apollo Docking

Figure 67 shows that, for 1/2-g artificial gravity, the maximum wobble angle is 0. 09 degrees and the maximum transverse body velocity is 0. 035 deg/sec. The maximum body angular acceleration is 0. 0165 deg/sec^2. The variation in the spin rate is negligible.

9.3. 2 Configuration Y-A: Apollo Docking

Figure 68 shows that, for 1/2-g artificial gravity, the maximum transverse body velocity is 0. 0055 deg/sec. The maximum body angular acceleration is 0. 0025 deg/sec^2. The wobble angle and the variation in the spin rate are negligible.

9.4 ANGULAR ACCELERATION OR DECELERATION AND CONTROL FORCES

Angular acceleration (spin-up) and deceleration (de-spin), about the spin axis of the space station, is achieved by application of an external rectangular moment pulse, M_x, about the spin axis, until the desired spin velocity, p, is developed. Spin up or de-spin of a vehicle in the absence of transverse body velocity components (q and r) does not present any particular difficulty since a moment about the spin axis will cause only a change in the spin velocity.

However, in the presence of small transverse body velocity components, an increase or decrease in the spin velocity will change the wobble amplitude and frequency. Several cases of spin-up with transverse body velocity are presented in graphical form in Figure 69 through 77. The period during which the spin-up pulse moment (M_x) is applied is indicated by the heavy portions of the curves; subsequently, the curves are light. The moments of inertia for each configuration are given in Section 2.0.

Figures 69 and 70 show the spin-up response of Configuration 1-A to 300,000 foot-pounds torque with 0.1 degrees per second initial transverse body velocity. The maximum wobble angle is 2.15 degrees. Note that the motion of the space station is shifted 90 degrees when the initial transverse body velocity is shifted 90 degrees.

Figures 71 and 72 show the spin-up response of Configuration 6-A to 60,000 foot-pounds and 120,000 foot-pounds torque, respectively, with 0.1 deg/sec initial transverse body velocity. The maximum wobble angles are 2.05 degrees and 1.45 degrees, respectively. In Figure 73, the response to 60,000 foot-pounds torque with 0.5 deg/sec initial transverse body velocity achieves 10.05 degrees maximum wobble angle.

Figure 74 shows the spin-up response of Configuration 6-A, where I_{xz} was arbitrarily set at 100,000 slug-ft^2, to 60,000 foot-pounds torque with 0.1 deg/sec initial transverse body velocity. The maximum wobble angle is 6.5 degrees. Note that the wobble motion and the transverse body velocities are greatly affected by the large degree of unbalance, while the time required to spin-up is identical to the case in Figure 71.

Figure 75 shows the spin-up response of Configuration 7-A to 60,000 foot-pounds torque with 0.1 deg/sec initial transverse body velocity. The maximum wobble angle is 2.12 degrees, which is slightly larger than for Configuration 6-A (Figure 71).

Figure 76 shows the spin-up response of Configuration Y to 60,000 foot-pounds torque with 0.1 deg/sec initial transverse body velocity. The maximum wobble angle is 1.25 degrees.

Figure 77 shows the spin-up response of Configuration Y-A to 90,000 foot-pounds torque with 0.1 deg/sec initial transverse body velocity. The maximum wobble angle is 1.9 degrees.

Reaction jets may be used to produce external moments on the space station for wobble damping and spin rate control. The proportional control laws which were investigated are functions of the body angular velocities. The general form of the control laws is

$$M_x = - k_1 (p - p_c)$$

$$M_y = - k_2 q$$

$$M_z = - k_3 r$$

Several cases are presented to show the effect of these control laws when used simultaneously.

Figures 78 and 79 show, for 1/2-g artificial gravity, the undamped and damped response, respectively, of Configuration 6-A with 0.1 deg/sec initial transverse body velocity. All wobble is damped after 18 seconds, the spin rate is controlled within 30 seconds, and the control moments become zero after damping is complete.

Figure 80 shows the controlled response of Configuration 1A to the disturbance arising from the same internal mass motion that produced uncontrolled response shown in Figure 54. The controlled wobble motions are almost entirely damped and the steady state control moments are nearly zero.

Figure 81 shows the controlled response of Configuration 1A corresponding to Figure 56. It is seen that the velocity proportioned control system cannot completely damp out the wobble. A further deficiency of the damping system is that constant moments must be applied to the unbalanced vehicle after the wobble has been damped to a minimum.

Figure 82 shows the controlled response of Configuration 6-A corresponding to Figure 57. Again, due to the unbalance of the vehicle, the wobble is not entirely damped out and constant moments must be applied after it is damped to a minimum.

The angular velocity proportional control laws presented here are not adequate for the wobble control of vehicles which are unbalanced such that I_{xy} or I_{xz} is not zero. They are, however, adequate for the control of balanced vehicles.

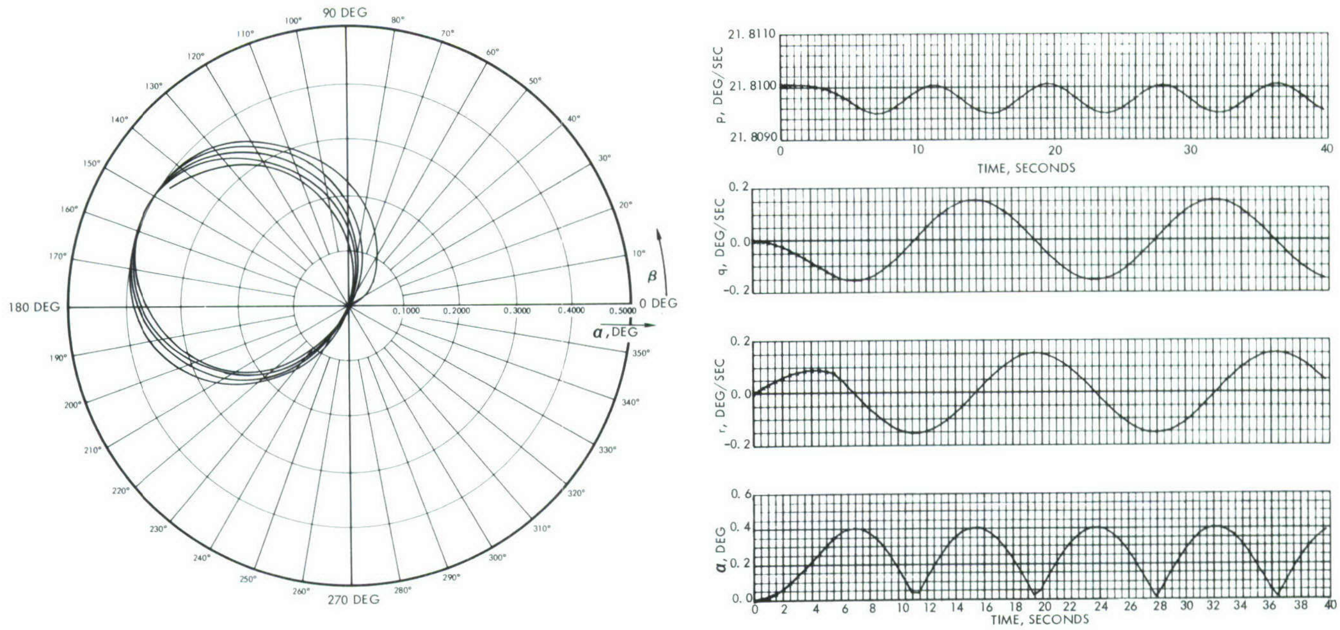

Figure 54. Internal Mass Motions, Artificial Gravity 1/2-g
(Configuration 1-A, Case 1)

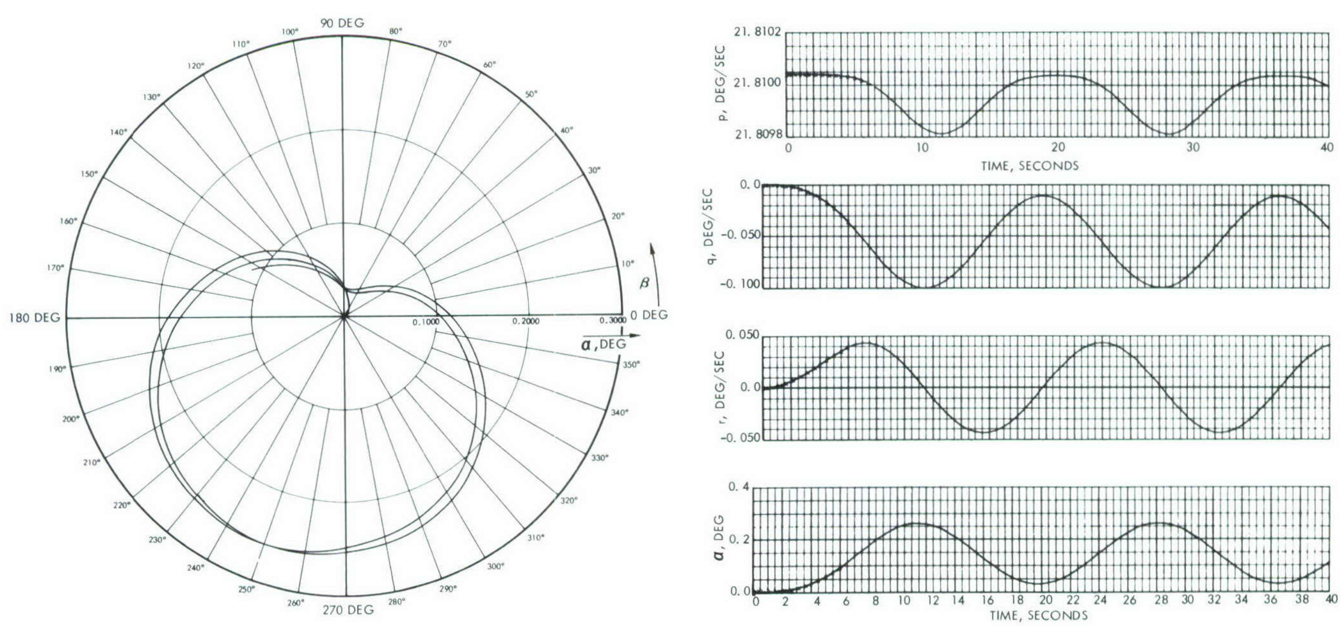

Figure 55. Internal Mass Motions, Artificial Gravity 1/2-g
(Configuration 1-A, Case 2)

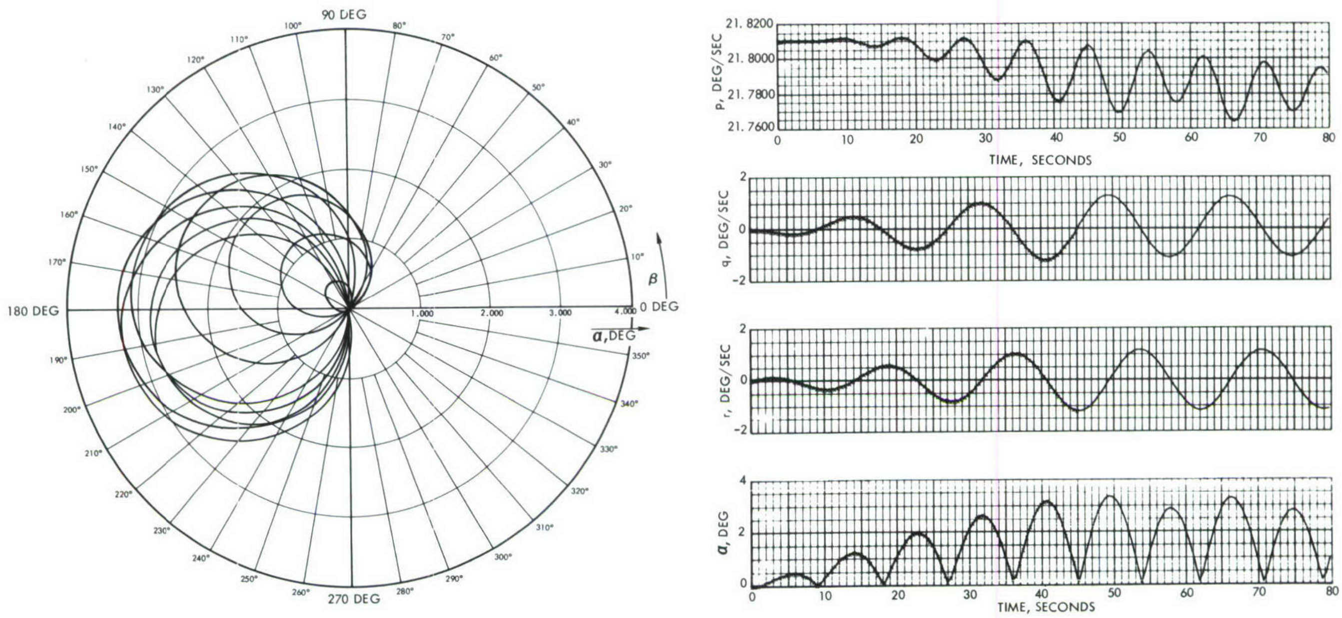

Figure 56. Internal Mass Motions, Artificial Gravity 1/2-g
(Configuration 1-A, Case 3)

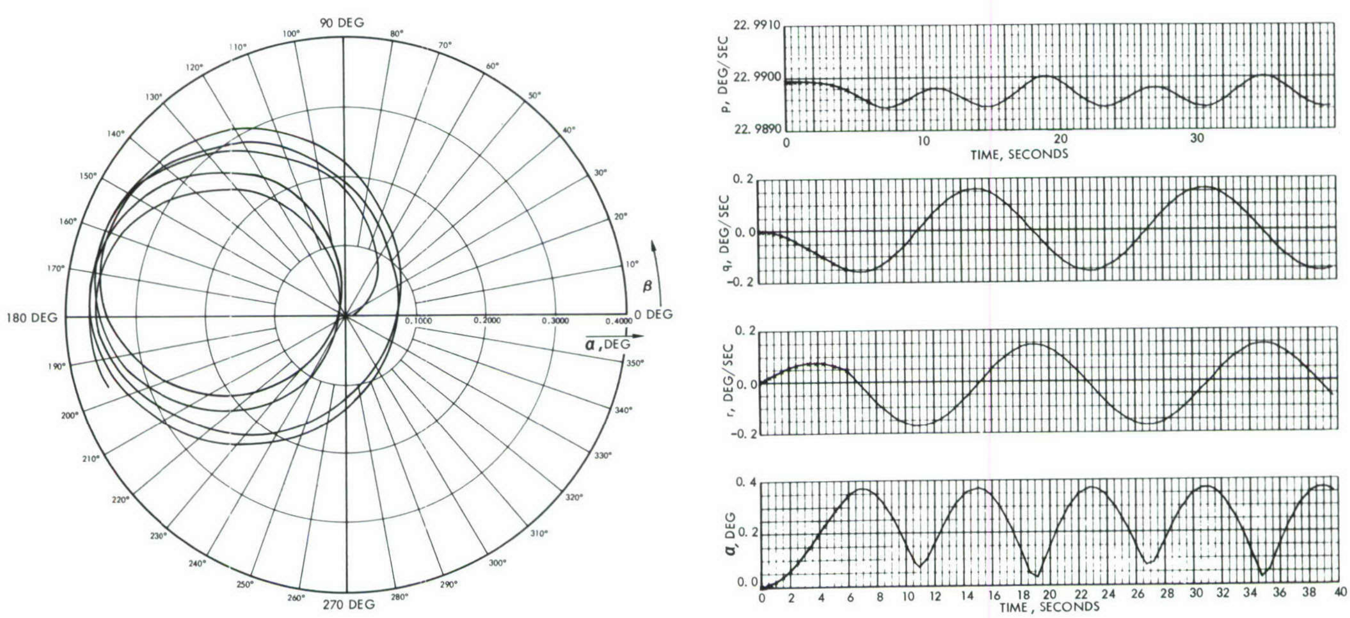

Figure 57. Internal Mass Motions, Artificial Gravity 1/2-g
(Configuration 6-A, Case 1)

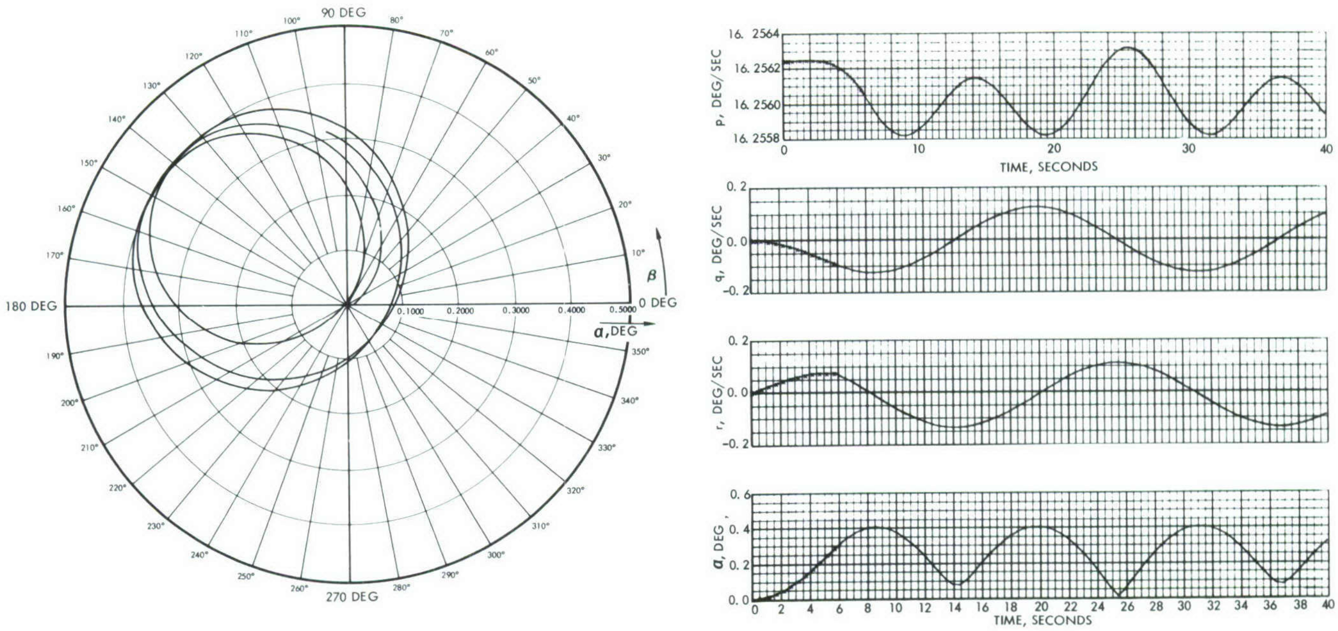

Figure 58. Internal Mass Motions, Artificial Gravity 1/4-g
(Configuration 6-A, Case 1)

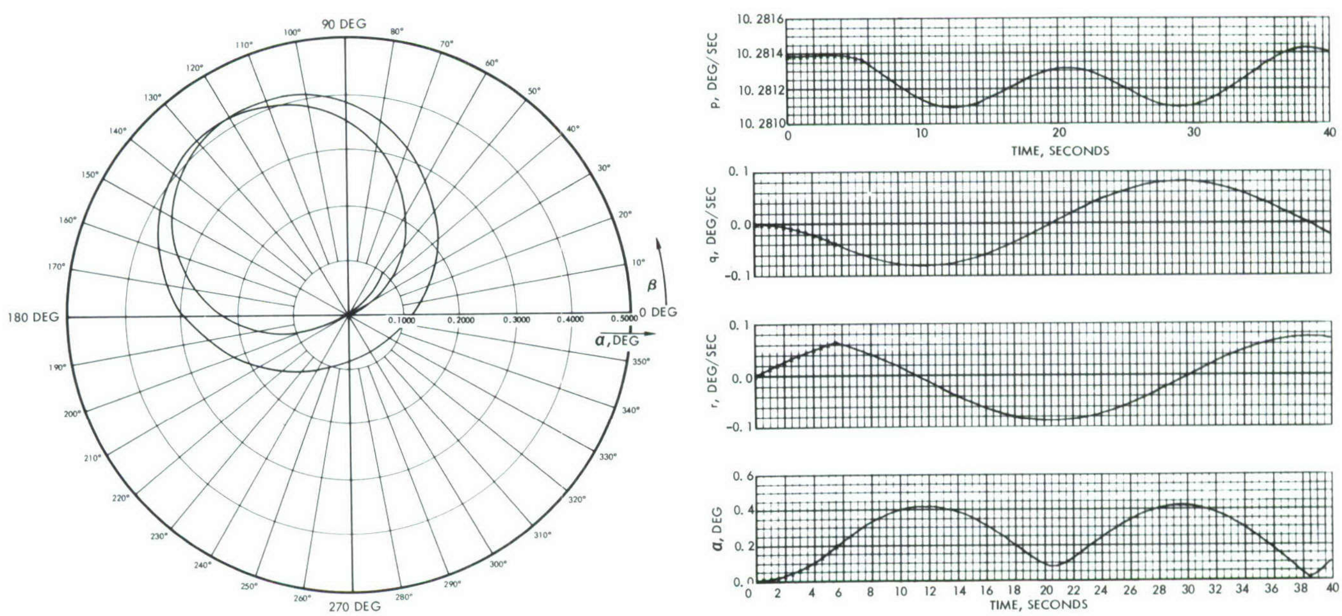

Figure 59. Internal Mass Motions, Artificial Gravity 1/10-g
(Configuration 6-A, Case 1)

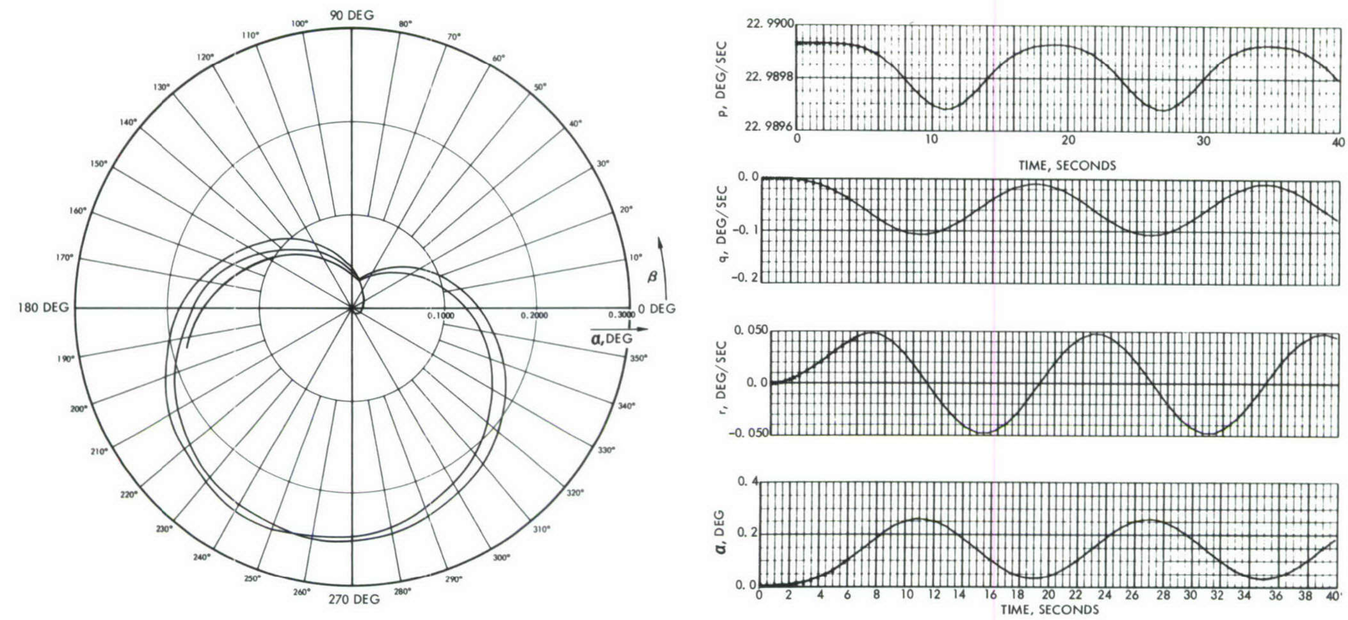

Figure 60. Internal Mass Motions, Artificial Gravity 1/2-g
(Configuration 6-A, Case 2)

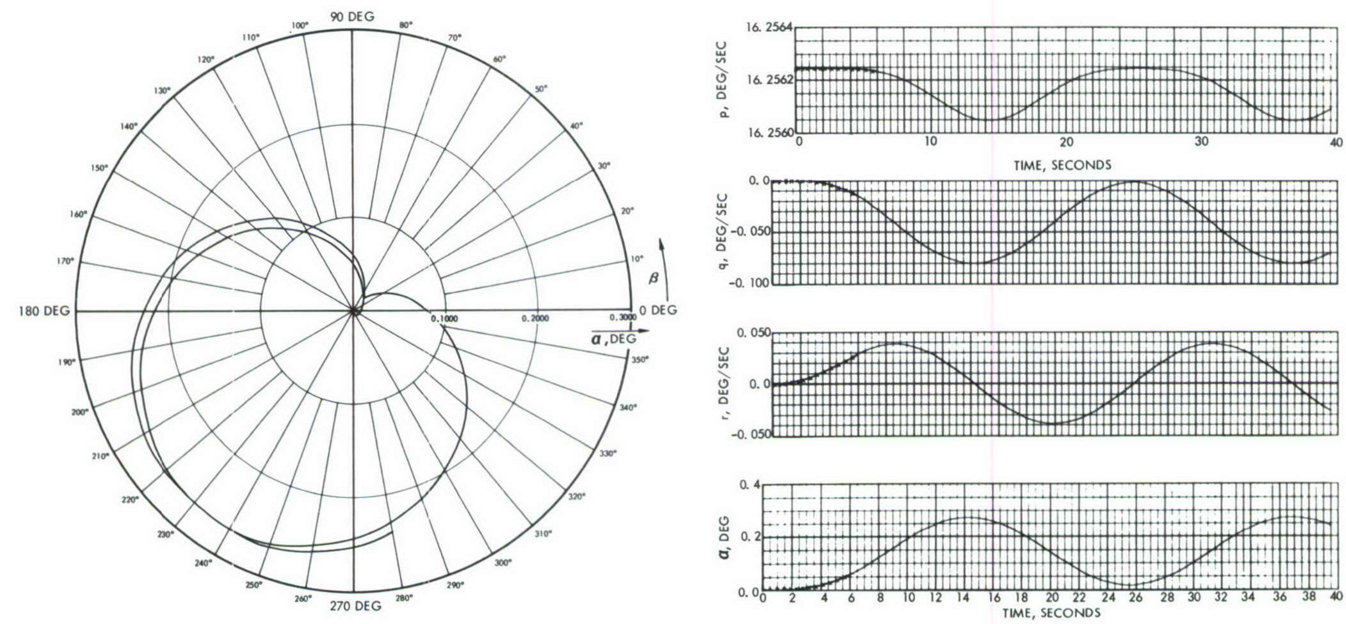

Figure 61. Internal Mass Motions, Artificial Gravity 1/4-g
(Configuration 6-A, Case 2)

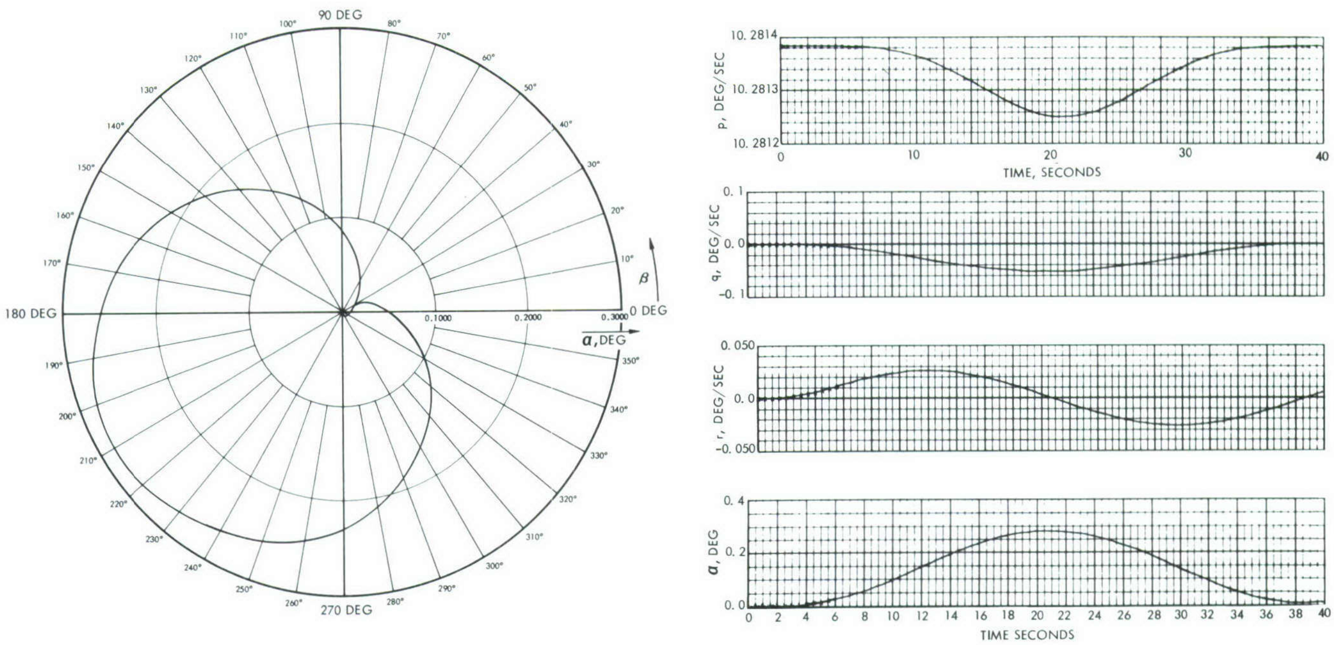

Figure 62. Internal Mass Motions, Artificial Gravity 1/10-g
(Configuration 6-A, Case 2)

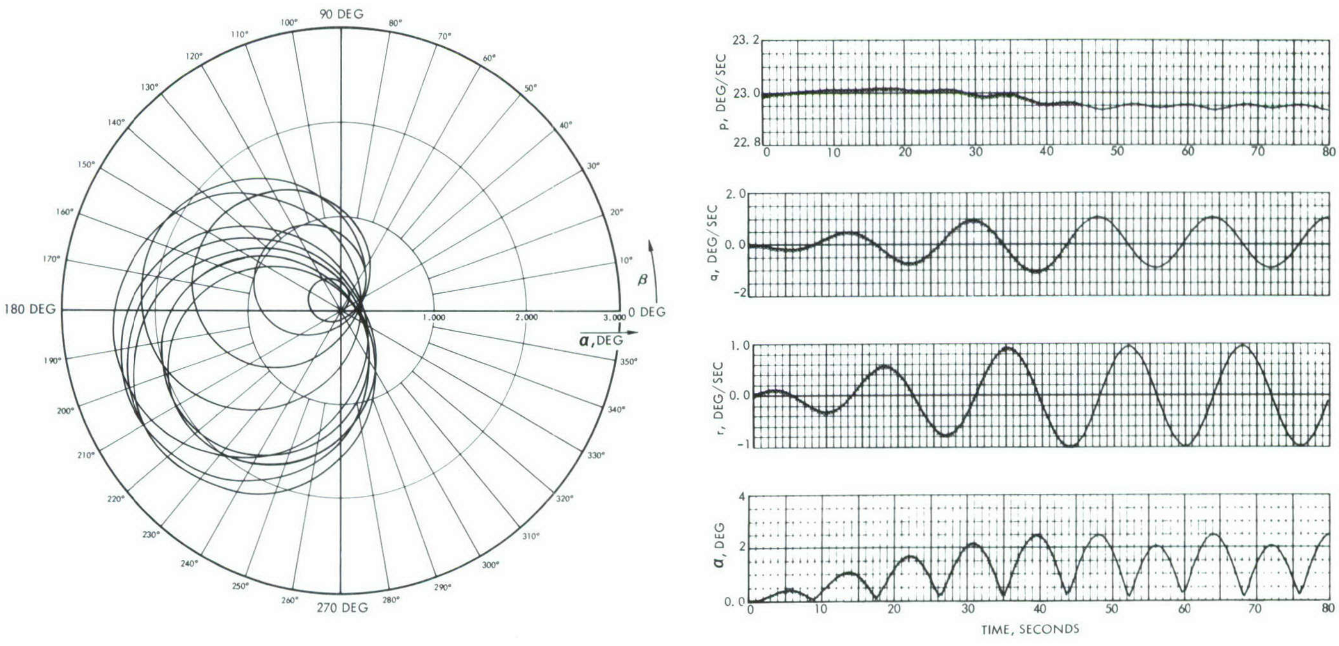

Figure 63. Internal Mass Motions, Artificial Gravity 1/2-g
(Configuration 6-A, Case 3)

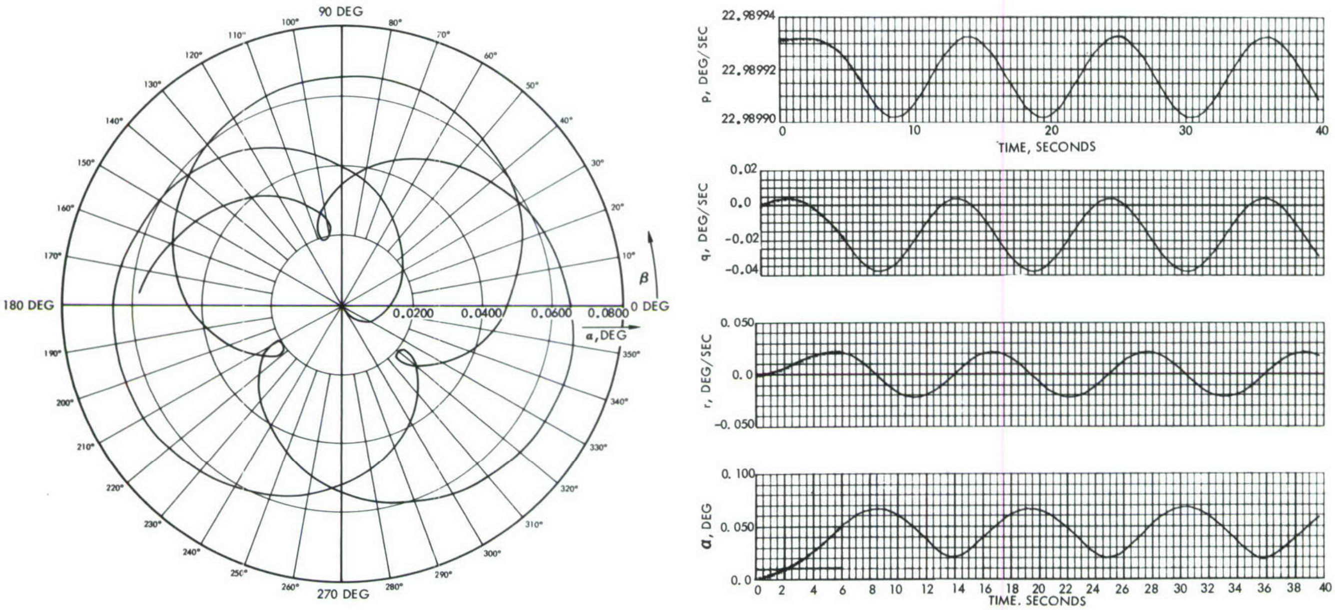

Figure 64. Internal Mass Motions, Artificial Gravity 1/2-g (Configuration Y-A, Case 1)

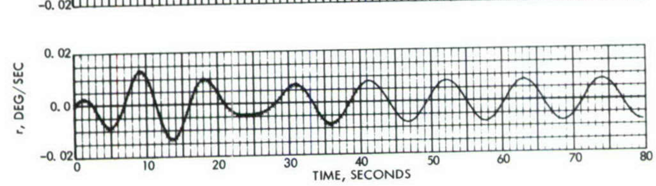

Figure 65. Internal Mass Motions, Artificial Gravity 1/2-g (Configuration Y-A, Case 2)

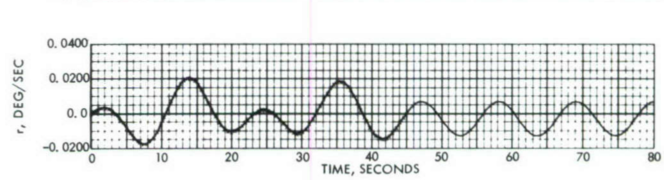

Figure 66. Internal Mass Motions, Artificial Gravity 1/2-g (Configuration Y-A, Case 3)

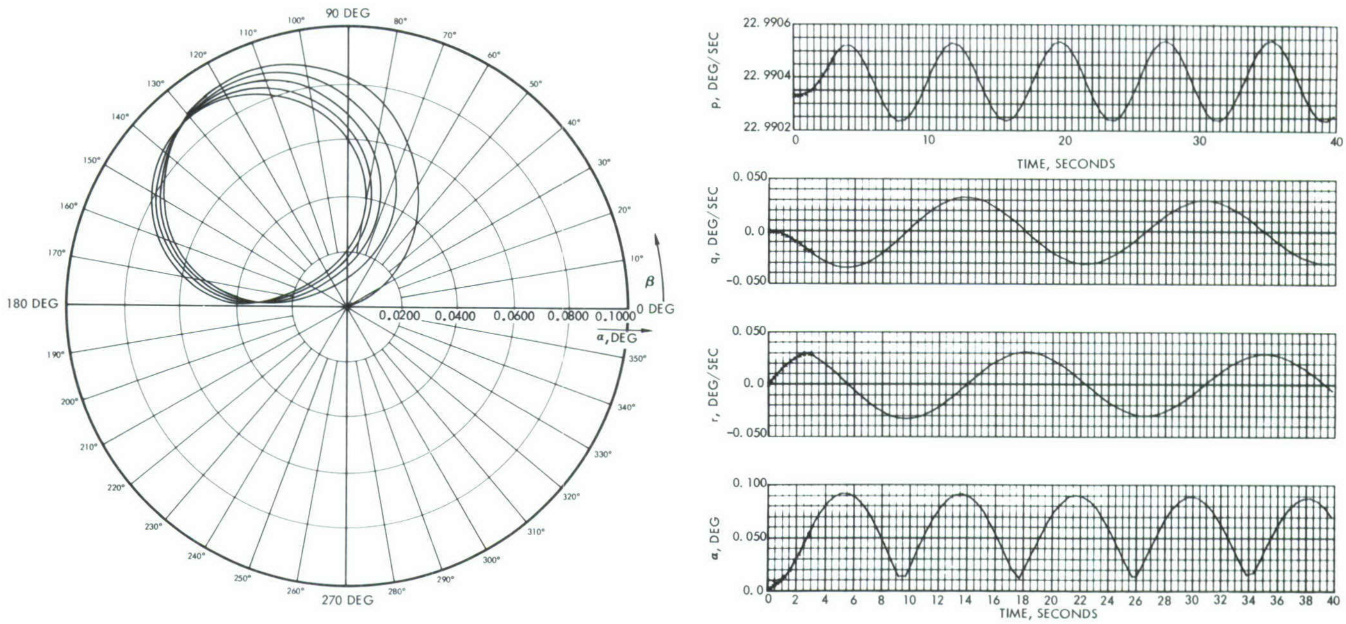

Figure 67. Apollo Docking, Artificial Gravity 1/2-g (Configuration 7-A)

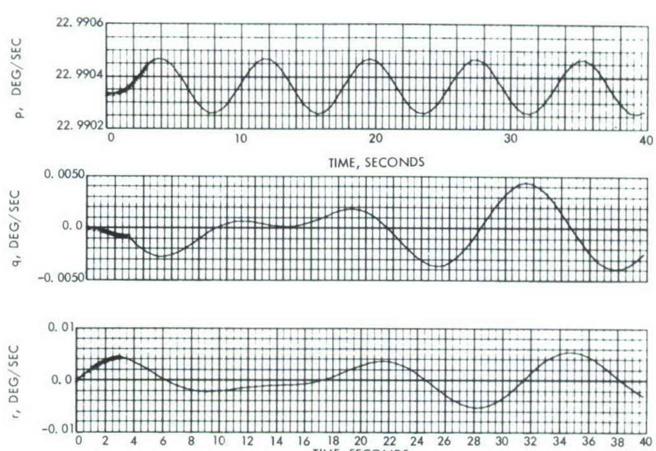

Figure 68. Apollo Docking, Artificial Gravity 1/2-g (Configuration Y-A)

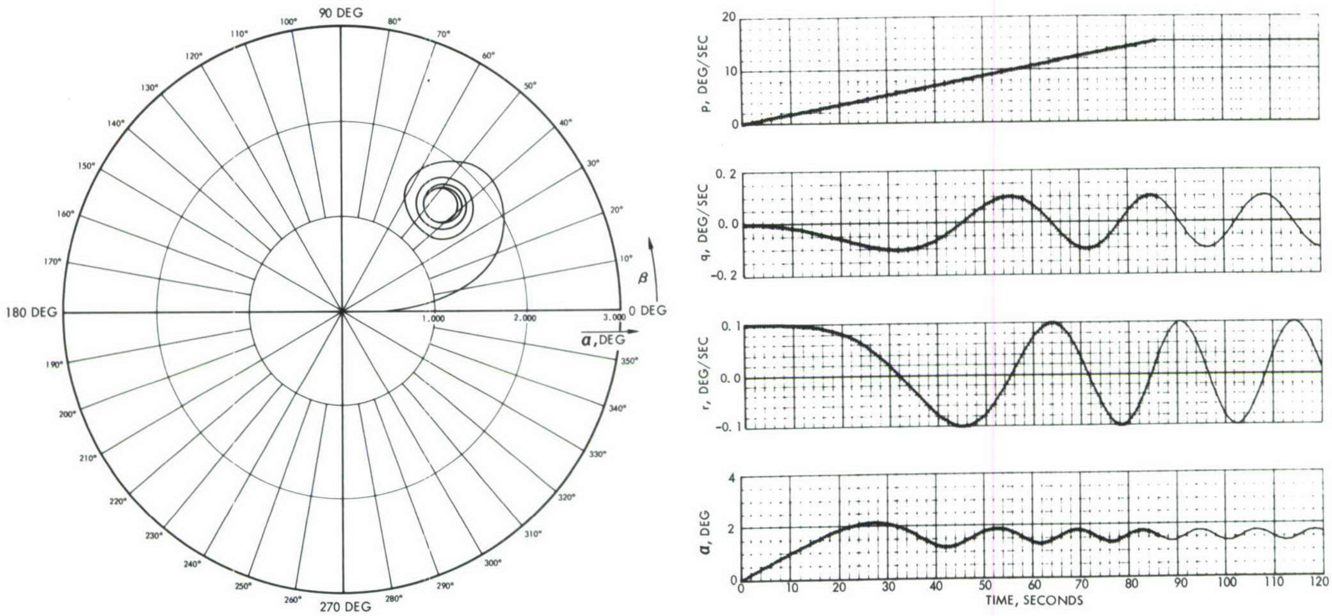

Figure 69. Spin-Up, M_x = 300, 000 Ft-lb (Configuration 1-A, Case 1)

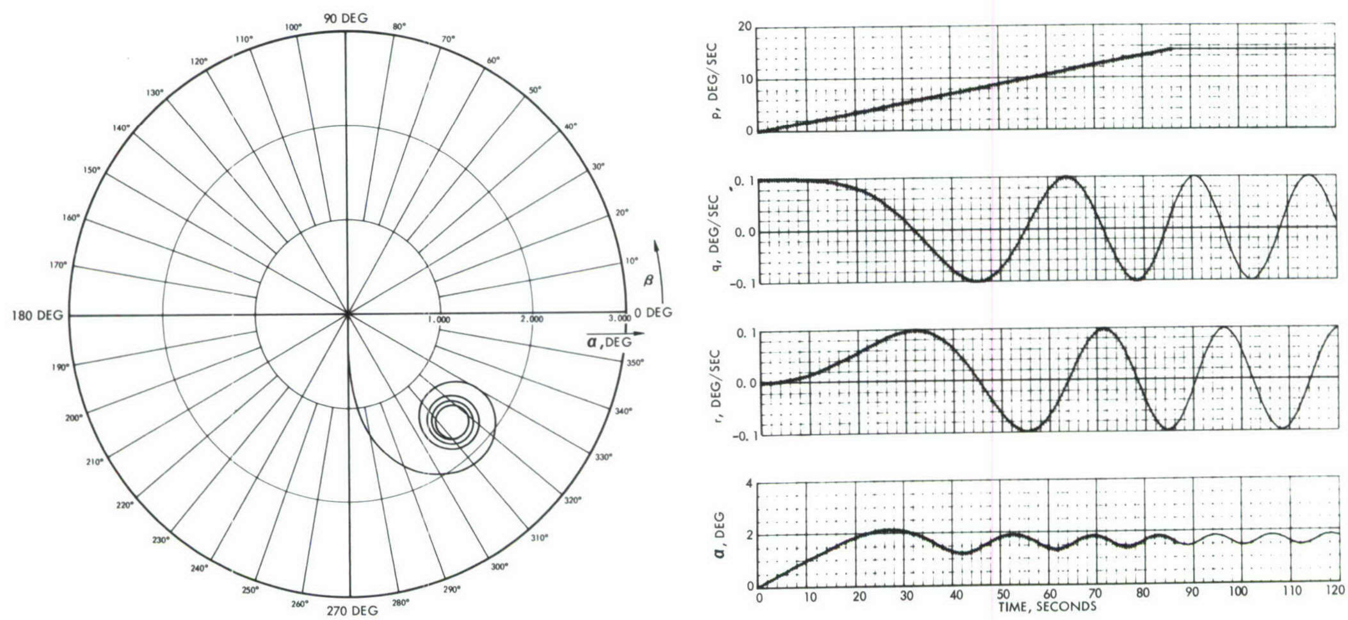

Figure 70. Spin-Up, M_x = 300, 000 Ft-lb (Configuration 1-A, Case 2)

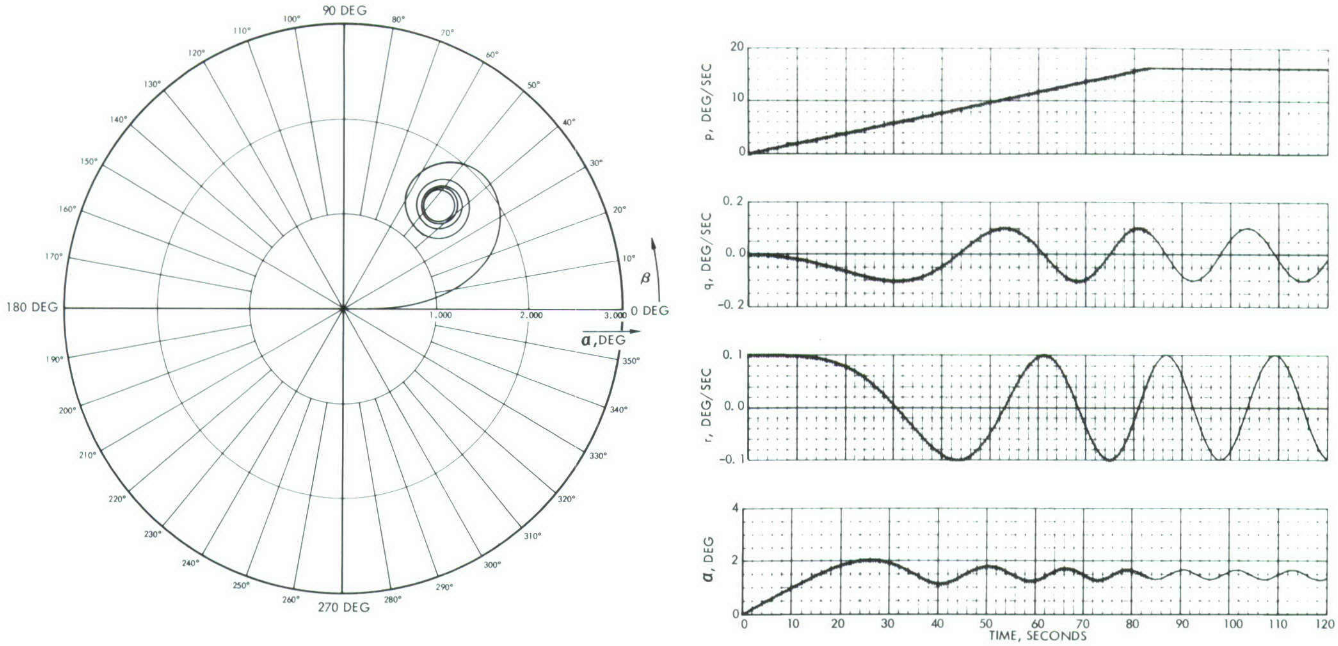

Figure 71. Spin-Up, M_x = 60,000 Ft-lb (Configuration 6-A, Case 1)

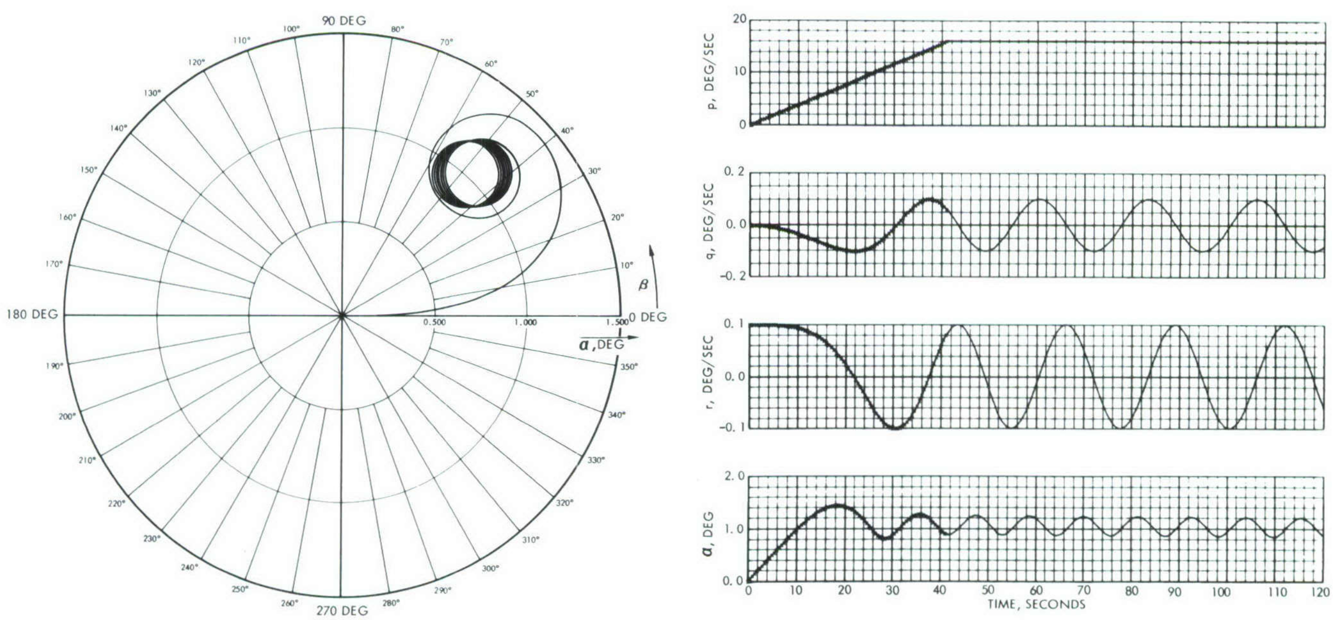

Figure 72. Spin-Up, M_x = 120,000 Ft-lb (Configuration 6-A, Case 1)

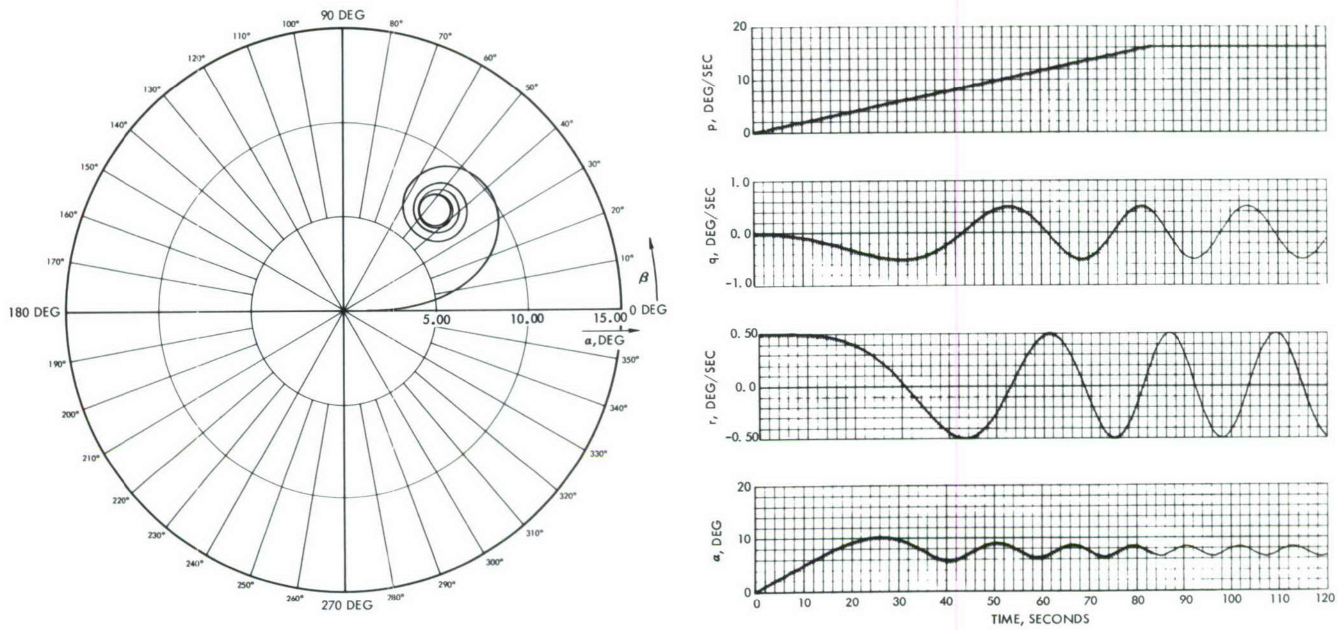

Figure 73. Spin-Up, M_x = 60, 000 Ft-lb (Configuration 6-A, Case 2)

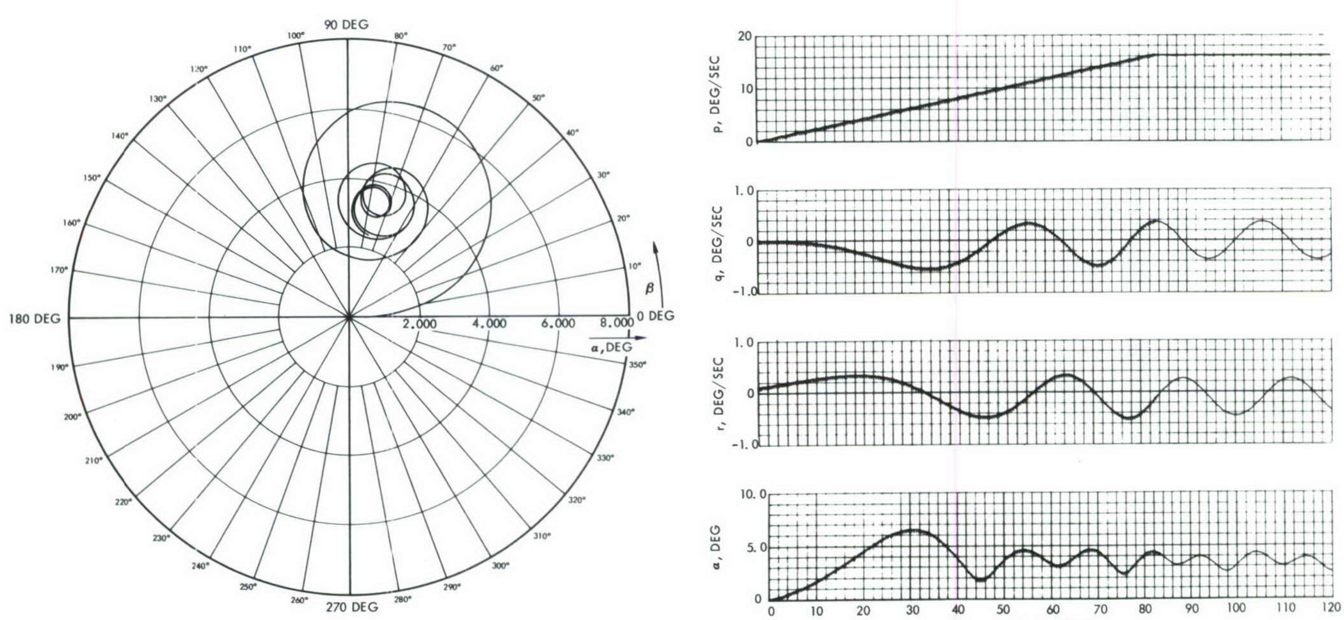

Figure 74. Spin-Up, M_x = 60, 000 Ft-lbs, I_{xz} = 100, 000 Slug-ft^2,
r = 0. 1 Degrees per Second at t = 0
(Configuration 6-A, Case 3)

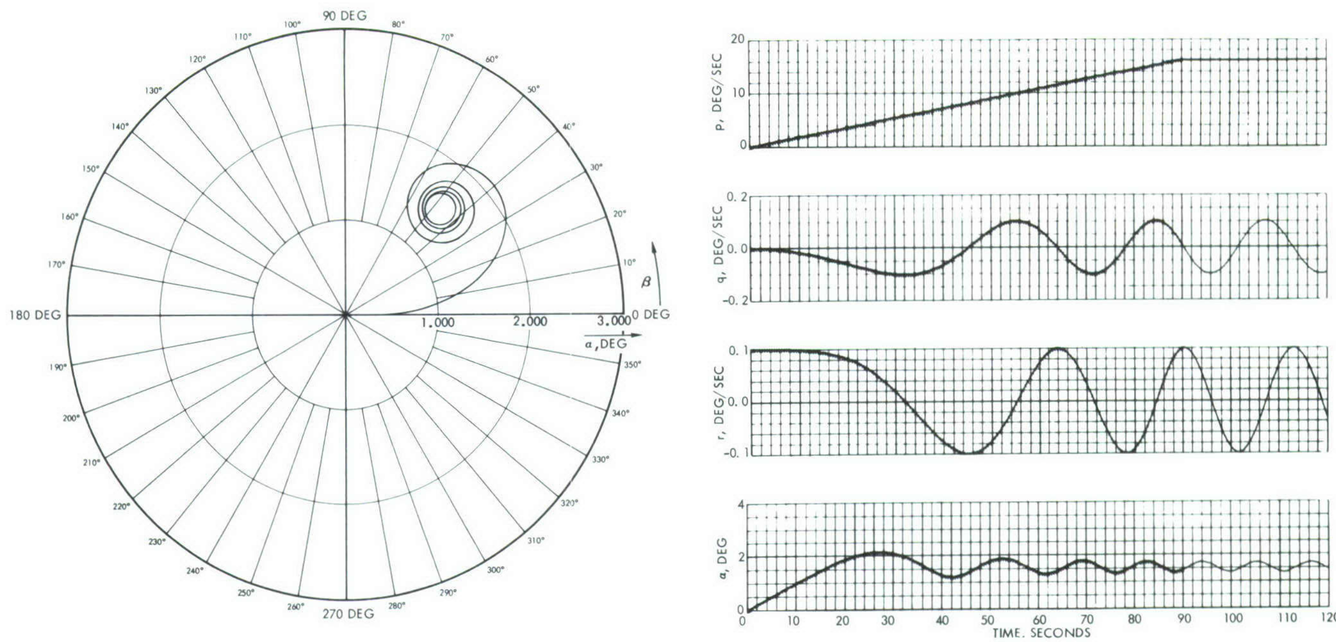

Figure 75. Spin-Up, M_X = 60, 000 Ft-lb (Configuration 7-A)

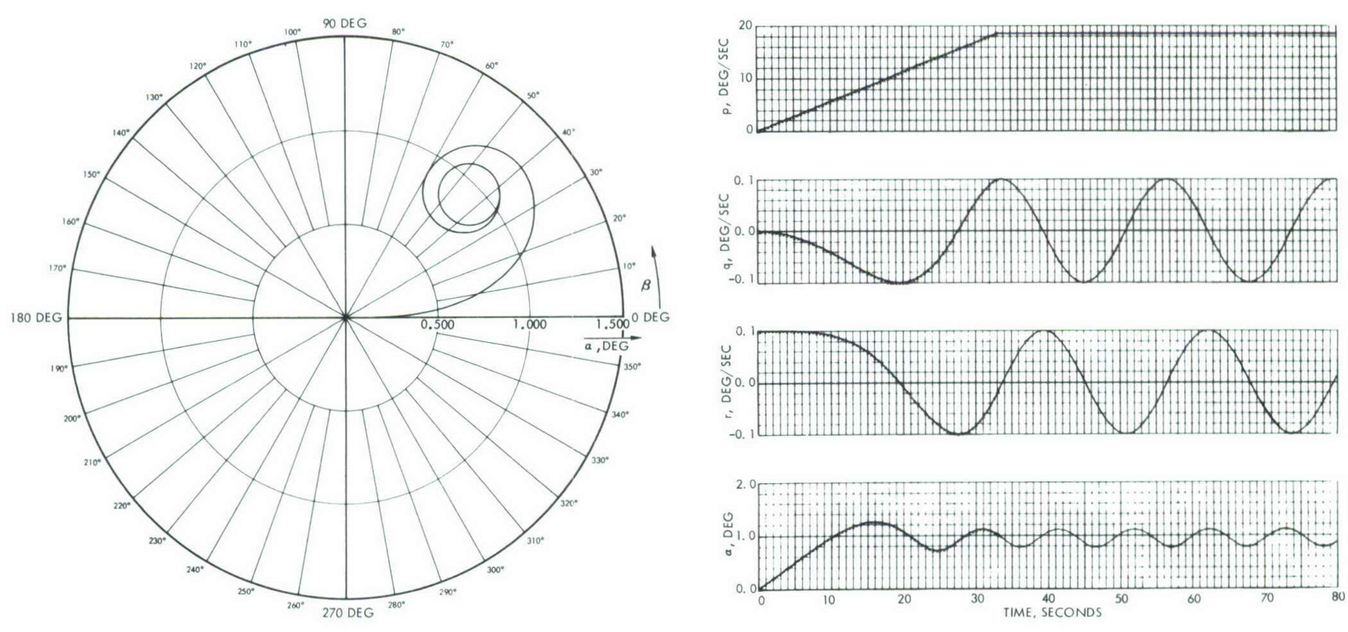

Figure 76. Spin-Up, M_X = 60, 000 Ft-lb (Configuration Y)

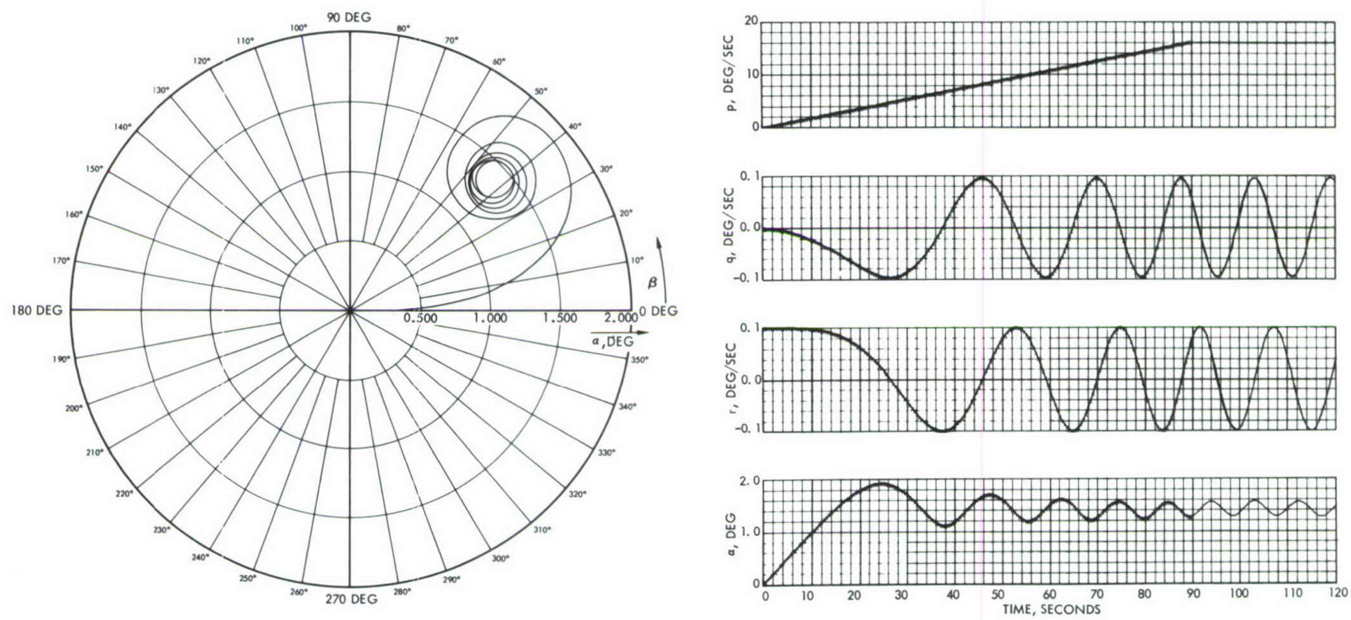

Figure 77. Spin-Up, M_x = 90, 000 Ft-lb (Configuration Y-A)

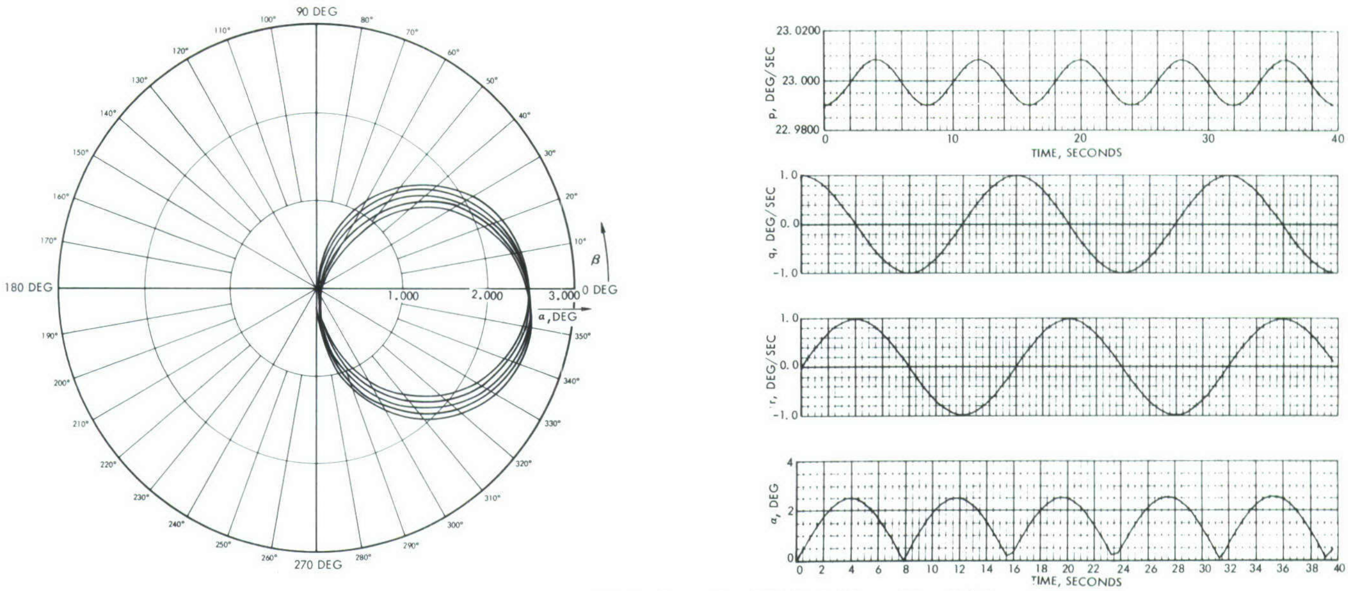

Figure 78. Moment-Free Wobble, Artificial Gravity 1/2-g (Configuration 6-A, q = 1.0 Degrees per Second at t = 0)

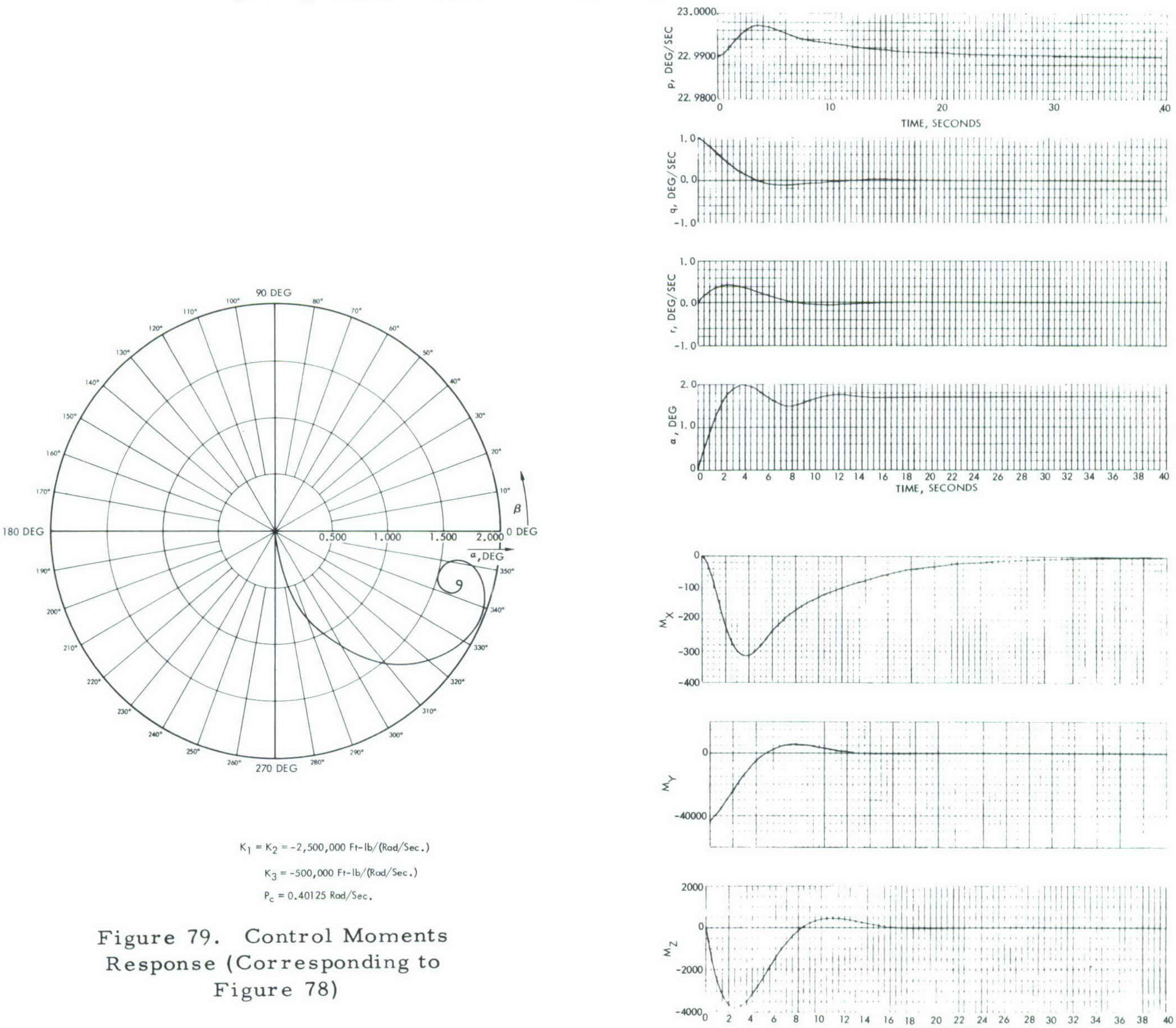

Figure 79. Control Moments Response (Corresponding to Figure 78)

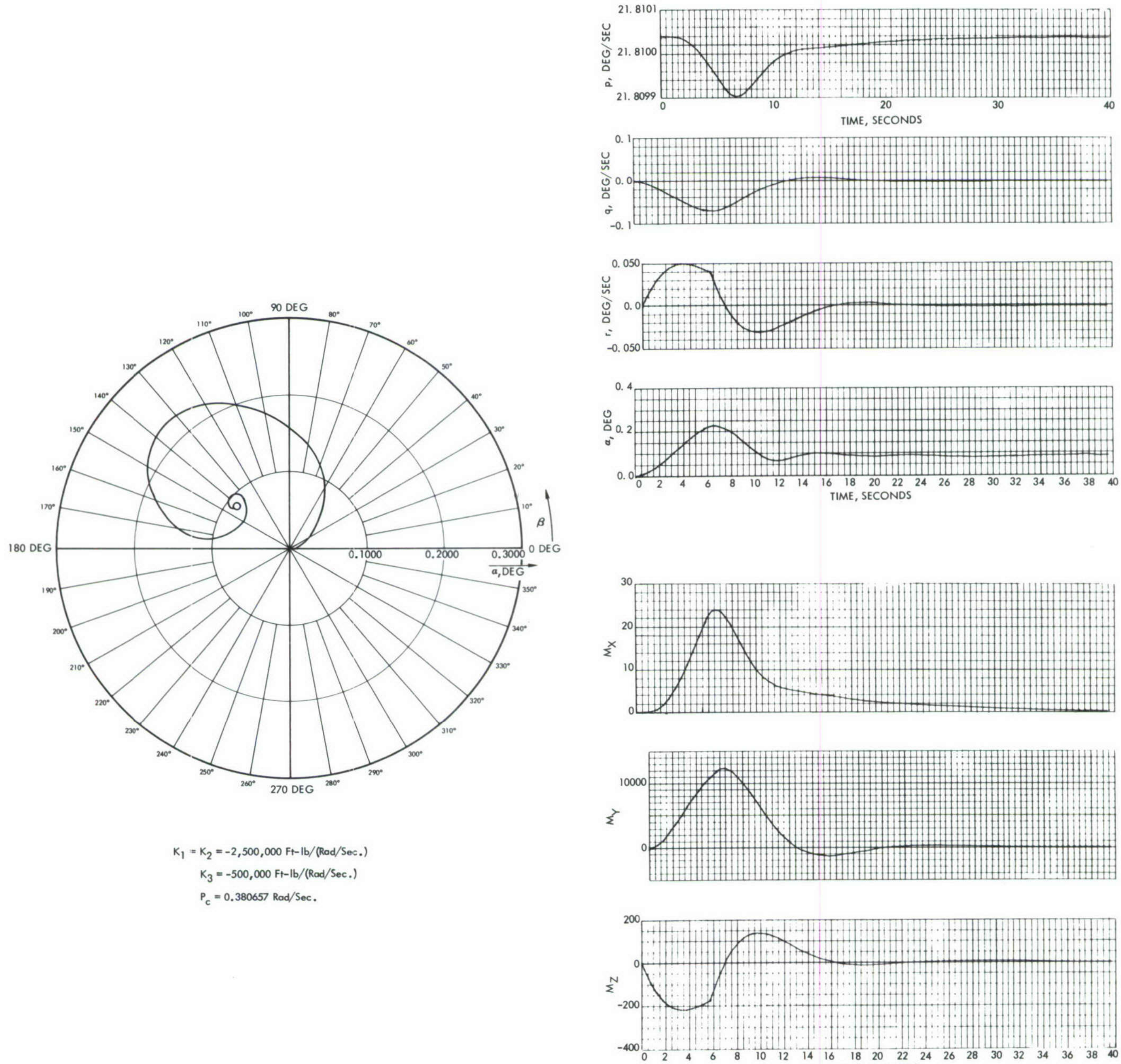

Figure 80. Control Moments Response (Corresponding to Figure 54)

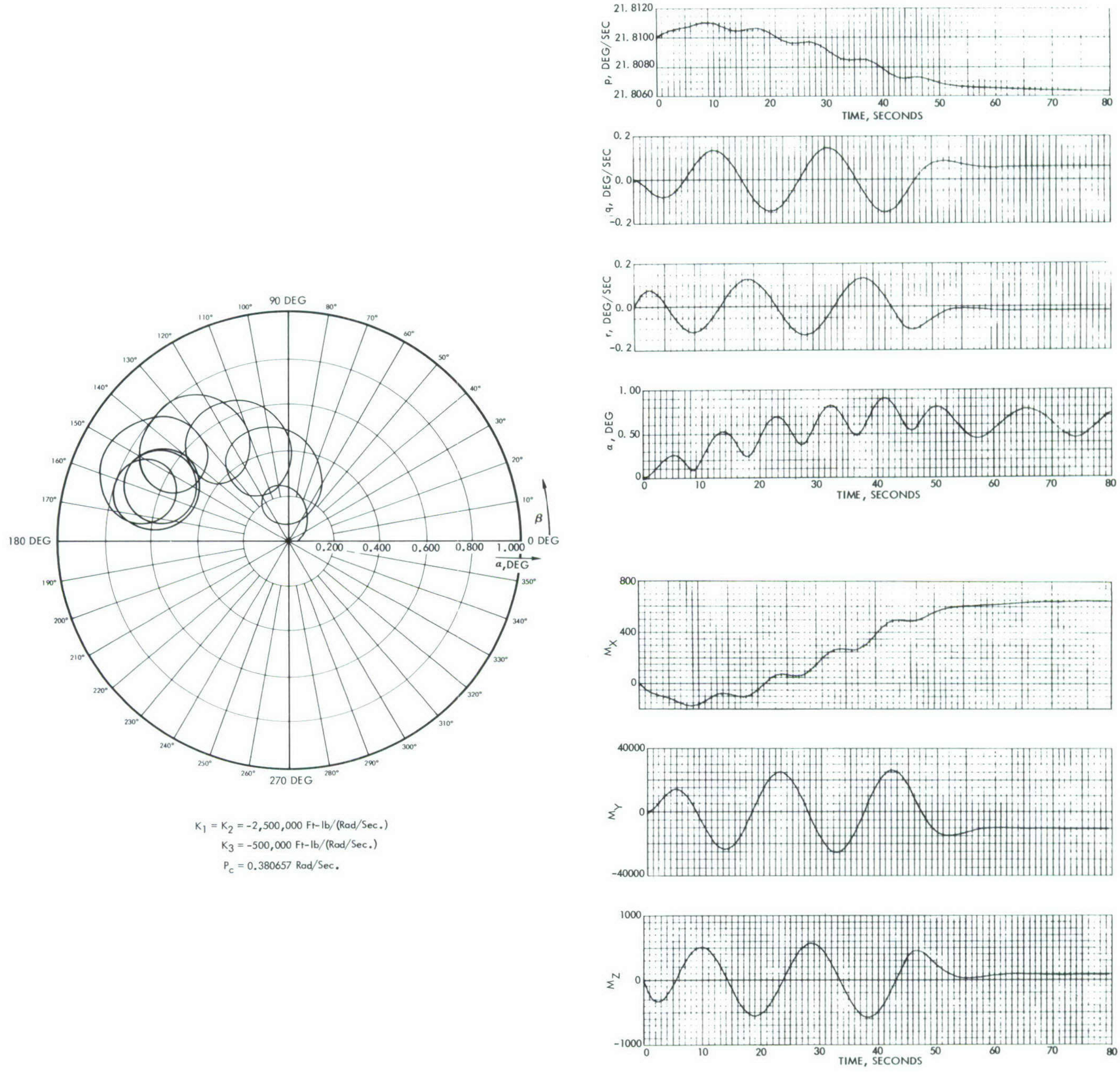

Figure 81. Control Moments Response (Corresponding to Figure 56)

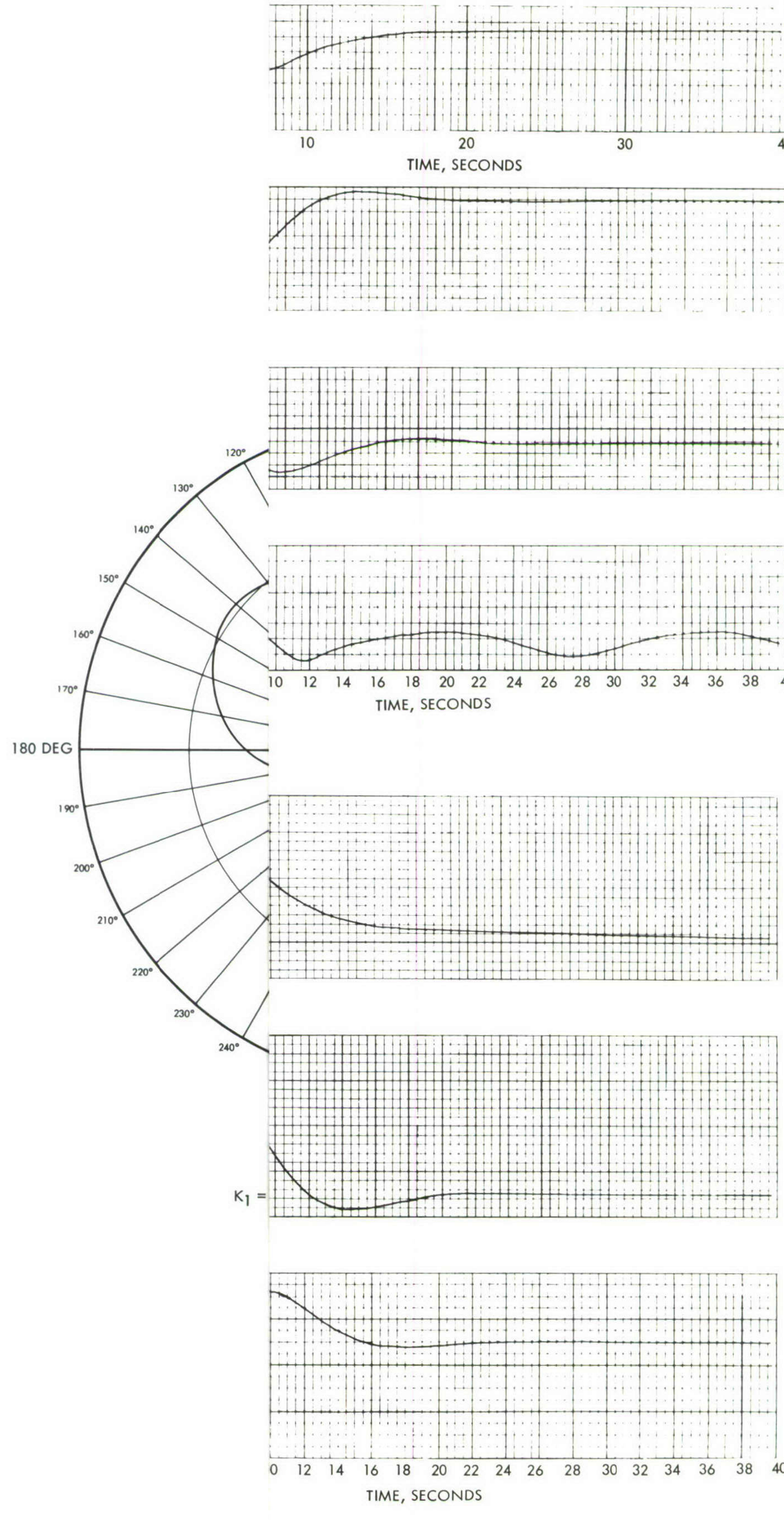

10
20
30
40
TIME, SECONDS
120°
130°
140°
150°
160°
170°
180 DEG
190°
200°
210°
220°
230°
240°
10 12 14 16 18 20 22 24 26 28 30 32 34 36 38 40
TIME, SECONDS
K_1 =
0 12 14 16 18 20 22 24 26 28 30 32 34 36 38 40
TIME, SECONDS

re 57)

BIBLIOGRAPHY

1. Adams, J. J. Study of an Active Control System for a Spinning Body. NASA TN D-905, (1961).

2. Andrew, L. V., C. L. Tai, M. M. H. Loh, M. Lukoff, and P. Kamrath, A Preliminary Investigation of the Motion of a Rotating Compartment-Cable-Counterweight Space Station in Orbit. NAA, SID 63-1036.

3. Chobotov, V. Gravity Gradient Excitation of a Rotating Cable-Counterweight Space Station in Orbit. Aerospace Corp. TDR-169 (3530-20) TN-1, (January 1963).

4. Dole, S. H. Design Criteria for Rotating Space Vehicles. Rand Corp. RM-2668 (October 1960).

5. Etkin, B. Dynamics of Flight. John Wiley & Sons (1959).

6. Frick, R. H. Optimum Stress Design of a Rotating Wire Antenna. The Rand Corp. RM-2640-ARPA, (27 September 1960).

7. Frick, R. H., and T. B. Garber General Equations of Motion of a Satellite in a Gravitational Gradient Field. Rand Corp. RM-2527, (December 1959).

8. Garber, T. B. The Precession of Spinning Bodies Due to Gravitational Gradient Torques. Rand Corp. RM-3191-PR,(June 1962).

9. Garber, T. B. A Preliminary Investigation of the Motion of a Long, Flexible Wire in Orbit. Rand Corp. RM-2705-ARPA, (March 1961).

10. Goldstein, H. Classical Mechanics. Addison-Wesley Publishing Company, (March 1956).

11. Grantham, W. D. Effects of Mass-Loading Variations and Applied Moments on Motion and Control of a Manned Rotating Space Vehicle. NASA TN D-803 (May 1961).

12. Isakson, G. Flight Simulation of Orbital and Re-entry Vehicles, Part I, Development of Equations of Motion in Six Degrees of Freedom. ASD Tech. Report 61-171 (I), (October 1961).

13. Jarmolow, K. Dynamics of a Spinning Rocket with Varying Inertia and Applied Moment. Journal Applied Physics. Vol. 28, No. 3, (March 1957).

14. Kuebler, M. E. Gyroscopic Motion of an Unsymmetric Satellite Under No External Forces. NASA, TND-596, (December 1960).

15. Kurzenberger, J. L. and J. H. Deh Lynch, Motion and Stability of a Rotating Dumbbell-Shaped Satellite Under the Influence of a Gravity Gradient Moment. Air Force Institute of Technology, WPAFB, (August 1963).

16. Kurzhals, P. R., and C. R. Keckler Spin Dynamics of Manned Space Stations. NASA TR R-155 (1963).

17. Leon, H. I. Spin Dynamics of Rockets, and Space Vehicles in Vacuum. Space Tech. Labs. Inc., (September 1959).

18. Loh, M. M. H. Vibration Modes of Radial and Hexagonal Space Stations. NAA, SID 63-256.

19. Loret, B. J., Optimization of Manned Orbital Satellite Vehicle Designs with Respect to Artificial Gravity, ASD, TR-61-688, USAF, Wright-Patterson AFB (December 1961)

20. MacMillan, W. D. Theoretical Mechanics - Dynamics of Rigid Bodies. Dover Publications Inc., (1936).

21. Manned Orbital Space Station - Stabilization and Control System Analysis and Design. NAA, SID 63-36-3.

22. Martz, C. W. Method for Approximating the Vacuum Motions of Spinning Symmetrical Bodies with Nonconstant Spin Rates. NASA TR-R-115, (1961).

23. Moran, J. P. The Effects of Plane Librations on the Orbital Motion of a Dumbbell Satellite. TAR-TN 603 Therm Advanced Research, N. Y., (August 1960).

24. Ordway, D. E. The Two-Dimensional Dumbbell Satellite. NAS-ARDC Special Study at Woods Hole, Mass. COMI-T25, (August 1958).

25. Paul, B. Planar Librations of an Extensible Dumbbell Satellite. AIAA Journal, Vol. 1, No. 2 (February 1963).

26. Reiger, Siegfried. Long Distance Communication via Reflection from Orbiting Long Wires. The Rand Corp. RM-2639-ARPA (February 1961).

27. Robinson, A. C. On the Three-Dimensional Librations of a Dumbbell-Shaped Satellite Over An Oblate Earth. WCLJY Internal Memo 58-54 WPAFB, Ohio (September 1948).

28. Roberson, R. E. Attitude Control of a Satellite Vehicle, An Outline of the Problems. 8th International Astronautical Congress, Barcelona, Spain, ARS Paper 485-57 (October 1957).

29. Routh, E. J. Advanced Dynamics of a System of Rigid Bodies. 6th ed., The Macmillan Book Co., London (1905), Reprinted by Dover.

30. Slager, Ursula T., Space Medicine, Prentice-Hall (1962)

31. Suddath, J. H. A Theoretical Study of the Angular Motions of Spinning Bodies in Space. NASA-TR-R83 (1961).

32. Tai, C. L. and M. M. H. Loh. Analysis of Free Vibration of Elastic Space Station of the Radial Element Configuration. NAA, SID 63-992.

33. Thomson, W. T. Introduction to Space Dynamics. John Wiley & Sons, N. Y. (1961).

34. Tiller, Perry R., Rotational Effects and Simulation, AIAA, 1963 Los Angeles Summer Meeting, No. 63-169.

35. Methods for the Control of Satellite and Space Vehicles. Edited by R. E. Roberson, WADD Tech Report 60-643.

36. Webster, A. G. The Dynamics of Particles. 2nd ed. B. G. Teubner, Leipsig, (1912), Reprinted by Dover Publications.

APPENDIX A

CONTROL FORCES ON THE CABLE-CONNECTED SPACE STATION

When control forces are introduced, the change in generalized force, ΔQ_j, caused by control effects, must be added to the right side of equations (176) to (180). The derivation of the components of ΔQ_j is presented below. For this purpose, some notation is added here (Figure A-1): x and y are inertial coordinates; $\bar{i}_3$ and $\bar{j}_3$ is the moving coordinate frame with an origin that passes through the center of mass of the system (m_1, m_2, and cable).

The coordinate system x_1, y_1 is determined by the slope of the cable at m_1, x_1 being parallel to the cable. Similarly x_2 and y_2 are determined at the point where mass m_2 is attached.

Control forces F_{x1}, F_{x2}, F_{y1}, F_{y2} and couples N, and N_2 are shown. Some of these are arbitrary, and different combinations have been used.

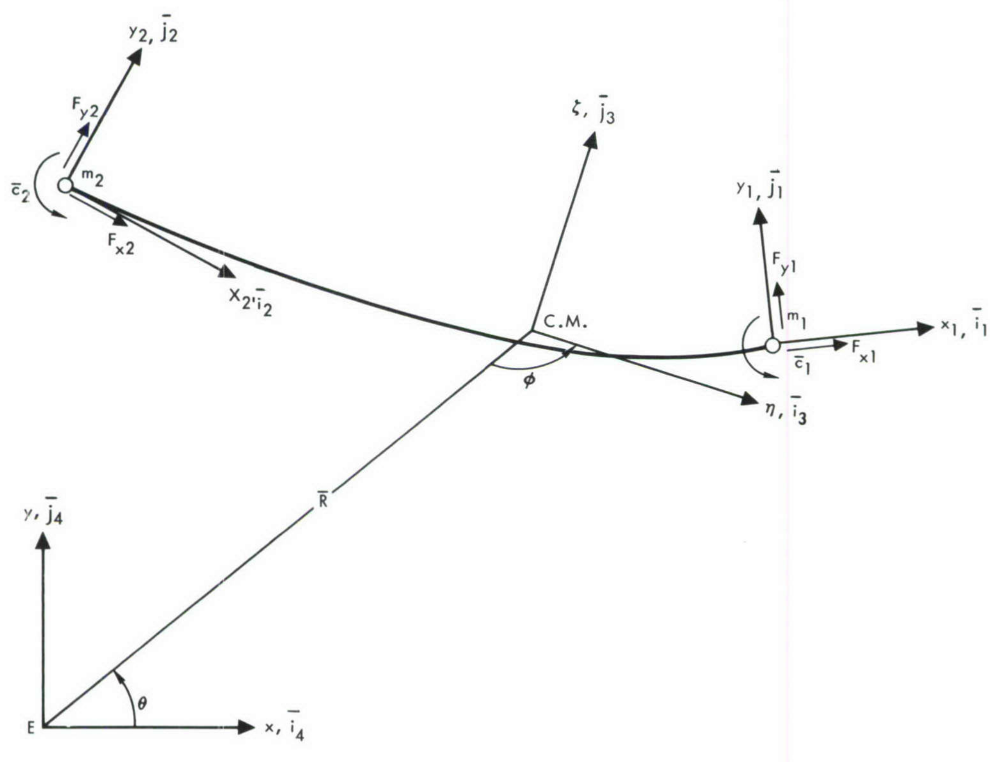

Figure A-1. Moving Coordinate Frame Through the Center of Mass of a Compartment-Cable Counterweight System

Using the relationships for inertial virtual displacements given in Section 8.0, the change in virtual work, caused by control forces and couples is given by equation (A-1) with the following shorthand notations:

$$C_o = \cos(\theta + \phi)$$

$$S_o = \sin(\theta + \phi)$$

$$S_1 = \sin(\theta + \phi + \Theta_1)$$

$$C_1 = \cos(\theta + \phi + \Theta_1)$$

$$S_2 = \sin(\theta + \phi + \Theta_2)$$

$$C_2 = \cos(\theta + \phi + \Theta_2)$$

and

$$\Theta_1 = \tan^{-1}\left(\frac{d\zeta}{d\eta}\right)_{\eta=\ell_1}$$

$$\Theta_2 = \tan^{-1}\left(\frac{d\zeta}{d\eta}\right)_{\eta=-\ell_2}$$

The equations are

$$\Delta \Sigma Q_j \,\delta q_j = [-F_{x1} C_1 + F_{y1} S_1] \left[\delta r \left(-\frac{\ell_1}{r_o} C_o\right) + S_o \Sigma \phi_n (\ell_1)\,\delta q_n\right.$$

$$+ \delta R \cos\phi + \delta\theta \left(\frac{\ell_1}{r_o} \; r\, S_o + \zeta_1 C_o - R \sin\theta\right)$$

$$\left. + \delta\phi \left(\frac{\ell_1}{r_o} r\, S_o + \zeta_1 C_o\right)\right] + [-F_{x2} C_2$$

$$+ F_{y2} S_2] \left[\delta r \frac{\ell_2}{r_o} C_o + S_o \Sigma \phi_n (-\ell_2)\,\delta q_n + \delta R \cos\theta\right.$$

$$+ \delta\theta \left(- \frac{\ell_2}{r_o} r S_o + \zeta_2 C_o - R \sin\theta\right) + \delta\phi \left(- \frac{\ell_2}{r_o} r S_o\right.$$

$$\left.\left. + \zeta_2 C_o\right)\right] + [- F_{x1} S_1 - F_{y1} C_1] \left[- \delta r \frac{\ell_1}{r_o} S_o\right.$$

$$- C_o \Sigma \phi_n (\ell_1) \delta q_n + \delta R \sin\theta + \delta\theta \left(- \frac{\ell_1}{r_o} r C_o + \zeta_1 S_o\right.$$

$$\left.\left. + R \cos\theta\right) + \delta\phi \left(- \frac{\ell_1}{r_o} r C_o + \zeta_1 S_o\right)\right] + [-F_{x2} S_2$$

$$- F_{y2} C_2] \left[\delta r \frac{\ell_2}{r_o} S_o - C_o \Sigma \phi_n (-\ell_2) \delta q_n + \delta R \sin\theta\right.$$

$$+ \delta\theta \left(\frac{\ell_2}{r_o} r C_o + \zeta_2 S_o + R \cos\theta\right) + S\phi \left(\frac{\ell_2}{r_o} r C_o\right.$$

$$\left.\left. + \zeta_2 S_o\right)\right] + N_1 \left[\delta\theta + \delta_\phi + \frac{\Sigma \phi'_n (\ell_1) \delta q_n}{1 + \left(\Sigma_n \phi'_n (\ell_1) q_n\right)^2}\right]$$

$$+ N_2 \left[\delta\theta + \delta\phi + \frac{\Sigma \phi'_n (-\ell_2) \delta q_n}{1 + \left(\Sigma \phi'_n (-\ell_2) q_n\right)^2}\right] \tag{A-1}$$

as before

$$\zeta = \Sigma \phi_n (\eta) q_n (t)$$

$$\phi'_n = \frac{d \phi_n}{d \eta}$$

Because of the definition of Θ, equation (A-1) reflects the facts that

$$\delta \Theta = \frac{\delta \left(\frac{d\zeta}{d\eta}\right)}{1 + \left(\frac{d\zeta}{d\eta}\right)^2} = \frac{\delta (\Sigma \phi'_n q_n)}{1 + (\Sigma \phi'_n q_n)^2}, \quad \delta \Theta = \frac{\Sigma \phi'_n \delta q_n}{1 + (\Sigma \phi'_n q_n)^2} \tag{A-2}$$

Equation (A-1) is easily reduced to equation (A-3).

$$\Delta(\Sigma Q_j\,\delta q_j) = +\,\delta R\,[-F_{x1}\cos(\phi+\Theta_1)+F_{y1}\sin(\phi+\Theta_1)-F_{x2}\cos(\phi+\Theta_2)$$

$$+F_{y2}\sin(\phi+\Theta_2)] + \delta\theta\left[F_{x1}\frac{\ell_1}{r_o}\,r\sin\Theta_1+F_{y1}\frac{\ell_1}{r_o}\,r\cos\Theta_1\right.$$

$$-F_{x2}\frac{\ell_2}{r_o}\,r\sin\Theta_2-F_{y2}\frac{\ell_2}{r_o}\,r\cos\Theta_2+N_1+N_2$$

$$-F_{x1}\zeta_1\cos\Theta_1+F_{y1}\zeta_1\sin\Theta_1-F_{x2}\zeta_2\cos\Theta_2$$

$$+F_{y2}\zeta_2\sin\Theta_2-F_{x1}R\sin(\phi+\Theta_1)-F_{y1}R\cos(\phi+\Theta_1)$$

$$\left.-F_{x2}R\sin(\phi+\Theta_2)-F_{y2}R\cos(\phi+\Theta_2)\right]+\delta r\left[F_{x1}\frac{\ell_1}{r_o}\cos\Theta_1\right.$$

$$\left.-F_{y1}\frac{\ell_1}{r_o}\sin\Theta_1-F_{x2}\frac{\ell_2}{r_o}\cos\Theta_2+F_{y2}\frac{\ell_2}{r_o}\sin\Theta_2\right]$$

$$+\,\delta\phi\left[F_{x1}\frac{\ell_1}{r_o}\,r\sin\Theta_1+F_{y1}\frac{\ell_1}{r_o}\,r\cos\Theta_1-F_{x2}\frac{\ell_2}{r_o}\,r\sin\Theta_2\right.$$

$$-F_{y2}\frac{\ell_2}{r_o}\,r\cos\Theta_2-F_{x1}\zeta_1\cos\Theta_1+F_{y1}\zeta_1\sin\Theta_1$$

$$\left.-F_{x2}\zeta_2\cos\Theta_2+F_{y2}\zeta_2\sin\Theta_2+N_1+N_2\right]$$

$$+\,\delta q_n\left[\phi_n(\ell_1)(F_{x1}\sin\Theta_1+F_{y1}\cos\Theta_1)+(F_{x2}\sin\Theta_2\right.$$

$$+F_{y2}\cos\Theta_2)\,\phi_n(-\ell_2)+\frac{N_1\,\phi'_n(\ell_1)}{1+\left(\Sigma\,\phi'_n(\ell_1)\,q_n\right)^2}$$

$$\left.+\frac{N_2\,\phi'_n(-\ell_2)}{1+\left(\Sigma\,\phi'_n(-\ell_2)\,q_n\right)^2}\right] \qquad (n = 1,\ 2,\ \ldots n). \qquad \text{(A-3)}$$

The bracketed terms are the changes in generalized forces that must be added to show the effects of control couples and forces.

It is now necessary to determine the control forces and couples. These forces and couples are resolved along inertial axes x and y to give the total force and total couple acting on the system.

$$F_x = - F_{x1}^{(c)} C_1 - F_{x2}^{(c)} C_2 + F_{y1}^{(c)} S_1 + F_{y2}^{(c)} S_2 \qquad \text{(A-4)}$$

$$F_y = - F_{y1}^{(c)} C_1 - F_{y2}^{(c)} C_2 - F_{x1}^{(c)} S_1 - F_{x2}^{(c)} S_2 \qquad \text{(A-5)}$$

$$\begin{aligned} N = {} & N_1^{(c)} + N_2^{(c)} + \ell_1 \left(F_{x1}^{(c)} \sin \Theta_1 + F_{y1}^{(c)} \cos \Theta_1\right) \\ & - \zeta_1 \left(F_{x1}^{(c)} \cos \Theta_1 - F_{y1}^{(c)} \sin \Theta_1 \right) \\ & - \ell_2 \left(F_{x2}^{(c)} \sin \Theta_2 + F_{y2}^{(c)} \cos \Theta_2\right) \\ & - \zeta_2 \left(F_{x2}^{(c)} \cos \Theta_2 - F_{y2}^{(c)} \sin \Theta_2 \right) \end{aligned} \qquad \text{(A-6)}$$

The superscript c represents computed values that differ from the actual control forces (F, previously given) according to the equation

$$F + \tau \dot{F} = \kappa F^{(c)} \qquad \text{(A-7)}$$

where τ is the time constant and κ is not quite 1. 000.

F_x, F_y, and N are computed from measured deviations from the standard trajectory and desired attitude, thus:

$$F_x = C_x \Delta x + C_{\dot{x}} \Delta \dot{x} + C_{\Delta x} \int dx \qquad \text{(A-8)}$$

$$F_y = C_y \Delta y + C_{\dot{y}} \Delta \dot{y} + C \Delta y \int dy \qquad \text{(A-9)}$$

$$N = C_\beta d\beta + C_{\dot{\beta}} d\dot{\beta} + C_{\Delta\psi} \int d\beta \qquad \text{(A-10)}$$

where the deviations from the predicted (p) standard trajectory

$$\Delta x = x - x^{(p)}$$

$$\Delta y = y - y^{(p)}$$

$$\beta = (\theta + \phi + \Theta) - (\theta + \phi + \Theta)^{(p)}$$

are discussed later in this section. Study might reveal that some of the gain constants (c) in these equations can be zero.

Two of the control forces and one of the control moments in equations (A-4, (A-5), and (A-6) are arbitrary. Because it is desired to investigate different combinations, the following may be used:

$$F_{x2}^{(c)} = f_6 F_{x1}^{(c)} + f_7 \tag{A-11}$$

$$F_{y2}^{(c)} = f_8 F_{y1}^{(c)} + f_9 \tag{A-12}$$

$$N_2^{(c)} = f_{10} N_1^{(c)} + f_{11} \tag{A-13}$$

where f_6, f_7, . . . f_{11} are numerical constants.

Substitution of the latter three equations and neglect of small order terms gives

$$F_x = - F_{x1}^{(c)} \left(C_1^{(s)} + f_6 C_2^{(s)}\right) - f_7 C_2^{(s)} + F_{y1} \left(S_1^{(s)} + f_8 S_2^{(s)}\right)$$
$$+ f_9 S_2^{(s)} \tag{A-14}$$

$$F_y = - F_{y1}^{(c)} \left(C_1^{(s)} + f_8 C_2^{(s)}\right) - f_9 C_2^{(s)} - F_{x1} \left(S_1^{(s)} + f_c S_2^{(s)}\right)$$
$$- f_7 S_2^{(s)} \tag{A-15}$$

$$- N = -N_1^{(c)} - f_{10} N_1^{(c)} - f_{11} + \ell_2 f_9 + F_{y1}^{(c)} (\ell_2 f_8 - \ell_1) \tag{A-16}$$

where

$$C_i^{(s)} = \cos (\theta_i + \phi_i + \Theta_i)^{(s)}$$

$$S_i^{(s)} = \sin (\theta_i + \phi_i + \Theta_i)^{(s)}$$

i = 1 or 2, and

$$(\theta_i + \phi_i + \Theta_i)^{(s)}$$

is the sensed or measured value of $(\theta_i + \phi_i + \Theta_i)$.

The actual control forces and couples for the equations of motion previously derived are given by equation (A-7). For example,

$$F_{x1} + \tau_{x1} \dot{F}_{x1} = \kappa_{x1} F_{x1}^{(c)} \tag{A-17}$$

where

τ_{x1} = time constant

κ_{x1} = not quite 1.000.

It is assumed that an "x-axis accelerometer" is mounted on mass m_1, measuring accelerations (minus gravity) along an axis which makes an angle of α_1 measured counterclockwise from axis x_1. A similar assumption is made for the "y-axis accelerometer" with respect to the y_1 axis, and therefore along an axis α_1 counterclockwise from y_1.

For mass m_2 replace subscript 1 by 2.

The inertial acceleration of mass m_1 or m_2 is given from previous work, by

$$\begin{aligned}\bar{a} = \bar{i}_3 \Big\{ & \ddot{\eta} - R\,\dot{\theta}\,\dot{\phi} \cos\phi + \sin\phi\,[-R\ddot{\theta} - \dot{R}\dot{\theta}] + \dot{R}\dot{\phi}\sin\phi - \ddot{R}\cos\phi - \dot{\zeta}\,(\dot{\theta} + \dot{\phi}) \\ & - \zeta\,(\ddot{\theta} + \ddot{\phi}) - (\dot{\theta} + \dot{\phi})\,[\dot{\zeta} + \dot{R}\sin\phi - R\dot{\theta}\cos\phi + \eta\,(\dot{\theta} + \dot{\phi})]\Big\} + \bar{j}_3 \Big\{\ddot{\zeta} \\ & + \ddot{R}\sin\phi + \dot{R}\,\dot{\phi}\cos\phi - \cos\phi\,[\dot{R}\dot{\theta} + R\ddot{\theta}] + R\,\dot{\theta}\,\dot{\phi}\sin\phi + \dot{\eta}\,(\dot{\theta} + \dot{\phi}) \\ & + \eta\,(\ddot{\theta} + \ddot{\phi}) + (\dot{\theta} + \dot{\phi})\,[\dot{\eta} - R\dot{\theta}\sin\phi - \dot{R}\cos\phi - \zeta\,(\dot{\theta} + \dot{\phi})]\Big\}\end{aligned} \tag{A-18}$$

Let us make the definition

$$\bar{a} = a_{3x}\,\bar{i}_3 + a_{3y}\,\bar{j}_3 \tag{A-19}$$

where unit vectors $\bar{i}_3$ and $\bar{j}_3$ correspond to η and ζ axes respectively.

It is necessary to subtract the gravitational acceleration to determine that acceleration which is an input to the accelerometers.

The gravitational acceleration for mass m_1 along inertial axes x and y is given by

$$\ddot{x}_{g1} = -\frac{g_h}{R}\left[-\ell_1 \frac{r}{r_o}\cos(\theta+\phi) + \zeta_1 \sin(\theta+\phi) + R\cos\theta\right] \quad \text{(A-20)}$$

$$\ddot{y}_{g1} = -\frac{g_h}{R}\left[-\ell_1 \frac{r}{r_o}\sin(\theta+\phi) - \zeta_1 \cos(\theta+\phi) + R\sin\theta\right] \quad \text{(A-21)}$$

where g_h is the artificial gravitational acceleration at the orbital height.

In equations (A-20) and (A-21), by replacing ℓ by $-\ell_2$, we have the gravitational acceleration for mass m_2 along the inertia axes. Thus the actual accelerations fed into the x and y accelerometers are

$$a_{xi} = a_{3xi}\cos(\Theta_i + \alpha_i) + a_{3yi}\sin(\Theta_i + \alpha_i) - \ddot{x}_{gi}\cos(\theta + \phi + \Theta_i + \alpha_i)$$
$$- \ddot{y}_{gi}\sin(\theta + \phi + \Theta_i + \alpha_i) \quad \text{(A-22)}$$

$$a_{yi} = a_{3yi}\cos(\Theta_i + \alpha_i) - a_{3xi}\sin(\Theta_i + \alpha_i) + \ddot{x}_{gi}\sin(\theta + \phi + \Theta_i + \alpha_i)$$
$$- \ddot{y}_{gi}\cos(\theta + \phi + \Theta_i + \alpha_i) \quad \text{(A-23)}$$

Subscript i is either 1 or 2, corresponding to m_1 or m_2.

The actual acceleration sensed $a_{xi}^{(s)}$ is given by

$$a_{xi}^{(s)} + \tau_{ai}\,\dot{a}_{xi}^{(s)} = \kappa_{ai}\,a_{xi} \quad \text{(A-24)}$$

This is similar for the y instrument. Again, τ is the time constant and κ is not quite 1.000.

The measured inertial components of acceleration (minus gravity) are given by

$$\ddot{x}_{ai} = a_{xi}^{(s)}\cos\left[(\theta + \phi + \Theta_i)^{(s)} + \alpha_i\right] - a_{yi}^{(s)}\sin\left[(\theta + \phi + \Theta_i)^{(s)} + \alpha_i\right]$$
(A-25)

$$\ddot{y}_{ai} = a_{yi}^{(s)}\cos\left[(\theta + \phi + \Theta_i)^{(s)} + \alpha_i\right] + a_{xi}\sin\left[(\theta + \phi + \Theta_i)^{(s)} + \alpha_i\right]$$
(A-26)

To obtain Δx and Δy computed values of gravitational acceleration have to be added.

The gravitational acceleration components (along the inertial axes) that are "to be computed" for mass m_1 are (using equations A-20 and A-21).

$$\ddot{x}_{g1}^{(tbc)} = \frac{g_h \ell_1}{R_o} \cos\left[(\theta + \phi + \Theta_i)^{(s)} - \Theta_1^{(p)}\right] - g_h \cos\theta^{(p)} \qquad \text{(A-27)}$$

$$\ddot{y}_{g1}^{(tbc)} = \frac{g_h \ell_1}{R_o} \sin\left[(\theta + \phi + \Theta_1)^{(s)} - \Theta_1^{(p)}\right] - g_h \sin\theta^{(p)} \qquad \text{(A-28)}$$

For mass m_2, replace subscript 1 by 2 and ℓ_1 by $-\ell_2$.

The superscript (p) indicates the predicted value.

The "actual computed" values are related to the inputs or "to-be-computed" values by

$$\ddot{x}_{g1}^{(ac)} + \tau_g \ddot{x}_{g1}^{(ac)} = \kappa_g \ddot{x}_{g1}^{(tbc)} \qquad \text{(A-29)}$$

etc.

We are now in a position to evaluate Δx and Δy.

$$\Delta x = f_1 \iint \ddot{x}_{a1} + (1 - f_1) \iint \ddot{x}_{a2} + f_1 \iint \ddot{x}_{g1}^{(ac)}$$

$$+ (1 - f_1) \iint \ddot{x}_{g2}^{(ac)} - x^{(p)} \qquad \text{(A-30)}$$

$$\Delta y = f_2 \iint \ddot{y}_{a1} + (1 - f_2) \iint \ddot{y}_{a2} + f_2 \iint \ddot{y}_{g1}^{(ac)} \qquad \text{(A-31)}$$

$$+ (1 - F_2) \iint \ddot{y}_{g2}^{(ac)} - y^{(p)}$$

Superscript (p) again refers to predicted value corresponding to a standard "trajectory."

f_1 and f_2 are weighting values to be optimized.

$\boldsymbol{\beta}$ is given by

$$\boldsymbol{\beta} = f_3 (\theta + \phi + \Theta_1)^{(s)} + (1 - f_3)(\theta + \phi + \Theta_2)^{(s)}$$

$$- f_3 (\theta + \phi + \Theta_1)^{(p)} - (1 - f_3)(\theta + \phi + \Theta_2)^{(p)} \qquad \text{(A-32)}$$

The calculations are now complete.

APPENDIX B

DEPLOYMENT OF A CABLE-CONNECTED COMPARTMENT AND COUNTER-WEIGHT SPACE STATION

Prior to the deploying operation, the cable is assumed to be wrapped around the cylindrical compartment in the neighborhood of the centroidal cross section of the compartment with the counterweight attached at the free end, and the system is assumed to have an initial spin Ω_o. The weight of the cable is neglected in this analysis. In the case where there is no external force acting on the system during deployment, the center of gravity of the system remains stationary. We attach a set of rotating unit vectors, $\bar{i}$, $\bar{j}$, $\bar{k}$ at the center of gravity of the system with $\bar{i}$ parallel to the deployed portion of the cable and with $\bar{k}$ parallel to the axis of rotation. Deployment of a cable-connected counterweight configuration is shown in Figure B-1.

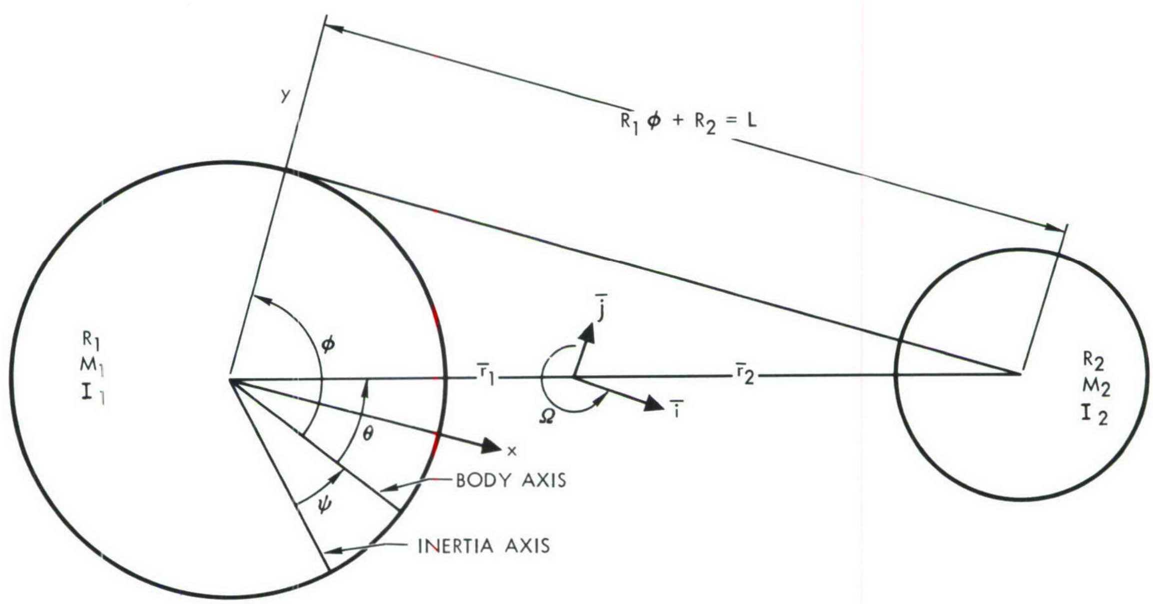

Figure B-1. Deployment of a Cable-Connected Counterweight

Designating the rotation of the system by Ω, it is observed from the above figure that

$$\text{rotation of } M_1 = (\Omega - \dot{\theta})\,\overline{k}$$

$$\text{rotation of } M_2 = (\Omega - \dot{\theta} + \dot{\phi})\,\overline{k}$$

$$\text{rotation of } \overline{ijk} = (\Omega)\overline{k} \qquad \text{(B-1)}$$

Let R_1, M_1, I_1, R_2, M_2, and I_2 represent the radius, mass, and the moment of inertia of the compartment and counterweight, respectively; the positions of M_1 and M_2 are then

$$\overline{r}_1 = -\frac{M_2}{M_1 + M_2}(R_1\,\phi + R_2)\,\overline{i} - \frac{M_2}{M_1 + M_2}R_1\,\overline{j}$$

$$\overline{r}_2 = \frac{M_1}{M_1 + M_2}(R_1\,\phi + R_2)\,\overline{i} + \frac{M_1}{M_1 + M_2}R_1\,\overline{j} \qquad \text{(B-2)}$$

with

$$n_1 = \frac{M_1}{M_1 + M_2}, \qquad n_2 = \frac{M_2}{M_1 + M_2} \qquad \text{(B-3)}$$

the velocities are

$$\overline{v}_1 = \dot{\overline{r}}_1 + (\Omega - \dot{\theta} + \dot{\phi})\,\overline{k} \times \overline{r}_1 = n_2\,[R_1\,(\Omega - \dot{\theta})]\,\overline{i}$$

$$- n_2\,[(R_1\,\phi + R_2)\,(\Omega - \dot{\theta} + \dot{\phi})]\,\overline{j}$$

$$\overline{v}_2 = \dot{\overline{r}}_2 + (\Omega - \dot{\theta} + \dot{\phi})\,\overline{k} \times \overline{r}_2 = n_1\,[-\,R_1\,(\Omega - \dot{\theta})]\,\overline{i}$$

$$+ n_1\,[(R_1\,\phi + R_2)\,(\Omega - \dot{\theta} + \dot{\phi})]\,\overline{j} \qquad \text{(B-4)}$$

The total kinetic energy T of the system is

$$2T = I_1 (\Omega - \dot{\theta})^2 + I_2 (\Omega - \dot{\theta} + \dot{\phi})^2 + M_1 \bar{v}_1 \cdot \bar{v}_1 + M_2 \bar{v}_2 \cdot \bar{v}_2$$

$$= I_1 (\Omega - \dot{\theta})^2 + I_2 (\Omega - \dot{\theta} + \dot{\phi})^2 + \left(M_1 n_2^2 + M_2 n_1^2\right) \left[R_1^2 (\Omega - \dot{\theta})^2 + (R_1 \phi + R_2)^2 (\Omega - \dot{\theta} + \dot{\phi})^2 \right] \quad \text{(B-5)}$$

The total angular momentum of the system is

$$H\bar{k} = \bar{k} \{I_1 (\Omega - \dot{\theta}) + I_2 (\Omega - \dot{\theta} + \dot{\phi})\} + \bar{r}_1 \times M_1 \bar{v}_1 + \bar{r}_2 \times M_1 \bar{v}_2$$

$$= \left\{ I_1 (\Omega - \dot{\theta}) + I_2 (\Omega - \dot{\theta} + \dot{\phi}) + \left(M_1 n_2^2 + M_2 n_1^2\right) \left[(R_1 \phi + R_2)^2 (\Omega - \dot{\theta} + \dot{\phi}) + R_1^2 (\Omega - \dot{\theta}) \right] \right\} \bar{k} \quad \text{(B-6)}$$

The system has no external forces, and assuming there is no dissipation of energy, the kinetic energy and angular momentum must remain constant and equal to their initial values.

At $t = 0$

$$2T_{t=0} = \left[I_1 + I_2 + M_1 n_2^2 (R_1 + R_2)^2 + M_2 n_1^2 (R_1 + R_2)^2 \right] \Omega_0^2$$

$$= \left[I_1 + I_2 + \left(M_1 n_2^2 + M_2 n_1^2\right) (R_1 + R_2)^2 \right] \Omega_0^2 \quad \text{(B-7)}$$

$$H_{t=0} = \left[I_1 + I_2 + M_1 n_2^2 (R_1 + R_2)^2 + M_2 n_1^2 (R_1 + R_2)^2 \right] \Omega_0$$

$$= \left[I_1 + I_2 + \left(M_1 n_2^2 + M_2 n_1^2\right) (R_1 + R_2)^2 \right] \Omega_0 \quad \text{(B-8)}$$

Thus,

$$H = \left[I_1 + I_2 + \left(M_1 n_2^2 + M_2 n_1^2\right) (R_1 + R_2)^2 \right] \Omega_0 = I_1 (\Omega - \dot{\theta}) + I_2 (\Omega - \dot{\theta} + \dot{\phi}) + \left(M_1 n_2^2 + M_2 n_1^2\right) \left[(R_1 \phi + R_2)^2 (\Omega - \dot{\theta} + \dot{\phi}) + R_1^2 (\Omega - \dot{\theta}) \right] \quad \text{(B-9)}$$

$$2T = \left[I_1 + I_2 + \left(M_1 n_2^2 + M_2 n_1^2\right) (R_1 + R_2)^2\right] \Omega_0^2 = I_1 (\Omega - \dot\theta)^2$$

$$+ I_2 (\Omega - \dot\theta + \dot\phi)^2 + \left(M_1 n_2^2 + M_2 n_1^2\right) \left[(R_1 \phi + R_2)^2 (\Omega - \dot\theta\right.$$

$$\left. + \dot\phi)^2 + R_1^2 (\Omega - \dot\theta)^2\right] \tag{B-10}$$

From the equation for H, with the notation,

$$C_1 = \frac{I_1}{M_1 n_2^2 + M_2 n_1^2} \qquad C_2 = \frac{I_2}{M_1 n_2^2 + M_2 n_1^2}$$

$$C_3 = C_1 + C_2 + (R_1 + R_2)^2 \qquad L = R_1 \phi + R_2 \tag{B-11}$$

we get

$$(\Omega - \dot\theta) = \frac{C_3 \Omega_0 - \dot\phi \left[C_2 + L^2\right]}{C_1 + C_2 + R_1^2 + L^2} \tag{B-12}$$

Substituting into the equation of T and simplifying, we have

$$\dot\phi^2 = \frac{C_3 \left[L^2 + R_1^2 - (R_1 + R_2)^2\right]}{\left(C_1 + R_1^2\right) \left(C_2 + L^2\right)} \Omega_0^2 \tag{B-13}$$

The relation between $\dot\theta$ and $\dot\phi$ is established from the geometrical configuration

$$\tan (\phi - \theta) = \frac{R_1 \phi + R_2}{R_1}$$

or

$$(\dot\phi - \dot\theta) = \frac{R_1^2 \dot\phi}{R_1^2 + (R_1 \phi + R_2)^2}$$

Therefore,

$$\dot{\theta} = \dot{\phi} - \frac{R_1^{\,2}\,\dot{\phi}}{R_1^{\,2} + (R_1\,\phi + R_2)^2} = \frac{L^2\,\dot{\phi}}{R_1^{\,2} + L^2} \tag{B-14}$$

Substituting equations (B-13) and (B-14) into (B-12), the spin rate Ω is obtained

$$\Omega = \frac{C_3\left(R_1^{\,2}+L^2\right)\left(C_1+R_1^{\,2}\right)^{\frac{1}{2}}\left(C_2+L^2\right)^{\frac{1}{2}} + \sqrt{C_3}\left(C_1\,L^2 - C_2\,R_1^{\,2}\right)\left[L^2+R_1^{\,2}-(R_1+R_2)^2\right]^{\frac{1}{2}}}{\left(R_1^{\,2}+L^2\right)\left(C_1+C_2+R_1^{\,2}+L^2\right)\left(C_1+R_1^{\,2}\right)^{\frac{1}{2}}\left(C_2+L^2\right)^{\frac{1}{2}}}\,\Omega_0 \tag{B-15}$$

The time required for deployment may be computed from equation (B-13).

$$t = \int_0^{\ell} \frac{d\ell}{R_1\,\dot{\phi}} = \int_0^{\Phi_1} \frac{R_1\,d\phi}{R_1\,\dot{\phi}} = \int_0^{\Phi_1} \frac{d\phi}{\dot{\phi}}$$

$$= \sqrt{\frac{C_1 + R_1^{\,2}}{C_3}}\;\frac{1}{R_1\,\Omega_0}\int_0^{\Phi_1}\sqrt{\frac{(R_1\,\phi + R_2)^2 + C_2}{(R_1\,\phi + R_2)^2 + R_1^{\,2} - (R_1 + R_2)^2}}\;d\,(R_1\,\phi + R_2) \tag{B-16}$$

This is an elliptic integral that may be used to find t (either from tables or by numerical integration).

When the length is large compared with R_1 and R_2, it can easily be seen from equations (B-13) and (B-14) that $\dot{\theta}$ and $\dot{\phi}$ are approximately equal to Ω_0 and Ω approaches zero. After being fully deployed, the compartment tends to wind up in the reversed sense. A jet couple should then be applied to avoid the reverse wind-up and to create a spin of the whole system for artificial gravitation.

With the physical data of the compartment-cable-counterweight configuration (M_1 = 103.52 lb - sec^2/in, M_2 = 12.94 lb - sec^2/in, R_1 = 90 in,

$R_2 = 60$ in, $I_1 = 838,000$ in-lb-sec^2, $I_2 = 31,000$ in-lb-sec^2), the results of calculation are shown in Figure B-2.

A preliminary investigation of the mechanics of deployment of a cable-connected space station has been completed. A clear relationship is shown between the deployed length of the cable and the rotational velocity of the system. An extension of the analysis to include the effect of dissipation of energy during the deployment and the effect of a control couple to avoid the reverse wind-up is suggested for future study. It is also suggested that other deployment procedures and mechanisms be studied.

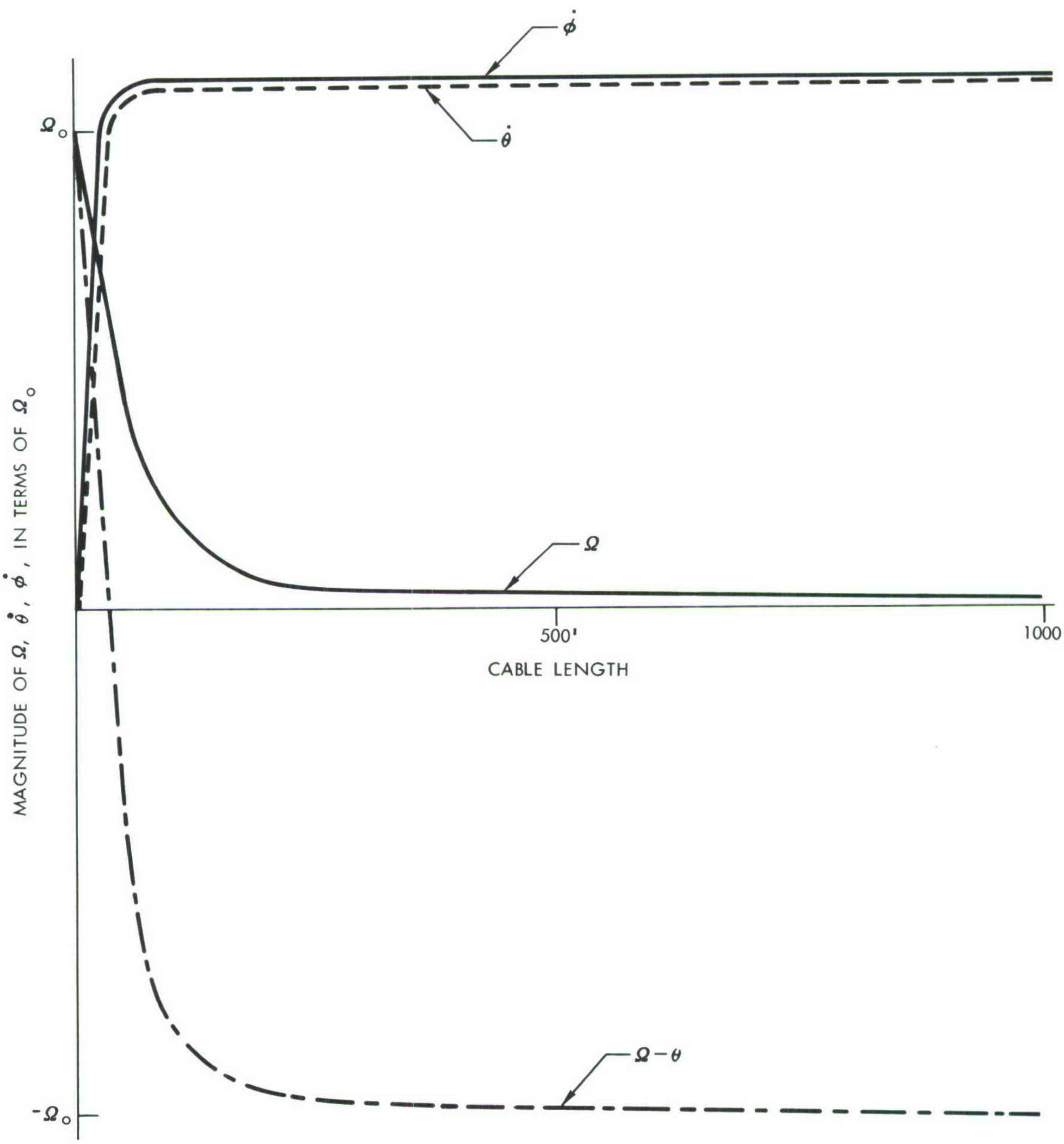

Figure B-2. Deployment of Compartment-Cable-Counter-Weight Configuration

APPENDIX C

HUMAN FACTORS RELATING TO AN ARTIFICIAL GRAVITY ENVIRONMENT

The purpose of a human factors investigation of the rotating space station is to establish conditions that are satisfactory with respect to the effect of the induced gravity environment on the crew. The problem is the creation of a design that will permit the crew to work with comfort, efficiency and safety. Since providing a favorable environment for the human occupants of a space station is the primary justification for creating artificial gravity, it is necessary to ensure that the induced environment does not create more problems than it solves. The psychological, medical, and physiological literature shows many examples of severe discomfort, major decrease in the performance of operators, and sickness which are all produced by experience of unusual gravity environments. However, it appears that there are conditions within the gravity stimuli that may be controlled to avoid undesirable response.

There has been a great deal of discussion regarding the requirement for artificial gravity provisions in a manned space station. To date, there is no conclusive evidence that man can or cannot survive in a weightless environment for extended periods of time. In fact, evidence can be found to support either argument. In reality, the question of artificial gravity provisions should be independent of man's ability to survive in the zero-gravity environment. The real question is what environment should be provided aboard a space station to enable the crew to perform their tasks most effectively. There is no doubt that the artificial-gravity environment is much more convenient for the crew members than the zero-gravity environment. This is not meant to imply that there is no need for a zero gravity environment aboard a space station. Rather it is believed that a fundamental advantage can be achieved if the same vehicle can provide both a zero-gravity and an artificial-gravity environment. The factors associated with the design of a zero-gravity vehicle are fairly well understood; however, the human-factors implications associated with a rotating vehicle; i.e., rotation radius, rotational rate, etc., must be further analyzed in order to conclusively establish these particular design parameters.

Rotation of the vehicle will produce a centrifugal acceleration which is dependent on the rotational speed and the distance from the spin axis. It has been postulated that many of the normal physiological functions will be complicated by weightless environment. Draining of sinus cavities may be reduced which may lead to minor infection; problems may arise concerning food retention and gas accumulation over long term periods; and elimination of body excreta is more complicated in the zero-gravity environment.

Artificial gravity would tend to minimize these problems, if not eliminate them entirely. In the artificial-gravity environment, task performance will not have to be relearned in the sense of compensating for the lack of gravity, as would be necessary in the zero-gravity environment, and experimental capacity is increased. For example, the gravitational acceleration can be altered by varying the rotational rate and, thus, supply pertinent data regarding the artificial gravity level necessary to establish comfort in any given space vehicle.

Rotation is not a cure-all, and there are many problems associated with man being exposed to this type of environment. As is well known, movement of the head while being rotated at a sufficient velocity produces a disturbance in the vestibular apparatus and viscera which often leads to nausea, regurgitation and, in some cases, complete immobilization. In addition, visual and other illusions of body position or motion can be induced by stimuli associated with the rotating system.

There is also the possibility that movement in any direction could cause a pitching sensation during acceleration and deceleration.

The semicircular canals are stimulated by angular accelerations. On earth, the semicircular canals should be stimulated by a Coriolis force each time the head is moved out of the plane of the earth's spin. However, the radius of the earth compared to the size of a man is so large that this force does not stimulate the cristae ampullaris. If the radius of rotation is smaller, rotation of the body in one plane and rotation of the head in another plane will produce stimulation of the semicircular canals. This can occur if a pirouetting ballerina nods her head, if a pilot nods or shakes his head during 3-g to 4-g pullout in an airplane, if a man moves in a rotating room, or tries to walk or move while being spun on a centrifuge. Similar motions occur in a ship rolling or pitching in a high sea, or in an airplane flying through turbulence. Locomotion in a small spinning spacecraft would produce the same effect.

Angular accelerations set up waves in the endolymph which displace the cupola of the cristae ampullaris of the semicircular canals. Stimulation of the semicircular canals produces an involuntary jerky motion of the eyes called nystagmus in which the eye moves slowly in a direction opposite to that of the rotation and then quickly in the same direction as the rotation. Since the eye movement is not felt, the tracking of the visual field across the retina during the slow component is interpreted as motion of the external objects in a direction opposite to that of the eye movement; i. e., in the direction of rotation. The fast component is so rapid that any visual sensations that occur during this period are disregarded. The result is a visual illusion, the oculo-gyral illusion, that an observed object is moving in the direction of the turn. The threshold for stimulation has been reported as 0.12 deg/sec^2 to 0.2 - 2.0 deg/sec^2. As soon as uniform rotation in only

one plane is resumed, the perceived object will return to its original position, or even move slightly in the opposite direction. This latter component of the oculo-gyral illusion is much weaker and is not observed by all subjects. With angular deceleration, the observed object and the cristae will be replaced by two minor pendulous motions. Displacement of the after-image is in a direction opposite to that of the object.

Stimulation of the semicircular canals also produces postural illusions and results in vertigo, a subjective sensation of rotation with respect to the environment. Vertigo can be inhibited by visual stimuli. It is most severe when there are conflicting stimuli, such as in the cabin of a tossing ship or plane, where vision suggests rest while vestibular stimuli suggest violent motion. Such a conflict also occurs in a spinning space cabin where turning of the head stimulates the semicircular canals and produces a sensation of tilt while vision, kinesthesis, and otoliths suggest no change in the body relation to its environment.

When such conflicting stimuli are severe, motion sickness may result. Motion sickness includes nausea, vomiting, headache, dizziness, prostration, excessive salivation, pallor, sweating, difficulty in walking, oliguria, and mental depression. Motion sickness is known as seasickness, airsickness, or spacesickness, depending on the situation under which it occurs. Since the condition is produced by the stimulation of the semicircular canals, the term canalsickness is often used.

Locomotion in the direction of rotation increases the angular velocity of the man in motion and, therefore, increases the artificial gravity level that he senses. Performance of tasks in a high-induced gravity field will cause unnecessary fatigue and should be avoided. Also, the artificial gravity level can be so low that locomotion is difficult due to the lack of traction. Devices such as hand rails and special shoes can be used as aids but they are, in general, inconvenient and will reduce the comfort and efficiency of the crew. The term locomotive effect is used for these conditions.

Differential accelerations or gravity gradient on the body could produce novel sensations. Since the artificial gravity is a function of distance from the spin axis for a constant rotational rate, a man in a standing position would experience a greater acceleration at his feet than at his head. Motion in the radial direction, as standing up from a reclining position, could add to the confusion of sensory inputs when the gravity gradient is large.

Figure C-1 denotes the human factors design envelope as adopted from the work of Loret[1]. The angular rotation rates, p, and the artificial gravity levels at distance, R_g, from the axis of rotation used in the analyses in this report were selected in such a manner that they bracket the design envelope.

---

1 Reference 19

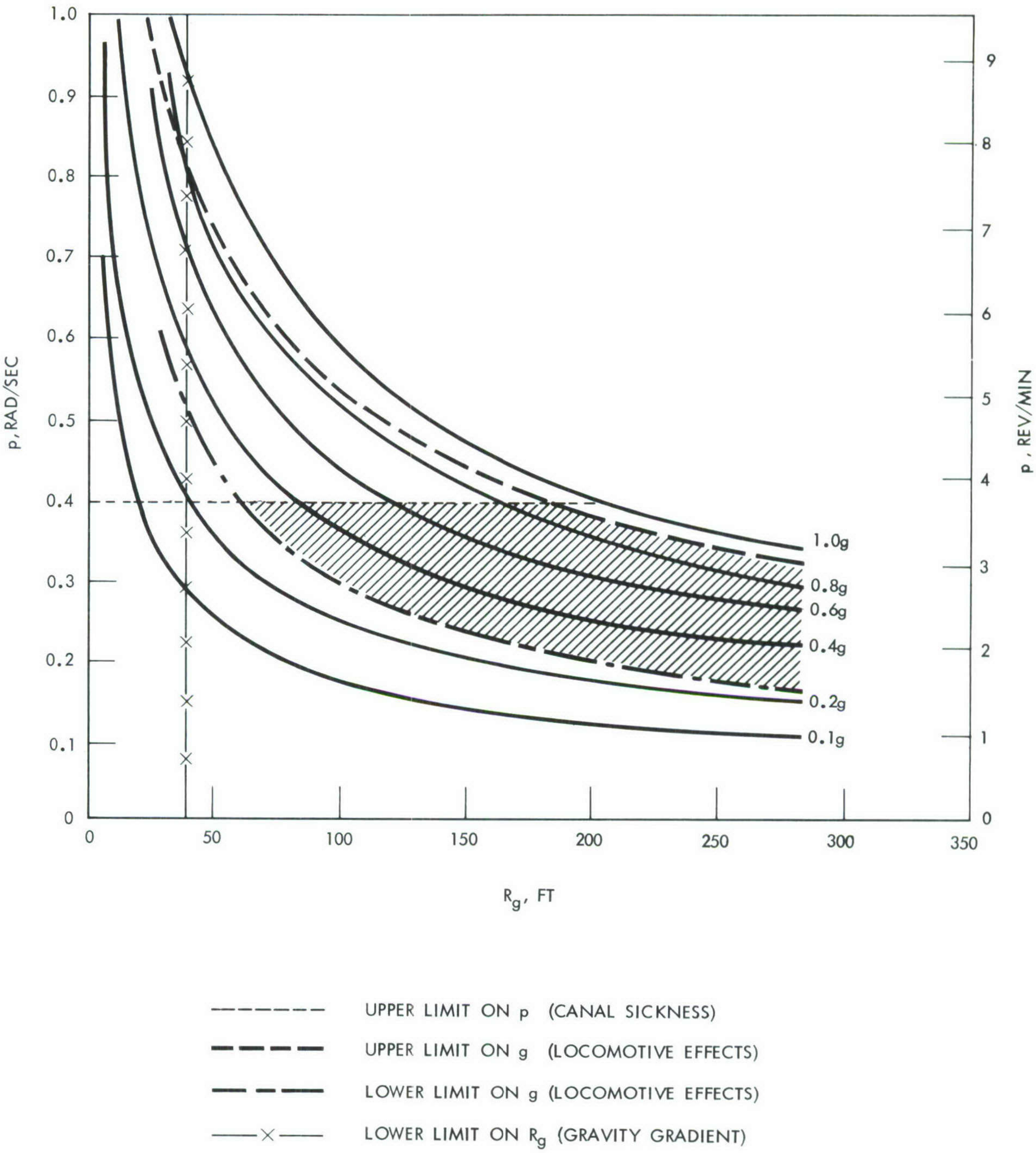

Figure C-1 Human Factors Design Envelope

APPENDIX D

PROGRAM FOR ROTATIONAL STABILITY OF A SPINNING ELASTIC SPACE STATION

An analysis of the rotational stability of a moment-free elastic space station spinning about its axis of maximum moment of inertia is presented in Section 4.3. The motion of the vehicle is described by relations between the nutation angle (depicted in Figure D-1) and the energy dissipation in the fixed-space system. In a finite time interval, the kinetic energy and the angular momentum of the moment-free rotating system are considered to be invariants. The FØRTRAN computer program written for this investigation is described in this appendix.

Figure D-2 depicts the logic of the program. The purpose of the program is to determine the relationship between the nutation angle α and the precession angle λ by step-wise integration of equation (34). This relationship is dependent on the moments of inertia of the vehicle and the energy-dissipation level $\Delta T/T_e$. The maximum and minimum values of the nutation angle α are given by equations (30) and (31), respectively.

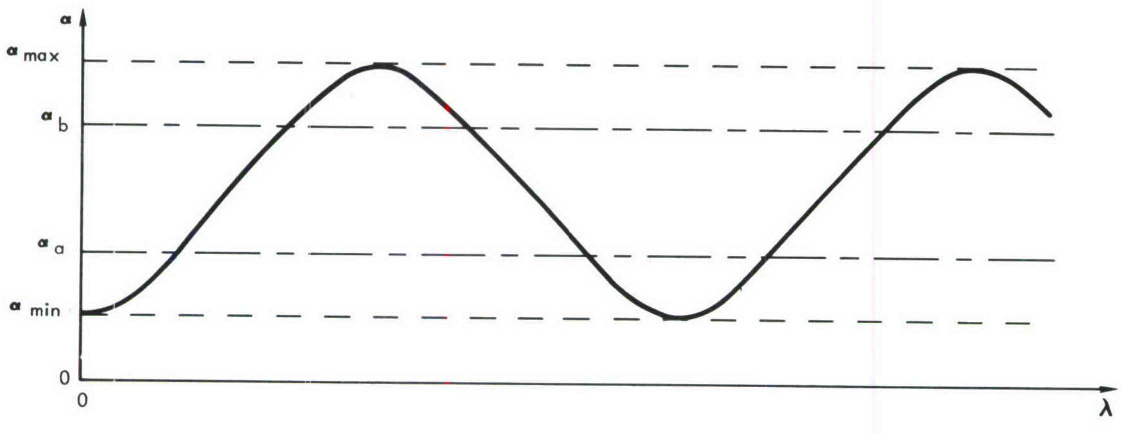

$$\alpha_a = \text{PCT(1)} * (\alpha_{max} - \alpha_{min}) + \alpha_{min}$$

$$\alpha_b = \text{PCT(2)} * (\alpha_{max} - \alpha_{min}) + \alpha_{min}$$

$$\text{PCT(1)} < \text{PCT(2)}$$

Figure D-1. Definition of α_a and α_b

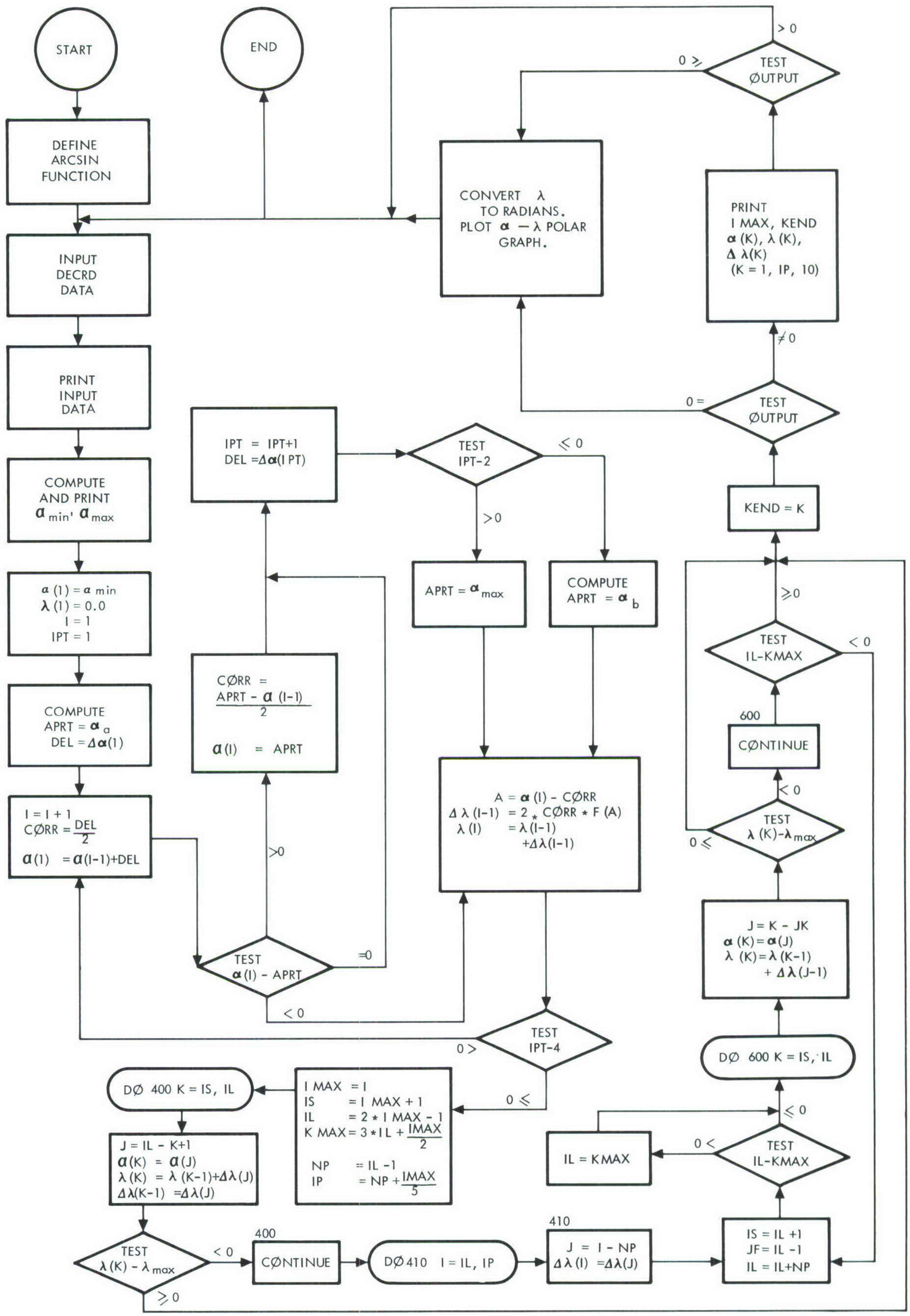

Figure D-2 Rotational Stability Program Logic

In the integration of equation (34), α is the independent variable, λ is the dependent variable, and the current values of the variables are α_i and λ_i. The interval of the next integration step is $\Delta\alpha_i$. Then, $\alpha = \alpha_i + 1/2\Delta\alpha_i$ and $d\alpha = \Delta\alpha_i$ are used in equation (34) to compute $d\lambda = \Delta\lambda_i$. The new values of the variables are thus $\alpha_{i+1} = \alpha_i + \Delta\alpha_i$ and $\lambda_{i+1} = \lambda_i + \Delta\lambda_i$.

Since the upper and lower limits of α are known and α is periodic, only the first half-cycle from α_{min} to α_{max} needs to be computed. The values of α and the corresponding values of $\Delta\lambda$ for the first half-cycle (starting with $\alpha(1) = \alpha_{min}$ and $\lambda(1) = 0.0$) are stored in arrays and are used to determine the coordinate points within successive half-cycles without further evaluation of equation (34).

Figure D-1 shows the relationships of α_a and α_b to α_{min} and to max. The values of PCT are selected by the user. It may become apparent from the results of a run that different integration intervals $\Delta\alpha$ are required within the three ranges of α. User-supplied values of $\Delta\alpha(1)$, $\Delta\alpha(2)$, and $\Delta\alpha(3)$ are used within the ranges α_{min} to α_a, α_a to α_b, and α_b to α_{max}, respectively.

Computations are terminated at λ_{max}, which is supplied by the user or at program-supplied KMAX, depending upon which is encountered first by the program. Upon completion of the computations, the stored values of α and λ are printed and/or plotted on a polar grid, depending upon the user-supplied value for ØUTPUT. Polar graphs are plotted on the S-C 4020 CRT plotter by using a subroutine package that requires the CAMRAV, PGRIDV, PPLØTV, PLABEL, and PLINE subroutines to be called by the program.

The floating-point input data are defined on the sample data sheet. Included on the sample data sheet are the data used to obtain the two polar graphs for Configuration 1-A in Figure 3.

The listing of the FØRTRAN II coded program is also included.

FORTRAN FIXED 10 DIGIT DECIMAL DATA

DECK NO. ______ PROGRAMMER ______ DATE ______ PAGE 1 of 1 JOB NO. ______

Col.		NUMBER	IDENTIFICATION	DESCRIPTION DO NOT KEY PUNCH	
1		1			
13		1.006935		I_x/I_y	RIXY
25		140.8452		I_x/I_z	RIXZ
37		0.0001		$\Delta T/T_e$	RT
49		0.001	73 80	$\Delta\alpha(1)$, degrees	DELTAA(1)
61		0.5	1	$\Delta\alpha(2)$, degrees	DELTAA(2)
1	—	6			
13		0.001		$\Delta\alpha(3)$, degrees	DELTAA(3)
25		0.01		$\%_1$	PCT(1)
37		0.995		$\%_2$	PCT(2)
49		2100.0	73 80	λ_{max}, degrees	BMAX
61		0.0	2	ØUTPUT: 1.0 = Print; 0.0 = CRT; -1.0 = Print & CRT	
1	—	3			
13		0.001		$\Delta T/T_e$	
25					
37					
49			73 80		
61			3		
1					
13					
25					
37					
49			73 80		
61					

Form 114-C-17 Rev. 7-58 (Vellum)

```
C     STABILITY OF SPINNING ELASTIC BODIES
C
C          * INPUT DATA AND CALCULATED VALUES ARE EXPRESSED IN DEGREES
C          * CODING OF VARIABLES
C              * RIXY = IX/IY
C              * RIXZ = IX/IZ
C              * RT = DELTA T/TE
C              * A = ALPHA
C              * B = LAMBDA = DALAMB
C              * DELTAA = DELTA ALPHA
C              * BMAX = LAMBDA MAX
C          * DEFINE THE ARCSIN FUNCTION IN DEGREES
      ASINDF(X) = ATANF(X/SQRTF(1.0 -  X**2))*57.29578
      COMMON RIXY,RIXZ,RT,DELTAA,PCT,BMAX,OUTPUT
      DIMENSION DALAMB(6000), ALPHA(6000), DELB(3500), DELTAA(3),
     X          PCT(2), RIXY(1)
   10 CALL DECRD(RIXY)
      WRITE OUTPUT TAPE 6, 15
   15 FORMAT(1H0,15X,    51H** STABILITY OF SPINNING ELASTIC BODIES IN S
     1PACE **/1H0)
      PRINT 20,RIXY,RIXZ,RT,DELTAA
   20 FORMAT(1H0,5X,10HINPUT DATA//8X, 5HIX/IY,12X,5HIX/IZ,10X,9HDELTAT/
     XTE,7X,14HDELTA ALPHA(3)/(/6E17.8))
   30 FORMAT(/6E17.8)
      PRINT 40,PCT,BMAX
   40 FORMAT(1H0,6X,9HPERCENT 1,7X,9HPERCENT 2,6X,10HLAMBDA MAX//3E17.8)
      WRITE OUTPUT TAPE 6, 50
   50 FORMAT(1H0,5X,17HCALCULATED VALUES//6X,9HALPHA MIN,8X,9HALPHA MAX)
      AMIN = ASINDF(SQRTF(RT/(RIXZ - 1.0)))
      AMAX = ASINDF(SQRTF(RT/(RIXY - 1.0)))
      WRITE OUTPUT TAPE 6, 30, AMIN, AMAX
C
      RANGE = AMAX - AMIN
      ALPHA(1) = AMIN
      DALAMB(1) = 0.0
      I = 1
      IPT = 1
      APRT = PCT(IPT) * RANGE + AMIN
      DEL = DELTAA(IPT)
  100 I=I+1
      CORR = DEL/2.0
      ALPHA(I) = ALPHA(I-1) + DEL
      IF(ALPHA(I) - APRT)160,130,110
  110 CORR= (APRT - ALPHA(I-1))/2.0
      ALPHA(I)=APRT
  130 IPT = IPT + 1
      DEL = DELTAA(IPT)
      IF(IPT - 2)140,140,150
  140 APRT = PCT(IPT) * RANGE  + AMIN
      GO TO 160
  150 APRT = AMAX
  160 A = ALPHA(I) - CORR
      SA2 = SINDF(A)**2
```

```
      CØTA2 = CØSDF(A)**2/SA2
      DELB(I-1) =(1.0 + (1.0 + CØTA2)*RT)* 2.0 * CØRR/SQRTF((RIXZ - 1.-R
     XT/SA2) * (RT -(RIXY-1.)*SA2))
      DALAMB(I)= DALAMB(I-1)+DELB(I-1)
      IF(IPT-4)100,200,200
  200 IMAX = I
      IS = IMAX+1
      IL=2 * IMAX-1
      KMAX= 3 * IL + IMAX/2
      NP = IL -1
      IP=NP + IMAX/5
      DØ 400 K = IS, IL
      J= IL - K +1
      ALPHA(K) = ALPHA(J)
      DALAMB(K)= DALAMB(K-1)+DELB(J)
      DELB(K-1) = DELB(J)
      IF(DALAMB(K)-BMAX)400,700,700
  400 CØNTINUE
      DØ 410 I=IL,IP
      J= I -NP
  410 DELB(I)=DELB(J)
  510 IS = IL+1
      JF = IL-1
      IL = IL+NP
      IF(IL - KMAX)530,530,520
  520 IL=KMAX
  530 DØ 600 K=IS,IL
      J=K-JF
      ALPHA(K) = ALPHA(J)
      DALAMB(K)= DALAMB(K-1)+ DELB(J-1)
      IF(DALAMB(K) - BMAX)600, 700,700
  600 CØNTINUE
      IF(IL-KMAX)510, 700, 700
  700 KEND = K
      IF(ØUTPUT)710, 3000, 710
  710 PRINT 720,IMAX,KEND,(ALPHA(K),DALAMB(K),DELB(K), K=1,IP,10 )
  720 FØRMAT(1H1,5X,6HIMAX =I5,6X,6HKEND =I5//5X,10HALPHA, DEG,7X,11HLAM
     XBDA, DEG,5X,12HDELTA LAMBDA/(/3E17.8))
      IF(ØUTPUT)3000,3000,5000
 3000 CØNTINUE
      AMAX = 5.0*INTF((AMAX + 5.0)/5.0)
      CALL CAMRAV (9)
      CALL PGRIDV(1, AMAX, 5.0, 2, 2, 3, 9, 3, -1)
      CALL PLABEL (10)
      DØ 3020 K = 1, KEND
 3020 DALAMB(K) = DALAMB(K)/57.29578
      CALL PPLØTV(K, ALPHA, DALAMB, 1, 1, -1, 1HX, IERR)
      CALL PLINE( K,ALPHA,DALAMB,1,1,1,IERR)
      CALL PRINTV(-36,36HSTABILITY ØF SPINNING ELASTIC BØDIES,368,1023)
      CALL PRINTV(-50,50HALPHA IS RADIUS                       LAMBDA IS AN
     1GLE,312,0)
      WRITE ØUTPUT TAPE 6, 4910
 4910 FØRMAT(1H0,10X,23H*** CRT ØUTPUT INCLUDED/20X,54HPØLAR GRAPH, ALPH
     1A IS RADIUS AND LAMBDA IS PØLAR ANGLE)
 5000 WRITE ØUTPUT TAPE 6, 5010
 5010 FØRMAT(1H0,5X,11HEND ØF CASE,15X,11HEND ØF CASE,15X,11HEND ØF CASE
     1/ 1H1)
      GØ TØ 10
      END
```

APPENDIX E

PROGRAM FOR LINEARIZED MOMENT EQUATIONS FOR PARTICULAR DISTURBANCES

A linearized analysis of the rigid body angular response of a space station rotating at a constant angular velocity about its axis of maximum moment of inertia is presented in Section 5.0. The FØRTRAN computer program written for this investigation is described in this appendix.

Figure E-1 depicts the logic of the program. The purpose of the program is to determine the angular response of the space station to externally applied moments through the solution of the linearized Euler moment equations (42) and (43). Externally applied moments are expressed as Fourier series in equations (47). Integration of the linearized Euler moment equations is accomplished through the use of Laplace transforms, which results in equations (49) and (50) for the body angular velocities q and r.

Orientation of the space station relative to inertial space is defined by the linearized equations (45), which relate the Euler angles and the body angular velocities. Expressions for the orthogonal wobble angle components θ and ψ are given by equations (51) and (52).

Storage locations are allocated for a maximum of 30 Fourier coefficients for each summation term in the external moments expressions and a maximum of 500 computed points per plotted variable. It should be noted that the Fourier coefficients that are read in as data describe periodic moment functions of unit amplitude; these input data are internally modified by the factors read in at EQUIVALENCE indexes 143 and 144 to obtain the desired moment function amplitudes.

The computed results are printed and/or plotted on rectilinear grids, depending upon the input value of ØUTPUT. Either the variables λ, $\dot{q}$, $\dot{r}$, θ, ψ and t or the variables λ, q, r, θ, ψ, and t are printed (when ØUTPUT $\neq 0$), depending upon the input value of CHECK. The graphs that are plotted when ØUTPUT $\leqslant 0$ are θ - ψ, θ - t, ψ - t, $\dot{\theta}$ - t, $\dot{\psi}$ - t, $\dot{q}$ - t, $\dot{r}$ - t, q - t, r - t, ϕ - t, and λ - t. An M_x - t graph is plotted when $(I_y - I_z) \neq 0$. The M_y - t and M_z - t graphs are also plotted when the input value of SERIES $\geqslant 0$. Dimensions of the printed and plotted output are optionally either in radians or in degrees, depending upon the input value of UNITS.

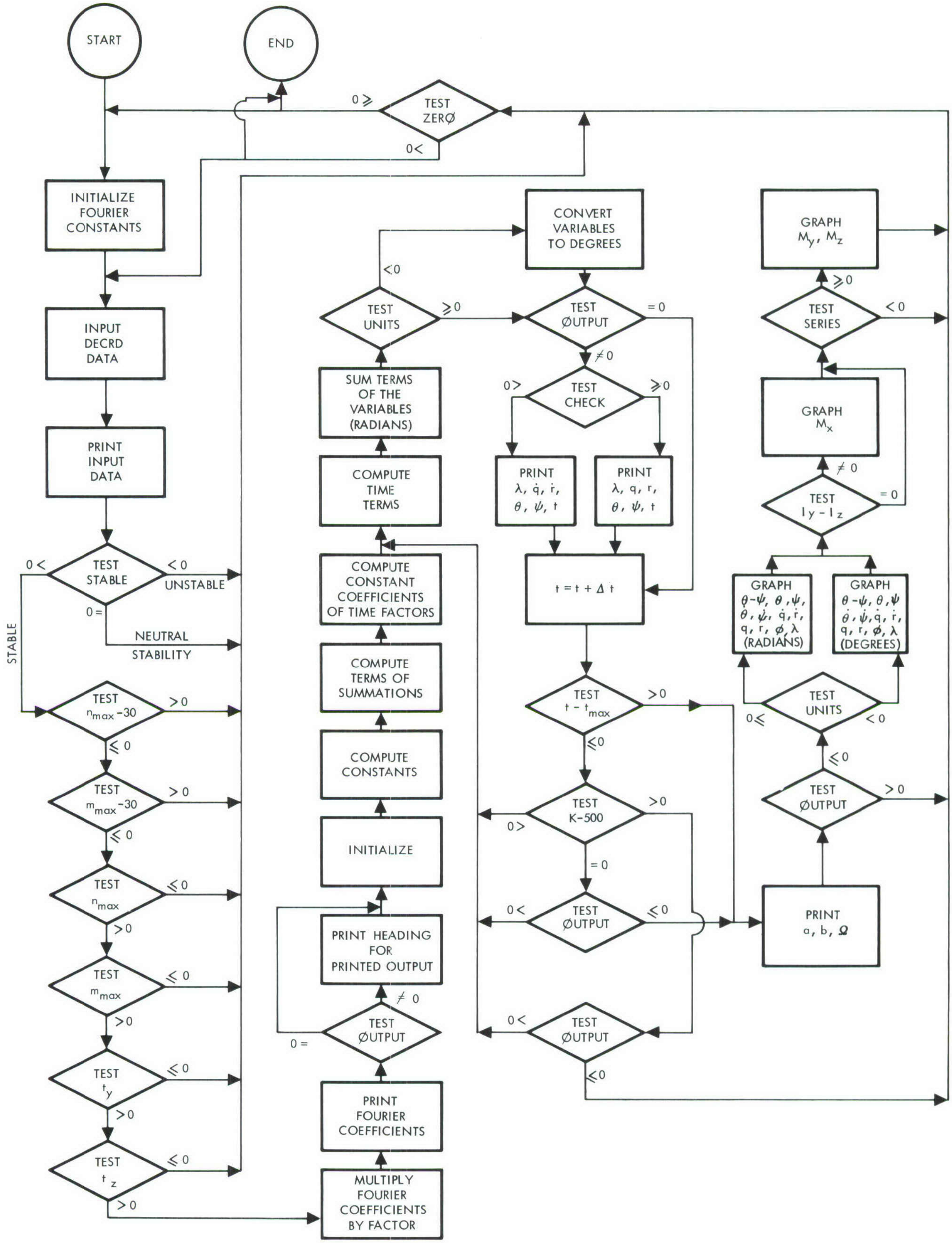

Figure E-1 Linearized Euler Moment Equations Program Logic

Computations are terminated at $t = t_{max}$ (input data) or when the number of points per variable to be plotted equals 500. Upon completion of the computations, the stored values of the variables are plotted (when ϕUTPUT ≤ 0) on the S-C 4020 CRT plotter by using the rectilinear graphing subroutine package GRAPH (S&ID Deck No. 9J - 400).

The floating-point input data are defined on the sample data sheets. Included on the sample data sheets are the data used to obtain the graphs for Configuration Y shown in Figure 15.

The listing of the FϕRTRAN II coded program is also included.

FORTRAN FIXED 10 DIGIT DECIMAL DATA

DECK NO. ________ PROGRAMMER ________ DATE ________ PAGE 1 of 8 JOB NO. ________

Col.	Sign	NUMBER	IDENTIFICATION	DESCRIPTION DO NOT KEY PUNCH	
1		1			
13		0.46332		p_o	= Constant spin rate about x-axis, Radians/second.
25		0.0		q_o	= Angular velocity about y-axis when t = 0, Rad/sec.
37		0.0		r_o	= Angular velocity about z-axis when t = 0, Rad/sec.
49		0.0	73 80	θ_o	Values of Euler angles when t = 0, Radians.
61		0.0	1	ψ_o	(Note: $\phi_o = 0$)
1		6			
13		0.0		t_o	= Initial value of time, seconds
25		0.5		Δt	= Time increment for computations, sec
37		20.0		t_{max}	= Time at which computations are terminated, Sec
49		16.240016	73 80	t_y	= 1/2 (Period of M_y), Sec > 0
61		1.0	2	t_z	= 1/2 (Period of M_z), Sec > 0
1		11			
13		5.52005 E+6		I_x	= Principal moment of inertia about x-axis, Slug-ft^2
25		3.00810 E+6		I_y	= Principal moment of inertia about y-axis, Slug-ft^2
37		3.00814 E+6		I_z	= Principal moment of inertia about z-axis, Slug-ft^2
49		30.0	73 80	n_{max}	= Maximum number of a_y (n) or b_y (n), $0 < n \leq 30$
61		1.0	3	m_{max}	= Maximum number of a_z (m) or b_z (m), $0 < m \leq 30$
1		16			
13		0.0		ØUTPUT:	>0, Print; = 0, CRT; <0, Print & CRT
25	—	1.0		UNITS:	≥ 0, Radians; <0, Degrees
37	—	1.0		CHECK:	≥ 0, Print λ, $\dot{q}$, $\dot{r}$, θ, ψ, t; <0, Print λ, q, r, θ, ψ, t
49		20000.0	73 80	a_{yo}	= 2(Constant term of M_y)
61		0.0	4	a_{zo}	= 2(Constant term of M_z)

Form 114-C-17 Rev. 7-58 (Vellum)

FORTRAN FIXED 10 DIGIT DECIMAL DATA

DECK NO. ______ PROGRAMMER ______ DATE 2 PAGE 8 of ______ JOB NO. ______

		NUMBER	IDENTIFICATION	DESCRIPTION DO NOT KEY PUNCH
1		21		
13		0.63661976		$a_y(n)$, n = 1: Coefficients of $\cos \frac{n\pi t}{t_y}$ in M_y
25		0.0		2
37	–	0.21220659		3
49		0.0	73 80	4
61		0.12732395	5	5
1		26		
13		0.0		$a_y(n)$, n = 6 $M_y = \frac{a_{yo}}{2} + \sum_{n=1}^{N} a_{yn} \cos \frac{n\pi t}{t_y} + \sum_{n=1}^{N} b_{yn} \sin \frac{n\pi t}{t_y}$
25	–	.90945680-1		7
37		0.0		8
49		.70735553-1	73 80	9
61		0.0	6	10
1		31		
13	–	.57874524-1		$a_y(n)$, n = 11
25		0.0		12
37		.48970751-1		13
49		0.0	73 80	14
61	–	.42441318-1	7	15
1		36		
13		0.0		$a_y(n)$, n = 16
25		.37448221-1		17
37		0.0		18
49	–	.33506303-1	73 80	19
61		0.0	8	20

Form 114-C-17 Rev. 7-58 (Vellum)

FORTRAN FIXED 10 DIGIT DECIMAL DATA

DECK NO. ______ PROGRAMMER ______ DATE ______ PAGE 3 of 8 JOB NO. ______

Col.	Sign	NUMBER	IDENTIFICATION	DESCRIPTION DO NOT KEY PUNCH
1		41		
13		.30315227-1		a_y (n), n = 21
25		0.0		22
37	—	.27679120-1		23
49		0.0	73 80	24
61		.25464791-1	9	25
1		46		
13		0.0		a_y (n), n = 26
25	—	.23578510-1		27
37		0.0		28
49		.21952406-1	73 80	29
61		0.0	10	30
1		51		
13		0.0		b_y (n), n = 1 :Coefficients of $\sin\frac{n\pi t}{t_y}$ in M_y
25		0.0		2
37		0.0		3
49		0.0	73 80	4
61			11	5
1		56		
13		0.0		b_y (n), n = 6
25		0.0		7
37		0.0		8
49		0.0	73 80	9
61		0.0	12	10

Form 11l-C-17 Rev. 7-58 (Vellum)

FORTRAN FIXED 10 DIGIT DECIMAL DATA

DECK NO. ______ PROGRAMMER ______ DATE ______ PAGE 4 of 8 JOB NO. ______

	NUMBER	IDENTIFICATION	DESCRIPTION DO NOT KEY PUNCH
1	6 1		
13	0 . 0		b_y (n), n = 11
25	0 . 0		12
37	0 . 0		13
49	0 . 0	73 80	14
61	0 . 0	1 3	15
1	6 6		
13	0 . 0		b_y (n), n = 16
25	0 . 0		17
37	0 . 0		18
49	0 . 0	73 80	19
61	0 . 0	1 4	20
1	7 1		
13	0 . 0		b_y (n), n = 21
25	0 . 0		22
37	0 . 0		23
49	0 . 0	73 80	24
61	0 . 0	1 5	25
1	7 6		
13	0 . 0		b_y (n), n = 26
25	0 . 0		27
37	0 . 0		28
49	0 . 0	73 80	29
61	0 . 0	1 6	30

Form 114-C-17 Rev. 7-58 (Vellum)

FORTRAN FIXED 10 DIGIT DECIMAL DATA

DECK NO. ______ PROGRAMMER ______ DATE ______ PAGE 5 of 8 JOB NO. ______

	NUMBER	IDENTIFICATION	DESCRIPTION DO NOT KEY PUNCH
1	8 1		
13	0 . 0		a_z (m), m = 1 : Coefficient of cos $\frac{m\pi t}{t_z}$ in M_z
25			2
37			3
49		73 80	4
61		1 7	5
1	8 6		
13			a_z (m), m = 6 $M_z = \frac{a_{zo}}{2} + \sum_{m=1}^{M} a_{zm} \cos \frac{m\pi t}{t_z} + \sum_{m=1}^{M} b_{zm} \sin \frac{m\pi t}{t_z}$
25			7
37			8
49		73 80	9
61		1 8	10
1	9 1		
13			a_z (m), m = 11
25			12
37			13
49		73 80	14
61		1 9	15
1	9 6		
13			a_z (m), m = 16
25			17
37			18
49		73 80	19
61		2 0	20

Form 114-C-17 Rev. 7-58 (Vellum)

FORTRAN FIXED 10 DIGIT DECIMAL DATA

DECK NO. ______ PROGRAMMER ______ DATE ______ PAGE 6 of 8 JOB NO. ______

	NUMBER	IDENTIFICATION	DESCRIPTION DO NOT KEY PUNCH
1	1 0 1		
13			a_z (m), m = 21
25			22
37			23
49		73 80	24
61		2 1	25
1	1 0 6		
13			a_z (m), m = 26
25			27
37			28
49		73 80	29
61		2 2	30
1	1 1 1		
13	0 0		b_z (m), m = 1: Coefficient of $\sin \frac{m\pi t}{t_z}$ in M_z
25			2
37			3
49		73 80	4
61		2 3	5
1	1 1 6		
13			b_z (m), m = 6
25			7
37			8
49		73 80	9
61		2 4	10

Form 114-C-17 Rev. 7-58 (Vellum)

FORTRAN FIXED 10 DIGIT DECIMAL DATA

DECK NO. ______ PROGRAMMER ______ DATE ______ PAGE 7 of 8 JOB NO. ______

	NUMBER	IDENTIFICATION	DESCRIPTION DO NOT KEY PUNCH
1	1 2 1		
13			b_z (m), m = 11
25			12
37			13
49		73 80	14
61		2 5	15
1	1 2 6		
13			b_z (m), m = 16
25			17
37			18
49		73 80	19
61		2 6	20
1	1 3 1		
13			b_z (m), m = 21
25			22
37			23
49		73 80	24
61		2 7	25
1	1 3 6		
13			b_z (m), m = 26
25			27
37			28
49		73 80	29
61		2 8	30

Form 114-C-17 Rev. 7-58 (Vellum)

FORTRAN FIXED 10 DIGIT DECIMAL DATA

DECK NO. ______ PROGRAMMER ______ DATE ______ PAGE 8 of 8 JOB NO. ______

	NUMBER	IDENTIFICATION	DESCRIPTION DO NOT KEY PUNCH
1	1 4 1		
13	1 . 0		*ZERØ: ≤ 0, Set Fourier moment coefficients
25			to zero before next data CALL
37			> 0, Let Fourier coefficients remain
49		73 80	unchanged for next data CALL
61		2 9	
1	1 4 2		
13	1 . 0		*SERIES: ≥ 0, Graph Fourier moment series
25			< 0, Do not graph Fourier moment series
37			
49		73 80	
61		3 0	
1	1 4 3		
13	2 0 0 0 0 . 0		*Multiplication factor of input data $a_y(n)$ and $b_y(n)$
25			
37			
49		73 80	
61		3 1	
1	– 1 4 4		
13	0 . 0		*Multiplication factor of input data $a_z(m)$ and $b_z(m)$
25			
37			
49		73 80	
61		3 2	

Form 114-C-17 Rev. 7-58 (Vellum)

```
C      ANGULAR MOTIONS, GENERAL FOURIER Y AND Z BODY MOMENTS
C       ** RIGID BODY ANGULAR MOTIONS OF SPINNING BODIES IN SPACE
C        * CONSTANT SPIN RATE, PO
C        * IX MAY NOT EQUAL IY AND/OR IZ
C        * MY = AYO/2 + AY(N)*COS(N*PI*T/TY) + BY(N)*SIN(N*PI*T/TY)
C        * MZ = AZO/2 + AZ(M)*COS(M*PI*T/TZ) + BZ(M)*SIN(M*PI*T/TZ)
C        * LAMBDA = PSIDOT*THETA/PO
      WRITE OUTPUT TAPE 6, 3
    3 FORMAT(1H0, 10X,   79H** RIGID BODY ANGULAR MOTIONS, GENERAL FOURI
     1ER Y AND Z BODY MOMENTS **          / 1H0)
      WRITE OUTPUT TAPE 6, 4
    4 FORMAT(1H0, 5X, 19HOUTPUT CONTROL DATA// 10X, 23HOUTPUT*  1 = PRIN
     1T ONLY/ 17X, 14H  0 = CRT ONLY/  17X, 24H -1 = BOTH PRINT AND CRT/
     2 10X, 20HUNITS *  1 = RADIANS/ 17X, 13H -1 = DEGREES/ 10X, 47HCHEC
     3K *  1 = PRINT(LAMBDA, Q, R, THETA, PSI, T)/ 17X, 46H -1 = PRINT(L
     4AMBDA, QDOT, RDOT, THETA, PSI, T)/ 10X,  80HZERO  *  1 = LET FOURI
     5ER MOMENT COEFFICIENTS REMAIN UNCHANGED FOR NEXT DATA CALL/ 17X,
     6 66H -1 = SET FOURIER MOMENT COEFFICIENTS TO ZERO BEFORE NEXT DATA
     7CALL/ 10X, 40HSERIES*  1 = GRAPH FOURIER MOMENT SERIES/ 17X ,
     8 40H -1 = DO NOT GRAPH FOURIER MOMENT SERIES)
      WRITE OUTPUT TAPE 6, 5
    5 FORMAT(1H-, 5X, 15HFOURIER MOMENTS// 10X, 56HMY = AYO/2 + AY(N)*CO
     1S(N*PI*T/TY) + BY(N)*SIN(N*PI*T/TY)/ 10X, 56HMZ = AZO/2 + AZ(M)*CO
     2S(M*PI*T/TZ) + BZ(M)*SIN(M*PI*T/TZ)///// 10X, 25HLAMBDA = PSI-DOT*
     3THETA/PO/ 1H1)
      DIMENSION          SN1(30),SN2(30),SN3(30),SN4(30),SN5(30),SM1(30),
     1 SM2(30),SM3(30),SM4(30),SM5(30),AY(30),BY(30),AZ(30),BZ(30)
     2,THETA(500),PSI(500),AT(500),AAMPY(500),AAMPZ(500)
     3 , ATHDOT(500), APSDOT(500), AQDOT(500), ARDOT(500), AQ(500)
     4 , AR(500), APHI(500), ALAMBD(500), AMX(500), EMPTY(10)
      EQUIVALENCE(D(1),PO),(D(2),QO), (D(3),RO),(D(4),THETAO),(D(5),PSIO
     1 ),(D(6),TO),(D(7),DELTAT),(D(8),TMAX),(D(9),TY),(D(10),TZ),(D(11)
     2 ,XI),(D(12),YI),(D(13),ZI),(D(14),ANMAX),(D(15),AMMAX),(D(16),
     3 OUTPUT),(D(17),UNITS),(D(18),CHECK),(D(19),AYO),(D(20),AZO),
     4 (D(21), AY),(D(51), BY),(D(81), AZ), (D(111), BZ) ,(D(141),ZERO)
     5 ,(D(142), SERIES),(D(143), CMY),(D(144), CMZ)
      ANMAX = 1.0
      AMMAX = 1.0
      TY = 1.0
      TZ = 1.0
      DELTAT = 1.0
      TMAX = 2.0
      CMY = 1.0
      CMZ = 1.0
    6 AYO = 0.0
      AZO = 0.0
      DO 7 N=1, 30
      AY(N) = 0.0
      BY(N) = 0.0
      AZ(N) = 0.0
    7 BZ(N) = 0.0
   10 CALL DECRD(D)
      NMAX = ANMAX
```

```
      MMAX = AMMAX
C     PRINT INPUT DATA
      WRITE ØUTPUT TAPE 6, 3
      WRITE ØUTPUT TAPE 6, 20
   20 FØRMAT(1H0, 4X, 10HINPUT DATA//  5X, 11HPØ, RAD/SEC, 6X, 11HQØ, RA
     1D/SEC, 6X, 11HRØ, RAD/SEC, 6X,11HTHETAØ, RAD, 7X, 9HPSIØ, RAD)
      WRITE ØUTPUT TAPE 6,30,PØ,QØ,RØ, THETAØ,PSIØ
   30 FØRMAT(/6E17.8)
      WRITE ØUTPUT TAPE 6, 32
   32 FØRMAT(1H0, 6X,  7HTØ, SEC, 8X,  12HDELTA T, SEC, 6X,10HT MAX, SEC
     1, 4X,14HIX, SLUG-FT**2, 3X, 14HIY, SLUG-FT**2, 3X,14HIZ, SLUG-FT**
     22)
      WRITE ØUTPUT TAPE 6, 30,TØ,DELTAT,TMAX,XI,YI ,ZI
      WRITE ØUTPUT TAPE 6, 33
   33 FØRMAT(1H0, 6X, 7HTY, SEC, 10X,  7HTZ, SEC, 11X, 5HN MAX, 12X,  5H
     1M MAX)
      WRITE ØUTPUT TAPE 6, 30, TY, TZ, ANMAX, AMMAX
      AYØ2 = AYØ/2.0
      AZØ2 = AZØ/2.0
      WRITE ØUTPUT TAPE 6, 34
   34 FØRMAT(1H0, 3X, 12HAYØ/2, FT-LB, 5X, 12HAZØ/2, FT-LB, 2X, 16HAY,BY
     1 MULTIPLIER,1X, 16HAZ,BZ MULTIPLIER)
      WRITE ØUTPUT TAPE 6, 30, AYØ2, AZØ2, CMY, CMZ
      STABLE = (XI - YI)*(XI - ZI)
      IF(STABLE) 41, 44, 47
   41 WRITE ØUTPUT TAPE 6, 42
   42 FØRMAT(1H0,4X,65H** IY LESS THAN IX LESS THAN IZ  ØR  IZ LESS THAN
     1 IX LESS THAN IY/5X,31H * CASE ØF UNSTABLE EQUILIBRIUM/5X,34H * CA
     2SE IS UNCØNDITIØNALLY DELETED)
      GØ TØ 5000
   44 WRITE ØUTPUT TAPE 6, 45
   45 FØRMAT(1H0,4X,42H** IX IS EQUAL TØ EITHER ØR BØTH IY AND IZ/5X,28H
     1 * CASE ØF NEUTRAL STABILITY/5X, 34H * CASE IS UNCØNDITIØNALLY DEL
     2ETED)
      GØ TØ 5000
   47 IF(NMAX - 30) 48, 48, 49
   48 IF(MMAX - 30) 51, 51, 49
   49 WRITE ØUTPUT TAPE 6, 50
   50 FØRMAT (1HØ, 4X, 36H** N MAX ØR M MAX IS GREATER THAN 30/ 5X,  34H
     1 * CASE IS UNCØNDITIØNALLY DELETED)
      GØ TØ 5000
   51 IF(NMAX) 53, 53, 52
   52 IF(MMAX) 53, 53, 55
   53 WRITE ØUTPUT TAPE 6, 54
   54 FØRMAT(1HØ, 4X, 37H** N MAX ØR M MAX IS NEGATIVE ØR ZERØ/ 5X,  34H
     1 * CASE IS UNCØNDITIØNALLY DELETED)
      GØ TØ 5000
   55 IF(TY) 57, 57, 56
   56 IF(TZ) 57, 57, 59
   57 WRITE ØUTPUT TAPE 6, 58
   58 FØRMAT(1HØ, 4X, 41H** TY ØR TZ IS LESS THAN ØR EQUAL TØ ZERØ/ 5X,
     1 34H * CASE IS UNCØNDITIØNALLY DELETED)
      GØ TØ 5000
   59 DØ 60 N = 1, NMAX
      AY(N) = AY(N)*CMY
   60 BY(N) = BY(N)*CMY
      DØ 61 M = 1, MMAX
      AZ(M) = AZ(M)*CMZ
   61 BZ(M) = BZ(M)*CMZ
      WRITE ØUTPUT TAPE 6, 78
   78 FØRMAT(1HØ,10X,25HAY(N), CØEFF ØF CØS IN MY)
      WRITE ØUTPUT TAPE 6, 30,(AY(N),N=1,NMAX)
```

```
      WRITE OUTPUT TAPE 6, 80
   80 FORMAT(1H0,10X,25HBY(N), COEFF OF SIN IN MY)
      WRITE OUTPUT TAPE 6, 30,(BY(N),N=1,NMAX)
      WRITE OUTPUT TAPE 6, 90
   90 FORMAT(1H0,10X,25HAZ(M), COEFF OF COS IN MZ)
      WRITE OUTPUT TAPE 6, 30,(AZ(M),M=1,MMAX)
      WRITE OUTPUT TAPE 6, 100
  100 FORMAT(1H0,10X,25HBZ(M), COEFF OF SIN IN MZ)
      WRITE OUTPUT TAPE 6, 30,(BZ(M),M=1,MMAX)
      IF(OUTPUT)110,300, 110
  110 IF(CHECK) 160 ,120,120
  120 IF(UNITS)148, 130, 130
  130 WRITE OUTPUT TAPE 6, 140
  140 FORMAT(1H0,5X,17HCALCULATED VALUES//7X,6HLAMBDA,9X,10HQ, RAD/SEC,7
     1X,10HR, RAD/SEC,7X,10HTHETA, RAD,8X,8HPSI, RAD,10X,6HT, SEC)
      GO TO 300
  148 WRITE OUTPUT TAPE 6, 150
  150 FORMAT(1H0,5X,17HCALCULATED VALUES//7X,6HLAMBDA,9X,10HQ, DEG/SEC,7
     1X,10HR, DEG/SEC,7X,10HTHETA, DEG,8X,8HPSI, DEG,10X,6HT, SEC)
      GO TO 300
  160 IF(UNITS) 190, 170,170
  170 WRITE OUTPUT TAPE 6, 180
  180 FORMAT(1H0,5X,17HCALCULATED VALUES//7X, 6HLAMBDA,5X,16HQDOT, RAD/S
     1EC**2,1X,16HRDOT, RAD/SEC**2, 5X, 10HTHETA, RAD, 8X, 8HPSI, RAD,
     2 10X, 6HT, SEC)
      GO TO 300
  190 WRITE OUTPUT TAPE 6, 200
  200 FORMAT(1H0,5X,17HCALCULATED VALUES//7X, 6HLAMBDA,5X,16HQDOT, DEG/S
     1EC**2,1X,16HRDOT, DEG/SEC**2, 5X, 10HTHETA, DEG, 8X, 8HPSI, DEG,
     2 10X, 6HT, SEC)
C     SET INITIAL VALUE OF SUMMATION TERMS TO ZERO
  300 SN1V= 0.0
      SN3V= 0.0
      SM1V= 0.0
      SM3V= 0.0
C     INITIAL VALUES
      T = T0
C                 ** K = NUMBER OF CALCULATIONS OF THETA AND PSI
      K = 0
C     CALCULATE  CONSTANTS
      A = P0*(XI-ZI)/YI
      B = P0*(XI-YI)/ZI
      OMEGA = SQRTF(A*B)
      OM = OMEGA
C     NAME OF OMEGA**2 = A*B IS  O
      O = A*B
      PI = 3.1415927
      C1 = 1. - A/OM
      C2 = 1. + A/OM
      C3 = 1. - B/OM
      C4 = 1. + B/OM
      C5 = P0 - OM
      C6 = P0 + OM
      C7 = 0.5/C5
      C8 = 0.5/C6
      C9 = 0.5/(B*P0)
      C10 = 0.5/(A*P0)
      C11 = 0.5/OM
      C12 = AY0/YI
      C13 = AZ0/ZI
      C14 = C12*C11
      C15 = C13*C11
```

```
      C16 = RØ*A/ØM
      C17 = QØ*B/ØM
      C18 = C14*B/ØM
      C19 = C15*A/ØM
      C20 = YI - ZI
      C21 = C20/XI
      C22 = C18/PØ
      C23 = C19/PØ
      C24 = 57.29578
C     CØMPUTE TERMS ØF SUMMATIØNS
      DØ 350N=1, NMAX
      AN = N
      AL =AN*PI/TY
      AL2 = AL**2
      E1= AL/(Ø - AL2)
      SN1(N) = AY(N)/(Ø - AL2)
      SN1V= SN1V+ SN1(N)
      SN2(N) = AY(N)*E1
      SN3(N) = BY(N)*E1
      SN3V= SN3V+ SN3(N)
      SN4(N) = 0.5*(1. - B/AL)/(PØ - AL)
  350 SN5(N) = 0.5*(1. + B/AL)/(PØ + AL)
      DØ 360M=1, MMAX
      AM = M
      BE =AM*PI/TZ
      BE2 = BE**2
      E2 = BE/(Ø - BE2)
      SM1(M) = AZ(M)/(Ø - BE2)
      SM1V= SM1V+ SM1(M)
      SM2(M) = AZ(M)*E2
      SM3(M) = BZ(M)*E2
      SM3V= SM3V+ SM3(M)
      SM4(M) = 0.5*(1. - A/BE)/(PØ - BE)
  360 SM5(M) = 0.5*(1. + A/BE)/(PØ + BE)
C     CØMBINED CØNSTANT CØEFFICIENTS ØF TIME FACTØRS IN THETA
      THC1 = (C3*(C14 +SN1V*ØM/YI) +  C1*(RØ -SM3V/ZI))*C7
      THC2 = -(C4*(C14 +SN1V*ØM/YI) +  C2*(SM3V/ZI- RØ))*C8
      THC3 = -(C1*(C15 +SM1V*ØM/ZI) + C3*(SN3V/YI- QØ))*C7
      THC4 = (C2*(C15 +SM1V*ØM/ZI) +   C4*(QØ -SN3V/YI))*C8
C     CØMBINED CØNSTANT CØEFFICIENTS ØF PSI
      PSC1 = (C1*(C15 +SM1V*ØM/ZI) +   C3*(SN3V/YI- QØ))*C7
      PSC2 = -(C2*(C15 +SM1V*ØM/ZI) +  C4*(QØ -SN3V/YI))*C8
      PSC3 = (C3*(C14 +SN1V*ØM/YI) +   C1*(RØ -SM3V/ZI))*C7
      PSC4 = -(C4*(C14 +SN1V*ØM/YI) +  C2*(SM3V/ZI- RØ))*C8
C     CØMBINED CØNSTANT CØEFFICIENTS ØF TIME FACTØRS IN Q AND R
      QC1 = C14 - C16
      QC2 = QØ + C19
      RC1 = C15 + C17
      RC2 = RØ - C18
C     CØMPUTE NØN-SUBSCRIPTED TIME FUNCTIØNS
  365 T1 = CØSF(C5 * T)
      T2 = CØSF(C6 * T)
      T3 = SINF(C5 * T)
      T4 = SINF(C6 * T)
      T5 = CØSF(PØ * T)
      T6 = SINF(PØ * T)
      T7 = CØSF(ØM * T)
      T8 = SINF(ØM * T)
      T9 = ØM * T8
      T10 = T8/ØM
C     CØMPUTE SUBSCRIPTED TIME FUNCTIØNS
      AMPY = 0.0
```

```
      TH6 = 0.0
      TH7 = 0.0
      TH8 = 0.0
      TH9 = 0.0
      PS6 = 0.0
      PS7 = 0.0
      PS8 = 0.0
      PS9 = 0.0
      Q3 = 0.0
      Q4 = 0.0
      R3 = 0.0
      R4 = 0.0
      DØ 370N=1, NMAX
      AN = N
      AL =AN*PI/TY
      G1 = PØ - AL
      G2 = PØ + AL
      AMPY      = AMPY + AY(N)*CØSF(AL * T) + BY(N)*SINF(AL * T)
      STN1     = CØSF(G1 * T)
      STN2     = CØSF(G2 * T)
      STN3     = SINF(G1 * T)
      STN4     = SINF(G2 * T)
      STN5     =  T9   - AL*SINF(AL * T)
      STN6     = T7 - CØSF(AL * T)
      STN7     =  T10  - SINF(AL * T)/AL
C     TIME-SUMMATIØN TERMS ØF THETA, PSI, Q AND R
      TH6 = TH6 - SN2(N)*SN4(N)*(STN1    - 1.)
      TH7 = TH7 + SN2(N)*SN5(N)*(STN2    - 1.)
      TH8 = TH8 + SN3(N)*SN4(N)*STN3
      TH9 = TH9 + SN3(N)*SN5(N)*STN4
      PS6 = PS6 - SN3(N)*SN4(N)*(STN1    - 1.)
      PS7 = PS7 - SN3(N)*SN5(N)*(STN2    - 1.)
      PS8 = PS8 - SN2(N)*SN4(N)*STN3
      PS9 = PS9 + SN2(N)*SN5(N)*STN4
      Q3 = Q3 + SN1(N)*STN5
      Q4 = Q4 - SN3(N)*STN6
      R3 = R3 - SN1(N)*STN6
  370 R4 = R4 - SN3(N)*STN7
      AMPZ = 0.0
      TH10 = 0.0
      TH11 = 0.0
      TH12 = 0.0
      TH13 = 0.0
      PS10 = 0.0
      PS11 = 0.0
      PS12 = 0.0
      PS13 = 0.0
      Q5 = 0.0
      Q6 = 0.0
      R5 = 0.0
      R6 = 0.0
      DØ 380M=1, MMAX
      AM = M
      BE = AM*PI/TZ
      G3 = PØ - BE
      G4 = PØ + BE
      AMPZ      = AMPZ + AZ(M)*CØSF(BE * T) + BZ(M)*SINF(BE * T)
      STM1     = CØSF(G3 * T)
      STM2     = CØSF(G4 * T)
      STM3     = SINF(G3 * T)
      STM4     = SINF(G4 * T)
      STM5     =  T9   - BE*SINF(BE * T)
```

```
      STM6    = T7 - CØSF(BE * T)
      STM7    =  T10  - SINF(BE * T)/BE
C     TIME-SUMMATIØN TERMS ØF THETA, PSI, Q AND R
      TH10 = TH10 + SM3(M)*SM4(M)*(STM1    - 1.)
      TH11 = TH11 + SM3(M)*SM5(M)*(STM2    - 1.)
      TH12 = TH12 + SM2(M)*SM4(M)*STM3
      TH13 = TH13 - SM2(M)*SM5(M)*STM4
      PS10 = PS10 - SM2(M)*SM4(M)*(STM1    - 1.)
      PS11 = PS11 + SM2(M)*SM5(M)*(STM2    - 1.)
      PS12 = PS12 + SM3(M)*SM4(M)*STM3
      PS13 = PS13 + SM3(M)*SM5(M)*STM4
      Q5 = Q5 + SM1(M)*STM6
      Q6 = Q6 + SM3(M)*STM7
      R5 = R5 + SM1(M)*STM5
  380 R6 = R6 - SM3(M)*STM6
C     SUM TERMS ØF THETA AND PSI       ** UNITS ARE RADIANS
      K = K + 1
      THETA(K)=THC1*(T1-1.) + THC2*(T2-1.) + THC3*T3 + THC4*T4 + C22*(T5
     1 -1.) - C23*T6 + (TH6 + TH7 + TH8 + TH9)/YI + (TH10 + TH11 + TH12
     2 + TH13)/ZI + THETAØ
      PSI(K)=PSC1*(T1-1.) + PSC2*(T2-1.) + PSC3*T3 + PSC4*T4 + C22*T6 +
     1 C23*(T5-1.) + (PS6 + PS7 + PS8 +PS9)/YI + (PS10 + PS11 + PS12 +
     2 PS13)/ZI + PSIØ
      AT(K) = T
C     SUM TERMS ØF Q AND R             ** UNITS ARE RADIANS/SECØND
      AQ(K) = QC1*T8 + QC2*T7 + (Q3 + Q4)/YI + (Q5 + Q6)*A/ZI
     1 - C19
      AR(K) = RC1*T8 + RC2*T7 + (R3 + R4)*B/YI + (R5 + R6)/ZI
     1 + C18
      ATHDØT(K) = AQ(K)*T5 - AR(K)*T6
      APSDØT(K) = AR(K)*T5 + AQ(K)*T6
      AAMPY(K) =  AYØ/2.0 + AMPY
      AAMPZ(K) =  AZØ/2.0 + AMPZ
      AQDØT(K) = AAMPY(K)/YI - A*AR(K)
      ARDØT(K) = AAMPZ(K)/ZI + B*AQ(K)
      ALAMBD(K) = APSDØT(K)*THETA(K)/PØ
      APHI(K) = PØ*AT(K)
      AMX(K) = - C20*AQ(K)*AR(K)
      IF(UNITS) 500, 510, 510
  500 THETA(K) = THETA(K) * C24
      PSI(K) = PSI(K) * C24
      AQ(K) = AQ(K) * C24
      AR(K) = AR(K) * C24
      ATHDØT(K) = ATHDØT(K) * C24
      APSDØT(K) = APSDØT(K) * C24
      AQDØT(K) =  AQDØT(K) * C24
      ARDØT(K) =  ARDØT(K) * C24
      APHI(K) = APHI(K) * C24
  510 IF(ØUTPUT) 520, 3000, 520
  520 IF(CHECK) 550, 530, 530
  530 WRITE ØUTPUT TAPE 6, 30, ALAMBD(K), AQ(K), AR(K), THETA(K), PSI(K)
     1, AT(K)
      GØ TØ 3000
  550 WRITE ØUTPUT TAPE 6, 30, ALAMBD(K), AQDØT(K), ARDØT(K), THETA(K),
     1 PSI(K), AT(K)
 3000 T = T + DELTAT
      IF(T - TMAX) 3010, 3010, 4000
 3010 IF(K - 500) 365, 3015, 3011
 3015 IF(ØUTPUT) 3020, 3020, 365
 3020 WRITE ØUTPUT TAPE 6, 3030
 3030 FØRMAT (1H0,4X,29HDIMENSIØNS FØR CRT ARE FILLED/
     1 10X,34HCASE IS UNCØNDITIØNALLY TERMINATED/10X,14HCRT IS PRINTED)
```

```
      GØ TØ 4000
 3011 IF(ØUTPUT) 3012, 3012, 365
 3012 WRITE ØUTPUT TAPE 6, 3013
 3013 FØRMAT(1H0,4X,33HDIMENSIØNS FØR CRT ARE ØVERLØADED/
     1   10X, 34HCASE IS UNCØNDITIØNALLY TERMINATED/ 10X, 18HCRT IS NØT
     2PRINTED/ 15X,      47HLØØK FØR ERRØRS IN CØMPUTATIØNS DUE TØ ØVERL
     3ØAD)
      GØ TØ 5000
 4000 WRITE ØUTPUT TAPE 6, 4001
 4001 FØRMAT(1H-, 4X, 10HA, RAD/SEC,7X, 10HB, RAD/SEC,5X,14HØMEGA, RAD/S
     1EC)
      WRITE ØUTPUT TAPE 6, 30, A, B, ØM
      WRITE ØUTPUT TAPE 6, 4002
 4002 FØRMAT(1H-)
      IF(ØUTPUT) 4010, 4010, 5000
 4010 IF(UNITS) 4030, 4020, 4020
 4020 CALL GRAPH(1,1HX,-K, PSI    , THETA   ,13H PSI, RADIANS,15H THETA,
     1RADIANS,61H RIGID BØDY ANGULAR MØTIØNS, GENERAL FØURIER Y,Z BØDY M
     2ØMENTS)
      CALL GRAPH(2,1HX, -K, AT, THETA, 14H TIME, SECØNDS, 15H THETA, RAD
     1IANS,    61H RIGID BØDY ANGULAR MØTIØNS, GENERAL FØURIER Y,Z BØDY M
     2ØMENTS)
      CALL GRAPH(2,1HX, -K, AT, PSI,    14H TIME, SECØNDS, 13H PSI, RADIA
     1NS, 1H )
      CALL GRAPH(2, 1HX, -K, AT, ATHDØT, 14H TIME, SECØNDS, 26H THETA-D0
     1T, RADIANS/SECØND, 61H RIGID BØDY ANGULAR MØTIØNS, GENERAL FØURIER
     2 Y,Z BØDY MØMENTS)
      CALL GRAPH(2, 1HX, -K, AT, APSDØT, 14H TIME, SECØNDS, 24H PSI-DØT,
     1 RADIANS/SECØND, 1H )
      CALL GRAPH(2, 1HX, -K, AT, AQDØT,  14H TIME, SECØNDS, 25H Q-DØT, R
     1ADIANS/SECØND**2,  61H RIGID BØDY ANGULAR MØTIØNS, GENERAL FØURIER
     2 Y,Z BØDY MØMENTS)
      CALL GRAPH(2, 1HX, -K, AT, ARDØT,  14H TIME, SECØNDS, 25H R-DØT, R
     1ADIANS/SECØND**2, 1H )
      CALL GRAPH(2, 1HX, -K, AT, AQ,     14H TIME, SECØNDS, 18H Q, RADIA
     1NS/SECØND,         61H RIGID BØDY ANGULAR MØTIØNS, GENERAL FØURIER
     2 Y,Z BØDY MØMENTS)
      CALL GRAPH(2, 1HX, -K, AT, AR,     14H TIME, SECØNDS, 18H R, RADIA
     1NS/SECØND, 1H )
      CALL GRAPH(2, 1HX, -K, AT, APHI,   14H TIME, SECØNDS, 13H PHI, RAD
     1IANS,              61H RIGID BØDY ANGULAR MØTIØNS, GENERAL FØURIER
     2 Y,Z BØDY MØMENTS)
      CALL GRAPH(2, 1HX, -K, AT, ALAMBD, 14H TIME, SECØNDS, 22H LAMBDA,
     1DIMENSIØNLESS,  1H )
      IF(C20) 4032, 4033, 4032
 4030 CALL GRAPH(1,1HX,-K, PSI    , THETA   ,13H PSI, DEGREES,15H THETA,
     1DEGREES,61H RIGID BØDY ANGULAR MØTIØNS, GENERAL FØURIER Y,Z BØDY M
     2ØMENTS)
      CALL GRAPH(2,1HX, -K, AT, THETA, 14H TIME, SECØNDS, 15H THETA, DEG
     1REES,    61H RIGID BØDY ANGULAR MØTIØNS, GENERAL FØURIER Y,Z BØDY M
     2ØMENTS)
      CALL GRAPH(2,1HX, -K, AT, PSI,    14H TIME, SECØNDS, 13H PSI, DEGRE
     1ES, 1H )
      CALL GRAPH(2, 1HX, -K, AT, ATHDØT, 14H TIME, SECØNDS, 26H THETA-D0
     1T, DEGREES/SECØND, 61H RIGID BØDY ANGULAR MØTIØNS, GENERAL FØURIER
     2 Y,Z BØDY MØMENTS)
      CALL GRAPH(2, 1HX, -K, AT, APSDØT, 14H TIME, SECØNDS, 24H PSI-DØT,
     1 DEGREES/SECØND, 1H )
      CALL GRAPH(2, 1HX, -K, AT, AQDØT,  14H TIME, SECØNDS, 25H Q-DØT, D
     1EGREES/SECØND**2,  61H RIGID BØDY ANGULAR MØTIØNS, GENERAL FØURIER
     2 Y,Z BØDY MØMENTS)
      CALL GRAPH(2, 1HX, -K, AT, ARDØT,  14H TIME, SECØNDS, 25H R-DØT, D
```

```
     1EGREES/SECOND**2, 1H )
      CALL GRAPH(2, 1HX, -K, AT, AQ,      14H TIME, SECONDS, 18H Q, DEGRE
     1ES/SECOND,            61H RIGID BODY ANGULAR MOTIONS, GENERAL FOURIER
     2 Y,Z BODY MOMENTS)
      CALL GRAPH(2, 1HX, -K, AT, AR,      14H TIME, SECONDS, 18H R, DEGRE
     1ES/SECOND, 1H )
      CALL GRAPH(2, 1HX, -K, AT, APHI,    14H TIME, SECONDS, 13H PHI, DEG
     1REES,                 61H RIGID BODY ANGULAR MOTIONS, GENERAL FOURIER
     2 Y,Z BODY MOMENTS)
      CALL GRAPH(2, 1HX, -K, AT, ALAMBD, 14H TIME, SECONDS, 22H LAMBDA,
     1DIMENSIONLESS, 1H )
      IF(C20) 4032, 4033, 4032
 4032 CALL GRAPH(1, 1HX, -K, AT, AMX,     14H TIME, SECONDS, 10H MX, FT-L
     1B,                    61H RIGID BODY ANGULAR MOTIONS, GENERAL FOURIER
     2 Y,Z BODY MOMENTS)
 4033 IF(SERIES) 4900, 4034, 4034
 4034 CALL GRAPH(2, 1HX, -K, AT, AAMPY,  14H TIME, SECONDS, 10H MY, FT-L
     1B,                    61H RIGID BODY ANGULAR MOTIONS, GENERAL FOURIER
     2 Y,Z BODY MOMENTS)
      CALL GRAPH(2, 1HX, -K, AT, AAMPZ,  14H TIME, SECONDS, 10H MZ, FT-L
     1B, 1H )
 4900 WRITE OUTPUT TAPE 6, 4910
 4910 FORMAT(1H0,10X,     23H*** CRT OUTPUT INCLUDED/ 20X, 19HTHETA VS PS
     1I GRAPH /20X,      36HTIME VS THETA AND TIME VS PSI GRAPHS/
     2 20X,    44HTIME VS THETA-DOT AND TIME VS PSI-DOT GRAPHS/ 20X,  38H
     3TIME VS Q-DOT AND TIME VS R-DOT GRAPHS/ 20X, 30HTIME VS Q AND TIME
     4 VS R GRAPHS/ 20X, 37HTIME VS PHI AND TIME VS LAMBDA GRAPHS)
      IF(C20) 4035, 4037, 4035
 4035 WRITE OUTPUT TAPE 6, 4036
 4036 FORMAT(1H , 19X,  16HTIME VS MX GRAPH)
 4037 IF(SERIES) 4040, 4038, 4038
 4038 WRITE OUTPUT TAPE 6, 4039
 4039 FORMAT(1H , 19X, 32HTIME VS MY AND TIME VS MZ GRAPHS)
 4040 IF(C20) 4043, 4041, 4043
 4041 WRITE OUTPUT TAPE 6, 4042
 4042 FORMAT(1H0, 25X, 38HMX IS IDENTICALLY ZERO SINCE (IY = IZ))
 4043 IF(SERIES) 4044, 5000, 5000
 4044 WRITE OUTPUT TAPE 6, 4045
 4045 FORMAT(1H0, 25X, 51HMY AND MZ ARE OF CONSTANT VALUE AND ARE NOT GR
     1APHED)
 5000 WRITE OUTPUT TAPE 6, 5010
 5010 FORMAT(1H0,5X,11HEND OF CASE,15X,11HEND OF CASE,15X,11HEND OF CASE
     1/ 1H1)
      IF(ZERO) 6, 6, 10
      END
```

APPENDIX F

PROGRAM FOR LATERAL VIBRATION MODES OF TWO-COMPARTMENT, SINGLE-CABLE-CONNECTED CONFIGURATION

A lumped parameter analysis of the free lateral vibration of a two-compartment configuration connected by a single cable is presented in Section 6.2.1.2. The FØRTRAN computer program written for this investigation is described in this appendix.

Figure F-1 depicts the logic of the program. The purpose of the program is to determine five consecutive natural frequencies and the corresponding modes of free lateral vibration for two-compartment, cable-connected configurations. Rotary inertia is neglected and, consequently, the frequency equation is the determinant of coefficients of λ. This determinant, D, is of the order $(n + 1)$, where n is the number of cable segments.

Diagonal elements of the determinant D contain the natural frequency of free lateral vibration p, and adjacent off-diagonal elements are constants, the values of which depend on the system parameters. Iteration on p is executed to determine the values of p—i.e., the natural frequencies of the system, which produce a zero-valued diagonalized determinant D.

Once the natural frequencies p are known, the systems of equations

$$[A]_{i,j}[\lambda]_{i+1,\ 1} = [B]_{i,\ 1}$$

where

$$[A]_{i,j} = [D]_{i,j+1}$$

$$[B]_i = [-D]_{i,\ 1}$$

$$i = 1, 2, \ldots, n$$

$$j = 1, 2, \ldots, n$$

are solved for n λ's by using the library mathematical function "XSIMEQ - Simultaneous Equation Solution." Upon successful execution of XSIMEQ, the value of λ_{i+1} is stored in $A_{i,\ 1}$.

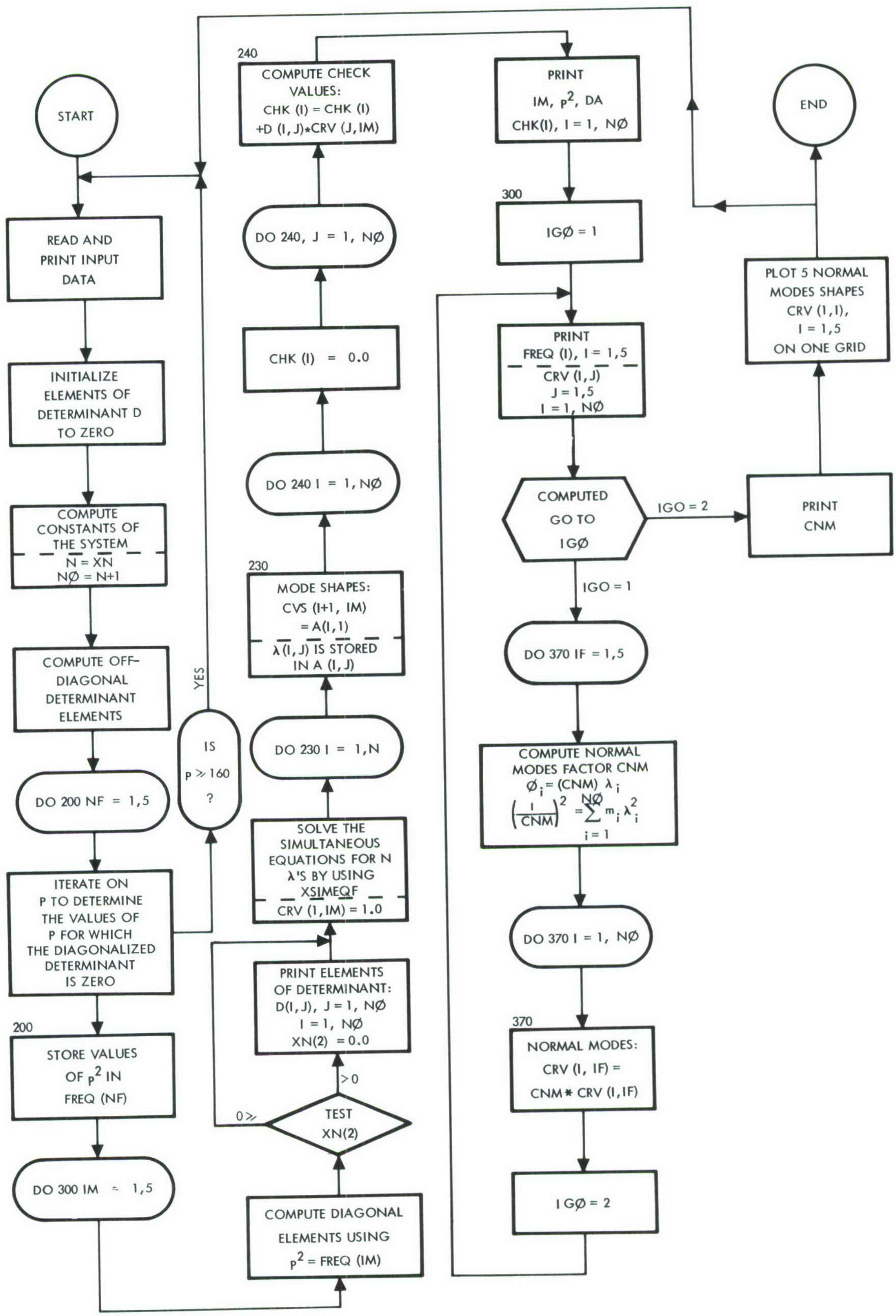

Figure F-1. Lateral Vibration Modes Program Logic

A check of the solution is made by computing and printing the values of $D\lambda$ in the $(n + 1)$ equations $D\lambda = 0$. The values of the $(n + 1)$ λ's for each of the five mode shapes are also printed. The values of the elements in D are optionally printed, depending on the input value of XN(2).

Normal modes ϕ are computed, printed and plotted, where

$$\phi_i = c\,\lambda_i$$

$$c^2 = \frac{1}{\sum_{i=1}^{n+1} m_i\,\lambda_i}$$

$$i = 1, 2, \ldots, n + 1$$

Upon completion of the normal mode computations, the stored values of ϕ_i are plotted on the S-C 4020 CRT plotter by using the rectilinear graphing subroutine package GRAPH (S&ID Deck No. 9J-400). The five normal modes are plotted on one grid.

The floating-point input data are defined on the sample data sheet. Included on the sample data sheet are the data used to obtain the five lowest normal modes for Configuration 1-A shown in Figure 24.

The listing of the FØRTRAN II coded program is also included.

FORTRAN FIXED 10 DIGIT DECIMAL DATA

DECK NO. 9J-210 PROGRAMMER ______ DATE ______ PAGE 1 of 1 JOB NO. ______

Col.	NUMBER	IDENTIFICATION	DESCRIPTION DO NOT KEY PUNCH
1	1		
13	50 0		XN(1) = n = Number of equal cable segments ≤ 100
25	0.0		XN(2) :≤0, No Print;>0, Print D(I, J), J = 1, NØ, I = 1, NØ
37			XN(3)
49		73 … 80	XN(4) - Reserve data locations - not used
61		10	XN(5)
1	6		
13	10944000.		AE = Extensional stiffness, lb.
25	12000.0		l = Unstressed length of cable, inches
37	103.52		M_1 = Mass of compartment 1, slug
49	12.94	73 … 80	M_2 = Mass of compartment 2, slug
61	.474464	20	m_u = Cable mass per unit length, slug/inch
1	− 11		
13	1.0		ρ = Starting frequency of vibration, rad/sec
25	1.0		Δp = Frequency increment, rad/sec
37			
49		73 … 80	
61		30	
1			
13			
25			
37			
49		73 … 80	
61			

Form 114-C-17 Rev. 7-58 (Vellum)

```
C                    DECK NO. 9J-210  -  LATERAL
C           TWO-COMPARTMENT CABLE CONNECTED CONFIGURATION
C                                 LUMPED MASS
C
      COMMON XN, AE, XL, XM1, XM2, XMU,PIN, DEL, S, B1, BN,  BT, CDIA,
     X         D, FREQ, A, B, TEMP, CRV, CHK, STA
      DIMENSION  XN(5), S(100), BT(101), CDIA(101), D(101,101),
     X           FREQ(5), A(100,100), B(100), TEMP(100), CRV(101,5),
     X           CHK(101), STA(101)
   10 CALL DECRD(XN)
      PRINT 11,  XN, AE, XL, XM1, XM2, XMU, PIN, DEL
   11 FORMAT(45X,14HDATA - LATERAL//37X,11HN TESTWORDS//37X,26HAE    L
     X   M1    M2     MU//37X,16HINITIAL P   INCR/(/5E19.8))
      N = XN
      NO = N+1
      DO 12 I = 1,NO
      DO 12 J=1,NO
   12 D(I,J) = 0.0
C                   CONSTANTS, B1, BN  AND BETAS
      XMUL = XMU * XL
      D1 = (XM2*XL + .5 * XMUL * XL)/(XM1 + XM2 + XMUL)
      D2 = XL - D1
      OMSQ = 386.4/D1
      AL = XL/XN + OMSQ/XN/AE *(D1**2 * (XM1 + XMU*D1/3.0) + D2**2 *(XM2
     X + XMU*D2/3.0))
      XM = XMUL/XN
      XMOM = XM * OMSQ
      CN1 = XM1 + .5 * XM
      CN2 = XM2 + .5 * XM
      S(1) = CN1 * OMSQ * D1
      DO 15  I=2,N
      IL = I-1
      XI = IL
      DA1 = D1 - XI * AL
      IF(DA1)17, 17, 15
   15 S(I) = S(IL) + XMOM * DA1
   17 S(N ) = CN2 * OMSQ * D2
      DO 18  I=1,N
      IL = N - I
      XI = I
      DA2 = D2 - XI * AL
      IF(DA2)19, 19, 18
   18 S(IL) = S(IL+1) + XMOM * DA2
   19 RMA = 1.0/XM/AL
      B1 = S(1)/(XM1 + .5 * XM) / AL
      BN  = S(N)/(XM2 + .5 * XM)/ AL
      DO 20  I=1,N
   20 BT(I) = S(I) * RMA
C                          CONSTANT ELEMENTS FOR D
      CDIA(1) = B1
      CDIA(NO) = BN
      DO 21 I=2,N
   21 CDIA(I) = BT(I-1) + BT(I)
```

```
      D(1,2)= -B1
      D(NO,N)= -BN
      DO 22  I= 2,N
      D(I,I-1) = - BT(I-1)
   22 D(I,I+1) = - BT(I)
      TST1 = 0.0
C                                 FREQUENCY LOOP
      DO 200 NF=1,5
      DINC = DEL
      CHG = 1.0
      P = PIN
C
   25 PSQ = P ** 2
      DO 30 I=1,NO
   30 D(I,I) =-PSQ + CDIA(I)
   33 FORMAT(1H1,5X,11HD - BY ROWS/(/6E17.8))
C                                 EVALUATE D
   35 DC = D(NO,NO)
      DO 60 K=1,N
   50 I= NO - K
      J= I + 1
      D(I,I) = D(I,I) - D(I,J) * D(J,I)/D(J,J)
      DC = DC * D(I,I)
   60 CONTINUE
      IF(TST1)90, 70, 90
   70 TST1 = 1.0
   80 DL = DC
      SVPSQ = PSQ
      IF(CHG - 1.0)88, 85, 88
   85 P=P+DINC
      IF(P-160.0)25, 25, 10
   88 SN = 1.0
      GO TO 130
   90 IF(DL * DC)100,80,80
  100 IF(CHG - 1.0)120, 110,120
  110 CHG = .5
      PIN = P + DEL
      DLNXT = DC
  120 SN = -1.0
  130 DINC = DINC/2.0
      PLST = P
      P = P + SN * DINC
      IF(PLST -P)25, 140, 25
  140 IF(ABSF(DL) - ABSF(DC))150, 150, 160
  150 FREQ(NF) = SVPSQ
      GO TO 170
  160 FREQ(NF) = PSQ
  170 DL = DLNXT
  200 CONTINUE
C                             SOLVE FOR LAMBDAS
C                   COL. 1 - CONSTANTS    ROW 11 OMITTED
      DO 300 IM=1,5
      PSQ = FREQ(IM)
      DO 210  I= 1,NO
  210 D(I,I) = -PSQ + CDIA(I)
      IF(XN(2))218,218,215
  215 PRINT 33,((D(I,J),J=1,NO),I=1,NO)
      XN(2) = 0.0
  218 DO 220 I=1,N
      B(I) =-D(I,1)
      DO 220 J=1,N
  220 A(I,J) = D(I, J+1)
```

```
      DA = 1.0
      MA = XSIMEQF(100, N, 1, A, B, DA,TEMP)
      CRV(1, IM) = 1.0
      DO 230 I=1,N
  230 CRV(I+1,IM) = A(I,1)
      DO 240 I=1,NO
      CHK(I) = 0.0
      DO 240 J=1,NO
  240 CHK(I) = CHK(I) + D(I,J) *  CRV(J,IM)
C
      PRINT 250, IM, PSQ, DA, (CHK(I), I=1,NO)
  250 FORMAT(1H-,5X,15HCHECK FOR FREQ-I2,2E17.8/(/6E17.8))
  300 CONTINUE
      IGO = 1
C
  305 PRINT  310, (FREQ(I), I=1,5)
  310 FORMAT(1H1,31X,38H LATERAL VIBRATION    -     MODE SHAPES//12X,7HFR
     XEQ. 1,11X,7HFREQ. 2,11X,7HFREQ. 3,11X,7HFREQ. 4,11X,7HFREQ. 5//E24
     X.5, 4E18.5/6H   STA)
      PRINT 320, (I,(CRV(I,J), J=1,5), I=1,NO)
  320 FORMAT(1HO, I5, 5E18.5)
      GO TO(340, 390), IGO
C                   COMPUTE C FOR NORMAL MODE
  340 DO 370 IF=1,5
      SUMN = 0.0
      DO 350 I=2,N
  350 SUMN = SUMN + CRV(I,IF)**2
      CNM=SQRTF(1.0/(CN1 * CRV(1,IF)**2 + XM * SUMN +CN2*CRV(NO,IF)**2))
      DO 360 I=1,NO
  360 CRV(I,IF)= CNM * CRV(I,IF)
  370 CONTINUE
      IGO = 2
      GO TO 305
  390 PRINT 395, CNM
  395 FORMAT(1H-,30X,3HC =E17.8/1H1)
C                               CRT  -  PLOT CURVES
  396 DO 400 I=1, NO
  400 STA(I) = I
      YB = CRV(1,1)
      YT = CRV(1,1)
      DO 410 I=1,5
      DO 410 J=1,NO
      YB = MIN1F(YB, CRV(J,I))
  410 YT = MAX1F(YT, CRV(J,I))
      CALL LIMITI(STA(1), STA(NO), YB, YT)
C
      CALL GRAPH(1,1H1, -NO, STA,CRV(1,1),8H STATION,7H LAMBDA,49H LATER
     XAL VIBRATION  -  NORMAL MODE       FIGURE 2)
      DO 500 I =2,5
  500 CALL GRAPH(0,I,-NO,STA,CRV(1,I))
      GO TO 10
      END
```

APPENDIX G

PROGRAM FOR SOLUTION OF SEVEN-DEGREE OF FREEDOM PLANAR EQUATIONS OF MOTION

The computer program of the numerical solution of the equations 176 through 180 of this report was written in FØRTRAN for an IBM 7094 computer. Figure G-1 shows the logical flow of the program. The input data are explained on the sample data sheets. The data shown are for an actual case, the output for which is shown in Figure 52 of this report. A more complete discussion of the results is given in the report.

The computer program uses three main subroutines—RUQ, SEQ, and GRAPH. SUBRØUTINE RUQ is a Runge-Kutta integration routine, which uses the equations as derived in "Discrete Variable Methods in Ordinary Differential Equations," by P. Henrici. SUBRØUTINE SEQ calculates the second derivatives needed by RUQ for the integration and is called only from RUQ. SUBRØUTINE GRAPH is a plotting routine used at North American Aviation's Space and Information Systems Division. The user may write a subroutine called GRAPH that presents the output data in any form suitable to the equipment he has available.

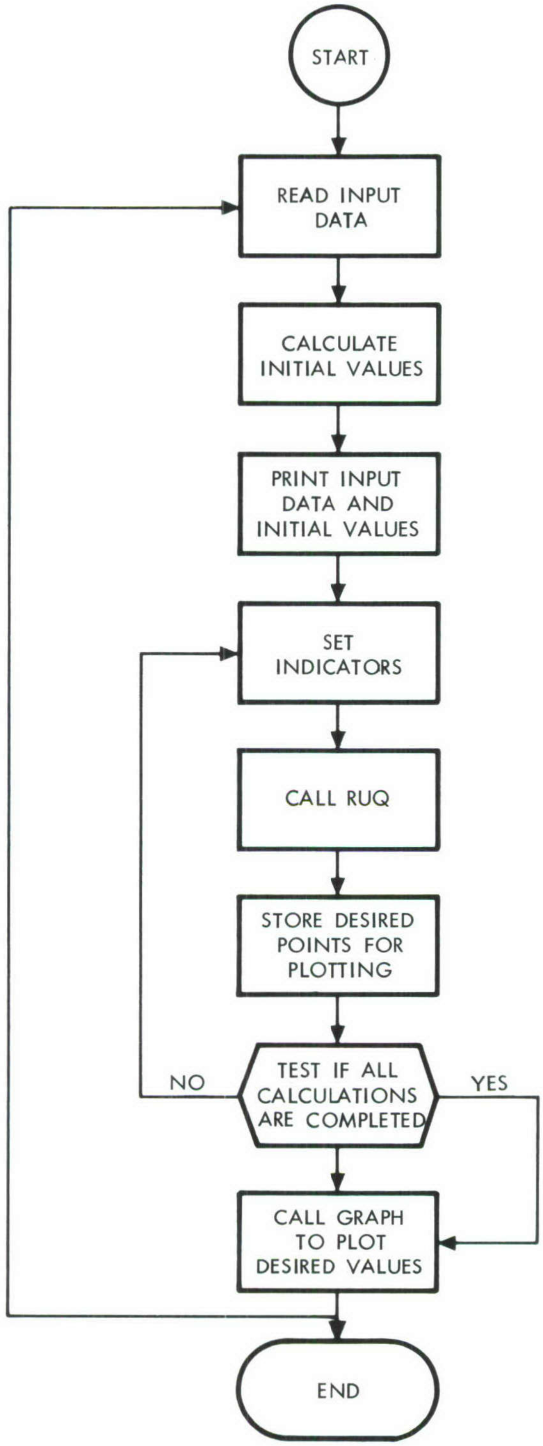

Figure G-1. Simplified Flow Chart (Sheet 1 of 2)

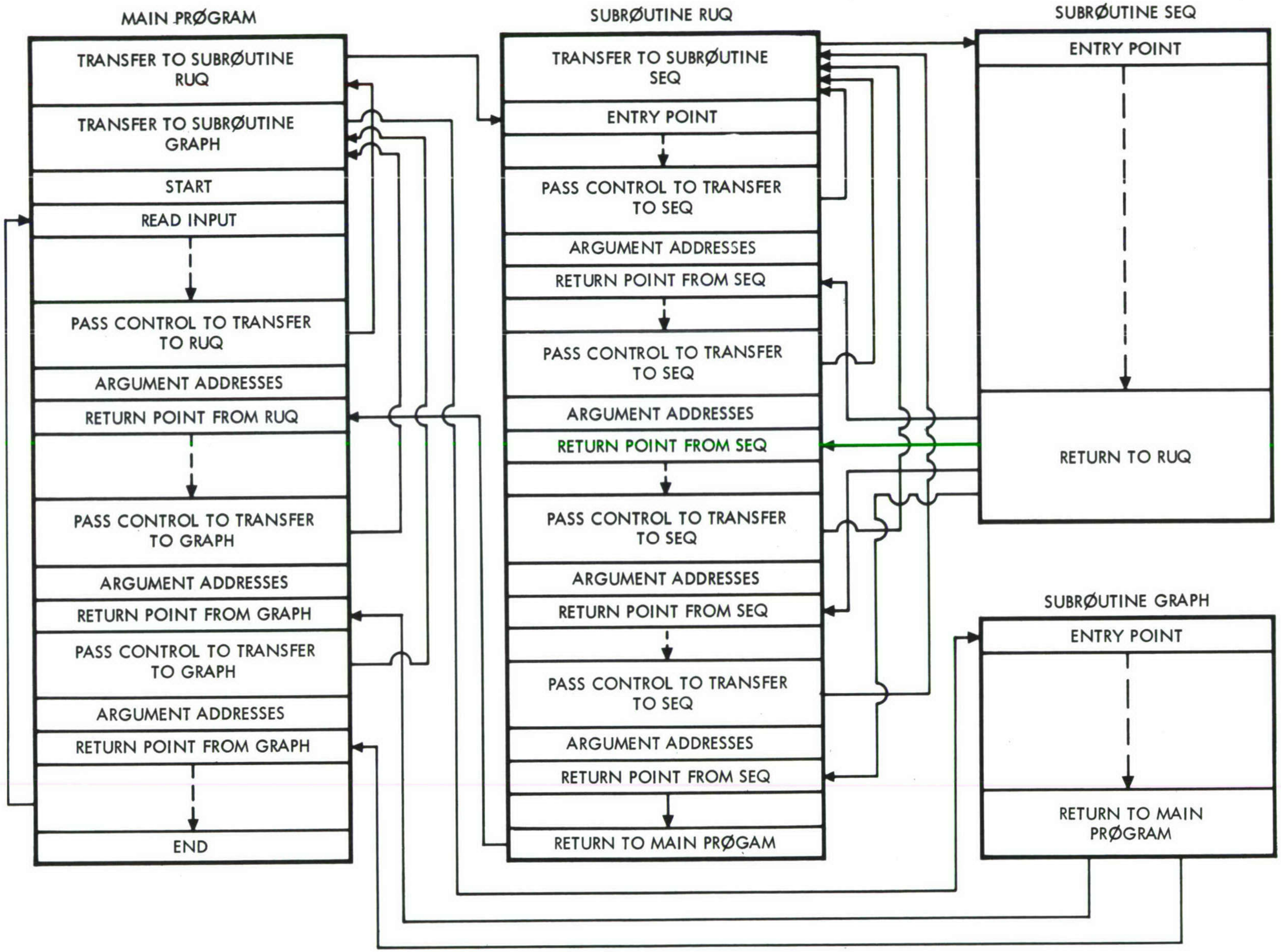

Figure G-1. Simplified Flow Chart (Sheet 2 of 2)

FORTRAN FIXED 10 DIGIT DECIMAL DATA

DECK NO. ______ PROGRAMMER ______ DATE ______ PAGE 1 of ______ JOB NO. ______

	NUMBER	IDENTIFICATION	DESCRIPTION DO NOT KEY PUNCH
1	1 0		KI = 1 Grid will occupy entire frame
13	1 2 2 1 0		ISYM = 0 Symbol used in plotting data points
25			M = 12 No. of subtitle cards
37			INC = 210 Increment in plotting points
49		73 80	
61			
1	T I M E - S E C .		Title cards on grid frames
13			
25			36 alpha numeric cards have
37			to be provided for use of
49		73 80	GRAPH with a Hollerith punch
61			in column 1
1	T I M E - S E C .		
13			
25			
37			
49		73 80	
61			
1	3 0 1 5 0 - 1 5 0		K = 30150 Total no. of points to be integrated
13			NP = 150 Total no. of points to be plotted
25			
37			
49		73 80	
61			

FORM 114-C-17 REV. 7-58

FORTRAN FIXED 10 DIGIT DECIMAL DATA

DECK NO. ______ PROGRAMMER ______ DATE ______ PAGE 2 of ______ JOB NO. ______

Col.	NUMBER	IDENTIFICATION	DESCRIPTION DO NOT KEY PUNCH
1	1 4 0 7 7 5 0 0 + 1 7		G_{me} = 14077500 + 17 - gravitational const.
13	2 1 4 5 4 4 2 7 + 0 8		R - Orbit radius at T = 0 (T → time)
25	4 9 9 1 5 3 3 8 + 0 0		$\dot{\phi}$ - Spin at T = 0
37	1 0 0 0 + 0 4		r - Cable length at T = 0, in ft.
49	1 2 9 2 3 7 2 9 + 0 3	73 … 80	ℓ_1 - Distance from C.G. to m_1
61	8 7 0 7 6 2 7 1 + 0 3		ℓ_2 - Distance from C.G. to m_2
1	5 7 6 0 0 + 0 0		A - Cross section area of cable
13	1 9 0 0 0 + 0 8		E - Modulus of elasticity
25	9 9 6 1 5 8 6 0 + 0 3		r_o - Cable length at zero tension
37	3 3 4 0 + 0 0		Damping factor for cable length
49	1 2 4 2 2 3 6 0 + 0 4	73 … 80	Mass of m_1
61	1 5 5 2 7 9 4 9 + 0 3		Mass of m_2
1	6 8 3 2 2 9 8 1 - 0 1		Cable density
13	0 0 0 + 0 0		Starting time
25	1 0 0 - 0 1		Time increment between integ. points
37	1 3 5 2 + 0 0		Damping factor for q_1
49	2 6 9 0 + 0 0	73 … 80	Damping factor for q_2
61	3 8 5 0 + 0 0		Damping factor for q_3
1	8 3 3 3 3 3 3 3 - 0 1		M_1 symbols referenced in report
13	8 3 3 3 3 3 3 3 - 0 1		M_2
25	8 3 3 3 3 3 3 3 - 0 1		M_3
37	1 9 9 7 5 3 3 3 + 0 1		N_{11}
49	2 9 6 3 4 3 6 5 - 0 2	73 … 80	N_{21}
61	4 5 7 8 6 0 9 8 - 0 2		N_{31}

FORM 114-C-17 REV. 7-58

FORTRAN FIXED 10 DIGIT DECIMAL DATA

DECK NO. ______ PROGRAMMER ______ DATE ______ PAGE 3 of ______ JOB NO. ______

		NUMBER	IDENTIFICATION	DESCRIPTION DO NOT KEY PUNCH
1		2 9 6 3 4 3 6 5 - 0 2		N_{12}
13		7 5 2 8 5 6 4 2 + 0 1		N_{22}
25		6 6 2 3 9 8 0 9 - 0 2		N_{32}
37		4 5 7 8 6 0 9 8 - 0 2		N_{13}
49		6 6 2 3 9 8 0 9 - 0 2	73 80	N_{23}
61		1 6 7 2 2 5 7 8 + 0 2		N_{33}
1		0 0 0 + 0 0		Radial deviation from R at T = 0
13		1 5 7 0 7 9 6 1 + 0 1		ϕ at T = 0
25		0 0 0 + 0 0		Cable length deviation from r at T = 0
37		5 1 4 + 0 2		q_1 at T = 0
49		5 8 8 + 0 2	73 80	q_2 at T = 0
61		5 4 2 + 0 2		q_3 at T = 0
1		0 0 0 + 0 0		$\dot{R}$ at T = 0
13		4 9 9 1 5 3 3 8 + 0 0		$\dot{\phi}$ at T = 0
25		0 0 0 + 0 0		$\dot{r}$ at T = 0
37	−	1 1 1 + 0 3		$\dot{q}_1$ at T = 0
49	−	2 7 9 + 0 3	73 80	$\dot{q}_2$ at T = 0
61	−	1 3 6 + 0 3		$\dot{q}_3$ at T = 0
1				
13				
25				
37				
49			73 80	
61				

FORM 114-C-17 REV. 7-60

MAIN PRØGRAM

```
      DIMENSIØN X(6),XD(6),XN(201,6),XDN(201,7),XDDN(201,6),TI(201),YV(2
     150,7),YD(250,6),A1(12,12),A2(12,12),A3(12,12),TX(250),VM(3),TN(3,3
     1)
      CØMMØN UK,RØ,PØ,SØ,D1,D2,DR,AR,ER,W1,W2,RØU,DAM,CØ,C1,C2,C3,VM,TN
     1,DA4,DA5,DA6
D     DIMENSIØN UK(1),RØ(1),PØ(1),SØ(1),D1(1),D2(1),W1(1),W2(1),RØU(1),
     1CØ(1),C1(1),C2(1)
      READ INPUT TAPE 5,7,KI,ISYM,M,INC
      WRITE ØUTPUT TAPE6,31,KI,ISYM,NP,M,INC
    7 FØRMAT(5I5)
    3 FØRMAT(12A6)
      READ INPUT TAPE5,3,((A1(I,J),I=1,12),J=1,M),((A2(I,J),I=1,12),J=1,
     1M),((A3(I,J),I=1,12),J=1,M)
      WRITE ØUTPUT TAPE6,32,((A1(I,J),I=1,12),J=1,M),((A2(I,J),I=1,12),J
     1=1,M),((A3(I,J),I=1,12),J=1,M)
   75 READ INPUT TAPE5,11,K,NP,UK,RØ,PØ,SØ,D1,D2,AR,ER,DR,DAM,W1,W2,RØU,
     1T,H,DA4,DA5,DA6
   11 FØRMAT(2I5/(6E12.8))
      READ INPUT TAPE5,10,(VM(I),I=1,3),((TN(I,J),I=1,3),J=1,3)
   10 FØRMAT(6E12.8)
      READ INPUT       TAPE5,10,(X(I),I=1,6),(XD(I),I=1,6)
      TET=SQRTF(UK/RØ**3)
D     C1=(W1*D1*D1+W2*D2*D2+RØU*(D1*D1*D1+D2*D2*D2)/3.0)/(SØ*SØ)
      SUM=VM(1)*X(4)**2+VM(2)*X(5)**2+ VM(3)*X(6)**2
D     C2=W1+W2+RØU*SØ
D     BR=(TET+PØ)
D     CØ=C2*RØ*RØ*TET+C1*BR*SØ*SØ+BR*SUM
   31 FØRMAT(1H0,5I5)
   32 FØRMAT(1H0,12A6)
      WRITE ØUTPUT TAPE6,20,K,UK,RØ,PØ,SØ,D1,D2,AR,ER,DR,DAM,W1,W2,RØU,T
     1,H,TET,CØ,C1,C2,C3,SUM,BR
   20 FØRMAT(1H0,7HINPUT   2HK=I5/(1H0,7E16.8))
      WRITE ØUTPUT TAPE6,22,(VM(I),I=1,3),((TN(I,J),I=1,3),J=1,3)
      WRITE ØUTPUT TAPE6,22,(X(I),I=1,6),(XD(I),I=1,6)
   22 FØRMAT(1H0,6E16.8)
      IA1=0
      IC1=0
      IB=0
      IC=0
      NM=XABSF(NP)
      IF(K-NM)18,18,17
   18 NP=XSIGNF(K,NP)
   17 IF(K-201)6,8,8
    6 L=K
      GØ TØ 82
    8 L=201
```

```
82    CALL RUQ(L,T,H,X,XD,XN,XDN,XDDN,TI)
      IF(IB+L/INC-250)23,24,24
24    WRITE OUTPUT TAPE6,89
89    FØRMAT(1HO,16HDIMENSIØN EXEDED)
      CALL EXIT
23    DØ70J=1,7
      IA=IA1
      DØ70I=1,L,INC
      IA=IA+1
70    YV(IA,J)=XDN(I,J)
      IA1=IA
      DØ72I=1,L,INC
      IB=IB+1
      YD(IB,1)=XN(I,3)
      YD(IB,2)=XN(I,1)
72    TX(IB)=TI(I)
      DØ74J=4,6
      IC=IC1
      J1=J-1
      DØ74I=1,L,INC
      IC=IC+1
74    YD(IC,J1)=XN(I,J)
      IC1=IC
      NN=XABSF(NP)
      IF(NN-IB)45,45,41
45    KT=K-L
      IR=0
      DØ62I=8,12
      IR=IR+1
62    CALL GRAPH(KI,ISYM,NP,TX(1),YD(1,IR),A1(1,I),A2(1,I),A3(1,I))
      DØ60I=1,7
60    CALL GRAPH(KI,ISYM,NP,TX(1),YV(1,I),A1(1,I),A2(1,I),A3(1,I))
      IA1=0
      IC1=0
      IB=0
      IC=0
      IF(KT-NN)43,43,41
43    NP=XSIGNF(KT,NP)
41    K=K-L
      IF(K)16,16,17
16    GØ TØ 75
      END(1,0,0,0,0,0,1,0,0,1,0,0,0,0,0)
```

SUBRØUTINE RUQ

```
      SUBRØUTINE RUQ(N,T,H,X,XD,XN,XDN,XDDN,TI)                         MP560000
      CØMMØN UK,RØ,PØ,SØ,D1,D2,DR,AR,ER,W1,W2,RØU,DAM,CØ,C1,C2,C3,VM,TN
     1,DA4,DA5,DA6
      DIMENSIØN X(6),XD(6),XN(201,6),XDN(201,7),XDDN(201,6),TI(201),XR(6MP560010
     1),XDR(6),Y1(6),Y2 (6),Y3(6),Y4(6),VM(3),TN(3,3)                  MP560015
D     DIMENSIØN UK(1),RØ(1),PØ(1),SØ(1),D1(1),D2(1),W1(1),W2(1),RØU(1),
     1CØ(1),C1(1),C2(1)
      DØ40I=1,N                                                         MP560020
      R=RØ+X(1)                                                         MP560025
      S=SØ+X(3)
      TI(I)=T
      E=VM(1)*X(4)**2+VM(2)*X(5)**2+VM(3)*X(6)**2
      E1=CØ-(C1*S*S+E)*XD(2)
      E2=C2*R**2+C1*S**2-E
      XDN(I,7)=E1/E2                                                    MP560045
      DØ7J=1,6                                                          MP560050
      XR(J)=X(J)                                                        MP560055
 7    XDR(J)=XD(J)                                                      MP560060
      CALL SEQ(XR,XDR,Y1,T)                                             MP560065
      DØ20J=1,6                                                         MP560070
      XN(I,J)=X(J)                                                      MP560075
      XDN(I,J)=XD(J)                                                    MP560080
      XDDN(I,J)=Y1(J)                                                   MP560085
      XDR(J)=XD(J)+H*Y1(J)/2.0                                          MP560090
 20   XR(J)=X(J)+H*XD(J)/2.0                                            MP560100
      T=T+H/2.0                                                         MP560105
      CALL SEQ(XR,XDR,Y2,T)                                             MP560110
      DØ30J=1,6                                                         MP560115
      XR(J)=X(J)+H*XD(J)/2.0+H**2*Y1(J)/4.0                             MP560120
 30   XDR(J)=XD(J)+H*Y2(J)/2.0                                          MP560125
      CALL SEQ(XR,XDR,Y3,T)                                             MP560130
      DØ35J=1,6                                                         MP560135
      XR(J)=X(J)+H*XD(J)+H**2*Y2(J)/2.0                                 MP560140
 35   XDR(J)=XD(J)+H*Y3(J)                                              MP560145
      T=T+H/2.0                                                         MP560150
      CALL SEQ(XR,XDR,Y4,T)                                             MP560155
      DØ40J=1,6                                                         MP560160
      X(J)=X(J)+H*(XD(J)+H*(Y1(J)+Y2(J)+Y3(J))/6.0)                     MP560165
 40   XD(J)=XD(J)+H*(Y1(J)+2.0*Y2(J)+2.0*Y3(J)+Y4(J))/6.0               MP560170
      RETURN                                                            MP560175
      END(1,0,0,0,0,0,1,0,0,1,0,0,0,0,0)
```

```
        SUBRØUTINE SEQ(X,XD,XDD,T)                                          MP560000
        DIMENSIØN X(6),XD(6),XDD(6),VM(3),TN(3,3)                           MP560005
        CØMMØN UK,RØ,PØ,SØ,D1,D2,DR,AR,ER,W1,W2,RØU,DAM,CØ,C1,C2,C3,VM,TN
       1,DA4,DA5,DA6
D       DIMENSIØN UK(1),RØ(1),PØ(1),SØ(1),D1(1),D2(1),W1(1),W2(1),RØU(1),
       1CØ(1),C1(1),C2(1)
 1      SF=SINF(X(2))                                                       MP560015
 2      CF=CØSF(X(2))                                                       MP560020
 3      R=RØ+X(1)                                                           MP560025
        S=SØ+X(3)
 4      Y=VM(1)*X(4)**2+VM(2)*X(5)**2+VM(3)*X(6)**2                         MP560030
        SX=VM(1)*X(4)*XD(4)+VM(2)*X(5)*XD(5)+VM(3)*X(6)*XD(6)
D       Y1=S*S
D       R2=R*R
        AA=XD(1)
        AB=XD(2)
        AC=XD(3)
D       A1=RØU*AC*AA/C2
D       A2=CØ-(C1*Y1+Y)*AB
D       A3=C2*R2+C1*Y1+Y
D       A4=A2/A3
D       A5=R*A4*A4
D       A6=UK/R2
 13     XDD(1)=A5-A1-A6                                                     MP560075
 14     B1=3.0*UK*SF*CF/R**3                                                MP560080
 15     B2=C1*Y1-Y                                                          MP560085
 16     B3=C1*Y1+Y                                                          MP560090
 17     B4=B2/B3                                                            MP560095
 18     B5=1.0+C1*Y1/(C2*R2)+Y/(C2*R2)                                      MP560100
        B6=2.0*XD(2)*(C1*S*XD(3)+SX)/(C2*R2)
        Q1=(C2*R*XD(1)+C1*S*XD(3)+SX)/(C2*R2)
        B7=B3*Q1*XD(2)/A3
        Q2=(2.0*C1*S*XD(3)+2.0*SX)
        B8=Q2/B3
        B9=2.0*CØ*Q1/A3
        Q3=CØ*(2.0*C1*S*XD(3)+SX)/(C2*R2)
        Q4=Q3/B3
        XDD(2)=B6-B7-B8+B9-Q4-B1*B4*B5
 20     E1=CØ+C2*R2*XD(2)                                                   MP560110
 22     E3=E1/A3                                                            MP560115
 23     E5=ER*AR*(S-DR)/(C1*DR)
 24     E6=UK*S*(3.0*CF**2-1.0)/R**3
        E4=S*E3**2-DAM*XD(3)*(A4+XD(2))
 26     XDD(3)=E4-E5+E6
 27     F1=UK*(3.0*SF**2-1.0)*X(4)/R**3-DA4*XD(4)*(A4+XD(2))
 28     F2=E3*(TN(1,1)/VM(1)-1.0)*X(4)                                      MP560145
```

```
29    F3=(TN(1,2)*X(5)+TN(1,3)*X(6))/VM(1)                              MP560150
30    F4=E3**2*F3                                                       MP560155
31    XDD(4)=F1-F2-F4
      Q5=UK*(3.0*SF**2-1.0)*X(5)/R**3-DA5*XD(5)*(A4+XD(2))
32    G1=E3*(TN(2,2)/VM(2)-1.0)*X(5)                                    MP560165
33    G2=(TN(2,1)*X(4)+TN(2,3)*X(6))/VM(2)                              MP560170
34    G3=E3**2*G2                                                       MP560175
      XDD(5)=Q5-G1-G3
      Q6=UK*(3.0*SF**2-1.0)*X(6)/R**3-DA6*XD(6)*(A4+XD(2))
36    H1=E3*(TN(3,3)/VM(3)-1.0)*X(6)                                    MP560185
37    H2=(TN(3,1)*X(4)+TN(3,2)*X(5))/VM(3)                              MP560190
38    H3=E3**2*H2                                                       MP560195
      XDD(6)=Q6-H1-H3
      RETURN                                                            MP560205
      END(1,0,0,0,0,0,1,0,0,1,0,0,0,0,0)
```

APPENDIX H

PROGRAM FOR SPIN DYNAMICS OF ROTATING SPACE STATIONS

An analysis of the rigid body angular motions of the space station is presented in Section 9.0. The FØRTRAN computer program written for this investigation is described in this appendix.

The program consists of a main program and several levels of subprograms. Figure H-1 shows the interrelationship among the main prøgram and six of the enclosed subroutine subprograms. The MAIN PRØGRAM communicates with SUBRØUTINE RKS3 (SHARE program D2*ATFRKS3, "FØRTRAN Floating-Point Runge-Kutta with Simpson's Rule check") and SUBRØUTINE CRVS. The RKS3 subroutine is written in FAP, and has been modified slightly to make it compatible with the FØRTRAN II system at NAA. RKS3 communicates only with SUBRØUTINE DERIV and SUBRØUTINE CNTRL. The DERIV subroutine in turn communicates with SUBRØUTINE XYZ and SUBRØUTINE EMXYZ. These enclosed subroutines utilize certain library and built-in subprograms; SUBRØUTINE CRVS also communicates with several subprograms used to plot polar and rectilinear graphs of the computed results.

RKS3 performs a fourth-order Runge-Kutta integration in the variable interval mode on the system of equations consisting of equations (253) and (254). DERIV computes the current values of the derivatives of the system, using equations (257) through (259). the current position coordinates and velocity components of the moving masses m_n as supplied by XYZ, and the current values of the time-dependent external moments M_x, M_y and M_z as supplied by EMXYZ. CNTRL outputs and stores the current values of the system and effects a normal exit from RKS3 to the MAIN PRØGRAM when the integration limit is reached.

In general, each case involving mass transfer requires a specially written XYZ subroutine. Storage has been allocated for a maximum of ten discrete moving masses m_n. It should be noted that the data location EM(10) = m_{10} is utilized for internal routing when multiple cases are run in one job. If no mass transfer takes place, Subrøutine XYZ is not called by the program.

Each case in which the external moments M_x, M_y, and M_z are functions of time—e.g., control moments and spin-up—requires a specially

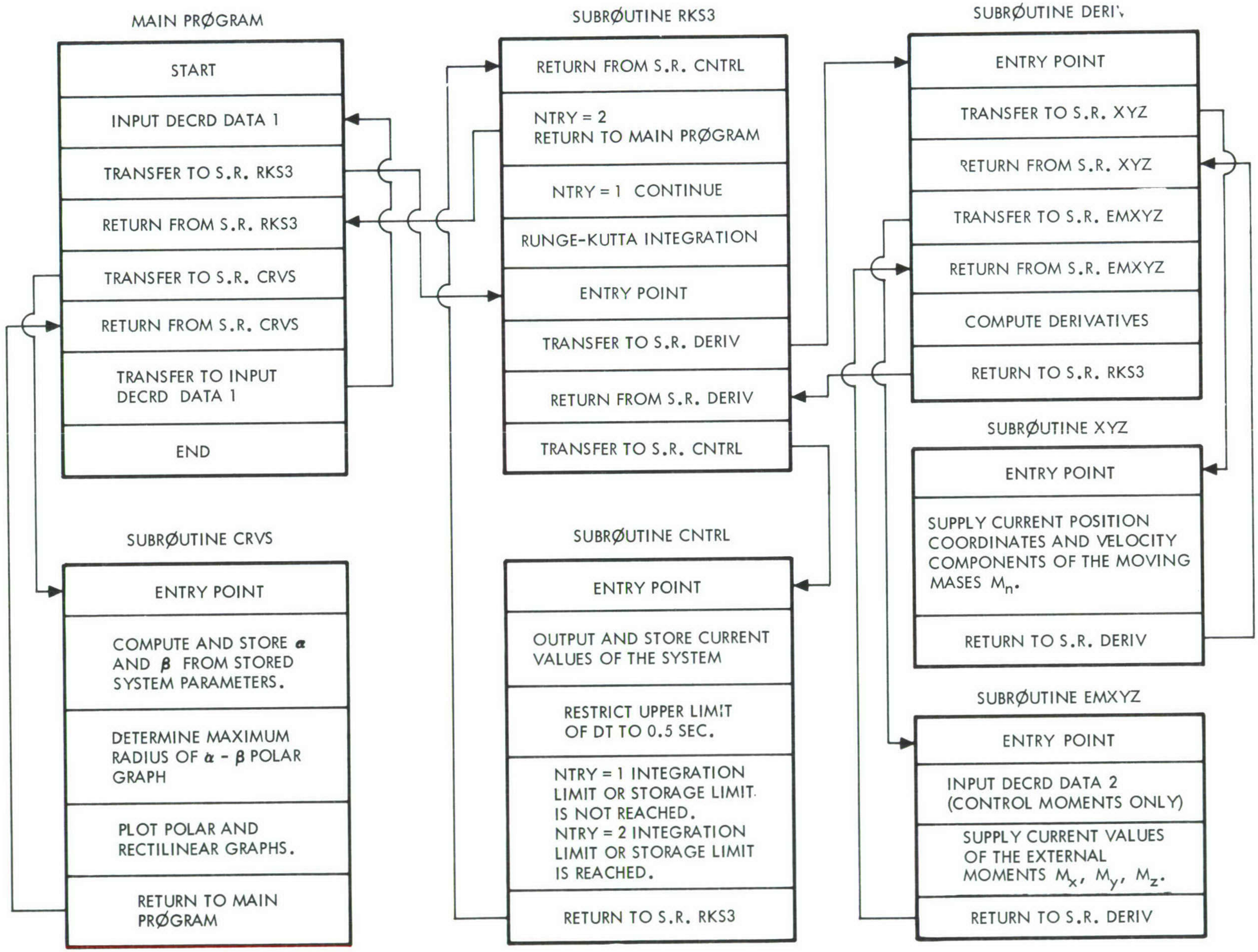

Figure H - 1 Logic Flow Between Subroutines

written EMXYZ subroutine. When the external moments are constants, a dummy EMXYZ subroutine is used and the values of the constant moments are read in as data.

Both polar and rectilinear graphs are plotted according to the instructions in SUBRØUTINE CRVS. CRVS also computes and stores the values of and by using equations (256). SUBRØUTINE GRAPH is a package routine that produces high-quality rectilinear graphical output on the S-C 4020 CRT plotter. The GRAPH subroutine package (Deck No. 9J-400) used in this program was written at S&ID. The polar graphs were plotted on the S-C 4020 CRT plotter by using a subroutine package that requires the CAMRAV, PGRIDV, PPLØTV, PLABEL and PLINE subroutines to be called by the program.

The floating-point input data are defined on the sample data sheets. The variables, including array names, appearing in CØMMØN from XN through EMZ are the FØRTRAN names of the input data (the order in CØMMØN has been retained) in the first call for the DECRD (decimal-read) subroutine. The second call for DECRD is made only when velocity proportional control moments are considered for wobble damping.

The listings of two program deck setups are included herein. The first set of listings and the input data were used to compute the results plotted in Figures 64, 65, and 66. These graphs represent the response of Configuration Y-A to three cases of internal mass motions. Following these listings are those of three subroutine decks that are used when velocity proportional control moments are used to damp wobble. These decks replace their respective decks in the first deck setup. Input data used to compute the results plotted in Figure 79, the damped wobble response of Configuration 6-A, are also listed.

The subprogram decks used in computing the response of the space station to docking and spin-up operations are very similar to the decks used to investigate internal mass motions and wobble damping. The listings of these decks are therefore not included.

FORTRAN FIXED 10 DIGIT DECIMAL DATA

DECK NO. ______ PROGRAMMER ______ DATE ______ PAGE 1 of 4 JOB NO. ______

SAMPLE DECRD DATA SHEETS
for
"Spin Dynamics of Rotating Space Stations"
Runge-Kutta numerical integration
* Internal mass motions
* Proportional control moments

Col.	NUMBER	IDENTIFICATION	DESCRIPTION DO NOT KEY PUNCH
1	1		
13			n = Number of moving masses m_n = 0, 1, 2, ..., 10
25			t_{max} = Time at which computation is terminated, seconds
37			dt = Initial time increment, seconds
49		73 80	t = Initial value of time, seconds
61		1 0	RSV = Reserve data location
1	6		
13			I_{mx} - Moments of Inertia — Inertial Values of
25			I_{my} — Space Station
37			I_{mz} — excluding moving
49		73 80	I_{mxy} - Products of Inertia — masses m_n,
61		2 0	I_{myz} — Slug-ft^2
1	1 1		
13			I_{mxz}
25			M = Mass of Space Station excluding moving masses m_n, Slugs
37			m_1
49		73 80	m_2
61		3 0	m_3
1	1 6		
13			m_4 - Mass of individual moving masses, m_n, Slugs
25			m_5
37			m_6
49		73 80	m_7
61		4 0	m_8

Form 114-C-17 Rev. 7-58 (Vellum)

FORTRAN FIXED 10 DIGIT DECIMAL DATA

DECK NO. ______ PROGRAMMER ______ DATE ______ PAGE 2 of 4 JOB NO. ______

	NUMBER	IDENTIFICATION	DESCRIPTION	DO NOT KEY PUNCH
1	2 1			
13			m_9	
25			m_{10}	Option: Internal routing number for multiple case jobs.
37			p	= Initial angular velocity about x-axis, Rad/sec.
49		73 80	q	= Initial angular velocity about y-axis, Rad/sec.
61		5 0	r	= Initial angular velocity about z-axis, Rad/sec.
1	2 6			
13			ϕ	
25			θ	- Initial values of the Euler angles, Radians
37			ψ	
49		73 80	ATABL (1)	
61		6 0	(2)	
1	3 1			Absolute interval control
13			(3)	numbers for variable interval mode.
25			(4)	
37			(5)	
49		73 80	(6)	
61		7 0	RTABL (1)	
1	3 6			
13			(2)	Relative interval control
25			(3)	numbers for interval mode.
37			(4)	
49		73 80	(5)	
61		8 0	(6)	

SAMPLE DECRD DATA SHEETS

Form 114-C-17 Rev. 7-58 (Vellum)

FORTRAN FIXED 10 DIGIT DECIMAL DATA

DECK NO. ______ PROGRAMMER ______ DATE ______ PAGE 3 of 4 JOB NO. ______

	NUMBER		IDENTIFICATION	DESCRIPTION DO NOT KEY PUNCH
1	–	4 1		
13				M_x = Constant moment about x-axis, Ft-lb.
25				M_y = Constant moment about y-axis, Ft-lb.
37				M_z = Constant moment about z-axis, Ft-lb.
49			73 80	
61			9 0	
1				
13				
25				
37				
49			73 80	
61				
1				
13				
25				
37				
49			73 80	
61				
1				
13				
25				
37				
49			73 80	
61				

SAMPLE DECRD DATA SHEETS

Form 1[illegible]-C-17 Rev. 7-58 (Vellum)

FORTRAN FIXED 10 DIGIT DECIMAL DATA

DECK NO. ______ PROGRAMMER ______ DATE ______ PAGE 4 of 4 JOB NO. ______

SAMPLE DECRD DATA

Second DECRD Call

Proportional Control Moment Coefficients

	NUMBER	IDENTIFICATION	DESCRIPTION DO NOT KEY PUNCH
1	1		
13			C_1
25			C_2
37			C_3
49		73 80	C_4
61		100	C_5
1	6		
13			C_6 $M_x = C_1p + C_2q + C_3r + C_4$
25			C_7
37			C_8 $M_y = C_5p + C_6q + C_7r + C_8$
49		73 80	C_9
61		110	C_{10} $M_z = C_9p + C_{10}q + C_{11}r + C_{12}$
1	11		
13			C_{11}
25			C_{12}
37			C_{13}
49		73 80	C_{14} - Reserve data locations
61		120	C_{15}
1			Note: (1) Second DECRD data is not called unless Control
13			Moment decks are used
25			(2) When Control Moment decks are used, index
37			locations 41, 42 and 43 of first DECRD data are
49		73 80	used to store the computed values of M_x, M_y, and
61			M_z from SUBRØUTINE EMXYZ

Form 114-C-17 Rev. 7-58 (Vellum)

MAIN PRØGRAM

```
C                DECK NØ. 9J-RKM              RUNGE-KUTTA METHØD
C                                  MAIN PRØGRAM
C                               NØ CØNTRØL MØMENTS
F      DERIV, CNTRL
       CØMMØN   XN, TMAX, DT, T, RSV,      AIMX, AIMY, AIMZ, AIMXY, AIMYZ,
     X          AIMXZ, EMASS, EM, VAR, ATABL, RTABL, EMX, EMY, EMZ,  TIME,
     X          WØRK, DRV, IFVD, IBKP, NTRY, IERR, I, N, YCRV,
     X     X,Y,Z,XD,YD,ZD,SX,SY,SZ,SXD,SYD,SZD,SXY,SYZ,SXZ,SXYD,SYZD,
     X     SXZD,SX2,SY2,SZ2,SXD2,SYD2,SZD2,SXY2,SYZ2,SXZ2,SXYD2,SYZD2,
     X     SXZD2,AIX,AIY,AIZ,AIXD,AIYD,AIZD,AIXY,AIYZ,AIXZ,AIXYD,AIXZD,
     X          T1,T2,T3,T4,T5,T6,A, B,SM1,SMM,SPHI,CPHI,CTHETA
C
       DIMENSIØN  XN(1), EM(10), VAR(6),ATABL(6), RTABL(6), WØRK(60),
     X           DRV(6), TIME(500), X(10), Y(10), Z(10), XD(10), YD(10),
     X             ZD(10), A(3,3), B(3), YCRV(6,500)
C
    10 CALL DECRD(XN)
       N=XN
C                                PRINT DATA
       PRINT 15, (XN(I), I=1, 42)
    15 FØRMAT(1H1,36X,27HDATA FØR RUNGE-KUTTA METHØD/(/1P6E17.7))
       PRINT 25
    25 FØRMAT(1H1,40X,19HRUNGE-KUTTA RESULTS/36X,28HTIME   VARIABLES   DERI
      XVATIVES)
C                INITILIZE AND CØMPUTE  CØNSTANTS
       I=C
       NØ=6
       IFVD = C
       IBKP = 1
       SM=EMASS
       DØ 30 I=1,N
    30 SM=SM+EM(I)
       SM1=1.C/SM
       SMM= EMASS * SM1
C
       CALL RKS3(DERIV, CNTRL, VAR, DRV, ATABL, RTABL, WØRK, T, DT, NØ, I
      XFVD, IBKP, NTRY, IERR)
       IF(IERR)40, 50, 40
    40 PRINT 45, IERR
    45 FØRMAT(1H1,40X,20HERRØR RETURN    IERR=,I3)
       GØ TØ 60
C                                PLØT CURVES
    50 CALL CRVS(I,YCRV,TIME)
    60 GØ TØ 10
       END
```

SUBRØUTINE RKS3

```
*       FAP                                                                     RKS30000
        COUNT   322                                                             RKS30010
*RUNGE-KUTTA INTEGRATIØN WITH SIMPSØN'S RULE CHECK                              RKS30020
        LBL     RKS3,X                                                          RKS30030
        ENTRY   RKS3 (DERIV,CNTRL,Y,DY,ATABL,RTABL,WØRK,X,DX,N,IFVD             RKS30040
        REM                          ,IBKP,NTRY,IERR)                           RKS30050
        ENTRY   SMP3 (DERIV,CNTRL,Y,DY,ATABL,RTABL,WØRK,X,DX,N,IFVD             RKS30060
        REM                          ,IBKP,NTRY,IERR)                           RKS30070
 DERIV  TTR     **                   TRANSFER VECTØR                            RKS30080
 CNTRL  TTR     **                   TRANSFER VECTØR                            RKS30090
        PZE                                                                     RKS30100
        BCI     1,RKS3                                                          RKS30110
 RKS3   CAL     =HRKS3                                                          RKS30120
        SLW     RKS3-1                                                          RKS30130
        CAL     RKI1                 SET VARIABLE INSTRUCTIØNS                  RKS30140
        LDQ     RKI2                 FØR RUNGE-KUTTA                            RKS30150
        TRA     SMP3+4                                                          RKS30160
 SMP3   CAL     =HSMP3                                                          RKS30170
        SLW     RKS3-1                                                          RKS30180
        CAL     RKI3                 SET VARIABLE INSTRUCTIØNS                  RKS30190
        LDQ     RKI4                 FØR SIMPSØN'S RULE                         RKS30200
        SLW     RKV1                                                            RKS30210
        STQ     RKV2                                                            RKS30220
        SXA     RKXT,1               SAVE STATUS                                RKS30230
        SXA     RKXT+1,2                                                        RKS30240
        SXD     RKS3-2,4                                                        RKS30250
 RKB    CAL     1,4                  SET DERIV                                  RKS30260
        STA     DERIV                                                           RKS30270
        CAL     2,4                  SET CØNTRØL                                RKS30280
        STA     CNTRL                                                           RKS30290
        CLA     3,4                  SET Y                                      RKS30300
        ADD     RKØNE                                                           RKS30310
        STA     RKL+7                                                           RKS30320
        CLA     4,4                  SET DY                                     RKS30330
        ADD     RKØNE                                                           RKS30340
        STA     RKL+8                                                           RKS30350
        CLA     5,4                  SET ABS. ERRØR TABLE                       RKS30360
        ADD     RKØNE                                                           RKS30370
        STA     RKL+6                                                           RKS30380
        CLA     6,4                  SET REL. ERRØR TABLE                       RKS30390
        ADD     RKØNE                                                           RKS30400
        STA     RKL+5                                                           RKS30410
        CLA     8,4                  SET X                                      RKS30420
        STA     RKL+3                                                           RKS30430
        CLA     9,4                  SET DELTA-X                                RKS30440
        STA     RKL+4                                                           RKS30450
        CLA     10,4                 GET N                                      RKS30460
        STA     *+1                                                             RKS30470
        LXD     **,1                                                            RKS30480
 RKFVE  PXA     5,1                                                             RKS30490
        STA     RKN                  SET IR1 LØADER                             RKS30500
        STØ     RKAS                 SET N ADDER                                RKS30510
```

```
         ALS     3                FORM 7N+5                          RKS30520
         SUB     RKAS                                                RKS30530
         ADD     RKFVE                                               RKS30540
         STA     RKW              SET CLEARS                         RKS30550
         CLA     7,4              GET WORK AREA                      RKS30560
         STA     RKW+1            SET CLEAR                          RKS30570
         AXT     6,1                                                 RKS30580
         TRA     *+2                                                 RKS30590
         SUB     RKONE                                               RKS30600
         STA     RKL+15,1         SET 1-WORD REGIONS                 RKS30610
         TIX     *-2,1,1                                             RKS30620
         TXI     *+2,1,8                                             RKS30630
         SUB     RKAS                                                RKS30640
         STA     RKL+24,1         SET N-WORD REGIONS                 RKS30650
         TIX     *-2,1,1                                             RKS30660
         CLA     11,4             SET F-V KEY                        RKS30670
         STA     RKL+2                                               RKS30680
         CLA     12,4                                                RKS30690
         STA     *+1                                                 RKS30700
         CLA     **                                                  RKS30710
         ARS     3                                                   RKS30720
         STT     RKOP             SET BAKUP LOOP CONTROL             RKS30730
         CLA     14,4             SET ERROR KEY                      RKS30740
         STA     RKL+1                                               RKS30750
         STZ*    RKL+1            SET TO NORMAL                      RKS30760
         CLA     13,4             GET RE-ENTRY KEY                   RKS30770
         STO     RKC1+3           SET CNTRL CALL                     RKS30780
         STA     RKC1+1                                              RKS30790
         STA     RKC1+6                                              RKS30800
         SXA     RKSW,1           SET STEP-SWITCH TO 1               RKS30810
RKW      AXT     **,1             GET 7N+5                           RKS30820
         STZ     **,1             CLEAR WORK-REGIONS                 RKS30830
         TIX     *-1,1,1                                             RKS30840
         CLA*    RKL+4            SET STARTING DELTA-X FOR           RKS30850
         STO*    RKL+9            POSSIBLE PRINT-OUT                 RKS30860
         TSX     DERIV,4          TO DERIV                           RKS30870
         TXI     *+2,,1                                              RKS30880
         PZE     RKS3-2                                              RKS30890
RKC1     CLA     RKDC1            SET NORMAL RE-ENTRY                RKS30900
         STO     **                                                  RKS30910
         TSX     CNTRL,4          TO CNTRL                           RKS30920
         TSX     **,0             CALL PARAMETER = NTRY              RKS30930
         TXI     *+2,,0                                              RKS30940
         PZE     RKS3-2                                              RKS30950
         LXD     **,4                                                RKS30960
         TRA     RKN+1,4          DO NTRY-CONTROLLED JUMP            RKS30970
         TRA     RKW              TO RE-START                        RKS30980
         TRA     RKBK             TO BAKUP                           RKS30990
         TRA     RKXT             TO FINAL EXIT                      RKS31000
RKN      AXT     **,1             GET N FOR STEP START               RKS31010
         CLA*    RKL+3            X TO X-ZERO                        RKS31020
         STO*    RKL+13                                              RKS31030
         CLA*    RKL+10           XL TO XL-ZERO                      RKS31040
         STO*    RKL+14                                              RKS31050
RKN3     CLA*    RKL+7            Y TO Y-ZERO                        RKS31060
         STO*    RKL+18                                              RKS31070
         CLA*    RKL+15           YL TO YL-ZERO                      RKS31080
         STO*    RKL+19                                              RKS31090
         CLA*    RKL+8            DY TO DY-ZERO                      RKS31100
         STO*    RKL+21                                              RKS31110
         STZ*    RKL+22           CLEAR DELTA-Y                      RKS31120
         TIX     RKN3,1,1                                            RKS31130
```

```
RKE9  CLA*   RKL+4           GET DELTA-X                      RKS31140
      TZE    RKDE            TO ZERO DELTA ERROR              RKS31150
      STO*   RKL+9           SAVE                             RKS31160
      FDP    RKC+2                                            RKS31170
      STQ    RKHD            SET DX/2                         RKS31180
      XCA                                                     RKS31190
      FDP    RKC+2                                            RKS31200
      STQ    RKQD            SET DX/4                         RKS31210
RKE7  LXA    RKN,1                                            RKS31220
      LDQ*   RKL+8           K1/2 TO CUMULATIVE               RKS31230
      FMP    RKQD                                             RKS31240
      STO*   RKL+23                                           RKS31250
      CLA*   RKL+15          YL TO YL-HALF                    RKS31260
      STO*   RKL+17                                           RKS31270
      CLA*   RKL+7           Y TO Y-HALF                      RKS31280
      STO*   RKL+16                                           RKS31290
      FAD*   RKL+23          STEP Y                           RKS31300
      STO*   RKL+7                                            RKS31310
      TIX    RKE7+1,1,1                                       RKS31320
      CLA*   RKL+10          XL TO XL-HALF                    RKS31330
      STO*   RKL+12                                           RKS31340
      CLA*   RKL+3           X TO X-HALF                      RKS31350
      STO*   RKL+11                                           RKS31360
      FAD    RKQD            STEP X                           RKS31370
      STO*   RKL+3                                            RKS31380
RKV1  AXC    **,4            VARIABLE RE-ENTRY SETTING        RKS31390
      TRA    DERIV           TO DERIV                         RKS31400
      TXI    *+2,,2                                           RKS31410
      PZE    RKS3-2                                           RKS31420
RKE3  LXA    RKN,1                                            RKS31430
      LDQ*   RKL+8           FORM K2/2                        RKS31440
      FMP    RKQD                                             RKS31450
      STO    RKAS            SAVE                             RKS31460
      FAD*   RKL+16                                           RKS31470
      STO*   RKL+7           STEP Y                           RKS31480
      CLA    RKAS                                             RKS31490
      FAD    RKAS            FORM K2                          RKS31500
      FAD*   RKL+23                                           RKS31510
      STO*   RKL+23          ADD TO CUMULATIVE                RKS31520
      TIX    RKE3+1,1,1                                       RKS31530
RKI3  AXC    *+1,4           SET RE-ENTRY KEY                 RKS31540
      TRA    DERIV           TO DERIV                         RKS31550
      TXI    *+2,,3                                           RKS31560
      PZE    RKS3-2                                           RKS31570
RKE4  LXA    RKN,1                                            RKS31580
      LDQ*   RKL+8           FORM K3                          RKS31590
RKV2  PZE    **              VARIABLE MULTIPLY                RKS31600
      STO    RKAS            SAVE                             RKS31610
      FAD*   RKL+16                                           RKS31620
      STO*   RKL+7           STEP Y                           RKS31630
      CLA    RKAS                                             RKS31640
      FAD*   RKL+23          ADD K3 TO CUMULATIVE             RKS31650
      STO*   RKL+23                                           RKS31660
      TIX    RKE4+1,1,1                                       RKS31670
      CLA    RKHD            DOUBLE PRECISION                 RKS31680
      FAD*   RKL+11          X-HALF + DELTA/2                 RKS31690
      STO    RKAS            TO X                             RKS31700
      XCA                                                     RKS31710
      FAD*   RKL+12                                           RKS31720
      FAD    RKAS                                             RKS31730
      STO*   RKL+3                                            RKS31740
      STQ*   RKL+10                                           RKS31750
```

```
         TSX   DERIV,4        TO DERIV                      RKS31760
         TXI   *+2,,4                                       RKS31770
         PZE   RKS3-2                                       RKS31780
RKE5     LXA   RKN,1                                        RKS31790
         LDQ*  RKL+8          DY * DELTA/4                  RKS31800
         FMP   RKQD                                         RKS31810
         FAD*  RKL+23         + CUMULATIVE                  RKS31820
         FDP   RKC+3          TOTAL / 3                     RKS31830
         STQ*  RKL+23         SAVE INCREMENT                RKS31840
         XCA                                                RKS31850
         FAD*  RKL+16         DOUBLE PRECISION              RKS31860
         STO   RKAS           Y-HALF + INCREMENT            RKS31870
         XCA                  TO Y                          RKS31880
         FAD*  RKL+17                                       RKS31890
         FAD   RKAS                                         RKS31900
         STO*  RKL+7                                        RKS31910
         STQ*  RKL+15                                       RKS31920
         CLA*  RKL+23         STEP DELTA-Y                  RKS31930
         FAD*  RKL+22                                       RKS31940
         STO*  RKL+22                                       RKS31950
         TIX   RKE5+1,1,1                                   RKS31960
         TSX   DERIV,4        TO DERIV                      RKS31970
         TXI   *+2,,5                                       RKS31980
         PZE   RKS3-2                                       RKS31990
RKSW     AXC   **,1           FLIP SWITCH                   RKS32000
         SXA   RKSW,1                                       RKS32010
         TXL   RKFV,1,1       IF 1ST HALF                   RKS32020
         LXA   RKN,1          MOVE DY TO DY-HALF            RKS32030
         CLA*  RKL+8                                        RKS32040
         STO*  RKL+20                                       RKS32050
         TIX   *-2,1,1                                      RKS32060
         TRA   RKE7           TO 2ND HALF                   RKS32070
RKFV     ZET*  RKL+2          TEST FIXED-VARIABLE KEY       RKS32080
         TRA   RKC1           FIXED, TO NEXT STEP           RKS32090
         STZ   RKAS           VARIABLE, CLEAR MAX           RKS32100
         LXA   RKN,1                                        RKS32110
RKE8     LDQ*  RKL+7          FORM REL ERROR TOLERANCE      RKS32120
         FMP*  RKL+5                                        RKS32130
         SSP                                                RKS32140
         FAM*  RKL+6          ADD ABS ERROR TOLERANCE       RKS32150
         TZE   RKTE           TO ZERO CONTROL ERROR         RKS32160
         STO   RKQD           SAVE                          RKS32170
         LDQ*  RKL+20         FORM SIMPSON DELTA-Y          RKS32180
         FMP   RKC+4          4 * DY-HALF                   RKS32190
         FAD*  RKL+8          + DY                          RKS32200
         FAD*  RKL+21         + DY-ZERO                     RKS32210
         FDP   RKC+3          TOTAL / 3                     RKS32220
         FMP   RKHD           QUOTIENT * DELTA/2            RKS32230
         FSB*  RKL+22         SR - RK DELTA-Y               RKS32240
         FDP   RKQD           FORM ERROR RATIO              RKS32250
         CLA   RKAS                                         RKS32260
         LRS   0              CLEAR SIGN                    RKS32270
         TLQ   *+2            TEST                          RKS32280
         STQ   RKAS           SET NEW MAX                   RKS32290
         TIX   RKE8,1,1                                     RKS32300
         CLA   RKAS           GET MAX ERROR                 RKS32310
         CAS   RKC+1          TEST 1.0                      RKS32320
         TRA   RKC2           TO DECREASE AND BAKUP         RKS32330
         TRA   RKC3           TO DECREASE AND CONTINUE      RKS32340
         CAS   RKK+1          TEST 0.75                     RKS32350
         TRA   RKC3           TO DECREASE AND CONTINUE      RKS32360
         TRA   RKC1           TO CONTINUE                   RKS32370
```

```
        CAS    RKK            TEST 0.075                          RKS32380
        TRA    RKC1           TO CONTINUE                         RKS32390
        TRA    RKC1           TO CONTINUE                         RKS32400
        LDQ*   RKL+4          INCREASE AND CONTINUE               RKS32410
        FMP    RKC                                                RKS32420
        STO*   RKL+4                                              RKS32430
        TRA    RKC1                                               RKS32440
RKC2    CLA*   RKL+4          DECREASE AND BAKUP                  RKS32450
        FDP    RKC                                                RKS32460
        STQ*   RKL+4                                              RKS32470
RKOP    TXL    RKBK,**,0      OPTIONAL DECREASE LOOP              RKS32480
        CLA    RKAS                                               RKS32490
        FDP    RKC+5          MAX/10                              RKS32500
        STQ    RKAS                                               RKS32510
        CLA    RKC+1          TEST 1.0                            RKS32520
        TLQ    RKBK           OK- TO BAKUP                        RKS32530
        TRA    RKC2           TO DECREASE AGAIN                   RKS32540
RKC3    CLA*   RKL+4          DECREASE AND CONTINUE               RKS32550
        FDP    RKC                                                RKS32560
        STQ*   RKL+4                                              RKS32570
        TRA    RKC1           TO CONTINUE                         RKS32580
RKBK    LXA    RKN,1          RESET TO REPEAT LAST STEP           RKS32590
        CLA*   RKL+21         WITH SMALLER INTERVAL               RKS32600
        STO*   RKL+8          DY-ZERO TO DY                       RKS32610
        CLA*   RKL+18                                             RKS32620
        STO*   RKL+7          Y-ZERO TO Y                         RKS32630
        CLA*   RKL+19                                             RKS32640
        STO*   RKL+15         YL-ZERO TO YL                       RKS32650
        STZ*   RKL+22         CLEAR DELTA-Y                       RKS32660
        TIX    RKBK+1,1,1                                         RKS32670
        CLA*   RKL+13         X-ZERO TO X                         RKS32680
        STO*   RKL+3                                              RKS32690
        CLA*   RKL+14         XL-ZERO TO XL                       RKS32700
        STO*   RKL+10                                             RKS32710
        TRA    RKE9           TO REPEAT STEP                      RKS32720
RKDE    CLS    RKDC1          SET NEG FOR ZERO DELTA ERROR EXIT   RKS32730
        STO*   RKL+1                                              RKS32740
        TSX    $ESCORT,4                                          RKS32750
        TSX    DERR,0                                             RKS32760
        TSX    =0.,0                                              RKS32770
        TXI    RKXT,,0                                            RKS32780
        PZE    RKS3-2                                             RKS32790
RKTE    CLA    RKDC1          SET POS FOR ZERO ERROR CONTROL EXIT RKS32800
        STO*   RKL+1                                              RKS32810
        TSX    $ESCORT,4                                          RKS32820
        TSX    ARERR,0                                            RKS32830
        TSX    =0.,0                                              RKS32840
        TXI    RKXT,,0                                            RKS32850
        PZE    RKS3-2                                             RKS32860
RKXT    AXT    **,1           RESTORE STATUS                      RKS32870
        AXT    **,2                                               RKS32880
        LXD    RKS3-2,4                                           RKS32890
        TRA    15,4           EXIT                                RKS32900
RKL            0              ADDRESSES OF DERIV                  RKS32910
               0              1      ERROR KEY                    RKS32920
               0              2      FIXED-VARIABLE DELTA KEY     RKS32930
               0              3      X                            RKS32940
               0              4      DELTA-X TO BE USED IN NEXT STEP RKS32950
               0,1            5      R(I), RELATIVE ERROR CONTROLS RKS32960
               0,1            6      A(I), ABSOLUTE ERROR CONTROLS RKS32970
               0,1            7      Y                            RKS32980
               0,1            8      DY                           RKS32990
```

```
               0                    9      DELTA-X USED IN COMPLETED STEP     RKS33000
               0                    10     LOW-ORDER X                        RKS33010
               0                    11     X-HALF                             RKS33020
               0                    12     L.O. X-HALF                        RKS33030
               0                    13     X-ZERO                             RKS33040
               0                    14     L.O. X-ZERO                        RKS33050
               0,1                  15     L.O. Y                             RKS33060
               0,1                  16     Y-HALF                             RKS33070
               0,1                  17     L.O. Y-HALF                        RKS33080
               0,1                  18     Y-ZERO                             RKS33090
               0,1                  19     L.O. Y-ZERO                        RKS33100
               0,1                  20     DY-HALF                            RKS33110
               0,1                  21     DY-ZERO                            RKS33120
               0,1                  22     DELTA-Y FOR STEP                   RKS33130
               0,1                  23     WORK REGION                        RKS33140
RKI1   AXC     RKV1+1,4             RK RE-ENTRY                               RKS33150
RKI2   FMP     RKHD                 FORM RK K3                                RKS33160
RKI4   FMP*    RKL+4                FORM SR K3                                RKS33170
RKC    DEC     1.5848932,1.0,2.0,3.0,4.0,10.0                                 RKS33180
RKK    DEC     0.075,0.75                                                     RKS33190
RKONE  PZE     1                                                              RKS33200
RKDC1  PZE     0,0,1                                                          RKS33210
RKAS   PZE     0                                                              RKS33220
RKHD   PZE     0                                                              RKS33230
RKQD   PZE     0                                                              RKS33240
 DERR  BCI     6,INTEGRATION INTERVAL EQUALS ZERO.                            RKS33250
       OCT     777777777777                                                   RKS33260
ARERR  BCI     5,PERMISSIBLE ERROR EQUALS ZERO.                               RKS33270
       OCT     777777777777                                                   RKS33280
       END                                                                    RKS33290
```

SUBRØUTINE DERIV

```
C                                DECK NØ. 9J-DRV
      SUBRØUTINE DERIV
C
C
      CØMMØN  XN, TMAX, DT, T, RSV,    AIMX, AIMY, AIMZ, AIMXY, AIMYZ,
     X        AIMXZ, EMASS, EM, VAR, ATABL, RTABL, EMX, EMY, EMZ,  TIME,
     X        WØRK, DRV, IFVD, IBKP, NTRY, IERR, I, N, YCRV,
     X    X,Y,Z,XD,YD,ZD,SX,SY,SZ,SXD,SYD,SZD,SXY,SYZ,SXZ,SXYD,SYZD,
     X    SXZD,SX2,SY2,SZ2,SXD2,SYD2,SZD2,SXY2,SYZ2,SXZ2,SXYD2,SYZD2,
     X    SXZD2,AIX,AIY,AIZ,AIXD,AIYD,AIZD,AIXY,AIYZ,AIXZ,AIXYD,AIXZD,
     X        T1,T2,T3,T4,T5,T6,A, B,SM1,SMM,SPHI,CPHI,CTHETA
     X      ,CMX,CMY,CMZ,C
C
      DIMENSIØN  XN(1), EM(10), VAR(6),ATABL(6), RTABL(6), WØRK(60),
     X           DRV(6), TIME(500),X(10), Y(10), Z(10), XD(10), YD(10),
     X           ZD(10), A(3,3), B(3), YCRV(6,500),C(15)
C                          CØMPUTE X,Y,Z, XDØT,YDØT AND ZDØT
      DIMENSIØN  XSQ(10),YSQ(10),ZSQ(10),YYD(10),ZZD(10),  XXD(10),
     X           XY(10),YZ(10),XZ(10),XYD(10),YZD(10), XZD(10),TEMP(3)
      PC=VAR(1)
      QC=VAR(2)
      RC=VAR(3)
      PHC=VAR(4)
      THC=VAR(5)
      PSC=VAR(6)
      IF(N)150,150,100
  100 CALL XYZ
      GØ TØ 210
  150 AIX=AIMX
      AIY=AIMY
      AIZ=AIMZ
      AIXY=AIMXY
      AIYZ=AIMYZ
      AIXZ=AIMXZ
      CALL EMXYZ
      GØ TØ 650
C                         CØMPUTE  MX, MY, MZ
  210 CALL EMXYZ
C          ** CØMPUTE MØMENTS AND PRØDUCTS ØF INERTIA
C             CØMPUTE TIME-RATES-ØF-CHANGE ØF MØM AND PRØD ØF INERTIA
C               ** USE EQUATIØNS APPEARING IN MØNTHLY REPØRT NØ. 8
C                 * THESE EQUATIØNS ARE EXPRESSED IN TERMS ØF THE PØSITIØN
C                       AND VELØCITY ØF THE INSTANTANEØUS MASS CENTER(CM)
      DØ 300 I=1,N
      XSQ(I)=X(I)**2
      YSQ(I)=Y(I)**2
      ZSQ(I)=Z(I)**2
      YYD(I)=Y(I)* YD(I)
      ZZD(I)=Z(I)* ZD(I)
      XXD(I)=X(I)* XD(I)
      XY(I)=X(I)* Y(I)
      YZ(I)=Y(I)* Z(I)
      XZ(I)=X(I)* Z(I)
```

```
      XYD(I)=X(I)* YD(I)+ XD(I)* Y(I)
      YZD(I)=Y(I)*ZD(I)+ YD(I)* Z(I)
  300 XZD(I)=Z(I)* XD(I)+ ZD(I)* X(I)
      SX = 0.0
      SY =0.0
      SZ =0.0
      SXD=0.0
      SYD=0.0
      SZD=0.0
      SXY=0.0
      SYZ=0.0
      SXZ=0.0
      SXYD=0.0
      SYZD=0.0
      SXZD=0.0
      DO 400 I=1,N
      SX=SX + EM(I)*(YSQ(I)+ZSQ(I))
      SY=SY + EM(I)*(ZSQ(I)+XSQ(I))
      SZ=SZ + EM(I)*(XSQ(I) + YSQ(I))
      SXD=SXD + EM(I)*(YYD(I)+ZZD(I))
      SYD=SYD + EM(I)*(ZZD(I)+XXD(I))
      SZD=SZD + EM(I)*(XXD(I)+YYD(I))
      SXY=SXY + EM(I)* XY(I)
      SYZ=SYZ + EM(I)* YZ(I)
      SXZ=SXZ + EM(I)* XZ(I)
      SXYD=SXYD + EM(I) * XYD(I)
      SYZD=SYZD + EM(I) * YZD(I)
  400 SXZD=SXZD + EM(I) * XZD(I)
C                 COMPUTE LOCATION OF CM
      SX2 = 0.0
      SY2 = 0.0
      SZ2 = 0.0
      SXD2 = 0.0
      SYD2 = 0.0
      SZD2 = 0.0
      DO 500 I=1,N
      SX2 = SX2 + EM(I)*X(I)
      SY2 = SY2 + EM(I)*Y(I)
      SZ2 = SZ2 + EM(I)*Z(I)
      SXD2 = SXD2 + EM(I)*XD(I)
      SYD2 = SYD2 + EM(I)*YD(I)
  500 SZD2 = SZD2 + EM(I)*ZD(I)
C                 COMPUTE MOMENTS AND PRODUCTS OF INERTIA ABOUT G
      AIX = AIMX + SX - SM1*(SY2*SY2 + SZ2*SZ2)
      AIY = AIMY + SY - SM1*(SX2*SX2 + SZ2*SZ2)
      AIZ = AIMZ + SZ - SM1*(SX2*SX2 + SY2*SY2)
C
      AIXD = 2.0*(SXD - SM1*(SY2*SYD2 + SZ2*SZD2))
      AIYD = 2.0*(SYD - SM1*(SX2*SXD2 + SZ2*SZD2))
      AIZD = 2.0*(SZD - SM1*(SX2*SXD2 + SY2*SYD2))
C
      AIXY = AIMXY + SXY - SM1*SX2*SY2
      AIXZ = AIMXZ + SXZ - SM1*SX2*SZ2
      AIYZ = AIMYZ + SYZ - SM1*SY2*SZ2
C
      AIXYD = SXYD - SM1*(SX2*SXD2 +   SXD2*SY2)
      AIXZD = SXZD - SM1*(SX2*SZD2 +   SXD2*SZD)
      AIYZD = SYZD - SM1*(SY2*SZD2 +   SYD2*SZ2)
C                 COMPUTE 6 TERMS OF EULER'S EQUATIONS
      T1 = AIXD * PC -AIXYD * QC -AIXZD* RC
      T2 = AIYD * QC -AIYZD * RC -AIXYD* PC
      T3 = AIZD * RC -AIXZD * PC -AIYZD* QC
```

```
  650 T4 = AIZ * RC - AIXZ * PC - AIYZ * QC                             00011300
      T5 = AIX * PC - AIXY * QC - AIXZ * RC                             00011400
      T6 = AIY * QC - AIYZ * RC - AIXY * PC                             00011500
C                           FORM  A(3X3) AND  B(3X1) FOR XSIMEQ         00011600
      A(1,1) = AIX                                                      00011700
      A(1,2) = -AIXY                                                    00011800
      A(1,3) = -AIXZ                                                    00011900
      A(2,2) = AIY                                                      00012000
      A(2,3) = -AIYZ                                                    00012100
      A(2,1) = -AIXY                                                    00012200
      A(3,3) = AIZ                                                      00012300
      A(3,1) = -AIXZ                                                    00012400
      A(3,2) = -AIYZ                                                    00012500
      B(1) = EMX -T1 - QC*T4 + RC*T6                                    00012600
      B(2) = EMY -T2 - RC*T5 + PC*T4                                    00012700
      B(3) = EMZ -T3 - PC*T6 + QC*T5                                    00012800
C                     SOLVE SIMULTANEOUSLY FOR NEXT PF, QF AND RF       00012900
      DV=1.0                                                            00013000
      M3=  XSIMEQF(3,3,1, A,B, DV,TEMP)                                 00013100
      PF = A(1,1)                                                       00013200
      QF = A(2,1)                                                       00013300
      RF = A(3,1)                                                       00013400
C                     COMPUTE PHI DOT, THETA DOT AND PSI DOT            00013410
      SPHI = SINF(PHC)                                                  00013420
      CPHI=COSF(PHC)                                                    00013430
      THF=QC* CPHI-RC* SPHI                                             00013440
      PSF=(QC*SPHI + RC*CPHI)/COSF(THC)                                 00013450
      PHF=PC+PSF * SINF(THC)                                            00013460
      DRV(1)=PF                                                         00013461
      DRV(2)=QF                                                         00013462
      DRV(3)=RF                                                         00013463
      DRV(4)=PHF                                                        00013464
      DRV(5)=THF                                                        00013465
      DRV(6)=PSF                                                        00013466
  900 RETURN                                                            00013500
      END                                                               00090000
```

SUBRØUTINE XYZ

```
C                                  DECK NØ. 9J-XYZ
      SUBRØUTINE  XYZ
      CØMMØN  XN, TMAX, DT, T, RSV,    AIMX, AIMY, AIMZ, AIMXY, AIMYZ,
     X        AIMXZ, EMASS, EM, VAR, ATABL, RTABL, EMX, EMY, EMZ,  TIME,
     X        WØRK, DRV, IFVD, IBKP, NTRY, IERR, I, N, YCRV,
     X    X,Y,Z,XD,YD,ZD,SX,SY,SZ,SXD,SYD,SZD,SXY,SYZ,SXZ,SXYD,SYZD,
     X    SXZD,SX2,SY2,SZ2,SXD2,SYD2,SZD2,SXY2,SYZ2,SXZ2,SXYD2,SYZD2,
     X    SXZD2,AIX,AIY,AIZ,AIXD,AIYD,AIZD,AIXY,AIYZ,AIXZ,AIXYD,AIXZD,
     X        T1,T2,T3,T4,T5,T6,A, B,SM1,SMM,SPHI,CPHI,CTHETA
C
      DIMENSIØN  XN(1), EM(10), VAR(6),ATABL(6), RTABL(6), WØRK(60),
     X           DRV(6), TIME(500),X(10), Y(10), Z(10), XD(10), YD(10),
     X           ZD(10), A(3,3), B(3), YCRV(6,500)
C
      IF(RSV)60,20,400
   20 ITØ=EM(10)
      RSV=-1.C
      GØ TØ(1C0,200,300),ITØ
   60 ITØ = ITØ
      GØ TØ(125,225,325),ITØ
C                                  CASE Y-A(1)
  100 DØ 110 IC=1,20
  110 YD(IC)=0.0

      DØ 115 IC=1,3
  115 Y(IC)= -100.0
      Y(4)= 11.03
      Y(5)= 50.0
      Y(6)= 88.97
      Y(7)= 88.97
      Y(8)=50.0
      Y(9)=11.03
      Z(1)= 45.0
      Z(2)= 0.0
      Z(3)=-45.0
      Z(4)=-109.1
      Z(5)=-86.6
      Z(6)=-64.1
      Z(7)= 64.1
      Z(8)= 86.6
      Z(9)=109.1
C
  125 IF(T-6.C)130,130,140
  130 DØ 135 IM=1,3
      X(IM)= -.5 * T
  135 XD(IM)=-.5
      DØ 138 IM=4,9
      X(IM)= .5 * T
  138 XD(IM)= .5
      GØ TØ 4C0
C
  140 RSV=I
      DØ 145 IS=1,3
```

```
      X(IS)= -3.0
  145 XD(IS)=0.0
      DØ 148 IS=4,9
      X(IS)= 3.0
  148 XD(IS)=0.0
      GØ TØ 400
C                                  CASE Y-A(2)
  200 DØ 210 IC=1,9
  210 X(IC)=0.0
      DØ 215 IC=1,30
  215 XD(IC)=0.0
      DØ 218 IC=1,3
  218 Y(IC)=-100.0
      Y(4)=11.03
      Y(6)=88.97
      Y(7)=88.97
      Y(9)=11.03
      Z(1)=45.0
      Z(2)=0.0
      Z(3)=-45.0
      Z(4)=-109.1
      Z(6)=-64.1
      Z(7)=64.1
      ØMG = .82467
      ØMGX = 1.237005
      Z(9)=109.1
C
  225 IF(T-40.0)230,230,240
  230 Y(5)= 50.0 - 1.25 * T
      Y(8)= 50.0 - 1.25 * T
      X(5) =-1.5 * SINF(ØMG * T)
      X(8) = -X(5)
      Z(5)=-86.6 + 2.165 * T
      Z(8)=86.6 -2.165 * T
      YD(5)= -1.25
      YD(8)= -1.25
      XD(5) = -ØMGX * CØSF(ØMG * T)
      XD(8) = -XD(5)
      ZD(5)= 2.165
      ZD(8)=-2.165
      GØ TØ 400
C
  240 RSV=I
      Y(5)=0.0
      Y(8)=0.0
      X(5) = -1.5
      X(8) = 1.5
      Z(5)=0.0
      Z(8)=0.0
      YD(5)=0.0
      YD(8)=0.0
      XD(5) = 0.0
      XD(8) = 0.0
      ZD(5)=0.0
      ZD(8)=0.0
      GØ TØ 400
C                                  CASE Y-A(3)
  300 DØ 310  IC=1,9
  310 X(IC)=0.0
      DØ 315 IC=1,30
  315 XD(IC)=0.0
      DØ 318 IC=1,3
```

```
  318 Y(IC)=-100.0
      Y(5)=50.0
      Y(6)=88.97
      Y(7)=88.97
      Y(8)=50.0
      Z(1)=45.0
      Z(2)=0.0
      Z(3)=-45.0
      Z(5)=-86.6
      Z(6)=-64.1
      Z(7)=64.1
      Z(8)=86.6
      ØMG = .31416
      ØMG3 = .94248
C
  325 IF(T-45.0)330,330,340
  330 Y(4)=11.03 +1.732 * T
      Y(9)=11.03 +1.732 * T
      X(4) = -3.0*SINF(ØMG*T)
      X(9) = -X(4)
      Z(4)=-109.1 + T
      Z(9)=109.1 - T
      YD(4)= 1.732
      YD(9)= 1.732
      XD(4) = -ØMG3*CØSF(ØMG*T)
      XD(9) = -XD(4)
      ZD(4)= 1.0
      ZD(9)=-1.0
      GØ TØ 400
  340 RSV=I
      Y(4)= 88.97
      Y(9)= 88.97
      X(4) = -3.0
      X(9) = 3.0
      Z(4)= -64.1
      Z(9)= 64.1
      YD(4)=0.0
      YD(9)=0.0
      XD(4) = 0.0
      XD(9) = 0.0
      ZD(4)=0.0
      ZD(9)=0.0
  400 RETURN
      END
```

SUBRØUTINE EMXYZ

```
C                                 DECK NØ. 9J-DV2                              00000100
      SUBRØUTINE EMXYZ                                                         00000200
C                                                                              00000300
      RETURN                                                                   00008000
      END
```

SUBRØUTINE CNTRL

```
C                                 DECK NØ. 9J-CNT                              00000100
      SUBRØUTINE CNTRL(NTRY)                                                   00000200
C                                                                              00000300
      CØMMØN  XN, TMAX, DT, T, RSV,     AIMX, AIMY, AIMZ, AIMXY, AIMYZ,        00000400
     X        AIMXZ, EMASS, EM, VAR, ATABL, RTABL, EMX, EMY, EMZ,  TIME,00000500
     X        WØRK, DRV, IFVD, IBKP, NTRY, IERR, I, N, YCRV,                   00000600
     X    X,Y,Z,XD,YD,ZD,SX,SY,SZ,SXD,SYD,SZD,SXY,SYZ,SXZ,SXYD,SYZD,           00000800
     X    SXZD,SX2,SY2,SZ2,SXD2,SYD2,SZD2,SXY2,SYZ2,SXZ2,SXYD2,SYZD2,          00000900
     X    SXZD2,AIX,AIY,AIZ,AIXD,AIYD,AIZD,AIXY,AIYZ,AIXZ,AIXYD,AIXZD,         00001000
     X        T1,T2,T3,T4,T5,T6,A, B,SM1,SMM,SPHI,CPHI,CTHETA                  00001100
C                                                                              00001200
      DIMENSIØN  XN(1), EM(10), VAR(6),ATABL(6), RTABL(6), WØRK(60),           00001300
     X           DRV(6), TIME(500),X(10), Y(10), Z(10), XD(10), YD(10),        00001400
     X           ZD(10), A(3,3), B(3), YCRV(6,500)                             00001500
C                                                                              00001600
      I=I+1                                                                    00002000
      PRINT 5,I,WØRK(1),T,VAR,DRV,AIX,AIY,AIZ,AIXY,AIXZ,AIYZ                   00002050
    5 FØRMAT(I13,1P2E18.7/(6E17.7))                                            00002100
      IF( DT    - .5)15,15,10                                                  00002150
   10 DT=.5                                                                    00002250
   15 TIME(I) = T                                                              00002375
C                                                                              00002400
      IF(T-TMAX)20, 30, 30                                                     00002500
C                                                                              00002600
   20 IF(I-500)40, 30, 30                                                      00002700
   30 NTRY=2                                                                   00002800
      GØ TØ 60                                                                 00002900
C                                                                              00003000
   40 DØ 50  J=1,6                                                             00003100
   50 YCRV(J,I)= VAR(J) * 57.29578                                             00003200
   60 RETURN                                                                   00003300
      END                                                                      00003400
```

SUBRØUTINE CRVS

```
C                                 DECK NØ. 9J-CRV
      SUBRØUTINE CRVS(NDT, YCRV,TIME)
      CØMMØN XN, RSV
      DIMENSIØN XN(4)
      DIMENSIØN  YCRV(6,500), TIME(500), P(500), PHI(500), THETA(500),
     X           PSI(500),Q(500),R(500),ALPHA(500),BETA(500)
C
      MT = RSV
      NDT=NDT-1
      DØ 20 J=1, NDT
      P(J)= YCRV(1,J)
      Q(J)= YCRV(2,J)
      R(J)= YCRV(3,J)
      PHI(J)=YCRV(4,J)
      THETA(J)=YCRV(5,J)
   20 PSI(J)  =YCRV(6,J)
C                           CØMPUTE ALPHA AND BETA
      DØ 60 I=1,NDT
      CTH=CØSDF(THETA(I))
      YB= -SINDF(THETA(I))
      XB=SINDF(PSI(I))* CTH
      IF(YB)50,30,50
   30 IF(XB)50,40,50
   40 ALPHA(I)=0.0
      BETA(I)=0.0
      GØ TØ 60
   50 BETA(I)= QATANF(YB,XB)
      XALF= CTH * CØSDF(PSI(I))
      ALPHA(I)=ATANDF(SQRTF(1.0 - XALF**2)/XALF)
   60 CØNTINUE
C                           PØLAR CURVES FØR ALPHA - BETA
C                 DETERMINE ALPHA MAX. AND AMAX
      AMAX=ALPHA(1)
      DØ 70 I=2,NDT
   70 AMAX= MAX1F(AMAX,ALPHA(I))
   90 IF(AMAX) 3000, 2000, 100
  100 IF(0.01 - AMAX) 110, 500, 500
  110 IF(0.02 - AMAX) 120, 510, 510
  120 IF(0.05 - AMAX) 130, 520, 520
  130 IF(0.1  - AMAX) 140, 530, 530
  140 IF(0.2  - AMAX) 150, 540, 540
  150 IF(0.5  - AMAX) 160, 550, 550
  160 IF(1.0  - AMAX) 170, 560, 560
  170 IF(2.0  - AMAX) 180, 570, 570
  180 IF(5.0  - AMAX) 190, 580, 580
  190 IF(10.0 - AMAX) 200, 590, 590
  200 IF(20.0 - AMAX) 210, 600, 600
  210 IF(40.0 - AMAX) 220, 610, 610
  220 IF(90.0 - AMAX) 3000, 620, 620
  500 V = 0.002
      GØ TØ 1000
  510 V = 0.005
      GØ TØ 1000
```

```
  520 V = 0.01                                                          00003840
      GØ TØ 1000                                                        00003841
  530 V = 0.02                                                          00003842
      GØ TØ 1000                                                        00003843
  540 V = 0.05                                                          00003844
      GØ TØ 1000                                                        00003845
  550 V = 0.1                                                           00003846
      GØ TØ 1000                                                        00003847
  560 V = 0.2                                                           00003848
      GØ TØ 1000                                                        00003849
  570 V = 0.5                                                           00003850
      GØ TØ 1000                                                        00003851
  580 V = 1.0                                                           00003852
      GØ TØ 1000                                                        00003853
  590 V = 2.0                                                           00003854
      GØ TØ 1000                                                        00003855
  600 V = 5.0                                                           00003856
      GØ TØ 1000                                                        00003857
  610 V = 10.0                                                          00003858
      GØ TØ 1000                                                        00003859
  620 V = 15.0                                                          00003860
 1000 AMAX = V* INTF((AMAX + V)/V)                                      00004000
      CALL CAMRAV(9)                                                    00004100
      CALL PGRIDV(1,AMAX,V,0,1, 5,9,3,-1)                               00004200
      CALL PLABEL(10)                                                   00004300
      CALL PPLØTV(NDT,ALPHA,BETA,1,1,-1,42,IERR)                        00004400
      CALL PLINE(NDT,ALPHA,BETA,1,1,1,IERR)                             00004500
      CALL PPLØTV(MT, ALPHA,BETA,1,1,-1,55,IERR)                        00004600
      CALL PLINE(MT,ALPHA,BETA,1,1,1,IERR)                              00004630
C                          CRT   PLØT CURVES                            00004650
 2000 CALL GRAPH(4,42,-NDT,TIME,P,14H TIME, SECØNDS,11H P, DEG/SEC,1H ) 00004800
      CALL GRAPH(0,55,-MT,TIME,P)                                       00004900
      CALL GRAPH(4,42,-NDT,TIME,Q,1H$,11H Q, DEG/SEC,1H )               00005000
      CALL GRAPH(0,55,-MT,TIME,Q)                                       00005100
      CALL GRAPH(4,42,-NDT,TIME,R,1H$,11H R, DEG/SEC,1H )               00005200
      CALL GRAPH(0,55,-MT,TIME,R)                                       00005300
      CALL GRAPH(4,42,-NDT,TIME,ALPHA,1H$,11H ALPHA, DEG,1H )           00005400
      CALL GRAPH(0,55,-MT,TIME,ALPHA)                                   00005500
 3000 RETURN                                                            00006000
      END                                                               00009000
```

INPUT DATA

```
        1 9.0          40.0         0.2          0.0          0.0          0YA10001
        6 27.91883  +6 12.99868  +6 9.96507   +6 0.0          0.0          0YA10002
       11 0.0          3512.42      6.21118      6.21118      6.21118      0YA10003
       16 6.21118      6.21118      6.21118      6.21118      6.21118      0YA10004
       21 6.21118      1.0          0.40125      0.0          0.0          0YA10005
       26 0.0          0.0          0.0          0.1       -9 0.1       -90YA10006
       31 0.1       -9 0.1       -9 0.1       -9 0.1       -9 0.1       -30YA10007
       36 0.1       -3 0.1       -3 0.1       -3 0.1       -3 0.1       -30YA10008
-      41 0.0          0.0          0.0                                    0YA10009
        1 9.0          80.0         0.2          0.0          0.0          0YA10010
        6 27.91883  +6 12.99868  +6 9.96507   +6 0.0          0.0          0YA10011
       11 0.0                                                              0YA10012
       21              2.0          0.40125      0.0          0.0          0YA10013
-      26 0.0          0.0          0.0                                    0YA10014
        1 9.0          80.0         0.2          0.0          0.0          0YA10015
        6 27.91883  +6 12.99868  +6 9.96507   +6 0.0          0.0          0YA10016
       11 0.0                                                              0YA10017
       21              3.0          0.40125      0.0          0.0          0YA10018
-      26 0.0          0.0          0.0                                    0YA10019
```

MAIN PRØGRAM

```
C                  DECK NØ. 9J-RKM             RUNGE-KUTTA METHØD            00000100
C                                    MAIN PRØGRAM                            00000200
F      DERIV, CNTRL                                                          00000300
       CØMMØN   XN, TMAX, DT, T, RSV,       AIMX, AIMY, AIMZ, AIMXY, AIMYZ,  00000400
     X          AIMXZ, EMASS, EM, VAR, ATABL, RTABL, EMX, EMY, EMZ,   TIME,00000500
     X          WØRK, DRV, IFVD, IBKP, NTRY, IERR, I, N, YCRV,               00000600
     X     X,Y,Z,XD,YD,ZD,SX,SY,SZ,SXD,SYD,SZD,SXY,SYZ,SXZ,SXYD,SYZD,        00000800
     X     SXZD,SX2,SY2,SZ2,SXD2,SYD2,SZD2,SXY2,SYZ2,SXZ2,SXYD2,SYZD2,       00000900
     X     SXZD2,AIX,AIY,AIZ,AIXD,AIYD,AIZD,AIXY,AIYZ,AIXZ,AIXYD,AIXZD,      00001000
     X          T1,T2,T3,T4,T5,T6,A, B,SM1,SMM,SPHI,CPHI,CTHETA              00001100
     X        ,CMX,CMY,CMZ                                                   00001150
C                                                                            00001200
       DIMENSIØN  XN(1), EM(10), VAR(6),ATABL(6), RTABL(6), WØRK(60),       00001300
     X              DRV(6), TIME(500), X(10), Y(10), Z(10), XD(10), YD(10), 00001400
     X               ZD(10), A(3,3), B(3), YCRV(6,500)                       00001500
     X        ,CMX(500),CMY(500),CMZ(500)                                    00001550
C                                                                            00002000
   10 CALL DECRD(XN)                                                         00002100
      N=XN                                                                   00002200
C                                     PRINT DATA                             00002400
      PRINT 15, (XN(I), I=1, 42)                                             00002500
   15 FØRMAT(1H1,36X,27HDATA FØR RUNGE-KUTTA METHØD/(/1P6E17.7))             00002600
      PRINT 25                                                               00002700
   25 FØRMAT(1H1,40X,19HRUNGE-KUTTA RESULTS/36X,28HTIME   VARIABLES   DERI00002800
     XVATIVES)                                                               00002900
C                  INITILIZE AND CØMPUTE  CØNSTANTS                          00003000
      I=0                                                                    00003100
      NØ=6                                                                   00003200
      IFVD = 0                                                               00003300
      IBKP = 1                                                               00003400
      SM=EMASS                                                               00003500
      DØ 30 I=1,N                                                            00003600
   30 SM=SM+EM(I)                                                            00003700
      SM1=1.0/SM                                                             00003800
      SMM= EMASS * SM1                                                       00003900
C                                                                            00004000
      CALL RKS3(DERIV, CNTRL, VAR, DRV, ATABL, RTABL, WØRK, T, DT, NØ, I00004100
     XFVD, IBKP, NTRY, IERR)                                                 00004200
      IF(IERR)40, 50, 40                                                     00004300
   40 PRINT 45, IERR                                                         00004400
   45 FØRMAT(1H1,40X,20HERRØR RETURN   IERR=,I3)                             00004500
      GØ TØ 60                                                               00004600
C                                    PLØT CURVES                             00004700
   50 CALL CRVS(I,YCRV,TIME, CMX,CMY,CMZ)                                    00004800
   60 GØ TØ 10                                                               00004900
      END                                                                    00009000
```

SUBRØUTINE CRVS

```
C                                      DECK NØ. 9J-CRV
      SUBRØUTINE CRVS(NDT, YCRV,TIME,CMX,CMY,CMZ)
      CØMMØN XN, RSV
      DIMENSIØN XN(4)
      DIMENSIØN  YCRV(6,500), TIME(500), P(500), PHI(500), THETA(500),
     X            PSI(500),Q(500),R(500),ALPHA(500),BETA(500)
      DIMENSIØN CMX(500), CMY(500), CMZ(500)
C
      MT = RSV
      NDT=NDT-1
      DØ 20 J=1, NDT
      P(J)= YCRV(1,J)
      Q(J)= YCRV(2,J)
      R(J)= YCRV(3,J)
      PHI(J)=YCRV(4,J)
      THETA(J)=YCRV(5,J)
   20 PSI(J)   =YCRV(6,J)
C                                 CØMPUTE ALPHA AND BETA
      DØ 60 I=1,NDT
      CTH=CØSDF(THETA(I))
      YB= -SINDF(THETA(I))
      XB=SINDF(PSI(I))* CTH
      IF(YB)50,30,50
   30 IF(XB)50,40,50
   40 ALPHA(I)=0.0
      BETA(I)=0.0
      GØ TØ 60
   50 BETA(I)= QATANF(YB,XB)
      XALF= CTH * CØSDF(PSI(I))
      ALPHA(I)=ATANDF(SQRTF(1.0 - XALF**2)/XALF)
   60 CØNTINUE
C                                 PØLAR CURVES FØR ALPHA - BETA
C                    DETERMINE    ALPHA MAX. AND AMAX
      AMAX=ALPHA(1)
      DØ 70 I=2,NDT
   70 AMAX= MAX1F(AMAX,ALPHA(I))
   90 IF(AMAX) 3000, 2000, 100
  100 IF(0.01 - AMAX) 110, 500, 500
  110 IF(0.02 - AMAX) 120, 510, 510
  120 IF(0.05 - AMAX) 130, 520, 520
  130 IF(0.1  - AMAX) 140, 530, 530
  140 IF(0.2  - AMAX) 150, 540, 540
  150 IF(0.5  - AMAX) 160, 550, 550
  160 IF(1.0  - AMAX) 170, 560, 560
  170 IF(2.0  - AMAX) 180, 570, 570
  180 IF(5.0  - AMAX) 190, 580, 580
  190 IF(10.0 - AMAX) 200, 590, 590
  200 IF(20.0 - AMAX) 210, 600, 600
  210 IF(40.0 - AMAX) 220, 610, 610
  220 IF(90.0 - AMAX) 3000, 620, 620
  500 V = 0.002
      GØ TØ 1000
  510 V = 0.005
```

```
      GO TO 1000                                                        00003839
  520 V = 0.01                                                          00003840
      GO TO 1000                                                        00003841
  530 V = 0.02                                                          00003842
      GO TO 1000                                                        00003843
  540 V = 0.05                                                          00003844
      GO TO 1000                                                        00003845
  550 V = 0.1                                                           00003846
      GO TO 1000                                                        00003847
  560 V = 0.2                                                           00003848
      GO TO 1000                                                        00003849
  570 V = 0.5                                                           00003850
      GO TO 1000                                                        00003851
  580 V = 1.0                                                           00003852
      GO TO 1000                                                        00003853
  590 V = 2.0                                                           00003854
      GO TO 1000                                                        00003855
  600 V = 5.0                                                           00003856
      GO TO 1000                                                        00003857
  610 V = 10.0                                                          00003858
      GO TO 1000                                                        00003859
  620 V = 15.0                                                          00003860
 1000 AMAX = V* INTF((AMAX + V)/V)                                      00004000
      CALL CAMRAV(9)                                                    00004100
      CALL PGRIDV(1,AMAX,V,0,1, 5,9,3,-1)                               00004200
      CALL PLABEL(10)                                                   00004300
      CALL PPLOTV(NDT,ALPHA,BETA,1,1,-1,42,IERR)                        00004400
      CALL PLINE(NDT,ALPHA,BETA,1,1,1,IERR)                             00004500
      CALL PPLOTV(MT, ALPHA,BETA,1,1,-1,55,IERR)                        00004600
      CALL PLINE(MT,ALPHA,BETA,1,1,1,IERR)                              00004630
C                              CRT   PLOT CURVES                        00004650
 2000 CALL GRAPH(4,42,-NDT,TIME,P,14H TIME, SECONDS,11H P, DEG/SEC,1H ) 00004800
      CALL GRAPH(0,55,-MT,TIME,P)                                       00004900
      CALL GRAPH(4,42,-NDT,TIME,Q,1H$,11H Q, DEG/SEC,1H )               00005000
      CALL GRAPH(0,55,-MT,TIME,Q)                                       00005100
      CALL GRAPH(4,42,-NDT,TIME,R,1H$,11H R, DEG/SEC,1H )               00005200
      CALL GRAPH(0,55,-MT,TIME,R)                                       00005300
      CALL GRAPH(4,42,-NDT,TIME,ALPHA,1H$,11H ALPHA, DEG,1H )           00005400
      CALL GRAPH(0,55,-MT,TIME,ALPHA)                                   00005500
C                              PLOT   MX MY MZ                          00005510
      CALL GRAPH(3,42,-NDT,TIME,CMX,14H TIME, SECONDS,3H MX,1H )        00005520
      CALL GRAPH(0,55,-MT,TIME,CMX)                                     00005530
      CALL GRAPH(3,42,-NDT,TIME,CMY,1H$,3H MY,1H )                      00005540
      CALL GRAPH(0,55,-MT,TIME,CMY)                                     00005550
      CALL GRAPH(3,42,-NDT,TIME,CMZ,1H$,3H MZ,1H )                      00005560
      CALL GRAPH(0,55,-MT,TIME,CMZ)                                     00005570
 3000 RETURN                                                            00006000
      END                                                               00009000
```

SUBRØUTINE EMXYZ

```
C                                DECK NØ. 9J-DV2                           00000100
      SUBRØUTINE EMXYZ                                                     00000200
C                                                CØNTRØL    MØMENTS        00000250
C                             CØMPUTE  MX  MY  MZ                          00000300
      CØMMØN   XN, TMAX, DT, T, RSV,    AIMX, AIMY, AIMZ, AIMXY, AIMYZ,    00000400
     X         AIMXZ, EMASS, EM, VAR, ATABL, RTABL, EMX, EMY, EMZ,  TIME,00000500
     X         WØRK, DRV, IFVD, IBKP, NTRY, IERR, I, N, YCRV,              00000600
     X     X,Y,Z,XD,YD,ZD,SX,SY,SZ,SXD,SYD,SZD,SXY,SYZ,SXZ,SXYD,SYZD,      00000800
     X     SXZD,SX2,SY2,SZ2,SXD2,SYD2,SZD2,SXY2,SYZ2,SXZ2,SXYD2,SYZD2,     00000900
     X     SXZD2,AIX,AIY,AIZ,AIXD,AIYD,AIZD,AIXY,AIYZ,AIXZ,AIXYD,AIXZD,    00001000
     X         T1,T2,T3,T4,T5,T6,A, B,SM1,SMM,SPHI,CPHI,CTHETA             00001100
     X       ,CMX,CMY,CMZ,C                                                00001150
C                                                                          00001200
      DIMENSIØN  XN(1), EM(10), VAR(6),ATABL(6), RTABL(6), WØRK(60),       00001300
     X           DRV(6), TIME(500),X(10), Y(10), Z(10), XD(10), YD(10),    00001400
     X           ZD(10), A(3,3), B(3), YCRV(6,500),C(15)                   00001500
C                                                                          00002000
      DIMENSIØN          CMX(500),CMY(500),CMZ(500)                        00002100
      IF(I)30 ,20,30                                                       00002300
   20 CALL DECRD(C)                                                        00002400
   30 EMX = C(1)*VAR(1) + C(2)*VAR(2) + C(3)*VAR(3) + C(4)                 00002500
      EMY = C(5)*VAR(1) + C(6)*VAR(2) + C(7)*VAR(3) + C(8)                 00002600
      EMZ = C(9)*VAR(1) + C(10)*VAR(2) + C(11)*VAR(3) + C(12)              00002700
      CMX(I+1) = EMX                                                       00002800
      CMY(I+1) = EMY                                                       00002900
      CMZ(I+1) = EMZ                                                       00003000
      RETURN                                                               00008000
      END                                                                  01000000
```

INPUT DATA

```
         1 0.0           40.0         0.2           0.0          0.0                 1
         6 17.5558    +6 16.2225   +6 1.38147    +6 0.0          0.0                 2
        11 0.0           2087.76      0.0           0.0          0.0                 3
        16 0.0           0.0          0.0           0.0          0.0                 4
        21 0.0           0.0          0.40125       .0174533     0.0                 5
        26 0.0           0.0          0.0           .1        -9 .1          -9      6
        31 .1         -9 .1        -9 .1         -9 .1        -9 .1          -3      7
        36 .1         -3 .1        -3 .1         -3 .1        -3 .1          -3      8
        41 0.0           0.0         0.0                                 MØMENTS
-        1                                                               STØP
         1-2.5        +6                        1.003125 +6                GAIN1 1
         6-2.5        +6                                                   GAIN1 2
-       11-0.5        +6                                                   GAIN1 3
```

UNCLASSIFIED

Security Classification

DOCUMENT CONTROL DATA - R&D

(Security classification of title, body of abstract and indexing annotation must be entered when the overall report is classified)

1. ORIGINATING ACTIVITY (Corporate author) North American Aviation, Inc., Space and Information Systems Division	2a. REPORT SECURITY CLASSIFICATION Unclassified 2b. GROUP

3. REPORT TITLE

Transient Dynamic Response of Orbiting Space Stations

4. DESCRIPTIVE NOTES (Type of report and inclusive dates)

5. AUTHOR(S) (Last name, first name, initial)

Tai, C. L., Andrew, L. V., Loh, M. M. H., Kamrath, P. C.

6. REPORT DATE February 1965	7a. TOTAL NO. OF PAGES 349	7b. NO. OF REFS 36
8a. CONTRACT OR GRANT NO. AF33(657)-10219 b. PROJECT NO. 1370 c. Task 137008 d.	9a. ORIGINATOR'S REPORT NUMBER(S) FDL-TDR-64-25 9b. OTHER REPORT NO(S) (Any other numbers that may be assigned this report)	

10. AVAILABILITY/LIMITATION NOTICES

11. SUPPLEMENTARY NOTES	12. SPONSORING MILITARY ACTIVITY Air Force Flight Dynamics Laboratory

13. ABSTRACT

The stability and dynamic response of thirteen rotating space station configurations when subjected to various applied disturbances were investigated first by approximate exploratory analyses to determine the significant configurations and the relative significance of transient inputs to each configuration. Detailed analyses of ten selected combinations of configurations and forcing functions were then carried out in depth with special attention given to internal mass motions, docking, angular acceleration, and control forces. In view of the unique dynamic response problems associated with the gravitational gradient and structural elasticity, separate detailed analyses of the cable-connected configuration, the Y-configuration, and the H-configuration were also conducted.

DD FORM 1 JAN 64 1473

UNCLASSIFIED

Security Classification

14. KEY WORDS	LINK A		LINK B		LINK C	
	ROLE	WT	ROLE	WT	ROLE	WT

INSTRUCTIONS

1. ORIGINATING ACTIVITY: Enter the name and address of the contractor, subcontractor, grantee, Department of Defense activity or other organization *(corporate author)* issuing the report.

2*a*. REPORT SECURITY CLASSIFICATION: Enter the overall security classification of the report. Indicate whether "Restricted Data" is included. Marking is to be in accordance with appropriate security regulations.

2*b*. GROUP: Automatic downgrading is specified in DoD Directive 5200.10 and Armed Forces Industrial Manual. Enter the group number. Also, when applicable, show that optional markings have been used for Group 3 and Group 4 as authorized.

3. REPORT TITLE: Enter the complete report title in all capital letters. Titles in all cases should be unclassified. If a meaningful title cannot be selected without classification, show title classification in all capitals in parenthesis immediately following the title.

4. DESCRIPTIVE NOTES: If appropriate, enter the type of report, e.g., interim, progress, summary, annual, or final. Give the inclusive dates when a specific reporting period is covered.

5. AUTHOR(S): Enter the name(s) of author(s) as shown on or in the report. Enter last name, first name, middle initial. If military, show rank and branch of service. The name of the principal author is an absolute minimum requirement.

6. REPORT DATE: Enter the date of the report as day, month, year; or month, year. If more than one date appears on the report, use date of publication.

7*a*. TOTAL NUMBER OF PAGES: The total page count should follow normal pagination procedures, i.e., enter the number of pages containing information.

7*b*. NUMBER OF REFERENCES: Enter the total number of references cited in the report.

8*a*. CONTRACT OR GRANT NUMBER: If appropriate, enter the applicable number of the contract or grant under which the report was written.

8*b*, 8*c*, & 8*d*. PROJECT NUMBER: Enter the appropriate military department identification, such as project number, subproject number, system numbers, task number, etc.

9*a*. ORIGINATOR'S REPORT NUMBER(S): Enter the official report number by which the document will be identified and controlled by the originating activity. This number must be unique to this report.

9*b*. OTHER REPORT NUMBER(S): If the report has been assigned any other report numbers *(either by the originator or by the sponsor)*, also enter this number(s).

10. AVAILABILITY/LIMITATION NOTICES: Enter any limitations on further dissemination of the report, other than those imposed by security classification, using standard statements such as:

(1) "Qualified requesters may obtain copies of this report from DDC."

(2) "Foreign announcement and dissemination of this report by DDC is not authorized."

(3) "U. S. Government agencies may obtain copies of this report directly from DDC. Other qualified DDC users shall request through
_______________________."

(4) "U. S. military agencies may obtain copies of this report directly from DDC. Other qualified users shall request through
_______________________."

(5) "All distribution of this report is controlled. Qualified DDC users shall request through
_______________________."

If the report has been furnished to the Office of Technical Services, Department of Commerce, for sale to the public, indicate this fact and enter the price, if known.

11. SUPPLEMENTARY NOTES: Use for additional explanatory notes.

12. SPONSORING MILITARY ACTIVITY: Enter the name of the departmental project office or laboratory sponsoring *(paying for)* the research and development. Include address.

13. ABSTRACT: Enter an abstract giving a brief and factual summary of the document indicative of the report, even though it may also appear elsewhere in the body of the technical report. If additional space is required, a continuation sheet shall be attached.

It is highly desirable that the abstract of classified reports be unclassified. Each paragraph of the abstract shall end with an indication of the military security classification of the information in the paragraph, represented as *(TS)*, *(S)*, *(C)*, or *(U)*

There is no limitation on the length of the abstract. However, the suggested length is from 150 to 225 words.

14. KEY WORDS: Key words are technically meaningful terms or short phrases that characterize a report and may be used as index entries for cataloging the report. Key words must be selected so that no security classification is required. Identifiers, such as equipment model designation, trade name, military project code name, geographic location, may be used as key words but will be followed by an indication of technical context. The assignment of links, rules, and weights is optional.